The 15th National Conference on Chemical Dynamics

第十五届全国化学动力学会议

主办单位：中国化学会

承办单位：南京大学

2017 年 8 月 18–22 日



会 议 论 文 集

中国•南京

大会报告

K1	刘国平	Direct mapping of the key feature of the reactive potential energy surface
K2	伍灼耀	New Paradigm in Photoionization and Photoelectron Spectroscopy: Quantum-State-Selected Unimolecular and Bimolecular Reaction Dynamics of Ions
K3	张东辉	Cl + CH_4 反应的态-态量子动力学研究
K4	杨金龙	金属团簇的超原子分子理论
K5	André Fielicke	Shedding IR light on gas-phase metal clusters: insights into structures and reactions
K6	周鸣飞	Infrared Spectroscopy of Donor-Acceptor Bonding Carbonyl Complexes
K7	齐　飞	面向航空发动机的燃烧基础研究
K8	王兴安	基于高分辨交叉分子束-离子速度成像技术的基元化学反应研究
K9	罗　毅	突破选择定则：光学暗态的直接探测
K10	王鸿飞	Novel Aspects of Nonlinear Spectroscopy Using Synchronized Ultrafast Laser Pulses at Time and Frequency Limit
K11	夏安东	凝聚相复杂分子聚集体的激发态溶剂化过程研究
K12	任泽峰	Fill the Pressure and Material Gap in Catalytic Studies by Sum Frequency Generation Vibrational Spectroscopy
K13	徐　昕	Towards the accurate and efficient microkinetic modelling in heterogeneous catalysis
K14	郭　华	Nonadiabatic Tunneling: Adiabatic or Diabatic and Why We Should Care?

邀请报告

I1	史　强	Convergence of high order perturbative expansions in open system quantum dynamics
I2	朱超原	Restoring electronic coherence/decoherence for a trajectory-based nonadiabatic molecular dynamics
I3	蒋　彬	Recent Progress on the Dissociative Chemisorption of Energy-relevant Molecules on Metal Surfaces
I4	边文生	典型化学反应的势能面和分子动态学

I5	孙志刚	三原子和四原子体系的态－态分辨含时量子波包理论
I6	崔刚龙	激发态电子结构和非绝热动力学方法发展和应用
I7	兰峥岗	On-the-fly Surface-Hopping Nonadiabatic Dynamics and Analysis of Geometrical Evolution with Dimensionality Reduction Approaches
I8	苏红梅	捕捉 DNA 鸟嘌呤氧化损伤反应的自由基离子对中间体
I9	何圣贵	团簇与惰性分子的反应研究
I10	赵　仪	有机半导体、光合作用等复杂体系中载流子量子动力学理论
I11	翟华金	“中国红灯笼分子”－硼球烯及其家族
I12	刘　剑	A semiclassical study on quantum dynamical effects in Raman spectra of liquid water
I13	李　辉	Recent Progress in Study of Superfluid in Doped Quantum Solution
I14	梅　晔	Computing Free Energy of States and Potential of Mean Force at High Levels from Low Level Simulations
I15	田善喜	Recent Progresses on Dissociative Electron Attachment Study
I16	曹剑炜	典型势阱控速反应的准经典轨线计算
I17	郭　庆	水在 TiO_2 表面的光化学
I18	周传耀	Electronic Structure at TiO_2 Interface
I19	庄　巍	Ion Effect on Hydrogen Bonding Network in Water
I20	邢小鹏	Adsorption and activation of O_2 or NO on heavy metal clusters
I21	傅　钢	表界面催化的动力学调控
I22	王雪峰	Metal － Hydrogen Bridge and Agostic Bonding: Infrared Spectra and Theoretical Calculations
I23	何　晓	Recent Advances in Fragment-based Quantum Mechanical Methods and Minnesota Density Functionals
I24	郑卫军	Microsolvation of Salts in Water: Photoelectron Spectroscopy and Theoretical Studies of Size-Selected Salt-Water Clusters
I25	张　贞	Interaction of Ca^{2+} with Sphingomyelin Membrane Studied by High-Resolution Broadband Sum Frequency Vibrational Spectroscopy

I26	胡水明	分子红外光谱的亚 kHz 精度测量
I27	陈雪波	Resonance Energy Transfer Pathways for the Photoluminescence of Europium Antenna Probes: Insights into the Mechanism via a Combined Computational, Synthesis and Time-resolved Spectra Study
I28	张　冰	激发态分子相干核波包运动的直接观测
I29	杨　阳	主/客配位笼状超分子的激发态动力学：全时尺度瞬态光谱揭示核/壳电荷迁移
I30	吴成印	强激光场下分子离子激发态动力学
I31	郑贤锋	Photoionization cross section measurements of the excited states of 3d transition metal atoms
I32	马玉臣	光合作用过程中新的暗态对能量传递调控
I33	王学斌	Photoelectron Spectroscopy and Theoretical Study of Aerosol Cluster
I34	翁羽翔	Coupling of multi-vibrational modes in bacteriochlorophyll a in solution observed with 2D electronic spectroscopy
I35	王凤燕	Imaging complex-forming reaction dynamics in the oxidation of aluminum atoms
I36	朱　华	Ab initio potential energy surface and rovibrational spectra of the H_2–HCCCN complex
I37	莫宇翔	D_2 分子光解：D_2 + XUV→D(2s，2p)+ D(1s) D(2s)和 D(2p)通道的量子干涉
I38	郑旭明	烯酮和嘧啶碱基激发态势能面交叉动力学--拉曼光谱和从头计算研究

口头报告

O1	王林军	Recent Progress in Large-Scale Nonadiabatic Dynamics
O2	姚　尧	Simulation of coherent exciton dynamics in organic semiconductors using time-dependent density matrix renormalization group method
O3	李永乐	Investigate chemical reaction rates with RPMD
O4	龙　闰	纳米尺度界面的光激发动力学
O5	William Glover	Polarizable QM/MM for excited-state dynamics
O6	朱　通	Force Field Development and Fragment based Ab Initio Molecular Dynamic Simulation for MetalloProteins

O7	杨栋元	Accidental Resonance Mediated Predissociation Pathway of Water Molecules Excited to the Electronic $\tilde{C}$ State
O8	叶树集	Ultrafast Vibrational Energy Transfer of Interfacial Membrane Proteins at the Membrane/Water Interface
O9	曾小庆	Kinetics of heterocumulene OCNSO in cryogenic matrixes
O10	边红涛	光催化还原二氧化碳超快红外光谱学研究
O11	陆　洲	界面化学反应时间分辨动力学的二阶非线性光学研究
O12	李明德	敏性药物分子酮洛芬（Ketoprofen）的超快光谱研究及其应用
O13	陈缙泉	Ultrafast Dynamics in DNA Model System
O14	张　峰	Terahertz Vibrational Spectroscopy in Molecular Crystalline Systems
O15	梁先庭	Simulating two-dimensional non-linear photon echo spectra: By using the normally ordered form of Hamiltonian
O16	林　珂	C-H 伸缩振动光谱的费米共振去除方法
O17	颜　波	Recent Progresses in Cold Molecule Physics
O18	刘　晶	Interface reaction kinetics for NH_3-SCR of NO_x over $CuMn_2O_4$ catalyst
O19	张春峰	相干空穴转移过程的二维电子光谱研究
O20	徐海峰	超快强激光诱导的原子分子中性里德堡态激发
O21	马晨生	Combined femtosecond time-resolved fluorescence and transient absorption of excited state dynamics of cytosine and derivatives
O22	董文锐	Kinetic study of CH_2OO Criegee intermediate relevant reactions using OH laser induced fluorescence
O23	冯　刚	A highly-integrated supersonic-jet Fourier-transform microwave spectrometer: Instrumental setup and Initial Molecular Results

墙报展讲

P-001	赵　臻	Calculation on Activation Energy for Decomposition of Magnesite by Congruent Dissociative Vaporization Theory
P-002	陈　俊	Potential Energy Surfaces and Dynamics Study of Al + O_2 Reaction
P-003	陈　骏	Co(0001)表面 H_2O 和 CO 的共吸附：分子间氢键的作用
P-004	陈玲玲	液体及其界面的反应动力学质谱装置
P-005	陈荣军	泛频激发效应对于 F+CH_4 反应的影响
P-006	陈浙宁	Enhanced Ab Initio Molecular Dynamics Simulation of the Temperature-Dependent Thermodynamics for the Diffusion of Carbon Monoxide on Ru(0001) Surface
P-007	陈　震	甲烷的氢同位素效应对于 Cl+CH_4/CHD_3 反应影响研究
P-008	代文帅	REMPI/MATI Spectra and Theoretical Calculations of 2-Methoxypyridine and 2-(N-methylamino)pyridine: The Conformational Effect
P-009	邓国海	Simplest N-sulfonylamine HNSO
P-010	丁　晨	吸附物相互作用对甲酸分解火山形曲面的影响
P-011	董　斌	二次谐波研究偶氮苯分子衍生物在石墨烯表面的电催化反应
P-012	董慧纺	Shell thickness dependence of plasmon-induced hot electron injection process in Core/Shell Au@CdS Nanocrystals
P-013	杜存斌	Kinetics of absorption of carbon dioxide in aqueous N,N-dimethylethanolamine solutions with carbonic anhydrase
P-014	杜莉莉	The Influence of Water in the Photogeneration and Properties of a Bifunctional Quinone Methide
P-015	费泽杰	The thermal decomposition of nitrate/nitrite based molten salt and observation of N_2O emitting
P-016	冯瑞娟	Difluoroacetyl Azide: Synthesis, Characterization, and Decomposition
P-017	高　治	Product-pairs correlations in molecule-molecule inelastic collisions
P-018	宫士炎	NaSCN 在水中溶解的微观机理研究
P-019	郭前进	Probing laser-induced heterogeneous microenvironment changes in room temperature ionic liquids

P-020	韩建慧	DPC 分子激发态分子间双质子转移的理论研究
P-021	何　胜	Controllable Synthesis and Excited-State Dynamics of Organometal Halide Perovskite Quantum Dots
P-022	霍妲雨佳	含脯氨酸多肽的气相解离动力学研究
P-023	姜延欢	基于 AND/甲醇推进剂的甲醇和 NOX 化学反应动力学研究
P-024	冷　静	钙钛矿薄膜与电荷受体之间界面电荷转移的超快动力学研究
P-025	李芳芳	State-to-state reaction dynamics of Al + O_2 → AlO + O studied by a crossed-beam time-sliced velocity map ion imaging apparatus
P-026	李丰毅	Neural Network-based Global ab initio Potential Energy Surface for the 2^1A" State of C(1D)+H_2 Reactive System
P-027	李　璐	Thermal decomposition mechanisms of three methyl anisoles
P-028	李元杰	Diffusion Pathways of Atomic Hydrogen Adsorption on Defective Iron Surfaces
P-029	刘洪涛	高温熔盐原位结构研究
P-030	刘清华	High-Dimensional Atomistic Neural Network for Potential Energy Surface of HCl Intereacting with Au (111)
P-031	刘雅兰	甲基环己烷高温裂解机理的理论研究
P-032	刘　洋	基于 C_2H_2-Ne 体系全维精确势能面的碰撞传能的理论
P-033	卢丹丹	HO + CO → H + CO_2 体系的化学反应动力学研究
P-034	卢晓晓	An accurate full-dimensional potential energy surface and quasiclassical trajectory study of the H + H_2O_2 reaction
P-035	罗　璇	Reactive and nonreactive scattering of CO_2 on Ni(100) with a Generalized Langevin Oscillator Model
P-036	吕　骥	CO_2 Diffusion in various carbonated beverages: A molecular dynamics study
P-037	吕美横	Insight into the excited-state intramolecular double proton transfer of the 2,5-bis(benzoxazol-2-yl)thiophene-3,4-diol: one-step or stepwise mechanism?
P-038	马滢雪	维生素 B2 对不饱和脂肪酸在气/液界面上氧化反应动力学影响的非线性光学研究
P-039	马玉杰	Reaction dynamics of Al + O_2 → AlO + O studied by a crossed-beam time-sliced velocity map ion imaging apparatus via selective state ionization

P-040	马志远	Reaction kinetics of two tertiary amines with CO_2 in aqueous solutions
P-041	孟庆勇	Lattice Effects of Surface Cell: ML-MCTDH Study on Surface Scattering of CO/Cu(100)
P-042	孟　双	溶剂调控的 3-氨基-1,2,4-三唑的基态及激发态结构动力学研究
P-043	聂兆刚	液相水分子的超快离化反应动力学
P-044	平磊磊	Dynamics studies on a new ab initio based potential energy surface of the H_2S+OH→HS+H_2O reaction
P-045	史亚荣	硅纳米颗粒大小对表面电荷特性的影响
P-046	宋辛黎	Minding the Gap: Variations on the Bergman Theme. Cycloaromatization of Penta-, Hepta- and Octa-diynes
P-047	王俊慧	Cation-Exchange-Induced Reversible Conversion between 3D Cubic Perovskite and 2D Layer-Structured Perovskite
P-048	王　萌	Construction of Diabatic and Adiabatic Potential Energy Surfaces of Li_2 by Multistate Density Functional Theory
P-049	王锐敏	The location of excess electrons on H_2O/TiO_2(110) surface and its role in the surface reactions
P-050	王天骏	吸附水对二氧化钛(110)表面本征缺陷激发态的影响
P-051	王旭东	氧气起源：二氧化碳分子的电子贴附解离
P-052	王玉奉	F+HD→DF+H 反应中 HD(v=1)振动激发得到 DF(v'=5)产物
P-053	魏千顺	Negligible Cation Effect on Rotational Dynamics of Water Molecules in Electrolyte Aqueous Solution
P-054	魏　馨	溶剂调控的 2-巯基苯并噻唑的激发态质子转移
P-055	吴亚楠	C(^{1}D)+H_2 反应体系的 RPMD 计算
P-056	谢斌斌	Photoinduced Curtius Rearrangement of Fluorocarbonyl Azide, FC(O)N_3: A QM/MM Nonadiabatic Dynamics Simulations Study
P-057	谢　华	低温催化合成氨的反应机理研究
P-058	谢雨润	F+H_2(v=0,j=0)→HF+H 中的分波共振

P-059	许　兵	Borylene Complex FB═CeF_2 and Inserted F_2B−CeF Molecules : Matrix Infrared Spectra and Quantum Chemical Calculations for the Reaction Products of the Laser-Ablated Cerium Atom with Boron Trifluoride
P-060	杨　波	铜基催化剂表面甲酸根覆盖度对二氧化碳加氢反应动力学的影响
P-061	杨　静	Genistein Binding to Copper (II). Solvent Dependence and Effects on Radical Scavenging
P-062	杨　梦	硝基扭转角对硝基萘及其衍生物激发态衰减动力学的影响
P-063	于　嫚	The charge transport/recombination dynamics in planar perovskite solar cells
P-064	俞　凡	CuAAC 法合成 1,2,3-三氮唑的双核铜催化机理研究
P-065	翟翌童	Experimental and modeling studies of small typical methyl esters pyrolysis: Methyl butanoate and methyl crotonate
P-066	张单单	Methane dissociation on Cu Surfaces: A DFT study
P-067	张　迪	硝基多环芳烃激发态在醇溶液中的夺氢反应研究
P-068	张瑞丹	Probe the Adsorption of Acetone on RutileTiO_2(110) Surfaces with High-Resolution Sum Frequency Generation
P-069	张喜庭	To Photoredox or Not in Neutral Aqueous Solutions for Selected Benzophenone and Anthraquinone Derivatives
P-070	郑　勇	离子液体电沉积制备纳米铝的反应动力学规律
P-071	周海强	尿嘧啶胸腺嘧啶水溶液中激发态动力学的研究
P-072	周淼淼	二碘-氟硼吡咯中系间交叉过程和能量转移过程的溶剂化效应
P-073	周司文	吡啶离子液体[OPy][BF_4]与乙腈二元体系的局部微观结构研究
P-074	周雪瑶	Scattering and Reaction Dynamics on Chemically Accurate 15D Potential Energy Surface for Methane Dissociation on Ni(111)
P-075	左俊祥	Construction of Potential Energy Surface for ClH_2O System and Its Application in Ring Polymer Molecular Dynamics Study
P-076	陈娇娇	纳米尺寸中性锰氧化物团簇的产生和反应性研究
P-077	陈　强	VB_3^+阳离子团簇与 CH_4 的反应研究
P-078	崔佳桐	$Fe_2O_3^+$阳离子团簇与苯的反应研究

P-079	丁迅雷	氧化钒团簇负载的单原子金上的氢气氧化反应
P-080	冯林雁	Wheel-like, elongated, circular, and linear geometries in boron-based C_nB_{7-n} (n = 0−7) clusters: structural transitions and aromaticity
P-081	韩英姿	Tracing of Multi-Site Acetal Reactions at Metal Clusters by HR-ESI-TOF-MS
P-082	胡继闯	Fe_2O^+正离子团簇与长链烷烃的反应性研究
P-083	姜利学	CO_2 与 FeH^-反应生成甲酸根离子 HCO_2^-
P-084	蒋述康	三甲胺二聚体中性团簇的 IR-VUV 光谱研究
P-085	李晓娜	$IrAlO_6^+$团簇催化氧化 CO
P-086	李艳丽	Probing thorium oxides and beryllium clusters by high resolution photoelectron imaging
P-087	李　志	Density Functional Study on Small Al-Zn-Mg-Cu-Zr Cluster
P-088	刘付轶	氯自由基加成 1-丁烯和异丁烯反应研究
P-089	刘清宇	TaC^-双原子阴离子的低温光电子速度成像研究
P-090	刘志凌	Rh-doped Hexadecagold Cluster
P-091	王丽娜	铜-钒氧化物团簇催化氧化 CO 反应中的自旋湮灭研究
P-092	王亭亭	Low-temperature adsorption of O_2 on Au_n^- (n = 2 - 36)
P-093	王迎进	Why nanoscale tank treads move? Structures, bonding, and molecular dynamics of a doped boron cluster $B_{10}C$
P-094	王宗莹	Chemisorption of Atomic Hydrogen, Oxygen and Carbon on Small Iron Clusters: A First-principle Study
P-095	徐西玲	$Mn_xC_y^-$ 团簇的结构和成键性质研究
P-096	许洪光	Investigation on Semiconductor Clusters Doped with Metal Atoms
P-097	杨　斌	光电子能谱与密度泛函方法对 $Cr_nSi_{12}^-$(n=1,2,3)团簇的研究
P-098	杨　冬	Reactions of Yttrium-oxygen Cation with Carbon Dioxide: An Infrared Photodissociation Spectroscopic and Theoretical Study
P-099	杨　岩	Channel resolved multiorbital double ionization of molecular Cl_2 in intense femtosecond laser field
P-100	殷保祺	CuO_n^-(n = 1−3)和 AgO_n^- (n = 1−3，5)团簇与 CO 的反应

P-101	于同坡	振动态选择的 NO_2^+离子解离动力学研究
P-102	翟　羽	Investigate HCN-$(pH_2)_N$ clusters with Multi-Dimension Morse/Long-Range Potential and Path Integral Monte Carlo Simulation
P-103	张菊梅	异核三金属羰基团簇负离子的光电子速度成像研究
P-104	张梅琦	氧化钴团簇上共吸附小分子的光诱导反应研究
P-105	张　婷	Au^+与直链烷烃(C2−C10)反应的研究
P-106	张　岳	含氮正离子与氢分子的反应势能面
P-107	赵艳霞	光辅助下 Rh-V 异核氧化物团簇催化转化甲烷的研究
P-108	赵　越	$VO_{1\text{-}4}^+$阳离子团簇与烷烃（$C_{1,3,5,7}$）反应的实验和理论研究
P-109	赵　志	Reactions of Copper and Silver Cations with Carbon Dioxide: an Infrared Photodissociation Spectroscopic and Theoretical Study
P-110	邹静涵	Probing the bonding of CO to heteronuclear group 4 metal–nickel clusters by photoelectron spectroscopy
P-111	曹丹丹	氮化碳薄膜材料的制备、表征和光物理性质的研究
P-112	昌玉强	The ultrafast photocarrier generation process in Y-form oxotitanium phthalocyanine films
P-113	陈　佳	苯甲醛 $S_3(\pi\pi^*)$态激发态动力学的共振拉曼和从头计算研究
P-114	陈军华	1,1-二氟乙烷二聚体的转动光谱研究
P-115	陈　晓	Formation from Photolysis of 2-Propanol on Anatase-TiO_2(101)
P-116	陈银娟	Infrared Photodissociation Spectroscopy of Scandium Oxide-Carbonyl Cation Complexes
P-117	陈志超	The Study of HNCO Photodissociation Dynamics
P-118	池　振	二维材料中载流子及激子超快动力学的研究
P-119	戴　玲	Thermochromatium tepidum 光合膜人工模拟体系的构造及其激发态能量传递动力学
P-120	邓罡华	FT-IR and ultrafast IR spectroscopic monitoring of potassium thiocyanate aqueous solution with fast freezing
P-121	杜艺杰	非金属硼掺杂氧化钛中缺陷态对光催化分解水的影响
P-122	杜　勇	Dynamic Study of Dehydration Study within Tri-hydroxy Benzoic Acid Monohydrate with Raman Vibrational Spectroscopy

P-123	范　伟	拉曼光谱技术原位测量丁二酰亚胺加速溶菌酶纤维化过程
P-124	方业广	Excited-State Decay Mechanism of 4-Methylbenzylidene Camphor: A CASPT2//CASSCF Study
P-125	葛志统	碳掺杂氮化碳光物理性质和光催化制氢机理的研究
P-126	郭　伟	金表面对苯二甲氰自组装膜的时间分辨和频光谱研究
P-127	韩山雨	G-MCTDH 方法研究 CH_2OH 2^2A 态光解动力学
P-128	何　胜	Controllable Synthesis and Photoexcited Dynamics of Organometal Halide Perovskite Quantum Dots
P-129	何玉韩	启发渐进式特征投影法分析金纳米粒子的瞬态吸收光谱
P-130	侯　建	高分辨和频振动光谱研究气-液界面温敏性高分子 pNIPAM 侧链异丙基取向角
P-131	花伟杰	Multi-configurational study of ultrafast nonlinear X-ray spectroscopy of molecules
P-132	黄红琴	碳量子点/TiO_2 纳米片复合材料的制备以及光催化动力学研究
P-133	金佳晔	Covalent and Noncovalent Interactions between Boron and Argon: an Infrared Photodissociation Spectroscopic Study of Argon-Boron Oxide Cation Complexes
P-134	金佩佩	4-硝基联苯及其衍生物三重态的反应动力学研究
P-135	金佩佩	5-硝基异喹啉三重态的反应动力学研究
P-136	金艳玲	氨气分子光解动力学研究
P-137	鞠思文	除谱在离子水溶液光谱中的应用
P-138	孔繁晨	Infrared Photodissociation Spectroscopy of Mass-Selected Dinuclear Vanadium Dinitrogen Complexes
P-139	孔祥涛	$H_5O_2^+$红外光解离光谱的 tagging 效应的理论研究
P-140	匡卓然	蒽醌基化合物激发态电荷转移相关的构象弛豫与热活化延迟荧光
P-141	雷　鑫	三甲胺团簇离子的红外光解离光谱研究
P-142	冷　轩	光合捕光复合物的二维电子光谱研究
P-143	李　刚	三甲胺-甲醇混合体系中性团簇的 IR-VUV 光谱研究
P-144	李洪敏	Direct Observation of Methoxycarbonylnitrene

P-145	李鹏丽	4-硫代胸腺嘧啶激发态结构及动力学研究
P-146	李萝园	Temperature Effect on Upconversion Luminescence in the Lanthanide-doped Nanoparticles
P-147	李　帅	电子激发态嘧啶分子的飞秒振动波包动力学研究
P-148	李　爽	CdSe/CdS 量子棒的核/壳结构的超快载流子动力学研究*
P-149	李　巍	Infrared Spectroscopic and Theoretical Study of the HC_nO^+ (n = 5-12) Cations
P-150	梁　昊	Ultraviolet photodissociation dynamics of bromo-fluorobenzenes
P-151	梁　昊	Photodissociation Dynamics of C_2H_5Br Between 200 and 210 nm
P-152	林　丹	CF_3I Photodissociation at 238 nm: Vibrational Distribution of CF_3 Fragments and Dynamics of Curve Crossing
P-153	凌丰姿	光激发的 2,4-二氟苯酚在不同构型间的相干核运动的直接观测
P-154	刘付轶	丙烯酸乙酯的真空紫外光电离解析
P-155	刘付轶	基于时间分辨光电离质谱研究 CH_3 与 O_2 的反应动力学
P-156	林广双木	苯硫酚光解的三维波包动力学理论研究
P-157	刘　凯	O ($^3P_{0,1,2}$, $^1D_2$) yield ratio measurement in VUV photodissociation of O_2
P-158	刘俊学	Observation of Internal Photoinduced Electron and Hole Separation in Hybrid 2-Dimentional Perovskite Films
P-159	刘玉柱	飞秒时间尺度研究挥发性有机物的光化学动力学
P-160	罗　健	植物防晒霜分子的光动力学
P-161	马慧中	Energy level alignment and exciton dynamics at the H_2O/g-C_3N_4 interface for photocatalytic water splitting
P-162	马佳妮	Competition between “Meta Effect” Photochemical Reactions of Selected Benzophenone Compounds Having Two Different Substituents at Meta Positions
P-163	裴克梅	Investigation of the short-time photodissociation dynamics of Furfural in S2 state by Resonance Raman and quantum chemistry calculations
P-164	秦　泰	环状亚硝酸烷基二酯的光解动力学研究
P-165	沈祥建	High-dimensional Quantum Dynamics Studies of Methane Dissociation on Ni Surfaces

P-166	宋　迪	5-碘代尿嘧啶（5-IU）的光解研究
P-167	宋宏伟	2’-羟基查尔酮的激发态电荷转移与质子转移的超快过程研究
P-168	宋文韬	Vibrational spectroscopy of the mass-selected tetrahydrofurfuryl alcohol monomers and its dimers in gas phase using IR depletion and VUV single photon ionization
P-169	谭黎明	利用 TPE 瞬态吸收光谱研究类胡萝卜素单重态均裂反应
P-170	徐安莉	A study of species formation of aqueous amines using NMR spectroscopy
P-171	万华斌	N-Methylcarbamoyl Azide: Spectroscopy, X-ray Structure and Decomposition via Methylcarbamoyl Nitrene
P-172	汪　杰	XUV 泵浦-UV 探测方法研究 HD 的预解离动力学
P-173	汪　杰	HD 直接解离产物的分支比震荡与量子干涉
P-174	王静静	宽带和频光谱技术对电子-声子相互作用的研究
P-175	王　恋	The photoluminescence properties of 1,1,2,3,4,5-Hexaphenylsilole (HPS)
P-176	王墨函	Experimental and Computational Assignment of FTIR Spectra of Dityrosine and Its Configuration
P-177	王　倩	非天然碱基对在 DNA 中光物理过程的理论研究
P-178	王　娴	作为电子给体材料的类寡聚噻吩小分子电荷分离效率的奇偶效应研究
P-179	王雅婷	Photochromic Mechanism of a Bridged Diarylethene: Combined Electronic Structure Calculations and Nonadiabatic Dynamics Simulations
P-180	王永天	光电子能谱研究镧系和锕系元素氟化物的电子结构
P-181	温　静	氮化碳中间体(Melem)及剥离产物的光物理性质研究
P-182	吴海铭	Selective Dehydrogenation of Diaminobenzenes by Deep Ultraviolet Single Photons
P-183	吴刘霞	苯酞激发态非辐射动力学的拉曼强度分析和理论计算研究
P-184	吴向坤	碳酸二甲酯解离光电离研究—阈值光电子-光离子符合技术的应用
P-185	吴晓楠	A Cryogenic Ion Trap Mass Spectrometer for Infrared Photodissociation Spectroscopy of Mass-Selected Ions
P-186	吴沛颖	Resonant Two-Photon Ionization and Mass-Analyzed Threshold Ionization Spectroscopy of 4-Chloro-2-fluoroanisole

P-187	吴　萱	Infrared Spectra Of Barium Carbonyls In Neon Matrice
P-188	许文文	拉曼光谱法研究 γ-己内酯短程有序结构和ν(C=O)振动耦合相互作用力
P-189	闫天民	Quantum state tomography of high temporal resolution with THz streaking-assisted photoelectronic momentum distribution
P-190	闫亚明	A simulation study on exciton dissociation in organic photovoltaic cells
P-191	杨崇鑫	Time-resolved Photodissociation of Acetaldehyde Molecules by Ultraviolet Excitation
P-192	杨　振	Insights into Structural Properties and Vibrational Spectra of Ethylammonium Nitrate Ionic Liquid Confined in Single-Walled Carbon Nanotubes
P-193	殷蓉蓉	No-planar photodissociation path way of bromo-2,6-difluorobenzene
P-194	于昂扬	Isotopic Effects on the Photodissociation of CH_3I: a Nonadiabatic Dynamics Study
P-195	喻远琴	C-H…O interaction in methanol-water solution revealed from Raman spectroscopy and theoretical calculations
P-196	袁开军	水在 C(010)态的光解动力学
P-197	张冰冰	Configuration Interconversion and Flipping of Hydrogen Bond in the Neutral Methylamine Dimer Revealed by Infrared Spectroscopy
P-198	张德萍	High-resolution electronic spectra of yttrium oxide (YO) I: identification of the $D^2\Sigma^+$ state
P-199	张　嵩	Effect of Vibronically Induced Spin-Orbit Coupling on Nonradiative S-T Intersystem Crossing
P-200	张　强	High-resolution electronic spectra of yttrium oxide (YO) II: spectroscopic study on the $[33.2]^2\Pi$ and $A'^2\Delta_{5/2}$ states
P-201	张文凯	利用重氮基团红外探针研究局部水合环境的氢键动力学
P-202	张逸竹	Precise phase determination in two-dimensional electronic spectroscopy
P-203	张永燕	飞秒反向拉曼光谱色散线型的研究
P-204	张腾烁	溶剂调控 2-环己烯酮双荧光现象的理论研究
P-205	周德霞	The Structure and Dynamics of Ions in Confined Water Environment Investigated by Infrared Spectroscopy
P-206	陈　征	SC-KMC：一种兼顾精度和效率的表面催化动力学新方法

P-207	官亚夫	Construction of potential energy surfaces for polyatomic molecules with Gaussian Process Regression: Active Data Selection
P-208	胡　婕	低能量离子-分子反应的离子速度成像装置
P-209	吉　琳	燃烧反应机理的多尺度粗粒化表达
P-210	李德彰	Stationary state distribution and efficiency analysis of Langevin dynamics in real dynamics and virtual dynamics regions
P-211	李路路	A novel time of flight spectrometer for crossed beam experiment of elementary chemical reactions
P-212	刘润泽	String Method Study on the Proton Transfer Process of a simplified model system from CcO D-channel
P-213	龙金友	Ultrafast Liquid-jet Photoelectron Spectroscopy of Hydrated Electron: A New Method for Directly Tracking Electrons in Aqueous Solutions
P-214	马建毅	微波化学反应动力学模型构建
P-215	祁文科	Application of weak accelerating field to ion velocity map imaging
P-216	商辰尧	超快时间分辨紫外光电子能谱装置
P-217	施再发	催化反应过程中反应中间体原位质谱探测系统的研制
P-218	汪　涛	量子态分辨的分子束-表面解离动力学实验研究装置
P-219	王　鹤	兼顾精度和效率的催化剂理性设计新策略——在理性设计双金属催化剂催化氨分解反应中的应用
P-220	王　佳	VUV 激光解吸/电离质谱成像（VUVDI-MSI）
P-221	王　颖	Revised M06-L Functional
P-222	杨东铮	双原子-双原子非弹性散射中改良的 CS 近似
P-223	杨家岳	原子、分子以及自由基的高效电离探测——大连相干光源光束线
P-224	于　锋	Double-Hybrid Density Functionals for Noncovalent Interactions
P-225	张超杰	双光子激发时间分辨成像技术原位监测纳米载体的活体输运过程
P-226	张　强	A single-longitudinal-mode optical parametric oscillator for high resolution spectroscopy of free radicals

P-227	张小闽	多氯代多环芳烃的电加热合成方法
P-228	张耀龙	A Hybrid Learning Algorithm for Atomistic Neural Networks to Fit Potential Energy Surface
P-229	戴　玲	Thermochromatium tepidum 光合膜人工模拟体系的构造及其激发态能量传递动力学
P-230	丁俊杰	葡萄球菌肠毒素 B 与亲和体的分子识别动力学模拟研究
P-231	冯　瑾	New energy transfer channel from carotenoids to chlorophylls in purple bacteria
P-232	高　川	蓖麻毒素与单链抗体的相互作用分子动力学模拟研究
P-233	胡勇军	激光解吸/后电离质谱在生物医学中的应用
P-234	李亦易	气液界面鞘磷脂与胆固醇相互作用的高分辨宽带和频振动光谱研究
P-235	李裕健	激光烧蚀分子束质谱法对生物药物分子及其团簇的探测研究
P-236	吴丽丹	6-硫代鸟嘌呤脱氨反应机理的理论研究
P-237	夏　飞	蛋白质超粗粒化模型的发展
P-238	邢　蕾	拉曼光谱研究溶菌酶纤维化结构与进程
P-239	于　洁	小分子多元醇对嗜热紫色光合细菌 *Tch.tepidum*-LH_2 激发态动力学的影响
P-240	张　璐	Dynamic Protein Conformations Preferentially Drive Energy Transfer along Active Chain of the Photosystem-II Reaction Center
P-241	周　璇	胆酸钠对 Rhodobacter (Rba.) sphaeroides 2.4.1 的 chromatophore 膜的通透性的影响

K1 Direct mapping of the key feature of the reactive potential energy surface

Huilin Pan,[1] Fengyan Wang,[1,2] and Kopin Liu[1]

[1] Institute of Atomic and Molecular Sciences (IAMS), Academia Sinica, P.O. Box 23-166, Taipei, Taiwan 10617.

[2] Department of Chemistry, Collaborative Innovation Centre of Chemistry for Energy Materials, Fudan University, Shanghai 200433, People's Republic of China.

Within the Born-Oppenheimer approximation, the geometry and property of a molecule are governed by the electronic structure or the potential energy surface (PES); likewise, the reactivity of a chemical reaction by the intermolecular interaction. Traditionally, what experimentalists can measure are the spectroscopy, the rate constant or cross section etc. – not the PES itself. Theorists then need to solve the nuclear quantum dynamics (QD) on a given PES. By simulating the experimentally measured quantity, the theory-experiment comparison can be made to validate the PES. As we move toward larger chemical systems, it becomes increasingly more difficult to calculate accurate PES and to perform exact QD in full dimensionality. Some approximate methods such as the quasiclassical trajectory or the reduced dimensionality QD are often employed, resulting in some uncertainty on the discrepancy being from the deficiencies of the PES used or from the dynamics approximations. It is therefore highly desirable to develop a new way of thinking or experimental approach that is capable of direct determination of the key features of the PES for comparison.

Here, we will present two such examples. First, using the benchmark reaction of Cl + $CHD_3(v_1 = 1)$ as an example, we show how to map the angle-dependent barrier directly from a polarized scattering experiment. The deduced bend potential of the Cl–H–C configuration at the transition state agrees with *ab initio* calculated ones, validating the method [1]. Second, we will present a different set of experiments on the ground-state reaction of F + CH_3D, which suggests the possibility of inferring the well depth of the vibrationally adiabatic well – one of the key features of the PES in characterizing the quantum dynamical resonances – from the experimentally sighted 'reactive rainbow' [2].

References:

[1] H. Pan, F. Wang, G. Czako, and K. Liu, Nat. Chem. (2017).

[2] H. Pan and K. Liu, J. Phys. Chem. A 120, 6712-6718 (2016).

K2 New Paradigm in Photoionization and photoelectron spectroscopy: quantum-State-Selected unimolecular and bimolecular reaction dynamics of Ions

Cheuk-Yiu Ng

Department of Chemistry, University of California, Davis, California 95616

*Email: cyng@ucdavis.edu

We have successfully developed a novel apparatus for quantum-state-selected unimolecular dissociation and ion-molecule reaction studies based on vacuum ultraviolet (VUV) or two-color laser pulsed field ionization-photon (PFI-PI) detection. This new apparatus can perform all traditional functions in photoionization and photoelectron spectroscopic measurements, and more. As a demonstration experiment, we have determined the 0 K appearance energy or the dissociative photoionization threshold for CH_3^+ from methane (CH_4), as $AE_0(CH_3^+/CH_4)$ =14.32271 ± 0.00013 eV. When combined with known ionization energies of CH_3 and CH_4, we have determined the 0 K bond dissociation energies $D_0(H\text{-}CH_3)$ = 432.463 ± 0.027 kJ/mol and $D_0(H\text{-}CH_3^+)$ = 164.701±0.038 kJ/mol with unprecedented accuracy. In a series of ion-molecule reaction studies, which involve measurements of state-selected integral cross sections for reactions of H_2O^+, N_2^+, H_2^+, and O_2^+ ions, we have shown that the sequential electric field pulsing scheme used is generally applicable for measurements of rovibronic-resolved PFI-PI spectra for gaseous ions; and the reactivity of quantum-rovibronic-state-selected ions thus prepared can be examined down to thermal energies.

References:

[1] Yih-Chung Chang, Bo Xiong, David H. Bross, Branko Ruscic, and C. Y. Ng, "A vacuum ultraviolet laser pulsed field ionization-photoion study of methane (CH_4): Determination of the appearance energy of methylium from methane with unprecedented precision and the resulting impact on the bond dissociation energies of CH_4 and CH_4^+," *Phys. Chem. Chem. Phys.* **19**, 9592-9605 (2017).

[2] Yuntao Xu, Bo Xiong, Yih-Chung Chang, Yi Pan, Po Kam Lo, Kai Chung Lau, C. Y. Ng , "A quantum-rovibrational-state-selected study of the $H_2O^+(X^2B_1; v_1^+v_2^+v_3^+; N^+_{Ka+Kc+})$ + CO reaction in the collision energy range of 0.05-10.00 eV: translational, rotational, and vibrational energy effects", *Phys. Chem. Chem. Phys.* **19**, 9778-9789 (2017).

[3]Yuntao Xu, Bo Xiong, Yih Chung Chang, and C. Y. Ng, "Isotopic and Quantum-rovibrational-state effects for the ion-molecule reaction $H_2O^+(X^2B_1: v_1^+v_2^+v_3^+; N^+_{Ka+Kc+})$ + HD in the collision energy range of 0.03-10.00 eV", *Phys. Chem. Chem. Phys.*, **19,** 8694-8705 (2017).

[4] Hongwei Song, Anyang Li, Hua Guo, Yuntao Xu, Bo Xiong, Yih-Chung Chang, and C. Y. Ng, "Comparison of Experimental and Theoretical Quantum-state-selected Integral Cross Sections for the $H_2O^+ + H_2$ (D_2) Reactions in the Collision Energy Range of 0.04-10.00 eV", *Phys. Chem. Chem. Phys.* **18**, 22509 (2016).

K3 $Cl + CH_4$ 反应的态-态量子动力学研究

张东辉

中国科学院大连化学物理研究所
分子反应动力学国家重点实验室
辽宁省大连市中山路 457 号， 116023
*Email: zhangdh@dicp.ac.cn

近些年来，由于刘国平老师等人的开拓性工作，Cl + CH4反应受到了广泛的关注，已成为多原子反应动力学研究的一个经典体系。最近，我们基于高精度从头算和神经网络拟合，构造了该体系的一个全新势能面，其精度远高于Bowman等人几年前构造的势能面。同时我们也实现了C3v限制下该反应的7维态-态量子动力学研究。新势能面上的态-态量子动力学计算不仅得到了与实验高度吻合的微分截面，并且对该体系低碰撞能条件下可能存在的共振现象提出一个新的解释。

K4 金属团簇的超原子分子理论

杨金龙

中国科学技术大学，合肥微尺度物质科学国家实验室，安徽省合肥市金寨路 96 号，230026

*Email: jlyang@ustc.edu.cn

选取合适的金属团簇（超原子）作为结构基元，进而组装形成新的团簇或晶体材料是团簇科学中一个有趣且充满挑战的课题，受到了实验和理论研究者的广泛关注。通过超原子组装这种“自下而上”的组装方式，可以获得具有特定物理化学性质的新材料。但是，长久以来就如何进行超原子组装并无清晰、统一的理论认识，超原子组装基本等同于超原子的任意堆砌或拼接。那么，超原子能否像原子那样通过特定化学键形成分子或晶体？超原子间如何成键？超原子组装是否有一定模式可循？为了回答这些问题，我们提出了一个唯象理论即：超原子分子理论。该理论的核心是构建超原子间的成键规则，将涉及超原子的“超级化学键”概括为三种类型，即超级共价键、超级杂化键和超级非键。超原子可以通过超级化学键结合形成超分子或超原子晶体。同时，超原子分子理论指出，超原子具有几何结构不同但电子结构相似的异构体，这些异构体称为“等同超原子”。等同超原子同样可以作为组装基元，通过超级化学键进行结合。另外，针对包含复杂成键类型的团簇体系，超原子分子理论概括出了两种超原子组装模式，分别称为超原子网络和杂化超原子网络。综上所述，超原子分子理论包含了对超原子间成键规则的理解，对超原子组装基元的思考，以及对超原子组装模式的认识。超原子分子理论的相关内容不仅可以为超原子组装提供系统的理论依据，而且可以对特殊团簇结构的稳定性给出合理解释，还可以为新型团簇的结构设计以及实验合成提供理论指导。

关键词：团簇；金属团簇；超原子；化学键；超原子组装

参考文献

[1] Cheng L., Yang J., J. Chem. Phys., 2013, 138(14):141101.

[2] Cheng L., Ren C., Zhang X., Yang J., Nanoscale, 2013, 5(4):1475

[3] Koyasu K., Tsukuda T., Phys. Chem. Chem. Phys., 2014, 16(39):21717

[4] Muñoz-Castro A., Chem. Sci., 2014, 5(12):4749

[5] Zubarev D. Y., Boldyrev A. I., J. Phys. Chem. A, 2009, 113(5):866

[6] Jin R., Liu C., Zhao S., et al. ACS Nano, 2015, 9(8): 8530-8536.

[7] Liu L., Li P., Yuan L. F., Yang J., Nanoscale, 2016, 8(25): 12787.

[8] Cheng L., Yuan Y., Zhang X., Yang J., Angew. Chem. Int. Ed., 2013, 52(34): 9035.

[9] Liu L., Yuan J., Cheng L., Yang J., Nanoscale, 2017, 9(2): 856.

K5 Shedding IR light on gas-phase metal clusters: insights into structures and reactions

André Fielicke
Fritz-Haber-Institut der Max-Planck-Gesellschaft, 14195 Berlin, Germany
*E-mail: fielicke@physik.tu-berlin.de

Transition metal clusters are frequently used as model systems for low coordinated sites of extended surfaces and their study can provide valuable insights into the mechanisms of surface reactions. In many cases, however, there is still a lack of information on their structures and the relationship between structure and chemical behaviour. Using vibrational spectroscopy of gas-phase clusters one can obtain information about the clusters' structure or the behaviour of adsorbed species. The latter provides valuable insights into the binding geometry, the activation of bonds within the ligands or reactions occurring on the clusters' surface. Cluster size specific data can be obtained using infrared multiple photon dissociation spectroscopy. To cover the required spectral range from the far to the mid-IR our experiments make use of IR free electron lasers. The talk will discuss exemplary studies about structures of clusters of the platinum group metals [1,2] and the activation of carbon dioxide by anionic cobalt [3], rhodium, and platinum clusters.

References:

[1] Harding, D.J.; Fielicke, A. Chem. Eur. J. 2014, 20: 3258.
[2] Kerpal, C.; Harding, D.J.; Rayner, D.M.; Lyon, J.T.; Fielicke, A. J. Phys. Chem. C .2015, 119: 10869.
[3] Yanagimachi, A..; et al. J. Phys. Chem. C. 2016,120: 14209.

K6 Infrared Spectroscopy of Donor-Acceptor Bonding Carbonyl Complexes

Mingfei Zhou

Department of Chemistry, Fudan University, Shanghai 200433
*Email: mfzhou@fudan.edu.cn

Carbon monoxide is one of the most important ligand in inorganic and organometallic chemistry. It can bind to a host of neutral and charged transition metal as well as main group metal centers in forming diverse metal carbonyl complexes. The bonding interactions between carbon monoxide and metal center can be described using the Dewar−Chatt−Duncanson model, which involves σ donation from the carbon lone-pair 5σ orbital to the metal and concomitant π back-donation of electron density from the metal d(p) orbitals into the 2π* antibonding orbitals of CO. This talk will present our recent results on the preparation of a number of neutral and charged metal carbonyl complexes either in gas phase or in solid noble gas matrices via donor-acceptor bonding strategy including the main group tricarbonyl complexes featuring a tilted one-electron donor carbonyl ligand[1], carbonyl complexes bonded with strong Lewis acids BeO and BeCO3[2], and metal carbonyl complexes featuring metal-metal triple bonding[3]. The complexes are studied by mass-selected infrared photodissociation spectroscopy and matrix isolation infrared absorption spectroscopy. Vibrational spectroscopic combined with state-of-the-art quantum chemical calculations unrevealed unusual structure and bonding properties of these complexes.

Keywords: carbonyl complexes; infrared photodissociation spectroscopy; donor-acceptor bonding

References:

[1] Jin, J. Y.; Jian, J. W.; Qu, Q.; Lin, H. L.; Wang, G. J.; Chen, M. H.; Zhou, M. F.; Andrada, D. M.; Hermann, M.; Frenking, G. Chem. Eur. J. 2016, 22, 2376.

[2] Chen, M. H.; Zhang, Q. N.; Zhou, M. F.; Andrada, D. M.; Frenking, G. Angew. Chem. Int. Ed. 2015, 54, 124.

[3] Chi, C. X.; Wang, J. Q.; Qu, H.; Li, W. L.; Meng, L. Y.; Luo, M. B.; Li, J.; Zhou, M. F. Angew. Chem. Int. Ed. DOI: 10.1002/anie.201703525.

K7

面向航空发动机的燃烧基础研究

齐飞[1]

[1] 上海交通大学机械与动力工程学院，上海，200240

*Email: fqi@sjtu.edu.cn

燃烧在能源、交通、国防、工业等诸多核心领域发挥着不可替代的作用。本报告将介绍航空发动机燃烧中的一些基础科学问题，以及基于激光和质谱的诊断技术在燃烧研究中的应用、燃烧反应动力学研究的难点与挑战性的问题等。

关键词：燃烧；诊断；燃烧反应动力学

K8　基于高分辨交叉分子束-离子速度成像技术的基元化学反应研究

袁道福[1]，俞盛锐[1,3]，陈文韬[1]，杨学明[2,1*]，王兴安[1*]

1.中国科学技术大学化学物理系及化学物理高等研究中心，安徽省合肥市金寨路 96 号，230026
2.中国科学院大连化学物理研究所分子反应动力学国家重点实验室, 大连市中山路 457 号， 116023
3.浙江师范大学杭州高等研究院，浙江省杭州市耕文路 1108 号，311231
*Email: xmyang@dicp.ac.cn; xawang@ustc.edu.cn

交叉分子束技术在化学反应动力学的发展进程中扮演着至关重要的角色。近年来，人们通过离子速度成像技术与交叉分子束技术相结合的方法，对诸如多原子化学反应动力学、立体动力学、离子-分子反应和分子间相互作用[1-4]等问题开展了深入的实验研究。

在常规的共振增强多光子电离过程中，由于激光提供的能量显著高于分子电离所需能量，探测分子在激光电离后表现出显著地电子反冲，极大地的限制了实验的分辨率。在中国科学技术大学，我们采用新研制的交叉分子束分子散射实验装置[5]，通过将离子速度成像技术与(真空紫外+紫外)双光子阈值电离技术相结合，我们对H+H2等基元化学反应开展了高分辨的实验研究，获得了具有转动量子态分辨的产物影像，同时实现了对反应产物质心散射角度的高分辨探测。

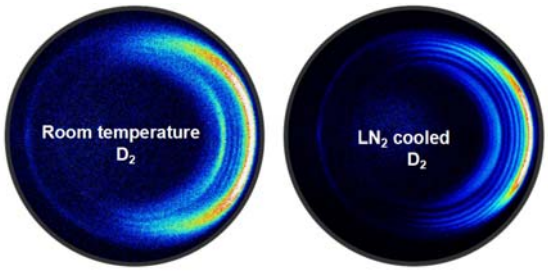

A)　　B)

Fig.1 H+D2 反应产物 D 原子的转动态分辨(对应 HD(v'，j'))的离子影像，A)图与 B)图分别对应室温和液氮温度下的 D2 分子束源。

参考文献

[1] W. Zhang, Y. Zhou, G. Wu, Y. Lu, H. Pan, B. Fu, Q. Shuai, L. Liu, S. Liu, L. Zhang, B. Jiang, D. Dai, S.-Y. Lee, Z. Xie, B. J. Braams, J. M. Bowman, M. A. Collins, D. H. Zhang, and X. M. Yang, PNAS, 107 (29) 12782-12785, (2010).

[2] F. Wang, Kopin Liu and T. P. Rakitzis, Nature Chemistry 4, 636-641, (2012).

[3] J. Mikosch, S. Trippel, C. Eichhorn, R. Otto , U. Lourderaj, J. X. Zhang, W. L. Hase, M. Weidemüller, R. Wester, Science 319, 183 (2008).

[4] S. N. Vogels, J. Onvlee, S. Chefdeville, A. van der Avoird, G. C. Groenenboom and S. Y.T. van de Meerakker, Science 350, 787 (2015).

[5] S. R. Yu, D. F. Yuan, W. T. Chen, X.M. Yang, and X.A. Wang, J. Phys. Chem. A, 119 (29), 8090 (2015).

K9 突破选择定则： 光学暗态的直接探测

罗毅

合肥微尺度物质科学国家实验室（筹），中国科学技术大学

*Email: yiluo@ustc.edu.cn

由于光学跃迁选择定则的限制，直接探测自旋禁戒激发三线态（“光学暗态”）的特性极其动力学演化过程，是光物理、光化学和光生物研究领域中颇为棘手的难题之一。本报告将介绍我们最近发展的两种突破跃迁选择定则的方法。 第一种方法是通过实现高激发单线态和三线态的能量共振，增强系间窜跃的速率，探测三线态的特性[1, 2]。同时用一种反常规的“时序反转飞秒泵浦–探测”技术，在模型分子体系中实现了对发生在“光学暗态”空间“纯净的”超快动力学演化过程的实时跟踪和刻画[1]。 另外一种方法，是利用空间高度局域的纳腔等离激元[3]，产生超强磁场，直接打破常规的对称和自旋跃迁选择规则， 实现对分子激发态的全谱探测[4]。

参考文献：

1. J. Ge, et al. *Phys. Chem. Chem. Phys.* 17 (2015) 13129
2. B. Wu, et al. *J. Am. Chem. Soc.,* 137 (2015) 8769
3. R. Zhang, et al. *Nature*, 498 (2013) 82; S. Duan, et al., *J. Am. Chem. Soc.*, 137(2015) 9515; S. Duan, et al., *Angew. Chem. Int. Ed.,* 128 (2016) 1053.
4. S. Duan, et al. to be published.

K10 Novel Aspects of Nonlinear Spectroscopy Using Synchronized Ultrafast Laser Pulses at Time and Frequency Limit

Hong-Fei Wang (王鸿飞)

Deapartment of Chemistry, Fudan University, 220 Handan Road, Yangpu District, Shanghai 200433
*Email: wanghongfei@fudan.edu.cn

The recent development of the sub-wavenumber resolution broadband sum frequency generation vibrational spectroscopy (HR-BB-SFG-VS) using synchronized ultrafast laser pulses of ~35fs and ~90ps allows direct measurements of accurate spectral lineshapes in the SFG vibrational spectra of complex molecular interfaces and provides a novel way to obtain coherent vibrational dynamics lifetimes of molecular surfaces and interfaces. This approach of using synchronized laser pulses for nonlinear spectroscopy can be extended to other Raman base nonlinear spectroscopy techniques for studying molecular vibrational spectroscopy and ultrafast dynamics in the condensed phase and at molecular interfaces at the time and frequency limit. Here I would like to discuss the novel aspects of this approach and to provide an overview for its future development and impact to broad scientific problems.

Keywords: Nonlinear spectroscopy; Spectral lineshape; Synchronized laser pulses; Sum-frequency generation vibrational spectroscopy; Spectral resolution.

References:

[1] Velarde, L.; Wang, H. F. *Phys.Chem. Chem. Phys.,* **2013, 15**, 19970-19984.
[2] Wang, H. F.; Velarde, L.; Gan, W.; Fu, L. *Annu. Rev. Phys. Chem.,* **2015, 66**, 189-216.
[3] Wang, H. F. *Prog. Surf. Sci.*, **2016, 91**, 155-182.

K11 凝聚相复杂分子聚集体的激发态溶剂化过程研究

夏安东

中国科学院化学研究所

*Email: andong@iccas.ac.cn

对于有机π共轭分子的聚集体来讲，为了保证激发态能量高效传递，其分子结构必须能够最大程度的保持激发态去局域、且不同去局域色团之间保持高度的相干。这种共轭π分子生色团之间的激发态去局域化过程受环境极性调控至关重要，可以改进化学反应的进程。该报告将系统介绍我们课题组在过去几年利用超快光谱技术在针对具有推－拉电子特性的超支化共轭π分子的激发态电荷转移动力学和溶剂化过程方面的研究进展。 主要介绍不同极性溶剂中的超支化分子激发态离域和定域化相关的溶剂化过程的光谱特点；介绍利用各向异性光谱方法估算超支化分子生色团之间的激发态定域与离域贡献比例的光谱方法等。

关键词：激发态过程，溶剂化，共轭π分子，激发态离域和定域化

参考文献

[1]Li, Y.; Hu, J. P.; He, G.-Y.; Zhu, H.-N.; Wnag, X.; Guo, Q.-J.; Xia, A.-D.*; Lin, Y.-Z.; Wang, J.-Y.; Zhan, X.-W.*, Influence of Thiophene Moiety on the Excited State Properties of Push-Pull Chromophores. *J. Phys. Chem. C,* 2016, 120,13922-13930.

[2]He,G.-Y.; Shao, J.-J.; Li, Y.; Hu, J.-P.; Zhu, H.-N.; Wang, X.; Guo, Q.-J.; Chi, C.-Y.*; and Xia, A.-D.*, Photophysical Properties of Octupolar Triazatruxene-Based Chromophores. *PhysChemChemPhys,* 2016, 18, 6789-6798.

[3]Li, Y.; He, G.-Y.; Wang, X.; Guo, Q.-J.; Niu, Y.-L.*; and Xia, A.-D.*, Determination of the Excitation Delocalization/Localization in Multibranched Chromophores by Means of Fluorescence Excitation Anisotropy Spectroscopy. *ChemPhysChem,* 2016*,* 17,406-411. (VIP article) .

[4]Li, Y.; Zhou, M.; Niu, Y.-L.; Guo, Q.-J.; Xia, A.-D.* Solvent-dependent intramolecular charge transfer delocalization/localization in multibranched push-pull chromophores. *J. Chem. Phys*. 2015,143, 034309.

[5]Hu, J.-P.; Li, Y.; Zhu, H.-N.; Qiu, S.-H.; He, G.-Y.; Zhu, X.-Z.*; Xia, A.-D.*. Photophysical Properties of Intramolecular Charge Transfer in a Tri-branched Donor-π-Acceptor Chromophore. *ChemPhysChem,* 2015,16, 2357-2365.

[6]Long, S.-R.; Zhou, M.; Tang, K.; Zeng, X.-L.; Niu, Y.-L.; Guo, Q.-J.;Zhao, K.-H.*; Xia, A.-D.* Single-Molecule Spectroscopy and Femtosecond Transient Absorption Studies on Excitation Energy Transfer Process in ApcE(1-240) Dimer. *PhysChemChemPhys,* 2015, 17, 13387-13396.

K12 Fill the Pressure and Material Gap in Catalytic Studies by Sum Frequency Generation Vibrational Spectroscopy

Ruidan Zhang[1,2], Xingxing Peng[1,2], Anan Liu[2], Ting Luo, Zefeng Ren[1,*]

[1]*Dalian Institute of Chemical Physics, Chinese Academy of Sciences, Dalian, 230026, P. R. China*
[2]*International Center for Quantum Materials (ICQM) and School of Physics, Peking University, Beijing 100871, P. R. China*
* Email: *zfren@dicp.ac.cn*

The photocatalytic reaction on TiO_2 material has attracted more and more attention since the photosplitting of water on TiO_2 was discovered in 1972. Here, we will present our recent studies of the adsorption structures of methanol and its photocatalytic reaction on TiO_2(110) by sum frequency generation (SFG) vibrational spectroscopy. SFG is an intrinsic surface-specific method, which enables us to probe the vibrational spectra under both ultrahigh vacuum (UHV) and near ambient pressure conditions.[1] We found that the adsorption structure of methanol on TiO_2(110) is not only dependent on the coverage of methanol under the vacuum condition,[2, 3] but also on the methanol pressure in the gas phase. The SFG spectra shows that under UHV condition the both molecular and dissociated methanol coexist at no more than one monolayer on the surface, while the dissociated methanol decreases as the coverage increasing, and even disappears at the multilayer coverage. Near the ambient methanol pressure condition, we also found the TiO_2(110) surface might reconstruct and some new reaction were induced. Our results not only provide a detailed insight into the adsorption structure of methanol on TiO_2(110), but also shed light on the photochemistry on this surface under real reaction condition. Recently we are setting up new instrument to fill the material gap in catalytic studies. I will briefly introduce our design and the idea.

[1] Liu S, Liu A-a, Zhang R, Ren Z. *Rev. Sci. Instrum.* **2016**, 87, 044101
[2] Liu A-a, Liu S, Zhang R, Ren Z. *J. Phys. Chem. C* **2015**, 119, 23486-23494
[3] Liu S, Liu A-a, Wen B, Zhang R, Zhou C, Liu L-M, Ren Z. *J. Phys. Chem. L* **2015**, 6, 3327-3334

K13 Towards the accurate and efficient microkinetic modelling in heterogeneous catalysis

Xin Xu*

Collaborative Innovation Center of Chemistry for Energy Materials, MOE Laboratory for Computational Physical Science, Department of Chemistry, Fudan University, Shanghai, 200433, China

*Email: xxchem@fudan.edu.cn

Electronic structure calculations based on density functional theory (DFT) provide valuable information on geometries, heats of reactions and reaction barrier heights, etc., for a catalytic system. To relate these atomic scale properties with the macroscopic variables of the catalytic system, however, one has to carry out reaction kinetics simulations. The central gateway to go from DFT energetics to reaction kinetics is microkinetics via kinetic Monte Carlo (KMC [1,2]) simulations in principle, but often mean-field modelings [3] in practice. Modern KMC techniques have the power to directly account for all studied surface processes on a lattice of all kinds of active sites on the catalyst surfaces by explicitly solving the master equation. The high dimensionality of this master equation and the large time-scale separation of various surface processes soon render the brute force KMC simulations intractable. The complexity can be efficiently reduced by applying the mean-field approximation to solving the reaction network with chemical rate equations. Nevertheless, the standard mean-field kinetics with chemical rate equations, though widely used, are unreliable in many circumstances of real catalytic systems.

Here we report a novel method, based on equation-free multiscale simulation strategy [4], where the reaction tendencies at a given surface coverage are extracted from an on-lattice KMC on the fast processes, while the evolutions of surface coverages are performed by an off-lattice KMC on the slow processes. The steady state is reached when the surface coverages and corresponding reaction tendencies are self-consistent. This so-called self-consistent KMC (SC-KMC) method is shown here to provide a useful tool that complex catalytic processes can be studied efficiently and yet accurately.

Case studies such as CO oxidation reactions, NH_3 decomposition reactions, HCOOH decomposition reactions, and CO activation in Fischer-Tropsch synthesis, etc., will be presented. Challenges and our future plans will be discussed.

Keywords: heterogeneous catalysis; microkinetics; kinetic Monte Carlo; time-scale separation; rate equation

References:

[1] Bortz, A. B.; Kalos, M. H.; Lebowitz, J. L. *J. Comput. Phys.* **1975**, **17**:10.

[2] Gillespie, D. T. *J. Comput. Phys.* **1976**, **22**: 403.

[3] Dumesic, J. A., Rudd, D. F., Aparicio, L. M., Rekoske, J. E., and Treviño, A. A., "The Microkinetics of Heterogeneous Catalysis." American Chemical Society, Washington, DC, **1993**.

[4] Kevrekidis, I. G.; Samaey, G. *Annu. Rev. Phys. Chem.* **2009**, **60**: 321

K14 Nonadiabatic Tunneling: Adiabatic or Diabatic and Why We Should Care?

Hua Guo

Department of Chemistry and Chemical Biology, University of New Mexico, Albuquerque, NM 87131

Within the familiar Born-Oppenheimer approximation, nuclear dynamics, including tunneling, is often envisioned to occur on an adiabatic potential energy surface. However, this single-state adiabatic picture needs be reconsidered if a conical intersection (CI) is present, even when the energy is nominally much lower than the CI. This is because the presence of CI introduces two additional terms into the adiabatic Hamiltonian, namely the geometric phase (GP) and diagonal Born-Oppenheimer correction (DBOC). The GP, which is a by-product of the Born-Oppenheimer separation of electronic and nuclear motion, can qualitatively alter the behavior of the system. In this talk, we discuss the nonadiabatic tunneling dynamics in the photodissociation of phenol near a CI between the S1 and S2 states. It is shown that the inclusion of GP in the one-state adiabatic Hamiltonian leads to interference between tunneling "trajectories" on the two sides of the CI, resulting in either retardation (destructive interference) or enhancement (constructive interference) of the tunneling rate. These interference effects manifest in the tunneling wavefunction as the appearance or disappearance of a node.

References:

[1]C. Xie, C., J. Ma, X. Zhu, D. R. Yarkony, D. Xie, H. Guo, Nonadiabatic tunneling in photodissociation of phenol. *J. Am. Chem. Soc.* **138**, 7828-7831, (2016).

[2]C. Xie, D. R. Yarkony, H. Guo, Nonadiabatic tunneling via conical intersections and the role of the geometric phase. *Phys. Rev. A* **95**, 022104 (2017).

[3]C. Xie, B. K. Kendrick, D. R. Yarkony, H. Guo, Constructive and destructive Interference in nonadiabatic tunneling via conical intersections. *J. Chem. Theo. Comput.* **13**, 1902-1910 (2017).

I1 Convergence of high order perturbative expansions in open system quantum dynamics

Qiang Shi, Meng Xu, Linze Song, and Kai Song
State Key Laboratory for Structural Chemistry of Unstable and Stable Species, Institute of Chemistry, Chinese Academy of Sciences, Zhongguancun, Beijing 100190, China

*Email: qshi@iccas.ac.cn

We present a new method to directly calculate high order perturbative expansion terms in open system quantum dynamics. By starting from their path integral expressions, a set of differential equations are then derived by extending the hierarchical equation of motion (HEOM) approach. As two typical examples for the bosonic and fermionic baths, specific forms of the extended HEOM are obtained for the spin-boson model, and the Anderson impurity model. Numerical results are then presented for these two models, and general trends of the high order perturbation terms, as well as the necessary order for the perturbative expansions to converge are analyzed. Then, by combining the above results with a previously obtained Dyson expansion of the memory kernel in the Nakajiama-Zwanzig generalized master equation (NZ-GME), high order expansions of the exact memory kernels in the NZ-GME are calculated and their convergence is examined. It is found that, the high order expansions does not necessarily converge in certain parameter regimes. High order rate constants beyond the Fermi's golden rule are also studied.

Keywords: open system quantum dynamics; high order perturbation; generalized master equation; memory kernel

References:

[1] Xu, M; Song, L.-Z.; Song, K.; Shi, Q. J. Chem. Phys. 2017, 146: 064102.
[2] Shi, Q.; Geva, E. J. Chem. Phys. 2003, 119: 12063-12076.
[3] Chen, H.-T.; Berkelbach, T. C.; Reichman, D. R. J. Chem. Phys. 2016, 144: 154106.
[4] Xu, M; Song, L.-Z.; Shi, Q. In preparation.

I2 Restoring electronic coherence/decoherence for a trajectory-based nonadiabatic molecular dynamics

Chaoyuan Zhu

Department of Applied Chemistry, National Chaio-Tung University,

Ta-Hsueh Rd. 1001, Taiwan 30010

*Email: cyzhu@mail.nctu.edu.tw

Trajectory-based molecular dynamics (MD) simulations assume nuclear motions governed by Newton equations associated with the potential energy surfaces. MD simulation on a single potential energy surface results in average reaction probability and rate constant in accordance with exact calculation of quantum wavepacket. This is because trajectory simulation averages out quantum interference from different vibrational quantum states. On the other hand, nonadiabatic MD simulation on coupled potential energy surfaces results in semiclassical nonadiabatic switching probability that may overestimate or underestimate nonadiabatic quantum interference of exact quantum wavepacket. As the result, semiclassical methods usually add electronic coherence/decoherence into simulation of nonadiabatic switching probability. This is because numerically obtained nonadiabatic switching probability suffers overcoherent problems and these coupled semiclassical electronic states must decohere. In particular, Tully's fewest switching and semicalssical Ehrenfest hopping algorithms that are suitable for large-scale nonadiabatic molecular dynamics simulations have attracted the great attention. Various efforts have been made to improve decoherence/coherence effects to some extent but at either high computational cost or through the use of complicated algorithms. We have recently figured out simple but accurate new coupled equations with minimum modification to original coupled electronic semiclassical equations, and within the new coupled equations both Tully's fewest switching and semicalssical Ehrenfest hopping algorithms present nonadiabatic switching probability in excellent agreement with exact quantum simulations [1].

Keywords: Coherence; Decoherence; Molecular dynamics; Nonadiabatic transition; Quantum wavepacket

References:

[1] Zhu, C. Sci. Rep. 2016, 6; 24198.

I3 Recent Progress on the Dissociative Chemisorption of Energy-relevant molecules on Metal Surfaces

Bin Jiang[1]

[1] Department of Chemical Physics, University of Science and Technology of China, Hefei, Anhui 230026, China

*Email: bjiangch@ustc.edu.cn

Dissociative chemisorption of small molecules is the obligate and often rate-limiting step in many heterogeneous processes. As a result, an in-depth understanding of the reaction dynamics of such processes is of great importance for the establishment of a predictive model of heterogeneous catalysis. Beyond the extensively studied CH_4 and H_2O molecules, in this talk, I will introduce our recent work on CO_2 dissociative chemisorption.[1, 2]. In addition, some progresses in fitting high dimensional potential energy surface including surface atoms and mode dependent friction tensor will be also addressed.

Keywords: potential energy surface; reaction dynamics; dissociative chemisorption; neural network;

References:

[1] B. Jiang and H. Guo, J. Chem. Phys. **144**, 091101 (2016).

[2] X. Zhou, B. Kolb, X. Luo, H. Guo and B. Jiang, J. Phys. Chem. C **121**, 5594 (2017).

I4 典型化学反应的势能面和分子动态学

吴亚楠[1]，吴锋[1]，曹剑炜[1]，马海涛[1]，边文生[1*]

[1] 中国科学院化学研究所，北京市海淀区中关村北一街 2 号，100190

*Email: bian@iccas.ac.cn

对于典型的氢参与的化学反应，由于涉及到最具“量子”特征的H原子，量子动力学(QD) 效应(如隧穿、几何相效应等)很重要。因此，对这些反应的正确的动力学认识不仅有赖于高精度从头算势能面的构建, 而且需要开展精确的QD计算。我们近年来发展建立了PBFC-Lanczos量子动力学方法[1, 2], 通过实施大规模并行计算，实现了对分步双氢转移反应的选模隧穿分裂的精确全维量子计算, 最近又首次实现了对丙二醛隧穿异构体(含9原子)中的隧穿分裂的精确非含时21维量子计算, 对更大体系中的氢转移隧穿分裂的计算也在进行中。另一方面，高精度电子激发态从头算势能面的研究也是当前的一个重要前沿，我们以$C(^1D)H_2$体系为典型，成功构建了该体系单重电子基态($\tilde{a}^1A'$)[3]和第一电子激发态($\tilde{b}^1A''$)[4]的高精度全局从头算势能面，其重要特色是对锥形交叉附近区域以及范德华作用区域的高精度描述，对更高电子激发态的研究最近也取得了进展。基于所构建的势能面，我们进行了大规模的动力学计算，得到了微分截面、产物态分布和反应速率常数等动力学信息。我们的研究揭示了氢转移过程的本质特征, 电子激发态和势能面锥形交叉以及范德华力在分子动态学中的作用。

关键词：化学反应；微观动态学计算；势能面

参考文献

[1] Ren, Y.; Bian, W. *J. Phys. Chem. Lett.* **2015**, **6**: 1824.

[2] Wu, F.; Ren, Y.; Bian, W. *J. Chem. Phys.* **2016**, **145**: 074309.

[3] Zhang, C.; Fu, M.; Shen, Z.; Ma, H.; Bian, W. *J. Chem. Phys.* **2014**, **140**: 234301.

[4] Shen, Z.; Ma, H.; Zhang, C.; Fu, M.; Wu, Y.; Bian, W.; Cao, J. *Nature Commun.* **2017**, **8**: 14094.

I5　三原子和四原子体系的态－态分辨含时量子量子波包理论

孙志刚

大连化学物理研究所分子反应动力学国家重点实验室

zsun@dicp.ac.cn

发展具有产物量子态分辨的反应动力学程序，以利用现有的计算资源，尽可能快速的完成对复杂体系的反应动力学研究，是反应动力学理论研究的重要方向。最近几年，针对三原子和四原子反应体系，我们发展了几种能够实现产物量子态分辨的反应动力学的量子动力学理论方法。所发展的理论方法包括：针对复杂势能面的基于反应物和产物坐标的理论方法，针对直接反应的 RPD 方法，以及能够一次计算中计算出全部态－态分辨信息的过渡态波包方法和基于 MCTDH 方法的态态分辨的动力学方法。报告将简述这些方法的基本内容和特点，及其相对的优缺点。

【参考文献：】

1. State-to-state mode selectivity in the HD + OH reaction: Perspectives from two product channels, Bin Zhao, Zhigang Sun, Hua Guo J. Chem. Phys. **144**, 214303 (2016)
2. State-to-state differential cross sections for D_2 + OH → D + DOH reaction: Influence of vibrational excitation of OH reactant, Bin Zhao, Zhigang Sun, Hua Guo, J. Chem. Phys. **145**, 134308 (2016)
3. Calculation of state-to-state cross sections for triatomic reaction by the multi-configuration time-dependent Hartree method, Bin Zhao, D. H. Zhang, S. Y. Lee, Zhigang Sun, J. Chem. Phys. **140**, 164108 (2014)
4. A reactant-coordinate-based wave packet method for full-dimensional state-to-state quantum dynamics of tetra-atomic reactions: Application to both the abstraction and exchange channels in the H + H_2O reaction, Bin Zhao, Zhigang Sun, Hua Guo, J. Chem. Phys. **144**, 064104 (2016)
5. Calculation of state-to-state differential and integral cross sections for atom-diatom reactions with transition-state wave packets, Bin Zhao, Zhigang Sun, Hua Guo, J. Chem. Phys. **140**, 234110 (2014)
6. State-to-State Mode Specificity: Energy Sequestration and Flow Gated by Transition State, Bin Zhao, Zhigang Sun, Hua Guo*, Journal of the American Chemical Society, **137** (2015) 15964
7. Calculation of the state-to-state S-matrix for tetra-atomic reactions with transition-state wave packets: H2/D2 + OH → H/D + H2O/HOD, Bin Zhao, Zhigang Sun*, Huo Guo*, J. Chem. Phys. **141** (2014) 154112
8. Extraction of state-to-state reactive scattering attributes from wave packet in reactant Jacobi coordinates Zhigang Sun, H. Guo*, D. H. Zhang*, J. Chem. Phys. **132** (2010) 084112
9. A Reactant-Coordinate-Based Time-Dependent Wave Packet Method for Triatomic State-to-State Reaction Dynamics: Application to the H + O2 Reaction，Zhigang Sun, Donghui Zhang, Soo-Y. Lee, J. Phys. Chem. A **113** (2009) 4145

I6 激发态电子结构和非绝热动力学方法发展和应用

崔刚龙

北京师范大学化学学院，北京，100875

*Email: ganglong.cui@bnu.edu.cn

化学、生物、材料等许多领域都涉及十分复杂的光物理过程和光化学反应，理论计算模拟在其中起着重要的角色[1-3]。在本报告中，主要介绍课题组近年来在激发态电子结构和非绝热动力学方法和计算模拟方面的一些工作, 包括势能面交叉结构优化算法[4]、蓝光光受体光化学反应机理[5]、DNA中偶氮苯发色团的光异构化、硅量子点的激发态弛豫动力学等。

关键词：光化学；激发态；电子结构；非绝热动力学；势能面交叉

参考文献

[1] Xie, B.B.; Liu, X.Y.; Fang, Q.; Fang, W.H.; Cui, G.L. J. Phys. Chem. Lett. 2017, 8, 1019.

[2] Xia, S.H.; Cui, G.L.; Fang, W.H.; Thiel, W. Angew. Chem. Int. Ed. 2016, 55, 2067.

[3] Wang, Y.T.; Liu, X.Y.; Cui, G.L.; Fang, W.H.; Thiel, W. Angew. Chem. Int. Ed. 2016, 55, 14009.

[4] Liu, X.Y.; Cui, G.L.; Fang, W.H.; Theor. Chem. Acc. 2017, 136, 8.

[5]Chang, X.P.; Gao, Y.J.; Fang, W.H.; Cui, G.L.; Thiel, W. Angew. Chem. Int. Ed. 10.1002/anie.201703487

I7 On-the-fly Surface-Hopping Nonadiabatic Dynamics and Analysis of Geometrical Evolution with Dimensionality Reduction Approaches

Zhenggang Lan[1*]

[1]Qingdao Institute of Bioenergy and Bioprocess Technology,
Chinese Academy of Sciences, Qingdao 266101, China
*Email:lanzg@qibebt.ac.cn

Our works focus on the theoretical description of nonadiabatic dynamics on molecular excited states.

One important topic of our group is to develop a user-friendly simulation package called "JADE", which performs the simulation of nonadiabatic dynamics within the framework of the on-the-fly trajectory surface-hopping dynamics. Our recent progress on the code development, particular the new analysis tool, is briefly discussed.

We show the possibility to analyze the geometrical evolution of trajectory-based nonadiabatic molecular dynamics by dimensionality reduction techniques (Classical Multidimensional Scaling and Isometric Mapping). These approaches allow us to extract the major molecular motion from the very complicated time-dependent evolution from many trajectories. This opens a very interesting research topic in the future.

Keywords: nonadiabatic molecular dynamics, MDS, ISOMAP, surface hopping, dimensionality reduction

I8　　捕捉 DNA 鸟嘌呤氧化损伤反应的自由基离子对中间体

苏红梅

北师大化学学院，北京市新街口外大街 19 号，100875

*Email: hongmei@bnu.edu.cn

鸟嘌呤G碱基氧化还原性质极为活泼，在DNA氧化损伤及DNA电荷传导等过程中扮演重要的角色。光照或强氧化自由基作用下，G碱基容易失去一个电子形成阳离子自由基(G+·)，引发DNA链上的空穴传输或系列的DNA氧化损伤反应，生成后续的损伤产物（8-OG、FAPY-G, imidazolone, oxazolone等）。然而，G+·的生成不单纯是直接的单电子氧化过程，而是经常涉及到一类重要的自由基离子对中间体参与反应。理论计算预测自由基离子对中间体寿命短（~ ps），稳定性极低，过去实验上一直难以对其探测表征。

我们通过低温稳定反应中间体的方法并结合时间分辨光谱探测，成功捕捉到DNA鸟嘌呤氧化损伤基元反应途径中的自由基离子对中间体。对于氯自由基与G碱基的反应体系，在低温瞬态吸收光谱上探测到中心位于570 nm的强吸收峰，结合理论计算归属为G+•…Cl-离子对中间体，这一可见光区域的特征吸收光谱是由离子对静电作用改变跃迁轨道空间重叠所致，与G+•本身在可见区吸收弱的光谱行为有明显区别。进一步在双链DNA的氧化反应体系中，观测到离子对中间体在570nm的特征光谱裂分为480nm和610nm两个吸收峰。 借助动力学分析，确定了这两个吸收峰对应于双链GC碱基对内质子转移平衡的两种离子对结构 Cl-…G+•:C ↔ Cl-…G(-H)•:C(+H+)，通过离子对特征光谱的裂分，进而清晰区分了双链DNA碱基对内质子转移平衡的两种质子化结构、并测得质子转移的反应能垒(Ea ~ 1.4 kcal/mol)。这些结果给出DNA鸟嘌呤氧化反应的自由基离子对机理的关键实验证据，对深入认识DNA质子耦合电子转移和DNA氧化损伤等过程具有重要意义。

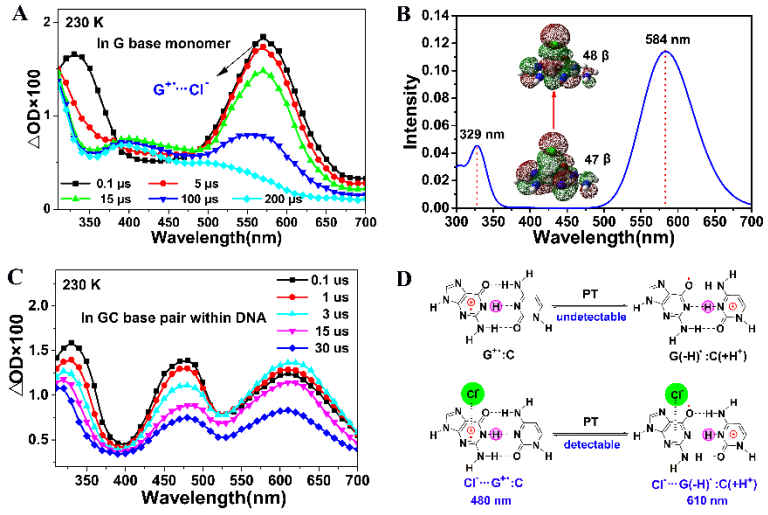

关键词：低温时间分辨光谱；自由基离子对；DNA氧化损伤反应；质子转移

参考文献

[1] 节家龙，刘坤辉，吴丽丹，赵红梅，宋迪，苏红梅. *Sci. Adv.* **2017,** 3: e1700171.

[2] J. Cadet, T. Douki, J.-L. Ravanat, *Acc. Chem. Res.* **2008,** 41: 1075

I9 团簇与惰性分子的反应研究

何圣贵

中国科学院化学研究所，北京市海淀区中关村北一街 2 号，北京 100190

*Email: shengguihe@iccas.ac.cn

甲烷、二氧化碳等惰性分子的活化与转化是化学研究的重要内容。研究团簇与相关分子的反应，可以在化学键和电子结构水平深入理解控制分子活化转化的关键因素，为设计新型分子催化过程提供研究基础。最近，通过研究一些金属氧化物和金属碳化物团簇的反应性，我们发现了CH4活化转化中的协同效应[1]、CO2的直接加氢反应机理[2]、异核金属氧化物团簇反应中的电负性阶梯效应[3]、纳米尺寸团簇中的热-电耦合现象[4]。这次会议将重点汇报我们近两年来的相关研究进展。

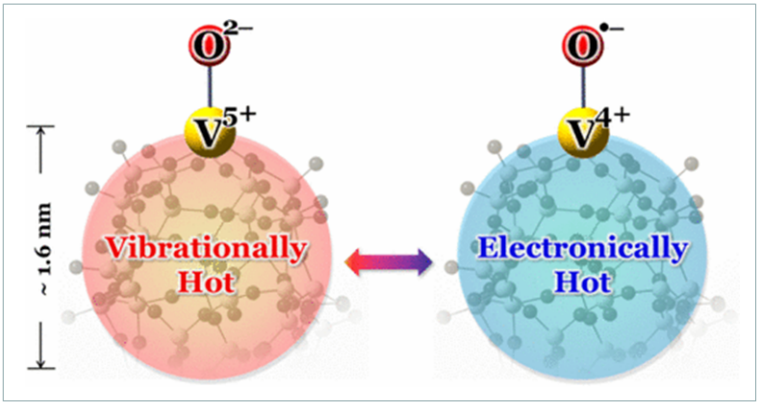

Fig.1 纳米尺寸氧化钒团簇中的热-电耦合。

参考文献

[1] (a) Li, H.-F.; Zhao, Y.-X.; Yuan, Z.; Liu, Q.-Y.; Li, Z.-Y.; Li, X.-N.; Ning, C.-G.; He, S.-G. *J. Phys. Chem. Lett.* **2017**, *8*, 605; (b) Zhao, Y.-X.; Li, X.-N.; Yuan, Z.; Liu, Q.-Y.; Shi, Q.; He, S.-G. *Chem. Sci.* **2016**, *7*, 4730; (c) Li, Y.-K.; Yuan Z.; Zhao Y.-X.; Zhao C.; Liu Q.-Y.; Chen H.; He S.-G. *J. Am. Chem. Soc.* **2016**, *138*, 12854; (d) Li, Z.-Y.; Li, H.-F.; Zhao, Y.-X.; He, S.-G. *J. Am. Chem. Soc.* **2016**, *138*, 9437; (e) Liu, Q.-Y.; Ma, J.-B.; Li, Z.-Y.; Zhao, C.; Ning, C.-G.; Chen, H.; He, S.-G. *Angew. Chem. Int. Ed.* **2016**, *55*, 5760.

[2] Jiang, L.-X.; Zhao, C.; Li, X.-N.; Chen, H.; He, S.-G. *Angew. Chem. Int. Ed.* **2017**, *56*, 4187.

[3] (a) Li, X.-N.; Zhang, H.-M.; Yuan, Z.; He, S.-G. *Nat. Commun.* **2016**, *7*, 11404; (b) Wang, L.-N.; Li, Z.-Y.; Liu, Q.-Y.; Meng, J.-H.; He, S.-G.; Ma, T.-M. *Angew. Chem. Int. Ed.* **2015**, *54*, 11720.

[4] Zhang, M.-Q.; Zhao, Y.-X.; Liu, Q.-Y.; Li, X.-N.; He, S.-G. *J. Am. Chem. Soc.* **2017**, *139*, 342.

I10　有机半导体、光合作用等复杂体系中载流子量子动力学理论

赵 仪

固体表面物理化学国家重点实验室，厦门大学化学化工学院，厦门，361005

*Email: yizhao@xmu.edu.cn

有机分子光电器件中的载流子动力学对控制器件效率起着至关重要的作用。2016 年12 月20 日，Nature Materials 在线发布的6篇与新能源材料相关的综述和展望论文中，其中一篇“灵感于光合系统相干效应的光伏概念”就专门探讨了如何模仿自然光合体系中载流子量子相干运动效应来制造出更好的人造光和作用体系。理论上，描述有机半导体内载流子运动的局域跳跃模型相对成熟，但如何将载流子的量子相干运动与跳跃模型结合起来是理论化学动力学领域的难点和热点之一。尽管面临诸多困难，人们已提出和发展了多种理论和计算方法，最近几年我们也在这方面做了一定的尝试，提出一个能够处理几万个分子体系中载流子量子动力学的含时波包扩散方法[1]，我们也从发展的杂化级联-随机薛定谔方程出发[2-4]，确认了波包扩散方法的应用范围。在此基础上，我们将其方法推广到具体应用，如计算并分析了有机聚合物PBDTTPD中热激子的超快能量弛豫过程，发现该过程实际上分两步：一个超快的退相干过程和较为缓慢的扩散过程，计算出的两个不同步骤的特征时间与Heeger等人的超快荧光光谱实验结果相符[5]；讨论了Singlet fission过程中载流子的相干与离域、电荷转移态对其速率的影响等[6]。

关键词：有机材料；载流子；量子动力学；波包扩散理论

参考文献

[1] Zhong, X.; Zhao, Y. *J. Chem. Phys.,* **2013, 138,** 014111.

[2] Ke, Y.; Zhao, Y. *J. Chem. Phys.,* **2016, 145,** 024101.

[3] Ke, Y.; Zhao, Y. *J. Chem. Phys.,* **2017, 146,** 174105.

[4] Ke, Y.; Zhao, Y. *J. Chem. Phys.,* **2017, 146,** 214105.

[5] Ke, Y.; Liu, Y.; Zhao, Y. *J. Phys. Chem. Lett.* **2015, 6,** 1741−1747.

[6] Zang, H.; Ke, Y.; Zhao, Y.; Liang W. *J. Phys. Chem. C* **2016, 120,** 13351-13359.

I11 “中国红灯笼分子”—硼球烯及其家族

翟华金 (Hua-Jin Zhai)

山西大学分子科学研究所纳米团簇实验室，山西太原，030006

*Email: hj.zhai@sxu.edu.cn

本报告涵盖作者与中美合作者在硼球烯 (borospherenes) 研究领域的若干进展。硼球烯亦称全硼富勒烯 (all-boron fullerenes), 是继碳富勒烯之后又一类共价笼形团簇体系。我们的研究手段基于高真空气相光电子能谱学实验和高精度量子化学理论计算的密切结合。报告的具体团簇体系包括: (1)首例硼球烯B40–/B40的实验发现，其总体构型酷似传统“中国红灯笼”; 由硼双链纵横交织而成, 含上下二个六边形和腰上4个七边形孔洞, 具有类立方结构, 呈D2d对称性; 成键分析展示独特的π和σ双离域, 包括均匀覆盖笼形表面的12个离域π键。(2)手性硼球烯B39–的实验观察与理论表征。(3)基于量子化学计算建立和拓展完整硼球烯家族: Bnq (q = n–40, n = 36–42), 包括C2 B422+, C1 B41+, D2d B40/B40–, C3/C2 B39–, Cs B382–, C1 B373–, Th B364–。其共性是均为类立方结构, 均含12个离域π键。(4)尺度最小的扇贝状硼球烯B28–的实验观察和理论表征。它由2个三角形密堆B15准平面单元融合而成, 有9个离域π键。

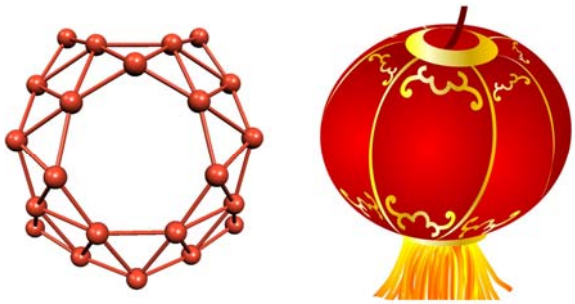

Fig. 1 Borospherene D_{2d} B_{40} (*left*) versus Chinese red lantern (*right*)

关键词： 硼球烯；纳米团簇；硼团簇；π和σ双离域；芳香性

参考文献

[1] Zhai, H.J., et al. *Nature Chem.* **2014**, **6**: 727–731.

[2] Chen, Q., et al. *ACS Nano* **2015**, **9**: 754–760.

[3] Wang Y.J., et al. *J. Chem. Phys.* **2016**, **144**: 064307.

I12 A semiclassical study on quantum dynamical effects in Raman spectra of liquid water

Xinzijian Liu[1], Jian Liu[1,*]

[1]Institute of Theoretical and Computational Chemistry, College of Chemistry and Molecular Engineering, Peking University, Beijing, 100871
*Email: jianliupku@pku.edu.cn

Liquid water is of great interest due to its important role in many processes in nature. We focus on quantum dynamical effects and the isotopic effects in Raman spectra of liquid water [1] using the linearized semiclassical initial value representation (LSC-IVR) with the local Gaussian approximation (LGA) [2-4] and an ab initio-based, polarizable water model for inter- and intramolecular vibrational spectroscopy (POLI2VS) [5]. Due to the physical decay in the condensed phase system, LSC-IVR is a good and practical approximate quantum approach for studying vibrational spectra of liquid water.

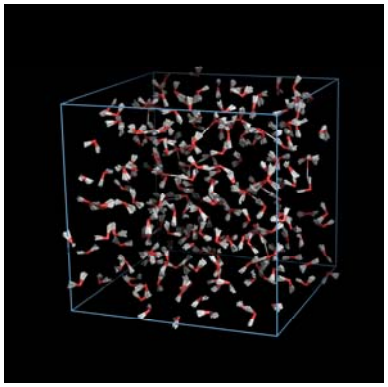

Fig. 1 Representation of the simulated water box.

Keywords: Semiclassical; quantum dynamical effect

References:

[1] Liu, X.; Liu, J. in preparation.
[2] Liu, J.; Miller, W. H. *J. Chem. Phys.* **2009**, **131**: 074113.
[3] Liu, J.; Miller, W. H.; Fanourgakis, G. S.; Xantheas, S. S.; Imoto, S.; Saito, S. J. *J. Chem. Phys.* **2001**, **135**: 224503.
[4] Liu, J.; Miller, W. H.; Paesani, F.; Zhang, W.; Case, D. A. *J. Chem. Phys.* **2009**, **131**: 164509.
[5] Hasegawa, T.; Tanimura, Y. *J. Phys. Chem. B* **2011**, **115**: 5545.

I13 Recent Progress in Study of Superfluid in doped quantum solution

Hui Li

Institute of Theoretical Chemistry, Laboratory of Theoretical and Computational Chemistry, Jilin University Liutiao Road 2, Changchun, 130023
*Email: prof_huili@jlu.edu.cn

Superfluidity is a remarkable manifestation of quantum mechanics at the macroscopic scale. When cooled to very low temperature, liquid helium exhibits the very peculiar property of flowing without friction or dissipation. This phenomenon has been observed and well characterized in the bulk liquid helium phase. In clusters and nanodroplets, 4He and pH2 have been shown to exhibit superfluid effects but a direct assessment of the superfluid response of mixtures of these two bosons remains an open area of investigation. To understand the properties of microscopic superfluid mixtures, we perform path integral Quantum Monte Carlo simulations of different rotors (HCN, CO2 and OCS) doped pH2 or 4He clusters. Size-dependent phase separation is observed and the onset thereof is characterized and attributed to a delicate interplay between interaction induced localization and the filling of solvation shells. Our findings shed new light on pioneering experiments performed on OCS with pH2 embedded in helium droplets where the disappearance of the Q-branch spectroscopic feature was attributed to the onset of the superfluidity of pH2. Our results rather suggest that the helium environment significantly suppresses the superfluid response of pH2 and that the disappearance of the Q-branch may very well instead be a sign of phase separation of the two bosonic species.

Keywords: Superfluid, Rovibrational spectra, Potential energy surface

I14 Computing Free Energy of States and Potential of Mean Force at High Levels from Low Level Simulations

Pengfei Li[1], Meiting Wang[1], Xiangyu Jia[1,2], Ye Mei[1,*]

[1]State Key Laboratory of Precision Spectroscopy, School of Physics and Materials Science, East China Normal University, Shanghai 200062, China

[2]Current Address: NYU-ECNU Center for Computational Chemistry at NYU Shanghai, Shanghai 200062, China

*Email: ymei@phy.ecnu.edu.cn

Free energy calculations at high levels such as QM(ai)/MM level are very expensive, due that extensive phase space sampling is always indispensable before the convergence can be reached and for most cases many intermediate states are required to make the conversion between two states smooth enough. We proposed an efficient method for the calculations of free energies at QM/MM levels. In this method, the QM/MM free energies are computed indirectly via a series of MM states and the MM-to-QM corrections were computed at two end points using thermodynamics perturbation (TP). This method provides the minimal variance for the results if expensive QM/MM simulations are avoided. We also proposed a quantity called reweighting entropy, which measures the reliability of TP calculations. Similarly, calculations of potentials of mean force (PMF), which are essential to the understanding of reaction mechanisms, are also expensive. We also proposed an efficient method for the calculations of PMF at high QM/MM levels using phase space sampling under low level Hamiltonians followed by free energy corrections.

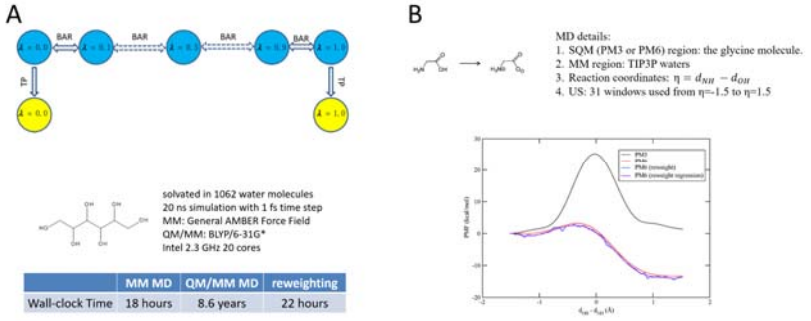

Fig. 1 (A) The computation of free energy difference between two states. (B) The computation of potential of mean force for a intramolecular proton transfer reaction.

Keywords: free energy; potential of mean force; QM/MM; WHAM; TP

References:

[1] Jia, X.Y; Wang, M.T.; Shao, Y.; Koenig, G.; Brooks, B.; Zhang, J.Z.H.; Mei, Y. J. Chem. Theory Comput., **2016, 12**: 499

[2] Wang, M.T.; Li, Pengfei; Jia, X.Y; Liu, W.; Shao, Y.; Mei, Y. J. Chem. Inf. Model., in revision

[3] Li, Pengfei; Jia, X.Y; Mei, Y., in preparation.

I15 Recent Progresses on Dissociative Electron Attachment Study

Shan Xi Tian（田善喜）

Department of Chemical Physics, University of Science and Technology of China, Hefei, China

*Email address: sxtian@ustc.edu.cn

When an electron is attached or transferred to an empty anti-bonding orbital of a molecule, a specific bond in this temporary electron-molecule system could be broken. This process is known as dissociative electron attachment (DEA). An anionic fragment and one or more neutral radicals will be produced in DEA, then they may be involved in the sub-reactions with the surrounding molecules or substance. DEA and its sub-reactions, noted as electron-induced process, play prominent roles in many contexts ranging from astro- and plasma physics, the atmosphere chemistry to radiation damage of living tissue. During the past decades, many research groups in the world put a lot of efforts into this subject. However, some fundamentals and dynamics details about DEA are still unrevealed. Furthermore, it is unclear about the potential applications of electron-induced process although few reports have concerned this process.

Three projects about the electron-induced chemical reaction are carried out in our laboratory: the gas-phase DEA process, the electron collision with the liquid/surface, and the gas-phase positive/negative ion-molecule reaction. These processes represent three typical electron-induced chemical reactions, namely, with the free-, hydrated- or bound-electron/charge, respectively. The first project started in 2012 by setting up a home-made anion time-sliced velocity map imaging (VMI) apparatus1, and some novel features of DEA dynamics were reported in the past five years2. To have insights into the molecular-vibration effects on the gas-phase DEA process, now we are developing a high-resolution anion time-sliced VMI apparatus. Here I will introduce our recent progress on this project.

References:

[1] Wu B., et al. *Rev. Sci. Instrum.* **83**, 013108 (2012). Xuan C.-J., et al. *Chin. J. Chem. Phys.* **27**, 628 (2014).

[2] Wu B., et al. *Phys. Rev. A* **85**, 052709 (2012). Xia L., et al. *J. Chem. Phys.* (communication) **137**, 151102 (2012). Xia L., et al. *Angew. Chem. -Int. Ed.* **52**, 1013 (2013). Zeng X.-J., et al. *Phys. Rev. A* **87**, 012711 (2013). Li H.-K., et al. *J. Phys. Chem. A* **117**, 3176 (2013). Tian S.X., et al. *Phys. Rev. A* **88**, 012708 (2013). Xia L., et al. *J. Chem. Phys.* (communication) **140**, 041106 (2014). Wang X.-D., et al. *J. Chem. Phys.* **142**, 064316 (2015). Tian S.X., et al. *Phys. Rev. A* **91**, 056702 (2015). Wang X.-D., et al. *J. Chem. Phys.* **143**, 066101 (2015). Li M.-Y., et al. *Int. J. Mass Spectrom.* (cover story) **404**, 20 (2016). Wang X.-D. et al. *Nature Chem.* **8**, 258 (2016).

I16 典型势阱控速反应的准经典轨线计算

曹剑炜[1*]，吴亚楠[1]，马海涛[1]，边文生[1*]

[1] 中国科学院化学研究所，北京市海淀区中关村北一街 2 号，100190

*Email: caojw@iccas.ac.cn, bian@iccas.ac.cn

准经典轨线计算不仅可以提供各种宏观和微观的反应动力学信息，还可以为研究反应机理提供直观图像。电子激发态反应动态学和范德华相互作用力对反应的影响是化学反应研究的两个重要前沿。C(1D)+H2体系是研究势阱控速反应的模型体系，同时在烃类燃烧和天体物理学中扮演着重要角色，因此长期以来一直为实验和理论工作者所关注。所在课题组成功构建了C(1D)H2体系单重电子基态(ã1A′)[1]和第一电子激发态(b̃1A″)[2]的高精度全局从头算势能面（Zhang-Ma-Bian，ZMB势能面），首次正确描述了锥形交叉附近区域以及范德华作用区域。基于所构建的势能面，我们对C(1D)+HD及其同位素反应进行了详细的准经典轨线计算，得到了积分截面、微分截面、产物态分布和反应速率常数等动力学信息。我们的研究揭示了势能面的锥形交叉和范德华鞍的动力学作用，并在量子态层次发现了新的反应机理，同时也澄清了以前理论计算和实验的分歧，将有助于深化人们对势阱控速反应以及电子激发态反应的认识。

关键词：势阱控速反应；准经典轨线计算；反应机理

参考文献

[1] Zhang, C.; Fu, M.; Shen, Z.; Ma, H.; Bian, W. J. Chem. Phys. 2014, 140: 234301.

[2] Shen, Z.; Ma, H.; Zhang, C.; Fu, M.; Wu, Y.; Bian, W.; Cao, J. Nature Commun. 2017, 8: 14094.

I17 水在 TiO_2 表面的光化学

郭庆，马志博，樊红军，杨学明*

大连化学物理研究所分子反应动力学国家重点实验室，大连市中山路 457 号，116023

*Email: xmyang@dicp.ac.cn

TiO_2 由于其广泛的应用价值吸引了众多科学家的注意，特别是在光解水制氢上的作用为人类获得清洁能源提供了可行的思路。为了更好的理解整个光化学过程，越来越多的物理化学工作围绕着TiO_2单晶表面特别是TiO_2(110)面展开。因此，研究水在TiO_2表面的光化学过程，以及表面光化学反应机理，对开发新光催化剂来实现光催化分解水起着重要的作用。我们研究组利用多套表面研究装置，分别从程序升温脱附谱（TPD）、扫描隧道显微镜（STM）等多方面对水在TiO_2上发生的光化学过程进行了研究，通过多种手段的结合，开展了一系列工作，较为清楚和全面的阐明了该体系在光诱导下发生的化学过程。

关键词： TiO_2；水；光催化

参考文献

[1] Yang , W.; Wei, D.; Jin, X.; Xu, C.; Geng, Z.; Guo, Q.; Ma, Z.; Dai, D.; Fan, H.; Yang, X. *J. Phys. Chem. Lett.* **2016**, **7**: 603.

Photolysis of water on TiO_2

Qing Guo, Zhibo Ma, Hongjun Fan, Xueming Yang*

Dalian Institute of Chemical Physics, 457, Zhongshan Road, Dalian, 116023

*Email: xmyang@dicp.ac.cn

TiO2 has attracted enormous attentions, because of its potential applications, especially in the hydrogen production from water splitting, which provides a feasible way for human to obtain clean energy. In order to better understand the whole photochemical process, more and more works around the TiO2 single crystal surface, especially the TiO2(110) surface. Therefore, the investigation of fundamental processes of water photolysis on TiO2 surfaces plays an important role in the development of new catalysts to achieve hydrogen production from water splitting. Combination programed desorption spectroscopy (TPD), scanning tunneling microscopy (STM) and density functional theory (DFT) calculation, the photochemical processes of water dissociation on TiO2 surface have been studied systematically in our group.

I18 Electronic Structure at TiO_2 Interface

Chuanyao Zhou,[1,*] Zhiqiang Wang,[1] Bo Wen,[2] Qunqing Hao,[1] Li-Min Liu,[2] Anabella Selloni,[3] Xueming Yang[1,*]

[1]State Key Laboratory of Molecular Reaction Dynamics, Dalian Institute of Chemical Physics, CAS

[2]Beijing Computational Science Research Center

[3]Department of Chemistry, Princeton University

*Email: chuanyaozhou@dicp.ac.cn, xmyang@dicp.ac.cn

In reduced TiO2, electronic transitions originating from the Ti3+- induced states in the band gap are known to contribute to the photoabsorption, being in fact responsible for the material's blue color and visible light photocatalysis, but the excited states accessed by these transitions have not been characterized in detail. In this work we investigate the excited state electronic structure of the prototypical rutile TiO2(110) surface using two-photon photoemission spectroscopy (2PPE) and density functional theory (DFT) calculations. Using 2PPE, an excited resonant state derived from Ti3+ species is identified at 2.5±0.2 eV above the Fermi level (EF) on both the reduced and hydroxylated surfaces. DFT calculations reveal that this excited state is closely related to the gap state at ~ 1.0 eV below EF, as they both result from the Jahn-Teller induced splitting of the 3d-t2g orbitals of Ti3+ ions in reduced TiO2. Localized excitation of Ti3+ ions via 3d→3d transitions from the gap state to this empty resonant state increases significantly the TiO2 photo-absorption and extends the absorbance to the visible region, consistent with the observed enhancement of the visible light induced photocatalytic activity of TiO2 through Ti3+ self-doping. Water adsorption can significantly increase the excited resonance in 2PPE. Possible reasons for such enhancement have been discussed. Our work reveals the physical origin of the Ti3+ related photoabsorption and visible light photocatalytic activity in prototypical TiO2, and also paves the way for the investigation of the electronic structure and photoabsorption of other metal oxides.

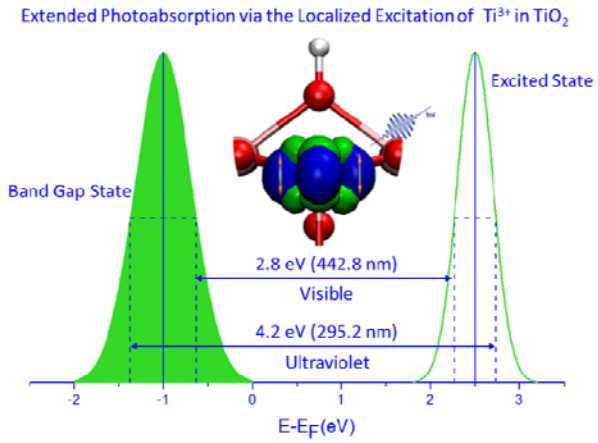

I19 Ion Effect on Hydrogen Bonding Network in Water

Wei Zhuang

State Key Lab of Structural Chemistry, Fujian Institute of Research on Structure of Matters, Fuzhou, China
*E-mail : wzhuang@fjirsm.ac.cn

Ions effect on water structure and dynamics have significant specificity which is far from being fully comprehended. Various vibrational spectroscopies are among the most powerful experimental tools to explore this issue. The interpretation of these spectroscopy signals is, however, usually non-trivial and requires the help from theoretical studies. We've developed a series of theoretical approaches to simulate the analyze the vibrational spectroscopies of the ionic solution, which reproduce nicely the spectra including THZ, Raman, fsIR,2DIR,IRPD and Raman-THZ. Based on these simulations, we attempt to address several important issues about the ion effect on water hydrogen bonding network, including 1) ion specificity in their effects on water dynamics and 2) spatial range of ion effects. Novel techniques including complex network recognition and gaussian field model are employed to assist the analysis.

I20 Adsorption and activation of O_2 or NO on heavy metal clusters

Xiaopeng Xing[1,*], Jun Ma[1], Baoqi Yin[1], Tingting Wang[1]

[1]School of Chemical Science and Engineering, Tongji University, No 1239, Siping Road, 200092
*Email: xingxp@tongji.edu.cn

We studied low-temperature adsorption and activation of O2 or NO on heavy metal clusters of Agn+/-, Aun+/-, Bin+/-, Pbn+/- etc., which contain two to tens of atoms. The reaction rates of Agn+/- and Agn+/- are closely related to their global electronic properties, while nearly independent on local structures of the adsorption sites. For Bin+/- and Pbn+/-, both the electronic properties and the local adsorption sites have significant effects. These observations imply different reaction mechanisms of these molecules on the heavy metal clusters, providing more profound views on the adsorption and activation processes on bulky metal surfaces. The reactions of O2 or NO on gold or silver clusters are also closely related to the processes on real catalysts containing dispersed gold or silver.

Keywords: cluster reactions; flow-reactor; heavy metals; adsorption of O_2; adsorption NO

References:

[1] Ma, J.; Cao, X.; Xing, X.; Wang, X.; Parks, J. *Phys. Chem. Chem. Phys.* **2016, 18:** 743.
[2] Ma, J.; Cao, X.; Liu, H.; Yin, B.; Xing, X. *Phys. Chem. Chem. Phys.* **2016, 18:** 12819.
[3] Ma, J.; Cao, X.; Chen, M.; Yin, B.; Xing, X.; Wang, X. *J. Phys. Chem. A* **2016, 120:** 9131.
[4] Cao, X.; Chen, M.; Ma, J.; Yin, B.; Xing, X. *Phys. Chem. Chem. Phys.* **2017, 19:** 196.

I21 表界面催化的动力学调控

傅钢

厦门大学化学化工学院，福建省厦门市思明南路 422 号，361005

*Email: gfu@xmu.edu.cn

多相催化是借助高性能材料，在分子和原子水平上对分子的化学键进行重排、对化学态进行重组，其根本是分子在催化剂表面以及载体（或配体）与其形成的多相界面上的相互作用。因此，界面区域的结构、电子特性、以及热力学和动力学特征可能是认识相关催化过程的关键。真实的催化剂的表界面非常复杂，不仅有不同配位的金属原子暴露，往往还存在金属/金属界面，金属/有机物界面和金属/氧化物界面，见Fig.1。本文应用密度泛函理论，系统研究了几个重要的表界面催化体系[1-6]：1)细致研究了合金等复杂催化体系表面的部分占据难题；2)考察了金属/金属氧化物界面对氧化和加氢反应的促进机制，揭示了界面羟基在催化反应中的重要作用；3)应用配位化学的概念深入研究有机物修饰对贵催化剂选择加氢的影响，发现有机胺/有机硫酚可以通过立体效应和/或电子效应来调控加氢反应的动力学； 4)阐明表面乙二醇基在光助Pd单原子分散催化剂生成过程中重要作用，细致研究了单原子Pd催化加氢和催化氧化机理。

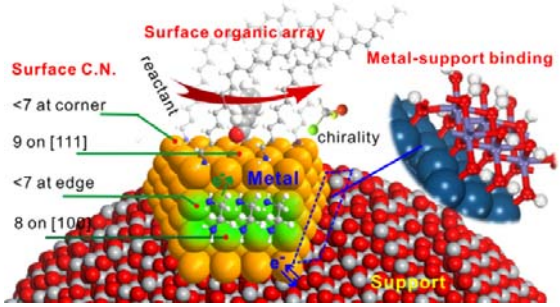

Fig. 1 A coordination chemistry view of surface/interface

关键词：密度泛函；催化氧化；催化加氢；单原子催化；表面配位化学

参考文献

[1] Chen, G. X.; Zhao, Y.; Fu, G.; Duchesne, P. N.; Gu, L.; Zheng, Y. P.; Weng, X. F.; Chen, M. S.; Zhang, P.; Pao, C.-W.; Lee, J.-F.; Zheng, N. F. Science 2014, 344, 495.

[2] Liu, P. X.; Zhao, Y.; Qin, R. X.; Mo, S. G.; Chen, G. X.; Lin, G.; Chevrier, D. M.; Zhang, P.; Guo, Q.; Zang, D. D.; Wu, B. H.; Fu, G.; Zheng, N. F. Science 2016, 352, 797.

[3] Wu, B. H.; Huang, H. Q.; Yang, J.; Zheng, N. F.; Fu, G. Angew. Chem. Int. Ed. 2012, 51, 3440.

[4] Chen, G. X.; Xu, C. F.; Huang, X. Q.; Ye, J. Y.; Gu, L.; Li, G.; Tang, Z. C.; Wu, B. H.; Yang, H. Y.; Zhao, Z. P.; Zhou, Z. Y.; Fu, G.; Zheng, N. F. Nature Mater. 2016, 15, 564.

[5] Cao, Z.; Chen, Q.; Zhang, J.; Li, H.; Jiang, Y.; Shen, S; Fu, G; Lu, B.; Xie, Z.; Zheng, L.，Nature Communications, DOI: 10.1038/NCOMMS15131

[6] Liu, P.;，Qin, R.; Zheng, N.; Fu G.,，J. Am. Chem. Soc.,2017，139(6), 2122-2131

I22 Metal－Hydrogen Bridge and Agostic Bonding: Infrared Spectra and Theoretical Calculations

Bing Xu, Jie Zhao, Wenjie Yu, Tengfei Huang, Xuefeng Wang

Department of Chemistry, Tongji University, Shanghai 200092

*Email: xfwang@tongji.edu.cn

Infrared spectra of matrix isolated dibridged Si(μ-H)2MH2 and tribridged Si(μ-H)3MH molecules (M = Zr and Hf, or Be and B) were observed following the laser-ablated metal atom reactions with SiH4 during condensation in excess argon and neon, but methylidene complex CH2＝MH2 with agostic bonding was formed in metal atom reactions with CH4. Assignments of the major vibrational modes, which included terminal MH, MH2 and hydrogen bridge stretching modes, were confirmed by the appropriate deuterium isotopic shifts and density functional vibrational frequency calculations (B3LYP and BPW91). The Si－H－M bridge bond is calculated as weak covalent interaction and compared with the C–H⋯M agostic interaction in terms of electron localization function (ELF) analysis and noncovalent interaction index (NCI) calculations.

References:

[1] B. Xu, P.P. Shi, T.F. Huang, X.F. Wang, L. Andrews, J. Phys. Chem. A, 2017, 121, 3898.

[2] J. Zhao, B. Xu, W.J. Yu, X.F. Wang, Organometallics, 2016, 35, 3272.

[3] J. Zhao, W.J. Yu, B. Xu, T.F. Huang, X.F. Wang, Chem. Phys. Lett. 2017, 672, 1.

[4] X.F. Wang, B.O. Roos, L. Andrews, Angew. Chem. Int. Ed. 2010, 49, 157.

[5] H.G. Cho, X.F. Wang, L. Andrews, J. Am. Chem. Soc., 2005, 127, 465.

I23 Recent Advances in Fragment-based Quantum Mechanical Methods and Minnesota Density Functionals

Xiao He[1,2*]

[1]School of Chemistry and Molecular Engineering, East China Normal University, Shanghai, China

[2]NYU-ECNU Center for Computational Chemistry at NYU Shanghai, Shanghai, China

*Email: xiaohe@phy.ecnu.edu.cn

The major computational limitation of conventional *ab initio* methods is the scaling problem, because the cost of *ab initio* calculation scales as *n*th power or worse with the system size. In the past two decades, the fragmentation method has opened a new door for the development of QM methods and their applications to large molecules. In the first half of this talk, I will present our recent *ab initio* molecular dynamics (AIMD) simulation of liquid water at ambient conditions using fragment-based second-order Møller-Plesset perturbation theory (MP2). The simulated structural and dynamical properties of liquid water are in excellent agreement with experimental observations. For the water oxygen-oxygen radial distribution function (RDF), our simulation accurately reproduces the first three experimental peaks of aqueous water for the first time using high-level *ab initio* theory. The calculated oxygen-oxygen-oxygen triplet angular distribution, self-diffusion coefficient, and molecular dipole moment of liquid water are also in good agreement with experimental results. Our AIMD simulation sheds light on the intriguing hydrogen-bond networks, and reveals the dynamic features of the aqueous environment, which are difficult to probe experimentally.

The M06-L density functional is one of the best local functionals to date, but still has room for improvement on numerical stability and overall accuracy. In the second half of this talk, I will present the revised M06-L functional, named revM06-L, for smoother potential energy curves and improved accuracy on chemical and physical databases. We optimized the revM06-L functional against the Minnesota Database 2015A using smoothness restraints. The mean unsigned error (MUE) of revM06-L on 422 chemical energies is 3.1 kcal/mol, which is improved from 3.6 kcal/mol calculated by M06-L. The MUEs of revM06-L for the chemical reaction barrier height database (BH76), the noncovalent interaction database (NC51), and the solid-state lattice constant database (LC17) are significantly reduced as compared to M06-L. The revM06-L functional also predicts more accurate results than M06-L in 7 out of 8 diversified test sets. Therefore, the revM06-L functional is well-suited for a broad range of applications in chemistry and solid-state physics.

References:

(1) He, X.; Zhu, T.; Wang, X.; Liu, J.; Zhang, J. Z. H. *Acc. Chem. Res.* **2014**, 47: 2748.

(2) Hirata, S.; Gilliard, K.; He, X.; Li, J. J.; Sode, O. *Acc. Chem. Res.* **2014**, 47: 2721.

(3) Liu, J. F.; He, X.; Zhang, J. Z. H. *Phys. Chem. Chem. Phys.* **2017**, 19: 11931.

(4) Liu, J. F.; Qi, L. W.; Zhang, J. Z. H.; He, X. *J. Chem. Theory Comput.* **2017**, 13: 2021.

(5) Liu, J. F.; Zhang, J. Z. H.; He, X. *Phys. Chem. Chem. Phys.* **2016**, 18: 1864.

(6)Liu, J. F.; Zhu, T.; Wang, X. W.; He, X.; Zhang, J.Z.H. *J. Chem. Theory Comput.* **2015**, 11: 5897.

(7) Wang, X. W.; Liu, J. F.; Zhang, J. Z. H.; He, X. *J. Phys. Chem. A* **2013**, 117: 7149.

(8) Wang, Y.; Jin, X. S.; Yu, H. S.; Truhlar, D. G.; He, X. *PNAS,* **2017**, in press.

(9) Yu, H. S.; He, X.; Li, S. L.; Truhlar, D. G. *Chem. Sci.* **2016**, 7: 5032.

(10) Yu, H. S.; He, X.; Truhlar, D. G. *J. Chem. Theory Comput.* **2016**, 12: 1280.

I24 Microsolvation of Salts in Water: Photoelectron Spectroscopy and Theoretical Studies of Size-Selected Salt-Water Clusters

Weijun Zheng

Beijing National Laboratory for Molecular Sciences (BNLMS), Institute of Chemistry, Chinese Academy of Sciences, Beijing 100190
*Email: zhengwj@iccas.ac.cn

In order to understand the microsolvation of salts in water, we investigated a series of salt-water clusters using photoelectron spectroscopy. The structures of these clusters and their corresponding neutrals were investigated with ab initio calculations and confirmed by the photoelectron spectroscopy experiments. Our studies show that the SSIP type of structures start to appear at n=5 in LiI(H2O)n clusters. However, the separation of the Cs+-I- ion pair by water is insignificant in CsI(H2O)n clusters. For neutral NaCl(H2O)n, the CIP structures are dominant at n < 9. At n = 9-12, the CIP structures and SSIP structures of NaCl(H2O)n are nearly degenerate in energy, coincident to the H2O:NaCl molar ratio of NaCl saturated solution and implying that the CIP and SSIP structures can coexist in concentrated solutions. For Li2SO4(H2O)n- cluster anions with n = 1–3, two kinds of isomers derived from the turtle-shaped and propeller-shaped structures of bare Li2SO4- were identified. These two kinds of isomers present similar structural and energetic features with increasing number of water molecules and thus are not distinguishable at n = 4–5. For the anionic Li2SO4(H2O)n clusters, the water molecules prefer to firstly interact with one Li atom until fully coordinating it. While for the neutral Li2SO4(H2O)n clusters, the water molecules interact with the two Li atoms alternately, therefore, show a pairwise solvation behavior. These results indicate that the structural variation and microsolvation in salt-water clusters are determined by the delicate balance between ion-ion, ion-water, and water-water interactions, which may have significant implications for the general understanding of salt effects in water solutions.

Keywords: microsolvation; salt-water clusters; size-selected; photoelectron;

References:

[1] Hou, G.-L.; Liu, C.-W.; Li, R.-Z.; Xu, H.-G.; Gao, Y. Q.; Zheng W. J. *J. Phys. Chem. Lett.* **2017, 8:** 13.

[2] Feng, G.; Liu, C. W.; Zeng, Z.; Hou, G.-L.; Xu, H.-G.; Zheng W. J. *Phys. Chem. Chem. Phys.* **2017, 19:** 15562.

[3] Li, R.-Z.; Zeng, Z.; Hou, G.-L.; Xu, H.-G.; Zhao, X.; Gao, Y. Q.; Zheng W. J. *J. Chem. Phys.* **2016, 145:** 184307.

[4] Zhang, W.-J.; Hou, G.-L.; Wang, P.; Xu, H.-G.; Feng, G.; Xu, X.-L.; Zheng W. J. *J. Chem. Phys.* **2015, 143:** 054302.

[5] Feng, G.; Hou, G.-L.; Xu, H.-G.; Zeng, Z.; Zheng W. J. *Phys. Chem. Chem. Phys.* **2015, 17:** 5624.

[6] Zeng, Z.; Gao-Lei Hou, Jian Song, Gang Feng, Xu, H.-G.; Zheng W. J. *Phys. Chem. Chem. Phys.* **2015, 17:** 9135.

[7] Liu, C.-W.; Wang, F.; Yang, L.-J.; Li, X.-Z.; Zheng W. J. and Yi Qin Gao, *J. Phys. Chem. B* **2014, 118:** 743.

[8] Li, R.-Z.; Liu, C.-W.; Gao, Y. Q.; Jiang, H.; Xu, H.-G.; Zheng W. J. *J. Am. Chem. Soc.* **2013, 135:** 5190.

I25 Interaction of Ca^{2+} with Sphingomyelin Membrane Studied by High-Resolution Broadband Sum Frequency Vibrational Spectroscopy

Zhen Zhang[1,*] Rong-juan Feng[1, 2], Yi-yi Li[1, 2,] Ming-hua Liu[3, 4,] Yuan Guo[1, 2,*]

[1] Beijing National Laboratory for Molecular Sciences, CAS Research/Education Center for Excellence in Molecular Sciences, Institute of Chemistry, Chinese Academy of Sciences, Beijing 100190
[2] University of Chinese Academy of Sciences, Beijing 100049
[3] National Center for Nanoscience and Technology, Beijing 100190
[4] Beijing National Laboratory for Molecular Sciences, CAS Key Laboratory of Colloid, Interface and Chemical Thermodynamics, Institute of Chemistry, Chinese Academy of Sciences, Beijing, 100190,
*Email: guoyuan@iccas.ac.cn; zhangz@iccas.ac.cn

Sphingomyelin(SM) is specifically enriched in the plasma membrane of mammalian cells. The functions of the SM molecules play crucial roles in the cellular activities by the interaction between the sphingomyelin and Ca^{2+} ions. In this report, we investigate the conformational differences between the egg sphingomyelin (ESM) and milk Sphingomyelin (MSM) monolayer caused by Ca^{2+} ions using sub-wavenumber high-resolution broadband sum frequency generation vibrational spectroscopy (HR-BB-SFG-VS). The HR-BB-SFG-VS spectra of one alkyl-chain-deuterated ESM and ESM revealed that the Ca^{2+} ions do not affect the N-linked saturated fatty acid chain, but they make the sphingosine backbone order. [1] Unlike ESM, Ca^{2+} ions can induce disordering of the acyl chains in the MSM monolayer. In addition, both ESM and MSM show the large blue shifts of the phosphate group at the $CaCl_2$ solution interface, which indicates new cation binding modes for ESM and MSM. The binding causes the phosphate moiety to dehydrate result in the conformation change of the phosphate moiety. From above results, we propose the interactional molecular mechanism between Ca^{2+} and ESM and MSM molecules: firstly, for both ESM and MSM polar headgroup, Ca^{2+} ions bind to the phosphate group and subsequently destroy the intramolecular hydrogen bond between the 3-hydroxyl group and the phosphate oxygen, which results in the conformation change of the alky chain. Secondly, in ESM monolayer, Ca^{2+} results in an ordering change of the sphingosine backbone. The interactions between ESM and Ca^{2+} ions make the orientation of the methyl group at the end of sphingosine backbone change from pointing downward to pointing upward. But in MSM monolayer, the Ca^{2+} bonded to the phosphate group to create a strong dipolar fields penetrating into the membrane interior. Such electric fields are large enough to induce more gauche-defects of the CH_2 groups closed to the head group. However, the addition of Ca^{2+} do not affect the conformation of the methyl located at the tail of the alky chain. This results shed lights on understanding the relationship on the interactions of complex molecules at surfaces and interfaces and also demonstrates the ability of HR-BB-SFG to probing complicated systems.

Keywords: high-resolution broadband sum frequency generation vibrational spectroscopy, sphingomyelin, conformation change, lipid–cation interactions

References:

[1] R-j Feng, L Lin, Y-y Li, M-h Liu, Y Guo*, and Z Zhang*. *Biophysical Journal.* 2017, 112, 2173-2183.

I26 分子红外光谱的亚 kHz 精度测量

胡水明*，王进，孙羽，陶雷刚，华天鹏，刘安雯

中国科学技术大学化学物理系，合肥微尺度物质科学国家实验室，合肥市金寨路 96 号，230026

*Email: smhu@ustc.edu.cn

分子的振转跃迁是天然的频率参考，被广泛应用于光谱测量、光通讯、计量以及天文观测等领域。分子跃迁的精密测量在基础物理研究中也得到越来越大的兴趣，例如检验物理常数变化[1]、研究基本对称性破缺[2]（如分子手性）等。然而由于实验上的困难，迄今为止，分子红外跃迁的最好精度大多在kHz水平（$\delta\nu/\nu \approx 10^{-11}$）。在高精细度的共振光腔内，有效吸收长度可以获得大幅度提高，同时光腔内激光强度的大幅增强，还有利于实现跃迁的饱和。我们利用该方法，使用毫瓦级的连续可调谐激光，实现了对分子跃迁无多普勒的兰姆凹陷测量[3]。实验表明，光谱测量的分辨率达到亚kHz、灵敏度（最小可探测吸收系数）达到10^{-12}/cm。基于该方法，并结合光频梳标定技术，我们示范性地测量了CO、C_2H_2等分子的泛频振转光谱，对跃迁绝对频率的测定精度达到0.5kHz（$\delta\nu/\nu \approx 3*10^{-12}$）。本报告还将展望其它相关的重要精密测量应用。

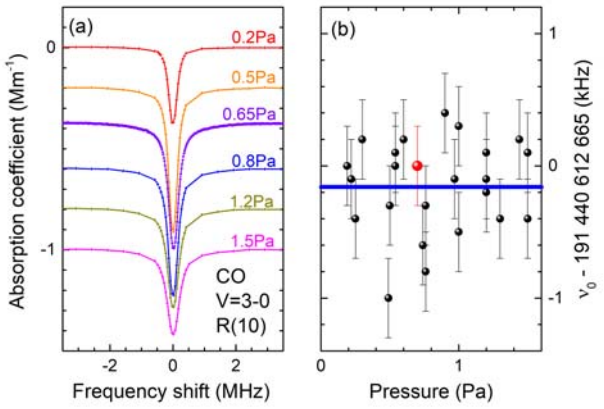

Fig. 1 (a) Cavity ring-down saturation spectra of the R(10) line in the (3-0) band of $^{12}C^{16}O$.
(b) Positions of the R(10) line determined from the spectra recorded with different sample pressures.

关键词：精密测量；分子振转跃迁；兰姆凹陷；光腔增强

参考文献

[1] Ubachs, W.; Bagdonaite, J.; Salumbides, E. J.; Murphy, M. T., Kaper, L. *Rev. Mod. Phys.* **2016**, **88**: 021003.

[2] Quack, M.; Stohner, J.; Willeke, M. "High-resolution spectroscopic studies and theory of parity violation in chiral molecules," in Annual Review of Physical Chemistry, Vol. 59 (2008) pp. 741–769.

[3] Wang, J.; Sun, Y. R.; Tao, L.-G.; Liu, A.-W.; Hua, T.-P.; Meng, F.; Hu, S.-M. *Rev. Sci. Instrum.* **2017**, **88**: 043108

I27 Resonance Energy Transfer Pathways for the Photoluminescence of Europium Antenna Probes: Insights into the Mechanism via a combined Computational, Synthesis and Time-resolved Spectra Study

Xuebo Chen[1,*], Haoling Sun [1], Weihai Fang [1], Yunliang Li[2,*]

[1]Key Laboratory of Theoretical and Computational Photochemistry of Ministry of Education, and College of Chemistry, Beijing Normal University, Beijing 100875, China
[2]Key Laboratory of Soft Matter Physics, Institute of Physics, Chinese Academy of Sciences, Beijing 100190, P. R. China
*Email: xuebochen@bnu.edu.cn; yunliangli@iphy.ac.cn

The energy transfer (ET) pathways in lanthanide antenna probes cannot be comprehensively rationalized by the currently available models, and their elucidation remains to be a challenging task. Based on CASSCF/CASPT2 computations of representative europium antenna complexes, we have reported an innovative ET model that is governed by the nonet–quintet intersystem crossing and spin–orbit couplings (SOCs) among the sublevels of the involved states to better elucidate the photoluminescence mechanism of lanthanide-based probes.[1] Guided by the proposed ET mechanism, we synthesized the coordination polymer of europium antenna complexes by using the acetylacetone type ligand, resulting in high luminescence quantum efficiency (up to 0.60). Accurate quantum chemical calculations together with the time-resolved spectra observations reveal the optimal performance of photoluminescence is ascribed to the enhanced SOC in presence of heavy atom Br, which facilitates the rate-determining ligand ISC concomitant with concerted 4f electron pairing on Eu^{3+}. These results contribute a complementary ET mechanism beyond the classical Förster and Dexter models,[2-3] and should motivate further studies and applications with lanthanide–based luminescent materials.

Keywords: ab initio calculations; antenna probes; energy transfer; luminescence; resonant crossing

References

[1] Q.Q. Zhang, L.L. Wu, X.Y. Cao, X.B. Chen, W.H. Fang and D. Michael. *Angew. Chem. Int. Ed.*, **2017**, *56*, 7986 –7990

[2] J. Han, X.B. Chen, L. Shen, Y. Chen, W.H. Fang and H.B. Wang. *Chem.-Eur.J.* **2011**, *17*, 13971-13977.

[3] J. Han, L. Shen, X.B. Chen and W.H. Fang. *J. Mater. Chem. C*, **2013**, *1*, 4227-4235

I28 激发态分子相干核波包运动的直接观测

凌丰姿， 李帅， 宋辛黎，唐颖，王艳梅，张冰*

波谱与原子分子物理国家重点实验室，武汉物理与数学研究所，武汉 430071

*Email: bzhang@wipm.ac.cn

相干激发相邻振动态时，会制备一个相干振动波包，波包运动所导致的能量流动过程，表现为量子拍频调制的衰减信号[1-2]。这种量子拍频来源于这些叠加态的干涉效应[3-4]。

光激发的2,4-二氟苯酚的相干振动波包的演化过程及其所导致的能量流动通过时间分辨的离子产率光谱和光电子影像技术被直接观测。从平面构型以及从非平面构型电离的信号在光电子谱中同时被采集，但是通过与不同的中间里德堡态发生偶然共振而在电子谱中进行区分。从平面构型以及从非平面构型电离得到的光电子峰的时间依赖线型，都表现出明显的拍频特征，频率相同，但是相位相差180°，描绘出一幅非常清楚的相干振动波包在不同构型间来回振荡的物理图像。

振动能在嘧啶S1态上6a1···6b2费米共振对中的流动,通过飞秒时间分辨的质谱技术结合光电子影像方法被直接追踪。从6a1和 6b2振动态电离得到的光电子峰的时间依赖线型都表现出明显的拍频特征，频率相同，但是相位相差180°，描绘出一幅非常清楚的能量在费米共振对中流动的物理图像。

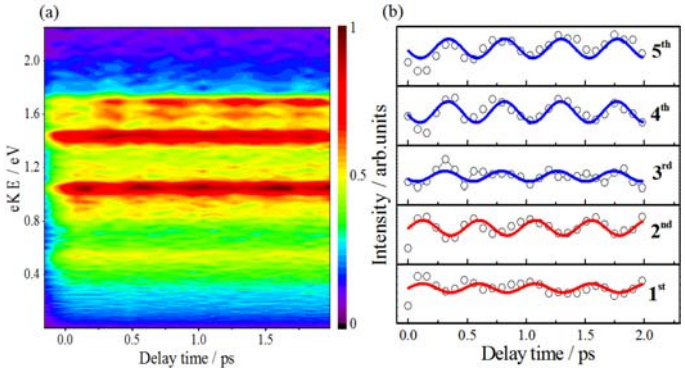

Fig. 1 (a) Photoelectron spectra of 2,4-difluorophenol as a function of delay time between pump laser at 279.9 nm and probe laser at 400 nm. (b) Time-resolved photoelectron intensities integrated over the five peaks as a function of delay time.

关键词： 量子拍频；相干振动波包；飞秒时间分辨的光电子影像

参考文献

[1] P. M. Felker and A. H. Zewail, Phys. Rev. Lett. **53**, 501 (1984).

[2] P. M. Felker and A. H. Zewail, J. Chem. Phys. **82**, 2961 (1985).

[3] H. Goto, H. Katsuki, H. Ibrahim, H. Chiba, and K. Ohmori, Nature Physics. **7**, 383 (2011).

[4] P. M. Felker and A. H. Zewail, J. Chem. Phys. **86**, 2460 (1987).

I29 主/客配位笼状超分子的激发态动力学：全时尺度瞬态光谱揭示核/壳电荷迁移

杨阳，韩克利*

中国科学院大连化学物理研究所分子反应动力学国家重点实验室，辽宁省大连市沙河口区中山路 457 号，116023

*Email: klhan@dicp.ac.cn

本研究工作利用稳态的吸收和发射光谱结合时间分辨光谱技术，定量地给出了一种笼状超分子（CC）的激发态光物理特性，通过 DFT/TDDFT 量子化学计算的手段，我们发现 CC 存在一种新型可见光触发的内核 coronene 向外壳 cage 的电荷转移过程，我们命名为 core-to-cage charge transfer (CCCT)。CCCT 产生了在可见光区的强吸收效应，拓展了光敏剂分子的响应光谱区间，同时，可见光照射产生的激发态 CC 以极高的系间窜越效率到达了激发三重态 CC，激发态寿命相比激发三重态 coronene 延长了 3 倍，重金属 Pt 作为结构部件，其参与到了激发态前线轨道中，因此 CC 具有高的激发单重态向激发三重态的系间窜越效率。飞秒光谱观测了超快的电荷迁移过程和能量传导过程。我们认为：可见光照射 cc 时，内核 coronene 的离域负电子由于强烈的静电排斥作用而具有了向外膨胀的趋势，外壳 cage 带有正电荷，异性电荷相吸导致了 coronene 离域电子向外层转移，即 CCCT。具有 CCCT 特性的金属有机超分子在光化学反应中具有潜在应用价值。

I30 强激光场下分子离子激发态动力学

吴成印

北京大学物理学院，北京，100871

*Email: cywu@pku.edu.cn

利用空气的主要成份氮气或者氧气作为增益介质的空气激光，由于在大气遥感探测方面的潜在应用而受到人们的广泛关注。2011年上海光机所程亚研究小组利用中红外的飞秒激光在空气中传输，在激光的传输方向上观察到波长391纳米附近的相干辐射[1]。该辐射对应的是空气中的氮气分子电离，氮气离子第二激发态到氮气离子基电子态的辐射跃迁，即$N_2^+(B^2\Sigma_u^+ \rightarrow X^2\Sigma_g^+)$。进一步地，作者认为该相干辐射产生要求氮气离子激发态布居大于基电子态布居，即布居数形成反转，但是现有的分子强场理论不能解释氮气离子布居数反转这一现象。

为了对强激光场下分子离子量子态进行研究，我们在北京大学建立了荧光光谱谱仪[2]、激光诱导荧光光谱谱仪[3]、以及瞬态吸收/荧光关联谱仪[4]。本报告将介绍近年来，我们利用飞秒激光电离氮气分子，氮气离子量子态方面的研究进展[5-7]。实验发现波长 800 纳米飞秒激光在充有氮气的气室中传输，当含有 391 纳米的种子光存在时，391 纳米种子光得到两个量级以上的放大。通过测量 391 纳米相干辐射的时间特性和光谱特性，提供了氮气离子布居数反转的直接证据[6]。结合理论模拟，发现电离产生的氮气离子基电子态被抽运到第一激发态，导致氮气离子第二激发态和基电子态间形成布居数反转[5]。进一步地，我们采用皮秒条纹相机测量了氮气离子激发态荧光衰减，发现自由电子碰撞导致氮气离子激发态荧光衰减较自发辐射寿命快两个量级[7]。该项研究不仅拓宽了强场原子分子物理的研究领域，而且对揭示氮气离子激光的形成机理具有重要意义。

关键词：空气激光；飞秒；电离；激发态

参考文献

[1] Yao, J.; *et al.*, *Phys. Rev. A* **2011, 84:** 051802.

[2] Wu, C.; *et al.*, *Phys. Rev. A* **2011, 83:** 033410.

[3] Wang, P.; *et al.*, *Phys. Rev. A* **2014, 90:** 033407.

[4] Wang, P.; *et al.*, *Phys. Rev. A* **2015, 92:** 063412.

[5] Yao, J.; *et al.*, *Phys. Rev. Lett.* **2016, 116:** 143007.

[6] Lei, M.; *et al., Opt. Express* **2017, 25:** 4535.

[7] Lei, M.; *et al., J. Phys. B: At. Mol. Phys.* **2017, 50:** 145101.

I31 Photoionization cross section measurements of the excited states of 3d transition metal atoms

Xianfeng Zheng*, Zhifeng Cui

Department of Physics, Anhui Normal University, Beijing East Road 1, Wuhu, 241000

*Email: xfzheng@mail.ahnu.edu.cn

3d transition metal atoms are multielectron system with open 3d subshell and the electronic excited states present mixed configuration to a large extent. Investigation on the photoionization of the excited states of 3d metal atoms can discover the electronic structure, electron correlation effects in multielectron syetem, and interference effects of ionization channels.

In this work, the threshold photoionization cross sections, dependence of the photoionization cross sections on the excess energy above the ionization threshold and on the atomic state will be investigated by the laser Pump-Probe scheme under the condition of saturated resonant excitation[Fig. 1]. The free atoms at low excitation states are produced using laser ablation combined with the supersonic molecular beam technique. The excited states of the atoms are populated by tunable dye laser radiaition and subsequently ionized by another tunable laser. The ions produced are detected by a TOF-MS spectrometer. The photoionization cross sections of the electronic states are finally obtained from the dependence of the ion yields on the ionization laser fluence.

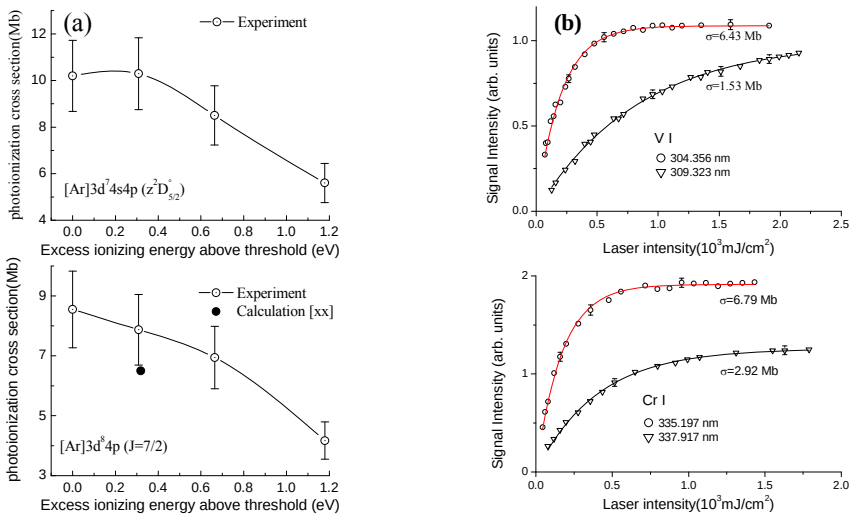

Fig. 1 (a) Dependence of the photoionization cross sections on the excess energy above the ionization threshold; (b) Photoionization data for V I and Cr I in different excited states.

Keywords: photoionization cross section; excited state; 3d-metal atom

References:

[1] Xianfeng Zheng, Ke Zhang, Zhifeng Cui, J. Chem. Phys. 2012, 136: 174304.

[2] Xianfeng Zheng*, Zehua Qu, Guanxin Yao, Xianyi Zhang, Zhifeng Cui, AIP advances 2014, 4: 107120.

I32 光合作用过程中新的暗态对能量传递的调控

马玉臣

山东大学化学与化工学院, 济南250100

*Email:myc@sdu.edu.cn

在光合作用体系中，类胡萝卜素的一个重要作用是收集太阳光，然后将能量传递给叶绿素。类胡萝卜素和叶绿素之间的能量传递已经研究了很长时间，但仍然存在很多争议。一直以来，人们普遍接受的能级模型是：太阳光被类胡萝卜素的S_2态吸收后部分传递给叶绿素的Q_x态，部分通过非辐射跃迁传递到自己的暗态S_1上。然而，包括二维电子光谱技术在内的实验表明，在S_2和S_1之间还有一个暗激发态参与了能量传递[1-3]。到目前为止，这个暗激发态的来源还没有确定下来。利用多体格林函数理论（包括GW方法和Bethe-Salpeter方程）和基于该理论的激发态动力学[4,5]，我们在类胡萝卜素中发现了一个新的暗激发态S_y，S_2态的能量通过非辐射跃迁可以传递给这个新的暗态[6]。根据我们的模型模拟的二维电子光谱与实验一致。在多体格林函数理论框架内，利用Förster-Dexter理论，我们研究了类胡萝卜素和叶绿素之间的能量传递速率，解释了先前的理论与实验之间的差异。

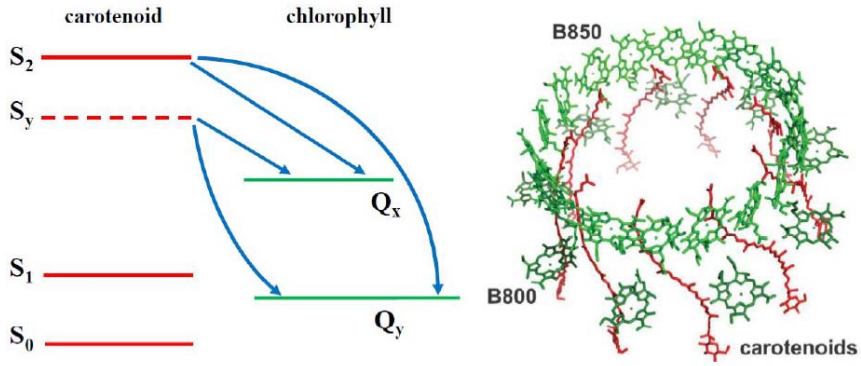

Fig.1 New excited state Syin carotenoids for energy transfer

参考文献

[1] Gradinaru, C.; Kennis, J. T. M.; Papagiannakis, E.; van Stokkum I. H. M.; Cogdell R. J.; Fleming, G. R.; Niederman, R. A.; van Grondelle, R. *PNAS***2001**, 98,2364.

[2] Cerullo, G.; Polli, D.; Lanzani, G.; De Silvestri, S.; Hashimoto, H.; Cogdell, R. J. *Science***2002**, 298,2395.

[3] Ostroumov, E. E.; Mulvaney, R. M.; Cogdell, R. J.; Scholes, G. D. *Science***2013**, 340,52.

[4] Leng, X.; Jin, F.; Wei, M.; Ma, Y. C. *WIREs Comput. Mol. Sci*. **2016**, 6, 532.

[5] Ma, Y. C.; Liu, C. B. *Prog. Chem.***2012**, 24, 981.

[6] Feng, J.; Tseng, C. W.; Chen, T. W.; Leng, X.; Yin, H. B.; Cheng, Y. C.; Rohlfing, M.; Ma, Y. C. *Nature Commun*. **2017**, DOI: 10.1038/s41467-017-00120-7.

I33 Photoelectron Spectroscopy and Theoretical Study of Aerosol Clusters

Xue-Bin Wang (王学斌)*

Physical Sciences Division, Pacific Northwest National Laboratory, 902 Battelle Boulevard, P. O. Box 999, MS K8-88, Richland, Washington 99352, USA

*Email: Xuebin.wang@pnnl.gov

Both field measurements and laboratory experiments have shown the significant roles of the clusters formed by sulfuric acid/bisulfate, oxidized organics, and/or water. The size of these clusters falls in about 1-2 nanometers, in which key steps of new particle formation (NPF) processes occur. To better understand NPF processes and develop more accurate climate models, we have been employing a cluster model approach-- integrated negative ion photoelectron spectroscopy (NIPES) and ab initio quantum computations to probing the structures, energetics, and thermochemistry of these clusters. The clusters we have studied include those formed by sulfuric acid/bisulfate and a wide range of organics from the oxidation products of both biogenic and anthropogenic emissions and their hydrates. We have obtained direct experimental evidence showing significant thermodynamic advantage of organics to promote formation and growth of the sulfuric acid/bisulfate clusters and aerosols, as well as the homogenous organic complexes. We employed the average carbon oxidation state and O/C ratio by taking into account of the carbon number and the type of functional groups (like hydroxyl, carbonyl, and carboxylic) to rationalize and predicate the extent of the enhanced roles of different organics in the aerosol formation and growth processes.

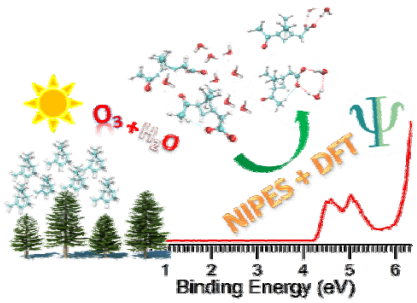

Fig. 1 Cluster model characterization of initial nucleation process of atmospheric aerosols

Keywords: photoelectron spectroscopy; molecular clusters; aerosols; proton transfer

References:

[1] Wang, X.-B. *J. Phys. Chem. A* **2017**, **121**: 1389.

[2] Qin, Z.; Hou, G.-L.; Yang, Z.; Valiev, M.; Wang, X.-B. *J. Chem. Phys.* **2016**, **145**: 214310.

[3] Hou, G.-L.; Zhang, J.; Valiev, M.; Wang, X.-B. *Phys. Chem. Chem. Phys.* **2017**, **19**: 10676.

[4] Wang, X.-B.; Kass, S. R. *J. Am. Chem. Soc.* **2014**, **136**: 17332.

[5] Hou, G.-L.; Lin, W.; Deng, S. H. M.; Zhang, J.; Zheng, W.-J.; Paesani, F.; Wang, X.-B. *J. Phys. Chem. Lett.* **2013**, **4**: 779.

I34 Coupling of multi-vibrational modes in bacteriochlorophyll a in solution observed with 2D electronic spectroscopy

Shuai Yue, Zhuan Wang, Xuan Leng, Rui-Dan Zhu, Hai-Long Chen, Yu-Xiang Weng*
Beijing National Laboratory for Condensed Matter Physics, CAS Key Laboratory of Soft Matter Physics, Institute of Physics, Chinese Academy of Sciences, Beijing 100190, China
University of Chinese Academy of Sciences, Beijing 100049, China
*Email: yxweng@iphy.ac.cn

Bacteriochlorophyll a (BChla) and B820 in ethanol were investigated with two dimensional electronic spectroscopy and transient grating methods. Low vibrational modes in a range of 80–400 cm−1 for BChla are excited and observed as beating dynamics in two-dimensional electronic spectra. A coupled multi-vibrational mode displaced oscillator model is proposed to account for the vibronic coherence. We found that these low frequency vibrational modes are coupled. By comparing the fitted lifetime of the vibrational modes appearing in the beating dynamics for bacteriochlorophyll a and a protein-bound bacteriochlorophyll a dimer B820 probed by transient grating method, it is suggested that the protein scaffold provides a protection effect on the vibronic coherence where no excitonic coherence has be excited.

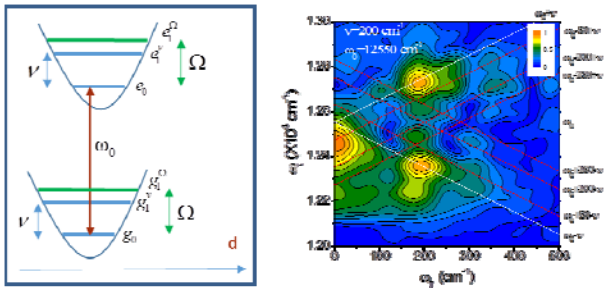

Fig. 1 Lft:Multi-vibrational mode-coupled displaced oscillator model with electronic transition energy w0 and two vibrational modes having a specific transition frequency of n and W respectively; right: Power spectrum for the beating frequency derived as a slice through the rephasing frequency wt from the 3DES at a given excitation frequency as indicated near the (0-0) transition energy.

Keywords: 2DES; BChla; B820; Coherence; Wave-packet

References:

[1] S. Yue, Z. Wang, X. Leng, R.D. Zhu, H.L. Chen, Y.X. Weng, Chem. Phys. Lett.

I35 maging complex-forming reaction dynamics in the oxidation of aluminum atoms

Fangfang Li, Yujie Ma, Changwu Dong, Jiaxing Liu, Fengyan Wang*

Department of Chemistry, Collaborative Innovation Centre of Chemistry for Energy Materials, Shanghai Key Laboratory of Molecular Catalysts and Innovative Materials, Fudan University, Shanghai, 200433

Email: fengyanwang@fudan.edu.cn

Through studies of chemical reaction dynamics, we seek to understand at the fundamental level how bonds are broken and reformed during chemical reactions. In the direct bimolecular reaction, the breaking of the old bond and the forming of the new bond proceed in a concerted way, and hence occurs over times of the duration of a vibrational period (fs scale). Comparatively, the complex forming reactions take a much long time (ps scale) with a duration comparable to a few rotational periods, which have attracted more attention in the last ten years both experimentally and theoretically. In a complex-forming reaction, it was proposed by Kim and Herschbach that the angular momentum disposal have a great influence on the angular distribution of products. This proposition has now been validated in our crossed-molecular-beam study of Al + O2 reaction with a state-to-state resolved high resolution. The time-sliced velocity-mapped ion imaging of AlO products at various rotational level N exhibits a clear shift in the angular distributions from forward-backward peaking to an isotropic distribution as N increases from zero to the maximum energetically available level. As a first experimental example to prove the theory, it is due to the small rotational constant of AlO radical followed by an easy rotational excitation to an extremely high level. A maximum impact parameter was also derived as 2.1-2.5 Å in our experiment and shows good agreement with the calculated intermolecular distance for electron transfer. The experimentally successful determination of electron transfer distance also strongly support the harpoon mechanism, which has long been proposed to explain the large reactive cross sections for the type of elementary reactions of metal atom. Such studies provide new insights into the factors that govern the reactivity for complex forming reactions.

Keywords: electron transfer, harpoon mechanism, slice imaging, crossed molecular beam

References:

[1] Herschbach D. R., *Angew. Chem. Int. Ed. Engl.*, **1987, 26:** 1221.

[2] Wang, F. Y., Lin J. S., Liu K. P., *J. Chem. Phys.*, **2014, 140:** 084202.

[3] Honma, K., Miyashita, K., Matsumoto, Y., *J. Chem. Phys.,* **2014, 140:** 214304.

[4] Wang, F. Y., Liu K. P., *J. Chem. Phys.*, **2016, 145**: 144305.

[5] Dong, C. W., Liu, J. X., Li, F. F., Wang, F. Y., *Chin. J. Chem. Phys.,* **2016, 29:** 99

I36 *Ab initio* potential energy surface and rovibrational spectra of the H_2–HCCCN complex

Hua Zhu

School of Chemistry, Sichuan University, Chengdu, 610064, China

zhuhua@scu.edu.cn

The spectra of the van der Waals (vdW) complexes provide useful information on the intermolecular potential energy surfaces (PESs) and dynamics of such weakly bound molecules. We report a new intermolecular potential energy surface of the H_2–HCCCN complex. The rather long HCCCN molecule causes the difficulty of the *ab initio* calculations and the convergence of the energies at points near linear configurations. The complex has a planar linear global minimum with the well depth of 199.366 cm^{-1}. The radial discrete variable representation (DVR)/angular finite basis representation (FBR) and the Lanczos algorithm were employed to calculate the rovibrational energy levels for four species of H_2–HCCCN ($p$$H_2$–HCCCN, $o$$H_2$–HCCCN, $p$$D_2$–HCCCN, $o$$D_2$–HCCCN). The calculated rotational transition frequencies and spectroscopic parameters are in excellent agreement with experiment. We further investigate the minimum-energy structures and energetics of the ($p$$H_2$)$_N$–HCCCN clusters with the number of $p$$H_2$. The first solvation shell is completed with number of $p$$H_2$ molecules (N)=20. The N dependence of the chemical potential $\mu(N)$ shows oscillatory behavior.

Keywords: H_2–HCCCN complex, rovibrational spectra, potential energy surface

I37 D_2 分子光解：D_2 + XUV→D(2*s*，2*p*)+ D(1*s*)

D(2*s*)和 D(2*p*)通道的量子干涉

汪杰，莫宇翔*

清华大学物理系 中国北京 邮编 100084

*Email: ymo@mail.tsinghua.edu.cn

氢气分子的光解是电子结构理论计算和光解动力学理论的试金石。对于标题中的 D_2 解离动力学，1987年的文献预测：生成 D(2*s*)和 D(2*p*)产物的分支比在解离阈值(14.76 eV)附近随产物平动能的变化发生振荡。[1] 我们在实验中第一次观测到了这个现象。[2]

对于解离产物 D(2*s*，2*p*)，与之相关的电子态是：$2p\sigma(B\ ^1\Sigma_u^+)$和 $3p\sigma(B'\ ^1\Sigma_u^+)$ 。由于非绝热相互作用，这两个态发生混合。一束 XUV 激光将分子泵浦到两个混合态，每一个混合态均可产生 D(2s)。这就形成了量子力学中普遍问题：结果来源于哪一条路径？如我们常见的，光学中的杨氏双缝干涉实验。当激发能量发生变化时， 这两个通道的相位发生变化， 由于两个通道的干涉效应，生成 D(2*s*)强度形成周期性变化。为了更好的了解其物理本质， 我们用两个球形势阱代替高精度的势能曲线。这样两个通道的相位差，可通过这个简单的模型求得。这个模型非常清晰的说明了，D(2s) 产物的周期性变化是由于相位差形成的。 通过实验结果的模拟，有效势阱的相关参数可得到，并与理论计算的势能曲线一致。

实验采取了 XUV 激光泵浦-UV 激光探测的方法。XUV 光通过两束激光四波混频获得。单光子电离方法探测解离产物 D(2*s*)和 D(2*p*)，并且利用它们寿命差异的特点加以区分。

参考文献

[1] J. A. Beswick and M.Glass-Maujean, *Phys. Rev. A*. 35, 8(1987).

[2] J. Wang, Q. Meng and Y. Mo, *Phys. Rev. Lett*., *in press*.

I38 烯酮和嘧啶碱基激发态势能面交叉动力学 --拉曼光谱和从头计算研究

郑旭明

浙江理工大学化学系，浙江省杭州市下沙 2 号大街 928 号，310018

*Email：zxm@zstu.edu.cn

α，β-烯酮和嘧啶碱基光吸收态的初始激发态动力学涉及 $S_2(\pi\pi^*)$与 $S_1(n\pi^*)$和 S_0 态间的快速内转换。[1-2] 在溶液中，该过程因溶剂的作用变得很十分复杂。由于，测不准原理的限制，实时时间分辨（吸收、荧光上转换等）飞秒超快光谱难以同时给出分子体系初始结构随时间演化的信息，这导致不同超快光谱在描述激发态衰变动力学机制时产生不确定性。例如，经过长期研究，目前给出嘧啶碱基在水中的 3 种激发态弛豫机制：(1)经 $S_2(\pi\pi^*)/S_1(n\pi^*)$势能面交叉，$S(\pi\pi^*)\rightarrow S(n\pi^*)\rightarrow S_0$；[3]；(2) $S_2(\pi\pi^*)\rightarrow S_1(n\pi^*)\leftrightarrow S_2(\pi\pi^*)\rightarrow S_0$, 这里 $S_1(n\pi^*)$只起中间态作用，不能直接从它返回基态, 而是回到 $S_2(\pi\pi^*)$态，并通过 $S_2(n\pi^*)/S_0$ 交叉点返回基态[4]；(3) $S_1(n\pi^*)$并不参与弛豫过程，$S_2(\pi\pi^*)$直接经 $S_2(n\pi^*)/S_0$ 交叉点回到基态。[5]

本文采用共振拉曼光谱强度分析技术，结合 CASSCF 从头计算方法，对α，β-烯酮和嘧啶碱基光吸收态的初始激发态动力学开展了较为系统的研究，取得如下进展：

1. 在α，β-烯酮的初始激发态动力学中，洞察到了 $S_2(\pi\pi^*)\rightarrow S_0$ 新弛豫通道；发现了 $S_2(\pi\pi^*)\rightarrow S_0$ 和 $S_2(\pi\pi^*)\rightarrow S_1(n\pi^*)$两条弛豫通道的拉曼光谱证据，以及与分子结构的相关性。
2. 尿嘧啶与胸腺嘧啶嘧啶水溶液的激发态初始动力学有重大差别，它们或与 $S_2(\pi\pi^*)\rightarrow S_0$ 和 $S_2(\pi\pi^*)\rightarrow S_1(n\pi^*)$弛豫通道相关。

关键词:胸腺嘧啶;尿嘧啶;弛豫;势能面

参考文献

[1] Lee, A. M. D.; Coe, J. D.; Ullrich, S.; Ho, M.-L.; Lee, S.-J.; Cheng, B.-M.; Zgierski, M. Z.; Chen, I. C.; Martinez, T. J.; Stolow, A. *J. Phys. Chem. A* **2007**, **111**, 11948.

[2] Crespo-Hernández, C. E.; Cohen, B.; Hara, P. M.; Kohler, B. *Chem. Rev*. **2004**, **104**, 1977.

[3] Nachtigallova, D.; Aquino, A. J. A.; Barbatti, M.; et al *J. Phys. Chem. A* **2011**, **115**, 5247–5255

[4] Mercier,Y.; Santoro, F.; Reguero, M. J. *J. Phys. Chem. B*, **2008**, **112(35)**, 10771

[5] Buchner, F.; Nakayama, A.;Yamazaki, S. *J. Am. Chem. Soc*. **2015**, **137**, 2931-2938

O1 Recent Progress in Large-Scale Nonadiabatic Dynamics

Linjun Wang

Department of Chemistry, Zhejiang University, Tianmushan Road 34, Hangzhou, 310028
*Email: ljwang@zju.edu.cn

With a mixed quantum-classical flavor, surface hopping[1] has been a popular choice when studying charge and exciton dynamics in various semiconductors and interfaces.[2] When dealing with many molecules, however, the traditional surface hopping suffers severely from the trivial crossing problem,[3] arising due to the high density of adiabatic potential energy surfaces. Charge transport is a typical example, where trivial crossings can easily induce artificial long-range charge transfer. Even a very small portion of trivial crossings is likely to make surface hopping results completely meaningless.[4-5] With a QM/MM-like idea, the flexible surface hopping (FSH) treats only the charge and its surrounding nuclear vibrations with surface hopping, and reproduces the crossover from hopping to band-like transport for the first time.[3] In 2014, the self-consistent fewest switches surface hopping (SC-FSSH)[6] has been proposed. It corrects the problematic surface hopping probabilities with the self-consistency of charge populations, and gives a more robust and clean description of trivial crossings. SC-FSSH has shown a high accuracy in small molecular aggregates.[6] Recently, we added proper decoherence corrections to SC-FSSH, and systematically investigate charge transport within hundreds of molecules. The obtained charge mobility converges very quickly with the time interval. Even a time interval as small as 0.2 fs is able to give converged results (see Fig. 1a). SC-FSSH reproduces perfectly the band-to-hopping crossover when decoherence is implemented (see Fig. 1b). The transition occurs when the charge is delocalized in about two molecules (see Fig. 1c). Due to the robustness of SC-FSSH, we further developed a novel series of flexible surface hopping methods based on SC-FSSH, e.g., SC-Fn-FSSH. All results from SC-FSSH have been reproduced with a two-fold reduction of computational cost. SC-Fn-FSSH with decoherence has shown great accuracy and efficiency in describing charge transport, and should be promising for general large-scale nonadiabatic dynamics.

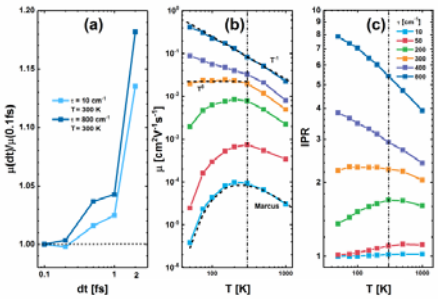

Fig. 1 (a) Convergence of charge mobility as a function of the time interval in two representative model molecular stacks, and temperature dependence of (b) mobility and (c) charge localization strength characterized by the inverse participation ratio.

Keywords: nonadiabatic dynamics; surface hopping; charge transport; trivial crossing problem

References:

[1] Tully, J. *J. Chem. Phys*. **1990**, **93**: 1061.
[2] Wang, L. J.; Long, R.; Prezhdo, O. V. *Annu. Rev. Phys. Chem.* **2015**, **66**: 549.
[3] Wang, L. J.; Beljonne, D. *J. Phys. Chem. Lett*. **2013**, **4**: 1888
[4] Wang, L. J.; Prezhdo, O. V.; Beljonne, D. *Phys. Chem. Chem. Phys.* **2015**, **17**: 12395.
[5] Wang, L. J.; Akimov, A.; Prezhdo, O. V. *J. Phys. Chem. Lett.* **2016**, **7**: 2100.
[6] Wang, L. J.; Prezhdo, O. V. *J. Phys. Chem. Lett*. **2014**, **5**: 713.

O2 Simulation of coherent exciton dynamics in organic semiconductors using time-dependent density matrix renormalization group method

Yao Yao
Department of Physics, South China University of Technology, Guangzhou, China
Yaoyao2016@scut.edu.cn

Benefiting from the recent development of time-resolved spectroscopy technology, people have observed numerous ultrafast excitonic processes in organic semiconductors with the timescale being of tens to hundreds femtoseconds and non-adiabatic phenomena caused by the crossing of potential-energy surfaces. In principle, an accurate solution of the coherent exciton dynamics in molecular systems can help understand these ultrafast non-adiabatic processes, however such kind of molecular dynamics comprising the electron-nuclear couplings is nontrivial and requires breaking the Born-Oppenheimer approximation, which is one of the basic assumptions in quantum chemistry. For the sake of properly dealing with this coherent dynamics, in the recent years several dynamical methodologies have been invoked, including full-quantum algorithms (multi-configuration time-dependent Hartree (MCTDH) appraoch, Full Multiple Spawning (FMS) , etc), semi-classical methods (Ehrenfest dynamics and surface hopping method, etc) and quantum dissipative approaches (Redfield theory, hierarchical equations of motion (HEOM) method, various stochastic differential equation methods). But the quantum dynamics simulation for systems with a large number of degrees of freedom is so far a great challenge due to the exponential divergence of the computational cost. In this work, we present a modified t-DMRG algorithm which can be used to simulate the non-adiabatic processes in realistic molecular system with discrete vibrational modes and vibronic coupling parameters for respective electronic states. Furthermore, transition of exciton to charge transfer state at C60/ot4 interface is simulated by virtue of t-DMRG as a realistic example to demonstrate its application.

O3 Investigate chemical reaction rates with RPMD

Yongle Li[1*], Hua Guo[2], Daiqian Xie[3]

[1]Department of Physics, International Center of Quantum and Material Structures, Shanghai University, Shanghai, 200444 China

[2]Department of Chemistry and Chemical Biology, University of New Mexico, Albuquerque, New Mexico 87131, United States

[3]Institute of Theoretical and Computational Chemistry, Key Laboratory of Mesoscopic Chemistry, School of Chemistry and Chemical Engineering, Nanjing University, Nanjing 210093, China

*Email: yongleli@shu.edu.cn

The determination of chemical reaction coefficients plays central role in the chemical kinetics modeling of combustion, atmospheric and interstellar chemistry by offering key parameters. But it's still formidable to confirm the rate coefficients for poly-atom reactions accurately and efficiently, either via experiment or popular theories such as quantum scattering theory or transition state theory. A recently developed full dimensional approximate quantum dynamics, ring-polymer molecular dynamics (RPMD) provides an alternative for achieving high accuracy with less computational cost. Now RPMD has been applied to various kinds of chemical reactions, confirmed it is an efficient and reliable method for theoretical studies in chemical reaction dynamics. And some new developments will also be introduced, such as the inclusion of novel enhanced sampling techniques to improve the efficiency of the calculation of potential of mean force in the procedure, and the thought of including the non-adiabatic effect into the RPMD chemical reaction rate calculations.

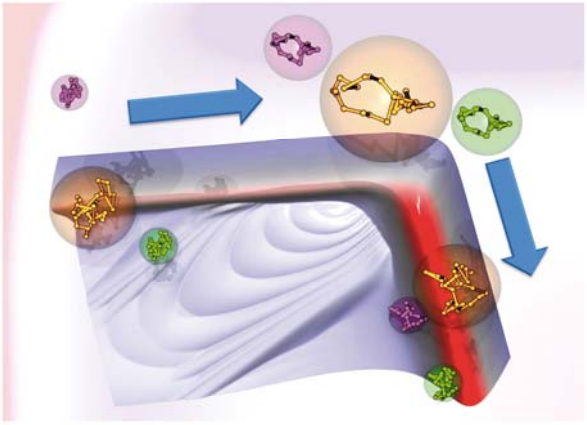

References:

[1] *Habershon, S.; Manolopoulos, D. E.; Markland, T. E.; Miller III, T. F. Ann. Rev. Phys. Chem. 2013, 64: 387*

[2] ***Li, Y.;*** *Suleimanov, Y. V.; Yang, M.; Green, W. H.; Guo, H. J. Phys. Chem. Letters 2013, 4: 48.* [3] ***Li, Y.;*** *Suleimanov, Y.; Guo, H.; J. Phys. Chem. Letters 2014, 5: 700.*

[4] *Zuo, J.;* ***Li, Y.;**** Guo, H.; Xie, D. Q.* J. Phys. Chem. A 2016, 120: 3433.*

[5] *Mengna Bai, Dandan Lu,* ***Y. Li,**** and Jun Li1,* Phys. Chem. Chem. Phys. 2016. 18:32031.*

O4 纳米尺度界面的光激发动力学

龙闰

北京师范大学化学学院，理论与计算光化学教育部重点实验室，北京市海淀区新街口外大街 19 号，100875
*Email: runlong@bnu.edu.cn

界面电子转移是决定太阳能电池光电转换效率的主要因素。通常认为电子施主-受主间的共价键相互作用强，绝热转移机制支配电子转移过程，弱范德瓦尔斯力促使非绝热转移机制主导电子转移过程。电子-空穴复合是影响光电转换效率的另一重要因素，复合率由能级差、非绝热耦合强度和纯退相三者协同决定。为了提高光电转换效率，必须实现快速有效的电荷分离，延缓电子-空穴复合。我们才用非绝热动力学结合含时密度泛函理论，在时域和原子尺度下模拟了一系列时间分辨的超快光谱实验，重点强调多种实际因素对真实材料中动力学的影响，包括缺陷、掺杂、化学键等。具体的体系包括半导体[1,-2]、金属[3]纳米颗粒、石墨烯[4]和MoS2[5]敏化的半导体，范德瓦尔斯异质节[6]，以及无机-有机杂化钙钛[8-9]。这些原子尺度的模拟结果得到了多种体系详尽的电子-振动动力学信息、解决了一些争议的问题，为提高具体材料光捕获能力提供了理论指导。

关键词： 二氧化钛；有机–无机杂化钙钛矿；电荷分离和复合；非绝热动力学；含时密度泛函理论

参考文献

[1] R. Long, et a., “Ab Initio Nonadiabatic Molecular Dynamics of the Ultrafast Electron Injection from a PbSe Quantum Dot into the TiO_2 Surface”, *J. Am. Chem. Soc.*, **2011**, 133, 19240-19249.

[2] R. Long, et al., Donor−Acceptor Interaction Determines the Mechanism of Photoinduced Electron Injection from Graphene Quantum Dots into TiO_2: π□Stacking Supersedes Covalent Bonding, *J. Am. Chem. Soc.* **2017**, 139, 219-2629.

[3] R. Long, et al., “Instantaneous Generation of Charge-Separated State on TiO_2 Surface Sensitized with Plasmonic Nanoparticles”, *J. Am. Chem. Soc.*, **2014**, 136, 4343-4354.

[4] R. Long, et al., “Photo-induced Charge Separation across the Graphene-TiO_2 Interface Is Faster than Energy Losses: A Time-Domain ab initio Analysis”, *J. Am. Chem. Soc.*, **2012**, 134, 14238-14248.

[5] Y. Q. Wei, W-H, Fang, R. Long et al., “Weak Donor–Acceptor Interaction and Interface Polarization Define Photoexcitation Dynamics in the MoS_2/TiO_2 Composite: Time-Domain Ab Initio Simulation”, *Nano Lett.* **2017**, DOI: 10.1021/acs.nanolett.7b00167

[6] R. Long, et al., “Quantum Coherence Facilitates Efficient Charge Separation at a MoS_2/$MoSe_2$ van der Waals Junction”, *Nano Lett.*, **2016**, 16, 1996-2003.

[8] R. Long, et al., “Unravelling the Effects of Grain Boundary and Chemical Doping on Electron−Hole Recombination in $CH_3NH_3PbI_3$ Perovskite by Time-Domain Atomistic Simulation”, *J. Am. Chem. Soc.*, **2016**, 138, 3884-3890.

[9] R. Long, et al., “Dopants Control Electron-Hole Recombination at Perovskite-TiO_2 Interfaces: Ab Initio Time-Domain Study” *ACS Nano*, **2015**, 9, 111143-11155.

O5 Polarizable QM/MM for excited-state dynamics

Prof. William J. Glover,
NYU-ECNU Center for Computational Chemistry at NYU Shanghai, Shanghai

Polarizable QM/MM has been shown to afford excellent vertical electronic excitation energies of molecules in a condensed-phase environment when implemented in a state-specific fashion, i.e. allowing the MM dipoles to polarize differently to each electronic state of the QM region. Unfortunately, a problem arises when attempting to extend Polarizable QM/MM to treat excited-state dynamics, since such a state-specific approach means each electronic state is of a different Hamiltonian, and therefore intersections between the electronic states are not described correctly.

We have developed a new polarizable QM/MM approach that solves the above issue by borrowing from our recently developed dynamically-weighted complete active space self-consistent field method[1]. The resulting QM/MM-DWpol method correctly describes the topology of a conical intersection between electronic states while retaining a state-specific polarization away from intersections. We have tested the method on the electronic structure of LiF, a simple system exhibiting a neutral and CT crossing, interacting with a polarizable atom. We show that our QM/MM-DWpol method reproduces well the entire potential energy surface compared to high-level multireference configuration interaction calculations on the full system. We expect this development will open the way to studying excited-state charge-transfer reactions in complex systems with a high-level of accuracy.

[1] W. J. Glover, *J. Chem. Phys.* **141**, 171102 (2014)

O6 Force Field Development and Fragment based Ab Initio Molecular Dynamic Simulation for MetalloProteins

Tong Zhu[1,2], John Z.H. Zhang[1,2,3]

[1]College of Chemistry and Molecular Engineering, East China Normal University, Shanghai, 200062, China

[2]*NYU-ECNU Cent*er for Computational Chemistry at NYU Shanghai, Shanghai, 200062, China

[3]Department of Chemistry, New York University, New York, NY 10003, USA

*Email: tzhu@lps.ecnu.edu.cn

A polarizable-charge transfer force field (QPCT) has been proposed to accurately describe the interaction dynamics of zinc–protein complexes. The parameters of the QPCT force field were calibrated by quantum chemistry calculation and can capture the polarization and charge transfer effect. QPCT are validated by molecular dynamic simulation of the hydration shell of the zinc ion, five proteins containing the most common zinc-binding sites, as well as protein–ligand binding energy in zinc protein MMP3. The calculated results show excellent agreement with the experimental measurement and with results from QM/MM simulations.

To further improve the theoretical treatment of metalloproteins, a fragment based ab initio molecular dynamics approach Metal-MFCC has been presented for practical application in protein dynamics study. In this approach, the energy and forces of the protein are calculated by a recently developed electrostatically embedded generalized molecular fractionation with conjugate caps method. For simulation in explicit solvent, polarizable embedding is introduced to treat protein interaction with explicit water molecules. This AIMD approach has been applied to the study of metal-Aβ coordination and build plausible Cu2+-Aβ models. This approach is linear-scaling, trivially parallel, and applicable to performing AIMD simulation of proteins of large size.

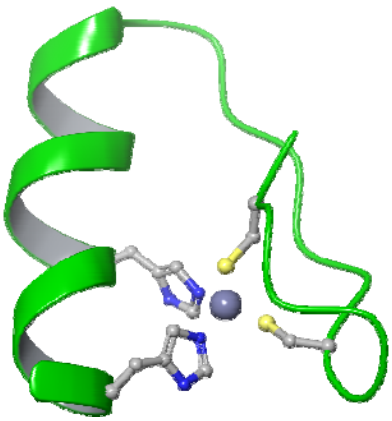

Reference:

[1] Zhu, T.; Xiao, X.D.; Ji, C.G.*; Zhang, J.Z.H*. *J. Chem. Theory Comput.* **2013**, *9*, 1788.

[2] Liu, J.F.; Zhu, T.*; Wang, X.W.; He, X.*; Zhang, J.Z.H.* *J. Chem. Theory Comput.* **2015**, *11*, 5897.

[3] Xu, M.Y.; Zhu, T.*; Zhang J.Z.H.*, *submitted*.

O7 Accidental Resonance Mediated Predissociation Pathway of Water Molecules Excited to the Electronic $\tilde{C}$ State

Dongyuan Yang[1,2], Zhigang He[1,2], Zhichao Chen[1], Guorong Wu[1,3,*] and Xueming Yang[1,3,*]

[1]State Key Laboratory of Molecular Reaction Dynamics, Dalian Institute of Chemical Physics, Chinese Acadamy of Sciences, 457 Zhongshan Road, Dalian, 116023
[2]University of Chinese Academy of Sciences, 19 Yuquan Road, Beijing, 100049
[3]Synergetic Innovation Center of Quantum Information & Quantum Physics, University of Science and Technology of China, 96 Jinzhai Road, Hefei, 230026
*Email: wugr@dicp.ac.cn, xmyang@dicp.ac.cn

Photo-induced molecular dynamics of water molecules in the gas phase is a very important, yet challenging polyatomic model system. Photodissociation of water in the vacuum ultraviolet (VUV) region is also of practical importance in the atmospheric and interstellar chemistry. Numerous experimental and theoretical studies have been devoted to this system from which many details of photochemical and photophysical processes of water molecules in electronically excited states, especially the lowest four singlet states, have been revealed. Among them, the $\tilde{C}$ state is the first one exhibiting rotationally resolved absorption band and shows very complicated and interesting predissociation dynamics. The $\tilde{C}$ state is found to be predissociative with a long lifetime on the same order of magnitude as 1 ps, but shows a clear dependence on rotational state. The relative long lifetime and partially rotationally resolved absorption spectrum of the#$\tilde{C}$ state provides a good opportunity of investigating the vibrational excitation effects on the predissociation dynamics of water in the $\tilde{C}$ state.

Here we present an experimental study of the predissociation dynamics of water molecules in the $\tilde{C}$ state using time-resolved photoelectron imaging (TRPEI) technique. The $\tilde{C}$ (000), $\tilde{C}$ (010) and $\tilde{C}$ (100) states of H_2O and D_2O excited by two-photon absorption at wavelength range of 248.0-239.0 nm are studied to investigate the vibrational excitation effects on the predissociation dynamics of the $\tilde{C}$ state. All vibrationally excited states show a moderate enhancement of the predissociation of the $\tilde{C}$ state, except the $\tilde{C}$ (010) state of H_2O which shows an "abnormal" high enhancement in the predissociation rate of the $\tilde{C}$ state. Further analysis reveals that this is due to an accidental resonance mediated pathway, highlighting a new decay mechanism of H_2O in the $\tilde{C}$ state.

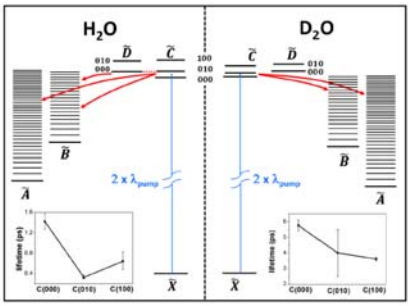

Fig. 1 The schematic view of the energy levels of water molecules for the related electronic states and the predissociation pathways of the $\tilde{C}$ state.

Keywords: vibrational excitation effect, predissociation dynamics, accidental resonance

O8 Ultrafast Vibrational Energy Transfer of Interfacial Membrane Proteins at the Membrane/Water Interface

Junjun Tan, Yi Luo, Shuji Ye

Hefei National Laboratory for Physical Sciences at the Microscale, University of Science and Technology of China, Hefei, Anhui 230026, China

Email: Shujiye@ustc.edu.cn

The vibrational energy transfer of proteins at cell membrane plays essential roles in controlling the functionalities of proteins, but its detection is severely restricted by limited experimental tools at hand. We have developed here a surface-sensitive femtosecond pump-probe scheme that employs an infrared pump followed by a sum frequency generation vibrational spectroscopy probe to detect the ultrafast vibrational energy relaxation in proteins at the cell membrane for the first time. This is the only optical detection method that is capable of elucidating the ultrafast vibrational dynamics of N-H stretching in the protein-H2O (D2O) interface. It is found that the N-H groups with strong hydrogen bonding gain faster relaxation time. The vibrational energy relaxation time of the N-H groups of the α-helical WALP23 located in the hydrophobic core of the lipid bilayer is determined to be 1.70(±0.05) ps whereas it decreases to 0.9(±0.05) ps for the β-sheet GP41 in lipid bilayer. The lifetime of the amide-I mode of WALP23 equals to 0.95(±0.05) ps. In the lipid/H2O interface, it is evident the N-H groups gain faster relaxation time when expose to water. By pumping the amide A band and probing the amide I band, the vibrational energy relaxation from N-H mode to C=O mode through two relaxation pathways (direct NH-CO coupling and coupling through intermediate states) is revealed. The NH/CO relaxation pathway depends on the hydrogen-bonding strength of NH···O=C. The strong NH···O=C hydrogen bonding favors the relaxation pathway through the intermediate states, which questions the simplified no-coupling approximation employed in current theoretical model for the amide I vibrations of proteins. Such important information will certainly help to improve the models to correctly interpret multidimensional infrared spectra, as well as to theoretically determine the potential energy surfaces of hydrogen-bonded peptides.

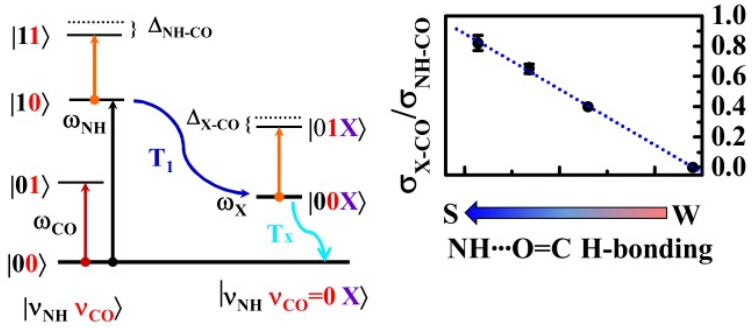

Fig. 1 Energy level diagram to describe the NH/CO coupling and the influence of hydrogen-bonding strength on the coupling pathway.

O9 Kinetics of heterocumulene OCNSO in cryogenic matrixes

Zhuang Wu, Xiaoqing Zeng*

College of Chemistry, Chemical Engineering and Materials Science, Soochow University,199 Ren-Ai Road, Suzhou Industrial Park,Suzhou, Jiangsu, 215123 Suzhou.
*Email: xqzeng@suda.edu.cn

Small inorganic molecules bearing multiple-bonding C, O, S, N atoms are of astrochemical and biological relevance that have been the targets of numerous experimental and theoretical studies. Particularly, simple species consisting of the triatomic pseudohalogens NNN and NCO are of fundamental importance due to interesting structural, conformational, and bonding properties. In contrast to N5 and OCNCO, the NSO-containing five-atomic heterocumulene OCNSO and its isoelectronic analogues OSNSO and OSNNN are completely unknown, neither experimentally nor theoretically.

Through flash vacuum pyrolysis of CF3S(O)NCO at ca. 1200 K, the novel cumulene radical OCNSO in two conformations have been generated in the gas phase and subsequently characterized in cryogenic matrices (Ar and N_2) and quantum chemical calculations for the first time. The reversible interconversion between the anti and the more stable syn conformation in cryogenic matrices were observed. The kinetics of conversion from anti to syn in solid Ar (13.0–15.5 K) and N2 (9.5–11.5 K) was studied, and very small activation barriers of 0.33 ± 0.03 (Ar matrix) and 0.46 ± 0.03 kcal mol–1 (N_2 matrix) were obtained. The change was found to be completely reversible (from syn to anti) when the matrix was irradiated with the 365 nm UV light. Similar to the photo-induced CO elimination of covalent isocyanates, upon 266 nm laser irradiation, OCNSO eliminates CO and furnishes NSO, and the latter undergoes photoisomerization into SNO.

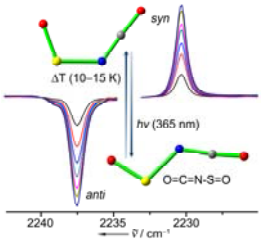

Fig. 1 The reversible interconversion between the *anti* and *syn* OCNSO.

Keywords: flash vacuum pyrolysis, matrix isolation, kinetics, activation barriers, photo-induced

References:

[1] Cacace, F.; Petris, G. D.; Troiani, A. *Science* **2002**, **295**; 480.

[2] Dixon, A. R.; Xue, T.; Sanov, A. *Angew. Chem. Int. Ed.* **2015**, **54**: 8764.

[3] Schreiner, P. R.; Reisenauer, H. P.; Romanski, J.; Mloston, G. *Angew. Chem. Int. Ed.* **2009**, **48**: 8133.

[4] Jerabek, P.; Frenking, G.; *Theor. Chem. Acc.* **2014**, **133**: 1.

[5] Ramos, L. A.; Ulic, S. E.; Romano, R. M.; Erben, M. F.; Lehmann, C. W.; Bernhardt, E.; Beckers, H.; Willner, H.; Védova, C. O. D. *Inorg. Chem.* **2010**, **49**: 11142.

[6] Wu, Z.; Liu, Q. F.; Xu, J.; Sun, H. L.; Li, D. Q.; Song, C.; Andrada, D. M.; Frenking, G.; Trabelsi, T.; Francisco, J. S.; Zeng, X. Q. *Angew. Chem. Int . Ed.* **2017**, **56**: 2140.

O10　　光催化还原二氧化碳催化剂超快红外光谱研究

刘芊辰，　周德霞，魏千顺，边红涛*

[1] 陕西师范大学化学化工学院，西安市长安区西长安街 620 号，710119

*Email: htbian@snnu.edu.cn

大量化石燃料的使用导致能源危机以及全球范围的温室效应，这使得光催化还原二氧化碳转化为一氧化碳或其它高附加值含碳能源的研究受到了极大的关注。1983年法国科学家Lehn等人首次报道了Re（bipy）（CO）$_3$X（X=Cl，Br）作为均相催化剂用于光催化还原二氧化碳产生一氧化碳，具有很高的选择性和催化活性。然而到目前为止，从微观分子层次上描述该催化反应机理还很缺乏，特别是不同配体X的选择对催化剂活性有着极大的影响。本研究利用多维超快红外光谱技术及前期工作发展的振动能量传递方法研究了Re（dcbpy）（CO）$_3$X（X=Cl，NCS）催化剂分子的三维分子构象以及其在不同溶剂中的超快动力学光谱。

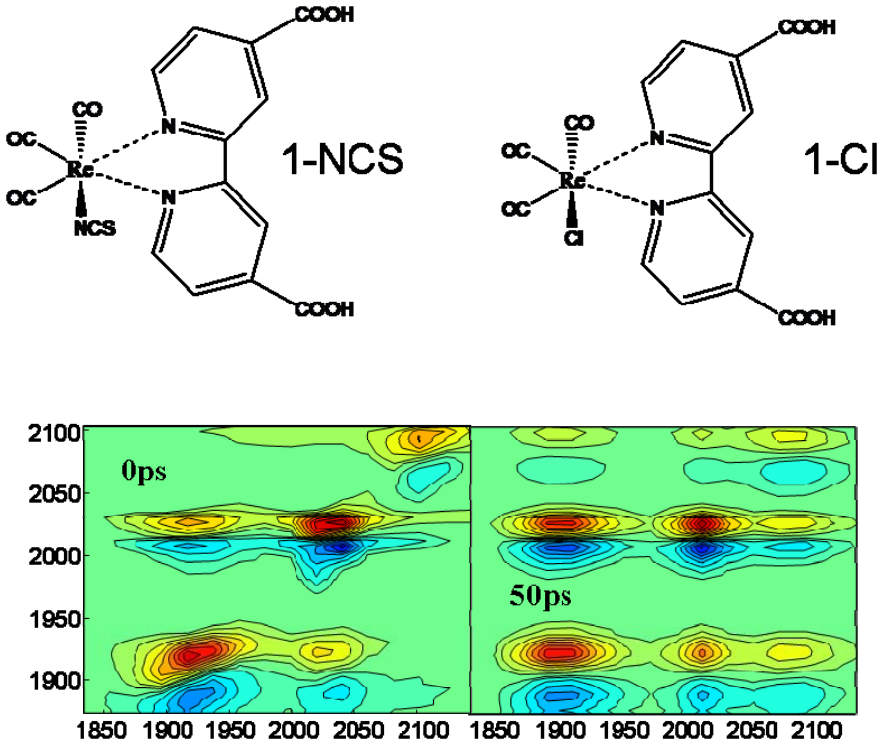

Fig. 1 (Top) Chemical structure for 1-NCS and 1-Cl; (Bottom) 2D-IR spectra of 1-NCS at different waiting times.

关键词： 多维超快红外光谱，光催化还原二氧化碳，分子构象

参考文献

[1] Bian, H.; Wen, X.; Li, J.; Chen, H.; Han, S.; Sun, X.; Song, J.; Zhuang, W.; Zheng, J.; *Proc. Natl. Acad. Sci.* **2011**, **108**: 4734.

[2] Chen, H.; Bian, H.; Zheng, J. *Acta Phys. Chim. Sin.*, **2017, 33:** 40.

O11　界面化学反应时间分辨动力学的二阶非线性光学研究

陆洲*

中国科学院化学研究所，北京市海淀区中关村北一街 2 号，100190

*Email: zhoulu@iccas.ac.cn

表/界面分子体系处于特殊的二维受限环境，其所受的空间位阻效应以及分子间作用力与体相分子有着很大区别，造成其截然不同的化学反应的动力学行为与分子机理。但由于传统光谱手段缺乏单层分子的检测灵敏度，长期以来人们对于表界面处的时间分辨化学反应动力学的认识还相当有限。近年来具有界面选择性与亚单分子层灵敏度的二阶非线性光学手段的飞速发展，为我们特异性地研究界面化学反应动态变化过程带来了希望。二阶非线性光学手段，包括和频振动光谱（sum frequency generation spectroscopy，SFG）与二次谐波技术（second harmonic generation，SHG）已经被广泛用于研究界面分子体系的组装结构、分子取向等。在本研究中，我们利用 SHG 与 SFG 分别研究了气/固界面 Langmuir- Blodgett （LB）单分子膜中苯乙烯基喹啉衍生物（SQC18）的光二聚反应动力学与气/液界面不饱和脂肪酸的氧化反应动力学过程。研究发现，LB 单分子膜中 SQC18 在双光子诱导下的[2+2]环加成反应速率为一级反应；其反应速率常数与反应单体的表面浓度呈非单调的依赖关系。经过结合原子力显微镜对 LB 膜的形貌测量与反应物与产物的量子化学计算，我们对该反应机理提出了合理的解释。对于气液界面不饱和脂肪酸的氧化反应，我们重点考察了维生素 B2 及其衍生物对不饱和脂肪酸-20 碳烯酸（11c-Eicosenoic acid, EA）在空气/水界面氧化动力学的影响。数据显示，相同分子面积下，亚相含有维生素 B2 可以减缓界面不饱和脂肪酸的氧化。通过高分辨和频光谱的静态光谱测量，我们发现在亚相中加入维生素 B2 可以增加界面上不饱和脂肪酸 EA 的排列致密度，从而保护有机长链中的不饱和双键，降低其在空气中的氧化速率。这些研究充分证明了 SFG 和 SHG 是研究各种表/界面上发生的化学反应动态变化过程的有力工具。

关键词：环加成反应；氧化动力学；不饱和脂肪酸；和频振动光谱；二次谐波

O12 光敏性药物分子酮洛芬（Ketoprofen）的超快光谱研究及其应用

李明德

汕头大学化学系，广东省汕头市大学路243号，515063

*Email: mdli@stu.edu.cn

酮洛芬（KP）是一种非甾体抗炎药，常用于类风湿性关节炎、风湿性关节炎、骨关节炎、关节强硬性脊椎炎及痛风等。但是，KP因具有二苯甲酮的母结构，因此KP也是一种光敏性药物分子，光照后会引起DNA双链损伤，脂质过氧化和光致溶血等光毒性副反应。[1] 然而对KP的光毒性反应机理、光物理和光化学过程中的激发态和活性反应中间体了解甚少。为了搞清楚KP的光物理和光化学过程，我们利用纳秒时间分辨共振拉曼光谱和飞秒/纳秒瞬态吸收光谱对KP及其衍生物进行了系统研究，结合DFT的理论计算，获得了KP在乙腈溶剂、异丙醇溶剂、中性乙腈/水溶液、酸性乙腈/水溶液和磷酸缓冲液（PBS）的飞秒瞬态吸收光谱和时间分辨共振拉曼光谱，捕捉到了KP受激发后的光物理和光化学反应的激发态和活性反应中间体，探索和阐明了KP在不同溶剂条件下的光化学反应机理。[2]

三重态的KP（T1，n,π*）在酸性溶液直接生成双自由基中间体而在PBS和碱性条件直接生成三重态的碳负离子，利用此特性，成功设计出基于KP为基底的清洁、高效、pH可调控的分子光控开关，在PBS和碱性条件下，三重态的碳负离子发生电荷转移（CT）释放出ibuprofen、氯、溴、碘、乙酸小分子基团，而在酸性时双自由基中间体不能释放离去基。[3]

另外，为了研究KP对DNA的光毒性机理，我们还研究了KP与尿嘧啶，腺嘧啶四种不同结构的二聚体的光化学反应机理，阐明了光照后KP与DNA的作用机制和作用活性位点，这些研究结果为更好的设计该类药物提供了非常有价值的依据。[4]

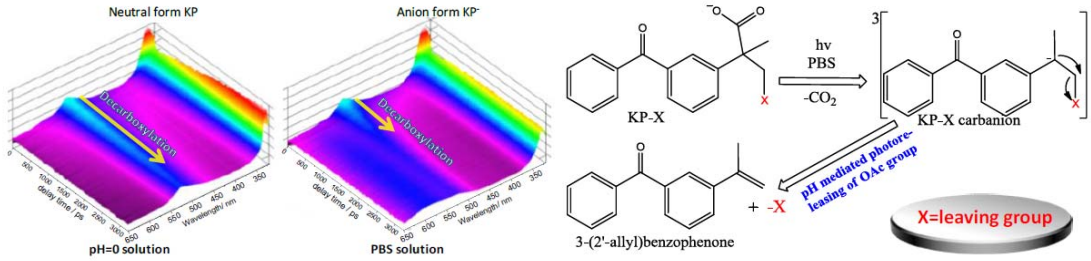

Fig. 1 Shown arefemtosecond transient absorption 3D image of KP in pH=0 and PBS solution (left) and pH mediated phototriggers platform of KP (right).

关键词：酮洛芬；飞秒瞬态吸收光谱；时间分辨共振拉曼光谱，光扳机，DNA

参考文献

[1] Bagheri, H.; Lhiaubet, V.; Montastruc, J. L.; Louis-Lalanne, N. *Drug Saf.* **2000**, ***22**:* 339.

[2] (a)Chuang, Y. P.; Xue, J.; Du, Y.; Li, M. D.; An, H. Y.; Phillips, D. L. *J. Phys. Chem. B* **2009**, ***113***:10530; (b) Li, M. D.; Du, Y.; Chuang, Y. P.; Xue, J.; Phillips, D. L. *Phys. Chem. Chem. Phys.* **2010**, ***12***:4800; (c) Li, M. D.; Yeung, C. S.; Guan, X.; Li, W.; Ma, J.; Ma, C.; Phillips, D. L. *Chem. Eur. J.* **2011**, ***17**:* 10935; (d) Li, M. D.; Ma, J.; Su, T.; Phillips, D. L. *J. Phys. Chem. B* **2012**, ***116***:5882.

[3]Li, M. D.; Su, T.; Ma, J., Liu, M.; Liu, H.; Li, X.; Phillips, D. L. *Chem. Eur. J.* **2013**, ***19***:11241; (b) Liu, M.; Li, M. D.; Su, T.; Huang, J.; Phillips, D. L. *Scientific Report.* **2016**, Accepted.

[4]Li, M. D.; Dang, L.; Liu, M.; Du, L.; Zheng, X.; Phillips, D. L. *J. Org. Chem.* **2015**, ***80**:* 3462.

O13 Ultrafast Dynamics in DNA Model System

Jinquan Chen
State Key Laboratory of Precision Spectroscopy, East China Normal University,
3663 N. Zhongshan Rd., Shanghai, 200062

Ultrafast laser experiments on carefully selected DNA model compounds probe the effects of base structure, base stacking, base pairing, and structural disorder on excited electronic states formed by UV absorption in single nucleic base as well as single and double DNA strands.

Ultrafast transient absorption experiments reveal that the long-lived excited states in a number of model compounds are charge transfer states formed by interbase electron transfer, which subsequently decay by charge recombination. The lifetimes of the charge transfer states are surprisingly independent of how the stacked bases are oriented, but disruption of π-stacking can completely eliminate this decay channel. In double strands, hydrogen bonding between bases perturbs, but does not quench, the long-lived excited states. By revealing how structure and non-covalent interactions affect excited-state dynamics, on-going experimental and theoretical studies of excited states in DNA strands can advance understanding of fundamental photophysics in other nanoscale systems.

O14 Terahertz Vibrational Spectroscopy in Molecular Crystalline Systems

Feng Zhang[1,*], Hong-Wei Wang [2], Keisuke Tominaga[1,*], Michitoshi Hayashi[2]

[1]Molecular Photoscience Research Center, Kobe University
[2]Center for Condensed Matter Science, National Taiwan University
*Email: fzhangseu@hotmail.com, tominaga@kobe-u.ac.jp

Thanks to the significant advance of terahertz (THz) technology in the past two decades, THz spectroscopy has become a routine characteristic tool in many laboratories. To the chemistry science, the most significant of THz spectroscopy is that it gives a direct access to non-covalent interactions. We have been dedicated to resolve the fundamental problem—mode assignment—of THz spectroscopy as applied to a broad spectrum of non-covalent systems. These systems involve fullerene, aromatic hydrocarbons, carbohydrates, pharmaceuticals, nucleobases, nucleosides, amino acids, short-chain peptides and polymers.

We have made progresses in primarily two respects. First, we have achieved accurate solid-state ab initial simulations of THz bands as shown in Fig. 1 by taking a few examples for illustration. Second, we developed an independent mode analysis method to evaluate the percentage contributions of external translations, librations, and a set of internal modes with unambiguous physical meaning to any THz mode of interest; so that we have achieved THz mode assignment at the quantitative level.[1, 2]

On this theoretical basis, we have illustrated several promising advantages of THz spectroscopy in crystallography, especially when hydrogen atoms, which are invisible to X-ray, play important roles in the determination of crystal structures. In particular, we examined the symmetry-conservation principle of polymer science[3] and studied elementary structural units of a disordered molecular system with using THz spectroscopy.

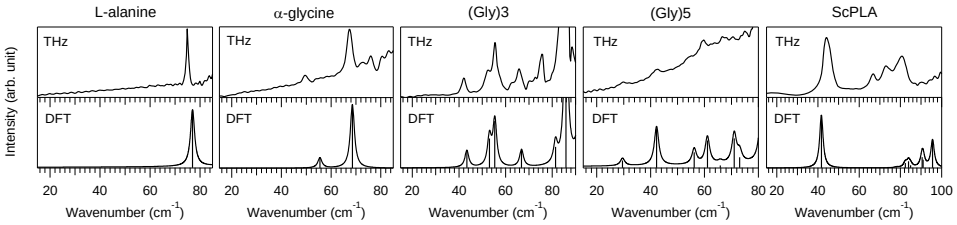

Fig. 1 Comparison between experiment and theory for five bio-molecular systems. THz spectra were measured with a time-domain THz spectrometer and at 78 K. DFT calculations were performed in the CRYSTAL14 software package and under the harmonic assumption. Lorentzian line shapes with an arbitrary haft width at half-maximum are convolved to all the simulated normal modes for visualization.

Keywords: terahertz spectroscopy, solid-state density functional theory, mode analysis,

References:

[1] F. Zhang, M. Hayashi, H.-W. Wang, K. Tominaga, O. Kambara, J.-i. Nishizawa and T. Sasaki, *J. Chem. Phys.*, **2014**, **140**, 174509.

[2] F. Zhang, H.-W. Wang, K. Tominaga and M. Hayashi, *WIREs Comput. Mol. Sci.,* **2016**, **6**, 386-409.

[3] F. Zhang, H.-W. Wang, K. Tominaga, M. Hayashi, S. Lee and T. Nishino, *J. Phys. Chem. Lett.*, **2016**, **7**, 4671-4676.

O15 Simulating two-dimensional non-linear photon echo spectra: By using the normally ordered form of Hamiltonian

Xian-Ting Liang

Department of Physics, Ningbo University, Ningbo, Zhejiang, China,315211
*Email: liangxianting@nbu.edu.cn

In this paper, we propose a method for theoretically simulating the response functions and then the 2D, third-order, non-linear, photon response spectra obtained from photon echo experiments of some complex molecular system. Here, we supposed that the exciton modes of the molecular system are coupled to their environments which are described with damped harmonic oscillators, and the Hamiltonian of the system-bath can be expressed into the normally ordered form. Two kinds of models of open molecules, the single-site molecule, and the coupled two-site molecule are investigated. It is shown that their 2D, third-order, non-linear, photon echo spectra calculated with this method are similar to the ones obtained from other methods. If only the normally ordered form of system-bath Hamiltonian can be obtained, this analytical method can also be used in other complex models.

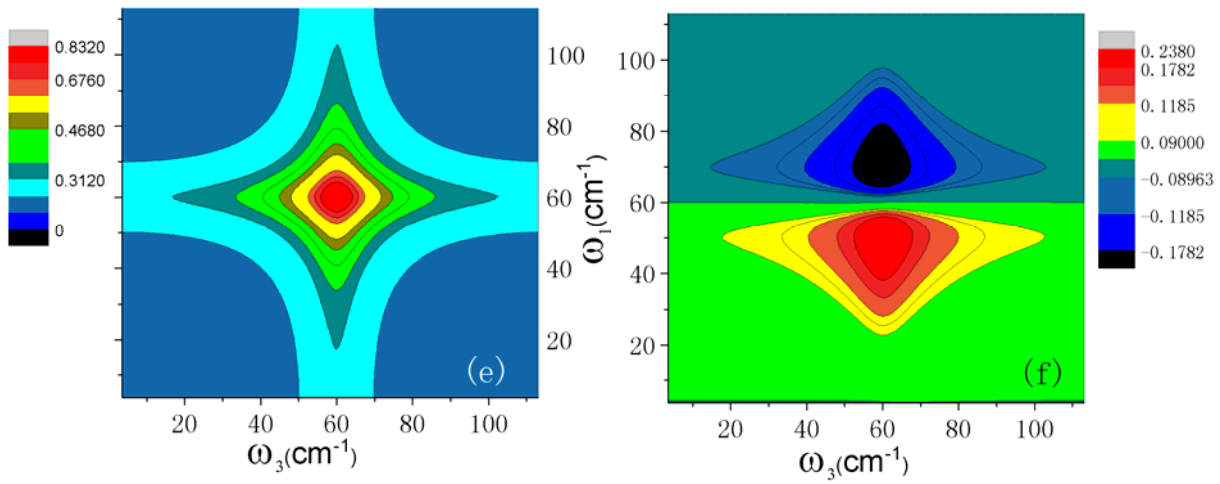

Fig. 1 2D, third-order, non-linear, photon echo purely absorptive spectra calculated with normally order form of Hamiltonian.

Keywords: Photon echo; Normally order form; 2D spectroscopy

References:

[1] Mukamel S, Mukamel S. Principles of nonlinear optical spectroscopy[M]. Oxford University Press, 1995.
[2] Fan, H.Y. Annals of Physics 2007, 322: 866.
[3] Chen, L.; Zheng, R.; Shi, Q.; et al. *Journal of Chemical Physics* **2010**, **132**: 227.
[4] Liang, X.T. *Journal of Chemical Physics* **2014**, **141***:* 044116.

O16 C-H 伸缩振动光谱的费米共振去除方法

林珂*，焦志润，但光宇，杨甫豪

西安电子科技大学，物理与光电工程学院，西安，710071

*Email: klin@xidian.edu.cn

C-H基团是生物有机分子中含量最多的基团，该基团的振动光谱常被用于研究生物有机分子。在CH伸缩区间的振动光谱中，常常伴随C-H 弯曲振动模式和C-H伸缩振动模式的费米共振。费米共振使得这个区间的光谱变得极为复杂，对这个区间的光谱归属带来了干扰，还阻碍了利用这段光谱研究生物有机分子的结构。我们发现利用一定的同位素取代方式可以使得费米共振消失。我们的拉曼光谱实验和理论结果都揭示，使用氘原子取代甲基/亚甲基中的氢原子，使得只留一下氢原子时，C-H伸缩振动谱段的费米共振就消失了。这是由于同位素取代后剩余的C-H弯曲振动的频率改变较大的缘故。基于这样的氘代方式，去除了费米共振，C-H伸缩振动光谱得以简化，这段光谱可以更简便的用于研究分子结构。我们计算了85种丝氨酸异构体的这种氘代分子，分析了其C-H伸缩振动频率与其结构的关联。发现C-H伸缩振动频率和C-H键长呈现非常好的负相关性，键长越长，C-H伸缩振动频率越低，利用这样的关系可以通过测量分子振动光谱定量化讨论C-H的键长。通过仔细分析这些丝氨酸异构体的结构和光谱，我们发现传统得把CH2当作C2v点群看待，把其伸缩振动光谱简单的归属为对称伸缩振动和反对称伸缩振动是不妥当的，具体的归属需要依靠对比两个CH的键长。只有当两个CH键长几乎一样时，才可以归属为称伸缩振动和反对称伸缩振动。我们的结果显示当通过同位素取代把费米共振去除后，C-H伸缩振动光谱可以被用于研究生物有机分子结构。

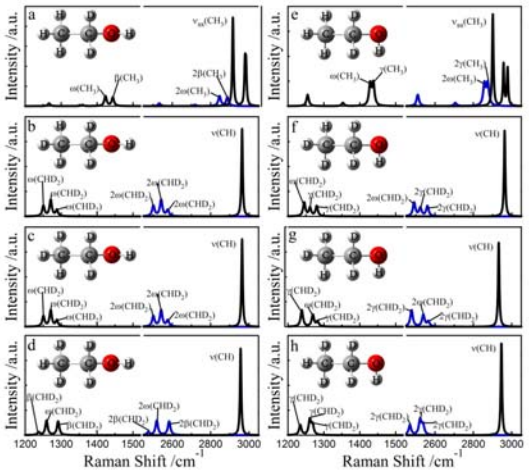

Fig. 1 乙醇同位素C-H伸缩振动光谱

关键词： C-H伸缩振动；费米共振；同位素取代；C-H键长；光谱归属

参考文献

[1] Chen, L.; Zhu, W.; Lin, K.; Hu, N.; et al. *J. Phys. Chem. A.,* **2015**, **119**: 3209.

[2] Yu, Y.; Wang, Y.; Hu, N.; Lin, K; et al. *Phys. Chem. Chem. Phys.*， **2016**, **18**: 10563

[3] He, K.; Allen, W.; *J. Chem. Theory Comput.,* **2016**, **12**: 3571

O17 Recent Progresses in Cold Molecule Physics

颜波 [1,*]

[1]Zhejiang University，No. 148, Tianmushan Road, Hangzhou, Zhejiang, China，310028

*Email: yanbohang@zju.edu.cn

As a nature development of cold atom physics, cold molecule physics have been developed for more than 20 yeas. It has valuable applications range from precision measurement, quantum chemistry to quantum many-body physics. However, due to the complexity of the molecular energy structure, molecular cooling has been facing many challenges. The traditional method (electric field, magnetic field, etc.) can not reduce the entropy of the system because they are conservative force. In recently years, new technologies such as laser cooling has been developed and made huge progress. This report will introduce some of the latest advances in cold molecules. Especially with regard to the progress of laser cooling of polar molecule. We believe the laser cooling technique can bring new breakthroughs in the near future .

Keywords: cold molecules, quantum chemistry, laser cooling.

Refereces:

[1] Bu, W., Chen, T., Lv, G., and Yan, B., *Phys. Rev. A* **2017**, **95**: 032701.

[2] Chen, T., Bu, W., and Yan, B., *Phys. Rev. A* **2016**, **94**: 063415.

[3] Yan, B., Moses, S., Gadway, B., Covey, J., Hazzard, K., Rey, A., Jin, D., and Ye, J., *Nature* **2013**, **501**: 521.

O18 Interface reaction kinetics for NH_3-SCR of NO_x over $CuMn_2O_4$ catalyst

Yingju Yang, Jing Liu*, Feng Liu, Zhen Wang, Sen Miao

State Key Laboratory of Coal Combustion, School of Energy and Power Engineering, Huazhong University of Science and Technology, Wuhan, 430074
*Email: liujing27@mail.hust.edu.cn (J. Liu)

Nitrogen oxides (NO_x) generated from stationary and automobile combustion sources are the primary atmospheric pollutants and have caused serious environmental problems [1]. Selective catalytic reduction (SCR) of NO_x with NH_3 has long been known to be the well-established and widely used technology controlling NO_x emission. $CuMn_2O_4$ spinel has been developed as the SCR catalyst, and significantly promotes the reduction of NO_x by NH_3. The catalytic reaction mechanism of NO_x reduction is closely associated with the SCR rate-enhancing capacity of $CuMn_2O_4$ catalyst. Therefore, the catalytic chemistry of the SCR process is investigated in detail.

The relationship among the microcosmic structure of $CuMn_2O_4$ spinel, the types of active sites, and the activity for SCR of NO_x with NH_3 were established through density functional theory (DFT) calculations. All possible elementary reaction steps involved in NH_3-SCR of NO_x over $CuMn_2O_4$ catalyst were systematically investigated. DFT calculation results show that the chemisorption mechanism is responsible for the adsorption of reactants, possible intermediates and products over $CuMn_2O_4$(100) surface. NH_3 can be strongly adsorbed on Cu active site, and subsequently dissociated into NH_2 and H through dehydrogenation reaction. NH_2 is very difficult to be further dissociated into NH and H because of the higher energy barrier of 275.30 kJ/mol. NH_2 easily reacts with the adsorbed NO to form N_2 and H_2O due to the lower energy barrier of 6.87 kJ/mol. Compared to the oxidation of NO into NO_2, NO prefers to be reduced by NH_2 to produce N_2 and H_2O via the reaction $NH_2 + NO \rightarrow N_2 + H_2O$, as shown in Fig.1. The energy barrier of N_2O formation over $CuMn_2O_4$ catalyst is much higher than that of N_2 formation, which indicates that $CuMn_2O_4$ catalyst shows a superior N_2 selectivity for NO_x reduction. The optimal reaction pathway of NH_3-SCR of NO_x over $CuMn_2O_4$(100) surface is a two-step process controlled by two reactions $NH_3 \rightarrow NH_2 + H$ and $NH_2 + NO \rightarrow N_2 + H_2O$. The rate-determining step of NH_3-SCR of NO_x over $CuMn_2O_4$(100) surface is the dehydrogenation reaction of NH_3.

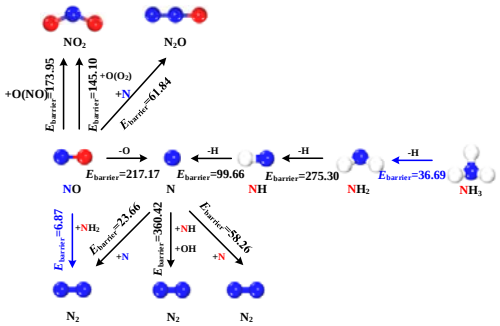

Fig. 1 Heterogeneous reaction pathway of NH_3-SCR of NO_x over $CuMn_2O_4$ catalyst.

Keywords: Interface reaction; Reaction pathway; NH_3-SCR; $CuMn_2O_4$ catalyst

References:

[1] Wang, X.; Lan, Z.; Zhang, K.; Chen, J.; Jiang, L.; Wang, R. *J. Phys. Chem. C* **2017**, **121**: 3339.

O19 相干空穴转移过程的二维电子光谱研究

张春峰 [1,*]

[1] 南京大学物理学院

*Email: cfzhang@nju.edu.cn

近年来，有机光伏器件取得了长足的进步，单节器件的效率已经突破13%，接近商用所需的效率阈值。富勒烯及其衍生物是传统有机光伏器件中的主要电子受体材料，其载流子输运性能极为出色，不过其吸收集中在紫外波段，在太阳能谱中占比很小，受体自身吸收的贡献微弱，机理的研究也主要关注在电子转移过程。非富勒烯受体材料的广泛采用是近期进步的重要原因，突破了传统观念的束缚，新的受体材料层出不从，性能提升有了更多期待。从机制上看，受体材料自身的吸收覆盖太阳能占比重要的可见近红外波段，贡献很重要的器件效率部分。前期工作，我们利用瞬态吸收光谱技术确认在非富勒烯基的聚合物/小分子[1]，小分子/小分子[2]等给受体混合物系统中亚皮秒尺度的空穴转移的重要作用。

为进一步理解空穴转移的物理机制，我们利用高时间分辨（< 10 fs）的二维电子光谱，研究了聚合物/小分子[1]有机光伏系统中的空穴转移过程。如Fig.1所示，我们发现在亚皮秒时间尺度的电荷转移过程中，动力学曲线显示~23fs为周期的明显量子拍频现象，其频率对应于C=C键等主要振动模式，显示电声相干性在空穴转移过程中扮演重要角色，与利用量子动力学理论模型计算结果吻合。电声相干性对于高效空穴转移起到关键作用，在此效应下，有效电荷转移可发生在能级差极小的分子界面之间，原则上可大幅提升开路电压，这一结果显示利用相干性进一步提升有机光电器件性能的可行性[3]。

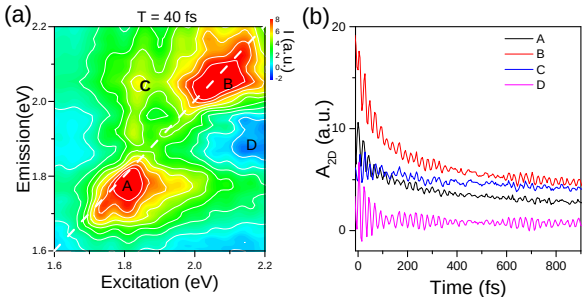

Fig. 1 (a) Absorptive two-dimensional electronic spectroscopy recorded on donor/acceptor blend. (b) The amplitudes of the two-dimensional electronic signals at points labeled in (a) are plotted versus decay time. The oscillations observed in the time-domain kinetics suggest a critical role played by vibronic coherence in the hole transfer process.

关键词： 二维电子光谱，电声相干，空穴转移，有机光伏，非富勒烯受体

参考文献

[1] Bin H. & et al., Nature Commun. 7, 13651 (2016).

[2] Bin H. & et al., J. Am. Chem. Soc. 139, 5085 (2017).

[3] J.-L. Bredas, E. H. Sargent, and G. D. Scholes, Nat. Mater. 16, 35-44 (2017)

O20 超快强激光诱导的原子分子中性里德堡态激发

徐海峰*

吉林大学原子与分子物理研究所，长春，130012

*Email: xuhf@jlu.edu.cn

当原子分子处于光强>10^{13}Wcm^{-2}的超快强激光场中，光电离电子在激光场和库仑势共同作用下可诱导很多新的高度非线性的物理现象，如高价高次谐波发射、高阶阈上电离、非序列多次电离等。最近的研究发现超快强激光场中能够产生处于高里德堡态的原子[1]，被认为是隧穿电离电子诱导的一种新的强场物理现象，将有助于完善超快强激光场与原子分子相互作用的物理图像，对相应理论的发展以及太赫兹、高次谐波、阿秒等新型光源研究亦具有重要的参考价值。

尽管超快强激光诱导的原子里德堡态激发已引起了很多理论和实验研究关注，但其背后的物理机制仍存在争议，同时分子的激发现象以及其中蕴含的分子结构效应或量子效应仍有待研究予以揭示。我们利用质量分辨脉冲场致电离、辐射荧光测量等方法，结合强场理论研究，围绕激发与电离等其它强场物理过程的关系、分子结构效应、量子效应等科学问题，开展了系统的研究。我们详细研究了椭偏光场中的原子里德堡态激发，测量了里德堡态产率对激光椭偏率的依赖，并与强场近似模型以及三维半经典计算结果进行对比，指出激发与阈上电离中低能或近零能结构是密切相关的[2]；通过对比电离限相近的原子和双原子分子的激发（Ar vs N2以及Xe vs O2），结合数值求解含时薛定谔方程的理论结果，指出分子不同HOMO结构导致隧穿电子出射角度分布不同，从而导致俘获到里德堡态的几率不同，发现了强场里德堡态激发过程中的分子轨道结构效应并给出了理论解释[3]；最近我们对强场激发过程中的量子轨道干涉效应开展了研究，进一步揭示了超快强激光诱导的里德堡态激发的物理机制[4]。

关键词：超快光场；里德堡态激发；量子效应

参考文献

[1] Nubbemeyer, T.; Gorling, K.; Saenz, A.; Eichmann, U.; Sandner W., *Phys. Rev. Lett.* **2008**, **101**: 233001.

[2] Zhao, L.; Dong, J.; Lv, H.; Yang, T.; Lian, Y.; Jin, M.; Xu, H.; Ding, D.; Hu, S.; Chen, J., *Phys. Rev. A.* **2016**, **93**: 053403.

[4] Lv, H.; Zuo, W.; Zhao, L.; Xu, H.; Jin, M.; Ding, D.; Hu, S.; Chen, J., *Phys. Rev. A.* **2016**, **93**: 033415.

[5] Hu, S.; Hao, X.; Lv, H.; Yang, T.; Xu, H.; Jin, M.; Ding, D.; Chen, J.; Becker, W., to be submitted.

O21 Combined femtosecond time-resolved fluorescence and transient absorption study of excited state dynamics of cytosine and derivatives

Chensheng Ma,[1*] C. T.-L. Chan,[1] C. C.-W. Cheng,[2] Wai-Ming Kwok[2]

[1]School of Chemistry and Environmental Engineering, Shenzhen University, Shenzhen, 518052
[2]Department of Applied Biology and Chemical Technology, The Hong Kong Polytechnic University Hung Hom, Kowloon, Hong Kong
*E-mail: macs@szu.edu.cn

Nucleobases, the building blocks and also the chromophores of the genetic materials, have been extensively studied both experimentally and theoretically. The ultra-short lifetime of electronically excited states of the bases formed after absorption of UV light has been considered the key factor for the vitally important photo-stability of the bases to protect against UV irradiation. However, due to the complex nature of the excited states, in particular the likely involvement of various dark natured states that are sensitive both to covalent modification and environmental condition, the precise timescale and elementary steps underlying the nonradiative process causing the very short excited state lifetime are not fully understood. Here we present ultrafast time-resolved study which we coupled femtosecond broadband time-resolved fluorescence with transient absorption to directly probe and monitor temporal evolution of UV-excited nucleobases[1-4] with an emphasize on cytosine and a range of its derivatives in solvents of different properties.[1] The results we obtained uncover remarkable roles of the solvents and the substitutions in altering significantly the lifetime of excited states as well as to control the participation or not of dark natured state during the course of excited state deactivation. Our study provides direct evidences and new insights for a clearer picture describing the mechanism of nonradiative dynamics of cytosine and derivatives.

Keywords: Nucleobase; excited state; nonradiative dynamics; ultrafast time-resolved fluorescence; fs transient absorption

References:

[1] Ma, C.; Cheng, C. C.-W.; Chan, C. T.-L.; Chan, R. C.-T.; Kwok, W.-M. *Phys. Chem. Chem. Phys.* **2015**, **17**: 19045.

[2] Cheng, C. C.-W.; Ma, C.; Chan, C. T.-L.; Ho, K. Y.-F.; Kwok, W.-M. *Photochem. Photobiol. Sci.* **2013**, **12**: 1351.

[3] Kwok, W.-M.; Ma, C.; Phillips, D. L. *J. Am. Chem. Soc.* **2006**, **128**: 11894.

[4] Kwok, W.-M.; Ma, C.; Phillips, D. L. *J. Am. Chem. Soc.* **2008**, **130**: 5131.

O22 Kinetic study of CH_2OO Criegee intermediate relevant reactions using OH laser induced fluorescence

Yiqiang Liu,[1,2] Fenghua Liu,[1] Siyue Liu,[1,2] Dongxu Dai,[1] Wenrui Dong,[1*] and Xueming Yang[1*]

[1] State Key Laboratory of Molecular Reaction Dynamics, Dalian Institute of Chemical Physics, Chinese Academy of Sciences, Dalian, Liaoning 116023, China.

[2] School of Physics and Optoelectric Engineering, Dalian University of Technology, Dalian, Liaoning 116023, China.

*Email: wrdong@dicp.ac.cn

The OH laser induced fluorescence method was used to study the kinetics of CH_2OO with SO_2, $(H_2O)_2$, CH_2I_2 and I atoms. Decay of CH_2OO is not strictly first-order since its self-reaction is rapid.[1]-[4] With this consideration, we derived the rate coefficient of CH_2OO + SO_2 / $(H_2O)_2$ / CH_2I_2 / I taking into account the contribution of CH_2OO self-reaction. For the CH_2OO + SO_2 reacton, the rate coefficient is measured to be $(3.88 \pm 0.13) \times 10^{-11}$ cm^3 $molecule^{-1}$ s^{-1} at 10 torr, which agrees very well with a previously reported value obtained by directly monitoring CH_2OO using the UV absorption method with CH_2OO self-reaction considered.[1] We did not observe obvious evidence of SO_2 catalysed CH_2OO isomerization or intersystem crossing effect in this reaction. CH_2OO + $(H_2O)_2$ is supposed to count for major sink of CH_2OO in the atmosphere, but previous rate coefficient measurements were not in good consistency. We have revisited this reaction including the self-reaction of CH_2OO and obtained the rate coefficient to be $(7.53 \pm 0.38) \times 10^{-12}$ cm^3 $molecule^{-1}$ s^{-1} at 60 torr and 300 K. The rate coefficients of CH_2OO + CH_2I_2 and CH_2OO + I were measured to be $(5.2 \pm 2.6) \times 10^{-14}$ and $(2.2 \pm 1.1) \times 10^{-12}$ cm^3 $molecule^{-1}$ s^{-1} respectively.

Keywords: Criegee Intermediate, Laser induced fluorescence, rate coefficient

References:

[1] R. Chhantyal-Pun, A. Davey, D. E. Shallcross, C. J. Percival and A. J. Orr-Ewing, *Phys Chem Chem Phys*, 2015, 17, 3617-3626.

[2] Y. T. Su, H. Y. Lin, R. Putikam, H. Matsui, M. C. Lin and Y. P. Lee, *Nat Chem*, 2014, 6, 477-483.

[3] W. L. Ting, C. H. Chang, Y. F. Lee, H. Matsui, Y. P. Lee and J. J. M. Lin, *J Chem Phys*, 2014, 141,104308.

[4] Z. J. Buras, R. M. I. Elsamra and W. H. Green, *J Phys Chem Lett*, 2014, 5, 2224-2228.

O23 A highly-integrated supersonic-jet Fourier-transform microwave spectrometer: Instrumental setup and Initial Molecular Results

Gang Feng[1,*], Qian Gou, Jens-Uwe Grabow

[1]School of Chemistry and Chemical Engineering, Chongqing University, No.55 Daxuecheng South Rd., Chongqing, 401331.
[2]Institut für Physikalische Chemie und Elektrochemie, Lehrgebiet A, Gottfried-Wilhelm-Leibniz-Universität, Callinstrasse 3A, D-30167 Hannover, Germany.
*Email: fengg@cqu.edu.cn

A highly integrated supersonic-jet Fourier-transform microwave spectrometer of coaxially oriented beam-resonator arrangement (COBRA) type, covering 2-20GHz, has been recently built at Chongqing University.

Built up almost entirely in an NI PXIe chassis, we take the advantage of the NI PXIe-5451 Dual-channel arbitrary waveform generator and the PXIe-5654 RF signal generator to create a spectrometer with wobbling capacity for fast resonator tuning. Based on the I/Q modulation, associate with PXI control and sequence boards built at the Leibniz Universitat Hannover, the design of the spectrometer is much simpler and very compact.

The Fabry–Pérot resonator is semi-confocal with a spherical reflector of 630 mm diameter and a radius of 900 mm curvature and one circulator plate reflector of 630 mm diameter. The vacuum is effectuated by a three-stage mechanical (two-stage rotary vane and roots booster) pump at the fore line of a DN630 ISO-F 20000 L/s oil-diffusion pump. The supersonic-jet expansion is pulsed by a general valve Series 9 solenoid valve which is controlled by a general valve IOTA one driver governed by the experiment-sequence generation.

First molecular examples on weakly bounded molecular complexes will be present.

Keywords: microwave spectroscopy; supersonic expansion; non-covalent interactions

Calculation on Activation Energy for Decomposition of Magnesite by Congruent Dissociative Vaporization Theory

Zhen Zhao[1,*], Zhi Li[2]

[1]School of Chemistry and Life Science, Anshan Normal University, No. 43 Ping'an Street Tiedong District, Anshan 114007

[2]School of Materials and Metallurgy, University of Science and Technology Liaoning, No. 185 Qianshan Road High-tech Zone, Anshan, 114051

*Email: zhaozhenlunwen@yeah.net

The activation energy *E* parameters for decomposition of $MgCO_3$ at CO_2 and N_2 atmosphere are calculated by the third-law method in subsequent comparison of these data with the values of the *E* parameters by experimental measurements and calculated prediction. The calculated *E* values of our data are slightly higher than those of the experimental and theoretical values. It can be found that the *E* values were increased with the pressure of temperature and carbon dioxide increased. It can also be found that the curves of activation energy *E* have an inflection point when CO_2 was added. This is mainly due to the diffusion process in the interface of reactant-product layer and the adsorption of CO_2 on the surface of magnesite.

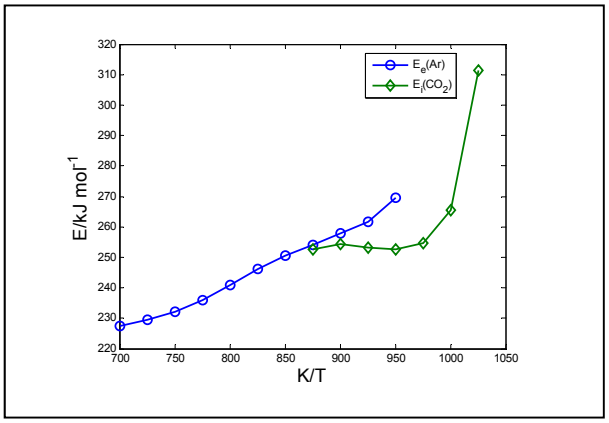

Fig. 1 The activation energy for magnesite decomposed at atmosphere pressure against K/T

Keywords: Magnesite; The third-law method; Decomposition; Activation energy; Congruent dissociative vaporization

References:

[1] L'vov, BV.; Polzik, LK.; Ugolkov, VL. *Thermochim. Acta*. **2002**, **390**: 5.

[2] Galan, I.; Glasser, FP.; Andrade, C. *J. Therm. Anal. Calorim*. **2013**, **111**: 1197.

[3] L'vov, BV.; Ugolkov, VL. *Thermochim. Acta*. **2004**, **410**: 47.

[4] L'vov, BV. *Thermochim. Acta*. **2002**, **386**: 1.

[5] Hurst, HJ. *Thermochim. Acta*. **1991**, **189**: 91.

[6] Galwey, AK.; Brown, ME.Thermal decomposition of ionic solids. Netherlands: Elsevier Science B.V. **1999**.

Potential Energy Surfaces and Dynamics Study of Al + O_2 Reaction

Jun Chen[1], Zichao Tang[1], Lansun Zheng[1] and Xin Xu[2,*]

[1]*i*ChEM, College of Chemistry and Chemical Engineering, Xiamen University, Xiamen 361005
[2]*i*ChEM, Department of Chemistry, Fudan University, Shanghai 200433
*Email: xxchem@fudan.edu.cn

The triatomic reaction Al + O_2 is regarded as the key step in aluminum combustion. In 2003 Gordon et al[1] performed a systematic multiconfigurational study of this reaction. Later in 2004 Lee et al[2] reported some potential energy surface (PES) features also with CASSCF method, but using different active space. The reaction mechanisms of AlO_2 complex formation and its decaying into AlO + O channel were analyzed in detail, while some discrepancies still exist in these two studies.

In this work, the potential energies of ^{2}A" state are calculated with the CASSCF method, the CCSD(T) method, and the XYG3 doubly hybrid density functional. The PESs are constructed with the neural network fitting, and quasi-classical trajectory calculations are performed on these PESs. Generally good agreements can be archived between theoretical and experimental results.

Keywords: potential energy surface; density functional; XYG3; AlO_2; reaction dynamics

References:

[1] Pak, M. V.; Gordon, M. S. *J. Chem. Phys.* **2003**, **118**: 4471.
[2] Ledentu, V.; Rahmouni, A.; Jeung, G.-H.; Lee, Y.-S. *Bull. Korean Chem. Soc.* **2004**, **25**: 1645.

Co(0001)表面 H_2O 和 CO 的共吸附：分子间氢键的作用

陈骏[1,2]，吴家伟[1]，郭庆[1,*]，苏海燕[1,*]，戴东旭[1]，杨学明[1]

[1] State Key Laboratory of Molecular Reaction Dynamics, Dalian Institute of Chemical Physics, 457 Zhongshan Road, Dalian 116023, Liaoning, P. R. China

[2] School of Physics and Optoelectric Engineering, Dalian University of Technology, Dalian, Liaoning 116023, P. R. China

*Email: guoqing@dicp.ac.cn

水煤气变换反应作为制氢，合成氨等工业过程中的重要反应，一直备受人们关注，Co基催化剂是该反应中常用的催化剂，理解在这个反应体系中吸附分子间的相互作用对理解和运用这个反应具有重要的意义。通过使用TPD（程序升温脱附谱）和DFT计算结合的方法，系统的研究了CO和H_2O在Co(0001)表面100K条件下的共吸附。CO的吸附几乎不受共吸附的H_2O的影响，但CO的存在会稳定水分子的吸附。当预吸附的CO的吸附量小于0.27ML时，原本H_2O（0.6ML）的TPD谱中的脱附单峰会分裂成3个脱附峰，其中一个向低温移动，另一个向高温移动。其中向低温移动的峰可以归属为由于H_2O分子间的排斥力作用，而向高温处移动的峰是由于H_2O和CO分子间的吸引作用。增加预吸附CO的量，H_2O的高温峰继续向高温移动（约15K），并且峰的强度也在增加，直到θ_{CO}=0.36 ML时达到最大。DFT计算认为H_2O和CO共吸附时的分子间吸引作用来源于H_2O和CO分子间形成的氢键作用。这一个研究促进了对水煤气变换反应中CO和H_2O分子间相互作用的认识。

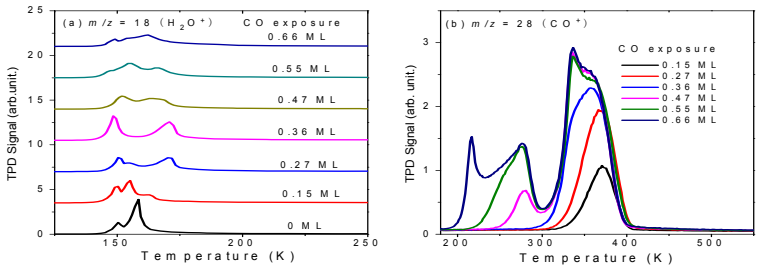

Fig. 1 Left panel: H2O (m/z = 18) TPD spectra from 0.6 ML H2O covered on various exposures of CO predosed Co(0001) at 100 K.Right panel: CO (m/z = 28) TPD spectra from 0.6 ML H2O covered on various exposures of CO predosed Co(0001) at 100 K.

关键词： Co(0001)表面；H_2O；CO；分子间氢键

参考文献

[1] Nagai, M. ; Matsuda, K. *Journal of Catalysis*, **2006, 238(2)**: 489-496..

[2] L.Xu, Y.Ma, Y.Zhang, B.Chen, Z.Wu, Z.Jiang, W.Huang. *J. Phys. Chem. C* **2010,114**:17023.

[3] M.E.Bridge, C.M.Comrie, R.M.Lambert. *J. Catal.* **1979,58**: 28.

[4] Jiawei W, Chen J, Guo Q, et al. *Surface Science*, **2017, 663**: 56-61.

液体及其界面的反应动力学质谱装置

陈玲玲，陈子伟，李子渊，胡婕，田善喜*

中国科学技术大学化学物理系，合肥微尺度物质科学国家实验室，安徽合肥，230026

*Email: sxtian@ustc.edu.cn

当前，气相分子的化学反应动力学已经研究得比较深入。但是，发生在液体及其界面的化学反应微观动力学机制还存在许多的疑问和研究空白。国际上的已有一些实验组开展液相及界面体系中的光电子能谱、原子散射动力学实验研究[1-3]。我们正在搭建一台液体及其界面的化学反应动力学装置，目前采用的关键技术是在真空中的微孔喷射（microjet）产生液柱以及质谱探测技术，拟开展液体及其界面的电子诱导（贴附、电离等）化学反应的实验研究。其中的飞行时间质谱部分可以进行正、负离子或分子团簇的探测，通过扫描电子束的电子能量，对不同分子团簇离子强度变化的测量分析，结合理论计算模拟，研究液体及其界面发生的反应过程。

关键词：电子碰撞；微孔喷射；飞行时间质谱

参考文献

[1] Faubel, M.; Steiner, B.; Toennies, J. P. *J. Chem. Phys.* **1997**, 106: 9013.

[2] Siefermann, K. R.; et al. *Nature Chem*. **2010**, 2(4): 274.

[3] Luckhaus, D.; et al. *Sci. Adv.* **2017**, 3: e1603224.

泛频激发效应对于 $F+CH_4$ 反应的影响

陈荣军，陈震，杨家岳，张冬，吴国荣*，杨学明*

中国科学院大连化学物理研究所分子反应动力学国家重点实验室，大连，116023

*Email: xmyang@dicp.ac.cn

我们已经知道，不同形式的能量对于反应会有不同的影响。对于$F+CH_4 \rightarrow CH_3+HF$这样的一个早期势垒反应，已经有人研究了$CH_4$在$v_3$=1时对于反应的影响[1]，这给予了我们灵感。于是我们使用自己搭建的交叉分子束设备[2]，用交叉分子束-时间切片的离子速度成像方法[3]，尝试进一步激发，使CH_4的v_3振动激发达到两个量子数——即在泛频激发下，再用2+1共振增强多光子电离（REMPI）的方式探测基态的CH_3基团，比较这种激发与在基态的反应结果，实验中使用的碰撞能约为8kcal/mol。初步的实验结果表明，泛频激发效应与基频激发效应类似，都会抑制反应的发生。当红外光开启（泛频激发）时，CH_3的整体信号会减小四分之一。

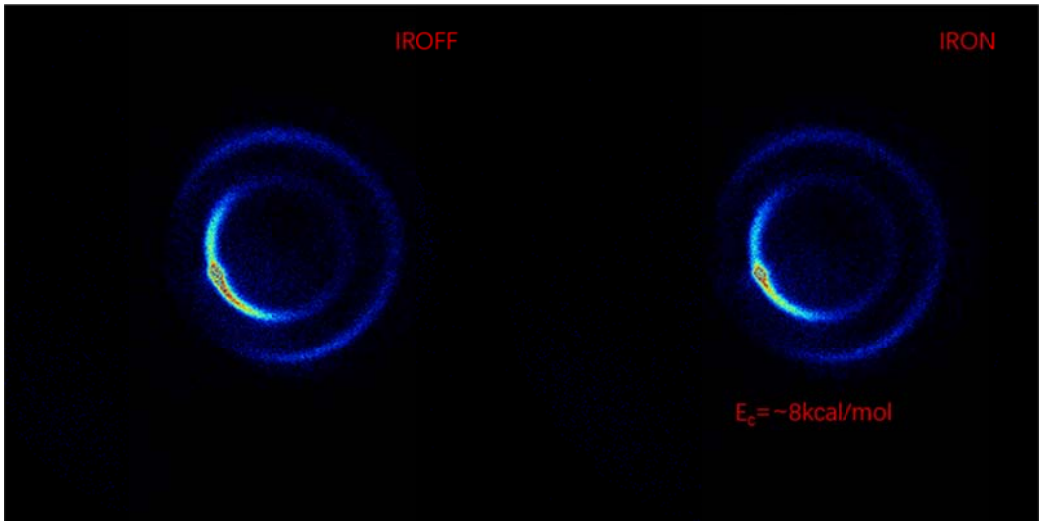

Fig. 1 Raw images of the CH_3 (v=0) product states acquired at Ec = 8 kcal/mol

关键词：交叉分子束；离子成像；泛频激发

参考文献

[1] Kawamata H, Zhang W, Liu K. *Faraday discussions*. **2012**, **157**: 89-100.

[2] Yang J, Zhang D, Jiang B, et al. *The journal of physical chemistry letters.* **2014**, **5(11)**: 1790-1794.

[3] Wu G, Zhang W, Pan H, et al. *Review of Scientific Instruments.* **2008**, **79(9)**: 094104.

Enhanced Ab Initio Molecular Dynamics Simulation of the Temperature-Dependent Thermodynamics for the Diffusion of Carbon Monoxide on Ru(0001) Surface

Zhe-Ning Chen[1*], Lin Shen[2], Mingjun Yang[2], Hao Hu[2*]

[1]State Key Laboratory of Structural Chemistry, Fujian Institute of Research on the Structure of Matter, Chinese Academy of Sciences, Fuzhou, Fujian 350002, China
[2]Department of Chemistry, The University of Hong Kong, Pokfulam Road, Hong Kong, China
*Email: znchen@fjirsm.ac.cn

CO diffusion on the metal surface is an elementary process in many heterogeneous catalytic reactions. The thermodynamics and the molecular mechanism of the diffusion process are key factors contributing to the kinetics of the catalysis. Theoretical study based on computer simulations can complement experimental studies to provide much needed thermodynamic and mechanistic information. Here, we report direct ab initio molecular dynamics (MD) simulation to investigate the temperature-dependent thermodynamics of CO diffusion on the Ru(0001) surface combined with an efficient sampling method based on integrated tempering to speed up phase space sampling. We show that reliable and smooth two-dimensional potential of mean force surfaces of CO diffusion can be obtained at different temperatures. As expected, with increasing temperature, the distribution of CO adsorbate at different surface sites becomes more and more uniform, while the height of the free energy barrier to CO diffusion decreases. The simulation results were used to elucidate the physics of the temperature-dependent in-plane diffusion. The good agreement between the results of current simulations and previous theoretical studies demonstrates the effectiveness and reliability of free energy simulation with the enhanced ab initio molecular dynamics in heterogeneous surface processes. For complex situations where a simple harmonic model becomes inappropriate and convergent phase space sampling is required, direct MD simulation with enhanced sampling methods can make important contributions to our understanding of the thermodynamics of the surface catalytic processes.

Keywords: AIMD; Enhanced sampling; ITS; Free energy; surface catalysis

References:

[1] Yang, L.; Liu, C.-W.; Shao, Q.; Zhang, J.; Gao, Y. Q. *Acc. Chem. Res.* **2015**, **48**: 947.
[2] Chen, Z.-N.; Shen, L.; Yang, M.; Fu, G.; Hu, H. *J. Phys. Chem. C* **2015**, **119**: 26422.
[3] Xie, L; Shen, L.; Chen, Z.-N.; Yang, M. *J. Chem. Phys.* **2017**, **146**: 024103.

甲烷的氢同位素效应对于 Cl+CH_4/CHD_3反应影响研究

陈震，陈荣军，杨家岳，张冬，吴国荣*，张东辉*，杨学明*

中国科学院大连化学物理研究所分子反应动力学国家重点实验室，大连，116023

*Email: xmyang@dicp.ac.cn

氯原子对于臭氧层有很强的破坏作用，因此氯原子相关的反应是大气化学中重要的一部分。近几十年来，随着交叉分子束技术和激光光谱技术的发展，我们能够更加深刻的揭示此类基元反应的特征和机理[1]。对于基元反应的认识，我们已经达到了从反应物分子的量子态到产物的量子态相关的态-态分辨的水平。我们利用自行搭建的交叉分子束设备[2]分别研究了2.3kcal/mol到6.9kcal/mol的碰撞能下，Cl+CH_4和Cl+CHD_3的反应。借助共振增强多光子电离(REMPI)和时间切片-离子速度成像技术(TS-VMI)，我们得到了基态产物CH_3和CD_3的速度分布和角分布图像。初步的实验结果表明，不论是CH_3还是CD_3，它们总的信号强度都会随着碰撞能的增加而增大，角分布的峰值也会逐渐向甲基的前向移动，但是相同碰撞能下CH_3和CD_3在角分布的具体细节略有不同。

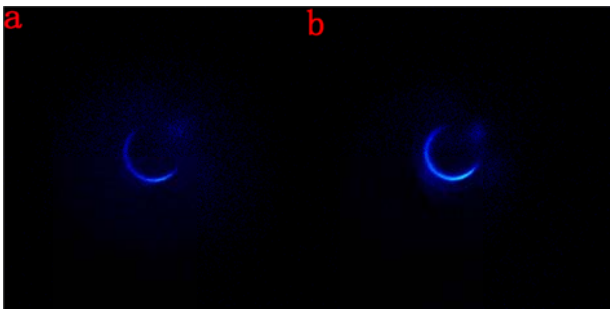

Fig. 1 Raw image of ground state CH_3 and CD_3 when E_c=3.9kcal/mol (a.CH_3 b.CD_3)

关键词：交叉分子束；离子成像；基元反应；同位素效应

参考文献

[1] J. Zhou, B. Zhang, J. J. Lin & K. Liu; Molecular Physics Vol. 103, Iss.13,2005

[2] Guorong Wu, Weiqing Zhang, Huilin Pan, Quan Shuai, Bo Jiang, Dongxu Dai, Xueming Yang; Rev. Sci. Instrum. 79, 094104 (2008).

REMPI/MATI Spectra and Theoretical Calculations of 2-Methoxypyridine and 2-(N-methylamino)pyridine: The Conformational Effect

Wenshuai Dai[1,2], Sheng Liu[1,2], Min Cheng[1], Yikui Du[1,*], Qihe Zhu[1]

[1] Beijing National laboratory of molecular Science, State Key laboratory of Molecular Reaction Dynamics, Institute of Chemistry, Chinese Academy of Sciences, Beijing, 100190, China

[2] University of Chinese Academy of Sciences, Beijing, 100049, China

*Email: ydu@iccas.ac.cn

The vibrational spectra of 2-methoxypyridine (2MOP) and 2-(N-methylamino)pyridine (2NMP) in the first electronically excited (S_1) and cationic ground (D_0) states are obtained by resonance-enhanced multi-photon ionization (REMPI) and mass-analyzed threshold ionization (MATI) spectroscopies. The experimental results reveal that there are *cis* and *trans* conformers in the S_0, S_1, and D_0 states of 2NMP. Whereas, only *cis* conformer can be detected for the 2MOP as predicted by the relaxed potential energy curve. The adiabatic ionization energies of 2MOP, *cis* 2NMP and *trans* 2NMP are measured to be 69379, 62518 and 62709 cm^{-1} with an uncertainty of about 5 cm^{-1}. Unlike 2MOP and *trans* 2NMP, more prominent low-frequency peaks in the REMPI spectrum of *cis* 2NMP are observed and most of them are due to the motions of methylamino, indicating remarkable geometrical changes at methylamino group between the S_1(or D_0) state and S_0 state of *cis* 2NMP. The *ab initio* and density functional theory calculations are performed to predict the optimized geometries and vibrational frequencies of 2MOP and the two 2NMP conformers. It is found that a geometrical distortion along $\tau(CH_3)$ mode has occurred distinctly during the electronic excitation of *cis* 2NMP, i.e. the almost staggered(s) methyl in the S_0 state becomes an eclipsed(e) conformer in the S_1 and D_0 state. The MATI spectra suggest that the molecular geometries of these conformers in the D_0 state are similar to those in the S_1 state. The natural bond orbital (NBO) and electron density topology are also performed to explain the s/e conformational effect in different electronic states of *cis* 2NMP.

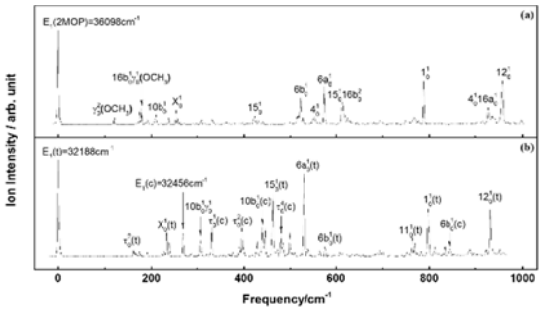

Fig. 1 Observed 1C-R2PI spectra of 2MOP, *cis* and *trans* 2NMP conformers

Keywords: 2-methoxypyridine; 2-(N-methylamino)pyridine; REMPI; MATI; conformer

Simplest *N*-sulfonylamine HNSO

Guohai Deng[1], Joseph S. Francisco[2,*], Xiaoqing Zeng[1,*]

[1]College of Chemistry, Chemical Engineering and Materials Science, Soochow University, Suzhou, 215123, China

[2]Department of Chemistry, Purdue University, West Lafayette, Indiana 47907, USA.

*Email: xqzeng@suda.edu.cn, francisc@purdue.edu.

The simplest *N*-sulfonylamine $HNSO_2$ has been generated in the gas phase through flash vacuum pyrolysis of methoxysulfonyl azide $CH_3OS(O)_2N_3$. Its identification was accomplished by combining matrix-isolation IR spectroscopy and quantum chemical calculations. Both experimental and theoretical evidences suggest a stepwise decomposition of the azide via the methoxysulfonyl nitrene $CH_3OS(O)_2N$, observed in the 193 nm laser photolysis of the azide, with concerted fragmentation into CH_2O and $HNSO_2$. Upon the 193 nm laser irradiation, $HNSO_2$ isomerizes into the novel *N*-hydroxysulfinylamine HONSO.

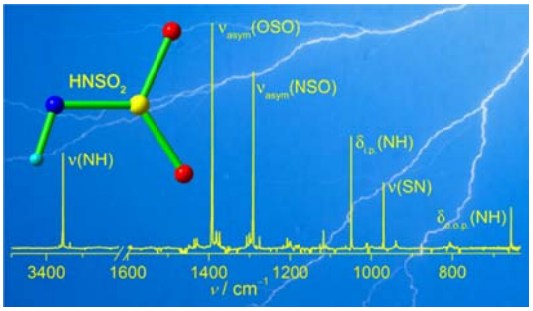

Fig. 1 Ne-matrix IR spectrum of the flash vacuum pyrolysis products of $CH_3OS(O)_2N_3$

Keywords: *N*-sulfonylamine; flash vacuum pyrolysis; sulfonyl azide; matrix-isolation IR spectroscopy; quantum chemical calculation.

References:

[1] Dyke, J. M.; Levita, G.; Morris, A.; Ogden, J. S.; Dias, A. A.; Algarra, M.; Santos, J. P.; Costa, M. L.; Rodrigues, P.; Andrade, M. M.; Barros, M. T. *Chem. –Eur. J.* **2005**, **11**, 1665.

[2] Zeng, X. Q.; Beckers, H.; Willner, H. *Angew. Chem., Int. Ed*. **2013**, **52**, 7981.

吸附物相互作用对甲酸分解火山形曲面的影响

丁晨[1]，陈征[1]，王鹤[1]，徐昕[1,*]

[1]复旦大学化学系，上海，200433

*Email：xxchem@fudan.edu.cn

甲酸可以通过多相催化分解生成 H_2，提供清洁、可再生的氢能源，但副反应会生成不期望的 CO[1]。因此研究甲酸催化分解的机理，对理性搜索设计兼顾活性和选择性的催化剂具有重要意义。Nørskov 课题组在不考虑吸附物相互作用的前提下，通过线性缩放关系结合微动力学模拟描绘了活性与选择性火山形曲面，并预测了金属、合金的催化性能，提供了理性设计催化剂的道路[2]。但已有研究显示，表面吸附物种的相互作用可能对反应的热力学与动力学产生显著影响[3]。基于此，我们在 Nørskov 课题组的工作基础之上，进一步引入吸附物相互作用，结合我们课题组最新开发的自洽动力学蒙特卡罗方法（Self-Consistent Kinetic Monte Carlo, SC-KMC）[4]，探究了这类作用对甲酸催化分解反应机理的影响。研究发现，在表面高 CO*或高 HCOO*覆盖度区域，相互作用会对物种吸附能力、物种覆盖度、反应路径、反应速率、活性、选择性均有不同程度的影响。与不考虑相互作用的火山形曲面相比，H_2 活性普遍显著提升，但 CO 选择性在很大范围内也有增大的现象，且趋势发生了根本性的变化。两者改变了火山形曲面上可选催化剂的范围。由此可见，吸附物相互作用的引入对理论上更准确地描述催化过程是必不可少的，为理性设计催化剂提供更进一步的基础。

关键词：甲酸；动力学模拟；吸附物相互作用

参考文献

[1] Singh, A. K.; Singh, S.; Kumar, A. *Catal. Sci. Technol.* **2016**, **338**: 12.

[2] Yoo, J. S.; Ablid-Pedersen, F.; Nørskov, J. K.; Studt, F. *ACS Catal.* **2014**, **4**: 1226.

[3] Li, H. P.; Fu, G.; Xu, X. *Phys. Chem. Chem. Phys.* **2012**, **14**: 16686.

[4] Chen Z.; Wang H.; Su N. Q.; Xu X. in preparing.

二次谐波研究偶氮苯分子衍生物在石墨烯表面的电催化反应

董斌[1, 2]，白锐朋[1, 2]，郭源[1, 2, *]，张贞[1, 2*]

[1] 中国科学院化学研究所北京分子科学国家实验室，北京市海淀区中关村北一街 2 号，100190

[2] 中国科学院大学，北京市石景山区玉泉路 19 号（甲），100049

[*]Email: guoyuan@iccas.ac.cn; zhangz@iccas.ac.cn

石墨烯是目前自然科学诸多领域研究得最为广泛的二维材料之一，其独特的晶格结构使得它在电子、信息、能源、环境和催化等领域具有广阔的应用前景。石墨烯的电化学活性位的分布均一，且具有良好的热导和电导特性，有利于催化反应的进行，因此在电催化领域研究中具有巨大的潜在应用价值。但石墨烯的表/界面电化学反应机理的原位研究尚不多见，光学非线性二次谐波技术能够在分子水平上原位、无损检测电极界面分子反应机理。目前，采用该技术研究石墨烯表面无机金属离子吸附以及质子转移的分子机理仅有两篇报道[1,2]。本文报道了使用光学二次谐波技术研究 Si(111) 单晶界面单层石墨烯电极反应机理。研究发现：该电极表面 SHG 信号随电极表面电势变化不同于单纯的 Si(111)电极表面的电势依赖规律。在此基础之上，我们使用该技术进一步研究石墨烯表面偶氮苯分子衍生物 DAAB 分子的原位电催化反应过程，期望进一步了解 DAAB 分子在石墨烯表面的吸附、分子取向及催化过程的分子机理。

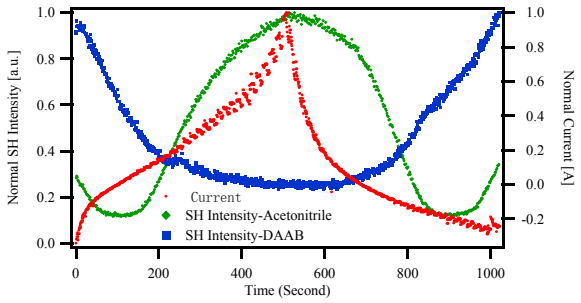

Fig.1 Second harmonic signals with p detection as a function of potential for acetonitrile and DAAB at the Si (111) and graphene interface. Red: Current changes with the potential changes; Blue: SH signals of DAAB on graphene interface; Green: SH signals of acetonitrile on Si (111) interface.

关键词：石墨烯；偶氮苯分子衍生物；电化学；二次谐波

参考文献

[1]Achtyl, J. L.; Vlassiouk, I. V.; Fulvio, P. F.; Mahurin, S. M.; 1Geiger, F. M., J Am Chem Soc 2013, 135, 979-981.

[2]Achtyl, J. L.; Unocic, R. R.; Xu, L. J.; Cai, Y.; Geiger, F. M., Nat Commum 2015, 6, 6539.

Shell thickness dependence of plasmon-induced hot electron injection process in Core/Shell Au@CdS Nanocrystals

Huifang Dong[1], Hailong Chen[1,*], Yuxiang Weng[1], Jingwen Feng[2], Jia Liu[2], Jiatao Zhang[2]

[1]Key Laboratory of Soft Matter Physics of CAS, Institute of Physics, Beijing, 100190, China.
[2]School of Materials Science, Beijing Institute of Technology, Beijing, 100081, China
*Email: hlchen@iphy.ac.cn

Finding the essential mechanism for hot electron injection of metal-semiconductor is of of vital importance for improving the solar energy utilization ratio in photocatalytic devices. Femtosecond transient absorption spectroscopy is used to detect a series of Au@CdS nanocrystals to explore the shell thickness dependence of plasmon-induced hot electron injection process. The interface of Au core and CdS shell forms a Schottky junction. As depicted in Figure 1: Plasmon induced hot electrons in Au core are excited from the occupied levels below the Fermi energy to unoccupied levels above the Fermi energy. Electron distribution joint density of state (EDJDOS) gives the distribution of hot electrons in Au core, but the hot electrons will cool down in a few 100fs due to electron-electron scattering. So hot electrons must arrive at the CdS shell before lossing energy, then the hot electrons with enough energy above Schottky barrier potential can inject into the CdS shell. A highly significant finding exists in our study: the shell thickness can change the height of the Schottky barrier, thus injection efficiency could be tuned by changing the CdS shell thickness.

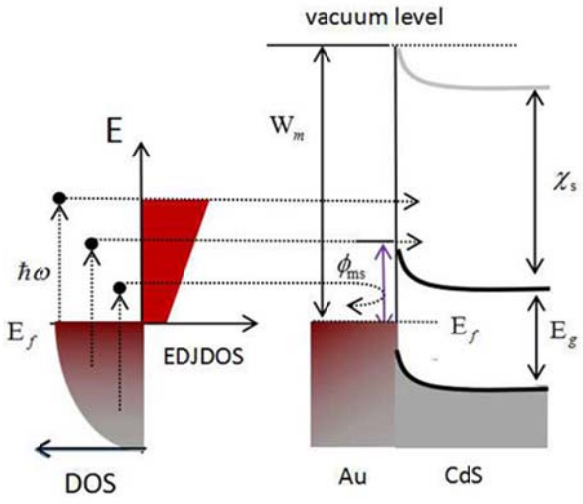

Fig. 1 Process of hot electrons' generation and injection in the Au@CdS.

Keywords: Plasmon; Femtosecond Transient Absorption Spectroscopy; EDJDOS; Schottky barrier; Hot electron injection.

References:

[1] Cesar Clavero, Nature Photonics. **2013**, **238**: 101038.
[2] Thomas P. White; Kylie R. Catchpole, Applied Physics letters. **2012**, **101**: 073905.

Kinetics of absorption of carbon dioxide in aqueous N,N-dimethylethanolamine solutions with carbonic anhydrase

Cunbin Du, Jian Wang*, Hongkun Zhao

College of Chemistry & Chemical Engineering, YangZhou University, YangZhou, Jiangsu 225002, People's Republic of China
*E-mail: wjhg@yzu.edu.cn

In the present work the absorption of carbon dioxide in 1000 $mol \cdot m^{-3}$ N,N-dimethylethanolamine (DMEA) solutions with carbonic anhydrase has been studied in a stirred cell reactor in the temperature range 278-343 K and carbonic anhydrase concentrations ranging from 0 to 1600 $g \cdot m^{-3}$. Based on the results with DMEA, the observed kinetics as a function of the CA concentration and temperature are described. The results showed that the empirical equation could predict the absorption rate constant within an acceptable accuracy.

Keywords: DMEA; Kinetics; Carbonic anhydrase

References:

[1] Alicia, G.; Diego, G.; Ana, B; Jose, M.; Antonio, R. *Ind. Eng. Chem. Res.* **2013**, **52**: 13432.

The Influence of Water in the Photogeneration and Properties of a Bifunctional Quinone Methide

Lili Du,[†] Xiting Zhang,[†] Jiadan Xue,[‡] Jiangrui Zhu,[§] Yuxiang Weng,[§] Yun-Liang Li,*[§] and David Lee Phillips*[†]

†Department of Chemistry, University of Hong Kong, Pokfulam Road, Hong Kong S.A.R., P. R. China

‡Department of Chemistry, Zhejiang Sci-Tech University, Hangzhou 310018, P. R. China

§Key Laboratory of Soft Matter Physics, Institute of Physics, Chinese Academy of Sciences, Beijing 100190, P. R. China

*Email: yunliangli@iphy.ac.cn; phillips@hku.hk

Quinone methides (QM) are crucial reactive species in molecular biology and organic chemistry, with little known regarding the mechanism(s) for the generation of short-lived reactive QM intermediates from relevant precursors in aqueous solutions. In this study, several time-resolved spectroscopy methods were used to directly examine the photophysics and photochemical pathways of 1,1′-(2,2′-dihydroxy-1,1′-binaphthyl-6,6′-diyl) bis (N,N,N-trimethylmethanaminium) bromide (BQMP-b) from initial photoexcitation to the generation of the key reactive binol QM intermediate (BQM) in aqueous solution. The fluorescence of BQMP-b is effectively quenched with a small amount of water which suggests an excited state intramolecular proton transfer (ESIPT) occurs. The kinetics isotope effects observed in femtosecond and nanosecond time-resolved transient absorption experiments provide evidence for the participation of water molecules in the BQMP-b singlet excited state ESIPT process and in the subsequent –HNMe3+ group release and ground state intramolecular proton transfer that give rise to production of the reactive BQM intermediate. Nanosecond time-resolved resonance Raman (ns-TR3) measurements were also employed to investigate the structure and properties of several intermediates including the key reactive BQM in aqueous solution. The ns-TR3 and density functional theory (DFT) computational results were compared and this indicates the binol moiety and water molecules both have important roles in the characteristics and structure of the key reactive BQM intermediate produced from BQMP-b. The results presented here also provide new benchmark characterization of bifunctional quinone methides intermediates that can be utilized to guide direct time-resolved spectroscopic study of the alkylation and interstrand cross-linking reactions of quinone methides with DNA in the future.

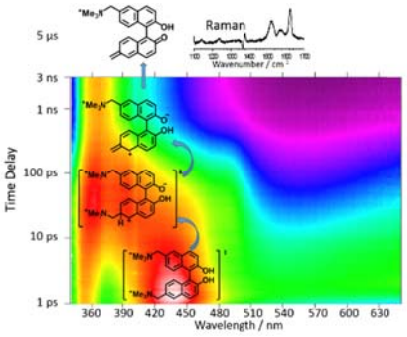

The thermal decomposition of nitrate/nitrite based molten salt and observation of N2O emitting

Zejie Fei[1], Yanli Li[1], Yu Zhang[2], Hongtao Liu[1*]

[1]Shanghai Institute of Applied Physics, Chinese Academy of Sciences, Shanghai 201800, China

[2]ShanghaiEBITlaboratory, Modernphysicsinstitute, FudanUniversity, Shanghai 200433, China

*Email: liuhongtao@sinap.ac.cn

The thermal stability of the solar salt (60%wt NaNO3-40%wt KNO3) and sodium nitrite was carried out from room temperature to a few degrees above the melting temperature (solar salt at 220℃and sodium nitrite at 271℃)in present work. A home-made in situ salt vaporization oven combined with time of flight mass spectrometer (TOF-MS) was designed for gas components detection. The evolution of gases from the molten nitrate/nitrite salt were investigated and the results of the mass spectrum shown that thermal decomposition reaction of the nitrate/nitrite salt took place above melting point, the gas products include N2, NO and N2O, the main production of the molten solar salt and molten sodium nitrite salt is NO and N2, respectively; No O2 or NO2 were detected by the TOF-MS in the intrinsic reaction at the temperature below 300℃; The possible salt decomposition reaction mechanisms were proposed to be , and .

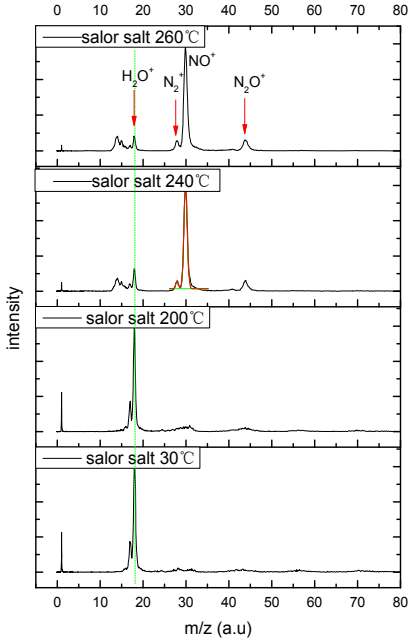

Fig.1 Mass spectra of the evolutions of gas from the molten solar salt (60%wt $NaNO_3$-40%wt KNO_3) change at different temperature points, the H_2O^+ is from the background and the new materials come out at the temperature above 220℃.

Keywords: Thermal energy storge; Thermal stability; Molten salts; Time of flight mass spectrometer; Thermal decomposition

Difluoroacetyl Azide: Synthesis, Characterization, and Decomposition

Ruijuan Feng[1], Zhuang Wu[1], Xiaoqing Zeng[1,*]

[1]College of Chemistry, Chemical Engineering and Materials Science, Soochow University, Suzhou 215123 (China).

*E-mail: xqzeng@suda.edu.cn

Difluoroacetyl azide, $CHF_2C(O)N_3$, has been synthesized and characterized. The azide decomposes slowly at room temperature (300 K) into N_2 and difluoromethyl isocyanate CHF_2NCO, which has also been isolated as neat substance and fully characterized. The elusive intermediate in the stepwise Curtius-rearrangement of the azide, difluoroacetyl nitrene $CHF_2C(O)N$, is observed by IR spectroscopy in the 193 nm laser photolysis of the azide in solid Ne matrix at 2.8 K. Unexpectedly, flash vacuum pyrolysis (FVP) of $CHF_2C(O)N_3$ in Ar (1:1000) at 500 K yields a novel carbonyl isocyanide FC(O)NC with N_2, HF, FCN, CO, and traces of CHF_2NCO. Subsequent irradiation (193 nm) of the pyrolysis products results in the rearrangement of FC(O)NC to FC(O)CN. According to the quantum chemical calculations (B3LYP and CCSD(T)), the azide $CHF_2C(O)N_3$ prefers concerted Curtius rearrangement with minor contribution of the stepwise decomposition. The thermally generated CHF_2NCO eliminates HF and forms FC(O)NC solely under the pyrolysis conditions, whereas, no HF-elimination occurs to isolated CHF_2NCO even at 1000 K due to a formidable activation barrier.

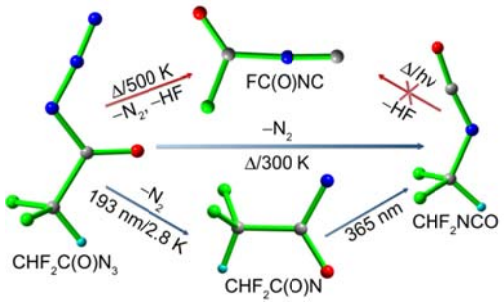

Keywords: Azides; Flash vacuum pyrolysis; Photochemistry; Reactive intermediates; Matrix isolation.

References:

[1] Zeng, X.Q.; Bernhardt, E.; Beckers, H.; Banert, K.; Hagedorn, M.; Liu, H.L. *Angew. Chem. Int. Ed*. **2013, 52**: 3503-3506.

[2] Sun, H.L.; Zhu, B.F.; Wu, Z.; Zeng, X.Q.; Beckers, H.; Jenks, W.S. *J. Org. Chem.* **2015, 80**: 2006–2009.

Product-pairs correlations in molecule-molecule inelastic collisions

Z. Gao, S. N. Vogels, Tijs Karman, Matthieu Besemer ,Gerrit Groenenboom, Ad van der Avoird, S. Y. T. van de Meerakker

Radboud University, The Netherlands

In molecule-molecule inelastic collision experiments, the added degree of complexity offers opportunities to address dynamical questions, product pair correlation is one of them. Measuring product pairs correlation have been proven extremely challenging, the measurement data of it is still lacking.

Our combination of Stark decelerator and velocity map imaging allow us to study molecule-atom collision at very high resolution(1, 2). Recently we extend this technique to molecule-molecule collision and the product pairs correlation was observed in several molecule-molecule inelastic collision systems.

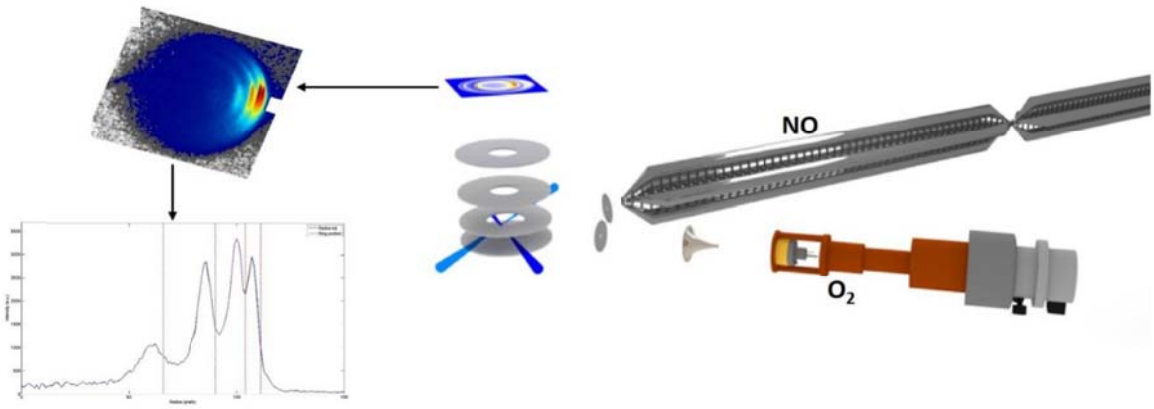

References:

[1].S. N. Vogels *et al.*, Imaging resonances in low-energy NO-He inelastic collisions. *Science* **350**, 787 (Nov 13, 2015).

[2].A. von Zastrow *et al.*, State-resolved diffraction oscillations imaged for inelastic collisions of NO radicals with He, Ne and Ar. *Nat Chem* **6**, 216 (Mar, 2014).

NaSCN 在水中溶解的微观机理研究

宫士炎[1]，杨斌[1]，王鹏[1]，徐西玲[1]，许洪光[1]，郑卫军[1,*]

[1] 中国科学院化学研究所，北京市海淀区中关村北一街 2 号，100190

*Email: zhengwj@iccas.ac.cn

采用激光溅射方法，将NaSCN溅射出来与水结合，再用质量门筛选出想要的离子，通过光电子能谱测量NaSCN加水团簇的垂直脱附能（VDE），之后采用密度泛函计算NaSCN+水团簇的能量，得到不同结构下VDE的值，与实验比对得到NaSCN和水结合较稳定的结构，可以知道Na正离子和SCN负离子之间的距离，从而得出NaSCN变为溶剂分离离子对最少需要几个水分子，进而研究离子与水分子之间的相互作用。

关键词：光电子能谱；密度泛函；NaSCN；离子对

Probing laser-induced heterogeneous microenvironment changes in room temperature ionic liquids

Renjun Ma,[1,2] Boxuan Li[*,1,2] ,Qianjin Guo[*,1,2] and Andong Xia[*,1,2]

[1]Beijing National Laboratory for Molecular Sciences (BNLMS), Key Laboratory of Photochemistry, Institute of Chemistry, Chinese Academy of Sciences, Beijing 100190, People's Republic of China

[2]University of Chinese Academy of Sciences, Beijing 100049, People's Republic of China

Modulating heterogeneous microenvironment in room temperature ionic liquids (RTILs) by external stimuli is an important approach for understanding and designing the external field induced chemical reactions in natural and applicable systems. Here, we report for the first time the redistribution of oxygen molecules related to microsctructure changes in RTILs induced by external laser field, which is probed simultaneously by triplet state dynamics of porphyrin. A remarkably long-lived triplet state of porphyrin is observed with the changes of microstructures after irradiation, suggesting that more charge-shifted O_2 induced by external field and/or rearranged intrinsic ions move from nonpolar domains into the polar domains of RTILs through electrostatic interactions. The results here suggest that the heterogeneous systems like ionic liquids upon external stimuli can be designed for those reaction systems associated with not only for O_2 but also for CO_2, CS_2, etc. and many other similar solvent molecules for many promising applications.

Keywords: Structural heterogeneity, room temperature ionic liquids (RTILs), molecular probe, porphyrin, triplet state

References:

[1].Wang, X. L. *et al.* Operando NMR spectroscopic analysis of proton transfer in heterogeneous photocatalytic reactions. *Nat. Commun.* **7**, 11918 (2016).

[2].Zhang, P., Gong, Y., Li, H., Chen, Z. & Wang, Y. Solvent-free aerobic oxidation of hydrocarbons and alcohols with Pd@N-doped carbon from glucose. *Nat. Commun.* **4**, 1593 (2013).

[3].Zhong, H. *et al.* Mass spectrometric monitoring of interfacial photoelectron transfer and imaging of active crystalline facets of semiconductors. *Nat. Commun.* **8**, 14524 (2017).

DPC 分子激发态分子间双质子转移的理论研究

韩建慧，刘晓春，石英*

吉林大学原子与分子物理研究所，吉林省长春市前进大街 2699 号，130012

*Email: shi_ying@jlu.edu.cn

激发 态分子间双质子转移过程是近年来物理和化学领域的热门研究课题之一。具有激发态双质子转移性质的分子可以用于开发有机发光材料，受到人们的广泛关注。我们采用密度泛函理论（DFT）和含时密度泛函理论（TD-DFT）对 dipyrido [2,3-a:3',2'-i] carbazole （DPC）分子在乙醇溶剂中的激发态双质子转移过程进行了研究。

研究结果表明：DPC 单体不能形成氢键，因此不发生质子转移反应。当加入乙醇溶剂后，单体与乙醇间形成了复合物 DPC-EtOH，该复合物具有 2 个分子间氢键。通过比较复合物基态和激发态氢键键长变化，红外光谱以及非共价相互作用，证实了激发态分子间氢键增强。DPC 单体的高对称性使得 HOMO、LUMO 轨道电荷对称分布（Fig. 1）。相比于单体，复合物 LUMO 轨道的电荷从苯环右侧移向了复合物 N_2 原子附近，使得左侧苯环电荷增多更易于质子转移。因此，乙醇溶剂的参与有助于激发态双质子转移的发生。

通过比较复合物在逐步、协同机理下的基态和激发态势能曲线，表明激发态分子间氢键能够降低反应的势垒，使得激发态双质子转移反应比基态更容易发生。在激发态中，双质子转移反应通过协同机理发生是最合理的模式。

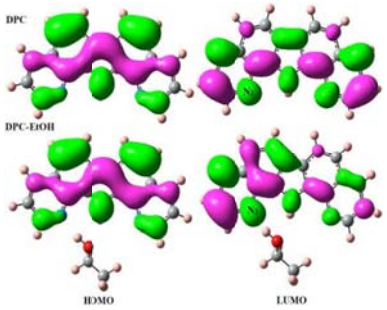

Fig. 1 Frontier molecular orbitals of DPC monomer and DPC-EtOH complex.

关键词： 激发态；双质子转移；氢键；含时密度泛函理论

Controllable Synthesis and Excited-State Dynamics of Organometal Halide Perovskite Quantum Dots

Sheng He, Shengye Jin*

Dalian Institute of Chemical Physics, Chinese Academy of Sciences, 457 Zhongshan Road, Dalian, 116023

*Email: sjin@dicp.ac.cn

Organometal halide perovskite quantum dot is one of the newly reported semiconductor materials with excellent photoelectric properties, such as high quantum yield, tunable band gap varying with size and consistent. With such characters, these quantum dots can make important contributions to the development of solar cells, photocatalysis and light-emitting device. However, the main barrier of its development is the weak stability. Thus, relevant photoelectric dynamics study are rare, which is, however, very meaningful and fundamental for these materials' application. In this article, we discussed various methods to prepare methylammonium lead halide($CH_3NH_3PbX_3$, $MAPbX_3$，X=Cl, Br, I) perovskite quantum dots and improved the reported synthesis method. We also put forward a new method to make anion-blended $MAPbX_3$ quantum dots by anion exchanging. Using transient absorption spectroscopy, we studied the lifetime(4.84±0.07 ns) of $MAPbBr_3$ quantum dots at excited state with only one exciton in every dot. Also, we observed charge transfer from $MAPbBr_3$ quantum dots to benzoquinone(as the electron acceptor). At the same time, we prepared nanowires self-assembled by $MAPbBr_3$ nanoplatelets with the wire length at the level of micrometer, and studied them with time-resolved and photoluminescence-scanned confocal microscopy, but no carrier diffusion along the nanowire was observed. These synthesis and photoelectric dynamics research will offer fundamental support for the application of the organolead halide perovskite quantum dots.

Keywords: perovskite; quantum dots; transient absorption spectroscopy

含脯氨酸多肽的气相解离动力学研究

霍妲雨佳，海滢，祖莉莉*

北京师范大学化学学院，北京，100875

*Email: zull@bnu.edu.cn

脯氨酸是20种常见氨基酸中唯一的亚氨基酸，其支链参与形成五元环，环状结构位于多肽的骨架上限制了N-C$^{\alpha}$键的转动；在能量上，脯氨酸的存在不利于β折叠构象的形成，进而影响蛋白质的结构及功能。碱性精氨酸与脯氨酸相邻的情况在一些具有应用前景的多肽类药物中普遍存在，如血管舒缓肽、神经肽substance P等。探究精氨酸等碱性氨基酸位于脯氨酸邻位的多肽解离动力学，可以为这类多肽药物在生物体内的降解提供信息，为其修饰提供依据，也可为含Arg-Pro的蛋白质质谱检测提供一定的帮助。

我们采用电喷雾电离技术研究了AAAPAA，AARPAA，AAKPAA等寡肽在气相碰撞诱导解离（CID）条件下的解离情况，通过研究不同解离能时碎片离子的种类和丰度得出精氨酸对脯氨酸N端指示作用的影响。实验结果表明：精氨酸在一定程度上抑制了脯氨酸的N端指示效应。另外，我们运用DFT理论计算方法获得了多肽及其解离产物的稳定构象，并结合质谱实验结果对多肽解离机理进行了推测。

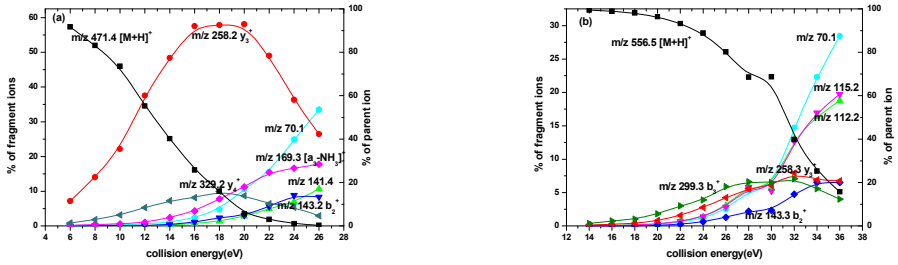

Fig. 1 CID breakdown graphs of protonated peptides: (a) AAAPAA, (b) AARPAA.

关键词： 脯氨酸；精氨酸；多肽；碰撞诱导解离；解离机理

参考文献

[1] Chiu, C. C.; Singh, S.; de Pablo, J. J. *Biophys. J.* **2013**, **5**: 1227-1235.

[2] Zeng, W. C.; Zhang, W. H.; He, Q.; Shi, B. *Process Biochem.* **2015**, **50**: 948-954.

[3] Bleiholder, C.; Suhai, S.; Harrison, A. G.; Paizs, B. *J. Am. Soc. Mass Spectr.* **2011**, **6**: 1032-1039.

[4] Deblase, A. F.; Harrilal, C. P.; Lawler, J. T.; Burke, N. L.; Mcluckey, S. A.; Zwiere, T. S. *J. Am. Chem. Soc.* **2017**, **139**: 5481-5493.

基于 AND/甲醇推进剂的甲醇和 NOX 化学反应动力学研究

姜延欢，李国岫*，刘星，李洪萌

北京交通大学，北京 100044

*Email: 14116371@bjtu.edu.cn

本文基于高性能绿色无毒AND/甲醇推进剂研究甲醇和NO_X的化学反应动力学。通过对气相AND分子进行量化计算，构建三种不同的分子结构，基于最稳定的最稳定的结构对展开AND的分解研究。并基于AND的分解产物，研究产物中的NO_X与甲醇的化学反应。研究表明：NO和NO_2是AND分解的主要产物，甲醇和NO_2反应更剧烈。初始温度大于900K时，甲醇和NO2反应稳定后的温度更高。且NO和NO_2与甲醇反应的主要消耗路径相同，均为CH_3OH→CH2OH（CH_3O）→CH_2O→CHO→CO→CO_2。

关键词：ADN； 甲醇； NOX； 分子结构； 量化计算

参考文献

[1] Jr AMF, Carberry J.J, Treacy J. C. *J AM Chem Soc*, **1953, 75(15)**:3786.

[2] Silverwood R, Thomas J H. Transactions of the Faraday Society,**1967,63**:2476.

[3] Sellchiro K, Kota Y, Jun O, Kazuo A, *Environ Sci Technol*.**1985,19**:262.

[4] Hajlme A, Hlroo T. *Environ Sci Technol*,**1986, 20(4)**:397.

[5] 宋蔷, 何百磊, 杨小勇, 陈昌和, 徐旭常.工程热物理学报, **2003, 24(1)**:145.

钙钛矿薄膜与电荷受体之间界面电荷转移的超快动力学研究

冷静，刘俊学，金盛烨*

中国科学院大连化学物理研究所，分子反应动力学国家重点实验室，大连，116023

*Email: sjin@dicp.ac.cn

钙钛矿（$MAPbX_3$, $MA=CH_3NH_3^+$, X=Cl, Br, I）材料由于在光电器件的优异表现引起了人们的广泛关注。在钙钛矿太阳能电池中，快速的电荷转移（CT）是实现高效电荷分离的一个重要条件。过去，人们已对钙钛矿薄膜与常见电荷受体之间的界面CT过程进行了大量研究，获得许多转移速率数据[1-4]；然而，这些不同研究小组报道的CT时间数据却相差很大，从亚皮秒到数百皮秒，甚至数纳秒。这些巨大的差异严重地阻碍了人们对钙钛矿太阳能电池中的界面CT过程及其本征作用的理解。

在钙钛矿太阳能电池中，光诱导的整个CT过程实际上包含电荷从薄膜内部到电极表面的迁移以及电荷在电极表面的转移两个过程；而前者明显与钙钛矿薄膜中的载流子迁移率和薄膜厚度有关。为了澄清这种薄膜内电荷扩散和本征的界面CT对整个光诱导的CT过程的贡献，我们采用飞秒瞬态吸收光谱（fs-TAS）技术研究了从钙钛矿薄膜到电子受体（PCBM）和空穴受体（spiro-OMeTAD）的CT动力学的薄膜厚度依赖性。结合扩散耦合的CT动力学模拟，我们发现钙钛矿薄膜到PCBM和spiro-OMeTAD的本征界面CT速率分别约为1.7×10^{11} s^{-1}（6 ps）和1.2×10^{11} s^{-1}（8 ps），而其光生电荷从薄膜内部扩散到界面大约需要200 ps到数纳秒（依赖于薄膜厚度），表明钙钛矿薄膜中的CT应该是一个扩散控制过程[5]。

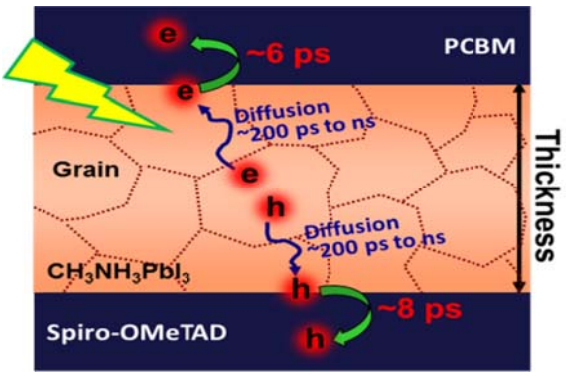

Fig. 1 Schematic diagram of charge diffusion and interfacial CT in perovskite solar cell.

关键词：钙钛矿；太阳能电池；电荷转移；飞秒瞬态吸收光谱

参考文献

[1] Xing, G. C.; Mathews, N.; Sun, S. Y.; Lim, S. S.; *et al.* ***Science***, 2013, 342, 344.

[2] Ponseca, C. S..; Hutter, E. M.; Piatkowski, P.; Cohen, B.; *et al.* ***J. Am. Chem. Soc.***, 2015, 137, 16043.

[3] Zhu, Z. L.; Ma, J. A.; Wang, Z. L.; Mu, C.; *et al.* ***J. Am. Chem. Soc.***, 2014, 136, 3760

[4] Marchioro, A.; Teuscher, J.; Friedrich, D.; Kunst, M.; *et al.* ***Nat. Photonics***, 2014, 8, 250.

[5] Leng, J., Liu, J., Zhang, J., Jin, S., ***J. Phys. Chem. Lett.***, **2016**, **7**: 5056.

State-to-state reaction dynamics of Al + O_2 → AlO + O studied by a crossed-beam time-sliced velocity map ion imaging apparatus

Fangfang Li, Changwu Dong, Jiaxing Liu, Yujie Ma, Fengyan Wang*
Department of Chemistry, Fudan University, Shanghai, 200433
*Email: fengyanwang@fudan.edu.cn

Dynamics of the reaction, Al($^2P_{1/2,3/2}$) + O_2($X^3\Sigma g$-) → AlO($X^2\Sigma^+$) + O(^3P_J), was studied at two collisional energies, 1.5 and 2.3 kcal/mol, with the newly built crossed molecular beam apparatus in combination with time-sliced velocity map ion imaging technique. The supersonic Al atomic beam was generated by laser ablation method with Ar or N_2 as carrier gas, and then crossed O_2 supersonic beam at an intersection angle of 90°. The formed AlO products were state-selectively detected by (1+1) resonance-enhanced multiphoton ionization via AlO ($D^2\Sigma^+$–$X^2\Sigma^+$) transition. Accordingly, the slice images of AlO ($X^2\Sigma^+$, *v', J'*) were recorded at various rotational and vibrational states. From the slice images the speed distributions and differential cross sections of state-specific AlO($X^2\Sigma^+$) and O(^3P_J) coproducts were directly obtained. The observed correlation between reactant velocity *k*, product velocity *k'* and rotational angular momentum *J'* will provide plentiful information on the oxidation dynamics of the Al atoms.

Keyword: slice imaging, crossed beam, laser ablation, state-to-state reaction dynamics

References:

[1] Changwu, Dong; Jia xing, Liu; Fangfang Li, Fengyan, Wang. *Chin. J. Chem. Phys.* 2016, 29(1): 109.
[2] Wang, Fengyan; Lin, Jui-San; Liu, Kopin. *J. Chem. Phys.* 2014,140(8): 084202

Neural Network-based Global *ab initio* Potential Energy Surface for the $2^1A''$ State of $C(^1D)+H_2$ Reactive System

Fengyi Li[1,2], H Ma[1,+], W Bian[1,2,*]

[1]Institute of Chemistry, Chinese Academy of Sciences,
No.2 Zhongguancun North First Street, Haidian District, Beijing, 100190
[2]University of Chinese Academy of Sciences,
No.19 (A) Yuquan Road,Shijingshan District, Beijing, 100049
[+]Email: mht@iccas.ac.cn
*Email: bian@iccas.ac.cn

The typical atom-diatom insertion reaction $C(^1D) + H_2 \rightarrow CH(^2\Pi) + H(^2S)$ plays a significant role in the hydrocarbon combustion and astrophysics of interstellar medium.[1,2] A new *ab initio* potential energy surface (PES) for the $2^1A''$ state of the $C(^1D)+H_2$ reactive system has been constructed in the present work. It is based upon *ab initio* calculations using the internally contracted multi-reference configuration interaction approach with the aug-cc-pVQZ basis set, performed at about 7000 symmetry unique geometries. [2] The Back-Propagation Neural Network [3] algorithm, which was widely used in different fields recently,[4] is employed and refined in the PES fitting processes. For different PES regions, variant numbers of network parameters have been employed to approach the best performance and avoid overfitting at the same time, and these regions were connected with switching functions to produce the final global PES. We found the fitted potentials to be smooth and without artificial oscillations. The root mean square error (RMSE) is less than 35.0 cm^{-1} for the global PES, and less than 10 cm^{-1} for the dynamically important regions. An accurate description of important regions around conical intersection were also achieved on this new surface (A cut of the PES in this region is shown in Fig.1).

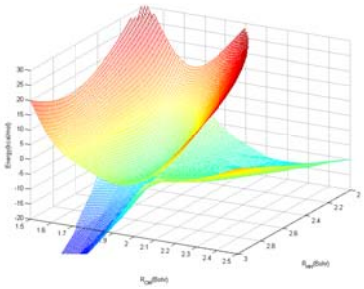

Fig. 1 A cut of the PES for the $2^1A''$ state (above) and the $1^1A''$ state (below) in the region around the HCH conical intersection as functions of R_{HH} and R_{CM} (distance between C atom and the center of H_2 molecule) . The energy of the $C(^1D)+H_2$ asymptote is taken to be zero.

Keywords: insertion reaction；potential energy surface；neural network；machine learning

References:

[1] Shen, Z.; Ma, H.; Zhang, C.; Fu, M.; Wu, Y.; Bian, W. Nature Communications, **2017, 8**:14094.
[2] Zhang, C.; Fu, M.; Shen, Z.; Ma, H.; Bian, W. *J. Chem. Phys*. **2014, 140**; 234301.
[3] Jiang, B.; Guo, H. *J. Chem. Phys.* **2013, 139**; 054112.
[4] M. T. Hagan and M. B. Menhaj. *IEEE Trans. Neural Netw.* **1994, 5**; 989.

Thermal decomposition mechanisms of three methyl anisoles

Lu Li[1], Gang Li [1], Hongjun Fan[1,*]

[1] State Key Laboratory of Molecular Reaction Dynamics, Dalian Institute of Chemical Physics, Chinese Academy of Sciences, Dalian, 116023

*Email: fanhj@dicp.ac.cn

Phenyl ethers serve as the model compounds for the low-rank coal and lignin from biomass.[1] The thermal decomposition of three methyl anisole isomers (*o*-, *m*-, and *p*-methyl anisole) were investigated at low pressure (below 15 Pa) within temperature range from 473 to 1473 K. The pyrolytic phenomena were studied by using vacuum ultraviolet single-photon ionization time-of-flight mass spectrometry (SPI-TOFMS) to identify the intermediates, radicals, and products, and the relative concentration profiles of the pyrolytic products were evaluated by the semiquantitative analysis method. Experimental results suggested that the pyrolytic pathways of three model compounds were analogous, and the bond homolysis of *o*-/*m*-/*p*-PhO-CH_3 to generate phenoxy radicals was the initial reaction for all three methyl substituted anisoles.Moreover, the concentration of m/z 106 showed extraordinary differences can be ascribed to the different position of substituted methyl group on the benzene ring. The energies required for abstracting a hydrogen atom from phenoxy radicals in this progress were calculated by theoretical methods, and the theoretical results gave satisfied explanation to the experimental phenomenon. Noteworthy, the isomerization reaction played a significant role in the pyrolysis of *m*-methyl anisole.

Keywords: methyl anisoles; thermal decomposition; SPI-TOFMS; theoretical methods

References:

[1] Li G.; Li, L.; Shi, L.; Ji, LJ. *Energy and Fuels.* **2014**, **28**: 980-986.

Diffusion Pathways of Atomic Hydrogen Adsorption on Defective Iron Surfaces

Yuanjie Li，Xiangjian Shen*，Yi-fan Han*

[1] Research Center of Heterogeneous Catalysis and Engineering Sciences, School of Chemical Engineering and Energy,Zhengzhou University, Zhengzhou 450001, China

*Email: xjshen85@zzu.edu.cn,yifanhan@ecust.edu.cn

Diffusion pathways of atomic hydrogen from surface into subsurface of defective iron with point defects have been shown due to its significance in heterogeneous hydrogenation catalytic surface reactions. To construct the highly-accurate potential energy surfaces(PESs) of hydrogen diffusion on defective iron surfaces, we interpolate *ab initio* energy points(1500~2000 for each surface) by using cubic spline approach. Through globally searching out the diffusion pathways of atomic hydrogen from surface into subsurface, it is found that atomic hydrogen diffusion pathways on defective iron surfaces are obviously enhanced with much lower adsorption energies. Importantly, the diffusion barriers of atomic hydrogen from surface into subsurface are decreased in comparison with that on perfect surface. Furthermore, these adsorbed energies and geometries of atomic hydrogen have been identified by using density functional theory method under considering the surface relaxation effect.

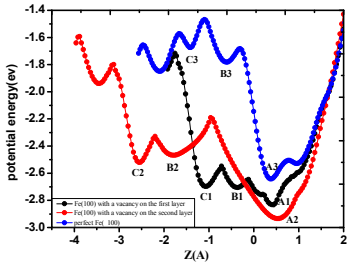

Fig. 1 Minimum energy diffusion pathways for hydrogen on Fe(100) from surface into subsurface

Keywords: diffusion pathways; defective surface; potential energy surface; hydrogen-Fe system

References:

[1] Shen, X.; Tanguy, D.; Connetable, D. *Phil. Mag.* **2014**,**94**: 2247.

[2] Shen, X.; Chen, J.; Sun, Y.; Liang, T. *Surf. Sci.* **2016**,**654**: 48.

[3] Shen, X.; Li, Y.; Liu, X.; Zhang, D.; Gao, J.; Liang, T. *Phys. Chem. Chem. Phys.* **2017**,**19**: 3557.

[4] Goikoetxea, I.; Alducin, M.; Diez Mui~no, R.; Juaristi, J. *Phys. Chem. Chem. Phys.* **2012**,**14**: 7471.

[5] Ferrin, P.; Kandoi, S.; Nilekar, A.; Mavrikakis, M. *Surf. Sci.* **2012**,**606**: 679

高温熔盐原位结构研究

苏涛，刘舒婷，刘一阳，刘洪涛*

中国科学院上海应用物理研究所，熔盐化学与工程技术部，上海，201800

*Email: liuhongtao@sinap.ac.cn

熔盐在电化学冶金、聚焦型太阳能热发电和第四代核能技术之一的熔盐反应堆等领域具有非常重要的应用价值。而开展熔盐物理化学研究，特别是高温熔盐微观结构的研究，对于深入认识熔盐的宏观热物性如粘度、电导率、传蓄热性能，新型多元熔盐的设计与制备，以及熔盐与材料相互作用和腐蚀防护技术有重要意义。高温熔融盐环境中，盐分子通常是以完全电离的离子形态存在而形成离子液体，正、负离子通过静电吸引形成动态壳层结构。但是很多配位性强的高价态金属离子在高温熔融环境中仍存在$[M^{a+}L_b]^{(b-a)-}$型配位结构。理论计算表明，熔盐中金属离子的配位结构存在配体-配体动态交换过程，配位结构稳定存在时间和中心离子极化能力以及与配体之间成键的“共价性”密切相关，配体负离子交换时间一般在皮秒量级。金属离子的配位数和多元熔盐体系的组成、温度等密切相关，另外一些共价性强的离子体系还存在具有M-L-M桥键的团簇结构以及网络结构的高粘度玻璃体。本文主要介绍熔盐原位结构的谱学方法，包括X-射线，紫外-可见和红外吸收光谱，激光拉曼和荧光光谱，高温熔盐核磁共振谱等。其中针对高温熔盐环境和强腐蚀性，设计和研制了相关熔盐原位结构研究的谱学装置，并开展了液态核燃料相关氟化熔盐吸收光谱初步研究，如图是四氟化铀在氟化锂-氟化钠-氟化钾（FLiNaK）三元盐中的吸收光谱，其中暴露在空气中的四价铀离子U^{4+}被氧化为铀酰离子UO_2^{2+}（左），

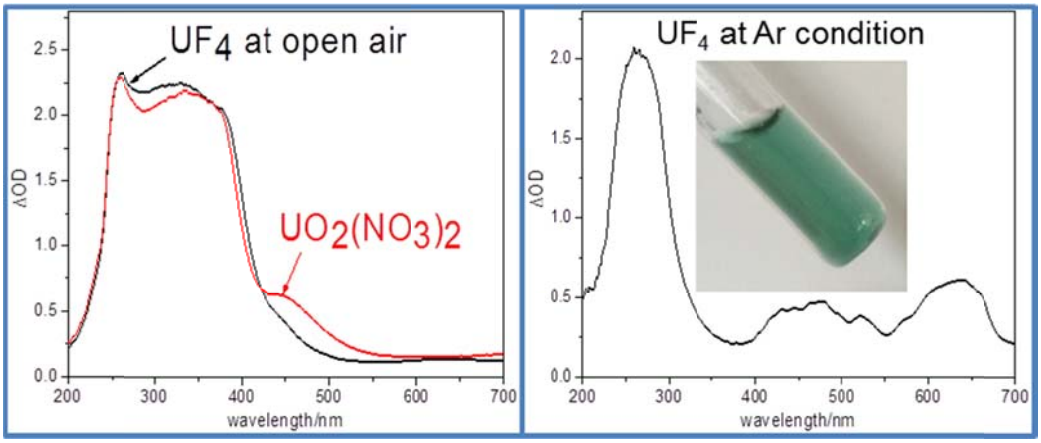

Fig. 1 Absorption spectra of UF_4 in FLiNaK molten salt

关键词：熔盐；吸收光谱；四氟化铀；铀酰离子；

High-Dimensional Atomistic Neural Network for Potential Energy Surface of HCl Intereacting with Au (111)

Qinghua Liu[1], Xueyao Zhou[1], Brain Kolb[2], Xuan Luo[1], Bin Jiang[1,*]

[1] Department of Chemical Physics, University of Science and Technology of China, Hefei, Anhui 230026, China

*Email: bjiangch@ustc.edu.cn

Ab initio molecular dynamics (AIMD) simulations of molecule−surface interactions allow first-principles characterization of the dynamics. However, the large number of density functional theory calculations along the trajectories is very costly, limiting simulations of long-time events and giving rise to poor statistics. To avoid this computational bottleneck, we constructed a high-dimensional potential energy surface (PES) for the interaction between Au (111) and HCl molecule using neural networks method based on roughly 180000 energies generated by extensive density functional theory (DFT) calculations. We focus on the reaction potential energy surface, and fit a potential energy surface which can well describe the reaction. Classical Trajectory calculations for the scattering and reaction are both studied, and it is found well in consistency with ab initio molecular methods dynamics (AIMD) results.

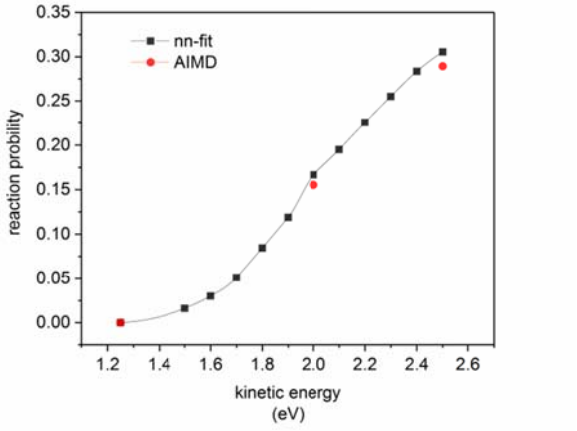

Fig 1. Zero coverage sticking probability (S0) of DCl on Au (111) surface using AIMD (red circles) compared to PES fitted by neural network

Keywords: potential energy surface; neural network; DFT calculations;

References:

[1] Brain Kolb; Xuan luo; Xueyao Zhou. *Journal of Physical Chemistry Letters,* **2017**, **8**: 666.

[2] Liu TianHui; FU BiNa ;Zhang DongH. *Science China Chemistry*. **2014, 57**:147.

[3] Gernot Fu chsel; Marcos del Cueto; Cristina Díaz; Geert-Jan Kroes. *Journal of Physical Chemistry C.* **2016, 120**:25760**.**

甲基环己烷高温裂解机理的理论研究

刘雅兰[1]，丁俊霞[1,*]

[1] 中国科学院大连化学物理研究所，辽宁省大连市沙河口区中山路 457 号，邮编 116023

*Email: liuyl@dicp.ac.cn

甲基环己烷是最简单的烷基化环烷烃，并且经常作为喷气发动机燃料中环烷烃的代表来进行研究[1]。本文主要采用ReaxFF [2]反应性力场研究了甲基环己烷的高温裂解的微观反应机理。其次采用B3LYP/6-311G(d,p)和ReaxFF的理论方法计算了主要的初始反应通道的能量。通过分析其裂解的初始反应通道及其比例，得到了甲基环己烷高温裂解的主要初始反应通道。接着对裂解过程中主要物种的分布，中间反应过程及其动力学行为的分析从而获得了甲基环己烷裂解的动态化学过程，尤其是对实验上尚不明晰的中间体的反应机制在原子水平上给予详尽的描述，并且为建立精确的燃烧动力学模型提供可靠的参考。

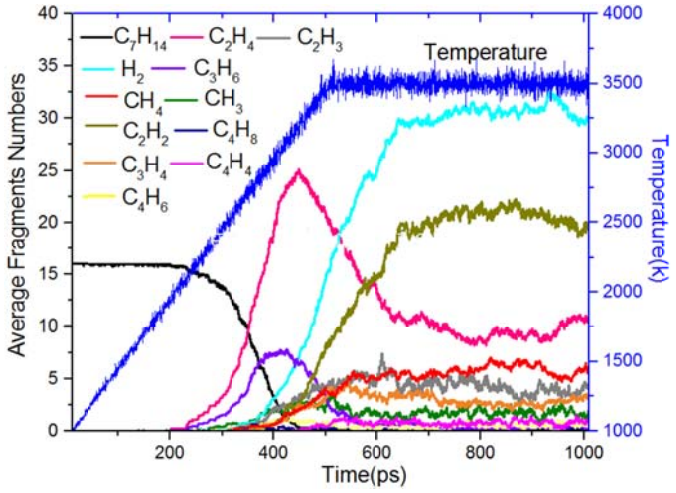

Fig. 1 Time evolution of the main compounds observed during RMD simulation of the sixteen MCH molecules at a density of 0.17g/cm^3. The blue line denotes the temperature profile during simulations.

关键词： 甲基环己烷；高温裂解；微观机理

参考文献

[1] Orme, J. P.; Curran, H. J.; Simmie, M. *J. Phys. Chem. A.* **2006**, 110: 114.

[2] Van Duin, A. C. T.; Dasgupta, S.; Lorant, F. et al. *J. Phys. Chem. A.* **2001**, 105, 9396.

基于 C_2H_2-Ne 体系全维精确势能面的碰撞传能的理论研究

刘洋，李军*

重庆大学化学化工学院, 401331

*Email: jli15@cqu.edu.cn

基于神经网络势能面(PIP-NN PES)和 Lennard-Jones 势能面，采用经典动力学方法研究两种势能面碰撞传能的情况。其中，总的势能面为 C_2H_2 的势能面加上 C_2H_2 和 Ne 相互作用势能面。[1]在 CCSD(T)-F12a/cc-pVTZ-F12 水平上计算相互作用部分的势能面，并且考虑了基组重叠误差 (BSSE)。[2]最终选取 41270 个结构，并进行从头算计算，采用 PIP-NN 方法拟合势能面，拟合均方根误差为 1.04meV。碰撞传能研究表明高能碰撞时 LJ 势能面和 PIP-NN 势能面的结果相差不大，低能碰撞时势能面影响明显。

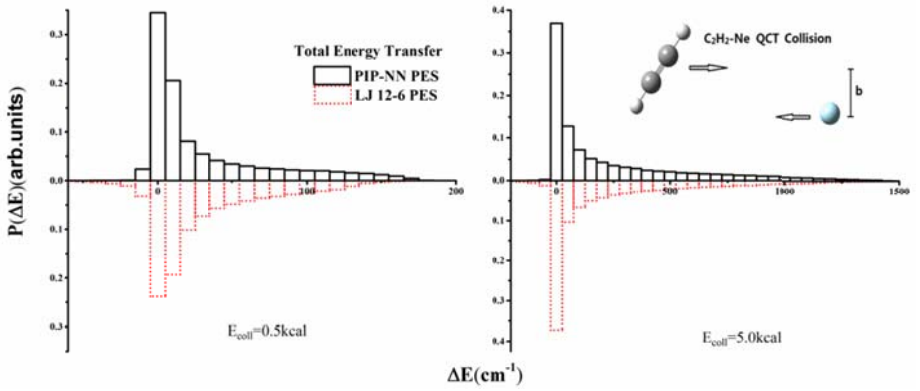

图 1. 振动能和转动能量变化之和的分布情况。

关键词：PIP-NN；碰撞传能；碰撞参数；Lennard-Jones 参数

参考文献

[1] J. Li and H. Guo, *J. Chem. Phys.* **2015, 143**:214304.

[2] M. Gutowski and G. Chalasinski, *J. Chem. Phys.* **1993, 98**:5540.

[3] R. Conte, P. L. Houston, and J. M. Bowman, *J. Phys. Chem. A* **2014, 161**:101.

$HO + CO \rightarrow H + CO_2$ 体系的化学反应动力学研究

卢丹丹，李军*

重庆大学化学化工学院 401331

*Email: jli15@cqu.edu.cn

$HO + CO \rightarrow H + CO_2$ 在燃烧和大气环境中扮演着重要角色。最近，我们采用对易不变多项式结合神经网络的方法重新构建了该体系的全维精确势能面。该势能面是该体系迄今为止最精确的全维势能面。基于该势能面，采用准经典轨线方法对该体系重新进行了反应动力学计算。具体地，起始反应物在振转基态，分别计算了 $H^{18}O + CO \rightarrow H + {}^{18}OCO$ 反应在碰撞能为 7、11.5、13.0、13.9、14.5、17.0、22.0 kcal/mol 时的积分截面(ICS)和微分截面(DCS)，并探讨了详细的微观动力学机理。理论模拟结果与实验吻合，特别地，理论计算的产物角度分布与实验吻合。

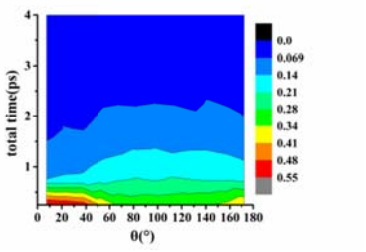

Fig. 1 . The correlation between the total simulation time and the scattering angle at Ec=13.9 kcal/mol for the reaction $H^{18}O + CO \rightarrow H + {}^{18}OCO$

关键词：积分截面；微分截面；化学反应动力学

参考文献

[1] Nguyen, T.L.; Xue, B.C.; Weston, R.E., J. Phys. Chem. Lett. 2012, 3: 1549−1553.

[2] Li, J.; Chen J.; Zhang, D.H., J. Chem. Phys. 2014, 140: 044327.

[3] Alagia, M.; Balucani, N.; Casavecchia, P., J. Chem. Phys. 1993, 98: 8341.

An accurate full-dimensional potential energy surface and quasiclassical trajectory study of the H + H_2O_2 reaction

Xiaoxiao Lu[1,2], Xing-an Wang[2], Bina Fu[1,*], Donghui Zhang[1,*]

[1]State Key Laboratory of Molecular Reaction Dynamics and Center for Theoretical and Computational Chemistry, Dalian Institute of Chemical Physics, Chinese Academy of Sciences, Zhongshan Road 457, Dalian, 116023

[2]Department of Chemical Physics, University of Science and Technology of China, Jinzhai Road 96, Hefei, 230026

*Email: bina@dicp.ac.cn, zhangdh@dicp.ac.cn

A new global, full-dimensional ground-state potential energy surface (PES) of the H+H_2O_2 multichannel reaction was constructed using fundamental invariant neural network (FI-NN) approach based on 114790 geometries. The corresponding *ab initio* energies were calculated at UCCSD(T)-F12b/aug-cc-pVTZ level of theory and the PES was accurately fitted with a root mean squre error (RMSE) of 5.7 meV. Extensive quasiclassical trajectory (QCT) calculations were carried out on the new PES at the collision energy (Ec) of 15.0 kcal/mol. The product branching ratios together with the scattering angular and translational energy distributions of H_2 + HO_2 and OH + H_2O product channels were calculated. It was found that the both reaction channels proceeds with the abstraction mechanism. The rate coefficients for the title reaction at 300K ≤T ≤1000K on the FI-NN PES were also calculated with the QCT approach, and were compared with the available experimental values.

Keywords: FI-NN; PES; QCT

References:

[1] Shao, K.; Chen, J.; Zhao, Z.; Zhang, D. H., *J. Chem. Phys.* **2016**, **145**: 071101.

Reactive and nonreactive scattering of CO_2 on Ni(100) with a Generalized Langevin Oscillator Model

Xuan Luo[1], Xueyao Zhou[1], Bin Jiang[1,*]

[1]Department of Chemical Physics, University of Science and Technology of China, Hefei, Anhui 230026

*Email: bjiangch@ustc.edu.cn

Dissociative chemisorption of CO_2 on the metal has attracted an increasing interest in recent years thanks to its importance in CO_2 reduction and activation related to global warming. We recently investigated the dissociation dynamics of CO_2 on Ni(100) based on a first-principles potential energy surface (PES)[1]. However, the calculations were based on adiabatic and rigid surface approximation neglecting energy transfer to electron-hole pairs (EHPs) and surface phonons. In order to account for the effect of energy exchange between the CO_2 and Ni(100) we present here the quasi-classical trajectory (QCT) calculations based on the generalized Langevin oscillator(GLO) model and local density friction approximation (LDFA). It has been shown that, in spite of its simplicity, the GLO model was able to qualitatively reproduce the energy transfer to surface phonon described by ab initio molecular dynamics[2]. Furthermore, the energy dissipation due to EHP excitations is generally small.

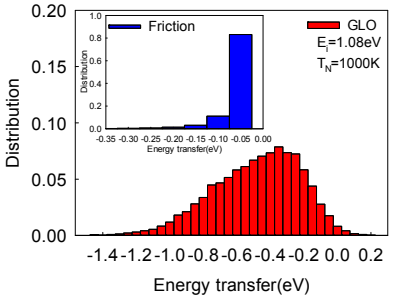

Fig.1 energy transfer distributions to the electron-hole pairs (LDFA, blue) and to surface phonons (GLO, red)

Keywords: CO_2; GLO; EHP(electron-hole pair)

References:

[1] J. I. Juaristi; M. Alducin; R. Díez Muiño; H. F. Busnengo; A. Salin, Phys.Rev. Lett.**2008, 100**, 116102

[2] L. Martin-Gondre; M. Alducin; G. A. Bocan, Phys.Rev.Lett.**2012, 108**, 096101.

CO_2 Diffusion in various carbonated beverages: A molecular dynamics study

Ji Lv[1,2], Jiali Gao[1,2], Yakun Chen[1,*]

[1] Theoretical Chemistry Institute, Jilin University, Changchun, China,130023

[2] Department of Chemistry and Supercomputing Institute, University of Minnesota, Minneapolis, Minnesota 55455

*Email: ykchen@jlu.edu.cn

Although carbonated beverages are mostly enjoyed at leisure, the many physical and chemical processes in them remain clouded at the molecular level. In this article, we employ the molecular dynamics to determine the diffusion coefficient of CO_2 in various carbonated beverages, includes champagne, coke and club soda and to study the structure and dynamics of water. It is clear that water plays an important role in determining the physical and chemical stability of solute in liquid. The addition of solute (such as sucrose) to water causes hydrogen bonding networks change and an increase in liquid viscosity. The resulting degradation in molecular mobility has significant effects on the rates of CO2 diffusion.

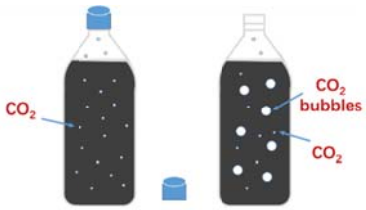

Keywords: Carbonated beverages; diffusion coefficient; CO_2

References:

[1]Liger-Belair, G., et al. Journal of Agricultural and Food Chemistry, 2003. **51**(26): p. 7560-7563.

[2]Bonhommeau, D.A., et al. J Phys Chem Lett, 2014. **5**(24): p. 4232-7.

Insight into the excited-state intramolecular double proton transfer of the 2,5-bis(benzoxazol-2-yl)thiophene-3,4-diol: one-step or stepwise mechanism?

Meiheng Lu[1,2,4], YunfanYang [1], Tianshu Chu[1,3,*]

[1]State Key Laboratory of Molecular Reaction Dynamics, Dalian Institute of Chemical Physics, Chinese Academy of Sciences, 457 Zhongshan Road, Dalian, 116023

[2]College of Applied Chemistry, Shenyang University of Chemical Technology, Eleventh Road, Zhangshi Development Zone, Shenyang, 110142

[3] Institute for Computational Sciences and Engineering, Laboratory of New Fiber Material and Modern Textile, the Growing Base for State Key Laboratory, Qingdao University, 308 Ningxia Road, Qingdao, 266071

[4] University of Chinese Academy of Sciences, No.19(A) Yuquan Road, Shijingshan District, Beijing, 100049

*Email: tschu@dicp.ac.cn

The excited state double proton transfer (ESDPT) mechanism of 2,5-bis(benzoxazol-2-yl)thiophene-3,4-diol, has been theoretically investigated based on the methods of density functional theory (DFT) and time-dependent density functional theory (TDDFT)[1, 2]. Geometric structure comparison and infrared (IR) vibrational spectra analysis confirm that the strengthening of the intramolecular hydrogen bond in the first excited state (S_1) has facilitated the proton transfer process. The frontier molecular orbitals (MOs) analysis illustrates that the nature of the hydrogen bond enhancement lies in the charge redistribution upon photo-excitation, which is further confirmed by NBO charge analysis quantitatively. The reduced dimensionality (two-dimensional) potential energy surfaces (PESs) have been scanned for both the ground state (S_0) and the first electronic excited state to reveal the mechanism and pathway of the two protons being transferred. Compared with the concerted path of proton transfer, the stepwise path with one proton being transferred first then a second one followed exhibits a relatively mild energy barrier and seems to be more rational and favorable.

Fig. 1 Scheme of the ESDPT mechanism

Keywords: Excited-state intramolecular double-proton transfer; Time-dependent density functional theory; Stepwise mechanism; Hydrogen bond strengthening

References:

[1] Lu, M.; Yang, Y.; Chu, T. *Theor. Chem. Acc.* **2017, 136**: 62.

[2] Hao, Y.; Chen, Y. *Dyes Pigment.* **2016, 129**: 186.

维生素 B2 对不饱和脂肪酸在气/液界面上氧化反应动力学影响的非线性光学研究

马滢雪[1]，侯健[1]，郝文英[1]，陆洲[1,*]

[1]中国科学院化学研究所，北京市海淀区中关村北一街 2 号，100190

*Email: zhoulu@iccas.ac.cn

维生素 B2 及其衍生物是生物体中重要的光敏剂，可以诱导许多生物分子光氧化[1]。在体相中，维生素 B2（Riboflavin）可以催化氧化不饱和脂肪酸[2]。本文利用和频振动光谱（SFG）研究了维生素 B2 对不饱和脂肪酸-20 碳烯酸（11c-Eicosenoic acid, EA）在气/液界面氧化动力学的影响。研究发现，EA 在空气/水界面会被逐渐氧化，使和频光谱强度随时间衰减。我们通过监测 2880 cm^{-1} 处 EA 分子的甲基对称伸缩特征峰的光谱强度变化，实时研究 EA 的氧化动力学。在紫外灯的照射下，当 EA 分子面积为 35 $Å^2$ 且亚相为水时，EA 在空气中的氧化速率为 1.54×10^{-4} s^{-1}；相同条件下，亚相为维生素 B2 水溶液时， EA 在空气中的氧化速率降低为 5.25×10^{-5} s^{-1}。当 EA 分子面积为 25 $Å^2$ 且亚相为水时，EA 的氧化速率为 4.2×10^{-5} s^{-1}。数据显示，相同分子面积下，亚相含有维生素 B2 可以减缓界面不饱和脂肪酸的氧化，另外，EA 分子面积为 35 $Å^2$ 且亚相为维生素 B2 时，EA 的氧化速率与 EA 分子面积为 25 $Å^2$ 且亚相为水时 EA 的氧化速率相当。据此，我们推测维生素 B2 降低 EA 的氧化速率的原因是增加了的 EA 在界面上的致密程度。Fig. 2 显示了 EA 在不同条件下的 SFG 光谱，其中 2846 cm^{-1} 和 2880 cm^{-1} 分别为 CH_2 和 CH_3 的对称伸缩振动，CH_3 与 CH_2 的伸缩振动强度的比值（r^+/d^+）越大，说明界面上的膜越致密[3]。由图可以看出，当分子面积 35 $Å^2$ 且亚相为维生素 B2 时的 r^+/d^+ 和分子面积为 25 $Å^2$ 且亚相为水时的 r^+/d^+几乎相当，所以亚相中的维生素 B2 可使膜变得更致密，证实了之前的推测。因此，维生素 B2 可以增加界面上不饱和脂肪酸 EA 的排列致密度，从而降低其在空气中的氧化速率。

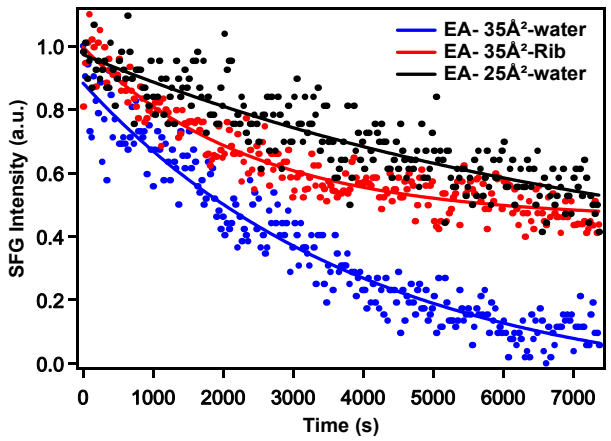

Fig. 1 The Effect of Riboflavin on the Oxidation Kinetics of EA

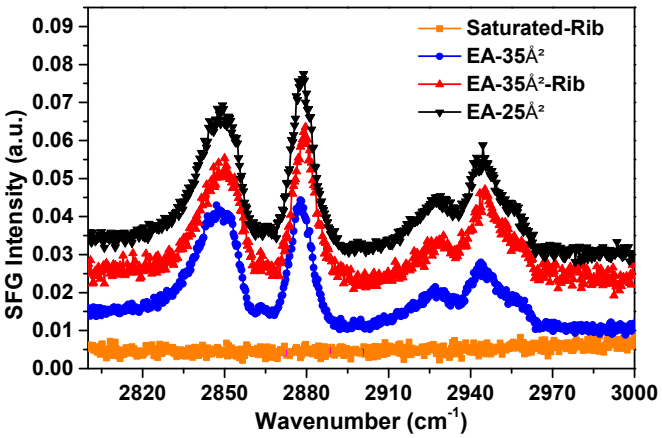

Fig. 2 The Effect of Riboflavin on the SFG spectrum of EA

关键词：氧化动力学；不饱和脂肪酸；和频振动光谱

参考文献

[1] Huvaere, K; Cardoso, D. R. *J. Phys. Chem. B*, **2010, 114**: 5583.

[2] Cardoso, D. R.; Scurachio R.S. *J. Agric. Food Chem.*, **2013**, **61**: 2268

[3] Feng, R.J.; Li, X. *J.Chem. Phys.*, **2016**, **145**: 244707

Reaction dynamics of Al + O_2 → AlO + O studied by a crossed-beam time-sliced velocity map ion imaging apparatus via selective state ionization

Fangfang Li[#], YuJie Ma[#], Jiaxing Liu, Changwu Dong, Fengyan Wang[*]
Department of Chemistry, Collaborative Innovation Centre of Chemistry for Energy Materials, Shanghai Key Laboratory of Molecular Catalysts and Innovative Materials, Fudan University, Shanghai, 200433
[#] These authors contributed equally to this work
*Email:fengyanwang@fudan.edu.cn

The ground state reaction, $Al(^2P_{1/2}) + O_2(X^3) \rightarrow AlO(X^2\Sigma^+) + O(^3P_J)$, was studied at collisional energy 2.4 kcal/mol in our crossed molecular beam and time sliced ion imaging apparatus. The rovibrational states of AlO products were detected via (1+1) resonance-enhanced multiphoton ionization through the intermediate state $D^2\Sigma^+$. Plentiful details were revealed by analyzing the velocity and angular distributions of AlO products. The AlO products were excited to a high vibrational level within the energetically allowed limit. The influence of polarization direction of probe laser to the scattered products were studied by changing the linear polarization direction of the laser from parallel to the reactant relative velocity ***v*** to perpendicular to ***v***. Little alignment effect of the rotational angular momentum of AlO products was observed by comparing the images recorded in the two different polarized directions. All the experimental observations are consistent with the oxidation reaction mechanism suggested with a long-lived complex in comparable with its rotational lifetime.

Keywords: slice imaging, crossed beam, laser ablation, state-to-state reaction dynamics

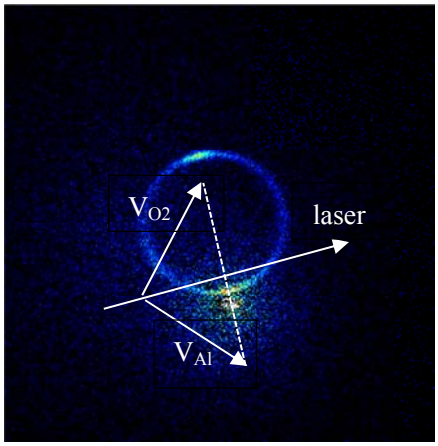

Reaction kinetics of two tertiary amines with CO_2 in aqueous solutions

Zhuangzhuang Yu, Zhiyuan Ma , Jian Wang*, Hongkun Zhao

College of Chemistry & Chemical Engineering, YangZhou University, YangZhou, Jiangsu 225002, People's Republic of China
*Email: wjhg@yzu.edu.cn

In the present work, a stopped-flow apparatus was used to determine the kinetics of the reaction between aqueous solutions of carbon dioxide and N,N-dimethylethanolamine (DMEA) and N-methyldiethanolamine (MDEA) in terms of observed pseudo-first-order rate constant (k_0) and second order reaction rate constant (k_2). The experiments were studied at 293-313 K, with amine concentrations ranging from 0.5 to 4 kmol· m^{-3}. The pK_a of two tertiary amines were also experimentally determined over a temperature range of 288-333 K. The Bronsted relationship between the reaction rate constant obtained from the stopped-flow apparatus and pK_a obtained from experimental determination was then evaluated.

Keywords: CO_2 kinetics; Tertiary amine; Stopped flow

References:

[1] Parag, N.; Prakash, D.; Eugeny, Y. *Chem. Eng. Sci.* **2013**, **100**: 234.

Lattice Effects of Surface Cell: ML-MCTDH Study on Surface Scattering of CO/Cu(100)

Qingyong Meng[1,*], Hans-Dieter Meyer[2,*]

[1] Department of Applied Chemistry, Northwestern Polytechnical University, Youyi West Road 127, 710072 Xi'an, China

[2] Theoretische Chemie, Physikalisch-Chemisches Institut, Ruprecht-Karls Universität, Im Neuenheimer Feld 229, D-69120 Heidelberg, Germany

Email: qingyong.meng@nwpu.edu.cn; hans-dieter.meyer@pci.uni-heidelberg.de

To study the scattering of CO on a movable Cu(100) surface, multilayer multiconfiguration time-dependent Hartree (ML-MCTDH) calculations were performed based on the SAP potential energy surface (PES) in conjunction with a recently developed expansion model for including lattice motion. The surface potential was constructed by a sum of Morse potentials where the parameters were determined through comparing the MCTDH vibration energies with the experimental results. By flux analysis of the ML-MCTDH propagated wave packets, we calculated the sticking probabilities for a series of models as shown in the following Figure 1. From these sticking probabilities, the 6D + 5D/15D calculations predict a slower decrease of sticking with increasing energy as compared to the sticking of the 6D + 0D/3D calculations. This is because the translational energy of CO is more easily transfered to surface vibrations, when the vibrational dimensionality of the surface is enlarged.

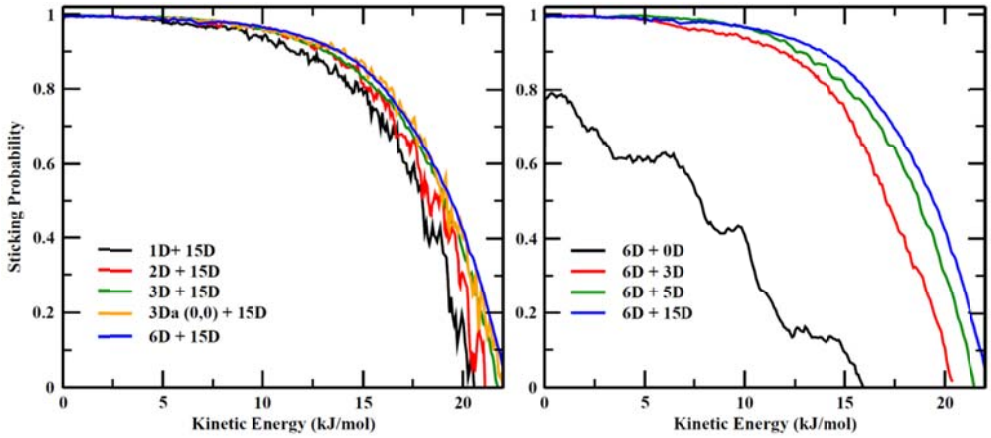

Fig. 1 ML-MCTDH flux analysis results on the CO/Cu(100) surface scattering

Keywords: ML-MCTDH; Molecule-surface coupling; Lattice motion; CO/Cu(100)

References:

[1] Marquardt, R. *et al*. *J. Chem. Phys.* **2010**, **132**: 074108.

[2] Meng, Q.; Meyer, H.-D. *J. Chem. Phys.* **2015**, **143**: 164310.

[3] Meng, Q.; Meyer, H.-D. *J. Chem. Phys.* **2017**, **146**: in press.

溶剂调控的 3-氨基-1, 2, 4-三唑的基态及激发态结构动力学研究

孟双，薛佳丹，赵彦英*，郑旭明*

浙江理工大学化学系，杭州，310018

*Email: yyzhao@zstu.edu.cn

拉曼光谱结合密度泛函理论计算研究研究了3-氨基-1,2,4-三唑(3AT)在不同环境中的构型。FT-IR和Raman光谱表明3AT固体以1H-3AT二聚体的形式存在，其计算结果与实验结果一致。488 nm Raman光谱实验结果发现溶剂中的3AT构型与晶态结构不同，这表明溶剂分子与3AT的相互作用导致了振动模式的位移，如图1所示。结理论计算表明在气相模型下1H-3AT的结构量比2H-3AT低低0.8 kcal/mol。结合PCM溶剂模型对3种能量最低的异构体进行的理论计算，确定了在溶剂中的存在的构象是2H-AT。通过显性溶剂模型计算表明3AT与质子性溶剂甲醇和水分子形成稳定的团簇结构，且溶剂分子有一定的饱和度，其振动模波数的位移及强度变化归因于3AT中的N和NH键与溶剂分子的氢键作用。

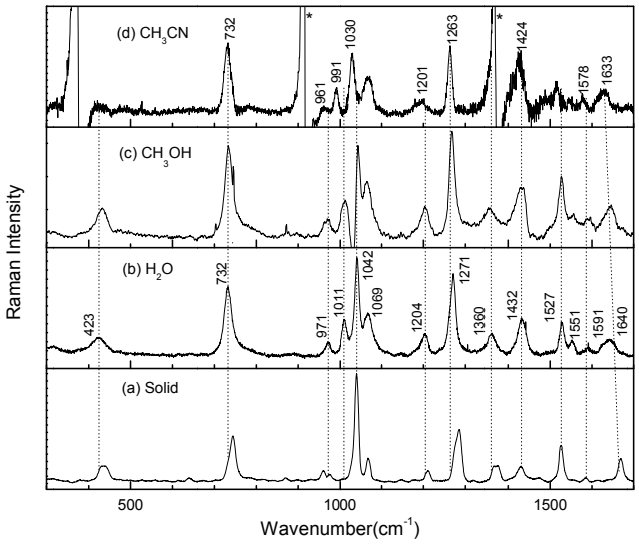

Fig 1. The 488 nm Raman spectra in (a) Solid, (b) CH_3CN, (c) CH_3OH and (d) H_2O of 3AT. (Asterisks mark regions where solvent subtraction artifacts are present.)

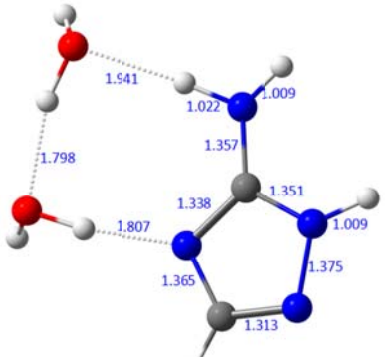

Fig 2. The Optimized cluster structural of 2H-3AT with H_2O.

关键词： 3-氨基-1,2,4-三唑；拉曼光谱；密度泛函计算；氢键作用

参考文献

[1] M. Pagacz-Kostrzewa; R. Bronisz; M. Wierzejewska; Chemical Physics Letters 473 (2009) 238-246.

[2] E.-S.M. Sherif; R. Erasmus; J. Comins; ; Journal of Colloid and Interface Science 309 (2007) 470-477.

液相水分子的超快离化反应动力学

聂兆刚 [1,*]，Loh Zhiheng[2]

[1]广东工业大学，物理与光电工程学院，广州市番禺区广州大学城外环西路 100 号，邮编 510006

[2]Division of Chemistry and Biological Chemistry, School of Physical and Mathematical Sciences, Nanyang Technological University, Singapore 637371, Singapore

*E-mail: zgniegdut@163.com

液相水分子的离化反应在辐射化学和辐射生物学现象中扮演非常重要的角色。然而，受到真空紫外离化激光脉冲贫乏的限制，其离化反应早期动力学过程的诸多细节需要进行更为清晰的描述。我们采用可见和近红外波段的飞秒激光脉冲，诱导了水分子的多光子离化反应，并结合飞秒相干光谱和偏振各项异性测试来观察在离化水分子中的超快电子和离子的动力学过程。首先采用800 nm，30-fs 的激光脉冲离化和检测了早期的包括水合s电子及其溶解前驱体的动力学过程。通过实验我们证实在水分子离化后存在纯的p电子，测定了它衰减到s电子所需要的时间。在水分子离化反应中，质子转移的过程极其短暂，试验上一直很难捕捉到。通过实验，我们得到了价电子运动和质子转移的时间常数。进一步采用500-750 nm，6-fs的激光脉冲离化和检测水合电子的动力学过程。实验观察到叠加在水合电子吸收峰之上的明显振荡(~300 cm^{-1})信号，并通过有窗光谱图(windowed spectrogram)计算发现了这种振荡的“泛音”模式，存在和谐和非和谐两种振荡。紧接着6-fs的激光脉冲和水分子相互作用后，这些属于H_3O^+与水分子之间振荡信号的出现，暗示O—H的解离过程发生在激光与水分子相互作用的6-fs以内。这与我们从头动力学模拟计算的结果(1.8–5.5-fs)高度吻合。观察到的液态水分子O—H键解离过程为我们提供了一个理解在短波脉冲辐照下水溶液和生物组织中光化学反应的切入点。

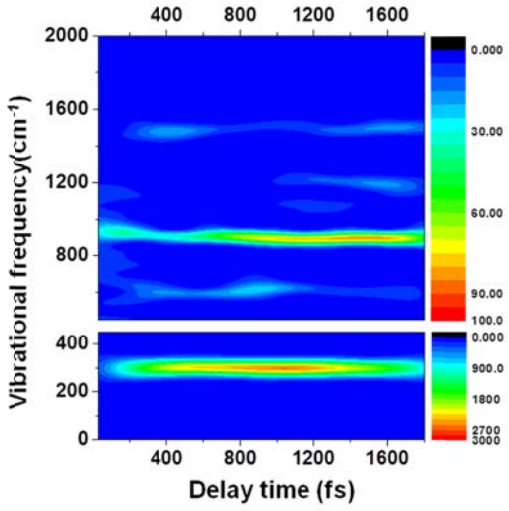

Fig. 1 Spectrogram calculation to show the intermolecular vibrational modes, including their overtones, as a function of delay time. The time trace used for the calculation is probed at 700 nm.

关键词：水分子；超短脉冲；超快激光；离化反应动力学；相干光谱

参考文献

[1] Li, J. L.; Nie, Z. G.; Zheng, Y. Y.; Dong, S. ; Loh, Z. H. *Chem. Phys.* **2011**, **135**: 14304.

[2] Nie, Z. G.; Low, P. J.; Debnath, T.; Chaban, V. V.; Prezhdo O. V.; Loh, Z. H. *J. Am. Chem. Soc.* **2017**, submitted.

Dynamics studies on a new ab initio based potential energy surface of the $H_2S+OH \rightarrow HS+H_2O$ reaction

Leilei Ping, Hongwei Song,* and Minghui Yang*

Wuhan Institute of Physics and Mathematics, Chinese Academy of Sciences, Wuhan 430071, China

hwsong@wipm.ac.cn and yangmh@wipm.ac.cn

The reaction between H_2S and OH to product HS and H_2O plays an important role in the elimination of H_2S in the atmosphere and in the solution of chemical air pollution and global warming[1]. In this work, ~64000 geometries are sampled and the energies are calculated at the level of unrestricted coupled cluster method with singles, doubles, and perturbative triples excitations with the augmented correlation-consistent polarized triple zeta basis set (UCCSD(T)-F12a/AVTZ). Then, the full-dimensional accurate potential energy surface (PES) are constructed by the neural network method. The total root mean squared error of the resulting PES is about 4.74 meV. Finally, the quasi-classical trajectory method is employed to study the reaction dynamics of the title reaction, in which the integral cross section, differential cross section and rate constants are calculated.

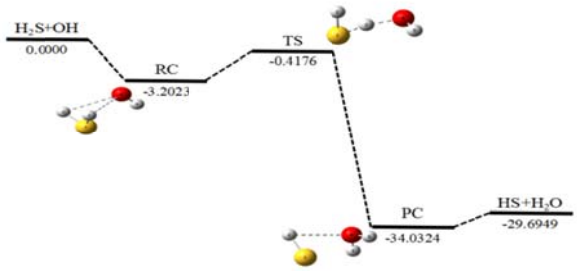

Fig.1 Schematic reaction path and energy (in kcal) for the title reaction.

Keywords: H_2S + OH reaction; full-dimensional; reaction dynamics; neural network

References:

[1] B.A. Ellingson, D.G. Truhlar, Explanation of the unusual temperature dependence of the atmospherically important OH + $H_2S \rightarrow H_2O$ + HS reaction and prediction of the rate constant at combustion temperatures, J. Am. Chem. Soc. 129 (2007) 12765–12771.

硅纳米颗粒大小对表面电荷特性的影响

史亚荣[1]，翁羽翔[1,*]

[1] 软物质实验室，中国科学院物理研究所，北京，100190

[1,*]软物质实验室，中国科学院物理研究所，北京，100190

*Email: yxweng@aphy.iphy.ac.cn

纳米颗粒表面电荷密度在药物输送和细胞吸收起着重要的作用。在本研究中,对不同粒径及浓度的纳米二氧化硅(SiO_2)的Zeta电位进行分析,探讨纳米二氧化硅Zeta电位和粒径大小与表面电荷大小的关系。通过文献可知，粒子表面质子化和去质子化反应通常被用于得到表面电荷，往往受粒子大小和溶液电解质性质的调控。如固定粒子大小，表面电荷的大小通常随pH值或背景盐浓度的增加而增加；本研究通过固定背景盐浓度和pH值, 测定不同粒径SiO_2的Zeta电位，由理论公式推算得到表面电荷的大小。结果表明表面电荷随着纳米粒径的增加而减小,当粒径超过一个临界值时达到一个常数，此变化趋势与理论预测基本一致。

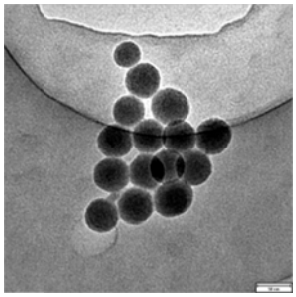

Fig. 1 TEM images of silica nanoparticles. The size of silica nanoparticles is about 60nm in diameter.

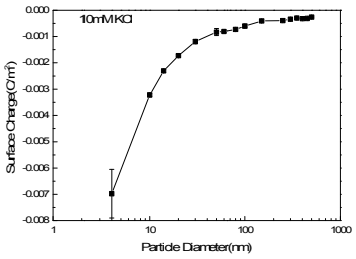

Fig. 2 Surface charge of silica nanoparticles of different sizes as a function of pH in 8.0 and 10mM KCl solutions

关键词：纳米二氧化硅；Zeta电位；表面电荷

参考文献

[1] Barisik M, Atalay S, Beskok A, et al. Size Dependent Surface Charge Properties of Silica Nanoparticles[J]. Journal of Physical Chemistry C, 2014, 118(4):1836-1842..

[2] Atalay S, Ma Y, Qian S. Analytical model for charge properties of silica particles.[J]. Journal of Colloid & Interface Science, 2014, 425(7):128-130.

[3] Behrens S H, Grier D G. The charge of glass and silica surfaces[J]. Journal of Chemical Physics, 2001, 115(14):6716-6721.

[4] Du L C, Huang Y F, Ren B, et al. Photosynthetic Bacterial Light-Harvesting Antenna Complexes Adsorbed on Silica Nanoparticles Revealed by Silica Shell-Isolated Au Nanoparticle-Enhanced Raman Spectroscopy[J]. The Journal of Physical Chemistry C, 2012, 116(12): 6993-6999.

Minding the Gap: Variations on the Bergman Theme.

Cycloaromatization of Penta-, Hepta- and Octa-diynes

Xinli Song, **Bing Zhang**

State key Laboratory of Magnetic Resonance and Atomic and Molecular Physics, Wuhan Institute of Physics and Mathematics, Chinese Academy of Sciences, Wuhan, 430071
*Email: xinli.song@wipm.ac.cn

It is well known that the Bergman Cyclization is one of the most intriguing unimolecular reactions in chemistry, with important applications in organic synthesis and pharmacology. We have studied cycloaromatization of penta-, hepta- and octa-diynes focusing on the effect of electronic and aromatization angle changes on the activation barrier and the heat of reaction. The geometry and frequency calculations were used by BLYP/6-31G* and UBS-BLYP/6-31G* methods; the results were improved through single-point energy coupled-cluster computations [CCSD(T), BD(T)]. As the increase of the aromatization angle, the barrier and reaction heat for cyclization reduced significantly. The cyclization barrier for 1, 6-heptadiyne cation is energetically comparable to that of Bergman Cyclization of (Z)-hexa-3-ene-1, 5-diyne, and the one for 1, 7-octadiyne dication is even much lower. Alternative cycloaromatization modes are predicted and await experimental realization. We try to identify an experimentally accessible system with a low enough cyclization barrier amenable to experimental conditions.

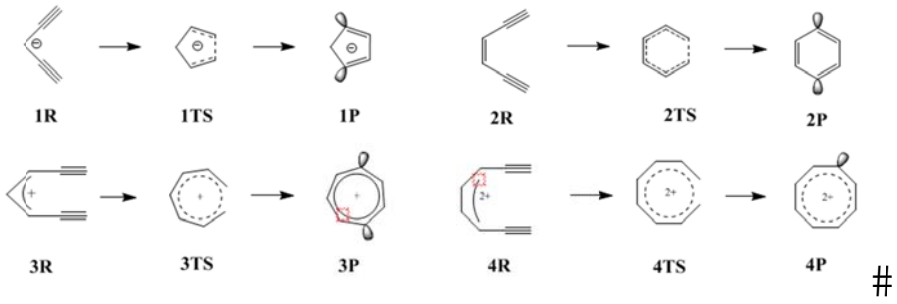

#

Scheme 1. Cycloaromatization of Penta-, Hexa-, Hepta-, and Octa-diynes.

Keywords: Bergman Cyclization, Diradicals, Activation energy, Heat of reaction

References:

[1] Jones, R. R..; Bergman, R. G., *J. Am. Chem. Soc.* **1972**, 94, 660
[2] Kawatkar, S. P.; Schreiner, P. R., *Org. Lett.* **2002**, **4**: 3643.

Cation-Exchange-Induced Reversible Conversion between 3D Cubic Perovskite and 2D Layer-Structured Perovskite

Junhui Wang, Jing Leng, Junxue Liu, Sheng He, Shengye Jin*
State Key Laboratory of Molecular Reaction Dynamics, Dalian Institute of Chemical Physics, Chinese Academy of Sciences, Dalian 116023, China
*Email: sjin@dicp.ac.cn

Two-dimensional (2D) organolead halide perovskites that incorporate hydrophobic organic interlayers offer improved resistance to degradation by moisture, which are proving to be strong contenders for solar cells and other optoelectronic applications. To explore the factors affecting the optoelectronic properties of these materials, we developed a facile cation-exchange method for the reversible transformation from 3D to hybrid or single phase 2D perovskite films. Based on this method, perovskite components in thin films can be tuned from pure 3D to 2D hybrid (containing n =1, 2, 3 and ∞), and pure single-phase (n = 1) by simply adjusting the cation-exchange time. Furthermore, this cation-exchange method is also applicable for the reversible conversion from 2D to 3D perovskite. More importantly, due to the sequential band alignment between different perovskite components in the hybrid 2D perovskite films, the excitons can dissociate by charge transfer into separated electrons and holes with longer lifetimes. Therefore, our cation-exchange reaction will be a promising strategy for 2D perovskite films fabrication and the fabricated hybrid 2D perovskite films with the self-charge-separation property and tunability in perovskite components and carrier dynamics should be more preferred for applications in photovoltaic devices.

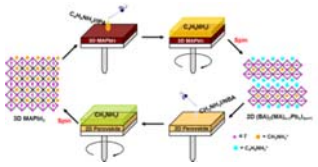

Fig. 1 Schematic diagram of the reversible conversion between 3D $MAPbI_3$ and layered 2D $(BA)_2(MA)_{n-1}Pb_nI_{3n+1}$ perovskites.

Keywords: 2D perovskite; ion-exchange; hybrid components; charge transfer

References:

[1] Tsai, H. H.; Nie, W. Y.; Blancon, J. C.; et al. *Nature* 2016, 536: 312.
[2] Liu, J.; Leng, J.; Wu, K.; Zhang, J.; Jin, S. *J. Am. Chem. Soc.* 2017, 139: 1432.

Construction of Diabatic and Adiabatic Potential Energy Surfaces of Li2 by Multistate Density Functional Theory

MengWang[1], Zexing Qu[1], Jiali Gao[1,2,*]
[1]Institute of theoretical chemistry, Jilin university
No.2 Liutiao Road, Changchun, 130023
[2]Department of Chemistry, Digital Technology Center and Supercomputing Institute
University of Minnesota, Minnesota, 55455
*Email: jiali@jialigao.org

In this study, we describe the total of 26 diabatic states for lithium dimer (Li2) to determine the adiabatic ground state and excited states and their potential energy surfaces using multistate density functional theory (MSDFT). The diabatic states are defined by block localization of Kohn-Sham orbitals, which constrain the valence electronic states for each diabatic state in active orbital space. Their configuration interaction produces the adiabatic ground and excited states. In our diabatic calculations, we use PBEC functional which contains 100% HF exchange and PBE correlation functional. The off-diagonal Hamiltonian matrix element of coupling of two diabatic states is obtained from our constructed transition density. Our obtained potential energy surfaces are in good agreement with the high level theoretical results.

Keywords: Diabatic potential energy surfaces; Adiabatic potential energy surfaces; Lithium dimer; Multistate density functional theory

References:

[1] A. Grofe; Z. Qu; D. G. Truhlar; H. Li and J. Gao. J. Chem. Theory Comput.. **2017, 13**: 1176
[2] Jasik P; Sienkiewicz J E. Chem. Phys. **2006, 323(2)**: 563.

The location of excess electrons on $H_2O/TiO_2(110)$ surface and its role in the surface reactions.

Ruiming Wang [1], Hongjun Fan[1,*]

[1] State Key Laboratory of Molecular Reaction Dynamics, Dalian Institute of Chemical Physics, Chinese Academy of Sciences, Dalian, Liaoning 116023, P. R. China

*Email: fanhj@dicp.ac.cn

Excess electrons play a key role in many of the properties of TiO_2. Understanding their behavior is important for improving the performance of TiO_2 in energy-related applications. Here we describe a DFT+U study of the locations of the unpaired electron (UPE) on rutile $TiO_2(110)$ (R-$TiO_2(110)$) surface and H_2O/R-$TiO_2(110)$ surface. In contrast to previous studies[1-4], we find that the UPE tends to migrate to the surface H_2O-Ti_{5c} with the increasing of H_2O coverage and UPE concentration. In addition, we have shown that the UPE plays an important role in the O-H bond dissociation and other important elementary reactions in photo-catalytic H_2O dissociation on R-$TiO_2(110)$.

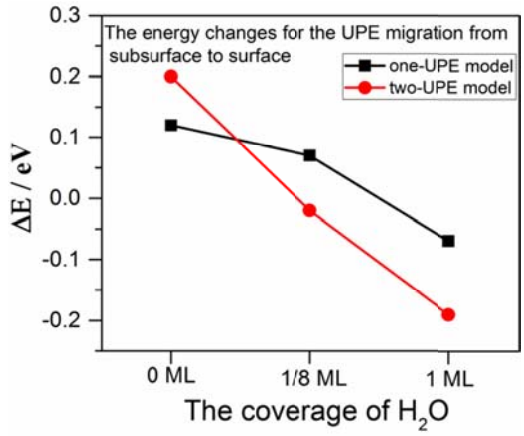

Fig. 1 The energy changes for the UPE migration from subsurface to surface.

Keywords: DFT, excess electrons, H_2O dissociation, $TiO_2(110)$ surface.

References:

[1] Di Valentin, C.; Pacchioni, G.; Selloni, A., *Phys. Rev. Lett.* **2006, 97**: 166803.

[2] Deskins, N. A.; Rousseau, R.; Dupuis, M., *J. Phys. Chem. C* **2010, 114**: 5891-5897.

[3] Chretien, S.; Metiu, H., *J. Phys. Chem. C* **2011, 115**:4696-4705.

[4] Deskins, N. A.; Rousseau, R.; Dupuis, M., *J. Phys. Chem. C* **2011, 115**:7562-7572**.**

吸附水对二氧化钛(110)表面本征缺陷激发态的影响

王天骏，郝群庆，王志强，周传耀*，杨学明*

大连化学物理研究所分子反应动力学国家重点实验室，辽宁省大连市中山路，116023

*Email: chuanyaozhou@dicp.ac.cn, xmyang@dicp.ac.cn

金红石型二氧化钛(110)表面由于氧空位及钛填隙的影响会形成能带结构中的带隙态。二氧化钛吸附ROH后,这一带隙态在紫外光的激发下可以产生一个寿命极短的激发态。我们使用双光子光电子能谱,对这一激发态进行了研究。我们的结果显示这一激发态来源于二氧化钛缺陷Ti^{3+}的d-d跃迁。通过改变入射光的偏振与入射角,我们发现这一过程受空间电场的调制。 造成这一现象的原因尚不明确，有待进一步研究。

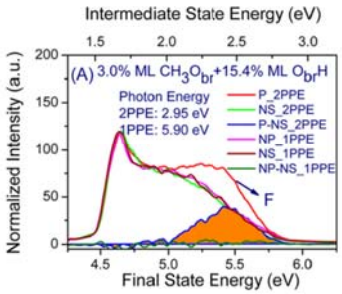

Fig. 1 Normalized PES spectra with different polarization, and incident energy.

关键词： 二氧化钛；光电子能谱；激发态电子结构；吸附质

参考文献

[1] Wang, Z.; Wen, B.; Hao, Q.; Liu, L.-M.; Zhou, C.; Mao, X.; Lang, X.; Yin, W.-J.; Dai, D.; Selloni, A.; Yang, X. Localized Excitation of Ti3+ Ions in the Photoabsorption and Photocatalytic Activity of Reduced Rutile TiO2. J. Am. Chem. Soc. 2015, 137, 9146−9152.

氧气起源：二氧化碳分子的电子贴附解离

王旭东，高小飞，李浩，田善喜*

中国科学技术大学化学物理系，合肥微尺度物质科学国家实验室，安徽合肥，230026

*Email: sxtian@ustc.edu.cn

地球上氧气（即稳定的氧分子O_2）的存在有许多未解之谜。不同于现在所熟知的光合作用产生氧，生命物质存在之前的地球原始大气中就存在氧气，它们是如何产生的呢？业已广泛认可的途径是三体复合反应[1,2]：即两个来自二氧化碳（CO_2）光解的O原子和一个媒介体原子分子M，三者共同作用而生成氧气分子O_2；最近的一个研究认为CO_2在能量范围为11.686~12.145eV的真空紫外光作用下可以直接解离产生O_2和原子碳C [3]。与之对比的是，在地球的上层大气或星际空间中存在大量低能量（几个至几十电子伏特）自由电子，它们产生于星际分子或尘埃曝照于极限真空紫外光或者与高能粒子的电离辐射。这些自由的低能量电子极易被星际分子捕获，即发生电子贴附过程。我们新近发现：CO_2分子捕获低能自由电子后发生解离（即低能电子贴附解离，Dissociative Electron Attachment），可以产生稳定的O_2分子。这是一个以前未被发现的“氧气起源”新途径[4]。

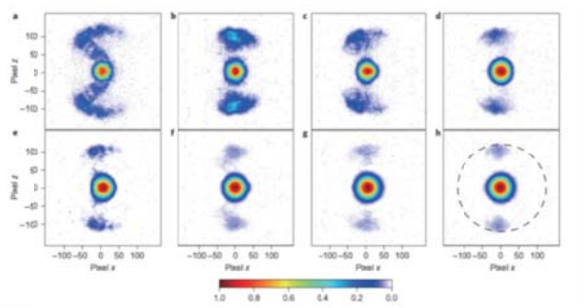

Fig. 1 碳负离子速度分布的时间切片成像。上图中贴附电子能量依次为15.9(a),16.2(b),16.5(c),16.8(d),17.4(e),18.0(f),18.6(g),19.0(h) eV。电子入射方向从左到右。

关键词：氧气起源；分子解离动力学；电子贴附

参考文献

[1] Holland, H. D. *Phil. Trans. R. Soc. B* **2006**, **361**: 903.

[2] Kasting, J. F.; Liu, S. C.; Donahue, T. M. *J. Geophys. Res.* **1979**, **84**: 3097.

[3] Lu, Z.; Chang, Y. C.; Yin, Q.-Z.; Ng, C. Y.; Jackson, W. M. *Science* **2014**, **346**: 61.

[4] Wang, X.-D.; Gao, X.-F.; Xuan, C.-J.; Tian, S. X. *Nat. Chem.* **2016**, **8**: 258.

F+HD→DF+H 反应中 HD(v=1)振动激发得到 DF(v′=5)产物

王玉奉，谢雨润，黄龙，汪涛，肖春雷*，戴东旭，杨学明

中国科学院大连化学物理研究所分子反应动力学国家重点实验室，大连，116023

*Email: chunleixiao@dicp.ac.cn

作为反应动力学中的一个非常典型的基元反应，F+H_2反应体系一直备受关注。其中的Feshbach共振现象给该体系的反应带来丰富的动力学行为[1]。另一方面，由于激发手段的限制，反应物振动激发对于动力学的影响一直鲜有研究。2013年[2]，我们通过受激拉曼激发的方式，以很高的效率得到了HD(v=1)反应物，研究了F + HD(v=1) → HF + D反应中Feshbach共振带来的特有的影响，并观测到仅能通过HD(v=1)振动激发才能得到的HF(v′=4)产物。2014年[3]，我们研究了Cl + HD(v=1) → DCl + H反应，并首次在该反应体系观测到共振现象。

近期，利用高分辨的氢里德堡标记飞行时间谱探测手段[4]，我们又进行了F + HD(v=1, j=0) → DF + H的研究，而HD(v=1)振动激发对于DF+H反应通道的影响暂无研究报导。在0.69 kcal/mol的碰撞能下，我们观测到了该反应中DF(v′=5)的产物，如此高的振动激发DF产物出乎我们的预料。相信HD振动激发还会给该反应带来更丰富的动力学行为。

关键词：振动激发；交叉分子束；氢里德堡标记飞行时间谱

参考文献

[1] Xueming Yang, Dong H. Zhang. *Accounts of Chemical Research*. **2007**, **41**: 981.

[2] Tao Wang, Jun Chen, Tiangang Yang, Chunlei Xiao *et al*. *Science*. **2013**, **342**: 1499.

[3] Tiangang Yang, Jun Chen, Long Huang, Tao Wang *et al. Science*. **2015**, **347**: 60.

[4] Minghui Qiu, Li Che, Zefeng Ren, Dongxu Dai *et al*. *Rev. Sci. Instrum*. **2005**, **76**: 083107-1.

Negligible Cation Effect on Rotational Dynamics of Water Molecules in Electrolyte Aqueous Solution

Qianshun Wei, **Dexia Zhou**, **Hongtao Bian***

Key Laboratory of Applied Surface and Colloid Chemistry, Ministry of Education, School of chemistry and Chemical Engineering, Shaanxi Normal University, Xi'an, 710119
*Email: htbian@snnu.edu.cn

The electrolyte aqueous solutions have been important subjects in chemistry, biology, and atmospheric environment sciences and extensively investigated for many years. One of the central topics in this field in recent years is about the correlations between ion hydrations and the resulting molecular dynamics and structures. It is generally believed that both cations and anions have significant effects on the water structure and rotational dynamics. Here, we used FTIR spectroscopy and ultrafast Infrared spectroscopy to study the structure and rotational dynamics of water molecules in concentrated $LiClO_4$ and $NaClO_4$ solutions. With the presence of ClO_4^-, the two distinct hydrogen bond configurations can be spectrally resolved and the specific ion effects can be studied accordingly. The vibrational relaxation and orientational anisotropy analysis showed that the anions have pronounced effects on the water structure and rotational dynamics. While the cations have negligible effects on the rotational dynamics of water molecules in the systems studied.

Keywords: FTIR spectroscopy, ultrafast Infrared spectroscopy, water molecules, $LiClO_4$ and $NaClO_4$ solutions

References:

[1] Omta, A. W.; Kropman, M. F.; Woutersen, S.; Bakker, H. J. *Science.* **2003, 301**: 347.
[2] Choi, J.-H. & Cho, M. *J. Chem. Phys.* **2016. 145**: 174501.
[3] Ji, M.; Gaffney, K. J. *J. Chem. Phys.* **2011, 134**: 044516.

溶剂调控的 2-巯基苯并噻唑的激发态质子转移

魏馨[1]，赵彦英[1*]

浙江理工大学化学系，中国杭州，310018

*Email:yyzhao@zstu.edu.com

通过2-巯基苯并噻唑（MBT）在不同溶剂中的吸收，发射光谱，结合含时密度泛函理论B3LYP/6-311++G（d,p），研究了MBT的激发态分子间和分子内质子转移（ESIPT）机理。研究结果表明激发态质子转移受溶剂性质影响很大，与质子行溶剂形成的分子间氢键在激发态质子转移反应中起着很重要的作用[1]。图1是MBT在乙腈和水两种溶剂中的吸收和发射光谱。如图1所示，乙腈和水溶剂中有两个吸收带。而230nm的荧光发射光谱在乙腈溶剂中给出了两个强吸收带，而在水中256nm处的谱带变得很弱，只有一个强的发射带位于330nm处。这些结果表明MBT在乙腈中发生激发态分子内质子转移反应，在水中由于水的参与发生激发态分子间质子转移反应。 结合DFT理论计算，提出了激发态分子内/分子间质子转移的机理。

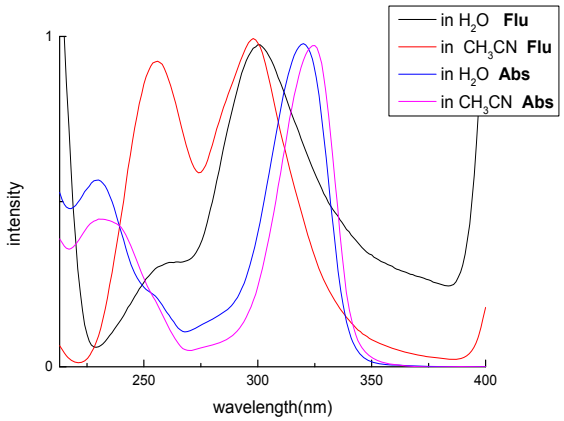

Fig.1: Normalized steady-state absorption and emission spectra in CH_3CN and H_2O of MBT

关键词： 激发态质子转移；含时密度泛函；2-巯基苯并噻唑

参考文献

[1] Zhao J, Yao H, Liu J, et al. New excited-state proton transfer mechanisms for 1, 8-dihydroxydibenzo [a, h] phenazine[J]. The Journal of Physical Chemistry A, 2015, 119(4): 681-688.

[2] An B,Yuan H, Zhu Q, et al. Theoretical insight into the excited-state intramolecular proton transfer mechanisms of three amino-type hydrogen-bonding molecules[J]. Spectrochimica Acta Part A: Molecular and Biomolecular Spectroscopy, 2017, 175: 36-42.

C(^{1}D)+H_2 反应体系的 RPMD 计算

吴亚楠 [1,2]，曹剑炜 [1]，边文生 [1,2*]

[1] 中国科学院化学研究所，北京市海淀区中关村北一街 2 号，100190

[2] 中国科学院大学，北京市石景山区玉泉路 19 号（甲），100049

*Email: bian@iccas.ac.cn

RPMD (Ring Polymer Molecular Dynamics)方法是近年来新发展的一种用于计算化学反应速率常数的量子动力学方法[1,2]。该方法能够处理含几个到几十个原子的反应体系，同时对零点能效应、隧道效应等量子效应都有较好的描述。C(^{1}D)+H_2 反应是势阱控速反应的一个典型例子，对于理解有机化学中 C 原子插入 C-H 或 C-C 键的反应动力学过程具有重要意义，同时在燃烧化学和天体物理中扮演着重要角色。所在课题组成功构建了关于该体系 $\tilde{a}^1A'$和 $\tilde{b}^1A''$电子态的高精度从头算全局势能面[3,4]，该势能面的特色在于对范德华相互作用以及锥形交叉区域的准确描述。基于该势能面，我们对 C(^{1}D)+H_2 及其同位素反应进行了 RPMD 计算，所获得的反应速率常数与实验结果吻合很好，揭示了隧道效应以及零点能效应的影响，表明 RPMD 方法在对势阱控速反应的研究中有较好的表现。

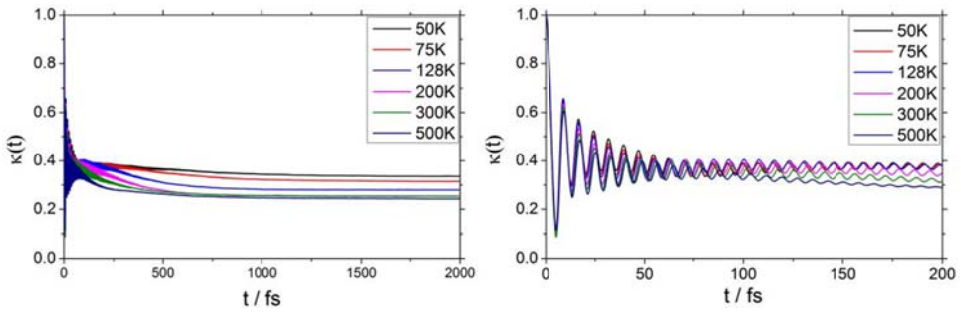

Fig. 1 Ring polymer time-dependent transmission coefficients (κ(t)) for the C(^{1}D)+H_2 reactions

关键词： RPMD；反应速率常数；势阱控速反应

参考文献

[1] Scott Habershon; David E. Manolopoulos; Thomas E. Markland; Thomas F. Miller III *Annu. Rev. Phys. Chem.* **2013**, **64**: 387.

[2] Yury V. Suleimanov; F. Javier Aoiz; Hua Guo *J. Phys. Chem. A* **2016**, **120**: 8488.

[3] Zhang, C.; Fu, M.; Shen, Z.; Ma, H.; Bian, W. *J. Chem. Phys.* **2014**, **140**: 234301.

[4] Shen, Zhitao; Ma, Haitao; Zhang, Chunfang; Fu, Mingkai; Wu, Yanan; Bian, Wensheng; Cao, Jianwei *Nature Commun.*. **2017**, **8**: 14094.

Photoinduced Curtius Rearrangement of Fluorocarbonyl Azide, $FC(O)N_3$: A QM/MM Nonadiabatic Dynamics Simulations Study

Bin-Bin Xie*, Ganglong Cui*, and Wei-Hai Fang

Key Laboratory of Theoretical and Computational Photochemistry, Ministry of Education, College of Chemistry, Beijing Normal University, Beijing 100875, China

*Email: binbinxie@mail.bnu.edu.cn

Upon either photolysis or pyrolysis, fluorocarbonyl azide $FC(O)N_3$ can eliminate molecular nitrogen and form isocyanate. Though two different pathways (i.e. stepwise and concerted patterns) have been proposed, the detailed decomposition mechanism is still elusive until now. In this work, we have employed combined electronic structure calculations and nonadiabatic dynamics simulations to study the radiationless deactivation mechanism of $FC(O)N_3$ in the S_3, S_2, S_1 and S_0 states in acetonitrile. On the basis of QM(CASPT2)/MM calculations, we have found that, upon □195 nm irradiation of $FC(O)N_3$, the excited-state decay from the S_3 state via S_2 and S_1 to S_0 state is a ultrafast process and can be completed within 100 fs, and subsequent Curtius rearrangement occurs in the period of ~300 fs; the elimination of N_2 and formation of carbonyl nitrene FC(O)N can take place both in the S_1 and S_0 states, but not in higher excited states; the isomerization from FC(O)N to FNCO involves a stepwise mechanism and can only be found in the ground state. On the contrary, thermal intramolecular rearrangement occurs in a concerted way without involvement of the carbonyl nitrene intermediate FC(O)N. This mechanistic scenario has been verified by both electronic structure calculations and full-dimensional trajectory-based nonadiabatic dynamics simulations. Finally, this work provides important mechanistic insights into similar carbonyl azide compounds.

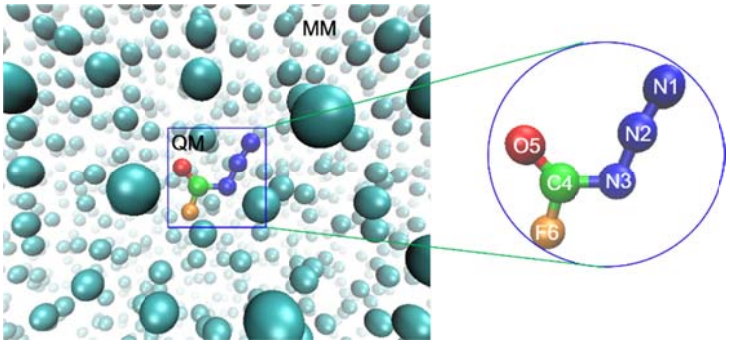

Fig. 1 The solvated QM/MM system used in this study. The $FC(O)N_3$ molecule is treated quantum mechanically; whereas the argon surrounding is done molecular mechanically.

Keywords: Nonadiabatic dynamics, Photolysis, Curtius rearrangement, Fluorocarbonyl azide

References:

[1] Sun, H. L.; Zhu, B. F.; Wu, Z.; Zeng, X. Q.; Beckers, H.; Jenks, W. S. *J. Org. Chem.* **2015**, *80*, 2006−2009.

[2] Zeng, X. Q.; Beckers, H.; Willner, H.; Grote, D.; Sander, W. *Chem. Eur. J.* **2011**, *17*, 3977–3984.

[3] Xia, S.-H.; Liu, X.-Y.; Fang, Q.; Cui, G. L. *J. Chem. Phys.* **2015**, *143*, 194303.

[4] Peng, X. L.; Ding, W. L.; Li, Q. S.; Li, Z. S. *Org. Chem. Front.*, **2017**, *4*, 1153.

[5] Mignolet, B.; Curchod, B. F. E.; Martínez, T. J. *Angew. Chem. Int. Ed.* **2016**, *55*, 14993–14996.

低温催化合成氨的反应机理研究

谢华，孔祥涛，赵志，江凌*

中国科学院大连化学物理研究所分子反应动力学国家重点实验室，辽宁大连，116023

*Email: ljiang@dicp.ac.cn

实现温和条件下氨的高效合成一直是催化领域的重要研究课题[1-5]。LiH-3d 过渡金属复合催化剂体系拥有优异的低温催化合成氨活性， 其“氮转移”催化机理可能是：LiH 作为第二催化中心，可以转移过渡金属表面的氮物种形成 $Li_2NH/LiNH_2$，继而加氢放氨。这种双中心的催化机制打破了单一过渡金属上反应物种之活化能垒和吸附能之间的限制关系，使得氨的低温低压合成成为可能[6]。然而该催化剂上氮的活化和转移转化的微观机制尚有待深入研究。

在本工作中，作者以 LiH-Fe 复合催化剂为研究对象，发现 Fe 与 LiH 在界面处存在强的相互作用。利用自主研制的团簇质谱与光谱联用实验装置，并与密度泛函理论计算紧密结合，成功探测到该催化剂表（界）面存在 Li-Fe-H 三元氢化物物种（如 Li_4FeH_6，Li_5FeH_6 等）[7]。更为有趣的是这些氢化物物种可与 N_2 反应直接转化为含有 Fe-(NH_2)-Li 和 $LiNH_2$ 的物质，实现了 N_2 的解离、向 Li 的转移和加氢；同时，三元氢化物中与 Fe 结合带负电荷的氢则转化为与 N 结合带正电荷的氢，完成了两电子转移。这些基于团簇反应的研究结果暗示了在 Fe-LiH 表（界）面形成的 Li_4FeH_6 很可能是催化活性中心，而 N_2 的活化则有可能从传统 Fe 基催化剂 C7 位上的均裂过程转变为“氢助解离”机制。这项研究加深了对 LiH-3*d* 过渡金属催化剂上合成氨反应机理的认识，为新型高效合成氨催化剂的设计开发提供了的思路。

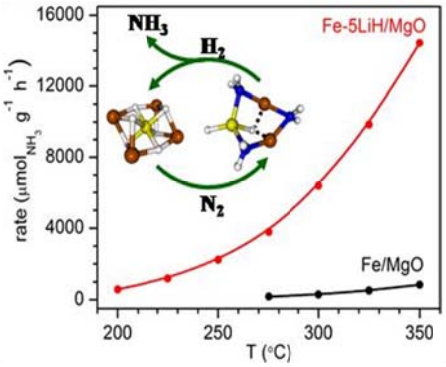

Fig. 1 The significant role of Li-Fe ternary hydrides in efficient low-temperature ammonia synthesis.

关键词：氮转移；三元氢化物；合成氨催化剂

参考文献

[1] Ertl, G. Catal. Rev. Sci. Eng. 1980, 21: 201.

[2] Yandulov, D. V.; Schrock, R. R. Science. 2003, 301: 76.

[3] Licht, S.; Cui, B. C.; Wang, B. H.; Li, F. F.; Lau. J.; Liu, S. Z. Science. 2014, 345: 637.

[4] Vojvodic, A.; Medford, A. J.; Studt, F.; Abild-Pedersen, F.; Khan, T. S.; Bligaard, T.; Norskov, J. K. Chem. Phys. Lett. 2014, 598: 108.

[5] Vojvodic, A.; Norskov. J. K. Natl. Sci. Rev. 2015, 2: 140.

[6] Wang, P. K.; Chang. F.; Gao, W. B.; Guo. J. P.; Wu, G. T.; He, T.; Chen, P. Nat. Chem. 2017, 9: 64.

[7] Wang, P. K.; Xie, H.; Guo, J. P.; Zhao, Z.; Kong, X. T.; Gao, W. B.; Chang, F.; He, T.; Chen, M. S.; Jiang, L.; Chen, P. Angew. Chem., Int. Ed. 2017, in press.

$F+H_2(v=0,j=0)\rightarrow HF+H$ 中的分波共振

谢雨润，黄龙，王玉奉，肖春雷，戴东旭，杨学明*

中国科学院大连化学物理研究所分子反应动力学国家重点实验室，大连，116023

*Email: xmyang@dicp.ac.cn

$F+H_2$反应体系是基元反应动力学研究中非常重要的一个体系，在过去几十年中对该反应中反应共振的研究一直是分子反应动力学领域备受关注的课题[1]。前人观察到的共振特征往往都是来自于许多分波的共同贡献，在实验上观测由特定分波引起的动力学现象，一直是化学动力学研究领域的一个极具挑战的课题[2]。利用高分辨的交叉分子束-氢里德堡标识时间飞行谱方法[3]，我们对$F+H_2(v=0,j=0)\rightarrow HF+H$反应在碰撞能为0.3-0.7kcal/mol范围内的散射结果进行了测量，结合进一步的理论计算分析表明，该碰撞能范围内的共振现象是由特定分波带来的结果。

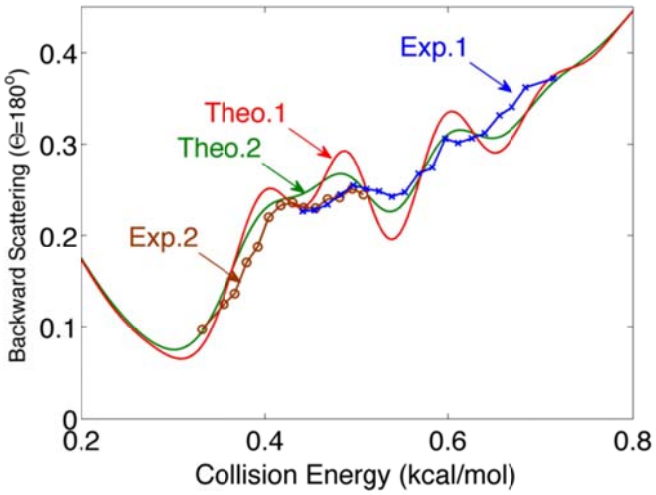

Fig. 1 Collision energy – dependent differential cross sections in the backward scattering direction in F(2P3/2) +H2(j = 0) reaction

关键词：反应动力学；分波共振

参考文献

[1] Neumark D M, Wodtke A M, Robinson G N, et al. Journal of Chemical Physics, 1985, v.82(7):3045-3066.

[2] Dong W, Xiao C, Wang T, et al. Science, 2010, 327(5972): 1501-1502.

[3] Qiu M, Che L, Ren Z, et al. Review of Scientific Instruments, 2005, 76(8):083107 - 083107-5.

Borylene Complex $FB{=}CeF_2$ and Inserted $F_2B{-}CeF$ Molecules : Matrix Infrared Spectra and Quantum Chemical Calculations for the Reaction Products of the Laser-Ablated Cerium Atom with Boron Trifluoride

Li Li[1], Tengfei Huang[2], Bing Xu[1,*]

Department of Chemistry, University of Tongji, School of Chemical Science and Engineering, Shanghai Key Lab of Chemical Assessment and Sustainability, Shanghai, 200092, China
*Email: xbrare@tongji.edu.cn

The experiments of laser-ablated cerium atoms with boron trifluoride were explored in excess solid argon or neno at 4 K through matrix isolation infrared spectroscopy and quantum chemical calculations [1]. The subject product molecules were trapped in inert gas and identified by the isotopic substitutions and DFT frequency calculations. The reaction products, borylene complex $FB{=}CeF_2$ and agostic $F_2B{-}CeF$, increased on annealing and nearly have no change on photolysis. The NBO analysis [2] suggested that B-Ce bond in $FB{=}CeF_2$ molecule contain a B−Ce σ bond and a π type one-electron bond donated from B to Ce. It is different with $FB{=}MF_2$ (M=Ti, Zr, Hf, Th)[3,4] which possesses two-center and two-electron bonds as we known. The agostic $F_2B{-}CeF$, which gives an 82 degree of the ∠Ce-B-F, mainly resulted from the donation of F-B electron to the vacant orbital of Ce atom. Electronic structure calculations reveal that the two product molecules are all in triplet ground state and the orbital composition analysis suggests that the 4*f* valence electron of Ce atom didn't participate in bonding. The electron localization function (ELF) [5] analysis and the theory of atoms-in-molecules (AIM)[6] are applied to investigate the bonding characters as well.

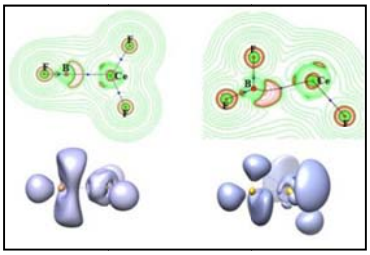

Fig.1 The AIM (top) and ELF of $FB{=}CeF_2$ and $F_2B{-}CeF$ product molecules

Keywords: borylene complex, agostic bonding, matrix isolation, infrared spectroscopy, density functional calculations

References:

[1] (a) Andrews, L.; Citra, A. *Chem. Rev.* **2002**, **102**: 885. (b) Andrews, L. *Chem. Soc. Rev.* **2004**, **33**: 123.

[2] (a) Reed, A. E.; R. B. Weinhold, W. F. *J. Chem. Phys.* **1985**, **83**: 735. (b) Reed, A. E.; Curtiss, L. A.; Weinhold, F. *Chem. Rev.* **1988**, **88**: 899.

[3] Wang, X. F.; Roos, Björn O.; Andrews, L. *Angew. Chem. Int. Ed.* **2010**, **49**: 157.

[4] Wang, X. F.; Roos, Björn O.; Andrews, L. *Chem. Commun.* **2010**, **46**: 1646.

[5] Savin, A.; Nesper, R.; Wengert, S.; Fassler, T. F. *Angew. Chem., Int. Ed. Engl.* **1997**, **36**: 1808.

[6] Bader, R. F. W. *Acc. Chem. Res.* **1985**, **18**: 9.

铜基催化剂表面甲酸根覆盖度对二氧化碳加氢反应动力学的影响

伍盼盼[1]，杨波[1,*]

[1] 上海科技大学物质科学与技术学院，上海，201210

*Email: yangbo1@shanghaitech.edu.cn

随着电子结构理论的快速发展，人们已经能够以较高的精度获得绝大部分多相催化剂表面吸附质的吸附能及基元反应的活化能，并用其对催化反应进行动力学模拟以计算相应的反应速率。当前表面反应动力学模拟中针对催化剂表面所作的假设主要包括两方面：一是催化剂表面结构确定且不随反应的进行发生变化；二是催化剂表面吸附质的浓度较低且吸附质之间的相互作用可以忽略。然而，真实反应条件下的催化剂表面结构及表面吸附质之间的相互作用远比目前绝大多数研究者假设的情况复杂得多[1-2]。报告将从表面覆盖度较高的吸附质的存在对催化反应动力学的影响方面，展示本课题组近年来在真实反应条件下表面催化反应的动态模拟方面所作的一些尝试[3]。主要研究采用的模型反应为铜催化二氧化碳催化加氢制甲醇，考虑的表面高覆盖度吸附质为大量实验所观察到的甲酸根。探究了甲酸根的覆盖度对甲醇合成反应速率和决速步骤等方面的影响。研究结果表明，采用接近真实反应条件下的表面吸附质浓度能够有效描述实验结果，并可在此基础上进一步基于理论计算进行多相催化剂的理性设计。

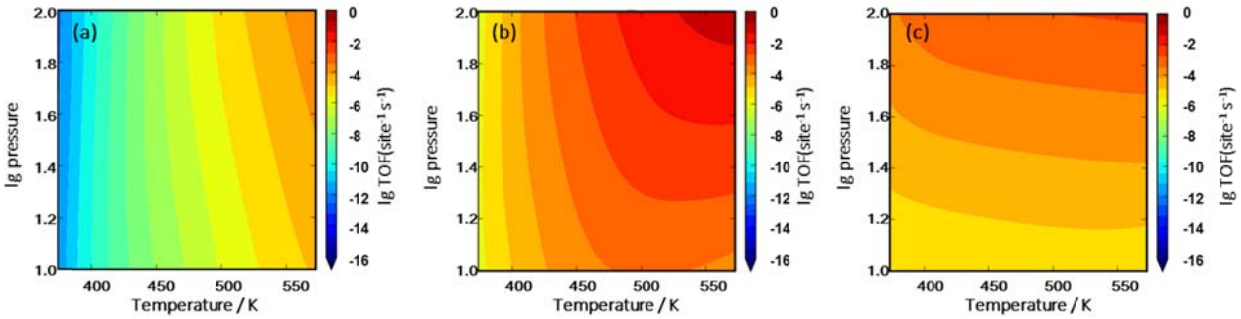

Fig. 1 Turn-over frequencies of methanol synthesis as a function of temperature and lg(pressure) on (a) clean and (b) one/ (c) two formate species pre-adsorbed Cu(211) surfaces.

关键词： 密度泛函理论；甲酸根覆盖度；二氧化碳加氢；反应速率；决速程度

参考文献

[1] Yang, B.; Burch, R.; Hardacre, C.; Headdock, G.; Hu, P. *J. Catal.* **2013**, **305**, 264

[2] Yang, K.; Yang, B. *Phys. Chem. Chem. Phys.* **2017**, DOI: 10.1039/C7CP02152F

[3] Wu, P.; Yang, B. *submitted*

Genistein Binding to Copper (II). Solvent Dependence and Effects on Radical Scavenging

Jing Yang [1], Yi Xu, Rui-Min Han[1*]

[1]Department of Chemistry, Renmin University of China, Beijing, 100872
*Email: rmhan@ruc.edu.cn

Flavonoids, as important micronutrients in fruit and vegetables, have many biological activities such as antioxidant, anti-inflammatory, antiatherosclerotic and antimutagenicity. Besides, flavonoids also exhibit antioxidant properties through chelation with transition metals. Metal-flavonoid complexes are recently found higher antioxidant properties than parent flavonoids. However, molecular mechanism of the interaction between flavonoids and metal ions, and radical scavenging capacity are poorly understood. In present study, isoflavonoid genistein but not daidzein binds to copper(II) with a 2:1 stoichiometry in ethanol and with a 1:1 stoichiometry in methanol indicating chelation by the 5-phenol and the 4-keto group of the isoflavonoid as demonstrated by Jobs method and UV-visible absorption spectroscopy. In ethanol the stability constants had the value 1.12×10^{11} $L^2\cdot mol^{-2}$ for the 2:1 complex and in methanol 6.0×10^5 $L\cdot mol^{-1}$ for the 1:1 complex at 25 °C. Binding was not detected in water, as confirmed by an upper limit for the 1:1 stability constant of K = 5 as calculated from the difference in solvation free energy of copper(II) between methanol and the more polar water. Genistein binding to copper(II) slightly increases the scavenging rate of the stable, neutral 2,2-diphenyl-1-picrylhydrazyl radical, and the generation rate of the short-lived and oxidizing *β*-carotene radical cation formed from laser flash photolysis in the presence of base. Minor effects in reacting with oxidizing radicals are supported by 0.016 V lower for the reduction potential of genistein binding to copper(II) than that of parent genistein.

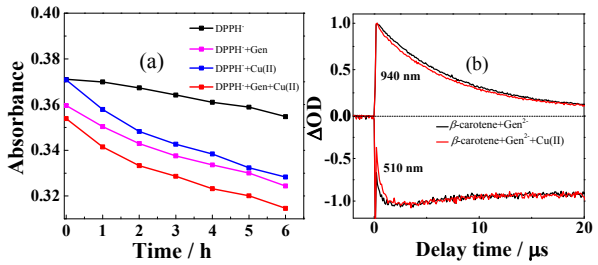

Fig.1 (a) Time profiles at 520 nm for bleaching of 35 μM DPPH• and of DPPH• by 100 μM genistein, 50 μM $CuSO_4$, and the mixture of 100 μM genistein and 50 μM $CuSO_4$ in ethanol. (b) Normalized time evolutions of absorbance at 940 and 510 nm for a solution of 40 μM *β*-Car with 40 μM genistein^{2-} and a solution of 40 μM *β*-Car with 40 μM genistein^{2-} and 40 μM $CuSO_4$ in methanol/chloroform (7/3, v/v) following 532 nm pulsed photoexcitation.

Keywords: genistein; copper; complex; DPPH•; *β*-Carotene

References:

[1] Dowling S; Regan F; Hughes H. *J. Inorg. Biochem*. **2010**, **104**: 1091.

[2] Lewandowski A. *Electrochim. Acta*. **1984**, **29**: 547.

[3] Jouyban A, Soltanpour S, Chan H K. *Int. J. Pharm*, **2004**, **269**: 353.

硝基扭转角对硝基萘及其衍生物激发态衰减动力学的影响

杨梦，薛佳丹，郑旭明*

浙江理工大学，浙江省杭州市下沙 2 号大街 928 号，310018

Email: 15151961552@163.com

硝基萘及其衍生物（NNDs）是含量丰富的基因毒性环境污染物，其主要消除途径是自身的光降解，主要产物是 T_1 态及 ArO·。而 ArO·的产生途径存在两种机制：1. S_1 态通过高效的系间穿越（ISC）衰减到三重态 Tn(nπ*)，部分发生分子内重排解离产生 ArO·，部分回到 T_1 态。2. S_1 发生构型驰豫到 S_{CT} 态[12]再经过分离重组机制产生 ArO·。

大量实验结果显示，硝基萘 T1 和 ArO·的产率因硝基取代位置的不同而有很大的差别。T_1 态的产率 2NN:0.93, 1NN:0.64, 2M1NN:0.33。ArO·的产率 2NN 很少以至于试验中观察不到，1NN 不到 37% 。对此 Carlos E. Crespo-Hernández [1,2]等人给出了 NNDs 的解离机制 Scheme1：ArO·的产生源于 S_{CT} 态的分离重组，硝基的扭转角越接近 90°三重态的量子产率月低，而 ArO·的产率越高。上述机制给出了一种看似合理的结论，但是关于 ArO·的产生路径、NNDs 的势能面情况及硝基扭转角的调控仍存在争论与模糊点。

因此，我们选取 1NN、2NN 和 2M1NN 作为研究体系，采用量子化学从头计算、密度泛函、TD-DFT、CASSCF 等计算方法，引入过渡态的想法，获得分子基态、激发态、过渡态及交叉点的结构和能量信息。经整理得出初步结论：S_1 态分别通过以下两条通道产生 T_1 态与解离态：1.S_1-FC(1NN) → S_1T_3(1NN) → T_3T_2(1NN) → T_2T_1(1NN) → T_1(1NN)。2. S_1-FC(1NN) → S_1T_3(1NN) → T_3T_2(1NN) → T_2T_1(1NN) → TS(T1) →T_1(ISO) → ArO·+ N-O·。即解离在 T_1 态上发生 Figure 1。同时，对 S_0（ISO）的刚性扫描及对 S1(1NN)的 Neb 计算结果均否定了在 S_0 与 S_1 态上进行解离的可能性。产生 T1 态亦或是 ArO·取决于 T_2T_1(1NN) 与 TS(T1)间的能垒高低，硝基的扭转角则是调控此能垒的因素之一。因此，接下来我们将围绕 NNDs 基态扭转角不同情况下动力学的差异进行研究。

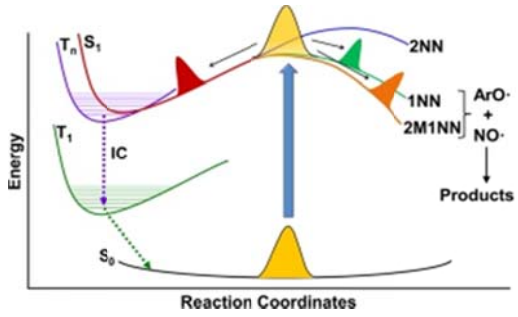

Scheme 1. The Structure−Photoreactivity Relationship Observed for the NND.

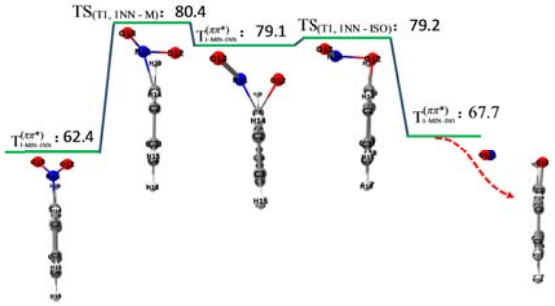

Fig. 1 Photo-dissociation mechanism on T1state.

关键词：NNDs；硝基扭转角；CASSCF

参考文献

[1] Zhang, S.; Li, S.; Zhou, W.; Zheng, L. Chem. Phys. 2011, 135: 14304.

[2] R. Aaron Vogt, Christian Reichardt, Carlos E. Crespo-Hernández. J. Phys. Chem. A 2013, 117, 6580−6588.

The charge transport/recombination dynamics in planar perovskite solar cells

于嫚

In the past few years, we have all witnessed the unprecedented zeal for the rapid growth of the organometal halide perovskite solar cell field. The tremendous efforts devoted to device fabrication and optimization have led to PCEs exceeding 20%. In spite of such an impressive development, an in-depth understanding of many of the physical properties of this class of eclectic materials remain elusive, including the energetic distribution of trap states, the dynamics of charge transport/recombination and light harvesting efficiency in the assembled planar solar cells. The underlying mechanism of the carrier transport/recombination processes are systematically studied by optoelectronic transient measurements. The transient photocurrent (TPC) and photovoltage (TPV)measurements are frequently used to elucidate the mechanism of photoelectrical conversion processes and evaluate charge transport/recombination lifetime in the planar perovskite solar cells. The photovoltaic performance of planar perovskite solar cell is significantly influenced by the morphology of perovskite film. We found that best morphology of perovskite film prepared from the moderate concentration of CH_3NH_3Cl in precursor solutions results the excellent photovoltaic performance with an average efficiency of 15.52% and a champion efficiency of 16.38%. The results of transient optoelectronic measurements, TPV and TPC, indicate that the morphology of perovskite film strongly influences the charge recombination and transport processes in planar perovskite solar cells, as proved by the derived charge collection efficiency. The cell with the best perovskite film exhibits slowest recombination and fastest transport dynamics. In addition, it is found that improper CH_3NH_3Cl may bring about more trap states. Density-of-state distribution is investigated by means of time-resolved charge extraction (TRCE). For TRCE measurements, photogenerated electrons under a given photovoltage are dumped out at specified timing by rapidly switching the solar cells from open- to short-circuit conditions. In a word, the preparation of high-quality perovskite film with controllable morphologies via chloride to optimize charge recombination and charge transport is significant for fabricating high-performance perovskite solar cells.

CuAAC 法合成 1,2,3-三氮唑的双核铜催化机理研究

俞凡，赵彦英*

浙江理工大学化学系，中国杭州，310018

*Email: yyzhao@zstu.edu.cn

过渡金属 Cu(I)催化的乙炔与叠氮化合物反应生成 1,2,3 三氮唑的 CuAAC(Cu-catalytic Azide-Alkyne Click)反应被广泛地应用到药物合成、有机合成、生物蛋白研究等领域[1-3]。目前，实验[4]证实了 CuAAC 反应是一个双金属 Cu(I)催化过程，为了深入了解 CuAAC 反应机理，本文选择了实验中用到的六种含取代基的乙炔和叠氮化合物反应，通过密度泛函理论计算了不同取代基对 CuAAC 反应机理的调控作用，结果表明不同取代基反应的决速步(rate determining step,RDS)不同，推电子取代基的 RDS 为乙炔化合物末端 C-H 键的活化生成 Alkyne-binuclear copper(I)中间体，吸电子取代基的 RDS 为叠氮化合物与该中间体的结合生成铜杂的 1,2,3 三氮唑六元环中间体。计算结果表明双铜核催化反应机理与 Watson 等的实验结果是一致的[5]。B3LYP/6-31+G 方法计算的 CuCl 做为催化剂的产物，中间体，过渡态及反应物的能量分布如 Fig. 1 所示。

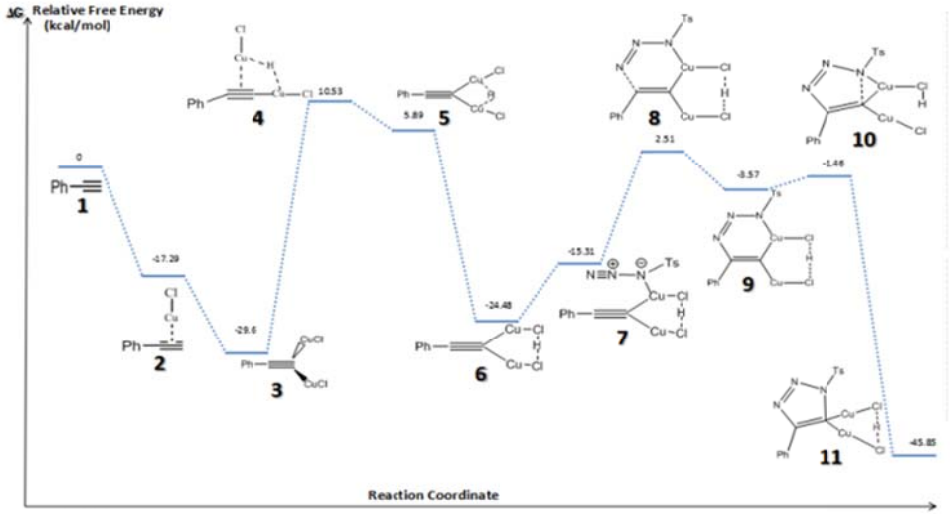

Fig1: Relative Free Energy (in kcal/mol) Profile of Generic Pathway (Shown in Blue) with Proposed Possible Mechanism in the CuAAC Process.

关键词：CuAAC；双核 Cu 催化；密度泛函理论；1,2,3 三氮唑

参考文献

[1] Kelvin,Pak ,Shing,Cheung;Gavin,Chit,Tsui.Org. Lett. **2017**, 19, 2881-2884.

[2] Ray, A.; Manoj,K.; Bhadbhade,M. M.;Bhattacharjya, A.Tetrahedron Lett. **2006**, 47, 2775-2778.

[3] Gong, D.; Bostic, H. E; Smith, M. D; Best, M. D.Eur.J. Org. Chem. **2009** ,24, 4170-4179.

[4] B. T. Worrell, J. A. Malik, V. V. Fokin. Science **2013**,340, 457-460.

[5] Ciaran,p.Seath;Glenn,A.Burley;Allan,J.B.Watson.Angew. Chem., Int. Ed.**2017**,129,1-6.

Experimental and modeling studies of small typical methyl esters pyrolysis: Methyl butanoate and methyl crotonate

Yitong Zhai[1]，Beibei Feng[1]，Wenhao Yuan[2]，Lidong Zhang[1]*

[1] National Synchrotron Radiation Laboratory, University of Science and Technology of China, Hefei, Anhui 230029

[2] Key Laboratory for Power Machinery and Engineering of MOE, Shanghai Jiao Tong University, Shanghai 200240

*Email: yizhai@mail.ustc.edu.cn

In order to examine in detail the effect of C=C bond on the combustion chemistry of biodiesel fuels, two C4 fatty acid methyl esters (FAMEs) were investigated, namely methyl butanoate (MB) and methyl crotonate (MC). Pyrolysis of these two FAMEs at 30, 150 and 780 Torr was conducted in a laminar flow reactor over the temperature range of 773-1323 K, using gas chromatography-mass spectrometry. A number of species including C1 to C4 hydrocarbons, oxygenated products, esters and aromatics, such as for methane, acetylene, carbon monoxide, methyl acrylate as well as benzene, were observed and quantified. A detailed kinetic model for esters pyrolysis at variable pressures containing 307 species and 1508 reactions was developed, and validated against the experimental data in the present work. Peak mole fraction of benzene, the initial and vital aromatic species leading to soot, as well as other unsaturated hydrocarbons in MC pyrolysis are slightly higher than those in MB pyrolysis. According to the reaction pathway analysis and sensitivity analysis, the vital source of propargyl radical, such as propyne and allene, mainly originates in 1-propenyl and allyl radical, which are the major decomposition intermediates and being produced abundantly during the MC pyrolysis. The detailed formation pathways of other unsaturated hydrocarbons also demonstrate that the C=C double bond in biodiesel fuels has significant implications for the formation of even more unsaturated species. To conclude, the effect of C=C double bond with its unsaturation would give rise the growing tendency of initial PAH and soot precursors.

Keywords: Methyl butanoate; Methyl crotonate; Pyrolysis; Kinetic model; Biodiesel

References:

[1] Lin, L; Zhou. C.S; V. Saritporn, Shen, X.Q; Dong, M.D. Opportunities and challenges for biodiesel fuel, *Appl. Energy* 2011 **88** 1020-1031.

[2]Wang, Z.D; Zhao, L; Wang, Y; Bian, H.T; Zhang, L.D; Zhang, F; Li, Y.Y.; S.M. Sarathy, Qi, F. Kinetics of ethylcyclohexane pyrolysis and oxidation: An experimental and detailed kinetic modeling study, *Combust. Flame* 2015 **162** 2873-2892.

[3]Zhang, Y.J; Cai, J.H; Zhao, L; Yang, J.Z; Jin, H.F; Cheng, Z.J; Li, Y.Y; Zhang, L.D; Qi, F. An experimental and kinetic modeling study of three butene isomers pyrolysis at low pressure, *Combust. Flame* 2012 **159** 905-917.

Methane dissociation on Cu Surfaces: A DFT study

Dandan Zhang, XiangjianShen*, Tianshui Liang*
School of Chemical Engineering and Energy, Zhengzhou University, Zhengzhou 450001, China
Email: xjshen85@zzu.edu.cn, liangtsh@zzu.edu.cn

The dissociative chemisorption of methane on Cu surfaces is widely investigated due to its potential application in industrial growth of graphene in a large scale. The first C-H chemical bond to break is a rate-limited step in all of fundamental reaction steps. Here, we present methane dissociation on three different copper surfaces by using first-principles density functional theory method. By analyzing the reactant, transition state and product, the reaction heat and the activation energy as well as geometric structures are given. Our results showed that, it is a endothermic reaction during methane dissociation on Cu surface ; the lattice atom motion can largely reduce the activation energy on these three surfaces; the dissociating C-H bond length is about 1.70-1.80Å; methane dissociation on Cu(110) has the lowest activation energy.

Keywords: Density functional theory; methane dissociation; Cu surfaces

References:

[1] Nave, S., Tiwari, A.K., Jackson B., J. Chem. Phys., **2010, 132**:054705
[2]Weaver, J.F., Carlsson, A.F., Madix, R.J., Surf. Sci. Rep., **2003, 50**:107

硝基多环芳烃激发态在醇溶液中的夺氢反应研究

张迪，薛佳丹*，郑旭明

浙江理工大学，杭州，310018

*Email: jenniexue@126.com

硝基多环芳烃(NPAHs)是致癌性有机污染物，存在于大气当中，主要来源于燃料的不完全燃烧和大气中多环芳烃与氮氧化物的反应，光降解是其主要降解路径[1,2]。硝基多环芳烃经光激发后S_1态的主要衰减通道有两条：一条是光解离生成芳氧自由基；另一条是发生超快系间蹿跃到三重态[1,2]。本文利用纳秒瞬态吸收光谱研究了1-氯-4-硝基萘和1-溴-5-硝基萘三重态的性质以及在醇溶液中的反应。0ns时在405nm和590nm处出现的吸收峰根据文献报道将其指认为最低三重态的吸收峰。随着三重态的衰减，在365nm处显露出一个尖峰。结合计算结果及文献报道，将其指认为夺氢自由基(NPAHsH•)[3]。我们利用纳秒瞬态吸收光谱结合量子化学计算，对其前驱体与生成机理进行了研究。

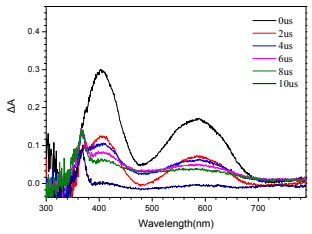

Fig. 1 Transient absorption spectra of 1Cl4NN in Argon-saturated isopropanol solvent

关键词： 硝基多环芳烃；三重态；纳秒瞬态吸收光谱

参考文献

[1] Vogt, R. A.; Reichardt, C.; Crespo-Hernández, C. E. *J. Phy. Chem. A,* **2013**, **117**: 6580-6588.

[2] Vogt R. A.; Crespo-Hernandez C. E. *J. Phys. Chem. A,* **2013, 117**: 14100–14108.

[3] Arce, R.; Pino, E. F.; Valle, C.; Ágreda, J. *J. Phy. Chem. A,* **2008, 112 (41)**: 10294-10304.

Probe the Adsorption of Acetone on RutileTiO_2(110) Surfaces with High-Resolution Sum Frequency Generation

Ruidan Zhang[1], Xingxing Peng[1], Zefeng Ren[2,*]

[1]International Center for Quantum Materials (ICQM) and School of Physics, University of Peking, No. 209 Chengfu Road,Beijing, 100871

[2]State Key Laboratory of Molecular Reaction Dynamics, Dalian Institute of Chemical Physics, Chinese Academy of Sciences, No.457 Zhongshan Road, Dalian 116023

*Email: zfren@dicp.ac.cn

In order to understand the adsorption behavior and photodegrade reactions of organic pollution on titanium dioxide at the molecular level, we have studied the vibrational spectra of acetone on TiO_2(110) by using surface-specific high-resolution (1cm^{-1}) broadband sum frequency generation (HR-BB-SFG) in combination with ultrahigh vacuum technique. As compared to vapor/liquid acetone interface[1-3], acetone on TiO_2(110) exhibits a much more complicated spectrum. The two methyl group have symmetric stretching mode similar to those at the air/liquid acetone interface, and also presents two intense antisymmetric stretching modes (out-of-plane and in-plane). Incredibly, both of the two antisymmetric stretching mode must use two opposite sign sub-peaks to fit well. The four peaks are assigned as out-plane-out-phase, out-plane-in-phase, in-plane-out-phase and in-plane-in phase antisymmetric stretching modes. Furthermore, the intensities of the out-plane antisymmetric stretching obviously decrease along with the IR exposure time increasing, while the intensities of the in-plane antisymmetric stretching significantly enhance. It provides evidence for the presence of polar ordering of acetone molecules in the films, and the ordering is induced by the laser. This work lays the foundation for further in situ studies of the surface chemistry of acetone on TiO_2(110). The results also demonstrate the ability of SFG vibrational spectroscopy for investigating complicated structures of adsorbates on single crystal oxides.

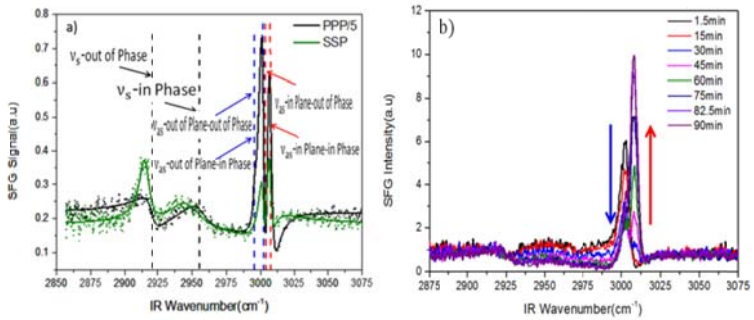

Fig. 1 a)SFG spectra of ppp and ssp polarizations for multilayer acetone on TiO_2(110) by dosing 6min 200Pa at 100K;b) ppp polarizations for multilayer acetone on TiO_2(110) along with exposure time.

Keywords: High Resolution; IR Induction; Polar Ordering

References:

[1] Chen, H.; Gan, W.; Wu, B.H.; Wang, H.F. *Chem. Phys.Lett.* **2005**, **408**: 284-289.

[2] G. DELLEPIANE.; J. OVEREND. *Spectrochimica Acta.* **1966**, **22**: 593-614.

[3] J. D. Rogers.; B. Rub.; S. Goldman.; W. B. Perso. *J. Phys. Chem.* **1981**, **85**: 3727-3729.

To Photoredox or Not in Neutral Aqueous Solutions for Selected Benzophenone and Anthraquinone Derivatives

Xiting Zhang[1], Jiani Ma*,[2] and David Lee Phillips*,[1]

[1] Department of Chemistry, The University of Hong Kong, Pokfulam Road, Hong Kong, P. R. China

[2] Key Laboratory of Synthetic and Natural Functional Molecule Chemistry of Ministry of Education, College of Chemistry and Materials Science, Northwest University, Xi'an, P. R. China

The experimental and theoretical results in neutral aqueous solutions reported here indicate that a proton-coupled electron transfer (PCET) from an alcohol C-H bond to the *para*-carbonyl is the initial and crucial process for the photoredox reaction of 2-(1-hydroxyethyl)-anthraquinone (HEAQ) to occur while the counterpart 3-(hydroxymethyl)-benzophenone (3-BPOH) compound displays a different PCET from an alcohol O-H bond to the carbonyl as the first step followed by an intersystem crossing process that does not lead to the analogous photoredox, which is caused by a subtle charge-radical coupled effect between HEAQ and 3-BPOH. This can account for experimental results in the literature that HEAQ can undergo efficient photoredox but 3-BPOH does not under neutral aqueous conditions. These results have implications for the pH dependent photochemical behavior of aromatic carbonyl compounds in aqueous media.

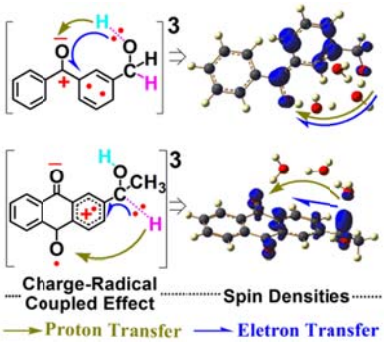

离子液体电沉积制备纳米铝的反应动力学规律

郑勇*，郑永军，王振，武卫明，侯绍刚

安阳工学院化学与环境工程学院，河南 安阳 455000

*Email: yzheng@ayit.edu.cn

作为一种新型的储能材料，纳米铝已被应用于火箭推进器、军工和航空航天等领域。目前，纳米铝的制备主要通过氮气雾化法进行，该方法虽然操作简单，但是存在着粉尘污染重、产品纯度低、能耗高和温度高等问题[1]。因此，开发新型的制备技术，特别是低温电解质是解决问题的关键。近年来的研究表明，从一些离子液体体系中也能够电沉积出纳米铝，这为技术的发展提供了新的方向[2]。然而，相关研究对电沉积过程的动力学规律认识不足，不利于有关应用工作的进一步开展。

本文从上述背景出发，深入研究了离子液体电沉积制备纳米铝过程的反应动力学规律。实验结果表明，铝的电沉积过程均为动力学上典型的准可逆过程，反应速率和效率受到离子扩散、离子传递的控制，符合三维瞬时成核机理，如图1所示。在较低的温度和适中的电流密度下，铝的择优晶型取向为（200），此时的沉积层较为均一、平整，平均粒径一般为纳米级。而当温度较高且电流密度较大时，铝的择优晶型为（111），所对应的沉积层大都比较粗糙，结构疏松，晶粒较大。所以说，制备纳米铝时，就需要适当地调整反应条件，引导铝在（200）型晶面上进行电沉积生长。同时还发现，离子与电极表面的相互作用是影响纳米铝制备的关键。当离子在电极表面分布较为均匀，电解形成较为均一致密的晶核，沉淀过程中晶核有序生长且不过度时，可获得纳米铝。而一些具有电化学活性的功能基团或者添加剂是促成该反应过程的重要因素。

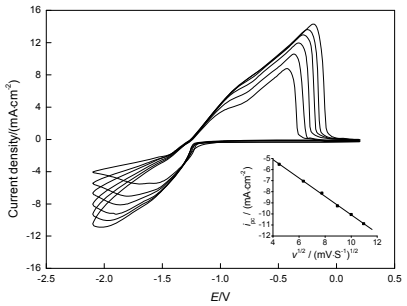

Fig. 1 Cyclic voltammograms recorded on the Pt electrode in ionic liquids with different potential scan rates

关键词：纳米铝，离子液体，电沉积，动力学

参考文献

[1] 宋丽, 宋美荣, 李庆华, 张治军. 纳米铝微粒制备的研究进展. 化学研究, **2008**, **19(2)**: 102.

[2] Zein El Abedin, S.; Moustafa, E.; Hempelmann, R.; Natter, H.; Endres, F. *Electrochem. Commun.* **2005**, **7**: 1111.

尿嘧啶胸腺嘧啶水溶液中激发态动力学的研究

周海强，薛佳丹，郑旭明*

浙江理工大学化学系，浙江省杭州市下沙 2 号大街 928 号，310018

*Email：zxm@zstu.edu.cn

至今，关于尿嘧啶和胸腺嘧啶在水溶液激发态衰变动力学，研究者提出了 3 种机制：第一种机制是从初始光吸收态 $^1(\pi\pi^*)$弛豫到暗态 $^1(n\pi^*)$，而后从 $^1(n\pi^*)$返回基态[1]；第二种机制是从 $^1(\pi\pi^*)$弛豫到 $^1(n\pi^*)$,但 $^1(n\pi^*)$只起中间态作用，不能直接从它返回基态,而是从它再回到 $^1(\pi\pi^*)$态，并通过 $^1(\pi\pi^*)$/GS 锥形交叉点返回基态[2]； 第三种机制是 $^1(n\pi^*)$并不参与弛豫过程，$^1(\pi\pi^*)$直接经 $^1(\pi\pi^*)$/GS 锥形交叉点到基态。第三种机制因计算过程没有考虑水溶剂作用的影响[3]，其可靠性受到质疑。

本文通过量子化学从头计算方法，结合共振拉曼光谱技术，对胸腺嘧啶、尿嘧啶在水溶液中的激发态弛豫路径进行了深入研究。在理论计算研究中，我们重点考虑水与嘧啶碱基的显式相互作用，考察了水与嘧啶碱基形成簇合物对 $^1(\pi\pi^*)$和 $^1(n\pi^*)$势能面的影响，提出了相应的弛豫机制，并得到共振拉曼光谱实验的有力印证。

图 1 是尿嘧啶水溶剂模型计算得到的,可以发现水溶液中的尿嘧啶有 2 条弛豫路径,第一条是从 $^1(\pi\pi^*)$经过 $^1(n\pi^*)/^1(\pi\pi^*)$交叉点,然后从 $^1(n\pi^*)$返回基态，另一条是从 $^1(\pi\pi^*)$经过 $^1(\pi\pi^*)$/GS 锥形交叉点直接返回基态。图 2 是胸腺嘧啶的水溶剂模型，可以看到对于胸腺嘧啶 $^1(n\pi^*)/^1(\pi\pi^*)$交叉点的能量(158Kcal/mol)远高于 $^1(\pi\pi^*)$FC(132Kcal/mol)点的能量，所以认为胸腺嘧啶弛豫路径是从 $^1(\pi\pi^*)$经过 $^1(\pi\pi^*)$/GS 锥形交叉点返回基态。

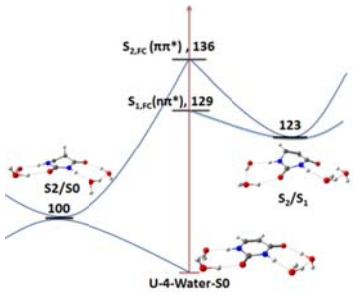

图 1. 尿嘧啶弛豫路径（单位：kcal/mol）

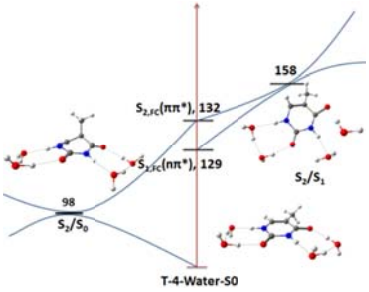

图 2. 胸腺嘧啶弛豫路径（单位：kcal/mol）

关键词：胸腺嘧啶；尿嘧啶；弛豫；势能面

参考文献

[1] Dana Nachtigallova.; Adelia J. A. Aquino.; Mario Barbatti J. Phys. Chem. A 2011, 115, 5247–5255

[2] Yannick Mercier.; Fabrizio Santoro.; Mar Reguero. J. Phys. Chem. B, Vol. 112, No. 35, 2008 10771

[3] Franziska Buchner.; Akira Nakayama.; Shohei Yamazaki.J. Am. Chem. Soc. 2015, 137, 2931-2938

二碘-氟硼吡咯中系间交叉过程和能量转移过程的溶剂化效应

周淼淼，王恋，张嵩，张冰

中国科学院武汉物理与数学研究所，武汉小洪山西 30 号，430071

Email：zackzm@mail.ustc.edu.cn

剂化效应在液相的光化学过程和能量转移过程中具有重要作用。然而，这种效应在三重态->三重态的湮灭（TTA） 上转换荧光实验中很少提及。在一个典型的 TTA 上转换体系——二碘-氟硼吡和二萘嵌苯中，我们研究了在五种不同的惰性溶剂：已烷、庚烷、甲苯、一四二氧六环、DMSO 之中，二碘-氟硼吡咯的溶剂化效应。我们使用了飞秒瞬态吸收的方法研究其系间交叉（ISC）和三重态到三重态能量转移过程。实验结果表明，随着溶剂极性增加，系间交叉过程变快，能量转移过程变快。

关键字：瞬态吸收，溶剂化效应

参考文献

[1] C. Zhang, J. Zhao, S. Wu, Z. Wang, W. Wu, J. Ma, S. Guo and L. Huang, J. Am. Chem. Soc., 2013, 135, 10566–10578.

吡啶离子液体[OPy][BF_4]与乙腈二元体系的局部微观结构研究

周司文，康贤取，朱光来*

安徽师范大学原子与分子物理研究所，安徽芜湖，241000

*Email: zhglai@mail.ahnu.edu.cn

离子液体是指在常温下呈液态的由阴、阳离子组成的化合物，其特点是蒸汽压小、不易挥发、熔点低、液态范围宽、热稳定性好等，作为一种新型的绿色溶剂正受到越来越多的研究者的关注[1, 2]。本文采用分子动力学模拟方法研究了吡啶离子液体 N-辛基吡啶四氟硼酸盐[OPy][BF_4]与乙腈(MeCN)二元体系的热力学性质和局部微观结构，获得了体系的密度、径向分布函数、空间分布函数等。二元体系各组分的扩散系数和密度随离子液体摩尔分数呈现出规律的变化。而阳离子上烷基链末端的碳原子(尾部)之间、吡啶环(头部)和阴离子之间的径向分布函数变化规律明显不同。空间分布也反映出类似的规律，说明分子溶剂乙腈与头尾的相互作用是不同的，也进一步证实离子液体内部极性与非极性区域的存在[3]。阴离子上的硼原子(B)在阳离子周围的空间分布如图 1 所示。在离子液体不同摩尔分数(x_i)下，B 原子大多聚集在阳离子的吡啶环周围，形成一个环状分布，与[BPy][BF_4]/MeCN 体系类似，但烷基链末端碳原子之间的径向分布函数的变化规律明显不同，这可能是由于[OPy][BF_4]具有更长的烷基链所导致的。

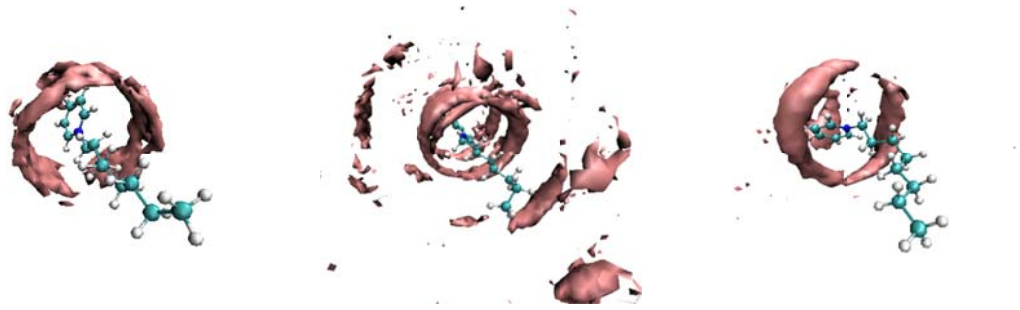

(a) (b) (c)

Fig. 1 SDFs for the B atoms on the anion around $[OPy]^+$ at (a) x_i=0.3, (b) x_i=0.5 and (c) x_i=0.7 with isovalues 35 respectively

关键词：离子液体；微观结构；径向分布函数；空间分布函数

参考文献

[1] Zhu, G.; Wang, Y.; Zhang, L.; Luo, Y.; Sha, M.; Xu, X. *J. Mol. Liq.* **2015, 203**: 153-158.

[2] Rogers, R. D.; Seddon, K. R. *Science*. **2003, 302**: 792-793.

[3] Zhu, G.; Kang, X.; Zhou, S.; Tang, X.; Sha, M.; Cui, Z.; Xu, X. *RSC Advances*. **2017, 7**: 4896-4903.

Scattering and Reaction Dynamics on Chemically Accurate 15D Potential Energy Surface for Methane Dissociation on Ni(111)

Xueyao Zhou[1], Francesco Nattino[2], Geert-Jan Kroes[2,*], and Hua Guo[3,*], Bin Jiang,[1,*]

[1]Department of Chemical Physics, University of science and Technology of China, Hefei, Anhui 230026, China

[2]Leiden Institute of Chemistry, Leiden University, Gorlaeus Laboratories, P.O. Box 9502, 2300 RA Leiden, The Netherlands

[3]Department of Chemistry and Chemical Biology, University of New Mexico, Albuquerque, New Mexico 87131, USA

[1]*Email: bjiangch@ustc.edu.cn

The dissociation of methane on metal surface has become one of the most studied gas-surface reactions due to its industrial significance. In the present work, we developed a chemically accurate, fifteen-dimensional potential energy surface (PES) for CH_4 on rigid Ni(111) surface with the (permutation invariant polynomial-neural network (PIP-NN) approach[1] based on the recently proposed SRP functional[2] with nearly 200 thousand DFT energy points. After that, quasi-classical trajectory (QCT) approach combined with the lattice relaxed sudden (LRS) model of Jackson[3] was employed to investigate the reaction characteristics of CHD_3 dissociation reaction. The realistic dissociative sticking coefficients agreed with AIMD data on movable surface and the experiment very well. In addition, the rovibrational state populations for scattering products were also compared with the state-to-state experimental measurements.

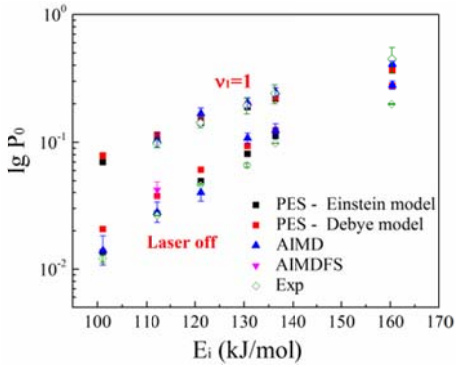

Fig.1 Comparison of CHD_3 dissociation probabilities on PES, AIMD calculations and experiments.

Keywords: Methane; Potential energy surface; Reaction dynamics; state-to-state Scattering dynamics;

References:

[1] Jiang, B.; Guo, H.; *J. Chem. Phys.* **2014, 141**: 034109.

[2] Nattino, F.; Migliorini, D.et al.; *J. Phys. Chem. Lett.* **2016, 7**: 2402.

[3] Tiwari, A. K.; Nave, S.; Jackson, B.; *J. Chem. Phys.* **2010, 132**: 134702.

Construction of Potential Energy Surface for ClH_2O System and Its Application in Ring Polymer Molecular Dynamics Study

Junxiang Zuo[1], Hua Guo[2,*], Daiqian Xie[1,3,*]

[1] Institute of Theoretical and Computational Chemistry, Key Laboratory of Mesoscopic Chemistry, School of Chemistry and Chemical Engineering, Nanjing University, Nanjing 210093, China

[2] Department of Chemistry and Chemical Biology, University of New Mexico, Albuquerque, New Mexico 87131, United States

[3] Synergetic Innovation Center of Quantum Information and Quantum Physics, University of Science and Technology of China, Hefei, Anhui 230026, China

* Email: hguo@unm.edu (H.G.) and dqxie@nju.edu.cn (D.X.).

A new and more accurate full-dimensional global permutation invariant polynomial-neural network (PIP-NN) potential energy surface (PES) for the ground electronic state of the ClH_2O system is developed by fitting 15777 points obtained using UCCSD(T)-F12b. Then the thermal rate coefficients are determined on this PES using ring polymer molecular dynamics (RPMD). It is shown that quantum effects such as tunneling and zero-point energy (ZPE) are of critical importance for the HCl + OH reaction at the low temperatures, while the heavier deuterium substitution renders tunneling less facile in the DCl + OH reaction. The self-consistency of the theoretical results allows a quality assessment of the experimental data.

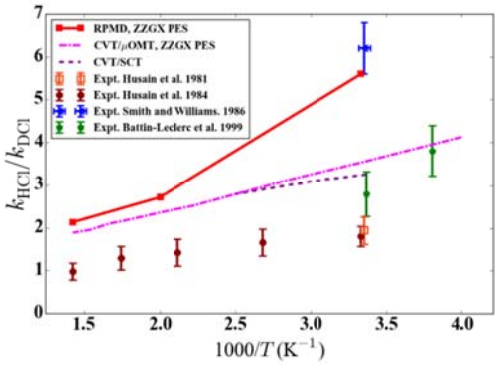

Fig.1 Comparison between calculated and measured KIEs for the HCl/DCl + OH reactions.

Keywords: Potential Energy Surface, Ring Polymer Molecular Dynamics, Rate Coefficient, Quantum Effects

References:

[1] B. Jiang and H. Guo, *J. Chem. Phys.*, 2013, **139**, 054112.

[2] Y. V. Suleimanov; J. W. Allen and W. H. Green, *Comput. Phys. Comm.* **2013,** *184*, 833-840.

[3] I. R. Craig; D. E. Manolopoulos, *J. Chem. Phys.* **2005,** *122*, 084106.

[4] S. Habershon; D. E. Manolopoulos; T. E.Markland and T. F.Miller III, *Annu. Rev. Phys. Chem.* **2013,** *64*, 387-413.

纳米尺寸中性锰氧化物团簇的产生和反应性研究

陈娇娇[1,2]，袁震[1]，李晓娜[1]，何圣贵[1,2*]

[1] 中国科学院化学研究所分子动态与稳态结构国家重点实验室，北京，100190

[2] 中国科学院大学，北京，100049

*Email: shengguihe@iccas.ac.cn

对中性氧化物团簇的结构及反应性研究有助于从分子水平上理解凝聚相表面的反应机理[1]。受限于真空紫外光（VUV）极低的产生效率，目前该领域的研究主要集中于产生中小尺寸团簇(<1 nm)[2,3],研究纳米尺寸氧化物团簇在技术上存在挑战。锰氧化物材料在生物医学、光催化等领域具有广泛的应用[4]，本研究采用激光溅射的方法制备中性锰氧化物团簇，并研究了其与C_2H_4在流动管中的反应，反应后中性锰氧化物团簇经VUV光电离后被飞行时间质谱检测。如图1所示，产生的中性锰氧化物团簇Mn_mO_n(m = 5–58; n = 8–82)达到了纳米尺寸，其中$Mn_{41}O_{59}$团簇（1.3 nm）的分辨率高达7270。在$(Mn_2O_3)_N$(N=2-22)团簇与C_2H_4的反应中发现，C_2H_4的吸附活性具有一定的尺寸效应。当N=3时，吸附活性最大，随后吸附活性随团簇尺寸增大而减小，当N>10时，吸附活性基本保持不变。该工作首次报道了纳米尺寸中性锰氧化物团簇的产生和反应，其研究结果为理解氧化锰材料的反应性和提高其性能提供了理论研究基础。

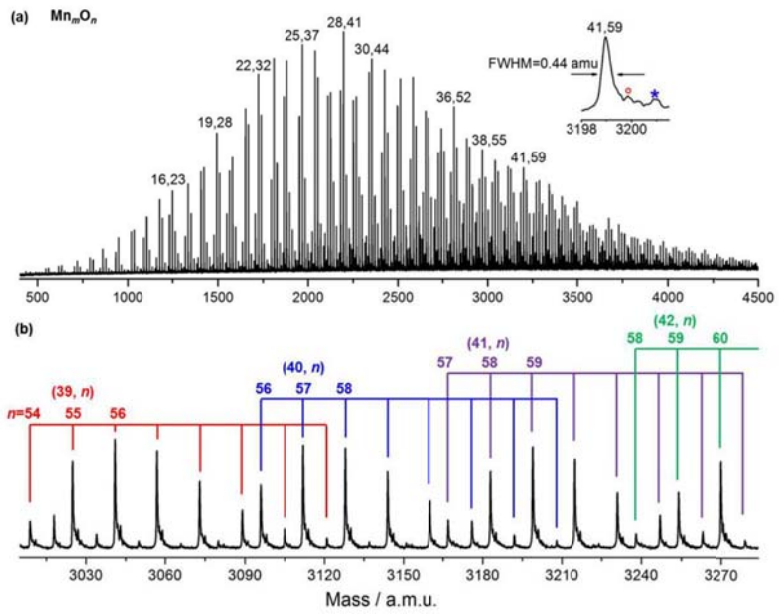

Fig. 1 An overview of a time-of-flight mass spectrum for the distribution of neutral manganese oxide clusters (a) and a portion of the spectrum with assignments of the peaks (b). The Mn_mO_n cluster is labeled as m, n.

关键词：纳米尺寸；中性锰氧化物团簇；高分辨质谱；VUV光电离

参考文献

[1] Muetterties, E. L.; Rhodin, T. N.; Band, E.; Brucker, C. F.; Pretzer, W. R. *chem. Rev.* **1979, 79**: 91.

[2] Yin, S.; Bernstein, E. R. *J. Phys. Chem. Lett*. **2016, 7**: 1709.

[3] Bernstein, E. R. *Int. J. Mass Spectrom.* **2015, 377**: 248.

[4] Nguyen, K.T.; Zhao, Y. *Nanoscale.* **2014, 6**: 6245.

VB_3^+阳离子团簇与 CH_4 的反应研究

陈强[1]，何圣贵[1,2*]

[1] 中国科学院化学研究所分子动态与稳态结构国家重点实验室，北京，100190

[2] 中国科学院大学，北京，100049

*Email: shengguihe@iccas.ac.cn

甲烷不仅是一种重要能源，也是生产高附加值化学品的重要原料，高度稳定的甲烷分子的活化转化一直是学术界的重大挑战之一。[1]。最新研究发现，甲烷的硼化反应可以将甲烷C-H键转化为B-C键[2-3]，但该类型甲烷活化过程需要在高压条件和贵金属基催化剂作用下进行，成本较高。本研究提出将廉价的过渡金属钒制备到硼原子形成的团簇中，研究钒硼化物团簇与甲烷的反应活性，探索其在温和条件活化转化甲烷的可行性。我们采用激光溅射方法产生钒硼阳离子团簇，通过四极杆质量分析器选出感兴趣的团簇，使其在离子阱中与甲烷分子反应，最后利用飞行时间质谱检测团簇分布。实验发现VB_3^+阳离子团簇与甲烷反应可以生成$VB_3CH_2^+$与VH^+阳离子(Fig. 1)，它们分别对应于H_2脱附和芳香性硼化物B_3CH_3消除反应通道。密度泛函理论计算结果与观测到的实验现象相吻合，其中H_2脱附反应在热力学上更有利。本研究可在分子层次上揭示甲烷C-H转化成B-C的微观机理，为非贵金属硼化物取代贵金属基催化剂提供研究基础。

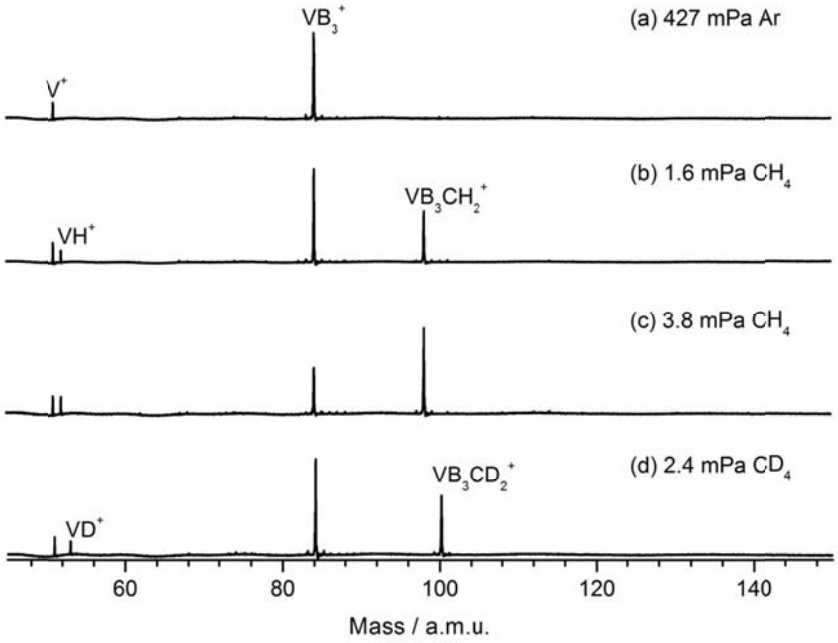

Fig. 1 TOF mass spectra for the reactions of VB_3^+ with 427 mPa Ar (a), 1.6 mPa CH_4 (b), 3.8 mPa CH_4 (c), and 2.4 mPa CD_4 (d) for 2.2 ms.

关键词： 甲烷活化；过渡金属硼化物；质谱；密度泛函计算

参考文献

[1] Arndtsen, B. A.; Bergman, R. G.; Mobley, T. A.; Peterson, T. H. *Acc. Chem. Res.*, **1995**, **28**: 154.

[2] Cook, A. K.; Schimler, S. D.; Matzger A. J.; Sanford, M. S. *Science,* **2016**, **351**:1421.

[3] Smith, K. T.; Berritt, S.; González-Moreiras, M.; Ahn, S.; Smith III, M. R.; Baik, M. H.; Mindiola, D. J., *Science,* **2016**, **351**: 1424.

$Fe_2O_3^+$阳离子团簇与苯的反应研究

崔佳桐，马嘉璧*

北京理工大学，北京市房山区良乡高教园区，102488

*Email: majiabi@bit.edu.cn

Fe_2O_3是大气中一种重要的矿尘气溶胶，约占矿尘气溶胶总质量的6%[1]；该物种可以为多种非均相反应提供场所[2]。苯是一类毒性较强的挥发性有机物（VOC），是典型的大气污染物。研究苯在Fe_2O_3上的活化氧化过程对于理解VOC的氧化反应具有重要意义。

我们利用团簇模型，可以从分子水平清晰认识铁氧化合物气溶胶表面活性位的构效关系，得到反应速率等重要信息，为大气模型的构建提供重要数据。通过原子分子团簇原位反应装置（四极杆-离子阱-反射式飞行时间质谱）对$Fe_2O_3^+$阳离子团簇与苯（C_6H_6）的反应活性进行了研究，发现存在以下两个反应通道，即氧转移通道（脱去水分子，反应1）和吸附通道（反应2），如图一所示：

$$Fe_2O_3^+ + C_6H_6 \rightarrow Fe_2O_2C_6H_4^+ + H_2O \quad (1)$$

$$Fe_2O_3^+ + C_6H_6 \rightarrow Fe_2O_3C_6H_6^+ \quad (2)$$

反应速率为 7.1×10^{-10} $cm^3 \cdot molecule^{-1} \cdot s^{-1}$，分支比为 64/36。我们进一步用 $^{18}O_2$ 同位素实验验证了上述反应。深入的理论研究还需深入进行。

此外，我们对其他 3d 过渡金属氧化物阳离子团簇(除了 Sc、Ti、Ni、Zn 之外）与苯的反应进行了系统研究，发生氧转移通道（脱去水分子）广泛存在，例如 $Cu_2O_2^+$，CrO_2^+，$Cr_2O_5^+$，$Cr_3O_2^+$，VO_3^+,$V_2O_5^+$,$V_3O_8^+$,$V_5O_{13}^+$团簇。

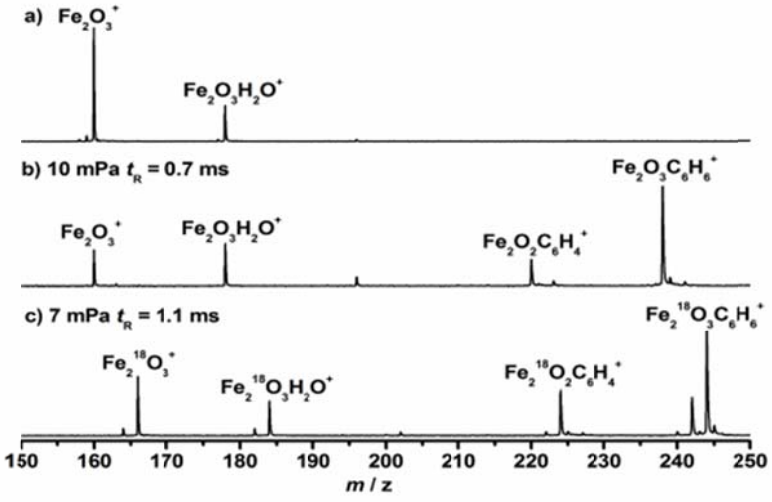

Fig. 1 Time-of-flight mass spectra for the reactions of mass-selected $Fe_2O_3^+$ (a) with C_6H_6 (b) for 0.7 ms, and $Fe_2{}^{18}O_3^+$ with C_6H_6 (c) for 1.1 ms. The effective reactant gas pressures are shown.

关键词： $Fe_2O_3^+$团簇；苯；催化氧化

参考文献

[1] Usher, C. R.; Michel, A. E.; Grassian, V. H. *Chem. Rev.* **2003**, **103**: 4883.

[2] Ling-Yan Wu; Sheng-Rui Tong; Li Zhou; Wei-Gang Wang; and Mao-Fa Ge. *J. Phys. Chem. A*. **2013**, **117**: 3972.

氧化钒团簇负载的单原子金上的氢气氧化反应

张岩[1]，丁迅雷[1*]，李子玉[2]，何圣贵[2]

1 华北电力大学数理学院，北京，102206 2 中国科学院化学研究所，北京，100190

*Email: dingxl@ncepu.edu.cn

单原子催化是近年来催化领域的一个研究热点 [1] 。氧化物团簇上负载单个贵金属原子可以作为模型体系，用于研究单原子催化的微观机理。氢气氧化反应在 H_2O_2 合成、碳氢化合物催化氧化等方面都具有要意义，金属氧化物担载金在此类反应中具有独特的催化活性。在本研究中，我们采用飞行时间质谱技术结合密度泛函理论，研究了 $AuV_2O_5^+$ 团簇上 H_2 的氧化反应，并通过与先前研究的 $AuCe_2O_4^+$ [2] 体系进行对比，揭示了单原子金在此类反应中所起的关键作用 [3] 。主要结果如下：

1. $AuV_2O_5^+$ 的基态机构中 Au 与一个 V 相连（端位金），其与 H_2 的反应活性优于 $AuCe_2O_4^+$ （基态结构中具有桥位金，即 Au 与两个 Ce 相连）。H_2 在 $AuV_2O_5^+$ 上的反应速率为 5.1×10^{-10}cm^3 molecule^{-1} s^{-1} ，比在$AuCe_2O_4^+$ 上的反应速率（5.6×10^{-12} cm^3 molecule^{-1} s^{-1} ）快约两个数量级。氢气在有桥位金结构的 $AuCe_2O_4^+$ 上的吸附能较小（0.04 eV），只有当桥位金转变为端位金之后，整个反应体系才能提供足够的能量来克服随后氢气解离的能垒。
2. 为了揭示两个体系上反应活性差异的微观机理，我们理论计算了两个体系上氢气氧化反应的完整路径，并对比研究了两个体系中相似的中间体(Fig. 1b)。NBO 分析（Fig. 1a）表明，随着反应的进行，Au 上的电子逐渐增多。由于 V 与 Ce 相比有更高的电负性（1.63/1.12），因此在氧化钒体系中，Au 较难得到电子，在 group3 中所带电荷仍为正值，而对于氧化铈体系，group3 中的 Au 上已经带了负电荷。带有正电荷的 Au 和 V 之间存在静电互斥，导致了相对较弱的 Au-V 键；相反，负价的 Au 和更高正价的 Ce之间具有较强的静电吸引，导致较强的 Au-Ce 键。较弱的 Au-V 键致使 Au 在钒体系中更容易脱落，而Au 的脱落将会阻碍氧化产物 H_2O 的生成。我们的研究表明，金和金属之间的键能强弱直接影响了 H_2氧化产物 H_2O 的形成。

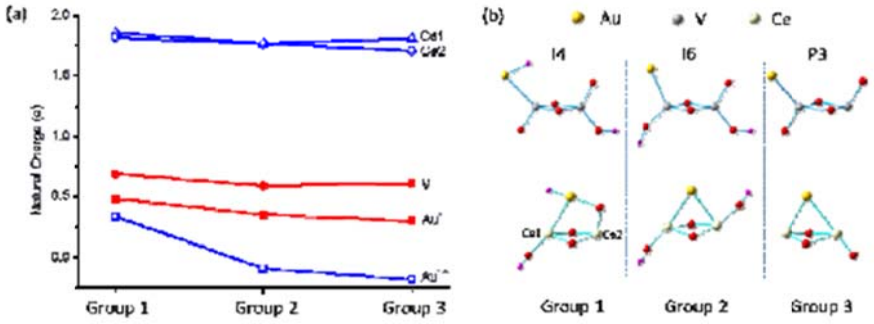

Fig.1 DFT calculated natural charge on the gold, vanadium, and cerium atoms during the reactions of $AuV_2O_5^+$ and $AuCe_2O_4^+$with H_2 (a). In each reaction three typical structures are selected, that with Au-H, without Au-H (instead,with two O-H groups), and the final product with H_2O releasing. The Group n (n = 1-3) contains two corresponding typical structures from the two reactions respectively (b).

关键词 ：单原子催化；飞行时间质谱；密度泛函理论；氢气氧化

参考文献

[1] Yang, X.-F.; Wang, A.; Qiao, B.; Li, J.; Liu, J.; Zhang, T., Acc. Chem. Res. 2013, 46: 1740-1748.

[2] Meng, J.-H.; He, S.-G. J. Phys. Chem. Lett. 2014, 5, 3890-3894.

[3] Zhang, Y.; Li, Z.-Y.; Zhao, Y.-X.; Li, H.-F.; Ding, X.-L.; Zhang, H.-Y.; He, S.-G., J Phys Chem A 2017, 121: 4069-4075.

Wheel-like, elongated, circular, and linear geometries in boron-based C_nB_{7-n} (n = 0–7) clusters: structural transitions and aromaticity

Lin-Yan Feng and Hua-Jin Zhai (翟华金)*

Nanocluster Laboratory, Institute of Molecular Science, Shanxi University, Taiyuan, 030006

*E-mail: hj.zhai@sxu.edu.cn

We report a quantum chemical study on the structural and bonding properties of a series of boron-carbon mixed clusters with seven atoms: C_nB_{7-n} (n = 0–7). Global-minimum structures were extensively searched and established using the Coalescence Kick (CK) method, followed by B3LYP/6-311+G(d) calculations for full optimizations and energetics. Top candidate structures were further benchmarked at single-point CCSD(T) level. Structural transitions were revealed to occur successively from wheel-like, elongated, circular, to linear geometries upon increasing of C contents in the clusters. Chemical bonding was elucidated via canonical molecular orbital (CMO) analyses and adaptive natural density partitioning (AdNDP). The number of delocalized electrons (σ plus π) in the clusters was shown to vary by one at a time from 5σ to 7σ, as well as from 3π to 7π, which allow aromaticity, antiaromaticity, and conflicting aromaticity to be precisely followed or tuned according to the ($4n$ + 2) and $4n$ Hückel rules. Delocalized π and σ bonds and their electron countings appear to dictate cluster structures of the whole series. Aromaticity in the systems was independently confirmed through nucleus-independent chemical shift (NICS) calculations. Monocyclic B_2C_5 cluster was shown to possess the greatest NICS values, consistent with its 6π and 6σ electron countings (that is, π and σ double aromaticity). Our analyses also shed light on the reason why C in filled-hexagonal B_6C cluster occupies a peripheral site rather than the center and why C avoids hypercoordination in B-C binary clusters. A similar argument should be extended to and apply for other B-C clusters in prior reports, such as B_6C^{2-}, B_7C^-, and B_8C.

Keywords: boron-carbon mixed clusters; structure and bonding; aromaticity; conflicting aromaticity; adaptive natural density partitioning (AdNDP)

References:

[1] Alexandrova, A. N.; Boldyrev, A. I.; Zhai, H. J.; Wang, L. S. *J. Phys. Chem. A* **2004**, **108**: 3509.

Tracing of Multi-Site Acetal Reactions at Metal Clusters by HR-ESI-TOF-MS

Ying-Zi Han, Jing (Jeanne) Yang, Hai-Feng Su, Shui-Chao Lin, Zi-Chao Tang* and Lan-Sun Zheng

State Key Laboratory of Physical Chemistry of Solid Surfaces, College of Chemistry and Chemical Engineering, Xiamen University, Xiamen 361005

*Email: zctang@xmu.edu.cn

In this work, using the post-modified metal clusters as molecular reactors, the progress of aldehyde ligands with methanol molecules forming hemiacetals and acetals under the catalysis of concentrated sulfuric acids was precisely traced with high resolution ESI-TOF Mass Spectrometry (HR-ESI-TOF-MS). It is indicated that as an effective tool to track chemical reactions, mass spectroscopy could provide some instructions in the designing of molecular reactors, and shows the ability to study the chemical reaction mechanisms.

Keywords: hemiacetal; acetal; metal cluster; reaction; mass spectrometry

References:

[1] Tangoulis, V.; Raptopoulou, C. P.; Paschalidou, S.; Tsohos, A. E.; Bakalbassis, E. G.; Terzis, A.; Perlepes, S. P. *Inorg. Chem.* **1997**, **36**: 5270.

[2] Kalita, A.; Gupta, S. K.; Murugavel, R. *Chem. Eur.J.* **2016**, **22**: 6863.

Fe_2O^+正离子团簇与长链烷烃的反应性研究

胡继闯，许琳琳，马嘉璧*

北京理工大学，北京市房山区良乡高教园区，102488

*majiabi@bit.edu.cn

矿尘颗粒物广泛存在于大气中，其表面可为大气非均相反应提供重要场所[1]。铁氧化物是矿尘颗粒物的重要组成物质，在地球化学和生态系统中起到关键作用[2]。目前，对铁氧化物在一些非均相物理化学反应中的研究较少，尤其在大气污染物中由挥发性有机物（VOC）向半挥发性有机物（SVOC）转变过程中铁氧化物起到的作用尚不十分清楚。

对于凝聚相研究的复杂性和不确定性，气相反应具有反应通道明确，活性位点清楚、反应可控等优点。因此，我们通过构建团簇模型，可以从分子水平清晰认识反应活性位点的构效关系等[3]。

我们利用在时间和空间上进行串联的四极杆质量选择器——线性离子阱——反射式飞行时间质谱连用装置[4]，对铁氧化物阳离子团簇与长链烷烃的反应进行了研究。其中Fe_2O^+可分别与C_3H_8、C_5H_{12}和C_7H_{16}发生脱H_2和吸附反应，同时与后两者还分别有生成C_2H_4、C_4H_8的反应通道，质谱图如Fig. 1所示，反应式如下：

$$Fe_2O^+ + C_3H_8 \rightarrow H_2 + Fe_2OC_3H_6^+$$

$$Fe_2O^+ + C_5H_{12} \rightarrow H_2 + C_2H_4 + Fe_2OC_3H_6^+ + Fe_2OC_5H_{10}^+$$

$$Fe_2O^+ + C_7H_{14} \rightarrow H_2 + C_4H_8 + Fe_2OC_3H_6^+ + Fe_2OC_7H_{14}^+$$

反应速率依次为：2.46E-10、3.59E-10、1.81E-9。

此外，我们结合密度泛函理论计算（DFT），对Fe_2O^+的构型和与C_3H_8的反应路径进行了计算，计算表明发生两步氢转移后，H_2以较低的能垒释放，反应能够发生。势能面如图Fig. 2所示：

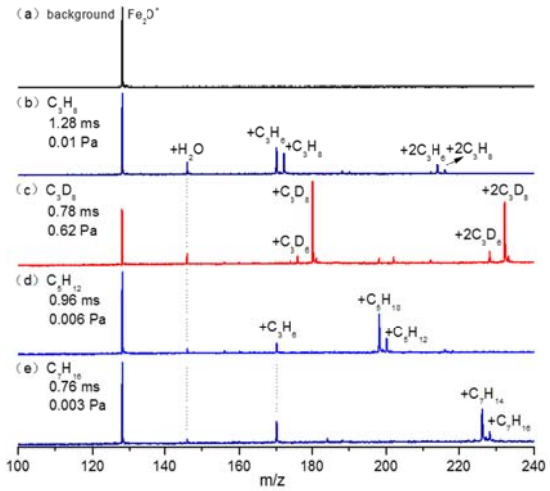

Fig. 1

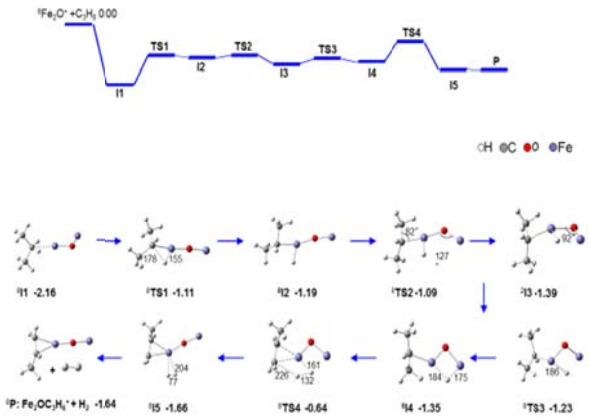

Fig. 2

参考文献

[1]Usher, C. R.; Michel, A. E.; Grassian, V. H. Chem. Rev. **2003, 103 (12)**, 4883.

[2] Dentener, F. J.; Carmichael, G. R.; Zhang, Y.; Lelieveld, J.; Crutzen, P. J.. J. Geophy. Res. Atmos. **1996, 101 (D17)**, 22869-22889.

[3] O'Hair, R. A. J.; Khairallah, G. N.. J. Cluster Sci. **2004, 15 (3)**, 331-363.

[4] Yuan, Z.; Li, Z. Y.; Zhou, Z. X.; Liu, Q. Y.; Zhao, Y. X.; He, S. G.. J. Phys. Chem. C **2014, 118 (27)**, 14967-14976.

CO_2 与 FeH^- 反应生成甲酸根离子 HCO_2^-

姜利学[1,3]，赵重阳[2,3]，李晓娜[1,*]，陈辉[2,*]，何圣贵[1,3,*]

[1] 中国科学院化学研究所分子动态与稳态结构国家重点实验室，北京，100190

[2] 中国科学院化学研究所光化学重点实验室，北京，100190

[3] 中国科学院大学，北京，100049

*Email: lxn@iccas.ac.cn, chenh@iccas.ac.cn, shengguihe@iccas.ac.cn

二氧化碳加氢转变为附加值更高的化学品是降低温室效应、实现碳循环的一条重要途径。CO_2加氢反应过程中，金属氢化物被认为是关键的反应中间体[1]，但其与CO_2反应形成C−H键的微观机理并不十分清楚。研究气相金属氢化物团簇与CO_2的反应可揭示C−H键的形成机理，但目前其反应性研究却鲜有报道[2]。本研究利用激光溅射方法，产生铁-氢团簇阴离子，利用四极杆对具有反应活性的FeH^-双原子离子进行选质，使用线性离子阱研究了FeH^-与CO_2的反应。本工作首次在气相条件下实验观测到碳酸根阴离子HCO_2^-产物的生成(图1)，这表明反应中生成了C−H键。理论计算结果表明，FeH^-离子中H^-离子直接转移是生成HCO_2^-最有效方式，这与凝聚相中铁基催化剂催化氢化CO_2的机理相吻合[3]；而CO_2直接吸附到铁原子上，更易将CO_2还原成CO(图2)。

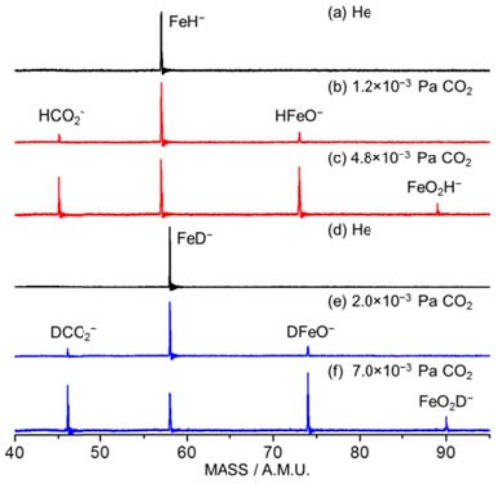

Fig.1 Time-of-flight mass spectra for reactions of FeH^- and FeD^- anions with He (a, d) and CO_2 (b, c, e, and f) for 1.5 ms. The reactant pressures are shown in Pa.

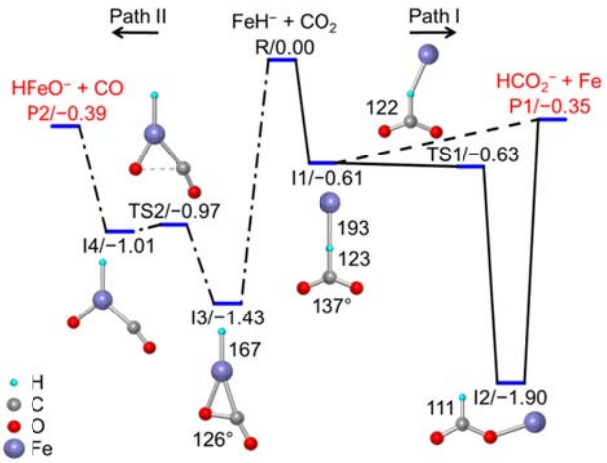

Fig.2 Quantum chemistry-calculated potential energy profiles for the reaction of FeH^- with CO_2 in the quintet state. The relative energies are given on unit of eV.

关键词： 二氧化碳；加氢反应；铁-氢离子；质谱；量化计算

参考文献

[1] S. Kato, S. K. Matam, P. Kerger, L. Bernard, C. Battaglia, D. Vogel, M. Rohwerder, A. Züttel, *Angew. Chem. Int. Ed.* **2016**, **55**: 6028-6032.

[2] H. Schwarz, *Coord. Chem. Rev.* **2017**, **334**: 112-123.

[3] R. Langer, Y. Diskin-Posner, G. Leitus, L. J. W. Shimon, Y. Ben-David, D. Milstein, *Angew. Chem. Int. Ed.* **2011**, **50**: 9948-9952.

三甲胺二聚体中性团簇的 IR-VUV 光谱研究

蒋述康[1]，孔祥涛[1]，张冰冰[1]，江凌[1,*]，…

[1] 中国科学院大连化学物理研究所分子反应动力学国家重点实验室，辽宁大连, 116023

*Email: ljiang@dicp.ac.cn

近年来随着环境问题的日益加重，对大气气溶胶颗粒的形成机理研究成为重要的研究热点，大气中胺类物质三甲胺的含量相对较多，在大气气溶胶的形成和转化过程扮演者重要的角色[1]。对三甲胺中性团簇的研究，将有利于我们从动力学角度认识大气颗粒的成核过程，以及胺类团簇分子的氢键相互作用机理[2]。我们利用自主研制的IR-VUV实验装置，与理论计算紧密结合，研究了三甲胺二聚体中性团簇[3]。实验发现，通过调节脉冲阀的松紧状态，可以在一定程度上控制生成的团簇尺寸大小；其次，通过改变红外激光能量的大小，确认红外谱图中泛频峰的指认；最后，将实验得到的红外光谱结合量子化学计算以及分子动力学模拟，揭示了三甲胺二聚体主要存在两种同分异构体，它们彼此之间可以相互转换。对三甲胺二聚体中性团簇的研究对我们进一步认识胺类氢键的相互作用有着重要的科学意义。

关键词：气溶胶；中性团簇；三甲胺

参考文献

[1] Qiu, C.; Zhang, R. Phys. Chem. Chem. Phys., 2013, 15, 5738-5752.

[2] Zhang, R. Khalizov, A.; Wang, L.; Hu, M.; Xu, W. Chem. Rev. 2012, 112, 1957-2011.

[3] Jiang, S.; Kong, X.; Zhang, B.; Jiang, L., et. al. to be submitted.

$IrAlO_6^+$团簇催化氧化 CO

李晓娜[1]，姜利学[1,2]，张婷[1,2]，何圣贵[1,2*]

[1] 中国科学院化学研究所分子动态与稳态结构国家重点实验室，北京，100190

[2] 中国科学院大学，北京，100190

Email: lxn@iccas.ac.cn, shengguihe@iccas.ac.cn

CO催化氧化是气相和凝聚相反应中的重要模型反应。利用气相团簇实验，在隔离、可控以及可重复条件下，在离子阱反应中研究发现异核金属团簇$IrAlO_6^+$可转移全部氧原子连续氧化六个CO分子，如图1所示（a-f）。$IrAlO_6^+$为目前为止报道的能氧化CO数目最多且能生成无氧产物的团簇离子。与同族的$RhAlO_6^+$和$CoAlO_6^+$团簇离子与CO的对比研究发现，$RhAlO_6^+$和$CoAlO_6^+$团簇离子与CO反应主要生成$RhAlO_4^+$和$CoAlO_4^+$，表明团簇$RhAlO_6^+$和$CoAlO_6^+$中含有弱吸附的分子氧单元。进一步研究表明，缺氧团簇$IrAlO_4^+$-$IrAlO_2^+$可进一步结合分子O_2生成产物$IrAlO_6^+$-$IrAlO_4^+$，其可进一步与CO反应，图1（g-i），而团簇$IrAlO^+$和$IrAl^+$与O_2反应剧烈放热，在离子阱实验中导致团簇碎裂，无法观测到O_2 吸附产物；而在高压快速流动管实验中，可观测到$IrAl^+$吸附三个O_2的反应。本研究表明，Ir-Al团簇特殊的催化模式，可作为探索氧储存材料中氧储存及释放过程反应机理的理想模型。

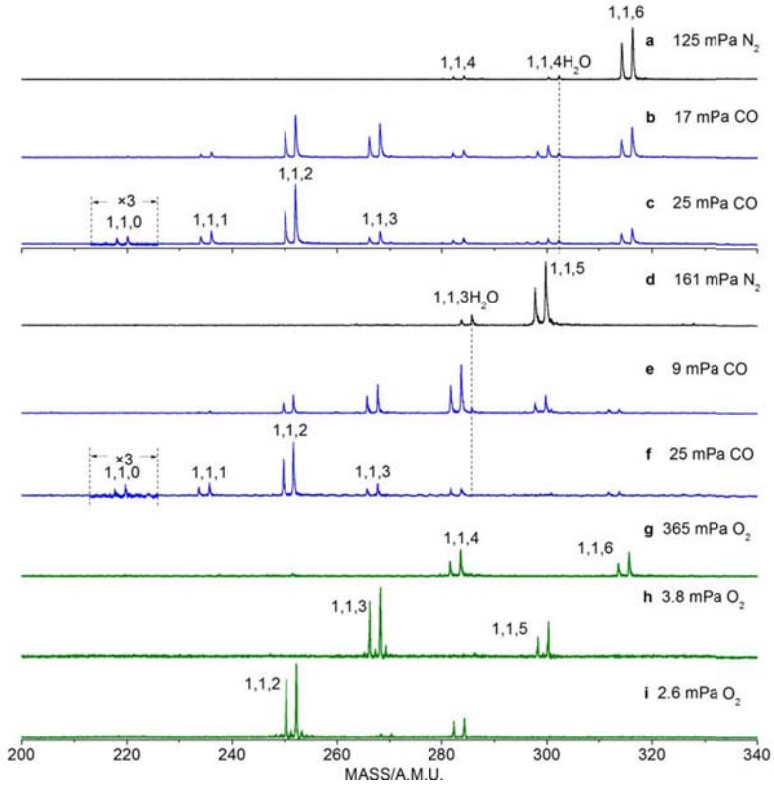

Fig.1 Time-of-flight mass spectra for the reactions of $IrAlO_6^+$ (b,c) and $IrAlO_5^+$ (e,f) clusters with CO, and $IrAlO_4^+$ (g), $IrAlO_3^+$ (h), and $IrAlO_2^+$ (i) clusters with O_2.

关键词： 一氧化碳；团簇；氧释放；氧储存；质谱

Probing thorium oxides and beryllium clusters by high resolution photoelectron imaging

Yanli Li, Xiao-Gen Xiong, Hongtao Liu*
Shanghai Institute of Applied Physics, Chinese Academy of Sciences, Shanghai 201800, P. R. China.
*Email: liuhongtao@sinap.ac.cn

In recent years, the development of velocity-map photoelectron imaging greatly improves the resolution of negative ion photoelectron spectroscopy (< 4 cm^{-1}), especially combined with low temperature ion trap technique, obtaining the fine structure of the molecular vibration comes true. We devoted to probe the electronic structures and chemical bondings of actinide complexes, and we have reported the investigation of the electronic structures and chemical bonding in gaseous thorium monoxide using anion photoelectron spectroscopy and quantum-chemical calculations. The electron affinity of ThO is firstly reported to be 0.71 ± 0.03 eV. Meanwhile, spectroscopic evidence is obtained for two-electron transition in ThO^-, indicating the strong electron correlation among the$(7s_\sigma)^2(6d_\delta)^1$ electrons in ThO^- and the $(7s_\sigma)^2$ electrons in ThO.[1] Still, we carried out the experiments of thorium polyoxide and corresponding calculation is underway. The chemistry of beryllium is known to be significantly different from the behavior exhibited by the heavier group ⅡA elements. Meanwhile, chemical bonding in beryllium clusters is dominated by electron correlation, such that they include significant contributions from doubly excited electron configurations, our group will attempt to carry out experimental and theoretical work on beryllium clusters to reveal the related electronic structures and chemical bonding.

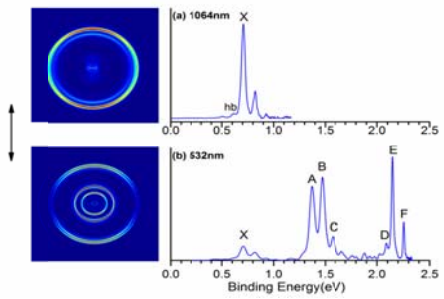

Fig. 1 Photoelectron images and spectra of ThO^- obtained at (a) 1064 nm, (b) 532 nm. The double arrow indicates the laser polarization.

Keywords: photoelectron imaging; thorium oxides; beryllium clusters

References:

[1] Li, Y. L., Zou, J. H., Xiong, X, G., Su, J., Xie, H., Fei, Z. J., Tang, Z. C., Liu, H. T. Probing Chemical Bonding and Electronic Structures in ThO^- by Anion Photoelectron Imaging and Theoretical Calculations. J. Phys. Chem. A, 2017, 121 (10)

Density Functional Study on Small Al-Zn-Mg-Cu-Zr Cluster

Zhi Li[1,*], Zhen Zhao[2], Hongbin Wang[1], Zhonghao Zhou[1]

[1]School of Materials and Metallurgy, University of Science and Technology Liaoning, No. 185 Qianshan Road High-tech Zone, Anshan, 114051

[2]School of Chemistry and Life Science, Anshan Normal University, No. 43 Ping'an Street Tiedong District, Anshan 114007

*Email: Lizhi81723700@163.com

The structures, electronic characters and the dissociation energies of small heteroatomic dimers, trimers, tetramers and pentamer of Al-Zn-Mg-Cu-Zr micro-clusters have been calculated by using the density functional B3LYP method. The calculated spectroscopic constants of single element dimers are in good agreement with the available experimental results. The results reveal that for the energetically most favorable pentamers of Al-Zn-Mg-Cu-Zr clusters, the Zn and Cu atom tends to be located on the two poles of cluster. For heteroatomic AlZnMgCuZr polyatomic system, the arrangement of atoms changes the electron adsorption ability of atoms by Mülliken population analysis. No trimers, tetramers and pentamers of Al-Zn-Mg-Cu-Zr micro-clusters prefers to loss a single Zr atom by the dissociation energies.

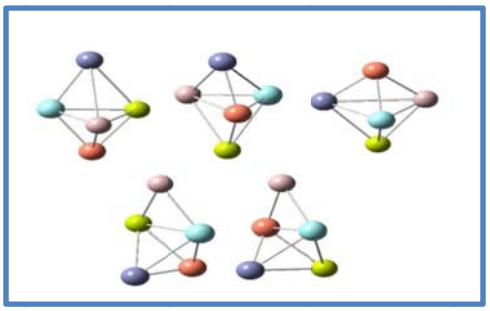

Fig. 1 Considered isomers for AlZnMgCuZr clusters at the B3LYP level

Keywords: Al-Zn-Mg-Cu-Zr Cluster; Density functional theory; Structure; Electronic Property

References:

[1] Li, CM.; Zeng, SM.; Chen, ZQ.; Cheng, NP.; Chen, TX. *Comp. Mater. Sci*. **2014**, **93**: 210.

[2] Ouyang, Y.; Zhai, D.; Wang, P.; Chen, H.; Du, Y.; He, Y. *Theor. Chem. Acc*. **2010**, **127**: 651.

[3] Taylor, S.; Spain, EM.; Morse, MD. *J. Chem. Phys*. **1990**, **93**: 8420.

[4] Morse, MD. *Chem. Rev*. **1986**, **86**: 1049.

[5] Huber, KP.; Herzberg, G. Molecular Spectra and Molecular Structure. IV. Constants of Diatomic Molecules, Van Nostrand Reinhold, New York, **1979**.

[6] Balfour, WJ.; Douglas, AE. *Can. J. Phys*. **2011**, **48**: 901.

[7] Ho, J.; Ervin, K.; Lineberger, WC. *J. Chem. Phys*. **1990**, **93**: 6987.

[8] Leopold, DG.; Ho, J.; Lineberger, WC. *J. Chem. Phys*. **1987**, **86**: 1715.

[9] Arrington, CA.; Blume, T.; Morse, MD.; Doverstål, M.; Sassenberg, U. *J. Phys. Chem*. **1994**, **98**: 1398.

[10] Hu, Z.; Zhou, Q.; Lombardi, JR.; Lindsay, DM.; in: Jena, P.; Khanna, SN.; Rao, BK.; (Eds.), Physics and Chemistry of Finite Systems: From Clusters to Crystals, Kluwer, Dordrecht, **1992**.

氯自由基加成 1-丁烯和异丁烯反应研究

储根柏,陈军,李淹博,余业鹏,李照辉,林煊,刘付轶*,单小斌,盛六四

中国科学技术大学国家同步辐射实验室，合肥市合作化南路 42 号，230029

*Email:fyliu@ustc.edu.cn

氯自由基在大气氧化有机物中起到重要作用，实验测得室温常压下 Cl 与 1-丁烯及异丁烯的速率常数分别为 3.38 和 3.40×10^{-10} cm^3 $molecule^{-1}s^{-1}$，氯自由基加成到 1-丁烯和异丁烯的反应速率[1]被预测为 2.60 和 2.64×10^{-10} cm^3 $molecule^{-1}s^{-1}$，此速率占了总反应速率的大部分。理论上曾预言了两个相似的氯加成到丙烯上的通道，反应经过过渡态 TS_{add}，此过渡态的能垒比 5 个消除通道对应的过渡态能垒低很多，这暗示加成形成氯丙烯烃自由基比消除形成的 C_3H_5 自由基更易发生。因此，氯自由基加成到 1-丁烯或异丁烯可能是主要的反应通道。

本文利用流动管反应器-激光闪光光解-同步辐射光电离质谱技术研究氯自由基与 1-丁烯和异丁烯的反应。能量 11 eV 下质谱减去非光解条件下的本底质谱同时观察到加成产物 C_4H_7Cl 和消去产物 C_4H_7 和 C_4H_6。实验测得 C_4H_7Cl 的电离能分别为 9.58 ± 0.10 和 9.56 ± 0.10 eV,同可能的异构体 $CH_3CH_2CCl=CH_2$, $CH_3CH=CHCH_2Cl$, $CH_3CH_2CH=CHCl$ (1-丁烯)及 $CH_2=C(CH_3)CH_2CI$ (异丁烯)的理论电离能一致。可能的加成和消去反应通道在 MP2/aug-cc-pvtz 水平下计算。两种（1-丁烯)和一种(异丁烯)可能的加成通道经历 Cl 自由基先加成到丁烯的不饱和键上再形成氯丁烷基自由基。一种(1-丁烯、异丁烯)可能的消去通道被证实为可行的。实验观察到的氯丁烯主要来源于 Cl 由基与所形成的氯丁烷基自由基的二次反应。

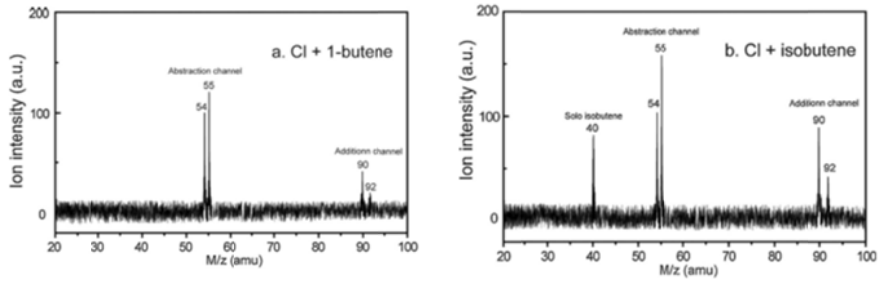

Fig.1 The mass spectra acquired at the photon energy of 11eV after subtracting the non-photolysis mass spectra for Cl radical with 1-butene (a) and isobutene (b), respectively.

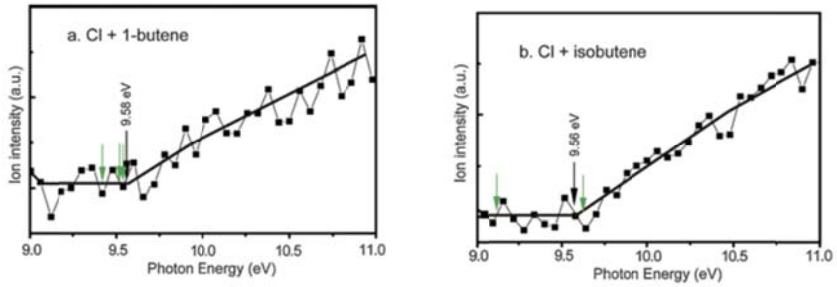

Fig. 2 The photoionization efficiency (PIE) curves of the addition products C_4H_7Cl species from Cl with1-butene **(**a) and isobutene (b), respectively.

关键词：同步辐射；光电离质谱；流动管反应器；闪光光解；自由基反应

参考文献

[1] M.J. Ezell,W.Wang, A.A. Ezell, G. Soskin, B.J.F. Pitts, Phys. Chem. Chem. Phys. 4(2002) 5813.

TaC^-双原子阴离子的低温光电子速度成像研究

刘清宇[1,2]，何圣贵[1,2,*]

[1] 中国科学院化学研究所北京分子科学国家实验室，北京，100190

[2] 中国科学院大学，北京，100049

*Email: shengguihe@iccas.ac.cn

过渡金属碳化物的电子结构和反应活性在众多研究领域内引起了广泛的兴趣，其双原子分子是研究成键性质和反应活性的最简单体系。[1-3] 本工作采用低温离子阱结合光电子速度成像方法研究了TaC^-双原子阴离子在常温与低温下的光电子能谱（如图1a），低温冷却有效消除了TaC^-光电子能谱中的热带。TaC的电子亲和能由实验准确测定为2.097 ± 0.003 eV，基态振动频率确定为766 ± 24 cm^{-1}。实验发现了TaC^-位于2.4 eV附近的Feshbach态（如图1b）。本研究表明低温对双原子阴离子的光电子速度成像研究具有重要意义。

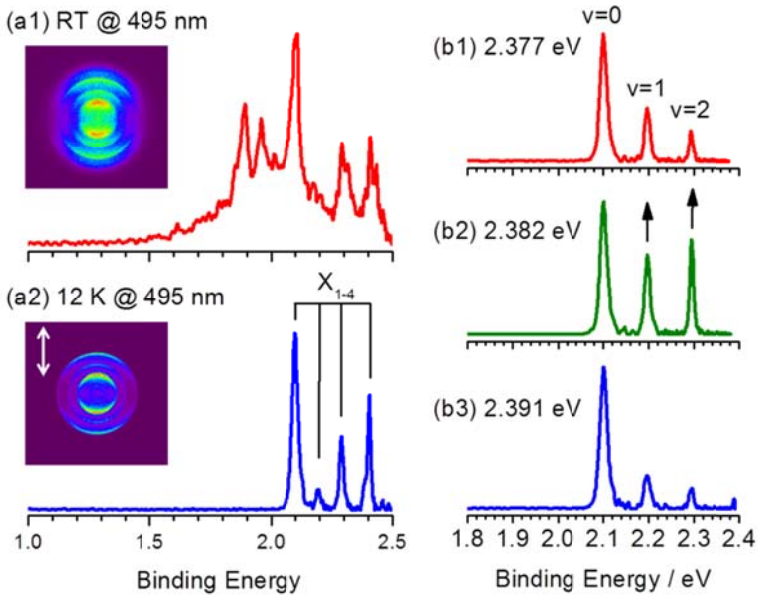

Fig. 1 Photoelectron images and spectra taken at 495 nm (2.505 eV) under room temperature and 12 K (a), and cold photoelectron spectra taken at 2.377 eV, 2.382 eV, and 2.391 eV (b).

关键词： TaC；低温离子阱；光电子速度成像

参考文献

[1] Li, H.-F.; Zhao, Y.-X.; Yuan, Z.; Liu, Q.-Y.; Li, Z.-Y.; Li, X.-N.; Ning, C.-G.; He, S.-G., *J. Phys. Chem. Lett.* **2017**, *8* , 605.

[2] Liu, Q.-Y.; Hu, L.; Li, Z.-Y.; Ning, C.-G.; Ma, J.-B.; Chen, H.; He, S.-G., *J. Chem. Phys.* **2015**, *142*, 164301.

[3] Luo, Z.; Huang, H.; Zhang, Z.; Chang, Y.-C.; Ng, C. Y., *J. Chem. Phys.* **2014**, *141*,024304.

Rh-doped Hexadecagold Cluster

Zhiling Liu[1,*], JinXun Liu[2]

[1]Key Laboratory of Magnetic Molecules & Magnetic Information Materials, Ministry of Education, The School of Chemical and Material Science, Shanxi Normal University. No. 1, Gongyuan Street, Linfen, 041004

[2]Inorganic Materials Chemistry, Department of Chemistry and Chemical Engineering, Eindhoven University of Technology, Eindhoven, 5600 MB, Netherlands.

*Email: lzling@sxnu.edu.cn

Gold has been at the center of the attention of the catalysis community, since pioneer reports of Haruta and Hutchings demonstrated the outstanding catalytic properties of nanoscale gold. An important corollary from the extensive follow-up work on heterogeneous gold systems is that size, morphology and oxidation state all profoundly affect gold's unique catalytic properties. Also doped gold clusters have received increasing attention, because doping presents a way to tune the electronic and catalytic properties. A cluster that has caught significant attention is the hollow hexadecagold cage with tetrahedral (T_d) point symmetry. We here use a genetic search algorithm based on DFT calculations to compute the energy of candidate structures to predict stable Au_{16} and neutral and anionic Rh-doped Au_{16} clusters. The algorithm correctly identifies the T_d cage as the most stable structure for the neutral Au_{16} cluster. These calculations also demonstrate the possibility of endohedral doping by Rh, in this way, and we show that neutral and anionic Rh–Au_{16} clusters (Rh@Au_{16}). Anionic Rh@Au_{16} (T_d) has a FCC Rh@Au_{12} octahedral core, and the other four gold atoms are above its four triangular faces. Magic electronic stability of the cluster is explained by the super valence bond model, of which it can be seen as a superatomic molecule in the electronic structure.

铜-钒氧化物团簇催化氧化 CO 反应中的自旋湮灭研究

王丽娜 [1,2]，李晓娜 [1*]，何圣贵 [1*]

[1] 中国科学院化学研究所分子动态与稳态结构国家重点实验室，北京，100190

[2] 中国科学院大学，北京，100049

*Email: lxn@iccas.ac.cn; shengguihe@iccas.ac.cn

CO氧化是异相催化中重要的模型反应，在很多实际过程中也具有重要应用[1]。CO催化氧化的反应机理一直备受科学家广泛研究[2]，然而CO催化氧化过程中的自旋湮灭问题（$2^1CO + {}^3O_2 \rightarrow 2^1CO_2$），却一直未被考虑。CO催化氧化过程中分子氧的三重态自旋在反应过程中如何发生改变并不清楚。本研究利用团簇模型阐述了O_2分子自旋湮灭的反应机理。我们利用激光溅射方法，制备了铜-钒氧化物团簇阴离子$Cu_2VO_{3\text{-}5}^-$。质谱实验研究发现$Cu_2VO_{3\text{-}5}^-$团簇离子可利用O_2分子催化氧化CO（图1）；而速率曲线拟合结果表明，整个催化氧化过程由六个活性物种构成，如图2b所示，而非三个（图2a）。理论计算结果指出基态$Cu_2VO_{3,4}^-$结构为单重态而$Cu_2VO_5^-$的基态电子结构为三重态，本研究也是首次报道的闭壳层团簇离子参与CO的催化氧化反应。结合团簇实验和理论计算，我们得出结论，需要两个O_2分子连续参与反应，才可导致CO催化氧化过程中三重态自旋的湮灭，即CO催化氧化公式应写成：$4^1CO + 2^3O_2 \rightarrow 4\ ^1CO_2$。

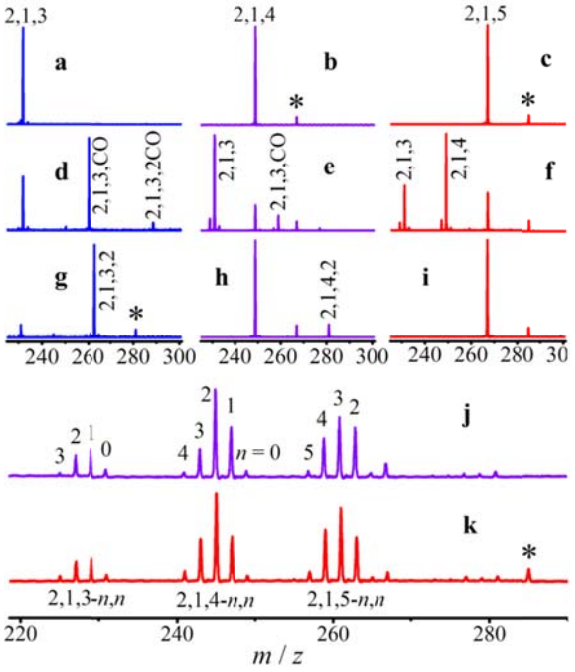

Fig. 1 Elementary (d-i) and catalytic (j,k) reactions of the atomic cluster ions

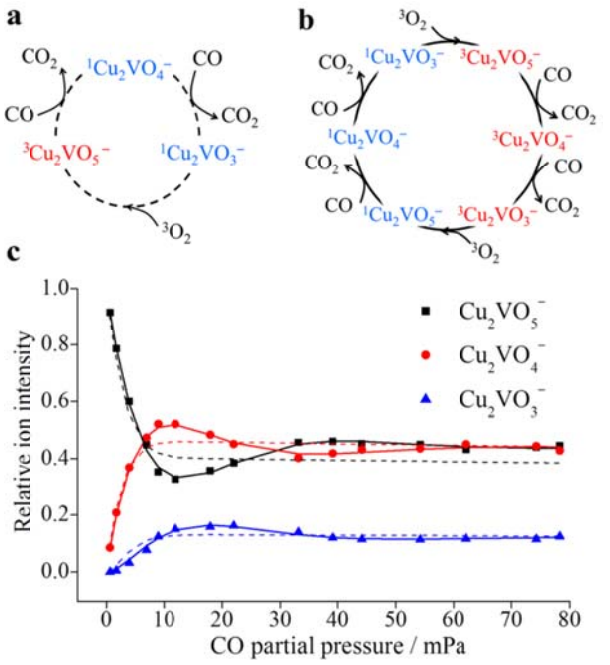

Fig. 2 Catalytic cycle (a,**b**) and the reaction kinetics (c)

关键词： 一氧化碳氧化；自旋湮灭；质谱；量子化学计算

参考文献

[1] Freund, H. J., Meijer, G., Scheffler, M., Schlogl, R.., Wolf, M. *Angew. Chem. Int. Ed.* **2011, 50**: 10064.

[2] Lin, J., Wang, X., Zhang, T. *Chinese J Catal* **2016, 37**: 1805.

Low-temperature adsorption of O_2 on Au_n^- (n = 2 - 36)

Tingting Wang[1], Jun Ma[1], Baoqi Yin[1], Xiaopeng Xing[1,*]

[1]School of Chemical Science and Engineering, Tongji University, No 1239, Siping Road, 200092
*Email: xingxp@tongji.edu.cn

We studied low-temperature adsorption of O_2 on Au_n^-, in which n ranges from 2 to 100. Only some even sizes can adsorb a single O_2 molecule to form $Au_nO_2^-$, and the largest active one is found to be Au_{36}^-. The kinetic measurements distinguished co-existing isomers of Au_{10}^-, Au_{18}^-, and Au_{22}^-, while the isomers of many other sizes including the co-existing 2D and 3D isomers of Au_{12}^- have nearly identical reaction rates. Analyses indicates that the global electronic properties of anionic gold clusters dominate the O_2 adsorption processes, while the local structures of the adsorption sites play no or negligible effects. These observations provide more profound views on the adsorption and activation of O_2 on real catalysts containing dispersed gold.

Keywords: cluster reactions; flow-reactor; gold clusters; adsorption of O_2; isomer titration

Why nanoscale tank treads move? Structures, bonding, and molecular dynamics of a doped boron cluster $B_{10}C$

Ying-Jin Wang, Jin-Chang Guo, Hua-Jin Zhai (翟华金)*

Nanocluster Laboratory, Institute of Molecular Science, Shanxi University, Taiyuan, 030006

*Email: hj.zhai@sxu.edu.cn

Planar boron clusters form dynamic rotors [1,2], either as molecular Wankel motors or subnanoscale tank treads, the latter being exemplified by an elongated B_{11}^- cluster [1]. For an in-depth mechanistic understanding of the rotors, we investigate herein a doped boron cluster, $B_{10}C$, in which a C atom isovalently substitutes B^- in the B_{11}^- tank tread. Two critical structures are reached: the C_s ($^1A'$) global minimum (GM) with C positioned in the peripheral ring and the C_{2v} ($^1A_1$) local minimum (LM) with C in diatomic core. In the GM the C atom completely halts the rotation of $B_{10}C$, whereas in the LM the dynamic fluxionality retains. The energy barriers for in-plane rotation differ markedly: 12.93/18.31 kcal mol^{-1} for GM versus 1.84 kcal mol^{-1} for LM at the single-point CCSD(T) level. The GM rotates via two transition states (TS), compared to one for the LM. Chemical bonding in the structures is elucidated via canonical molecular orbital (CMO) analysis, adaptive natural density partitioning (AdNDP), electron localization functions (ELFs), and Wiberg bond indices (WBI). Electron delocalization is shown to be essential for structural fluxionality. In particular, the variation of WBI from the GM or LM geometries to their TS structures correlates positively to the energy barrier, which offers a quasi-quantitative measure of the barrier height and hence controls the dynamics. The finding should be extended to and applicable for all molecular rotors, as well as elucidate why a strongly covalent bound nanosystem and a weakly bound one can behave similarly.

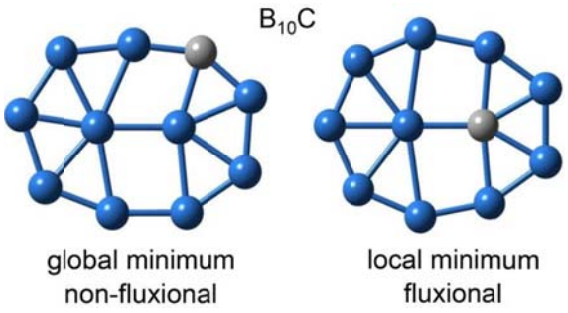

Fig. 1 Optimized structures of C_s ($^1A'$) global minimum (GM) and C_{2v} ($^1A_1$) local minimum (LM) of $B_{10}C$

Keywords: subnanoscale tank treads; boron clusters; structural fluxionality; molecular dynamics; aromaticity

References:

[1] Wang, Y.J.; Zhao, X.Y.; Chen, Q.; Zhai, H.J.; Li, S.D. *Nanoscale* **2015**, **7**: 16054.

[2] Jiménez-Halla, J.O.C.; Islas, R.; Heine, T.; Merino, G. *Angew. Chem. Int. Ed.* **2010**, **49**: 5668.

Chemisorption of Atomic Hydrogen, Oxygen and Carbon on Small Iron Clusters: A First-principle Study

Zongying Wang, XiangjianShen*, Tianshui Liang*

School of Chemical Engineering and Energy, Zhengzhou University, Zhengzhou 450001, China

Email: xjshen85@zzu.edu.cn, liangtsh@zzu.edu.cn

The chemisorption of light element atoms on transition metal clusters is of great significance in studying surface/interface reaction dynamics. Here, the atomic interactions between three light elements(i.e., hydrogen, oxygen and carbon) and small Fe clusters (n=1,2,3,4) were investigated based on ab initio density functional theory calculations. Our theoretical results clearly show that, the one gas-phase Fe atom can absorb mostly ten H atoms and five O atoms. A long carbon chain is formed among these Fe clusters as increasing of C atoms number. The structures of bare iron cluster containing four Fe atoms are destroyed by increasing enough number of H, O, and C atoms. Furthermore, the mechanism of atomic adsorption of H,O and C are drawn according to the structure symmetry, magnetic moments and adsorption energy.

Keywords: small iron clusters; atomic chemisorption; first-principle calculation

References:

[1]Keisuke Takahashi; Shigehito Isobe; Somei Ohnuki. Appl .Phys. Lett. **2013, 102**: 113108.

$Mn_xC_y^-$ 团簇的结构和成键性质研究

徐西玲，杨斌，许洪光，郑卫军*

中国科学院化学研究所，分子反应动力学国家重点实验室，北京市海淀区中关村北一街 2 号，100190

*Email: zhengwj@iccas.ac.cn

过渡金属碳化物具有独特的物理和化学性质，如高熔点、高硬度、高导电性和高导热性。它们在切割工具和硬质涂层材料方面有着广泛的应用。研究表明一些前过渡金属碳化物展现出了独特而有趣的类似于金属铂的催化性质，特别是涉及到C-H键活化的反应。过渡金属不仅可以位于碳笼的内部形成内嵌金属富勒烯，而且可以作为碳笼的一部分，其中金属碳笼met-cars[1]是以M_8C_{12}形式存在，具有极高稳定性。已有的研究指出形成met-cars的金属原子主要是前3d过渡金属原子 (Ti,V,Cr)。最近的研究发现，前过渡金属形成的一系列二维金属碳化物可以作为锂离子电池、非锂离子电池和超级电容器的电极材料[2,3]。而后3d过渡金属原子(Fe, Co, Ni)是单壁碳纳米管生长过程中的催化剂。有关于锰碳团簇的研究十分欠缺。为了研究锰碳团簇的结构演化、电子性质和成键特性，我们测量了$Mn_xC_y^-$ (x = 1-5; m = 3,4)团簇的光电子能谱，获得了它们的垂直脱附能和绝热脱附能，并利用密度泛函计算了它们的结构。通过比较实验和理论结果，确定了他们的最稳定结构：$Mn_{1-4}C_3^-$都是平面结构，$Mn_5C_3^-$是三维结构；其中MnC_3^-是C_{2v}对称的扇形结构，$Mn_{2-5}C_3^-$团簇中，3个C原子被Mn原子分开成为一个C原子和一个C_2二聚体；MnC_4^-是$C_{\infty v}$对称的线性结构，$Mn_{2-4}C_4^-$团簇中，4个C原子被Mn原子分开成为2个C_2二聚体，而$Mn_5C_4^-$团簇中4个C原子是以1个C_2二聚体和2个C原子的形式存在。$Mn_4C_4^-$的结构不同于$V_4C_4^-$ [4]和$Co_4C_4^-$[5]的结构, $Mn_5C_4^-$的结构不同于$V_5C_4^-$ [4]的结构。具体分析将在海报中给出。

关键词：过渡金属碳化物；光电子能谱

参考文献

[1] Guo, B. C.; Kerns, K. P.; Castleman, A. W. *Science*. **1992**, **255**: 1411.

[2] Naguib, M.; Come, J.; Dyatkin, B.; Presser, V.; Taberna, P.-L.; Simon, P.; Barsoum, M. W.; Gogotsi, Y. *Electrochem. Commun*. **2012**, **16**: 61.

[3] Byeon, A.; Zhao, M. Q.; Ren, C. E.; Halim, J.; Kota, S.; Urbankowski, P.; Anasori, B.; Barsoum, M. W.; Gogotsi, Y. *ACS Appl. Mater. Interfaces*. **2017**, **9**: 4296.

[4] Yuan, J. Y.; Wang, P.; Hou, G. L.; Feng, G.; Zhang, W. J.; Xu, X. L.; Xu, H. G.; Yang, J. L.; Zheng, W. J. *J. Phys. Chem. A* **2016**, **120**: 1520.

[5] Xu, X. L.; Yuan, J. Y.; Yang, B.; Xu, H. G.; Zheng, W. J. under review.

Investigation on Semiconductor Clusters Doped with Metal Atoms

Hong-Guang Xu,*, Sheng-Jie Lu, Xiao-Jiao Deng, Wei-Jun Zheng*
Beijing National Laboratory for Molecular Sciences, State Key Laboratory of Molecular Reaction Dynamics, Institute of Chemistry, Chinese Academy of Sciences, Beijing, 100190
*E-mail: xuhong@iccas.ac.cn

Semiconductor clusters doped with metal atoms have potential applications in nanomaterials and microelectronics. Doping metal atoms into semiconductor clusters can stabilize cage structures of these clusters and modulate the physical chemical properties of these clusters, therefore, can produce materials with novel properties. We generate metal-doped semiconductor by the laser ablation source, and investigate their structures and properties using time-of-flight mass spectrometry and photoelectron spectroscopy combined with quantum chemistry calculations. Our studies found several clusters with novel structures and properties, such as the smallest fullerene-like silicon cage $V_2@Si_{20}$, the wheel-like structure V_3Si_{12} with ferromagnetic properties, and the I_h symmetric icosahedral structure $Au@Ge_{12}$. These findings for novel clusters will provide valuable information for the development of semiconductor nanotubers and self-assembled functional materials.

Keywords: Semiconductor clusters; anion photoelectron spectroscopy; DFT calculations; cage structure;

光电子能谱与密度泛函方法对 $Cr_nSi_{12}^-$(n=1,2,3)团簇的研究

杨斌[1]，王鹏[1]，徐西玲[1]，卢胜杰[1]，许洪光[1]，郑卫军[1,*]

[1] 中国科学院化学研究所，北京市海淀区中关村北一街 2 号，100190

*Email: zhengwj@iccas.ac.cn

采用激光溅射的方法产生了铬掺杂硅 $Cr_nSi_{12}^-$(n=1,2,3)系列负离子团簇，通过对 $Cr_nSi_{12}^-$(n=1,2,3)负离子团簇进行光电子能谱研究获得该系列团簇的垂直脱附能 VDEs 和绝热脱附能 ADEs。采用密度泛函方法计算光电子能谱与密度泛函方法研究 $Cr_nSi_{12}^-$(n=1,2,3)，获得 $Cr_nSi_{12}^-$(n=1,2,3)团簇的结构，认识到 $Cr_nSi_{12}^-$(n=1,2,3)团簇电子分布、芳香性、磁性等性质，阐明了多个过渡金属对硅笼结构的稳定作用。

关键词：光电子能谱；密度泛函；铬硅团簇

Reactions of Yttrium-oxygen Cation with Carbon Dioxide: An Infrared Photodissociation Spectroscopic and Theoretical Study

Dong Yang, Zhi Zhao, Xiangtao Kong, Ling Jiang*

State Key Laboratory of Molecular Reaction Dynamics, Dalian Institute of Chemical Physics, Chinese Academy of Sciences, 457 Zhongshan Road, Dalian 116023, China

The reaction of Yttrium-oxygen cation with carbon dioxide has been studied by mass-selected infrared photodissociation spectroscopy. Quantum chemical calculations have been performed on these products, which aid the experimental assignments of the infrared spectra and help to elucidate the geometrical and electronic structures. Results reveal that YO^+ cation can bind to an oxygen atom of CO_2 in an ''end-on'' configuration or react with CO_2 to form yttrium-carbonate structure. The transform starts at n = 4. Then, yttrium-carbonate structures become dominating. On the other hand, the electrostatic interaction between oxygen atoms of $[YCO_3]^+$ and carbon atoms of CO_2 is very weak and flexible, so dynamic effect could be also very important in this system.

Keywords: metal; carbon dioxide; infrared photodissociation spectroscopy; quantum chemical calculation

References:

[1] Freund, H. J.; Roberts, M. W. *Surf. Sci. Rep.* **1996**, *25*, 225-273.

[2] Gibson, D. H. *Chem. Rev.* **1996**, *96*, 2063-2095.

[3] Taifan, W.; Boily, J.-F.; Baltrusaitis, J. *Surf. Sci. Rep.* **2016**, *71*, 595-671.

[4] Ricks, A. M.; Brathwaite, A. D.; Duncan, M. A. *J. Phys. Chem. A* **2013**, *117*, 11490-11498.

[5] Zhao, Z.; Kong, X.-T.; Yang, D.; Yuan, Q.-Q.; Xie, H.; Fan, H.-J.; Zhao, J.-J.; Jiang, L. *J. Phys.Chem. A* **2017**, *121*, 3220-3226.

Channel resolved multiorbital double ionization of molecular Cl_2 in intense femtosecond laser field

Jian Zhang[1], Zhipeng Li[2], Haitao Sun[2], Shian Zhang[2], Zhenrong Sun[2] and Yan Yang[2,3,*]

[1]College of Chemistry, Chemical Engineering and Biotechnology, Donghua University, Shanghai, 201620, China

[2]State Key Laboratory of Precision Spectroscopy, School of Physics and Materials Science, East China Normal University, Shanghai 200062, China

[3]State Key Laboratory of High Field Laser Physics, Shanghai Institute of Optics and Fine Mechanics, Chinese Academy of Sciences, Shanghai 201800, China

We experimentally study the sequential double ionization and the subsequent Coulomb explosion of molecular Cl_2 in intense femtosecond laser field by using dc-sliced ion imaging technique. The measurement results indicate not only highest occupied molecule orbital (HOMO) but also the next two lower-lying molecular orbitals are involved in three distinguished reaction pathways. For pathway I and III, in which the two electrons remove from HOMO and HOMO-2 with reverse sequence, the ionic excited states $^1\Pi_g$ and $^3\Pi_g$ are populated, respectively. The kinetic energy releases difference observed in these two channels is ascribed to the nuclear motion during the ionization process. For pathway II, the isotropic angular distribution of fragment ions is contributed to the combination of electron density distribution of HOMO-1, vibrational electronic wave packets evolution and field excitation. Our results propose a feasible method to manipulate the electronic dynamics which takes place in attosecond time domain by femtosecond laser field by accurately tuning laser parameters.

CuO_n^-(n = 1_ 3)和 AgO_n^- (n = 1_ 3，5)团簇与 CO 的反应

殷保祺[1]，王亭亭[2]，马骏，邢小鹏[1,*]

[1] 同济大学化学科学与工程学院，上海市四平路 1239 号，200092

*Email: xingxp@tongji.edu.cn

我们利用磁控溅射团簇源产生了CuO_n^-和AgO_n^-团簇，并将其引入流动管反应器，研究了其在150K条件下与CO的反应。由于Cu、Ag元素电子结构的差异，同样团簇源条件下两种金属分别形成了CuO_n^-(n = 1−3)和AgO_n^- (n = 1−3，5)。在低温反应管中，CuO^-、CuO_3^-、AgO^-、AgO_3^-和AgO_5^-都能氧化CO，生成单金属离子，但CuO_2^-和AgO_2^-和CO几乎不反应。我们通过理论计算很好的解释了观察到的实验现象，从分子水平揭示Cu、Ag离子表面各种氧物种与CO的反应机理，为理解相关催化剂表面的物理化学过程提供了理论基础。

关键词：铜氧化物团簇；银氧化物团簇；CO低温氧化

振动态选择的 NO_2^+离子解离动力学研究

于同坡 [1]，吴向坤 [1]，徐磊 [1]，周晓国 [1*]，刘世林 [1*]，

刘付轶 [2]，盛六四 [2]

1 微尺度物质科学国家实验室(筹)，中国科学技术大学化学物理系，安徽合肥，230026

2 国家同步辐射实验室，中国科学技术大学，安徽合肥，230027

*Email: xzhou@ustc.edu.cn (X. Zhou), slliu@ustc.edu.cn (S. Liu)

结合阈值光电子-光离子符合成像和同步辐射光电离技术[1]，我们开展了 NO_2^+离子的 a^3B_2 和 b^3A_2 电子态的解离动力学研究。在 12.8-14.0 eV 范围内测量得到的 NO_2^+离子 a^3B_2 和 b^3A_2 态的振动分辨阈值光电子谱（TPE）主要包含弯曲振动 ν_2^+激发。由电子-离子符合的飞行时间（TOF）质谱可以清楚看出，NO_2^+离子的解离是从 a^3B_2（0,2,0）开始的，并且 NO^+碎片离子的质谱宽度随着振动激发而逐渐加宽。通过测量处于 a^3B_2（0,3,0）和（0,4,0）态以及 b^3A_2（0,0,0）振动态的 NO_2^+离子解离生成的 NO^+碎片离子的符合速度聚焦影像，我们得到了解离过程中释放的总的平动能分布和 NO^+离子的角度分布。结合量子化学理论计算的势能面[2]，我们得到了 NO_2^+离子的 a^3B_2 和 b^3A_2 电子态的解离机理。

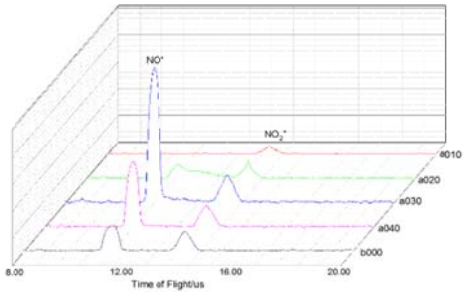

Fig. 1 Vibrational state-selected TPEPICO TOF mass spectra for the DPI process of NO_2

关键词： 解离动力学；光电离；阈值光电子谱；光电子-光离子符合；速度成像

参考文献

[1] Xiaofeng.Tang, Xiaoguo . Zhou*, Mingli Niu, Shilin. Liu*, Jinda Sun, Xiaobin .Shan, Fuyi .Liu, Liusi .Sheng. *Rev. Sci. Instrum.,* **2009, 80**: 113101

[2] HaiBo.Chang and MingBao.Huang. *Chem. Phys. Chem,***2009**,**10**:582-589

Investigate HCN-(pH_2)$_N$ clusters with Multi-Dimension Morse/Long-Range Potential and Path Integral Monte Carlo Simulation

Yu Zhai[1], and Hui Li[1, *]

[1]Institute of Theoretical Chemistry, Jilin University, 2519 Jiefang Road, Changchun, 130023
*Email: prof_huili@jlu.edu.cn

In this work, we present an accurate five-dimension (5D) intermolecular Potential Energy Surface (PES) including the intramolecular C-H vibrational normal coordinate. Approximation is made that intramolecular vibration can be separated from the total motions, and what we call 'vibrational averaging' is performed to obtain two 4D intermolecular PES corresponding to the vibrational ground and excited state of HCN interacting with the molecular hydrogen, and the pointwise energies are fitted to Multi-Dimension Morse/Long-Range potential energy model.[1, 2] Considering the rotational constant of hydrogen is much larger than HCN and the complex, 'Adiabatic-Hindered-Rotor' approximation[3], in which the rotational Schrodinger of H_2 is solved ahead of other parts, are made to get two effective 2D intermolecular HCN-(pH_2) interaction potential, for the ground and excited state of HCN, respectively. Based on these PES's, the infrared spectrum of HCN-H_2 complex and the band origin shifts of HCN-(pH_2)$_N$ are calculated using hybrid Discrete Variable Representation (DVR) – Finite Basis Representation (FBR) method with Lanczos algorithm[2] and Path Integral Monte Carlo (PIMC) simulation[4]. The 2D density distributions of HCN-(pH_2)$_N$ clusters are also provided with comparison with the band origin shifts.

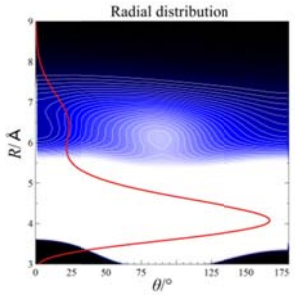

Fig. 1 The beginning of second solvent shell: HCN-(pH_2)$_{18}$.

Keywords: Morse/Long-Range Model; Cluster; Path Integral Monte Carlo; Adiabatic hindered-rotor; Solvent structure

References:

[1] J.-M. Liu, Y. Zhai, and H. Li, *J. Chem. Phys.*, accepted (2017).
[2] H. Li, P.-N. Roy, and R. J. Le Roy, *J. Chem. Phys.*, **132**, 214309 (2010).
[3] H. Li, P.-N. Roy, and R. J. Le Roy, *J. Chem. Phys.*, **133**, 104305 (2010).
[4] T. Zeng, N. Blinov, G. Guillin, H. Li, and P.-N. Roy, *Comp. Phys. Comm.*, **204**, 170 (2016).

异核三金属羰基团簇负离子的光电子速度成像研究

张菊梅，谢华，邹静涵，江凌*

中国科学院大连化学物理研究所分子反应动力学国家重点实验室, 辽宁大连, 116023

*Email: ljiang@dicp.ac.cn

CO 与过渡金属的反应在催化过程中有着非常广泛的实际应用价值[1]。金属团簇可以反映催化剂在反应过程中的活性位点及配位数，协同作用使异核过渡金属具有更高效催化活性[2-7]。金属羰基化合物对于研究异核过渡金属催化反应中的协同作用是一个十分合适的模型。对于异核双金属羰基化合物已有很多研究，而异核三金属羰基化合物的报道甚少。异核三金属与羰基的配位方式，及活性位如何可以更好地模拟金属表面与 CO 的相互作用。本文研究利用光电子速度成像实验方法，并与理论计算相结合，研究了 $V_2Ni(CO)_n^-$ (n=6-10) 团簇结构的生长规律[8]。研究表明，n=6 团簇含有两个端式两个桥式两个侧配位的 CO，n=7-9 团簇分别是在 n=6 的基础上成键，后续的 CO 与 V 配位。在 n=10 团簇中，形成了 7 个端式 3 个桥式，以两个 V 原子为中心形成八面体结构，以 Ni 原子为中心形成四面体结构。

关键词：羰基，团簇，光电子速度成像

参考文献

[1] Ricks, A. M.; Bakker, J. M.; Douberly, G. E.; Duncan, M. A. *J Phys Chem A* **2009**, *113*, 4701-4708.

[2] Freund, H. J.; Meijer, G.; Scheffler, M.; Schlogl, R.; Wolf, M. *Angew. Chem., Int. Ed.* **2011**, *50*, 10064-10094.

[3] Qu, H.; Kong, F.; Wang, G.; Zhou, M. *J Phys Chem A* **2017**, *121*, 1627-1632.

[4] Xie, H.; Zou, J.; Yuan, Q.; Fan, H.; Tang, Z.; Jiang, L. *J. Chem. Phys.* **2016**, *144*, 124303.

[5] Zou, J.; Xie, H.; Dai, D.; Tang, Z.; Jiang, L. *J. Chem. Phys.* **2016**, *145*, 184302.

[6] Zou, J.; Xie, H.; Yuan, Q.; Zhang, J.; Dai, D.; Fan, H.; Tang, Z.; Jiang, L. *Phys. Chem. Chem. Phys.* **2017**, *19*, 9790-9797.

[7] Wang, P.; Xie, H.; Guo, J.; Zhao, Z.; Kong, X.; Gao, W.; Chang, F.; He, T.; Wu, G.; Chen, M.; Jiang, L.; Chen, P. *Angew. Chem., Int. Ed.* **2017**, in press.

[8] Zhang, J.; Xie, H.; Zou, J.; Jiang, L. *to be submitted*.

氧化钴团簇上共吸附小分子的光诱导反应研究

张梅琦 [1,2]，何圣贵 [1,2*]

[1] 北京分子科学国家实验室，中国科学院化学研究所分子动态与稳态结构实验室，北京，100190

[2] 中国科学院大学，北京，100049

*Email: shengguihe@iccas.ac.cn

光催化反应是一种在温和条件下活化转化小分子的重要手段。作为一类重要的半导体光催化材料，过渡金属氧化物在水的光解、一氧化碳的光诱导氧化等方面应用广泛[1-3]。气态条件下的过渡金属氧化物团簇具有元素组分和原子数目确定的特点，研究其吸附小分子后的光诱导反应，有助于进一步探索小分子活化转化的新方式以及深入认识光催化反应的微观图像[4-7]。通过激光溅射法制备的氧化钴团簇阳离子，在快速流动管中共吸附一个H_2O分子和一个CO分子后进入飞行时间质谱，质量选择后与不同波长的激光相互作用。检测光诱导反应产物与未反应的反应物，如图1所示。在紫外光（355nm）的作用下，$(Co_3O_4)_2H_2OCO^+$与$(Co_3O_4)_4H_2OCO^+$团簇上依次发生CO分子、H_2O分子的脱附（图1a，图1c）；而$(Co_3O_4)_3H_2OCO^+$团簇上无单一分子脱附，表明H_2O分子与CO分子发生了光诱导耦合，很有可能形成HCOOH分子（图1b）。进一步研究发现，该反应不能被可见光引发，如图1d所示，在600nm激光的作用下，$(Co_3O_4)_3H_2OCO^+$团簇上依次发生CO分子、H_2O分子的脱附。本工作表明在特定结构的氧化钴团簇上，可以发生H_2O分子与CO分子的紫外光诱导耦合反应。

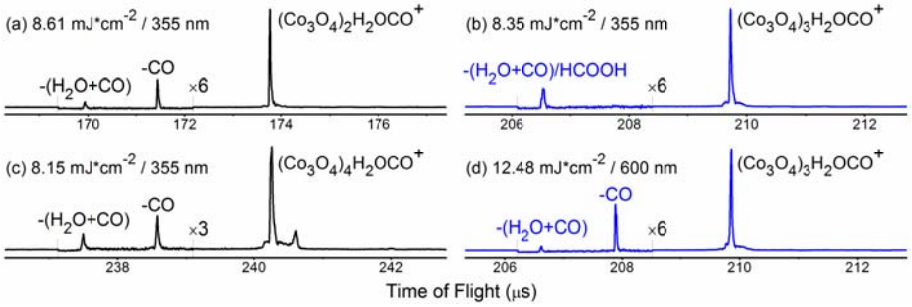

Fig. 1 Time-of-flight mass spectra for the photo-reaction of mass-selected $(Co_3O_4)_nH_2OCO^+$ clusters.

关键词： 氧化钴团簇；一氧化碳；水；甲酸；光诱导反应

参考文献

[1] Kudo, A.; Miseki, Y. *Chem. Soc. Rev.* **2009**, **38**: 253.

[2] Sahoo, D. P.; Rath, D.; Nanda, B.; Parida, K. M. *RSC Adv.* **2015**, **5**: 83707.

[3] Boyjoo, Y.; Sun, H.; Liu, J.; Pareek, V. K.; Wang, S. *Chem. Eng. J.* **2017**, **310**: 537.

[4] Xue, W.; Wang, Z. C.; He, S. G.; Xie, Y.; Bernstein, E. R. *J. Am. Chem. Soc.* **2008**, **130**: 15879.

[5] Castleman, A. W. *Catal. Lett.* **2011**, **141**: 1243.

[6] Dietl, N.; Schlangen, M.; Schwarz, H. *Angew. Chem. Int. Ed.* **2012**, **51**: 5544.

[7] Ding, X. L.; Wu, X. N.; Zhao, Y. X.; He, S. G. *Acc. Chem. Res.* **2012**, **45**: 382.

Au^+与直链烷烃(C2_ C10)反应的研究

张婷[1,2]，李子玉[1]，何圣贵[1,2*]

[1] 中国科学院化学研究所分子动态与稳态结构国家重点实验室，北京，100190；

[2] 中国科学院大学，北京，100049

*Email: shengguihe@iccas.ac.cn

挥发性有机物（VOC）的高灵敏度检测一直以来都是人们特别关注的课题[1]。其中烷烃(C_nH_{2n+2})作为一种重要的大气VOC，由于其极性弱、没有官能团和碳链易断裂的特点，烷烃的化学电离检测面临着巨大的挑战。常用于VOC检测的试剂离子为H_3O^+[2]，由于短链烷烃的质子亲和能小于H_2O，且长链烷烃易碎裂，以H_3O^+的质子转移反应不适用于烷烃的化学电离[3]。为了寻找合适的试剂离子，人们发现单个金属离子或配体保护的金属离子可与烷烃反应[4]。其中，Au^+反应活性较高，早期的文献报道[5]表明，Au^+能与烷烃（C2−C7）发生高效的氢负离子转移反应，产生烷烃的分子离子峰，然而，长链烷烃（C7）很容易发生碎裂。为了解决长链烷烃易碎裂的问题，我们研究了Au^+与直链烷烃（C2−C10）的反应，不仅确定了Au^+和烷烃分子反应的机理，还测定了反应速率，重要的是，根据理论计算分析发现，长链烷烃（n≥7）离子富含较高的内能，当缓冲气体压力较低时（~6 Pa），其与烷烃的碰撞不足以带走此能量，导致烷烃碎裂。因此我们通过增加缓冲气体压力，利用高气压（~1200 Pa）缓冲气体的碰撞冷却，使得碳链不断裂。这对烷烃的离子化及大气VOC的检测分析具有重要的意义。

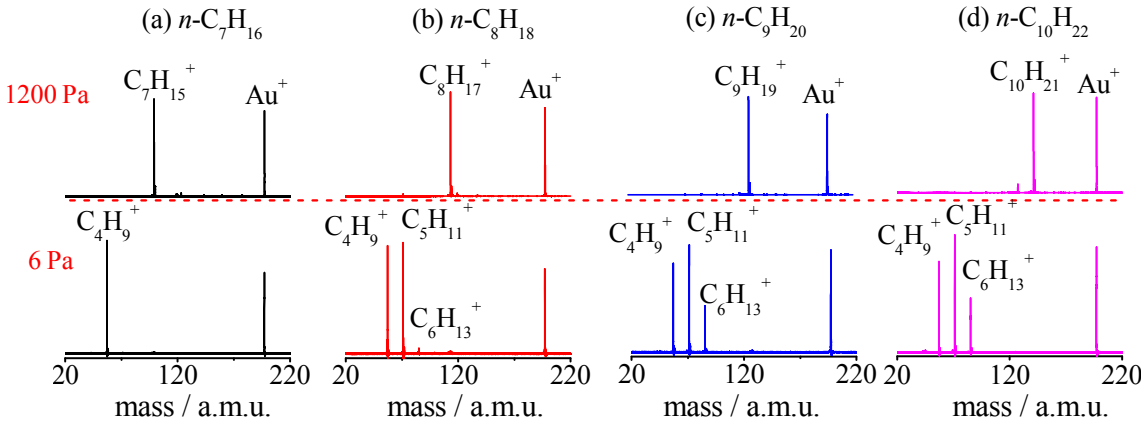

Fig. 1 TOF mass spectra for of $Au^+ + C_nH_{2n+2}$ (n = 7−10) with the buffer gas of 1200 Pa (above) and 6 Pa (below)

关键词： 化学电离；烷烃；金；质谱；密度泛函计算

参考文献

[1] Atkinson, R. Atmos. Environ. **2000, 34**: 2063.

[2] Blake, R. S.; Monks, P. S.; Ellis, A. M. Chem. Rev. **2009, 109**: 861.

[3] Gueneron, M.; Erickson, M. H.; VanderSchelden, G. S.; Jobson, B. T. Int. J. Mass Spectrom. **2015, 379**: 97.

[4] Roithova, J.; Schroder, D. Chem. Rev. **2010, 110**: 1170.

[5] Chowdhury, A. K.; Wilkins, C. L. J. Am. Chem. Soc. **1987, 109**: 5336.

含氮正离子与氢分子的反应势能面

张岳[1]，王海兴[1,*]，李安阳[2,*]

[1] 北京航空航天大学宇航学院，北京市海淀区学院路 37 号，100191

[2] 西北大学化学与材料科学学院，陕西省西安市长安学府大道 1 号，710127

*Email: whx@buaa.edu.cn, liay@nwu.edu.cn

氨气是星际空间第一个被发现的多原子分子，通过如下含氮正离子与氢分子的系列反应，氨气在气相中合成已经被证实[1]：

$$N^+ + H_2 \rightarrow NH^+ + H \quad (R1)$$
$$NH^+ + H_2 \rightarrow NH_2^+ + H \quad (R2)$$
$$NH_2^+ + H_2 \rightarrow NH_3^+ + H \quad (R3)$$
$$NH_3^+ + H_2 \rightarrow NH_4^+ + H \quad (R4)$$
$$NH_4^+ + e \rightarrow NH_3 + H \quad (R5)$$

全部的反应过程均快速高效，无需催化剂。揭示这系列反应的微观机制，对氨气的气相合成以及大气中此类离子分子反应的理解有重要的意思。

利用高级别的从头算方法（MRCI, UCCSD(T)等），R1-R4的反应路径被仔细梳理。对于R1, 产物NH^+最低的二重态$(\tilde{X}^2\Pi)$和四重态$(\tilde{a}^4\Sigma^-)$能量非常接近，其绝热势能面对应NH_2^+体系的$1^3A''$和$2^3A''$态，而在反应物端，这两个态简并，反应路径中，存在多个非绝热耦合区域。在反应R2中，副反应产物通道$N + H_3^+$能量低于反应物通道，NH_3^+离子体系的三个不同的通道得到了细致的分类考察。此外，对反应R3和R4的反应路径的初步研究，获得其中的过渡态和稳定中间产物结构和能量，由反应物直接生成NH_n^+的情况也已被考虑。

目标反应的反应物通道中均没有能垒或只有低于反应物能量极限的潜入式鞍点，反应路径类似于无能垒的复合物生成反应[2]，因此产物的能量分布，反应速率随温度变化，同位素效应等可能出现非常规的特征。现有的工作为进一步精确势能面的构建及动力学研究提供了基础。

关键词：势能面；反应路径；离子分子反应

参考文献

[1] Scott G. B. I.; Freeman C. G.; McEwan M. J. *Mon. Not. R. Astron. Soc.* **1997, 290(4)**: 636.

[2] Guo H. *Int. Rev. Phys. Chem.* **2012, 31**: 1.

光辅助下 Rh-V 异核氧化物团簇催化转化甲烷的研究

赵艳霞*，李海方，何圣贵*

中国科学院化学研究所，北京市海淀区中关村北一街 2 号，100190

*Email: chemzyx@iccas.ac.cn, shengguihe@iccas.ac.cn

作为天然气的主要成分，甲烷具有四面体对称性及零偶极矩，碳-氢键能大，是一种非常惰性的分子，很难在温和条件下实现向高附加值产品的直接转化。国际上关于人工合成材料高效催化甲烷直接转化的诸多研究需要在高温、高压、强酸等苛刻条件下进行[1]，不仅生产成本高，而且易造成催化剂失活、产物难分离等问题。因此，如何实现甲烷在温和条件下的选择性活化及直接定向转化是能源转化利用亟待解决的一个关键问题。光诱导反应因其温和的反应条件有望成为甲烷直接转化的一种新的技术手段[2]。过去人们采用团簇方法对甲烷转化的基元反应开展广泛研究[3,4]发现，活性较高的反应物团簇在室温下转化甲烷后，产物团簇往往处于较稳定的状态，不易转化为反应物团簇实现完整的催化循环。本研究首次通过光诱导反应与热反应（室温）的协同，实现了 Rh-V 异核氧化物团簇催化甲烷直接转化为甲醛（Fig. 1），为利用光诱导实现甲烷在温和条件下的直接催化转化提供了分子层次上的认识。

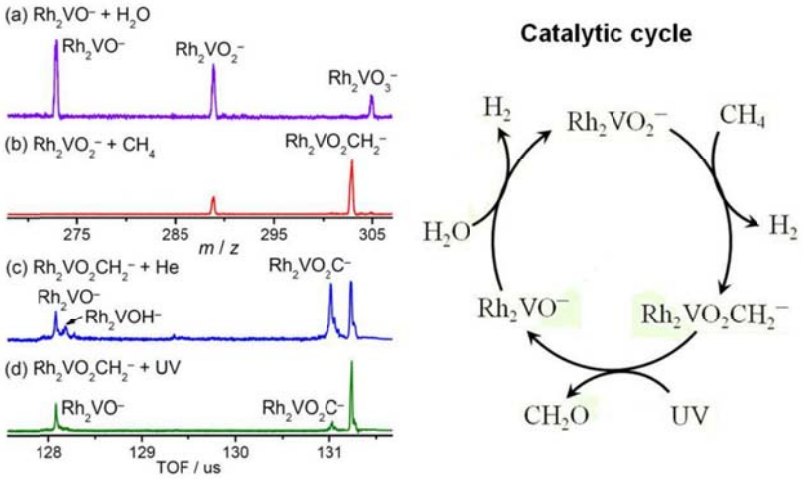

Fig. 1 Photon-assisted conversion of methane into formaldehyde catalyzed by Rhodium-Vanadium heteronuclear oxide cluster anions.

关键词： 原子团簇；甲烷催化转化；光诱导反应；热反应；质谱

参考文献

[1] Guo, X.; Fang, G.; Li, G.; Ma, H.; Fan, H. et al. *Science* **2014**, **344**: 616.

[2] Yuliati; L.; Yoshida; H. *Chem. Soc. Rev.* **2008**, **37**: 1592.

[3] Ding, X.-L.; Wu, X.-N.; Zhao, Y.-X.; He, S.-G. *Acc. Chem. Res.* **2012, 45**: 382.

[4] Zhao, Y.-X.; Liu, Q.-Y.; Zhang, M.-Q.; He, S.-G. *Dalton Trans.* **2016**, **45**: 11471.

VO_{1-4}^+阳离子团簇与烷烃（$C_{1,3,5,7}$）反应的实验和理论研究

赵越，马嘉璧*

北京理工大学，北京市房山区良乡高教园区，102488

*Email: majiabi@bit.edu.cn

近年来我国雾霾事件频发。矿尘气溶胶是我国大气的主要成分之一，该类气溶胶可以为非均相反应提供反应场所。钒氧化合物是大气中一种典型的重金属氧化物[1]，我国北方地区大气中烷烃约占30%。在此，我们利用原子分子原位反应装置（四极杆-离子阱-反射式飞行时间质谱）结合密度泛函理论（DFT）计算对VO_{1-4}^+与系列烷烃（C_3H_8、C_5H_{12}和C_7H_{16}）的反应，得到了有趣的结论。

VO_{1-3}^+与烷烃的反应主要存在两条通道，即：C-H键和C-C键的活化；VO_4^+与烷烃反应时主要为团簇失去O_2单元。图示以VO_3^+和C_5H_{12}反应为例，左侧为反应质谱图，右侧为反应势能面图。质谱实验结果表明VO_3^+团簇与C_5H_{12}的反应速率为3.45×10^{-10} $cm^3\cdot molecule^{-1}\cdot s^{-1}$，按照反应速率的快慢可以发生以下反应：a) $VO_3^+ + C_5H_{12} \rightarrow VO_3H_2^+ + C_5H_{10}$; b) $VO_3^+ + C_5H_{12} \rightarrow VO_2C_2H_4^+ + C_3H_6 + H_2O$; c) $VO_3^+ + C_5H_{12} \rightarrow VO_3C_4H_{10}^+ + CH_2$。DFT结果表明：反应a经历了两步氢转移；反应b首先经历两步氢转移发生脱水反应，脱水后的产物经过C-C键的活化最终生成$VO_2C_2H_4^+$和C_3H_6；反应c在三步氢转移的基础上活化端位的C-C键，生成$VO_2C_4H_9^+$和CH_2OH。CH_2OH进一步经过C-O键的活化生成CH_2自由基。该研究表明，VO_{1-3}^+团簇可以活化长链烷烃，其为凝聚体系表面相关物种的反应机理提供了理论支持。

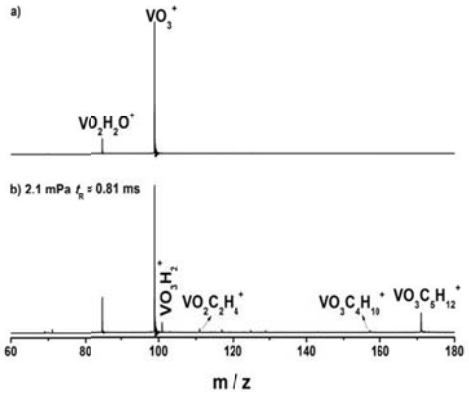

Fig. 1 Time-of-flight mass spectra for the reactions of mass-selected VO_3^+ (a) with C_5H_{12} (b) for 0.81 ms

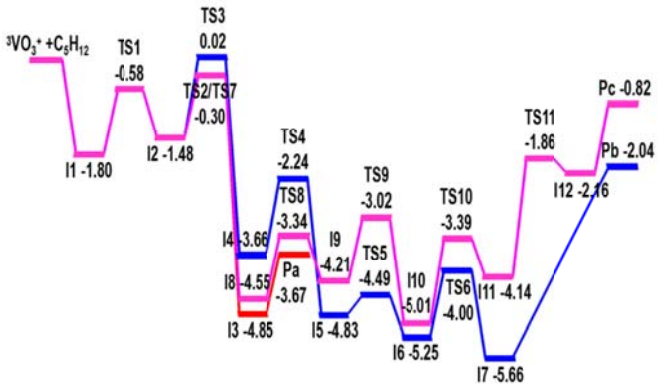

Fig. 2 DFT calculated potential-energy profile for the reaction of $VO_3^+$with C_5H_{12} in the triplet spin state.

关键词： VO_{1-4}^+团簇；DFT；质谱；反应机理

参考文献

[1] Jingchun Duan [a]; Jihua Tan [b,*]. *Atmos. Environ.* **2013**, **74**: 93-101.

Reactions of Copper and Silver Cations with Carbon Dioxide: an Infrared Photodissociation Spectroscopic and Theoretical Study

Zhi Zhao, Xiangtao Kong, Dong Yang, Hua Xie, Ling Jiang*

State Key Laboratory of Molecular Reaction Dynamics, Dalian Institute of Chemical Physics, Chinese Academy of Sciences, Dalian 116023, Liaoning, P. R. China
*Email: ljiang@dicp.ac.cn

The study of the interaction of carbon dioxide with metals is of considerable interest because CO_2 doubles as an abundant renewable resource for the production of fine chemicals and clean fuels and a main contributor to global warming [1-4]. The reaction of copper and silver cations with carbon dioxide has been studied by mass-selected infrared photodissociation spectroscopy [5]. Quantum chemical calculations have been performed on these products, which aid the experimental assignments of the infrared spectra and help to elucidate the geometrical and electronic structures. The Cu^+ and Ag^+ cations bind to an oxygen atom of CO_2 in an ''end-on'' configuration via a charge-quadrupole electrostatic interaction in the $[M(CO_2)_n]^+$ complexes. The formation of oxide-carbonyl and carbonyl-carbonate structures is not favored for the interaction of CO_2 with Cu^+ and Ag^+. For n = 3 and 4, the n+0 structure is preferred. The two nearly energy-identical n+0 and (n-1)+1 structures coexist in n = 5 and 6. While the six-coordinated structure is favored for $[Cu(CO_2)_{n=7,8}]^+$, the n+0 configuration is dominated in $[Ag(CO_2)_{n=7,8}]^+$. The reaction of CO_2 with the cationic metal atoms has been compared to that with the neutral and anionic metal atoms, which would have important implications for understanding the interaction of CO_2 with reduction catalysts and rationally designing catalysts for CO_2 reduction based on cost-effective transition metals.

Keywords: metal; carbon dioxide; infrared photodissociation spectroscopy; quantum chemical calculation

References:

[1] Freund, H. J.; Roberts, M. W. *Surf. Sci. Rep.* **1996**, *25*, 225-273.
[2] Gibson, D. H. *Chem. Rev.* **1996**, *96*, 2063-2095.
[3] Taifan, W.; Boily, J.-F.; Baltrusaitis, J. *Surf. Sci. Rep.* **2016**, *71*, 595-671.
[4] Ricks, A. M.; Brathwaite, A. D.; Duncan, M. A. *J. Phys. Chem. A* **2013**, *117*, 11490-11498.
[5] Zhao, Z.; Kong, X.-T.; Yang, D.; Yuan, Q.-Q.; Xie, H.; Fan, H.-J.; Zhao, J.-J.; Jiang, L. *J. Phys. Chem. A* **2017**, *121*, 3220-3226.

Probing the bonding of CO to heteronuclear group 4 metal–nickel clusters by photoelectron spectroscopy

Jinghan Zou, Hua Xie, Jumei Zhang, Ling Jiang*

State Key Laboratory of Molecular Reaction Dynamics, Dalian Institute of Chemical Physics, Chinese Academy of Sciences, Dalian 116023, Liaoning, P. R. China

*Email: ljiang@dicp.ac.cn

The interaction of carbon monoxide with transition metals is of considerable interest due to its importance in heterogeneous and homogeneous catalysis such as Fischer–Tropsch chemistry, hydroformylation, alcohol synthesis, and acetic acid synthesis[1]. Metal clusters are often regarded as models for the surface of bulk materials, which provide a nice correlation with the elemental reactions on the most active or least coordinated site of a catalyst[2]. Heteronuclear TM carbonyls are of particular interest because of the excellent chemical reactivity of bimetallic clusters in various important processes[3,4]. A series of heterobinuclear group 4 metal–nickel carbonyls $MNi(CO)_n^-$ (M = Ti, Zr, Hf; n = 3–7) has been generated via a laser vaporization supersonic cluster source and characterized by mass-selected photoelectron velocity-map imaging spectroscopy[5]. Quantum chemical calculations have been carried out to elucidate the geometric and electronic structures and support the spectral assignments. The n = 3 cluster is determined to be capable of simultaneously accommodating three different types of CO bonds (i.e., side-on-bonded, bridging, and terminal modes), resulting in a $MNi[\eta^2\ (\mu_2\text{-C,O})](\ \mu\text{-CO})(CO)^-$ structure, which represents the smallest metal carbonyl with the involvement of all the main modes of metal–CO coordination to date. The building block of three bridging CO molecules is favored at n = 4, the structure of which persists up to n = 7. The additional CO ligands are bonded terminally to the metal atoms. The present findings provide important new insight into the structure and bonding mechanisms of CO molecules with heteronuclear transition metals, which would have important implications for understanding chemisorbed CO molecules on alloy surfaces.

Keywords: photoelectron velocity-map imaging; Quantum chemical calculations; heteronuclear transition metal carbonyl anions

References:

[1] F. A. Cotton, G. Wilkinson, C. A. Murillo, and M. Bochmann, *Advanced inorganic chemistry*, John Wiley & Sons, New York, **1999**.

[2] H. J. Freund, G. Meijer, M. Scheffler, R. Schlogl, and M. Wolf, *Angew. Chem. Int. Ed.*, **2011**, *50*, 10064-10094.

[3] N. Zhang, M. B. Luo, C. X. Chi, G. J. Wang, J. M. Cui, andM. F. Zhou, *J. Phys. Chem. A*, **2015**, *119*, 4142–4150.

[4] Z. L. Liu, J. H. Zou, Z. B. Qin, H. Xie, H. J. Fan, and Z. C. Tang, *J. Phys. Chem. A*, **2016**, *120*, 3533–3538.

[5] J. H. Zou, H. Xie, Q. Q. Yuan, J.M. Zhang, D.X. Dai, H.J. Fan, Z. C. Tang, and L. Jiang, *Phys. Chem. Chem. Phys.*, **2017**, *19*, 9790-9797.

氮化碳薄膜材料的制备、表征和光物理性质的研究

曹丹丹[1]，吕荣[1]，于安池[1,*]

中国人民大学，北京， 100872

Email:a.yu@ruc.edu.cn

氮化碳作为非金属的半导体光催化材料，具有对可见光响应、热稳定性好等特点，可利用其太阳光光解水制氢、污染物降解，CO_2 捕获和还原等，所以成为目前光催化领域研究的热点。然而氮化碳本体对可见光的利用率低以及载流子复合速率高等缺点，很大程度上限制了其应用，所以基于光催化的一些光物理性质以及对载流子动力学的探究尤为重要。[1] [2] 但由于氮化碳不易溶于水、微溶于有机溶剂，并且本体粒径较大，较难得到能够光学探测的样品，所以现阶段对其光物理性质和载流子动力学研究较少。本工作尝试制备了可以用来泵浦探测的氮化碳薄膜样品，使用氮化碳粉末作为前驱体，通过热蒸汽法，在 ITO 玻璃上获得了均一致密的 g-CN 膜，如图（a）中插图。通过 SEM、EDS 以及 AFM 对本样品进行了表征，发现制备的薄膜表面较光滑，厚度约为 300 nm， 其 C / N 比例为 0.66 ± 0.02，基本接近本体；同时运用飞秒瞬态吸收光谱技术对氮化碳的载流子动力学进行了研究，在 550 nm 到 750 nm 的波长范围内，检测到一个较宽，并且连续的吸收峰，推测为光生空穴的吸收，这与 Ye 等人得到的瞬态吸收光谱类似。[3]

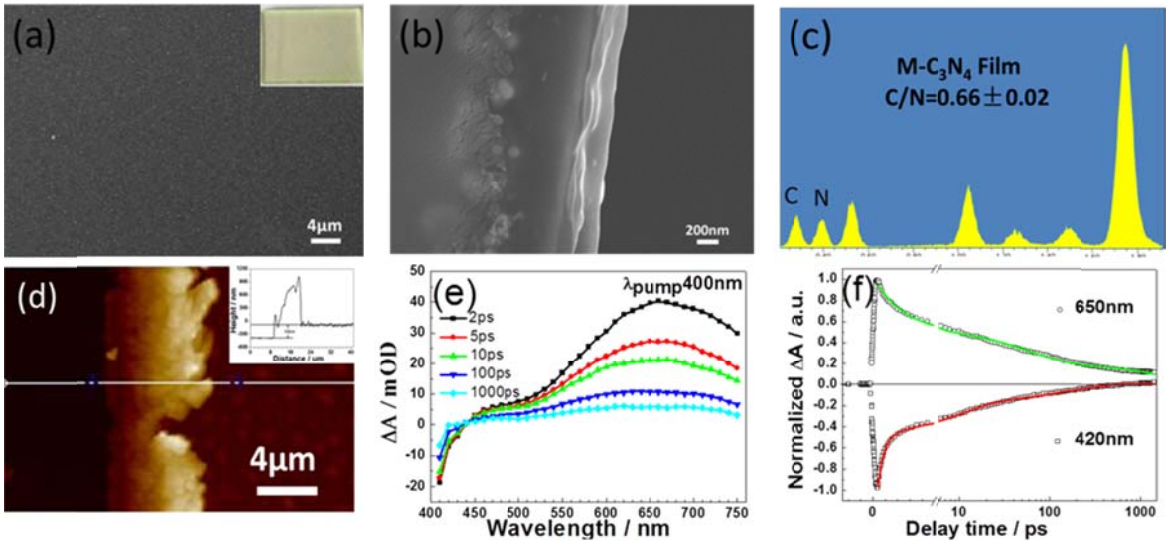

Fig.1 (a) Typical top view SEM imageand the insets in (a) show the optical photos of the g-CN film. (b) The cross-sectional view SEM image. (c) EDS spectra of g-CN film. (d) AFM image of the cross-sectional and the insets show the corresponding height image of one random film. (e) Femtosecond transient absorption spectra of the CN film at various time delays under a 400 nm pump. (f) The magic-angle pump-probe transient decays of g-CN film at a probe wavelength of 420 and 650 nm , respectively.

关键词： 氮化碳；薄膜；载流子

参考文献

[1] Wang, X.; Maeda, K.; Thomas, A.; Takanabe, K.; Xin, G.; Carlsson, J. M.; Domen, K.; Antonietti, M.. *Nature Materials* 2009, 8 (1), 76-80.

[2] Godin, R.; Wang, Y.; Zwijnenburg, M. A.; Tang, J.; Durrant, J. R. *Journal of the American Chemical Society*, 2017, 139 (14), 5216–5224

[3]Ye, C.; Li, J.-X.; Li, Z.-J.; Li, X.-B.; Fan, X.-B.; Zhang, L.-P.; Chen, B.; Tung, C.-H.; Wu, L.-Z. *ACS Catal.* 2015, 5, 6973

The ultrafast photocarrier generation process in Y-form oxotitanium phthalocyanine films

Yuqiang Chang[1], Chuanxi Wang[2], Jie Yu[3], Yuan Wang[2,*], Jian-Ping Zhang[3,*]

[1]Department of Physics, Harbin Institute of Technology, Harbin, 150001, PR China

[2]Beijing National Laboratory for Molecular Science, State Key Laboratory for Structural Chemistry of Unstable and Stable Species, College of Chemistry and Molecular Engineering, and Academy for Advanced Interdisciplinary Studies, Peking University, Beijing, 100871, PR China

[3]Department of Chemistry, Renmin University of China, Beijing, 100872, PR China

*Email: jpzhang@iccas.ac.cn;wangy@pku.edu.cn

The ultrafast photocarrier generation process of Y-form titanyl-phthalocyanine(Y-TiOPc) films was investigated by femtosecond transient absorption spectroscopy, nanosecond flash photolysis spectroscopy, and electrochemistry spectroscopy. A rapid change of the transient absorption spectra at different delay times from the excitation of 800 nm revealed that two kinds of charge-transfer states appeared immediately after the excitation. The S_{CT1} state with the absorption peak at 450 nm was localized, which could turn into localized charges (425 nm) [1]. However, the S_{CT2} state with the absorption from 590 nm to 650 nm was delocalized, which would produce delocalized charges (700-770 nm). Meanwhile, the lifetime of localized charges was not affected by oxygen or water ($\tau_{aerobic}$=5.14 μs, $\tau_{degassed}$=4.58 μs), but the lifetime of delocalized charges was greatly prolonged after degassing ($\tau_{aerobic}$=3.38 μs, $\tau_{degassed}$=6.6 μs). Regular arrangements between adjacent molecules are critical for photogeneration of delocalized charges [2].

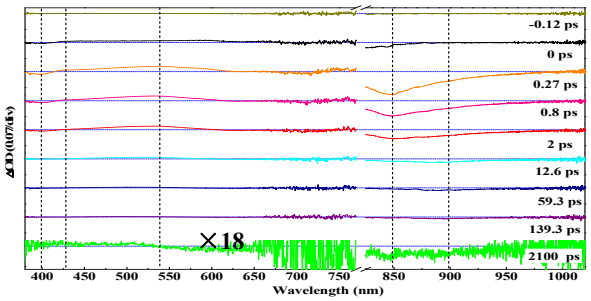

Fig. 1 Representative femtosecond vis-NIR transient absorption spectra obtained for Y-TiOPc/PC-19% film at pump-probe time delays noted.

Keywords: Y-form titanyl-phthalocyanine; charge photogeneration; femtosecond transient absorption spectra; charge-transfer states

References:

[1] Minoru, T., Noriaki, I., Hisatomo, Y., Chyongjin, P., Takeshi, O., *Coordination Chem Rev*, 2002, 229: 3–8.

[2] Jaehong, P.; Obadiah, G.R.; Garry, R.; *J Phys Chem B,* **2015**, **119**: 7729-7739.

苯甲醛 $S_3(\pi\pi^*)$态激发态动力学的共振拉曼和从头计算研究

陈佳，江雪莲，郑旭明*

[1]浙江理工大学，杭州市下沙 2 号大街 928 号，310018

Email: zxm@zstu.edu.cn

苯甲醛是最简单的芳香醛，其$S_1(n\pi^*)$暗态上衰变动力学机制已有研究报道[1]，大量研究致力于确定最低$^3n\pi^*$ 态和$^3\pi\pi^*$态的位置，这两个三态已经被确认位于S_1态极小下方 2000cm^{-1}处，且彼此靠的很近。但更高能级上激发态动力学研究非常稀少。本文开展苯甲醛$S_3(\pi\pi^*)$光吸收态衰变动力学研究，以揭示苯甲醛的激发态衰变通道。具体取得如下结果：

1.通过共振拉曼光谱强度分析定量拟合(见图1)，从而获得了Franck-Condon区域的结构动力学信息。研究结果显示，苯甲醛激发态初始反应坐标具有多维性，主要沿着C=O伸缩振动(ν_7,1697cm^{-1})，苯环对称伸缩振动(ν_8,1592cm^{-1})2个主要的活性振动模展开，二者的振动重组能之和为1150cm^{-1}（=734 cm^{-1}+416 cm^{-1}），约占总振动重组能的76%。根据苯甲醛在甲醇溶液和环己烷溶液中的简正坐标位移量|Δ|和振动重组能，我们发现，这些变化较大的振动模都与苯环的振动有关，说明在激发态光解动力学过程中，极性溶剂甲醇对苯环的振动影响较大；

2.采用CASSCF方法计算了苯甲醛的各激发态的最低能量结构，各势能面(内转换和系间窜越)交叉点的最低能量结构,如单重激发态S_1、S_2、S_3、S_4，三重激发态T_1、T_3、T_4,圆锥交叉点（CI）S_3S_2、S_1S_0、S_2S_1，系间蹿越点S_1T_1、S1T2、S_3T_1、S_3T_2、S_3T_3等能量极小点的结构和相对于基态S_0的势能，见图2.

3.提出了$S_3(\pi\pi^*)$态衰变机理

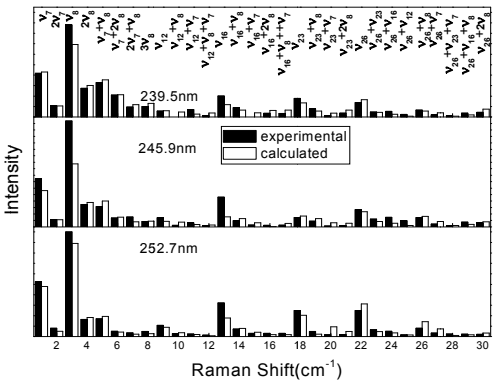

图1 绝对拉曼横截面实验值与计算值的拟合（甲醇作溶剂）

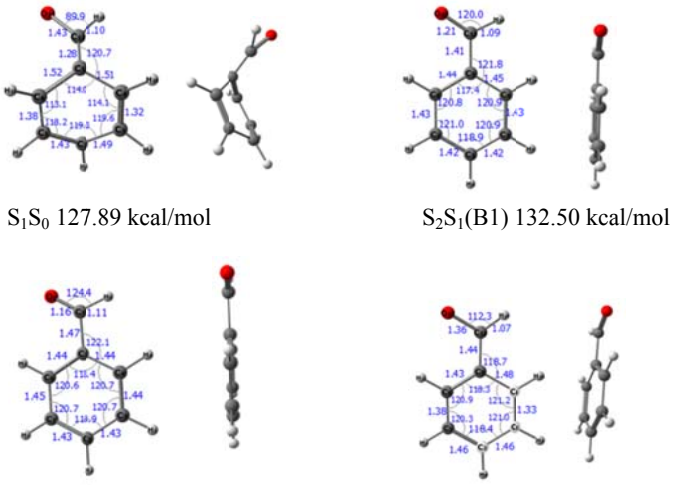

图2 CASSCF（8,7）/6-31G(d)计算水平下获得的苯甲醛圆锥交叉点结构与MS-CASPT2/cc-pvDZ矫正后的能量

关键词：苯甲醛；共振拉曼强度；激发态结构

参考文献

[1]Weihai Fang. Accounts of chemical research ,**2008, Vol. 41 No. 3**:452-457.

[2]Yufang Ma, Kemei Pei, Xuming Zheng, Haiyang Li. Chem Phys Lett, **2007, 449:**107-**1**14.

1,1-二氟乙烷二聚体的转动光谱研究

陈军华，郑阳，汪娟，冯刚，夏之宁，勾茜*

重庆大学化学化工学院，重庆市沙坪坝大学城南路 55 号，401331

*Email: qian.gou@cqu.edu.cn

微波波谱是研究气态分子内部动力学和超精细结构的有力工具，它可以提供配合物内分子的超精细结构、内部动力学、能量关系及构象平衡等信息。本研究中，我们采用新搭建的超声喷射傅里叶变换微波波谱研究了 1,1 二氟乙烷二聚体。实验测定了理论计算中最稳定的两个构型(见图 1)，两个构型均以 3 个 C-H···F-C 弱氢键相互作用，并且只有 F8 原子形成的这一个弱相互作用位点不同，其余两个弱氢键则是以相同的原子相互作用。除了母体体系，还测定了构型 I 在自然丰度下 4 个 ^{13}C 同位素的转动光谱，由此计算得到配合物分子碳原子的键长和距离：r(C1C2)=1.47(5) Å， r(C9C10)=1.50(1) Å， r(C9C2)=3.732(5) Å，分子间碳原子的夹角：∠C9C2C1=90(1)°。改变构型 I 的 5 个参数，其余参数固定在理论计算值(MP2/6-311++(d,p))，可以使它的转动常数很好的符合实验值，进而得到构型 I 的 3 个弱氢键键长 $r(H_5F_{11})$ = 2.664(2) Å，$r(H_6F_{12})$ = 2.572(2) Å 和 $r(F_8H_{13})$ = 2.586(2) Å。改变构型 **II** 的 2 个参数，其余参数固定在理论计算值，得到构型 II 的弱氢键键长 $r(H_5F_{11})$ = 3.005(5) Å， $r(H_6F_{12})$ = 2.485(5) Å 和 $r(F_8H_{14})$ = 2.452(5) Å。计算得到两个配合物的解离能分别为 9.1 kJ mol^{-1}(I)和 3.2 kJ mol^{-1}(II)，表明构型 I 的 3 个弱氢键相互作用更强。对超声膨胀中观察到的两个配合物的布局数分析表明，两个配合物的布局比 N_I/N_{II} ~ 6/1。

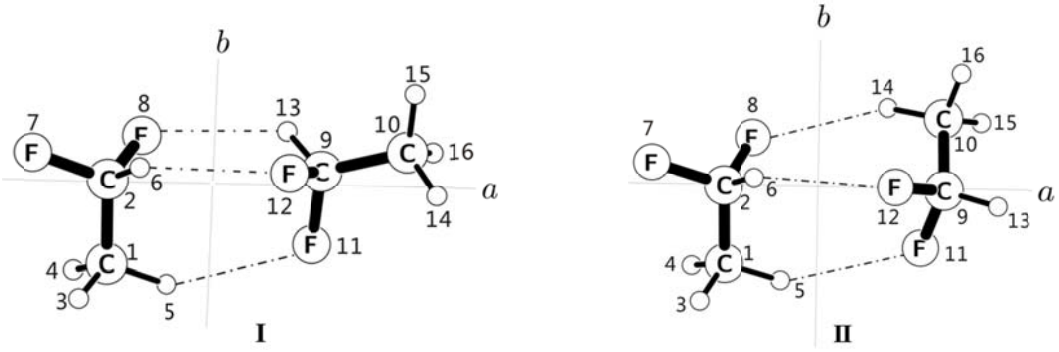

Fig. 1 Sketch of the observed conformer I and II of $(CH_3CHF_2)_2$ with principal axes and atom numbering.

关键词：转动光谱； 1,1-二氟乙烷；弱氢键；氟利昂

Formation from Photolysis of 2-Propanol on Anatase-TiO_2(101)

Chen Xiao[1, 2], Zhen-hua Geng [1,2], Qing Guo[1,2*], Xueming Yang[1,2*]

[1]State Key Laboratory of Molecular Reaction Dynamics, Dalian Institute of Chemical Physics, Dalian, 116023

[2]University of Chinese Academy of Sciences, Beijing, 100049

*Email: guoqing@dicp.ac.cn, xmyang@dicp.ac.cn

Photocatalysis of 2-propanol on A-TiO_2(101) has been investigated using a temperature programmed desorption (TPD) method under UV irradiation. A clear mechanism is proposed for the photodissociation of 2-propanol on A-TiO_2(101). Acetone product on five coordinate Ti^{4+} sites is formed in a stepwise manner in which the O-H dissociation proceeds first and then is followed by secondary C-H dissociation of 2-propanol while H atoms are transferred to the adjacent bridge bonding oxygen (BBO) sites. Low temperature water is formed in a thermally driven process via H-atom on BBO in exchange with isopropyl groups of molecule 2-propanol, while isopropyl radical desorbs at high temperature during the TPD process. The observation further demonstrates the prospect of TiO_2 as a photocatalyst for degradation of organics.

Keywords: 2-propanol; A-TiO_2(101); temperature programmed desorption; photocatalysis

References:

[1] Geng Z; Chen X; Guo Q; Dai D; Yang, X. Chinese Journal of Chemical Physics, **2017**, **30(1)**: 1-6.

Infrared Photodissociation Spectroscopy of Scandium Oxide-Carbonyl Cation Complexes

Yinjuan Chen[1], H. QU[2], K. XIN[1], G. WANG[2], M. ZHOU[2*], and X. WANG[1*]

[1]School of Chemical Science and Engineering, Tongji University, 1239 Siping Road, Shanghai, 200092

[2]Department of Chemistry, Shanghai Key Laboratory of Molecular Catalysis and Innovative Materials, Collaborative Innovation Center of Chemistry for Energy Materials, Fudan University, Shanghai 200433

*Email: mfzhou@fudan.edu.cn; xfwang@tongji.edu.cn

Mass selected scandium oxide-carbonyl cations $ScO(CO)_n^+$ (n=4-6) produced in pulsed laser vaporization supersonic cluster source are studied by infrared photodissociation (IRPD) spectroscopy in CO stretching frequency region in the gas phase. Insight into the structure and bonding of these cations can be obtained from their infrared active bands and their geometrical structures and theoretical frequencies are also provided by density functional theory calculations to further support and analyze the experimental results. The $ScO(CO)_4^+$ cation is determined to be C_{4v} structure, while $ScO(CO)_5^+$ is probably assigned to C_{4v} structure instead of C_{5v} on the basis of the two experimental vibration bands and these are in good agreement with theoretical results. $ScO(CO)_6^+$ has a pentagonal bipyramidal structure with C_{5v} symmetry, which includes five equatorial CO ligands and one axial CO ligand.

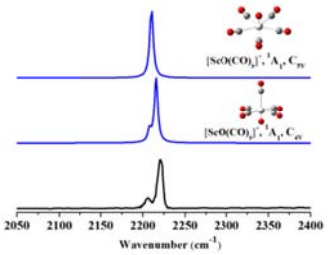

Fig. 1 The experimental (black) and simulated (blue) vibrational spectra of $ScO(CO)_5^+$ in carbonyl stretching frequency region.

Keywords: infrared photodissociation spectroscopy; scandium oxide-carbonyl cation complexes; quantum chemical calculation

References:

[1] Qu, H.; Wang, G. J.; Zhou, M. F. *J. Phys. Chem. A.* **2016, 120**: 1987-1984.

[2] Zhou, X. J.; Cui, J. M.; Li, Z. H.; Wang, G. J.; Liu, Z. P.; Zhou, M. F. *J. Phys. Chem. A.* **2013,117:** 1514-1521.

[3] Brathwaite, A. D.; Ricks, A. M. Duncan. M. A. J. *J. Phys. Chem. A.* **2013, 117:** 13435-13442.

[4] Xie, H.; Liu, Z. L.; Xing, X. P.; Tang, Z. C. *Chem. Phys. Lett.* **2015, 628:** 66 - 70.

The Study of HNCO Photodissociation Dynamics

Zhiguo Zhang[1, 2], Yanling Jin[1], Dongxu Dai[1], Zhichao Chen[1,*], Xueming Yang[1,*]

[1]State Key Laboratory of Molecular Reaction Dynamics, Dalian Institute of Chemical Physics, Chinese Academy of Sciences, Dalian,116023, Liaoning, China

[2]School of Physics and Electronic Engineering, Fuyang Normal University, Fuyang,236041, Anhui, , China

Email: czc@dicp.ac.cn; xmyang@dicp.ac.cn

Isocyanic acid (HNCO) photodissociation has attracted much attention because of its important role in combustion and interstellar space. The first UV absorption band of HNCO (180-280 nm) has been analyzed and assigned by Dixon and Kirby and by Rabalais *et al*. as an $S_1(^1A'')\leftarrow S_0(^1A')$ transition. At least three electronic states (S_0, S_1, and T_1) participate in the dissociation processes, which leads to three dissociation channels:

$$HNCO(S_1) \rightarrow NH\ (X^3\Sigma^-) + CO(X^1\Sigma^+) \qquad D_0 = 30060 \pm 30\ cm^{-1} \qquad (1)$$

$$H\ (^2S) + NCO\ (X^2\Pi) \qquad D_0 = 38370 \pm 30\ cm^{-1} \qquad (2)$$

$$NH\ (a^1\Delta) + CO\ (X^1\Sigma^+) \qquad D_0 = 42750 \pm 30\ cm^{-1} \qquad (3)$$

Channel (1) is a spin-forbidden dissociation pathway. Zyrianov *et al*. detected CO around 230 nm using the ion imaging technique. They found that the angular distribution of CO originating from channel (1) is essentially isotropic and suggested that dissociation in this channel follows IC from S_1 to S_0 and then ISC from S_0 to T_1. Channel (2) dissociation up to the channel (3) threshold is thought to occur via IC to S_0. Yu *et al*. using the high resolution HRTOF technique found that two competitive dissociation pathways have been observed: one is the indirect dissociation pathway through S_1 /S_0 coupling, the other is the direct dissociation pathway on the S_1 surface. Channel (3) is a spin-allowed dissociation pathway. Recently, we investigate channel (3) of HNCO photodissociation dynamics using time-sliced velocity map ion imaging technique combined with the molecular beam apparatus. We probed the NH($a^1\Delta$) fragment of channel (3). The new results obtained in this study are also compared with the results of previous related works [1-5].

Keywords: HNCO, Photodissociation, Time-sliced velocity map ion imaging

References:

[1] T.A. Spiglanin, D.W. Chandler, J. Chem. Phys. 87, 1577 (1987).

[2] M. Zyrianov, T. Droz-Georget, H. Reisler, J. Chem. Phys. 110, 2059 (1999).

[3] M. Zyrianov, A. Sanov, T. Droz-Georget, H. Reisler, J. Chem. Phys. 110, 10774 (1999).

[4] Z. G. Zhang, Z. Chen, C. S. Huang, Y. Chen, D. X. Dai, D. H. Parker and X. M. Yang. J. Phys. Chem. A. 118, 2413 (2014).

[5] M. Zyrianov, T.H. DrozGeorget, H. Reisler, J. Chem. Phys. 106, 7454 (1997).

二维材料中载流子及激子超快动力学的研究

池振 [a,b]，陈海龙 [*,a]，赵清 [b]，翁羽翔 [a]

[a] 中国科学院物理研究所，北京凝聚态物理国家实验室（筹）和中科院软物质物理重点实验室

[b] 北京理工大学，物理学院，量子技术研究中心

*Email: hlchen@iphy.ac.cn

过渡金属硫化物(TMDC)是继石墨烯之后又一可通过机械剥离获得单层的二维材料，随着块体变化到单层，其带隙也由间接带隙过渡到直接带隙 [1]。通过可见 pump-probe 技术已经发现 TMDC 材料具有很多新奇现象 [2-4]，但是对于泵浦诱导的光响应分析起来却十分困难，因为一个孤立的共振就可以对光谱产生极大的影响。目前，人们对 TMDC 材料基本的光物理特性的认识还没有完全达成共识。此外，溶液法处理获得的半导体过渡金属硫化合物二维材料，在光电子和光催化方面的应用引起了人们的广泛关注 [5]。我们利用飞秒可见/中红外瞬态吸收光谱深入研究了溶液剥离法制备的 TMDC 材料光生载流子的超快动力学过程。通过二维材料中不同光生载流子对红外光的感应差异，对于热电子气的弛豫、激子的形成以及缺陷态对激子的捕获各时间尺度进行了详细的分析。

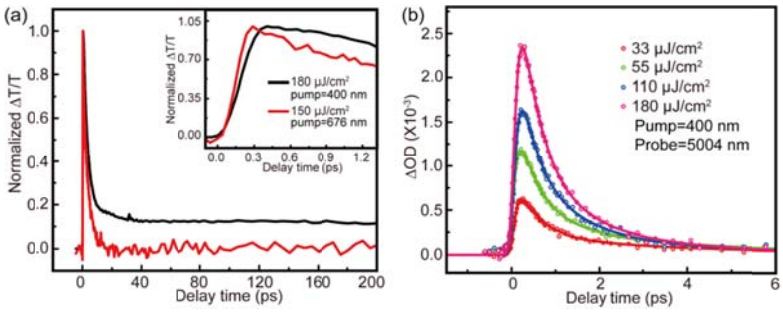

Fig. 1 (a) Normalized fluence-dependent A exciton dynamics in few-layer TMDC nanoflakes in ethanol probe at 676 nm (~1.83 eV) and pump wavelengths and fluence as marked. Inset is the zoom in for the first 1.25 ps. (b) Fluence-dependent temporal evolutions of the 400 nm (3.10 eV) excitation-induced absorption changes probed at 5004 nm (~0.25 eV) of the TMDC nanoflakes in ethanol.

关键词： 二维材料；自由载流子；可见/中红外超快光谱；激子动力学

参考文献：

[1] Jin, W.; Yeh, P. C.; Zaki, N.; Zhang, D.; Sadowski, J. T.; Almahboob, A.; Am, V. D. Z.; Chenet, D. A.; Dadap, J. I.; Herman, I. P. *Phys.rev.lett.* **2013, 111,** (10), 106801.

[2] Vega-Mayoral, V.; Vella, D.; Borzda, T.; Prijatelj, M.; Tempra, I.; Pogna, E. A.; Dal Conte, S.; Topolovsek, P.; Vujicic, N.; Cerullo, G.; Mihailovic, D.; Gadermaier, C. *Nanoscale* **2016, 8,** (10), 5428-34.

[3] Chen, H.; Wen, X.; Zhang, J.; Wu, T.; Gong, Y.; Zhang, X.; Yuan, J.; Yi, C.; Lou, J.; Ajayan, P. M.; Zhuang, W.; Zhang, G.; Zheng, J. *Nat Commun* **2016, 7,** 12512.

[4] Cunningham, P. D.; McCreary, K. M.; Jonker, B. T. *J Phys Chem Lett* **2016, 7,** (24), 5242-5246.

[5] Yu, X.; Prévot, M. S.; Sivula, K. *Chem. Mater.* **2014, 26,** (20), 5892-5899.

Thermochromatium tepidum 光合膜人工模拟体系的构造及其激发态能量传递动力学

戴玲[1]，谭黎明[1]，石莹[1]，王鹏[1*]，张建平[1] ，王征宇[2]

[1] 中国人民大学化学系，北京市中关村大街 59 号，100872；
[2] 茨城大学理学部，日本水户市文京 2-1-1，310-8512

紫色光合细菌光合膜 chromatophore 是由外周捕光天线蛋白 LH2，核心复合物 LH1-RC 以一定比例形成的高度有序、二维平面阵列结构，承担着光吸收、激发态能量传递及电荷分离等功能。用细胞膜模拟体系——脂质体将不同的光合膜蛋白以不同比例重新组装成人工膜体系，再与天然 chromatophore 对比研究，可以进一步阐明光合膜超分子组装的构-效关系。本研究将中等嗜热紫色光合细菌 *Thermochromatium （Tch.）tepidum* 的 LH2 及 LH1-RC 以不同比例组装进由大豆卵磷脂构成的脂质体中（样品 S1、S2），采用一系列稳态和瞬态光谱手段将它们与 *Tch. tepidum* 的 chromatophore（样品 S3）对比研究，结果表明：人工膜 S1 和 S2 样品的 LH1-RC/LH2 比例分别高于和低于天然膜 chromatophore（样品 S3）；飞秒时间分辨吸收动力学结果表明，选择性激 LH2 的 B800，人工脂质体的 LH2 内 B800→B850、LH2→LH1（B850→B915）激发态能量传递速率都比 chromatophore 中相应的过程快，而三种样品中 LH1→RC（B915→RC）激发态能量传递速率则非常接近；B800、B850、B915 间的激发态能量传递效率对比研究表明，两种人工膜体系的 LH2 内 B800→B850 激发态能量传递效率均比天然膜 chromatophore 中高，而 LH2→LH1、LH1→RC 的激发态能量传递效率则都比 chromatophore 中低，其中样品 S1 更为接近 chromatophore；人工膜体系中 LH2 的取向不像天然膜体系中保持完全一致，以及光合膜蛋白的不同混合比例（S1 和 S2）导致人工膜上蛋白宏观二维阵列的疏密程度不同，是造成三种样品在激发态动力学上产生不同规律的根本原因。

FT-IR and ultrafast IR spectroscopic monitoring of potassium thiocyanate aqueous solution with fast freezing

Gang-Hua Deng, Yuhuan Tian, Yanfeng Yin, Yuneng Shen, Xueming Yang, Kaijun Yuan*
State Key Laboratory of Molecular Reaction Dynamics, Dalian Institute of the Chemical Physics, Chinese Academy of Sciences, Dalian 116023, Liaoning, China
*Email: kjyuan@dicp.ac.cn

According to former studies[1-3], with the method of fast freezing, solutes and macromolecules could be fixed within non-crystalline, glass-like solid water without the dramatic shifts and segregation effects caused by crystallization. Herein, we investigated potassium thiocyanate (KSCN) aqueous solution at atmospheric pressure and temperatures from 295 to 10 K with fast freezing. From the FTIR spectra and ultrafast IR pump-probe data, the observed three peaks (2047 cm^{-1}, 2052 cm^{-1}, 2071 cm^{-1}) are assigned to octamer, crystals and cluster (ion pair, isolated anion), respectively. The percent of octamer, crystals and cluster (ion pair, isolated anion) are estimated to be 1.64%, 0.65% and 97.72%, respectively. It is concluded that KSCN can keep the morphology at room temperature (liquid solution) mostly with the method of fast freezing.

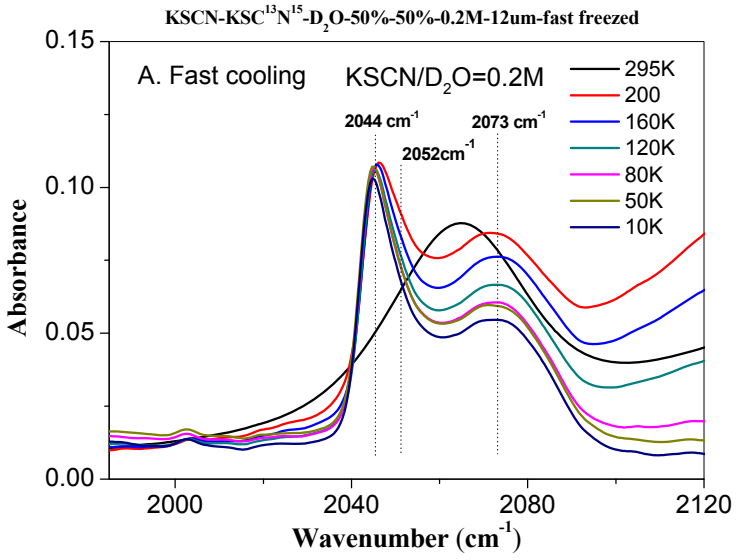

Fig. 1 FTIR of 0.2M KSCN aqueous solution with fast freezing

References:

[1] Baoyou Liu, Jingjing Zhao, FuxiangWei. Effects of water on the properties of acetamide-KSCN eutectic ionic liquids at several temperatures[J]. J. Mol . Liq, 187 (2013) 309-313.

[2] Baoyou Liu, Yaru Liu. Properties for binary mixtures of (acetamide + KSCN) eutectic ionicliquid with ethanol at several temperatures [J]. J. Chem. Thermodynamics, 92 (2016) 1–7.

[3] J. E. Tanner. Observations of Rapid Freezing of Salt Solutions [J]. Cryobiology 12 (1975) 353-363.

非金属硼掺杂氧化钛中缺陷态对光催化分解水的影响

杜艺杰[1]，王专[1]，刘岗[2]，翁羽翔[1,*]，

[1]北京凝聚态物理国家实验室（筹），中国科学院物理研究所，北京，100190

[2]沈阳材料科学国家（联合）实验室，中国科学院金属研究所，沈阳，110016

*Email: yxweng@aphy.iphy.cn

光催化分解水反应被认为是解决能源危机的潜在途径之一。近年来，研究人员投入大量精力开发高效的光催化材料并探寻光催化机理。光催化的最终效率是由材料的吸光率，光生载流子的产生及分离效率和表面的化学反应效率共同决定的。对于提高材料的吸光率而言，掺杂往往是拓宽材料吸光范围的主要手段。但是，因为光生载流子的产生与分离过程往往发生在非常快的时间尺度上（10^{-15}~10^{-3} s），一般的探测手段很难捕捉到其动力学行为。此外，光催化材料通常是半导体材料，半导体中有大量的缺陷态存在，缺陷态的存在往往会对材料的性质产生重要影响。本工作主要利用纳秒（带隙扫描激发-瞬态红外吸收光谱，Transient IR absorption – Excitation energy scanning spectroscopy, TIRA-ESS）[1-2]和飞秒时间分辨光谱技术（ Femtosecond time-resolved IR absorption spectroscopy ）[3]对非金属硼掺杂的主要含有{001}面的锐钛矿相氧化钛微米球[4]进行了研究，主要根据表面无硼(B-free surface)和表面含硼(B-containing surface)两种样品的光生电子的动力学行为讨论了其对光催化分解水的影响。使人们对硼掺杂氧化钛光解水的认识更加深入，为日后理性设计高效的光催化材料提供了参考依据。

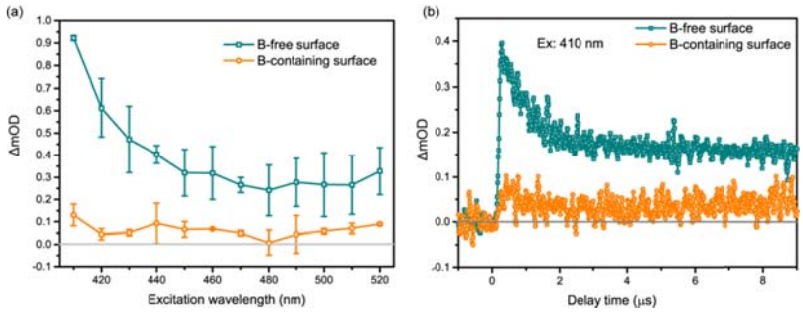

Fig. 1 (a) Typical nanosecond domain TIRA-ESS spectra and (b) kinetics delay for the B-free and B-containing surface anatase TiO_2 microspheres with exposed {001} facets.

关键词： 二氧化钛；缺陷态；光解水；硼掺杂

参考文献

[1] Zhu, M.; Mi, Y.; Zhu, G.; Li, D.; Wang, Y.; Weng, Y. J. Phys. Chem. C 2013, 117, 18863.

[2] Li, R.; Weng, Y.; Zhou, X.; Wang, X.; Mi, Y.; Chong, R.; Han, H.; Li, C. Energy Environ. Sci. 2015, 8, 2377.

[3] He, X.; Zhu, G.; Yang, J.; Chang, H.; Meng, Q.; Zhao, H.; Zhou, X.; Yue, S.; Wang, Z.; Shi, J.; Gu, L.; Yan, D.; Weng, Y., Sci Rep 2015, 5, 17076.

[4] Liu, G.; Pan, J.; Yin, L.; Irvine, J. T. S.; Li, F.; Tan, J.; Wormald, P.; Cheng, H.-M., Adv. Funct. Mater. 2012, 22, 3233.

Dynamic Study of Dehydration Study within Tri-hydroxy Benzoic Acid Monohydrate with Raman Vibrational Spectroscopy

Qiang Cai [1], Jiadan Xue [2], Qiqi Wang [1], Yong Du [1*]

[1] Centre for THz Research, China Jiliang University, No. 258, Xueyuan Street, Higher Education District of Xiasha, Hangzhou, 310018

[2] Department of Chemistry, Zhejiang Sci-Tech University, No. 928, 2nd Street, Higher Education District of Xiasha, Hangzhou, 310018

*Email: yongdu@cjlu.edu.cn

Vibrational spectroscopic techniques like Raman and infrared spectroscopy represent one of the most useful tools for obtaining information about structure and dynamic properties of molecules [1-2]. Tri-hydroxy benzoic acid (THBA), an intermediate component of plant metabolism from the hydrolysis of tannins, is distributed in plants and foods widely, which has been associated with a variety of biological actions including antioxidant, antibacterial, antiviral and antimicrobial [3]. In this work, the dynamic dehydration process of THBA monohydrate was carried out by heating method and characterized based on Raman vibrational spectroscopy. Raman spectra show that the vibrational modes of the THBA monohydrate are different from those of anhydrous one. The dynamic dehydration process of THBA monohydrate could be observed and monitored directly with Raman spectra. The results can offer us the experimental and theoretical benchmark for identifying pharmaceutical polymorphs and characterizing its conformation, and also useful information about the process of dynamic dehydration at the microscopic molecular level.

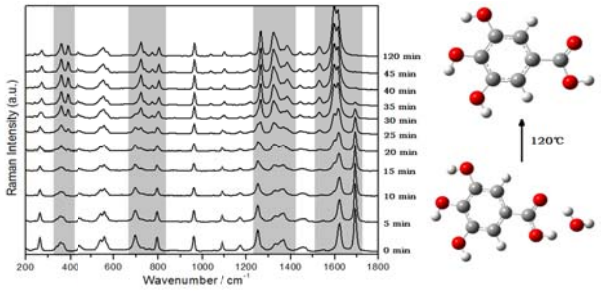

Fig. 1 Raman spectra of dehydration process of THBA monohydrate samples stored at the temperature 105 ℃ from 0 minute to the final 120 minutes (distinctive vibrational regions are shown with grey shadows).

Keywords: Tri-hydroxy benzoic acid (THBA); monohydrate; dynamic dehydration process; Raman spectroscopy

References:

[1] Du, Y.; Cai, Q.; Xue, J.; Zhang, Q. *Crtstals.* **2016**, **6**: 164.

[2] Du, Y.; Cai, Q.; Xue, J.; Zhang, Q.; Qin, D. *Spectrochim. Acta. A.* **2017**, **178**: 251.

[3] Doris, E.; Rajni, M.; Alastair, J.; Derek. A.; Sarah, L. *Cryst. Growth. Des.* **2013**, **13**: 19.

拉曼光谱技术原位测量丁二酰亚胺加速溶菌酶纤维化过程

范伟 [1]，邢蕾 [1]，周晓国 [1,*]，刘世林 [1,*]

[1] 微尺度物质科学国家实验室(筹)，中国科学技术大学化学物理系，安徽合肥，230026

*Email: xzhou@ustc.edu.cn

蛋白质的纤维化会引起老年痴呆症、帕金森症等一系列疾病 [1]，其中主要涉及成核过程、α-helix 结构、random coil、ß-sheet 结构的渐变过程。已有的研究表明在成核过程中产生的低聚物可能是主要的细胞毒性来源 [2]，而不可溶的成熟纤维样相对无毒，因此，减少低聚物的含量有可能降低纤维化过程对细胞的毒害作用。为此，我们以模型蛋白分子-溶菌酶的纤维化过程作为范例，通过应用高分辨的拉曼光谱技术观察溶菌酶纤维化过程中分子层次上的结构改变。通过对特征官能团的光谱指针峰 Trp(758cm^{-1})，Trp(1341-1361cm^{-1})，Trp(1552cm^{-1})，$NC_{\alpha}C$(933cm^{-1})，以及 Amide I 强度和位置的定量分析，我们证实了溶菌酶纤维化过程中 α-helix 结构优先转化成 random coil，继而转化成 ß-sheet 结构的 step-by-step 机制，并且丁二酰亚胺分子能够直接作用在 random coil 上，加速了其向 ß-sheet 结构的转变，从而打破原有的 step-by-step 机制，有效促进溶菌酶纤维化过程，减少毒性的低聚物存在的时间。

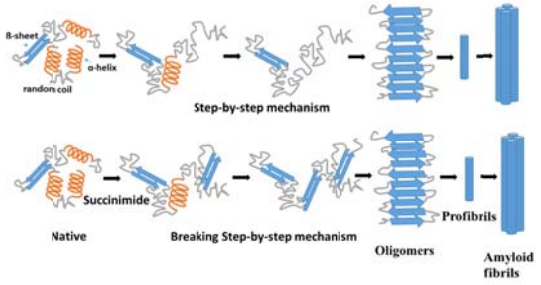

Fig. 1 Succinimide breaks a step-by-step mechanism

关键词：纤维化；丁二酰亚胺；拉曼光谱；step-by-step机制

参考文献

[1]Uversky, V. N.; Fink, A. L. *Biochimica et biophysica acta* **2004, *1698***, 131.

[2]Walsh, D. M.; Selkoe, D. *J. Journal of neurochemistry* **2007, 101**, 1172.

Excited-State Decay Mechanism of 4-Methylbenzylidene Camphor: A CASPT2//CASSCF Study

Ye-Guang Fang, Xue-Ping Chang, Wei-Hai Fang, and Ganglong Cui*
Key Laboratory of Theoretical and Computational Photochemistry, Ministry of Education, College of Chemistry, Beijing Normal University, Beijing 100875, China
yeguang.fang@mail.bnu.edu.cn

The growing awareness of the harmful effects of the sun's UV radiation (280–400 nm) has led to an increase in the use of sunscreens. These compounds composed of sunscreens are able to absorb, reflect or scatter UV radiation 280–320 nm for UVB and 320–400 nm for UVA, thus minimizing health problems such as sunburn, photo-aging and skin diseases (such as skin cancer). [1] In this study, a theoretical approach was used to study the excited state properties and decay dynamics of the UVB filter, 4-methylbenzylidene camphor (4-MBC). 4-MBC can exist as a (E)- or (Z)- isomer due to an exocyclic carbon–carbon double bond. [2,3] In 4-MBC configurations the (E) isomer predominates but under light exposure isomerization occurs from (E) to (Z). Herein we have employed multi-reference complete active space self-consistent field (CASSCF) and multistate complete active-space second order perturbation (MS-CASPT2) methods to scrutinize the photophysical and photochemical mechanism of E-4MBC. We have optimized the stationary point structures on the $^1\pi\pi^*$, $^1n\pi^*$, and S_0 potential surfaces to locate the $^1\pi\pi^*/^1n\pi^*$ and $^1n\pi^*/S_0$ conical intersections and to map $^1\pi\pi^*$ and $^1n\pi^*$ relaxation paths[4]. To explore the excited-state decay dynamics of E-4MBC, we study several possible $^1\pi\pi^*$ state deactivation channels with respect to the rotation of carbon-carbon double bond, and the linearly interpolated internal coordinate (LIIC) paths connecting the $^1\pi\pi^*$ minima and the $^1n\pi^*$ minima[5].Finally, the present work contributes a lot to understanding the photoprotection mechanism of 4-MBC.

Key words: Photochemistry; MS-CASPT2//CASSCF; 4-MBC; Isomerization

Reference:

[1] da Silva, L. P.; Ferreira, P. J. O.; Miranda, M. S. et al. *Photochem. Photobiol. Sci*., **2015, 14**, 465-472.
[2] Ferreira, P. J. O.; da Silva, L. P.; Miranda, M. S. et al. *Comput. Theor. Chem*., **2014, 1033**, 67-73.
[3] Kikuchi, A.; Shibata, K.; Kumasaka, R. et al. *J. Phys. Chem. A*, **2013, 117,** 1413-1419.
[4] Xie, X.-Y.; Li, C.-X.; Fang, Q. et al. *J. Phys. Chem. A*, **2016, 120**, 6014-6022.
[5] Chang, X.-P.; Li, C.-X.; Xie, B.-B. et al. *J. Phys. Chem. A*, **2015, 119,** 11488-11497.

碳掺杂氮化碳光物理性质和光催化制氢机理的研究

葛志统[1]，于安池[1]，吕荣[1,*]

[1] 中国人民大学理学院化学系，北京 ，100872

*Email: lvrong@chem.ruc.edu.cn

半导体光催化剂材料g-C_3N_4的研究已有大量报道，非金属元素B、P、S、N、O等的引入会不同程度改变其光物理性质和光催化活性，但目前对其掺杂机理的研究还相对匮乏。电子转移机理的研究对我们更好地理解光催化原理至关重要，它可以为我们以后的研究指出更明确的方向。本工作采用传统的热处理法合成了一系列不同掺杂量的Cring-C_3N_4[1]，采用DRS、XRD、EDS、FT-IR、TCSPC等测试手段对合成样品的结构、形貌、光催化性能及其构效关系进行了初步的研究。结果显示，样品随着掺杂量的增加在可见光区的吸收依次增加（图a）；随着碳含量的增加，掺杂后的样品在大约13°的衍射峰变得越来越弱，而在27.4°左右的衍射峰峰高逐渐降低，峰宽逐渐增加，峰位置向右稍有移动（图b），推测合成的样品物质种类并未改变，而晶粒的大小有所改变，掺杂后的平面结构可能发生褶皱，样品的层间距变得越来越小[1-2]；通过EDS证实了掺杂后的样品随着掺杂量的增加C/N比例依次增加；在皮秒时间分辨TCSPC系统下，460 nm激发，530 nm检测时，各掺杂样品与本体寿命相比，会不同程度的变短（图c）；此外，样品的光催化制氢效率也对应的发生了改变。

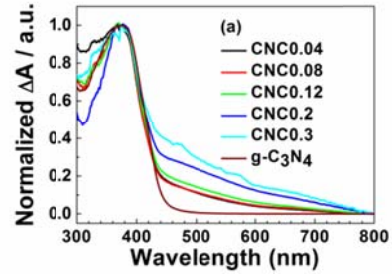

Fig. 1 XRD pattern

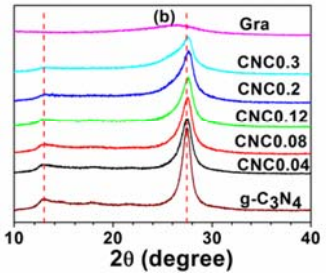

Fig. 2 UV-visible absorption

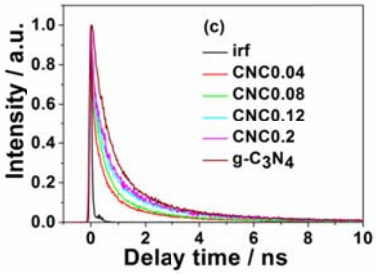

Fig. 3 Fluorescence decay lifetime date

关键词：氮化碳；掺杂；可见光；光催化

参考文献

[1] Che, W.; Cheng, W.; Yao, T.; Tang, F. M.; Liu, W.; Su, H.; Huang, Y. Y.; Liu, Q. H.* ; Liu, J.k.; Hu, F.C.; Pan, Z.Y.; Sun,Z.H.; Wei,S.Q.*. *J. Am. Chem. Soc*, **2017**, **139 (8)**, 3021–3026.

[2] Zhang, H. Y.; Yu, A. C.**J. Phys. Chem. C*, **2014**, **118**,11628–11635.

金表面对苯二甲氰自组装膜的时间分辨和频光谱研究

郭伟，何玉韩，王静静，张永燕，刘晨西，王朝晖*

固体表面物理化学国家重点实验室，谱学分析与仪器教育部重点实验室，厦门大学化学化工学院化学系，厦门，361005

*Email: zhwang@xmu.edu.cn

本文利用时间分辨和频光谱对金膜表面自组装对苯二甲氰（1,4-Phenylene diisocyanide, PDI）分子进行了研究。研究中发现，当可见光（皮秒光）为高斯线型时，难于获得没有金基底信号的 PDI 分子和频光谱；而当可见光为时域不对称线型（由 Eatlon 产生）时，则能得到 PDI 分子完整的振动去相位曲线（结果如图 1A 所示）。从图 1A 中可知，金膜表面自组装 PDI 分子自由-NC 振动去相位时间为 0.23 ps，而与金属结合的-NC 振动去相位时间为 0.12 ps。使用频域非线性回归算法对 PDI 的和频光谱进行拟合与分解发现，PDI 的和频光谱由一个正峰（与金属结合的-NC）和一个负峰（自由的-NC）构成（如图 1B 所示）。同时采用频域非线性回归算法可以得到更准确的 PDI 分子-NC 伸缩振动峰位信息。该研究结果表明，PDI 分子只有一端端位吸附在金原子上，从而导致 PDI 分子的-NC 相位相反。

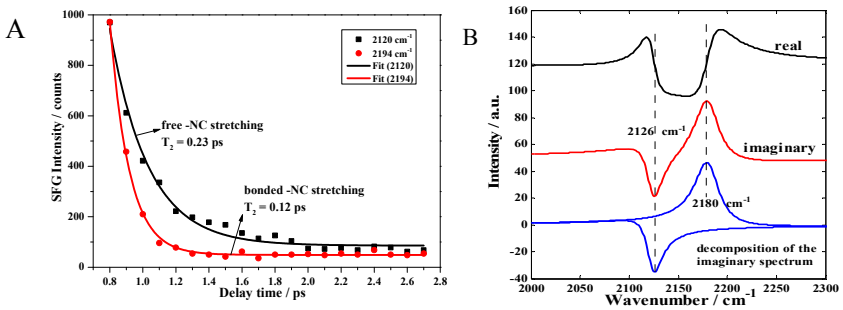

Fig. 1 (A) The SFG Intensity changes of different vibration modes of PDI. (B) The real part of the SFG spectrum, imaginary part, and decomposition of the fitted imaginary spectrum into two vibrational modes.

关键词：时间分辨和频光谱；对苯二甲氰；自组装；振动去相位

参考文献

[1] Ito M, Noguchi H, Ikeda K, Uosaki K. *PCCP*, **2010**, **12(13)**, 3156.

[2] Laaser J E, Xiong W, Zanni M T. *J. Phys. Chem. B*, **2011**, **115(11)**, 2536.

G-MCTDH 方法研究 CH_2OH 2^2A 态光解动力学

韩山雨[1]，谢长健[2]，郭华[1,2*]，谢代前[1,*]

[1] 南京大学化学化工学院理论与计算化学研究所，介观化学教育部重点实验室，江苏省南京市，210093

[2] 新墨西哥州大学化学与化学生物系，美国新墨西哥州阿尔伯克基，87131

*Email: dqxie@nju.edu.cn,hguo@unm.edu and jingsong@ucr.edu

受限于计算标度，以格点为基的量子波包方法很难用于多原子高维体系。而基于高斯波包的一类半经典方法具有优异的标度性质，并且理论上能够正确描述部分量子效应[1-3]。其基函数由随时间变化的参数决定，并且参数演化满足经典运动方程。G-MCTDH[4]方法是一类高斯波包方法，其将高斯基函数运用到MCTDH理论框架下，理论计算表明在短时间内传播G-MCTDH计算结果逼近MCTDH方法。本文用G-MCTDH方法在全维非绝热势能面上计算了CH_2OH 2^2A态吸收谱并与精确的全维量子波包动力学结果进行了比对，结果吻合非常好。相比于量子波包方法所用内存800GB，G-MCTDH方法只需要几兆。

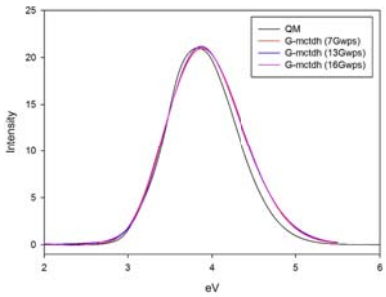

Fig. 1 G-MCTDH calculated absorption spectrum compared with TDWP

关键词： G-MCTDH；高斯波包；全维动力学

参考文献

[1] M. Sepúlveda, S. Tomsovic, and E. Heller. Phys. Rev. Lett. **69** (3), 402–405 (**1992**)

[2] T.J. Martínez, M. Ben-Nun, and R.D. Levine, J. Phys. Chem. **100**, 7884–7895 (**1996**).

[3] D.V. Shalashilin and M.S. Child, Chem. Phys. **304** (1–2), 103–120 (**2004**)

[4] G.W. Richings, I. Polyak, K.E. Spinlove, G.A. Worth, I. Burghardt and B. Lasorne, Inter. Rev. Phys. Chem. **34**, 269-308 (**2015**)

Controllable Synthesis and Photoexcited Dynamics of Organometal Halide Perovskite Quantum Dots

Sheng He, Shengye Jin*

Dalian Institute of Chemical Physics, Chinese Academy of Sciences, 457 Zhongshan Road, Dalian, 116023

*Email: sjin@dicp.ac.cn

Organometal halide perovskite quantum dot is one of the newly reported semiconductor materials with excellent photoelectric properties, such as high quantum yield, tunable band gap varying with size and consistent. With such characters, these quantum dots can make important contributions to the development of solar cells, photocatalysis and light-emitting device. However, the main barrier of its development is the weak stability. Thus, relevant photoelectric dynamics study are rare, which is, however, very meaningful and fundamental for these materials' application. In this article, we discussed various methods to prepare methylammonium lead halide($CH_3NH_3PbX_3$, $MAPbX_3$，X=Cl, Br, I) perovskite quantum dots and improved the reported synthesis method. We also put forward a new method to make anion-blended $MAPbX_3$ quantum dots by anion exchanging. Using transient absorption spectroscopy, we studied the lifetime(4.84±0.07 ns) of $MAPbBr_3$ quantum dots at excited state with only one exciton in every dot. Also, we observed charge transfer from $MAPbBr_3$ quantum dots to benzoquinone(as the electron acceptor). At the same time, we prepared nanowires self-assembled by $MAPbBr_3$ nanoplatelets with the wire length at the level of micrometer, and studied them with time-resolved and photoluminescence-scanned confocal microscopy, but no carrier diffusion along the nanowire was observed. These synthesis and photoelectric dynamics research will offer fundamental support for the application of the organolead halide perovskite quantum dots.

Keywords: Perovskite; Quantum Dots; Transient Absorption Spectroscopy

启发渐进式特征投影法分析金纳米粒子的瞬态吸收光谱

何玉韩，张檬，郭伟，王静静，张永燕，王朝晖*，孙世刚

厦门大学化学化工学院，厦门，361005

*Email: zhwang@xmu.edu.cn

瞬态吸收光谱(Transient absorption, TA)是研究凝聚态电子、质子和声子等相关超快动力学过程的有力工具。由于不同动力学过程的光谱相互重叠，研究常常需要根据假设模型分离不同过程的动力学光谱[1]。然而凝聚态动力学过程较为复杂，直接提出动力学过程较为困难，并容易引入模型误差。为了解决这个问题，本研究使用启发渐进式特征投影法(heuristic evolving latent projection, HELP)[2]对瞬态吸收光谱进行分析。该方法假定一个动力学过程的光谱线型不随延时而变化，动力学曲线不随波长而变化(即双线性条件)。HELP方法无需进一步假设，根据二维光谱矩阵秩的信息对不同动力学过程的时域和频域曲线进行分离。图1给出了HELP方法用于55 nm金纳米粒子TA光谱的分析结果，研究直接分离得到了带间跃迁、表面等离激元(SPR)漂白和电荷分离三个过程的光谱和动力学曲线。

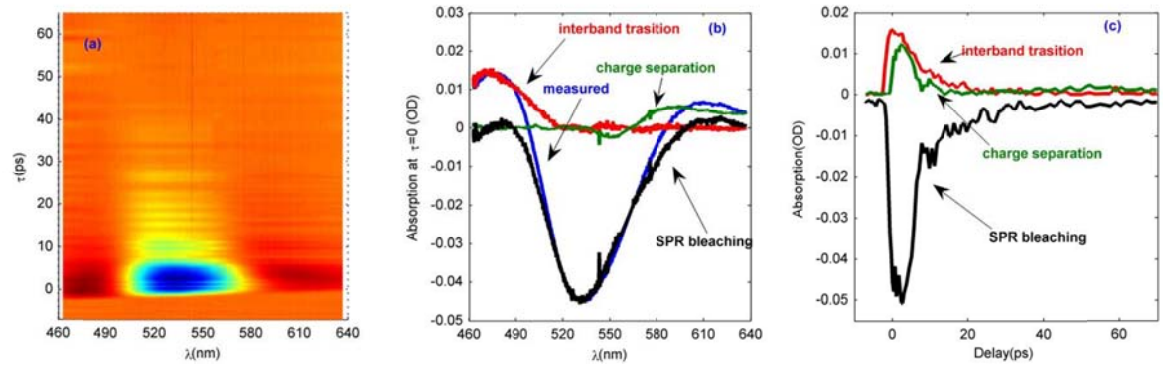

Fig. 1 HELP方法解析结果(a)原始光谱(b)不同过程频域光谱(c)不同过程时域光谱

关键词：启发渐进式特征投影法；金纳米粒子；瞬态吸收光谱

参考文献

[1] 翁羽翔, 陈海龙等. 超快激光光谱原理与技术基础 [M].北京:化学工业出版社, **2013**: 305-309.

[2] 许禄, 邵学广. 化学计量学方法 [M]. 北京: 科学出版社, **2004**: 196-199.

高分辨和频振动光谱研究气-液界面温敏性高分子 pNIPAM 侧链异丙基取向角

侯建，陆洲*

中国科学院化学研究所，中关村北一街 2 号，100190

*Email: zhoulu@iccas.ac.cn

高分子聚（N-异丙基丙烯酰胺）（pNIPAM）具有温度敏感性，在临界溶解温度 32℃左右时可发生相变，因此可利用温度变化实现对其亲疏水性及溶解度的有效调控。pNIPAM 已经被广泛用于药物的负载与释放、生物分子的分离以及智能仿生界面材料的设计等[1]，其性质在很大程度上取决于界面上的相变反应。对温敏性高聚物在水溶液界面的结构与相变机理进行原位检测具有重要的意义。和频振动光谱（sum frequency generation spectroscopy, SFG）具有界面选择性与亚单分子层灵敏度，是原位研究气/液和固/液等界面上的分子结构与基团取向的有力工具。Miyamae 等人利用 SFG 研究了固/液和固/气界面 pNIPAM 侧链异丙基取向角随温度的变化[2]，其数据分析的关键为异丙基基团在碳-氢伸缩波段的 SFG 光谱细节。根据 Miyamae 和 Cremer[3] 对异丙基的超极化率的理论推导，预测了异丙基中的甲基反对称伸缩振动存在三种模式,属于三种不同的对称性，但限于以往有限的光谱分辨率，尚未在实验中得到证实。我们在本研究中利用国内首台光谱分辨率高达 0.5 cm^{-1} 的皮秒-飞秒联用式高分辨超快 SFG 光谱仪，并结合二阶非线性光学中的偏振依赖测量技术，对空气/水界面 pNIPAM 的侧链异丙基的空间取向进行了系统研究。在光谱测量中。我们获取了不同分子量的高分子链在不同的表面膜压下的碳-氢伸缩波段的精细 SFG 光谱结构，首次发现了一系列新的光谱分裂；经过与理论预测进行对比，力图准确地计算异丙基的取向角和扭转角。

关键词：和频振动光谱；聚（N-异丙基丙烯酰胺）；界面取向；空气/水界面

参考文献

[1] Cheng, C ; Wei, H ; Shi, BX; Cheng, H ; Li, C; Gu, ZW ; Cheng, SX ; Zhang, XZ ; Zhuo, RX . *Biomaterials.* **2008**, **29**: 497.

[2] Miyamae, T; Akiyama, H; Yoshida, M; Tamaoki, N. *Macromolecules*. **2007**, **40**: 4601.

[3] Sho Kataoka, Paul S. Cremer. *J. Am. Chem. Soc*. **2006**, **9**: 5517.

Multi-configurational study of ultrafast nonlinear X-ray spectroscopy of molecules

Weijie Hua[1, 2, 3], Yi Luo,[2,4*] Shaul Mukamel[1*]

[1]Department of Chemistry, University of California, Irvine, CA 92697-2025, USA
[2]Department of Theoretical Chemistry and Biology, KTH Royal Institute of Technology, S-10691 Stockholm, Sweden
[3]Present address: Department of Applied Physics, School of Sciences, Nanjing University of Science and Technology, Nanjing 210094, P. R. China
[4]Hefei National Laboratory for Physical Sciences at the Microscale, University of Science and Technology of China, Hefei, Anhui 230026, China
*Email: luo@kth.se, smukamel@uci.edu

Bright, ultrashort pulses generated by X-ray free-electron laser (XFEL) and high harmonic generation (HHG) light sources enabled the possibility of ultrafast nonlinear X-ray spectroscopy, which can provide higher-level information than linear absorption and emission spectroscopy.[1,2,3] We have employed multi-configurational quantum chemistry methods to simulate the core excited states of conical intersection (CoIn) structures and double core hole (DCH) states and developed our in-house program to calculate and analyze the signals. We demonstrate that the attosecond stimulated X-ray Raman spectroscopy (ASRS) can be used in detecting the ultrafast passage of CoIns in a photochemical reaction, which can capture information in their very time locality. [4] The X-ray double-quantum coherence (XDQC) spectroscopy can be used in probing the correlation of two atoms in a molecule (Fig. 1).[5] We have developed a new model to simulate the transient X-ray absorption spectroscopy (TXAS) which is helpful for distinguishing the photo-decay mechanisms of uracil.[6] Our theoretical studies provide fundamental insights for experimental design and implementation of novel X-ray spectroscopies.

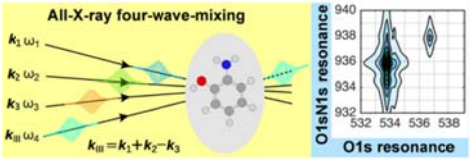

Fig. 1. Schematic illustration of the XDQC spectroscopy set-up for aminophenol (left) and the calculated signal (right). This signal shows the correlation between the O1s single core excited states and the O1sN1s double core excited states which maps the correlation of N and O atoms in the molecule.

Keywords: ultrafast nonlinear x-ray spectroscopy; quantum chemistry; molecular dynamics; photochemistry; multiconfigurational method

References:

[1] Bennett, K. et al., *Phys. Scr.* **2016, T169**: 014002.
[2] Zhang, Y; Hua, W.; Bennet, K; Mukamel, S. *Top. Curr. Chem.* **2016, 368**: 273.
[3] Mukamel, S; Healion, D; Y. Zhang, Y; Biggs, J. D. *Annu. Rev. Phys. Chem.* **2013, 64**:101.
[4] Hua, W. et al., *Struct. Dyn.* **2016, 3**: 023601.
[5] Hua, W; Bennet, K.; Zhang, Y. ; Luo, Y. ; Mukamel, S., *Chem. Sci.* **2016, 7**: 5922.

[6] Hua, W.; Mukamel, S.; Luo, Y. In manuscript.

碳量子点/TiO_2纳米片复合材料的制备以及光催化动力学研究

黄红琴[1]，郑旭明[2]，王惠钢[1,*]

[1]浙江理工大学理学院，杭州 310018

[2]浙江理工大学理学院，杭州 310018

*Email: zdwhg@163.com

TiO_2纳米片（TNS）拥有高结晶度且具有较大比例的（001）晶面，因此在光催化方面有巨大的应用潜能[1]，但其禁带能隙较宽，不能充分利用太阳光。因此，用绿色光催化促进剂碳量子点（CDs）修饰 TNS 提高其催化性能。本文通过水热法将 TNS 分散到 N-CDs 溶液中制备 N-CDs/TNS 复合材料[2] (如图 1 所示)，并对催化剂做了 SEM、TEM、XRD、XPS 等表征。在可见光照射下（λ>400nm），通过降解罗丹明 B（RhB）来测试 N-CDs/TNS 的催化性能。发现掺杂 6mLN-CDs 时，复合物的催化性能最好！(如图 2 所示)。

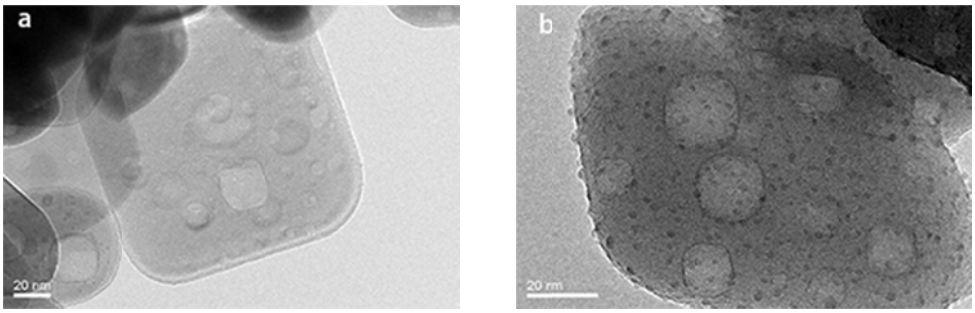

Fig. 1 TEM images of (a) TNS, (b) N-CDs/TNS composites

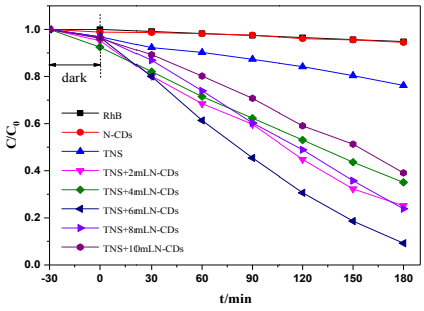

Fig. 2 Photocatalytic degradation of RhB solution by N-CDs/TNS composites with different amount of N-CDs under visible light irradiation.

关键词：碳量子点；TiO_2纳米片；光催化

参考文献

[1]Han X, Kuang Q, Jin M, Zhao X. Journal of the American Chemical Society, **2009**,**131(9)**: 3152-3153.

[2]Xue Y, Jian L, Ying Y, Sheng Z, Carbon,**2014**, **68(3)**:718–724.

Covalent and Noncovalent Interactions between Boron and Argon: an Infrared Photodissociation Spectroscopic Study of Argon-Boron Oxide Cation Complexes

Jiaye Jin, Wei Li , Yuhong Liu, Guanjun Wang and Mingfei Zhou*

Department of Chemistry, Fudan University, 220 Handan Rd, Shanghai, 200433
*mfzhou@fudan.edu.cn

Although a wide range of compounds of the heavy rare-gas elements are experimentally known, very few chemically bound molecules have been observed for the lighter noble gases. Here we report an infrared photodissociation spectroscopic and theoretical study on a series of argon-boron oxide cation complexes prepared via a laser vaporization supersonic ion source in the gas phase. Infrared spectroscopic combined with state-of-the-art quantum chemical calculations indicate that the $[ArB_3O_5]^+$, $[ArB_4O_5]^+$, $[ArB_4O_6]^+$, and $[ArB_5O_7]^+$ cation complexes have planar structures each involving an argon-boron covalent bond and an aromatic boroxol ring. The argon-boron bond is formed between the 2p lone-pair electrons of argon and in-plane orbital of boroxol ring. On the contrary, the $[ArB_3O_4]^+$ cation complex is characterized to have a weakly bound argon atom and a BO chain structure.

Keywords: noble gas bonding; argon-boron oxide complex; gas phase vibrational spectra; dative bonding; quantum chemical calculations

4-硝基联苯及其衍生物三重态的反应动力学研究

金佩佩，薛佳丹[1,*]，郑旭明

[1] 浙江理工大学化学系，杭州，310018

*Email: jenniexue@126.com

硝基多环芳烃具有强烈的光致毒性和基因毒性，对人类生产和生活有强烈影响，而硝基多环芳烃的主要降解途径是光降解[1,2]，因此研究其光化学反应具有重要的意义。本文利用瞬态吸收和时间分辨拉曼光谱研究了4-硝基联苯(NBP)和 4-硝基-4′-氨基联苯（ANBP）的最低激发三重态的反应动力学及在水溶液和醇溶液中的反应。

4-硝基联苯（NBP）受光激发后经过内转换(IC)跃迁至最低激发单重态S_1，S_1可经系间窜跃(ISC)至三重态 T_1。纳秒瞬态吸收动力学实验发现NBP在不同溶剂中的其三重态寿命均很短（sub-100ns），并且其寿命随着溶剂极性的增大而增大（在乙腈-水体积比为1的溶液中寿命为690ns）。造成这一现象的原因可能是弱极性溶剂中， S_0与T_1存在势能面交叉点，导致其$T_1 \rightarrow S_0$的ISC效率高，T_1寿命短；而在强极性溶剂中， S_0与T_1之间的能差大，ISC效率低。通过在乙腈-水混合溶液（体积比为1:1）中加二茂铁猝灭剂的动力学实验，得到其二级反应速率常数为1.27×10^{10} M^{-1} s^{-1}。从NBP在甲醇、异丙醇溶液中的瞬态吸收光谱观察到在470nm处有一尖峰，根据Rafael Arce等[3]报道，指认为NBP夺氢自由基。而在水溶液中的瞬态吸收光谱发现在350nm处有一尖峰，根据Brigante, M.等[4]报道，指认为NBP阴离子自由基。

除此之外，我们还对4-硝基-4′-氨基联苯（ANBP）进行了研究。与NBP不同的是，ANBP三重态的寿命很长（~3μs），这是由于对位的氨基使激发态分子更易形成push-pull结构，能够稳定能级，使得S_0与T_1之间的能差增大，三重态寿命增加。另外，我们还利用时间分辨拉曼光谱研究了ANBP在醇溶液中的反应，发现ANBP在醇溶液中的反应与NBP的完全不同。

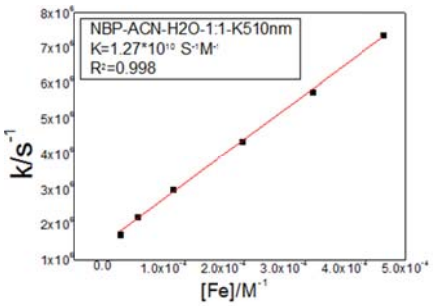

Fig. 1 Pseudofirst order decay of ^{3}NBP (monitored at 510 nm) as a function of ferrocene concentration.

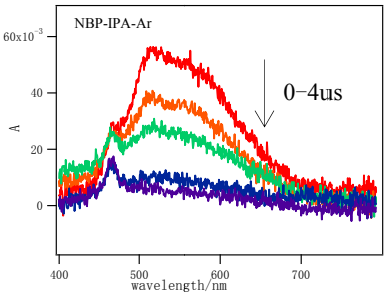

Fig. 2 Transient absorption spectra of NBP(2.0×10-4 M) in deaerated.

关键词：4-硝基联苯；光化学；三重态

参考文献

[1] Vogt R. A.; Crespo-Hernandez C. E. *J. Phys. Chem. A*, **2013**, **117**:14100.

[2] Vogt R. A.; Reichardt C.; Crespo-Hernandez C. E. *J. Phys. Chem. A*, **2013**, **117:**6580.

[3] Arce, R., et al. *J. Phys. Chem. A*, **2008**, **113**:10294.

[4] Brigante, M., et al. *J. Phys. Chem. A*, **2010**, **114:**2830.

5-硝基异喹啉三重态的反应动力学研究

金佩佩，薛佳丹[1,*]，郑旭明

[1] 浙江理工大学化学系，杭州，310018

*Email: jenniexue@126.com

人类社会大量排放的硝基多环芳烃对生物和环境有较大影响，光化学分解是其主要的降解路径[1,2]，因此研究其光化学反应具有重要的意义。本文利用纳秒瞬态吸收光谱研究了5-硝基异喹啉（NIQ）的最低激发三重态的反应动力学及在酸溶液、水溶液和醇溶液中的反应。

5-硝基异喹啉（NIQ）受光激发后经过内转换(IC)跃迁至最低激发单重态S_1，S_1可经系间窜跃(ISC)、内转换（IC）至三重态 T_1。通过纳秒时间分辨动力学实验测得NIQ在乙腈中能被二茂铁（$k=1.72\times10^{10}\ s^{-1}M^{-1}$）和NaI（$k=1.19\times10^{10}\ s^{-1}M^{-1}$）以扩散速率猝灭。从NIQ在甲醇、异丙醇溶液中的瞬态吸收光谱（t=1μs）观察到在365nm处有一尖峰，根据Rafael Arce等[3]报道1-硝基芘夺氢自由基的峰形（425nm），指认为NIQ夺氢自由基，并且根据TD-DFT（B3LYP/cc-PVDZ/PCM）计算NIQH·的吸收在362nm（f=0.2106）。以三级反应拟合甲醇浓度-衰减速率常数，得到反应速率常数$k=2.4\times10^{3}M^{-2}s^{-1}$（图1）。我们推测其机理为在T态与醇通过氢键结合，发生质子转移，且从图1可知，当醇浓度大于3.3M时，开始反应。NIQ在水溶液中的瞬态吸收光谱（t=50μs）发现在385nm处有一尖峰，根据Brigante, M.等[4]报道1-硝基萘阴离子自由基（$1NN^{-}\cdot$）的峰形（380nm），指认其为NIQ阴离子自由基，根据TD-DFT（BPW91/cc-PVDZ/PCM）计算$NIQ^{-}\cdot$的吸收在376nm（f=0.1001）。另外根据pH-^{3}NIQ衰减速率常数图（图2）可知，当pH>4.2时，^{3}NIQ的衰减可用准一级反应拟合，其速率常数为$1.16\times10^{6}\ s^{-1}$；当pH<4.2时，其衰减速率常数随pH减小而增加，这是由于生成了$NIQH^{+}$（类似$1NNH^{+}$[4]）。氢离子除了会与硝基上的O原子结合外，还会与环上的N原子结合，根据TD-DFT（B3LYP/cc-PVDZ）计算，N原子上结合H^{+}时的能量比O原子上结合时更低，相信H^{+}优先与N原子结合，再与O原子结合。

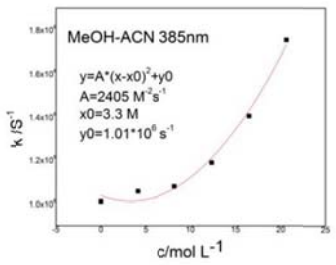

Fig. 1 Pseudofirst order decay of ^{3}NIQ (monitored at 385 nm) as a function of methanol concentration.

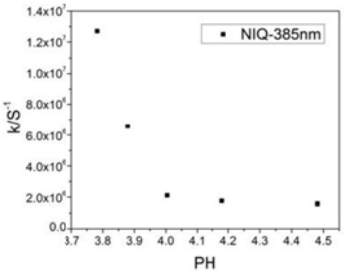

Fig. 2 Pseudofirst order decay of ^{3}NIQ (monitored at 385 nm) as a function of PH.

关键词：5-硝基异喹啉；光化学；三重态

参考文献

[1] Vogt R. A.; Crespo-Hernandez C. E. *J. Phys. Chem. A*, **2013**, **117**:14100.

[2] Vogt R. A.; Reichardt C.; Crespo-Hernandez C. E. *J. Phys. Chem. A*, **2013**, **117:**6580.

[3] Arce, R., et al. *J. Phys. Chem. A*, **2008**, **113**:10294.

[4] Brigante, M., et al. *J. Phys. Chem. A*, **2010**, **114:**2830.

氨气分子光解动力学研究

金艳玲[1]，张志国[1,2]，戴东旭[1]，陈志超[1,*]，郭华[3,*]，杨学明[1,*]

[1] 中国科学院大连化学物理研究所，大连，中国，116023

[2] 阜阳师范学院，阜阳，安徽，236041

[3] 新墨西哥大学，阿尔布开克，美国，87131

*Email: czc@ dicp.ac.cn，hguo@unm.edu，xmyang@dicp.ac.cn

氨气是大气中含量最多的碱性气体。研究表明它是 PM2.5 形成的“催化剂”，重污染天气中硫酸铵和硝酸铵占 PM2.5 质量浓度总和的一半以上。氨气在紫外波段的光解是大气氮循环中非常重要的过程。最近，我们应用离子速度成像技术对氨气分子（NH_3）进行了光解动力学的实验研究。我们在转动量子态分辨的水平上观测了 $NH+H_2$ 解离通道。产物量子态相关的实验结果表明：H_2 产物转动量子态分布具有明确的奇偶倾向性；空间角分布趋于各项同性，是比较慢的解离过程。理论计算结果表明 $NH+H_2$ 通道中存在“漫游机理”通道，其所占分支比为 30%。

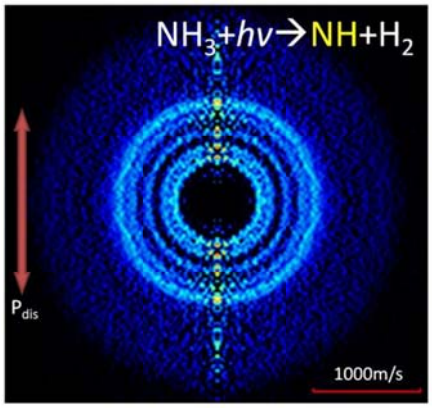

Fig. 1 Inverted image of the NH product from the photodissociation of NH_3.
The double arrow indicates the polarization of the pump laser.

关键词：氨气分子, 光解动力学, 离子速度成像

参考文献

[1] Eppink, A. T. J. B.; Parker, D. H. *Rev. Sci. Instrum*. **1997**, **68**: 3477.

[2] Behera, S. N.; Sharma, M.; Aneja, V.P.; Balasubramanian R. *Environ. Sci. Pollut. Res*. **2013**, **20**: 8092.

[3] Xie, C.; Ma, J.; Zhu, X.; Zhang, D. H; Yarkony, D. R.; Xie, D.; Guo, H. *J. Phys. Chem. Lett*. **2014**, **5**: 1055.

[4] Xie, C.; Zhu, X.; Ma, J.; Yarkony, D. R.; Xie, D.; Guo, H. *J. Chem. Phys*. **2015**, **142**: 091101.

除谱在离子水溶液光谱中的应用

鞠思文[1]，张宁[2]，张睿挺[1]，王志强[1]，曾德文[3]，林珂[1,*]

[1] 西安电子科技大学 物理与光电工程学院，陕西 西安，710071

[2] 中南大学 材料科学与工程学院，湖南 长沙 410004

[3] 中南大学 化学化工学院，湖南 长沙 410083

*Email: klin@xidian.edu.cn

离子水溶液的微观结构一直是人们关注的重点，如水与水、水与离子、离子与离子之间的相互作用等，但至今很多问题仍存在争议。研究离子水溶液微观结构常用技术有稳态谱学和超快谱学，但是这些技术较少可以对离子水溶液进行量化分析。我们新提出的除谱方法可以揭示一些原本很难观察到的光谱成分，例如，水OH伸缩振动谱段拉曼光谱中的自由OH伸缩振动谱峰，蛋白质水溶液OH伸缩振动谱段拉曼光谱中的amide A谱峰，离子水溶液的OH伸缩谱段拉曼光谱中阴离子第一水合层光谱。基于这一除谱方法，我们对不同温度下$NaClO_4$水溶液以及水的OH伸缩振动谱段拉曼光谱进行分析。结果表明，盐溶液中阴离子水合层水分子数目随温度的改变而保持不变，水合层光谱特征说明温度的增加只是削弱水与离子之间的氢键而并没有使之断裂。类似的光谱现象也在水的光谱中观测到，这也间接说明温度升高的过程中液体水的氢键没有明显断裂，仅是氢键强度减弱。这个结果支持液体水的氢键连续微观结构模型。除此之外，我们还利用除谱结合差谱的分析方法对不同浓度的$CuCl_2$水溶液薄膜紫外吸收光谱进行分析，在~230 nm和~380 nm处发现了之前没有观察到的光谱成分，结合TD-DFT计算结果，推断出其可能对应于$[CuCl_3(H_2O)_n]^-$和$[CuCl_4(H_2O)_n]^{2-}$两种离子对结构。以上研究结果充分说明除谱方法是分析离子水溶液微观结构的有效工具。

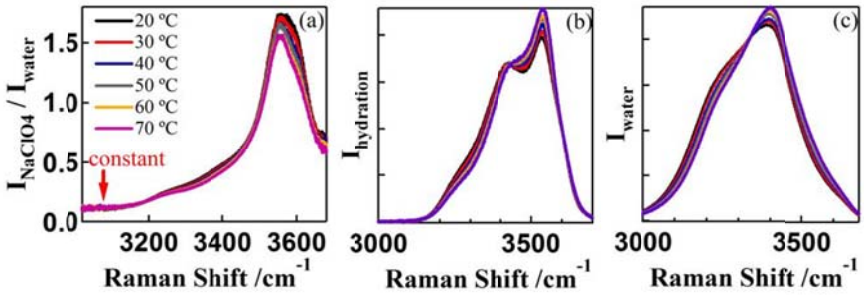

Fig. 1 Ratio Raman Spectra (a) of $NaClO_4$ aqueous solution and water, Raman Spectra (b) of water in the hydration shell of ClO_4^-, and Raman Spectra (c) of water from 20 °C to 70 °C.

关键词： 除谱；离子水溶液；溶剂层结构；氢键连续模型；离子对

参考文献

[1] K. Lin, X. G. Zhou, S. L. Liu and Y. Luo. Chin. J. Chem. Phys. **2013, 26 (2)**: 121-126.

[2] C. Q. Tang, K. Lin, X. G. Zhou and S. L. Liu. Chin. J. Chem. Phys. **2016. 29 (1)**: 129-134.

[3] Y. Wang, W. Zhu, K. Lin, L. Yuan, X. Zhou and S. Liu. J. Raman Spectrosc. **2016. 47 (10)**: 1231-1238.

[4] N. Zhang, D. W. Zeng, G. Hefter and Q. Y. Chen. J. Mol. Liq. **2014. 198**: 200-203.

[5] H. B. Yi, F. F. Xia, Q. B. Zhou and D. W. Zeng. J. Phys. Chem. A. **2011. 115 (17):** 4416-4426.

Infrared Photodissociation Spectroscopy of Mass-Selected Dinuclear Vanadium Dinitrogen Complexes

Fanchen Kong, Hui Qu , Guanjun Wang, Mingfei Zhou*
Department of Chemistry, Shanghai Key Laboratory of Molecular Catalysis and Innovative Materials, Fudan University, Shanghai, 200433, China

Dinitrogen activation by transition metals is of great interest. The coordination of N_2 to a single metal center often results in mild activation, while deep activation is found among N_2 complexes with multi metal centers. Searching for functional dinitrogen complexes coordinated with multiple metal centers is a potential route of dinitrogen activation.[1]

Dinuclear vanadium dinitrogen cation complexes $V_2(N_2)_n^+$ are produced by a laser vaporization supersonic cluster ion source in the gas phase. The ions are mass selected by time-of-flight mass-spectrometer and studied by infrared photodissociation spectroscopy.[2] The infrared spectrum of the $V_2(N_2)_8^+$ cation complex is shown in Figure 1. The strong bands above 2100 cm^{-1} are attributed to the N-N stretching vibrations of the end-on coordinated N_2 ligands. Deep activation of N_2 is found to occur with the observation of IR bands at 1737 and 1805 cm^{-1}. Geometric optimizations have been performed on various possible structures to determine the geometric and electronic structure of the experimentally observed cation complex. The $V_2(N_2)_8^+$ cation is determined to be a mixture of two close-lying structural isomers each involving a linear bridged N_2 ligand (Figure 1).

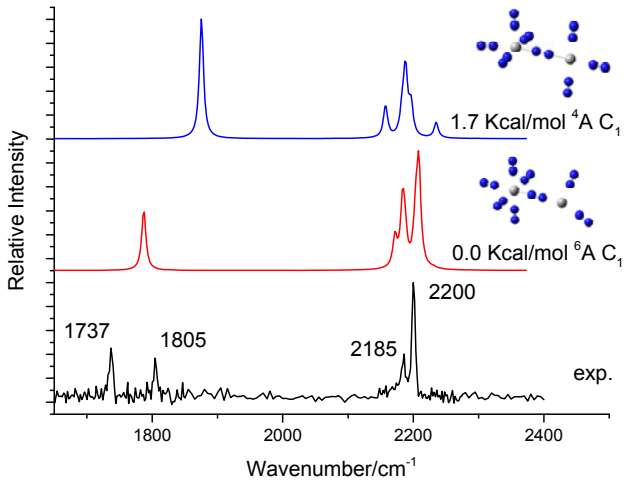

Fig.1 Experimental (black) infrared spectrum of $V_2(N_2)_8^+$ and simulated (red and blue) vibrational spectra of the two most stable structures of $V_2(N_2)_8^+$ in the frequency range of 1650-2400 cm^{-1}.

Keywords: infrared dissociation spectroscopy, dinitrogen activation, dinuclear dinitrogen complex

Reference:

[1] M.D. Fryzuk, *Science* **2013**, **340**:1530-1531.
[2]Wang, G.; Chi, C.; Cui, J.; Xing, X.; Zhou, M., *The Journal of Physical Chemistry A* **2012,** *116* (10), 2484-2489;

$H_5O_2^+$红外光解离光谱的 tagging 效应的理论研究

孔祥涛[1]，刘志锋[2]，江凌[1,*]

[1] 中国科学院大连化学物理研究所分子反应动力学国家重点实验室, 辽宁大连, 116023

[2] 香港中文大学化学系，香港沙田

*Email: ljiang@dicp.ac.cn

实验表明，$H_5O_2^+ \cdot Rg_n$ (Rg=Ar和Ne)团簇的红外光解离光谱有着明显的tagging效应[1]。我们使用从头算分子动力学模拟（AIMD）[2]，计算了$H_5O_2^+ \cdot Rg_n$ (Rg=Ar和Ne)团簇结构和红外光谱。研究表明，Ne和Ar与$H_5O_2^+$相互作用的位置有细微的差异，Ne位于两个水分子中间，未打破$H_5O_2^+$的对称性；而Ar位于H^+和H_2O的一个氢原子之间，打破了$H_5O_2^+$的对称性。同时AIMD模拟显示Ar标记的$H_5O_2^+$的团簇温度要比Ne标记的$H_5O_2^+$团簇温度偏高，这也与实验结果相符合[3]。虽然AIMD的微观温度并不对应宏观体系的真实温度，但可以推断不同tagging的团簇温度是不一样的，从头算分子动力学模拟对深层次理解氢键作用体系的团簇结构与动力学具有重要的科学意义[4]。

关键词：水合质子团簇；红外光解离光谱；分子动力学模拟

参考文献

[1] Hammer, N. I.; Diken, E. G.; Roscioli, J. R.; et.al. *J. Chem. Phys*. **2005**, *122*, 244301.
[2] CP2K website, http://www.cp2k.org/.
[3] Mizuse, K.; Fujii, A. *Phys. Chem. Chem. Phys.* **2011**, *13,* 7129.
[4] Kong, X.; Liu, Z.; Jiang, L. *to be submitted*.

蒽醌基化合物激发态电荷转移相关的构象弛豫与热活化延迟荧光

匡卓然，夏安东*

中国科学院化学研究所，北京市中关村北一街 2 号，100190

*Email: andong@iccas.ac.cn

具有电子给受体结构的双二苯胺基苯基蒽醌（2,6-bis[4-(diphenylamino)phenyl]-9,10-anthraquinone，AQ(PhDPA)$_2$）已被报道具有高效的红光热活化延迟荧光现象。分子的结构与构象直接决定的其激发态电子结构，进而影响反向系间窜越产生延迟荧光的效率。本文利用飞秒和纳秒瞬态吸收光谱的方法，结合量子化学计算，研究了 AQ(PhDPA)$_2$ 分子由光激发后、直到产生热活化延迟荧光的一系列完整的激发态去活化过程。通过稳态光谱和理论计算，详细研究了该分子激发态演化过程中各构象的电子态结构，发现其 S_0 和 S_1 的稳定构象有较小的最低单重态—三重态能级差（ΔE_{ST}），而 T_1 的扭曲构象使得 ΔE_{ST} 显著增加。飞秒瞬态吸收光谱显示，在非极性的甲苯溶液中 AQ(PhDPA)$_2$ 的电荷转移态在溶剂化稳定后具有较高的荧光效率；而在极性的四氢呋喃溶液中由于强烈的溶剂化效应使得电荷转移态的荧光发生淬灭。纳秒瞬态吸收光谱研究进一步发现，在甲苯溶液中构象自由演化的 AQ(PhDPA)$_2$ 分子由于扭曲弛豫导致部分处在三重态的分子不能返回单重态产生延迟荧光；而在掺杂薄膜中转动受限的分子则可以保持 ΔE_{ST} 较小的构象，使得三重态分子反向系间窜越产生延迟荧光的几率显著增加。本工作对具有分子内电荷转移特征的热活化延迟荧光体的超快激发态动力学的研究结果，有助于理解分子构象弛豫与反向系间窜越的关系，并为设计合成热活化延迟荧光材料提供了重要参考。

关键词：分子内电荷转移；热活化延迟荧光；反向系间窜越；激发态动力学；瞬态吸收光谱

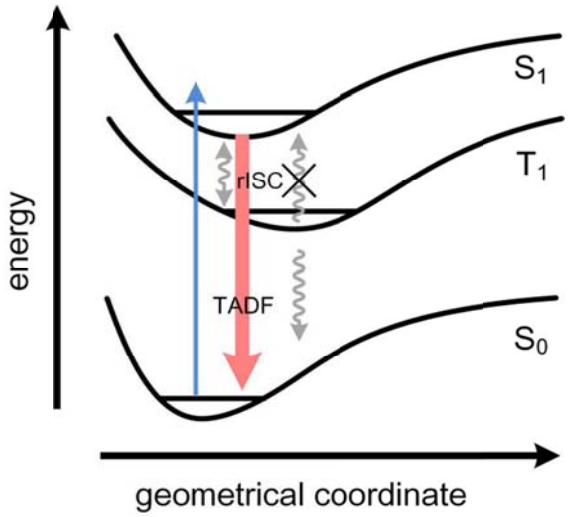

参考文献

[1] Q. Zhang, H. Kuwabara, W. J. Potscavage, Jr., S. Huang, Y. Hatae, T. Shibata, and C. Adachi, *J. Am. Chem. Soc.* **136**, 18070 (2014).

三甲胺团簇离子的红外光解离光谱研究

雷鑫，孔祥涛，江凌*

中国科学院大连化学物理研究所分子反应动力学国家重点实验室, 辽宁大连, 116023

*Email: smilelx@dicp.ac.cn

近年来随着环境问题的日益加重，对大气气溶胶颗粒的形成机理研究成为重要的研究热点，大气中胺类物质三甲胺的含量相对较多，在大气气溶胶的形成和转化过程扮演者重要的角色[1]。我们运用自主研制的 IRPD 装置研究了 2500-3600cm^{-1} 范围内的三甲胺团簇离子碳氢振动。与理论计算结合，我们指认了各相应峰，建立了三甲胺团簇离子结构模型。三甲胺团簇离子的研究对我们理解大气溶胶组成及形成机理有重要意义，对三甲胺团簇离子的研究，将有利于我们从动力学角度认识大气颗粒的成核过程[2]。

参考文献

[1] Qiu, C.; Zhang, R. *Phys. Chem. Chem. Phys.*, **2013**, *15*, 5738-5752.

[2] Zhang, R. Khalizov, A.; Wang, L.; Hu, M.; Xu, W. *Chem. Rev*. **2012**, *112*, 1957-2011.

光合捕光复合物的二维电子光谱研究

冷轩[1,2]，朱锐丹[1]，王专[1]，翁羽翔[1*]，史强[2*]

[1] 中国科学院物理研究所, 北京凝聚态物理国家实验室（筹）, 中科院软物质物理重点实验室, 北京 100190;
[2] 中国科学院化学研究所, 北京分子国家实验室（筹），分子动态与稳态结构国家重点实验室, 北京 100190;
*Email: yxweng@iphy.ac.cn; qshi@iphy.ac.cn

光合作用对地球上的生命是至关重要的，它把太阳光转换为人们可以使用的生物能和化学能。捕光天线捕获太阳光子能量并以激发态的形式传递到反应中心用于分解水则是光合作用的第一步[1]。在进化的压力下，捕光天线中的激发态传能效率被发展接近 100%[2,3]。 光合捕光天线是由一系列的捕光蛋白色素复合物构成，而其中LHCII（Light harvesting complex II）占据了地球含量的 50% 以上[2]。我们将二维电子光谱实验和理论结合起来研究LHCII中的激发态能量传递及相干现象。实验方面，首先我们对二维电子光谱系统做了相关的技术指标表征，如：相位稳定性、时间零点校准等；并初步获得相关实验数据[4]。理论方面，我们将级联运动方程和运动方程相匹配方法（Equation of motion phase matching approach）结合起来模拟二维电子光谱 [5]。我们模拟了激发叶绿素 b （Chl b）宽谱探测叶绿素 a (Chl a) 和宽谱激发、宽谱探测两种情形，并和先前实验做了比较分析。我们研究结果表明电子振动耦合可能在光合捕光天线传能过程中起着重要作用。

关键词： 二维电子光谱；LHCII；能量传递；级联运动方程；运动方程相匹配方法

参考文献

[1] B. Green and W. Parson, Light-Harvesting Antennas in Photosynthesis, Vol. 13 (Springer Science & Business Media, 2003).
[2] R. E. Blankenship, ed., Molecular Mechanisms of Photosynthesis (Blackwell Science, London, 2000).
[3] R. E. Blankenship, D. M. Tiede, J. Barber, G. W. Brudvig, G. Fleming, M. Ghirardi, M. Gunner, W. Junge, D. M. Kramer, A. Melis, et al., “Comparing photosynthetic and photovoltaic efficiencies and recognizing the potential for improvement,” Science 332, 805–809 (2011).
[4] S. Yue, Z. Wang, X. Leng, R.-D. Zhu, H.-L. Chen, and Y.-X. Weng, “Coupling of multi-vibrational modes in bacteriochloro-phyll a in solution observed with 2d electronic spectroscopy,” Chem. Phys. Lett. (2017).
[5] X. Leng, S. Yue, Y.-X. Weng, K. Song, and Q. Shi, “Effects of finite laser pulse width on two-dimensional electronic spectroscopy,” Chem. Phys. Lett. 667, 79–86 (2017).

三甲胺-甲醇混合体系中性团簇的 IR-VUV 光谱研究

李刚，张冰冰，孔祥涛，蒋述康，江凌*

中国科学院大连化学物理研究所分子反应动力学国家重点实验室, 辽宁大连, 116023

*Email: ljiang@dicp.ac.cn

由于能源利用引起的环境问题中，对大气颗粒物污染（如 PM2.5 等）研究的最大难点是对其来源和在大气中的化学变化机制的了解。有机气溶胶占大气细粒子总量的 20-50%，它们直接影响自然环境和人类健康，由于其化学成分复杂以及缺乏有效的实时分析仪器，目前人们还不十分了解这些有机颗粒物在大气中非均相反应的过程。大气中胺类物质三甲胺的含量相对较多，在大气气溶胶的形成和转化过程扮演者重要的角色[1]。对三甲胺中性团簇的研究，将有利于我们从动力学角度认识大气颗粒的成核过程，以及胺类团簇分子的氢键相互作用机理[2]。我们利用自主研制的 IR-VUV 实验装置，与理论计算紧密结合，研究了三甲胺与甲醇混合气体团簇，建立了三甲胺与醇类物质的相互作用模型[3]。

参考文献

[1] Qiu, C.; Zhang, R. *Phys. Chem. Chem. Phys.*, **2013**, *15*, 5738-5752.

[2] Zhang, R. Khalizov, A.; Wang, L.; Hu, M.; Xu, W. *Chem. Rev*. **2012**, *112*, 1957-2011.

[3] Li, G.; Zhang, B.; Kong, X.; Jiang, S.; Jiang, L., et. al. *to be submitted*.

Direct Observation of Methoxycarbonylnitrene

Hongmin Li[1], Xiaoqing Zeng[1,*]

[1] College of Chemistry, Chemical Engineering and Materials Science, Soochow University, Suzhou, Jiangsu, China. 215123

*Email: xqzeng@stu.suda.edu.cn

The simplest alkoxycarbonylnitrene, $CH_3OC(O)N$, has been generated through laser (266 and 193 nm) photolysis of $CH_3OC(O)N_3$ and $CH_3OC(O)NCO$ and subsequently characterized by IR (^{15}N, D-labelling) and EPR ($|D/hc| = 1.66$ cm^{-1} and $|E/hc| = 0.020$ cm^{-1}) spectroscopy in cryogenic matrices. Two conformers of the nitrene, with the CH_3 group being in *syn* or *anti* configuration to the C=O bond, have been unambiguously identified. Further UV light irradiation (365 nm) of the nitrene results in isomerization to CH_3ONCO, completing the frequently explored mechanism for the Curtius-rearrangement of $CH_3OC(O)N_3$.

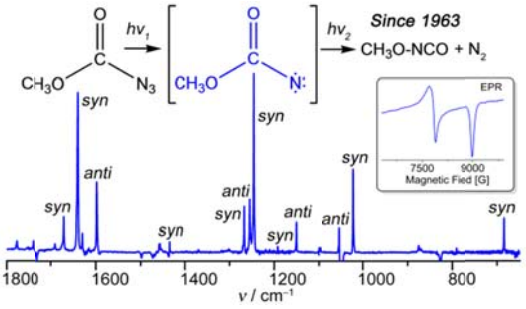

Fig. Methoxycarbonylnitrene $CH_3OC(O)N$, the missing link in the frequently studied Curtius-rearrangement of $CH_3OC(O)N$ has been directly observed by using matrix-isolation IR and EPR spectroscopy.

Keywords： matrix-isolation; nitrene； photolysis

References:

[1] Li, H. M.; Wu, Z.; Li, D. Q.; Wan, H. B. Xu, J. Abe, M.; Zeng, X. Q. *Chem. Commun.* **2017**, 53: 4783.

[2] R. S. Berry, D. Cornell, W. Lwowski, *J. Am. Chem. Soc.*, **1963**, 85: 1199.

[3] R. E. Wilde, T. K. K. Srinivasan, W. Lwowski, *J. Am. Chem. Soc.*, **1971**, 93: 860.

[4] J. Liu, S. Mandel, C. M. Hadad and M. S. Platz, *J. Org. Chem.*, **2004**, 69: 8583.

[5] J. M. Dyke, G. Levita, A. Morris, J. S. Ogden, A. A. Dias, M. Algarra, J. P. Santos, M. L. Costa, P. Rodrigues, M. M. Andrade, M. T. Barros, *Chem. Eur. J.*, **2005**, 11: 1665.

4-硫代胸腺嘧啶激发态结构及动力学研究

李鹏丽，姜杰，郑旭明*

浙江理工大学，浙江省杭州市下沙 2 号大街 928 号，310018

*Email: zhengxuming126@126.com

2-硫代胸腺嘧啶激发态动力学已有广泛的实验和理论计算研究[1]。Cui 等人开展了 CASSCF 计算研究，提出了三条可能的激发态弛豫路径[2]：

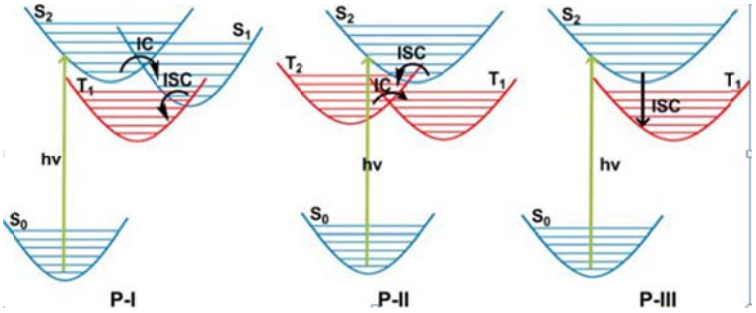

Fig. 1 The three excited state decay channels of 2-thiothymine

本文采用共振拉曼光谱技术，结合 CASSCF 计算方法，探究 4-硫代胸腺嘧啶和 2-硫代胸苷的激发态弛豫路径，以探究三条弛豫通道在不同硫代胸腺嘧啶激发态衰变动力学中的作用以及溶剂效应。结果如下：

(1)指认了研究体系在乙腈和水中的振动光谱、电子光谱和共振拉曼光谱。获取了两种物质的紫外吸收光谱、傅立叶拉曼光谱(FT-Raman)、傅立叶红外光谱(FT-IR)和共振拉曼光谱(resonance Raman)。采用密度泛函理论(DFT)计算了电子基态的分子结构和振动光谱，完成了实验振动光谱的指认。采用含时密度泛函理论(TD-DFT)计算了电子吸收带的跃迁性质及跃迁振子强度，指认了紫外光谱吸收带电子跃迁的归属。

(2)获取了 4-硫代胸腺嘧啶 S_2 态 Franck-Condon 区域结构动力学。采用含时波包理论单势能面模型对 4-硫代胸腺嘧啶在乙腈溶剂中 319.9 和 341.5 nm 激发波长的共振拉曼光谱进行定量拟合，通过 CASSCF 计算方法得到的 4-硫代胸腺嘧啶 S_2-min、S_2S_1、S_1T_2 等激发态以及交叉点结构的比较,得出的弛豫路径：$S_2 \rightarrow CI(S_2/S_1) \rightarrow S_1 \rightarrow CI(S_1/T_2) \rightarrow T_2 \rightarrow CI(T_2/T_1) \rightarrow T_1$。

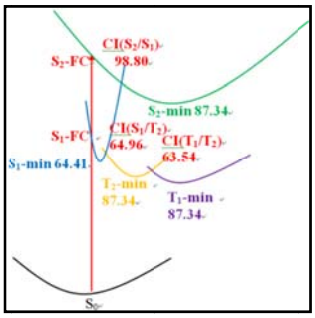

Fig. 2 The excited state decay channel of 4-thiothymine

关键词：4-硫代胸腺嘧啶；2-硫代胸苷；共振拉曼光谱； CASSCF；激发态衰变动力学

参考文献

[1] Jiang J, Zhang T, Xue J, et al. J. Chem. Phys. **2015**, **143(17)**: 1751.

[2] Cui.G, Fang.W, J. Chem. Phys. **2013**, **138**, 044315.

Temperature Effect on Upconversion Luminescence in the Lanthanide-doped Nanoparticles

Luoyuan Li[1], Limin Fu[1,*]

[1]Department of Chemistry, Renmin University of China, Zhongguancun Street No. 59, Beijing, 100872

The upconversion luminescence in rare-earth doped nanomaterials is a complicated process [1]. The luminescence performance is mainly determined by the competition among electron energy level distribution, multi-phonon nonradiative relaxation and radiative transition. There are a couple of factors affecting the three parts, such as temperature and doping concentration [2]. In this report, we devise a series of upconversion nanoparticles (UCNPs). The environment-temperature changing in the range of 77 K ~300 K of UCNPs was controlled by OptistatDN-V2 (Oxford Instruments). The steady-state luminescence spectra were measured by FLS 980 fluorescence spectroscopy and nanosecond time-resolved luminescence spectra under 974 nm pulsed laser by YAG laser (355 nm, 7 ns, 10 MHz) pumped optical parametric oscillator. The steady-state luminescence spectra showed different changes at different temperatures. And the nanosecond time-resolved fluorescence spectra were also conducted to demonstrate the different luminescence characteristics as varying the temperature. The results provide a fundamental understanding for the increasing of 655 nm UCL intensities resulted by the quenching of 542 nm emissions.

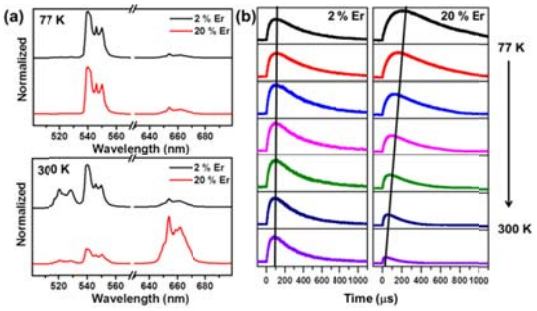

Fig. 1 (a) The steady-state luminescence spectra of the UCNPs with doping 2 % and 20 % Er^{3+} at 77K and 300K. (b) The nanosecond time-resolved luminescence spectra of the UCNPs with doping 2 % and 20 % Er^{3+} with the temperature in the range of 77 K ~ 300 K.

Keywords: upconversion luminescence; temperature effect; lanthanide-doped nanoparticles; four; five

References:

[1] Auzel, F. *Chem. Rev.* **2004, 104**: 139.

[2] Wei, W.; Chen, G. Y.; Baev, A.; He, G. S.; Shao, W.; Damasco, J.; Prasad, P. N. *J. Am. Chem. Soc.* **2016**, **138**: 15130

电子激发态嘧啶分子的飞秒振动波包动力学研究

李帅 [1,2]，龙金友 [1,2]，凌丰姿 [1,2]，张冰 [1,2*]

[1] 武汉物理与数学研究所，湖北省武汉市小洪山西 30 号，430071

[2] 中国科学院大学, 北京市，100049

*Email: bzhang@wipm.ac.cn

振动能在嘧啶S_1态上$6a_1$···$6b_2$费米共振对中的流动,通过飞秒时间分辨的质谱技术结合光电子影像方法被直接追踪。飞秒激光制备了由$6a_1$和$6b_2$两个费米共振组分组成的相干叠加态，导致生成了一个相干振动波包。这个相干振动波包的时间演化，通过叠加在母体离子产率线型中的量子拍频直接被可视化，拍频频率正好对应了两个本征态之间的能量差。从$6a_1$和 $6b_2$振动态电离得到的光电子峰的时间依赖线型都表现出明显的拍频特征，频率相同，但是相位相差180°，描绘出一幅非常清楚的能量在费米共振对中流动的物理图像。更重要的是，从实验上阐述了如何利用波包组分与离子振动态之间的可变的弗朗克康顿因子来过滤一个演化中的多维波包的不同组分。这样的一个实验，提供了一种跟踪激发态振动能流动的有效探测方法。

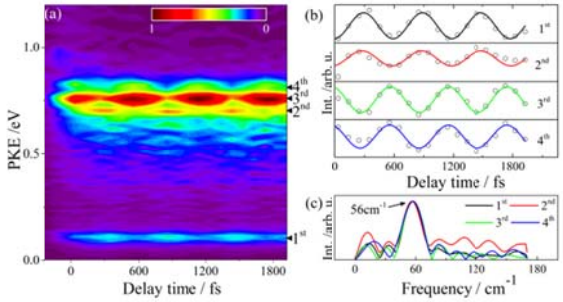

Fig. 1 (a) The time-resolved photoelectron spectra extracted from a series of images after excitation at 315.3 nm. (b) The time-dependent photoelectron intensities of the four peaks as a function of the delay time. The circles represent experimental data points and the colored lines represent sinusoidal fits of the data. (c) The FFT for the transients in Fig. 1b.

关键词：振动波包；光电子影像；量子拍频

CdSe/CdS 量子棒的核/壳结构的超快载流子动力学研究*

李爽[1]，吕荣[1]，于安池[1,*]

[1] 中国人民大学化学系，北京，100872

*Email：a.yu@chem.ruc.edu.cn

量子点作为一种新型发光材料，既可作为光催化剂、发光二级管，还可敏化太阳能电池，应用前景广阔，其光学特性也引起了广泛的关注。[1] 而核/壳异质结构的量子点具有较高的光致发光量子产率和电荷分离速率的优势，可进一步提高敏化太阳能电池的效率。[2] 本工作选取了 CdSe/CdS 核/壳量子棒作为研究对象，运用飞秒时间分辨吸收光谱、稳态吸收与荧光光谱技术对 CdSe/CdS 量子棒的核/壳异质结构间的相互作用进行了动力学机理研究。我们采用了不同的激发波长来探究（即 400 nm 可激发 CdSe 及 CdS，而 460 nm 只激发 CdSe）。经实验发现 CdSe/CdS 在 400 nm 激发波长下的瞬态吸收光谱比 460 nm 激发的更宽。为对其机理进一步探究，借助了苯醌（benzoquinone，BQ）及吡啶(pyridine，Py)在 550 nm 处探测，由瞬态吸收光谱及 CdSe 基态恢复动力学曲线发现 BQ 对 CdSe 的荧光有一定的猝灭作用，而 Py 却未发现此现象。其原因可能是当激发波长为 400 nm 时，尽管 CdSe 及 CdS 同时被激发，但由于 CdSe/CdS 核壳之间的相互作用很强，存在荧光共振能量转移过程，并且 CdSe 到 CdS 的电子转移速率快于 Py 与 CdS 之间的空穴捕获速率，所以并未看到 Py 对 CdSe/CdS 的荧光猝灭现象。

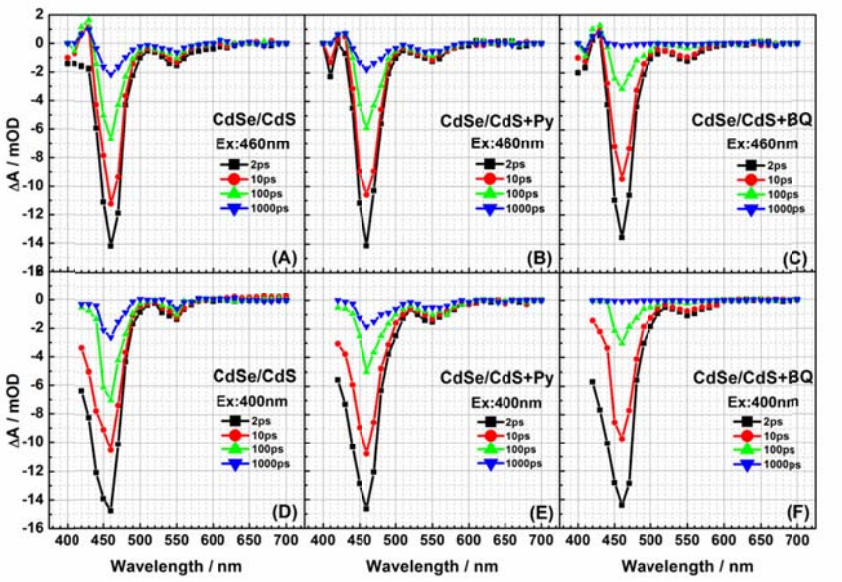

Fig.1 Femtosecond transient absorption spectra of CdSe/CdS in absence of any quencher(A) (D) , in the presence of hole quencher Py (B) (E), in the absence of electron quencher BQ (C) (F) in hexane at various time delays after 460 nm (top panel), 400 nm (bottom panel) laser excitation.

关键词：CdSe/CdS；BQ；Py；飞秒时间分辨吸收光谱；荧光猝灭

参考文献

[1] Alexey L. Kaledin,*,§Tianquan Lian, *,† Craig L. Hill, † and Djamaladdin G. Musaev*,§ J. Phy. Chem. B. **2015,**119, 7651-7658

[2] Partha Maity, Tushar Debnath, and Hirendra N.Ghosh* J. Phy. Chem. C. **2015,**119, 26202-26211.

Infrared Spectroscopic and Theoretical Study of the HC_nO^+ (n = 5-12) Cations

Wei li, Jiaye Jin, Guanjun Wang, Mingfei Zhou*
Department of Chemistry, Shanghai Key Laboratory of Molecular Catalysis and Innovative Materials, Fudan University, Shanghai, 200433, China

Carbon chains and derivatives are highly active species, which are widely existed as reactive intermediates in many chemical processes including atmospheric chemistry, hydrocarbon combustion, as well as interstellar chemistry. The carbon chain cations, HC_nO^+ (n = 5-12) are produced via pulsed laser vaporization of a graphite target in supersonic expansions containing carbon monoxide and hydrogen. The infrared spectra are measured via mass-selected infrared photodissociation spectroscopy of the CO "tagged" $[HC_nO{\cdot}CO]^+$ cation complexes in the 1600-3500 cm^{-1} region. The geometries and electronic ground states of these cation complexes are determined by their infrared spectra compared to the predications of theoretical calculations. All the HC_nO^+ (n = 5-12) core cations are characterized to be linear carbon chain derivatives terminated by hydrogen and oxygen. The HC_nO^+ cations with odd numbers of carbon atoms have closed-shell singlet ground states with polyyne-like structures, while those with even numbers of carbon atoms have triplet ground states with allene-like structures.

Keywords: Carbon chain cations, infrared photodissociation spectroscopy, theoretical calculations, polyyne-like carbon chain, allene-like carbon chain

References:

[1] Herrmann, H.; Ervens, B.; Wolke, H. W. R.; Nowacki, P.; Zellner, R. *J. Atmos. Chem.* **2000, 36 (3):** 231-284.
[2] Wang, G. J.; Chi, C. X.; Cui, J. M.; Xing, X. P. Zhou, M. F. *J. Phys. Chem. A*. **2012, 116:** 2484.
[3] Stanca-Kaposta, E. C.; Schwaneberg, F.; Fagiani, M. R.; Lalanne, M.; Wöste, L.; Asmis, K R. *ChemPhysChem*. **2016, 17:** 1.

Ultraviolet photodissociation dynamics of bromo-fluorobenzenes

Hao Liang, Chao He, Min Chen, Zhengfang Zhou, Yang Chen*, and Dongfeng Zhao*

Hefei National Laboratory for Physical Sciences at the Microscale, Department of Chemical Physics, University of Science and Technology of China, Hefei, Anhui 230026, PR China.

*Email: dzhao@ustc.edu.cn.

In the past few decades, because of the importance in atmospheric chemistry, experimental and theoretical studies on the photodissociation dynamics of organic halides have attracted great interest to physical chemists. Here, we present a detailed experimental study on the photodissociation dynamics of seven different fluorinated bromobenzenes at UV wavelengths corresponding to their first UV absorption band, aiming to validate our understanding in the dissociation mechanisms of lager aromatic molecules upon fluorine substitution effect. Recoiling velocity distributions of photofragmented Br($^2P_{3/2}$) and Br($^2P_{1/2}$) atoms have been measured using velocity map imaging technique combined with (2 + 1) resonance-enhanced multiphoton ionization (REMPI). It is found that the fragmented Br($^2P_{3/2}$) from 266 nm photodissociation of 1-Br-2,6-FPh and 1-Br-2,4,6-FPh shows a different behavior from other bromo-fluorobenzenes, which cannot be explained by the commonly known $S_0 \rightarrow S_1(^1\pi\pi^*) \rightarrow {}^1\pi\sigma^*$ predissociation mechanism. Accurate three-dimensional potential energy surfaces (PESs) of the low-lying electronic states of 1-Br-2,6-FPh, have been calculated. Based on the newly calculations, subtleties in addition to $S_0 \rightarrow S_1(^1\pi\pi^*) \rightarrow {}^1\pi\sigma^*$ mechanism, a charge-transfer state resulting from electron transfer from nonbonding electrons to the π^* orbitals of the phenyl ring, have been proposed to provide a renewed understanding of the present experimental results.

Keywords: velocity map imaging; fluorinated bromobenzenes; photodissociation dynamics

Photodissociation Dynamics of C_2H_5Br **Between 200 and 210 nm**

Hao Liang, Zhengfang Zhou, Yang Chen*, and Dongfeng Zhao*
Hefei National Laboratory for Physical Sciences at the Microscale, Department of Chemical Physics, University of Science and Technology of China, Hefei, Anhui 230026, PR China.
Email: lianhao@mail.ustc.edu.cn

The photodissociation dynamics of the ethyl bromide (C_2H_5Br) molecule in the 200-210 nm deep-UV wavelength range has been studied in a collision-free molecular beam. The Br*($^2P_{1/2}$) and Br($^2P_{3/2}$) fragments are ionized via (2+1) resonance-enhanced multiphoton ionization and then probed using time-sliced velocity map imaging to determine their recoiling velocity distributions. The present experimental results suggest that the Br* photofragments are produced as a result of direct dissociation via a repulsive potential energy surface (PES), and the low anisotropy parameter β of Br reveals the existence of a dissociation barrier on the PES. Previously reported PESs by high level ab initio calculations have provided a theoretical support in understanding the deep-UV photochemistry of C_2H_5Br.

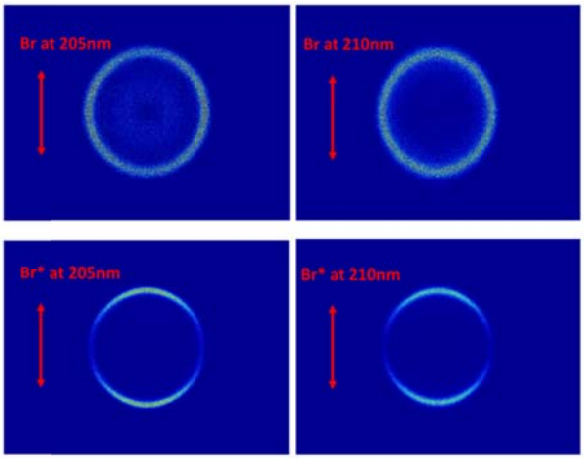

Figure 1. Ion-velocity images of Br fragments from the photodissociation of C_2H_5Br at a) 205nm,b) 210nm,and of Br* fragments at c) 205nm,d) 210nm. In all images the linear polarization vector of the UV laser is vertical.

Key words: ethyl bromide (C_2H_5Br), photodissociation dynamics, velocity map imaging, deep ultraviolet

CF_3I Photodissociation at 238 nm: Vibrational Distribution of CF_3 Fragments and Dynamics of Curve Crossing

Dan Lin[1,2], Min Cheng [1,*], Yikui Du[1], Qihe Zhu[1]

[1]Beijing National Laboratory of Molecular Sciences, State Key Laboratory of Molecular Reaction Dynamics, Institute of Chemistry, Chinese Academy of Sciences, Beijing 100190, China
[2]University of Chinese Academy of Sciences, Beijing 100049, China
*Email: chengmin@iccas.ac.cn

The photodissociation dynamics of CF_3I at 238 nm has been studied using our high resolution mini-TOF photofragment translational spectrometer. There are four pathways involved in the photodissociation process. Only in the pathway for the I* channel from the $^3Q_0$ parallel transition (i.e. I* ← $^3Q_0$ ← X), the signals are strong and the vibrational states of CF_3 fragments have been partially resolved in the photodissociation translational spectra. From the peak gap in the spectrum, both overtone bands (v_1, v_2 = 0) and combination bands (v_1, v_2 = 1) of CF_3 fragments are partially resolved, with $\sum P(v_1, 1)/\sum P(v_1, 0)$ = 0.48/0.52. Based on the theoretical calculations of Clary[1] and of Bowman[2] *et al.*, now we assign 701 cm^{-1} to the CF_3 symmetric stretch (breathing) v_1 mode, and 1086 cm^{-1} to the umbrella v_2 mode of the CF_3 fragment. The branching fractions of the four pathways are 0.664 for I*← $^3Q_0$ ← X, 0.084 for I ← $^1Q_1$ ← $^3Q_0$ ← X, 0.178 for I ← $^1Q_1$ ← X, and 0.074 for I* ← $^3Q_0$ ← $^1Q_1$ ← X. The back-jump of the curve crossing (c.c.) molecules is possible. It causes the experimental curve crossing fraction being lower than the Landau-Zener curve crossing probability. The experimental curve crossing fraction (F_{cc}) for $^1Q_1$ ← $^3Q_0$ is 0.11 and for $^3Q_0$ ← $^1Q_1$ is 0.29.

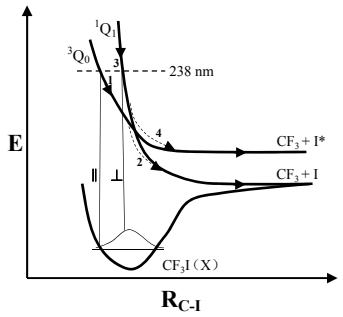

Fig. 1 Four pathways of CF_3I photodissociation near the blue edge of the A band. 1: direct dissociation from $^3Q_0$ ← X to I*, 2: dissociation from curve crossing $^1Q_1$ ← $^3Q_0$ ← X to I, 3: direct dissociation from $^1Q_1$ ← X to I, 4: dissociation from curve crossing $^3Q_0$ ← $^1Q_1$ ← X to I*.

Keywords: Photodissociation; Trifluoromethyl iodide; Vibrational energy excitation; Curve crossing fraction

References:

[1] Clary, D. C. *J. Chem. Phys.* **1986**, **84**, 4288-4298.
[2] Bowman, J. M.; Huang, X. C.; Harding, L. B.; Carter, S. *Mol. Phys.* **2006**, **104**, 33-45.

光激发的 2,4-二氟苯酚在不同构型间的相干核运动的直接观测

凌丰姿 [1,2]，李帅 [1,2]，宋辛黎 [1,2]，张冰 [1,2]

[1] 武汉物理与数学研究所，湖北省武汉市小洪山西 30 号，430071

[2] 中国科学院大学, 北京市，100049

*Email: bzhang@wipm.ac.cn

光激发的2,4-二氟苯酚的相干振动波包的演化过程及其所导致的能量流动通过时间分辨的离子产率光谱和光电子影像技术被直接观测。利用电离时构型发生改变的优势，通过选择合适的探测波长，使得只有在平面构型附近的波包才被电离，导致在母体离子线型中叠加了明显的量子拍频信号。更重要的是，从平面构型以及从非平面构型电离的信号在光电子谱中同时被采集，但是通过与不同的中间里德堡态发生偶然共振而在电子谱中进行区分。从平面构型以及从非平面构型电离得到的光电子峰的时间依赖线型，都表现出明显的拍频特征，频率相同，但是相位相差180°，描绘出一幅非常清楚的相干振动波包在不同构型间来回振荡的物理图像。

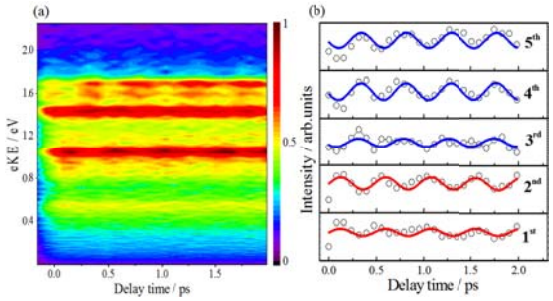

Fig. 1. (a) Photoelectron spectra of 2,4-difluorophenol as **a** function of delay time between pump laser at 280.4 nm and probe laser at 400 nm. (b) Time-resolved photoelectron intensities integrated over the five peaks as a function of delay time.

关键词：2,4-二氟苯酚，量子拍频，构型

参考文献

[1] Feng, L.; Shuai, L.; Xin, S.; Ying, T.; Yan, W.; Bing, Z. *Phys. Rev. A* **2017**, 95: 043421.

丙烯酸乙酯的真空紫外光电离解析

宋艳林,李淹博,张航,余业鹏,李照辉,刘付轶*,单晓斌,盛六四

中国科学技术大学国家同步辐射实验室，安徽省合肥市合作化南路 42 号，230029

*Email:fyliu@ustc.edu.cn

丙烯酸乙酯(Ethyl Aciylate)是聚合物和共聚物中的重要单体，它也是许多商品的重要组成成分，被广泛用作涂装过程中的保护液体等。由于它的高饱和蒸气压和挥发性，EA 主要以气相的形式存在于生产和应用的过程之中。在大气中，丙烯酸乙酯和其他挥发性有机化合物(VOCs)—样，可以与 OH 自由基，NO_3 自由基，卤素原子和臭氧分子反应，这有助于二次有机气溶胶(SOA)的形成。此外，丙烯酸乙酯与臭氧的反应可以生成 Criegee 中间体，例如 CH2OO[1]，它是对流层化学中一个重要的双自由基，极有可能改变以前我们对大气中臭氧清除通道的认识。

在这项工作中，我们利用光电离质谱技术(PIMS)，在 9.0-20.0 eV 的真空紫外光范围内，开展了对 EA 进行光电离解离的研究。根据理论和实验的结果对其解离机制也进行了研究，我们对于主要的光电离产物提出了九个可能的解离通道,分别是:R1: $C_3H_3O^+ + C_2H_5O$, R2: $C_2H_5^+ + C_3H_3O_2$, R3:$C_2H_5O^+ + C_3H_3O$, R4: $C_5H_7O_2^+ + H$, R5: $C_4H_5O_2^+ + CH_3$, R6: $C_3H_5O_2^+ + C_2H_3$, R7:$C_3H_4O^+ + C_2H_4O$, R8: $C_2H_3O^+ + C_3H_5O$, R9: $C_2H_4^+ + C_3H_4O_2$。值得一提的是,我们理论计算的结果基本上与试验值是相符合的。与此同时,我们也给出了产物,中间体,过渡态以及共生产物在 G3B3 下的几何结构,这也将有助于我们理解丙烯酸乙酯的光电离解离过程。这项工作的结果有助于更好地了解大环境下的丙烯酸乙酯的光电离解离过程，为以后的相关研究奠定了一定的基础。

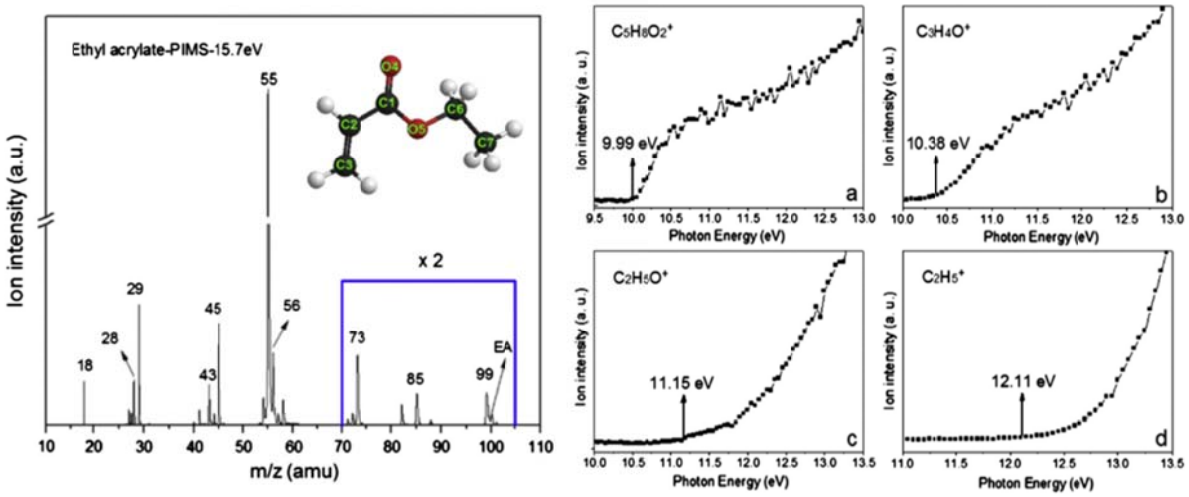

Fig. 1. Photoionization mass spectrum of EA at the photon energy of 15.7 eV (left), and the PIE curves (right) of parent ion $C_5H_8O_2^+$, themain fragments $C_3H_4O^+$, $C_2H_5O^+$ and $C_2H_5^+$.

关键词：同步辐射；光电离质谱；量子化学；丙烯酸乙酯

参考文献

[1] T.L. Nguyen, J. Peeters, L. Vereecken, Phys. Chem. Chem. Phys. 11 (2009) 5643.

基于时间分辨光电离质谱研究 CH_3 与 O_2 的反应动力学

王明,费维飞,李照辉,余业鹏,林烜,单晓斌,刘付轶*,盛六四

中国科学技术大学国家同步辐射实验室，合肥 230029

Email: fyliu@ustc.edu.cn

CH_3 自由基与 O_2 的反应是大气中烷烃氧化和燃烧的重要过程，实验和理论研究该反应动力学具有重要意义。利用 193 nm 激光光解反应流动管中丙酮, 产生 CH_3 自由基；利用同步辐射光电离和自制的多通道时间分辨质谱，获得 CH_3 自由基与 O_2 的反应产物及其时间分辨特性。实验获得反应产物 m/z 为 30、47、48 的光电离效率谱（9.7-12.0 eV），其电离能分别为 11.68 ± 0.10 eV、10.32 ± 0.15 eV、9.95 ± 0.10 eV。结合量化计算，确定产物依次为 C_2H_6、CH_3OO 和 CH_3OOH，其反应通道分别对应于 CH_3 的自反应、CH_3 与 O_2 的反应和 CH_3OO 的夺 H 反应。时间分辨光电离质谱获得了 CH_3 和 CH_3OO 的信号强度随时间变化的特性；通过改变 O_2 浓度，获得常温常压下 CH_3 和 CH_3OO 的准一级衰减速率常数。由此推导出 $CH_3 + O_2$ 反应速率常数为 $(2.3\pm0.3) \times10^{-13}$ cm^3 $molecule^{-1}$ s^{-1}，与 Hochanade 等人[1]的实验结果一致。这是用质谱的方法直接测量 CH_3 与 O_2 的反应速率常数，并首次探测到 CH_3OOH 产物。本实验室建立的同步辐射光电离-时间分辨质谱的自由基反应系统，可开展较大较复杂的自由基反应体系。

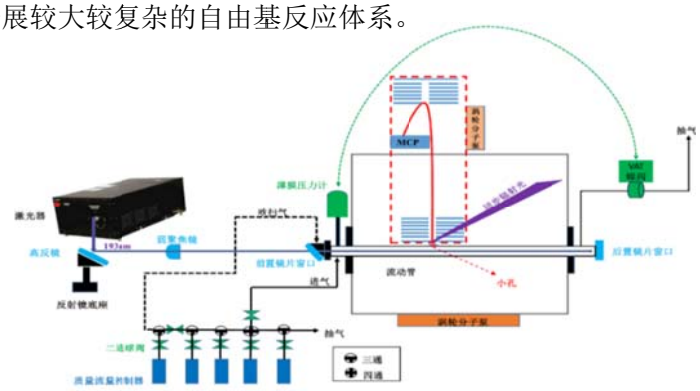

图 1 同步辐射光电离-时间分辨质谱的自由基反应系统

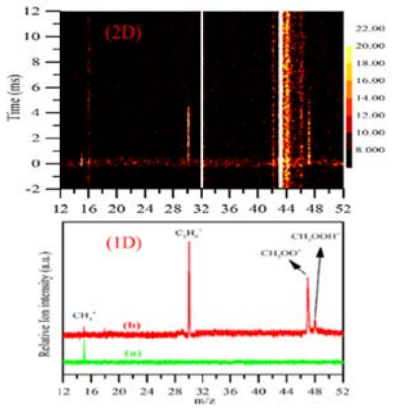

图 2 CH_3+O_2 反应的时间分辨 PIMS 谱

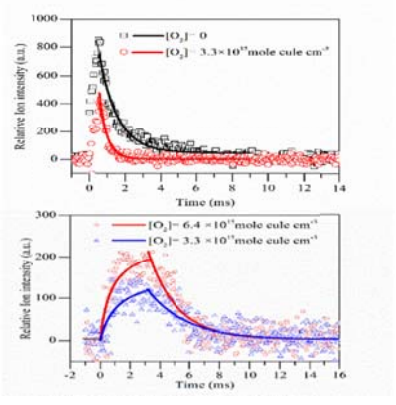

图 3 CH_3, CH_3OO 的时间分辨质谱

关键词：同步辐射光电离质谱,自由基反应,CH_3OOH,CH_3,CH_3OO

参考文献

[1] Hochanadel C J, Ghormley J A, Boyle J W, et al. Absorption Spectrum and Rates of Formation and Decay of the CH_3O_2 Radical [J]. Journal of Physical Chemistry, 1977, 81(5):3−7.

Three-dimensional Photodissociation Dynamics of Thiophenol

Guang-shuang-mu Lin[1], Daiqian Xie[1,*]

[1] Institute of Theoretical and Computational Chemistry, School of Chemistry and Chemical Engineering, Nanjing University, Nanjing 210093, China
*Email: dqxie@nju.edu.cn

Aromatic molecules with dissociative X-H (X=N, O, S, etc) stretch coordinate always hold a conical intersection between the repulsive electronic excited state and ground state along the X-H vibrational mode. Two radical products are generated with distinct alignment of intramolecular orbital through hydrogen atom elimination. Thiophenol and substituted thiophenol are paradigms to investigate the dynamics of non-radiative transition of electronic excited molecules. We constructed a three-dimensional diabatic potential energy surface including the S-H stretch, C-S-H bending and C-C-S-H torsional modes. Quantum wavepacket dynamics were performed with the method of second-order split operator. Both the absorption cross section of state and evolution of diabatic electronic population for the three states as function of time gave a short lifetime of the first excited state, which makes a qualitative agreement with the previous experiment measurement. The branching ratios of thiophenoxyl products were obtained by flux analysis at the S-H bond length of 10a.u. after 50000a.u. time's propagation. More excited product was achieved without any vibrational coordinates excited in the initial wavepacket. This result was consistent with the up-to-date experiment. Two obvious peaks appears in the X/A branching ratios as function of excitation energies above state. The wavefuntion calculated in the specific energy shows a resonance state structure. It is possible to control the product branching ratios and the corresponding structure-based stereo reactions by choosing a specific excitation energy.

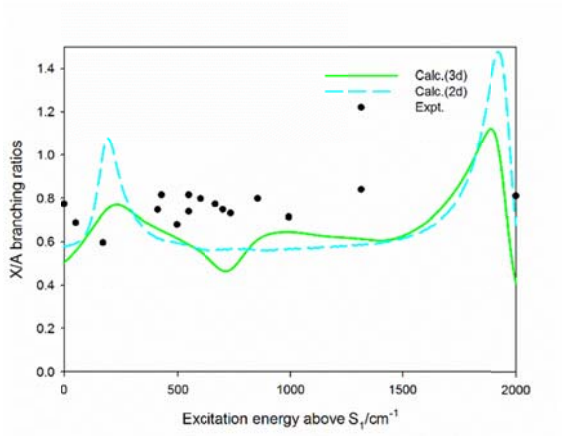

Fig. 1 Calculated X/A branching ratios as function of excitation energies compared with the experiment results.

Keywords: wavepacket dynamics; resonance states; diabatic; short lifetime

References:

[1] You, H.; Han, S.; Lim, J.; Kim, S. *J. Phys. Chem. Lett.* **2015**, **6**: 3202.
[2] Koppel, H.; Gronki, J.; Mahapatra, S. *J. Chem. Phys.* **2001**, **115**: 2377.

O ($^3P_{0,1,2}$, $^1D_2$) yield ratio measurement in VUV photodissociation of O_2

Kai Liu[1,2], Yih Chung Chang[1], Konstantinos S. Kalogerakis[3], Tom G. Slanger[3], Bing Zhang[2], William M. Jackson[1,*], and Cheuk Yiu Ng[1,*]

[1] Department of Chemistry, University of California, Davis, CA 95616, USA
[2] State Key Laboratory of Magnetic Resonance and Atomic and Molecular Physics, Wuhan Institute of Physics and Mathematics, Chinese Academy of Sciences, Wuhan 430071, China
[3] Physical Sciences Division, SRI International, Menlo Park, CA 94025, USA

The quantum yield of a VUV-induced photodissociation is defined as the ratio of the number of dissociative fragment created to the number of photons absorbed. Neutral photodissociation cross sections often remain significant for several electron volts above the ionization threshold and may be composed of contributions from both direct and indirect processes.

We developed a method to measure the yield ratios of O atoms in different spin-orbital state, using VUV-VUV pump-probe lasers and the time-sliced velocity-map-imaging photoion (VMI-PI) method. Combining the quantum dissociation cross section data[1], we calculated the quantum yield for O $^3P_0$, $^3P_1$, $^3P_2$, $^1D_2$ and $^1S_0$ in VUV photodissociation of O_2 ($H^3\Pi_u$, v'=2) is 0.24(2), 0.31(2), 0.26(2), 0.38(2), 0, respectively.

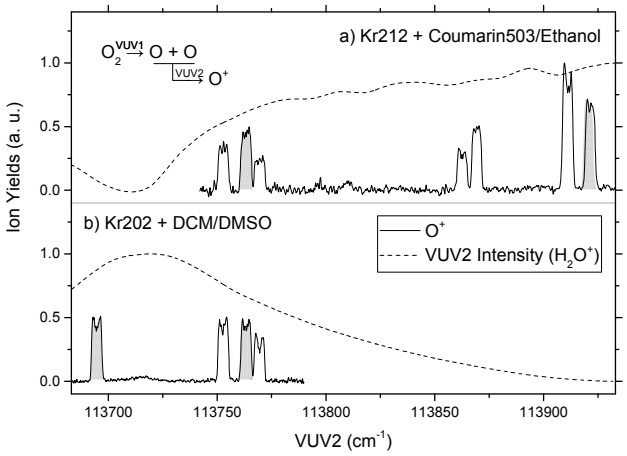

Fig. 1 The O atom PHOPEX spectrum observed by VUV2 excitations. Each O^+ curve (solid line) was the accumulation of four different measurements. O^+ ion signals are corrected by the VUV intensity curve (dash line). The structure of each peak is due to Doppler scan effect.

Keywords: superexcited oxygen; quantum yield; VUV; photodissociation

References:

[1] D. M. P. Holland, D. A. Shaw, S. M. Mcsweeney, M. A. Macdonald, A. Hopkirk and M. A. Hayes, *Chem Phys* .1993,173:315

Observation of Internal Photoinduced Electron and Hole Separation in Hybrid 2-Dimentional Perovskite Films

Junxue Liu[1, 2], Jing Leng [1], Jun Zhang[2], Shengye Jin[1*]

[1]State Key Laboratory of Molecular Reaction Dynamics, Dalian Institute of Chemical Physics, Chinese Academy of Sciences, 457 Zhongshan Rd., Dalian, 116023

[2]State Key Laboratory of Heavy Oil Processing, College of Chemical Engineering, China University of Petroleum, 66 Changjiang West Rd., Huangdao District, Qingdao, 266580

*Email: sjin@dicp.ac.cn

Two-dimensional (2D) organolead halide perovskites have recently emerged as an attractive material for applications in photovoltaics and other optoelectronic devices. The structural formula of the 2D perovskite is generally given as $(A)_2(CH_3NH_3)_{n-1}M_nX_{3n+1}$, where A is a large aliphatic or aromatic alkylammonium cation working as an insulating layer, M is the metal cation, and X is the halide anion. Recent reports have demonstrated that the 2D multi-layered perovskite films actually comprised multiple perovskite phases (with various *n* values from 1, 2, 3 and 4 to near ∞), even though the films were intended to be prepared as a single-phase. This hybrid feature seems to be ineluctable in fabricating 2D films. However, two important questions remain yet-to-be-answered: first, how the different perovskite phases align in the hybrid films; second, whether the band alignment between different phases induces energy funneling or instead charge separation. The latter is especially important because it dictates the application of these hybrid 2D perovskite films: energy funneling is useful for light-emitting applications, whereas charge separation would be more beneficial for light conversion or detection.

Here we report a unique spontaneous charge (electron/hole) separation property in multi-layered 2D perovskite films by studying the charge carrier dynamics using ultrafast transient absorption and photoluminescence spectroscopy. We find that indeed multiple perovskite phases with various *n* values co-existed in the 2D perovskite films, and more interestingly, these perovskite phases were naturally aligned in the order of *n* along the growth direction perpendicular to the substrate. Driven by the built-in band alignment between different perovskite phases, consecutive internal electron transfer from small-*n* to large-*n* perovskite phases and hole transfer in the opposite direction were observed in a film of ~358 nm thickness. This unique self-charge-separation property of the 2D perovskite films can facilitate their applications in photovoltaics and other optoelectronics devices.

Keywords: perovskites; quantum confinement; 2D materials; solar cell; charge separation

References:

[1] Tsai, H. H.; Nie, W. Y.; Blancon, J. C.; Toumpos, C. C. S.; *et al.* Nature **2016, 536**: 312.

[2] Dou, L. T.; Wong, A. B.; Yu, Y.; Lai, M. L.; *et al. Science* **2015**, **349**: 1518.

[3] Yuan, M.; Quan, L. N.; Comin, R.; Walters, G.; *et al.* Nat. Nanotech. **2016, 11**: 872.

[4] Wang, N.; Cheng, L.; Ge, R.; Zhang, S.; Miao, Y.; *et al.* Nat. Photonics **2016, 10**: 699.

[5] Liu, J., Leng, J., Wu, K., Zhang, J., Jin, S., *J. Am. Chem. Soc.*, **2017**, **139**: 1432.

飞秒时间尺度研究挥发性有机物的光化学动力学

刘玉柱[1,*]，尹文怡[1]，Thomas Gerber[2]，Gregor Knopp[2]

[1] 南京信息工程大学物理与光电工程学院，南京，210044

[2] Paul Scherrer Institute，Villigen (Switzerland)，5232

* Email: yuzhu.liu@gmail.com

大气污染物，尤其是有机挥发污染物VOCs (Volatile Organic Compounds)，在太阳光辐射下发生光物理光化学反应，对大气环境有严重破坏作用。借助于飞秒激光泵浦-探测技术和光电子成像探测技术，可以在飞秒时间尺度和分子空间尺度追踪VOCs分子在吸收光子后发生的微观光物理光化学反应过程，深入认识其动力学过程，对大气环境的进一步保护有着一定的参考意义。

本文介绍了我们在近年研究芳香烃、呋喃和氟利昂等VOCs体系的光物理和光化学动力学，描述了为该实验搭建的双极光电子/光离子速度成像实验平台，并介绍以下几个最新的实验研究成果：（1）呋喃、二甲基呋喃分子的激发态光化学动力学;（2）氟利昂分子的飞秒多光子电离和解离动力学；（3）乙苯、二甲苯、丙苯分子的超快光弛豫动力学。

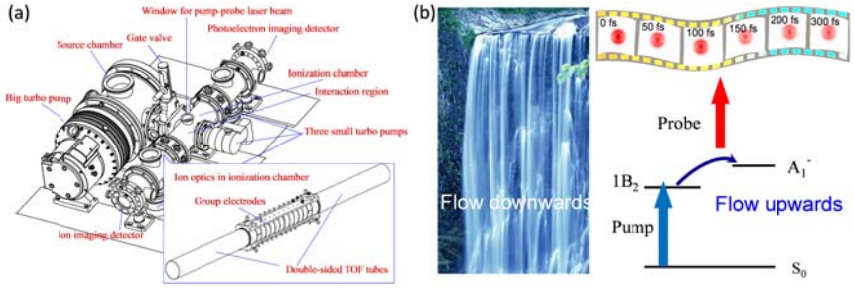

Fig. 1 (a) A home-built double sided photoelectron/ion imaging setup; (b) The up-conversion process observed in 2methy-furan system via femtosecond photoelectron imaging

关键词： 光化学；光电子成像；VOCs；飞秒泵浦-探测；光解离

参考文献

[1] Y. Liu*, T. Gerber, G. Zheng, S. Xiao, Q. Cheng, G. Knopp, *Journal of Molecular Spectroscopy* 331, 66, 2017.

[2] Y. Liu*, T. Gerber, C. Qin, F. Jin, G. Knopp, *Journal of Chemical Physics* 144, 084201, 2016.

[3] Y. Liu*, T. Gerber, P. Radi, G. Knopp, *Spectrochimica Acta Part A* 149, 54, 2015.

[4] Y. Liu*, G. Knopp, C. Qin, T. Gerber, *Chem. Phys.* 446, 142, 2015.

[5] Y. Liu*, G. Knopp, S. Xiao, T. Gerber, *Chin. Phys. Lett.* 31, 127802, 2014.

[6] Y. Liu*, G. Knopp, T. Gerber, *J. Mol. Stru.* 1076, 26, 2014.

[7] Y. Liu, T. Gerber, P. Radi, Y. Sych, G. Knopp*, *Chem. Phys. Lett.* 610-611, 153, 2014.

[8] Y. Liu*, T. Gerber, G. Knopp, *Acta Phys. Sin.* 63, 244208, 2014.

[9] Y. Liu*, T. Gerber, P. Radi, Y. Sych, G. Knopp, *Chem. Phys.* 442, 48, 2014.

[10] Y. Liu*, T. Gerber, P. Radi, Y. Sych, G. Knopp, *Opt. Express* 22, 9115, 2014.

[11] Y. Liu*, G. Knopp, P. Hemberger, Y. Sych, P. Radi, A. Bodi, T. Gerber, *Phys. Chem. Chem. Phys.* 15, 18101, 2013.

[12] Y. Liu*, T. Gerber, P. Radi, Y. Sych, G. Knopp, *Opt. Express* 21, 16639, 2013.

植物防晒霜分子的光动力学

罗健[1]，韩克利[1,*]

[1] 中国科学院大连化学物理研究所分子反应动力学国家重点实验室，辽宁省大连市中山路457号，116023

*Email: klhan@dicp.ac.cn

紫外线照射到生物体上会引起DNA损伤，相对于动物，植物所受的光照时间更长。为防止紫外线造成不良影响，十字花科植物表面均匀分布了一层苹果酸类似物（Sinapoyl Malate，SM），其为一种芥子酸（Sinapic Acid，SA）的脂衍生物，可有效将紫外线的能量耗散到环境中，从而防止紫外线的破坏作用。但是，在溶液环境中，SM抵抗紫外线损伤的机理尚不清楚。该研究团队利用飞秒瞬态吸收光谱技术和时间相关的密度泛函理论计算，发现在中性水溶液中，SM和SA都是去质子化的，它们吸收紫外线到达电子激发态后，会通过超快的光异构化方式内转换回到基态，有效地将紫外线的能量传递到环境中，避免了对遗传物质的伤害。但是，去质子化的SA发生光异构化后吸收紫外线的能力大大降低，而SM几乎没有变化，从而解释了自然选择SM作为防晒霜的原因。此外，该团队还发现处于质子化状态的SA能够在6个皮秒内通过反式-顺式光异构化的方式回到基态，生成的顺式产物也具有良好的吸收紫外线能力，为开发新型防晒霜指明了方向。

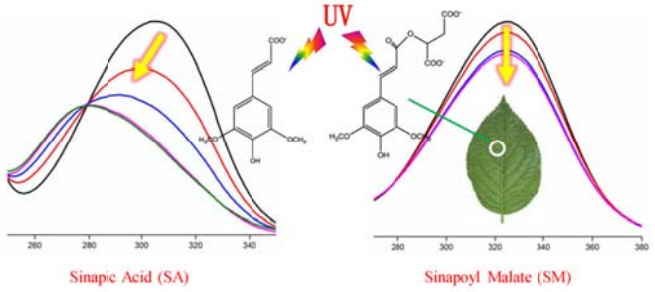

关键词： 飞秒；非辐射弛豫；光异构化

参考文献

[1] Luo, J.; Liu, Y.; Yang, S.; Flourat, A. L.; Allais, F.; Han, K. *J. Phys. Chem. Lett.*2017, *8*, 1025.

Energy level alignment and exciton dynamics at the $H_2O/g\text{-}C_3N_4$ interface for photocatalytic water splitting

Huizhong Ma, Yuchen Ma*

School of Chemistry and Chemical Engineering, Shandong University, Jinan 250100
*Email: myc@sdu.edu.cn

Graphitic carbon nitride ($g\text{-}C_3N_4$) has drawn increasing attention due to its hydrogen reduction capability under visible light. We investigate the energy level alignment at the $H_2O/g\text{-}C_3N_4$ interface within the many-body Green's function theory[1,2] and the decay of electron-hole pair by the time-dependent Schrödinger equation[3]. We find that the highest occupied molecular orbital of water molecule is much deeper in energy than that of $g\text{-}C_3N_4$, while the electronic level of OH^- appears at the top of the valence band of the whole system. This means that the photon-induced hole from $g\text{-}C_3N_4$ cannot migrate to the neutral H_2O but the OH^- instead. However, if taking into account the interaction between electron and hole, the hole cannot stay stably on the OH^- but be still mostly confined in $g\text{-}C_3N_4$ since the lowest excited state of the $H_2O/g\text{-}C_3N_4$ interface is with the hole delocalized on $g\text{-}C_3N_4$. This may explain why the quantum efficiency of $g\text{-}C_3N_4$ for hydrogen production is very low. There is also some probability for the electron in OH^- to be excited to the conduction band of $g\text{-}C_3N_4$ by ultraviolet light, leaving a neutral hydroxyl radical.

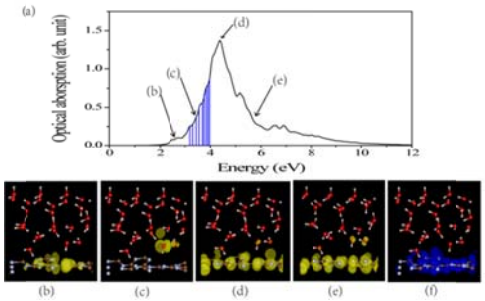

Fig. 1 Optical spectrum and electron-hole distributions of the $H_2O/g\text{-}C_3N_4$ interface.

Keywords: $H_2O/g\text{-}C_3N_4$ interface; many-body Green's function theory; exciton dynamics

References:

[1] Leng, X.; Jin,F.; Wei, M. and Ma, Y.C.; *WIREs Comput. Mol. Sci*, **2016**, **6**, 532
[2] Ma, Y. C.; Liu, C. B.; *Prog. Chem*., **2012**, **24**, 981
[3] Wang, N. P; Rohlfing, M; *Phys. Rev. B*, **2005**, **71(4)**: 045407

Competition between "*Meta* Effect" Photochemical Reactions of Selected Benzophenone Compounds Having Two Different Substituents at Meta Positions

马佳妮,*† 张喜庭,‡李明德,‡ **David Lee Phillips**[*,‡]
†西北大学　化学与材料科学学院
‡香港大学　化学系

Recent studies conducted on some "*meta* effect" photochemical reactions focused on aromatic carbonyls having a substitution on one *meta* position of the benzophenone (BP) and anthraquinone parent compound. In this paper, two different substitutions were introduced with one at each *meta* position of the BP parent compound to investigate possible competition between different types of meta effect photochemistry observed in acidic solutions containing water. The photochemical pathways of 3-hydroxymethyl-3'-fluorobenzophenone (**1**) and 3-fluoro-3'-methylbenzophenone (**2**) were explored in several solvents, including acidic water-containing solutions, using time-resolved spectroscopic experiments and density functional theory computations. It is observed that 1 can undergo a photoredox reaction and **2** can undergo a *meta*-methyl deprotonation reaction in acidic water-containing solutions. Comparison of these results to those previously reported for the analogous BP derivatives that contain only one substituent at a meta position indicates the introduction of electron-donating (such as hydroxyl) and electron-withdrawing groups (such as F) on the meta positions of BP can influence the meta effect photochemical reactions. It was found that involvement of an electron-donating moiety facilitates the *meta* effect photochemical reactions by stabilizing the crucial reactive biradical intermediate associated with the meta effect photochemical reactions.

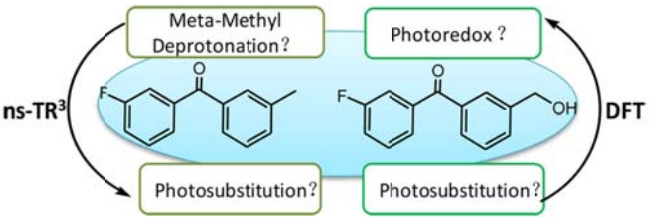

Investigation of the short-time photodissociation dynamics of Furfural in S2 state by Resonance Raman and quantum chemistry calculations

Kemei Pei *, Xuming Zheng

Engineering Research Center for Eco-Dyeing & Finishing of Textiles, Ministry of Education and Department of chemistry, Zhejiang Sci-Tech University, Hangzhou 310018, China

*Email:peikemei@zstu.edu.cn

Raman (Resonance Raman, FT-Raman), IR and UV-visible Spectroscopy and quantum chemistry calculations were used to investigate the photodissociation dynamics of furfural in S2 state. The RR spectra indicate that the photorelaxation dynamics for the S0→S2 excited state is predominantly along nine motions: C=O stretch ν_5 (1667 cm−1), Ring C=C antisymmetric stretch ν_6 (1570 cm−1), Ring C=C symmetric stretch ν_7 (1472 cm−1), C2-O6-C5 symmetric stretch/C1-H8 rock in plane ν_8 (1389 cm−1), C3-C4 stretch/ C1-H8 rock in plane ν_9 (1370 cm−1), C5-O6 stretch in plane ν_{12} (1154 cm−1), Ring breath ν_{13} (1077 cm−1), C3-C4 stretch ν_{14} (1020 cm−1), C3-C2-O6 symmetric stretch ν_{16} (928 cm−1). Stable structures of S0,S1 ,S2 ,T1 and T2 states with Cs point group were optimized at CASSCF method In Franck-Condon region there are S2/S1 conical intersection was found by state average method and RR spectra.

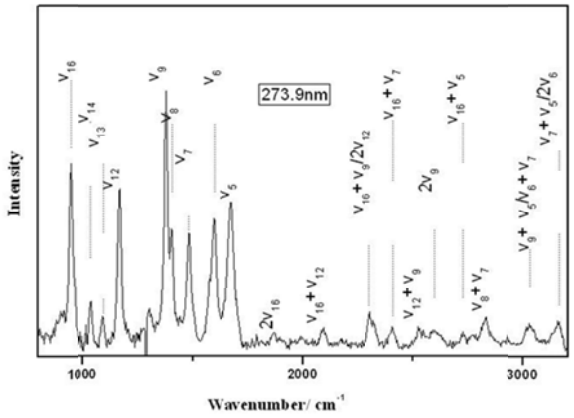

Fig. 1 Vibrational assignments of the resonance Raman spectra of furfural in water obtained with the 273.9 nm excitation wavelengths. The asterisks [*] mark solvent subtraction artifacts.

Keywords: Furfural; Resonance Raman; Quantum chemistry calculation; Excited state structural dynamics

References:

[1]Iliev,V. ; Mihaylova,A.; Bilyarska, L. J. Mol.Cataly. A: Chemical,**2002**,184: 121.

[2]A.Gorski,A.Starukhin,S.Stavrov,S.Gawinkowski,J.Waluk,Spectrochim.Acta A,**2017**,173:350.

环状亚硝酸烷基二酯的光解动力学研究

秦泰[1]，薛军非[2]，祖莉莉[1,*]

[1] 北京师范大学，北京，100875

*Email: zull@bnu.edu.cn

亚硝酸烷基二酯是大气中烷氧自由基和氮氧化物的主要光化学来源，同时也是碳氢化合物氧化反应过程的重要中间体[1]-[2]。此外，在生理pH或碱性范围内，亚硝酸烷基二酯也被作为一种亚硝酸化试剂以及神经缓释剂广泛使用[3]。研究亚硝酸烷基二酯的光解动力学对于监测大气中的化学过程以及防止污染改善环境具有重要意义，也可为医药科学提供理论基础。

本工作在超声射流条件下，研究了1,2-、1,3-、1,4-亚硝酸环已二酯在355nm激光光解时产物的激光诱导荧光（LIF）光谱，同时采用理论计算方法对三种二酯进行基态构象的优化，并且在此基础上，对其进行激发态计算、频率分析以及解离路径的计算。结合振动谱峰及理论计算结果，对谱峰进行标识和分析，尝试提出光触发环状亚硝酸烷基二酯的解离路径，为研究环状化合物在大气对流层中的化学过程提供依据。

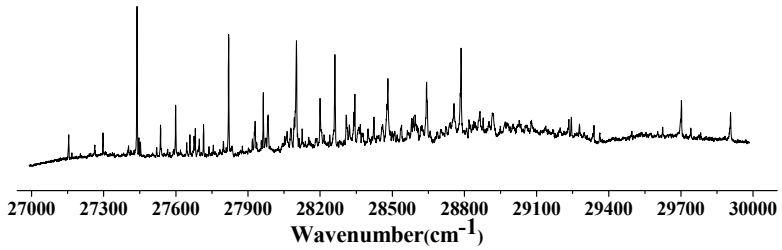

Fig. 1 LIF spectra obtained upon photolysis of 1,3-cyclohexyl dinitrite

关键词：激光诱导荧光；亚硝酸烷基二酯；光解动力学

参考文献

[1] Wang L, Zu L. Phys Chem Chem Phys. 2016; 18(36): 25249-25256.

[2] Wenge AM, Schmaunz A, Kensy U, Phys Chem Chem Phys. 2012; 14(19): 7076-7089.

[3] Cha HJ, Kim YJ, Jeon SY, et al. Neurosci Lett. 2016; 619: 79-85.

High-dimensional Quantum Dynamics Studies of Methane Dissociation on Ni Surfaces

Xiangjian Shen[1,2], Zhaojun Zhang[2,*], Donghui Zhang[2,*]

[1]School of Chemical Engineering and Energy, Zhengzhou University, Zhengzhou,450001

[2] State Key Laboratory of Molecular Reaction Dynamics and Center for Theoretical Computational Chemistry, Dalian Institute of Chemical Physics, Dalian, 116023

Email: zhangzhj@dicp.ac.cn; zhangdh@dicp.ac.cn

Gas-surface interaction is a very important branch in the field of surface chemical reaction dynamics. We present some quantum dynamics results about the role of molecular degrees of freedom(DOFs) of reagent CH_4 dissociation on Nickel surfaces from seven-dimensional to nine-dimensional quantum models. It is quantitatively found that, the DOF of stretching CH limitted in C3v symmetry weakly enhances the final sticking probability(S_0); the DOF of azimuth strongly weakens the final S_0; two lateral DOFs of surface impact sites largely decrease the final S_0; and the DOF of lattice thermal motion strongly increases the final S_0. These important roles of reaction coordinates clearly show the complex but interesting surface reaction dynamics features in polyatomic gas-surface reaction systems.

Keywords: high-dimensional quantum dynamics; degree of freedom; CH_4/Ni system;

References:

[1] Shen, X.J., Zhang, Zhaojun, Zhang, Dong H., *J. Chem. Phys.* **2017**,accepted

[2] Shen, X.J., Zhang, Zhaojun, Zhang, Dong H., *J. Chem. Phys.* **2016, 144**: 101101.

[3] Shen, X.J., Zhang, Zhaojun, Zhang, Dong H., *J. Phys. Chem. C.*, **2016, 120**: 20199.

[4] Shen, X.J., Chen, J., Zhang, Zhaojun, Shao, K. J., Zhang, Dong H., *J. Chem. Phys.* **2015, 143**:144701.

[5] Shen, X.J., Zhang, Zhaojun, Zhang, Dong H., *Phys. Chem. Chem. Phys.*, **2015, 17**: 25499.

[6] Shen, X. J., Lozano, A., Dong, W., Busnengo, H.F., Yan, X.H., *Phys. Rev. Lett.*, **2014, 112**: 046101.

5-碘代尿嘧啶（5-IU）的光解研究

代小娟[a]　宋 迪*,[a]　刘坤辉[b]　苏红梅*,[a,b]

[a]中国科学院化学研究所　北京分子科学国家实验室　北京 100190
[c]北京师范大学　化学学院　北京 100875

取代碱基分子由于其增强的光化学活性，吸引了分子生物学及药物学等相关领域的广泛关注。但以往的研究主要集中在硫代碱基，侧重于内转换、系间窜越等光物理过程的研究，而对另一类重要的卤代碱基分子的研究较少，主要是因为卤代碱基光激发后涉及复杂的光化学反应。本文利用时间分辨傅里叶变换红外吸收光谱（TR-FTIR）及CASPT2//CASSCF理论计算相结合的方法对5-碘代尿嘧啶（5-IU）的光化学反应机理进行了深入研究。在瞬态红外吸收光谱上观察到了266 nm激光照射5-IU 乙腈溶液的反应产物尿嘧啶U。由于乙腈溶剂是氢原子给体， U的生成是（U·）自由基从乙腈上抽氢产生的，由于溶液中并没有电子给体存在，这个抽氢的前体（U·）自由基只能来自于C-I键断裂，从而在实验上证实了5-IU发生了C-I键解离。理论上，利用CASPT2//CASSCF方法计算了单重态5-IU的解离势能曲线。计算结果揭示了一个单重态预解离机理：5-IU分子被初始激发到$^1(\pi\pi^*)$态，该态势能曲线与排斥态$^1(\pi\sigma^*)$或 $^1(n_I\sigma^*)$的势能曲线在Franck-Condon (FC)附近有交叉点，使得5-IU分子可以快速布居到这两个态上，无势垒解离生成基态（U·）自由基和碘原子。此外，我们还考察了5-IU发生系间窜越（ISC）布居到三重态上的可能性。$^1(\pi\pi^*)$ 态系间窜越到$^3(n_O\pi^*)$在能量及跃迁类型上是允许的，但是考虑到$^1(\pi\pi^*)$与两个排斥态的交叉点在FC区域，解离通常发生在几十到几百飞秒时间内，$^1(\pi\pi^*)$发生ISC的可能性很小。这些计算结果表明三重态对于5-IU光化学反应的贡献很少。我们的结果在量子态层次上揭示了5-IU的光化学反应机理，为5-IU作为光探针及辐射治疗癌症等应用提供了重要的理论基础。

2’-羟基查尔酮的激发态电荷转移与质子转移的超快过程研究

宋宏伟，郭前进，夏安东*

中国科学院化学研究所

*Email: andong@iccas.ac.cn

利用飞秒瞬态吸收技术结合理论计算的方法研究具有激发态质子转移和电荷转移特性的羟基查尔酮衍生物 4-dimethylamino-hydroxychalcone（DMAHC）和 4-dimethylamino-methoxychalcones（DMAMC）在不同溶剂中的激发态弛豫动力学。密度泛函（DFT/TDDFT）量化计算的结果表明 DMAHC 由于存在分子内氢键，其分子基态与激发态存在良好的平面共轭性；DMAMC 分子在弛豫过程中存在扭转态。同时，稳态和瞬态吸收光谱以及发光光谱结果发现，DMAHC 在极性和非极性溶剂中均不发光，而 DMAMC 发光产率随着极性的增加而增加。

DMAMC 的瞬态吸收证明，随着溶剂极性增加，DMAMC 分子局部的微粘度升高，限制分子转动等非辐射弛豫路径的发生，导致发光产率的升高。DMAHC 的瞬态吸收结果表明当体系存在质子转移和电荷转移耦合时，随着溶剂极性的增加质子转移的速率会迅速减小，因为体系存在溶剂化与质子转移的竞争过程，溶剂化稳定的 N 态发生质子转移需要翻越更大的势垒。

关键词：分子内氢键，溶剂化，激发态质子转移，激发态电荷转移

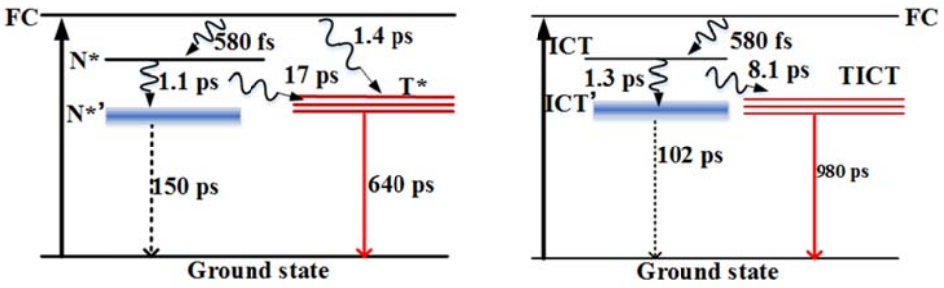

Fig. 1 The proposed relaxation pathways of DMAHC and DMAMC in THF.

参考文献

[1] Hu, J.; Zhu, H.; Li, Y.; Wang, X.; Ma, R.; Guo, Q.; Xia, A., *Physical Chemistry Chemical Physics* **2016,** *18* (28), 18750-18757.

[2] Cheng, X.; Wang, K.; Huang, S.; Zhang, H.; Zhang, H.; Wang, Y., *Angewandte Chemie International Edition* **2015,** *54* (29), 8369-8373.

Vibrational spectroscopy of the mass-selected tetrahydrofurfuryl alcohol monomers and its dimers in gas phase using IR depletion and VUV single photon ionization

Wentao Song, Yujian Li, Yongjun Hu*

MOE Key Laboratory of Laser Life Science & Institute of Laser Life Science, College of Biophotonics, South China Normal University, Guangzhou 510631, P. R. China
*Email: yjhu@scnu.edu.cn

Tetrahydrofurfuryl alcohol (THFA, $C_5H_{10}O_2$) is a close chemical analog of the sugar rings present in the phosphate-deoxyribose backbone structure of the nucleic acids. In present report, the infrared (IR) spectra of the size-selected THFA monomer and its dimer have been investigated in a pulsed supersonic jet using infrared-vacuumultraviolet (VUV) ionization. Herein, the laser light at 118 nmwavelength served as the source of "soft" ionization in a time-of-flight mass spectrometer. The IR features for the monomers located at 3622 cm^{-1} can be assigned to the intramolecular hydrogen bonding stretch vibrations mainly referring to A and C conformers. Compared with the monomer, however, characteristic peaks for the dimer centered at 3415 and 3453 cm^{-1}, red shifted 207 and 169 cm^{-1}, respectively, were associated with the intermolecular hydrogen bonding stretch vibrations. Combined with the quantum-chemical calculations, the dimer in the gas phase preferred cyclic AC conformer stabled by forming two strong intermolecular hydrogen bonds, which shown the high hydrogen bond selectivity in the cluster. The conclusions drawn from the role played in the conformational flexibility by the hydroxyl and ether groups may be extended to other biomolecules.

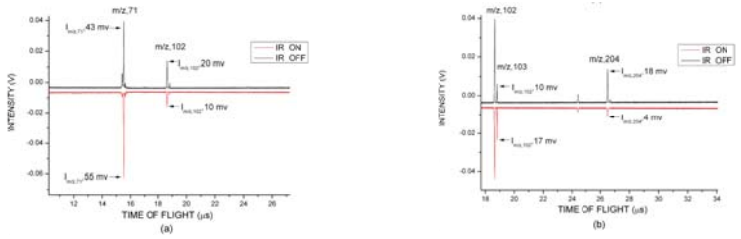

Fig. 1. (a) TOF mass spectrum showing intensity changes in THFA cation and its fragmentions under the 118 nm light with the IR light on/off at 3622 cm−1. (b) TOFmass spectrum showing intensity changes in THFA dimer and its fragment ions under the 118 nm light with the IR light on/off at 3453 cm−1. I represents the absolute value of the signal intensity.

Keywords: Tetrahydrofurfuryl alcohol; Tetrahydrofurfuryl alcohol's dimer; Gas-phase; IR spectroscopy; Hydrogen bonding

References:

[1] E.J. Bieske, J.P. Maier, Chem. Rev. 93 (**1993**) 2603.
[2] B. Brutschy, Chem. Rev. 100 (**2000**) 3891.
[3] M.S. de Vries, P. Hobza, Annu. Rev. Phys. Chem. 58 (**2007**) 585.

利用 TPE 瞬态吸收光谱研究类胡萝卜素单重态均裂反应

谭黎明 王鹏 于洁 周璇 张建平*

中国人民大学化学系 北京市海淀区中关村大街 59 号 100872

E-Mail: jpzhang@chem.ruc.edu.cn

紫色嗜热光合硫细菌 Thermochromatium (Tch.) tepidum，生长在 50℃的温泉中，光谱利用范围超过 900 nm，其热稳定性和近红外捕光特性引起人们广泛研究。近期研究中发现细菌天线蛋白中共轭程度较高的类胡萝卜素(如 spirilloxanthin, Spx, n=13)能够通过单重态均裂反应生成两个三重激发态，而且反应发生在<1 ps 的超快时间尺度上。光合细菌中的类胡萝卜素的共轭长度(n)一般为 9–13，最低单重激发态为 $S_1(2A_g^-)$ 的能级约为三重态 $T_1(B_u^+)$的两倍，即 $E_{S1}=2E_{T1}$ 。另外，就电子结构而言，两态之间符合 $S_1(2A_g^-) \leftrightarrow 2 \otimes T_1(B_u^+)$。因此 $S_1(2A_g^-)$态具备单重态均裂反应前驱物的条件。类胡萝卜素的基态 $S_0(1A_g^-)$ 和最低单重激发态 $S_1(2A_g^-)$之间是偶极跃迁禁戒的，也就是说 $S_1(2A_g^-)$态不能由单光子激发直接布居。但是，$S_1(2A_g^-)$态可以被双光子激发。由于双光子激发效率取决于光脉冲的峰值功率，我们采用飞秒激光脉冲激发类胡萝卜素。通过双光子激发飞秒时间分辨吸收光谱研究类胡萝卜素 $S_1(2A_g^-)$态的反应活性，甄别单重态均裂反应前驱物。

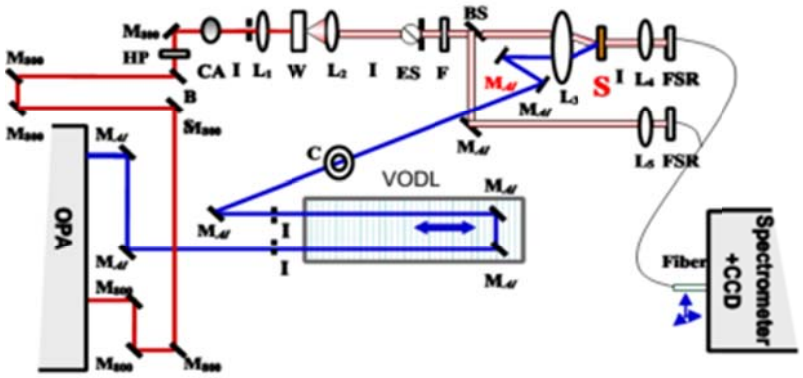

Fig.1 Schematic diagram of femtosecond time resolved absorption spectrometer

关键词 ： 双光子激发，单重态裂分，时间分辨光谱，类胡萝卜素

参考文献

[1] Gradinaru C C, Kennis J T M, Papagiannakis E, et al.Proc. Natl. Acad. Sci. USA., 2001, 98:2364

[2] Kimura Y, Kawakami T, Yu L J, et al. FEBS Lett, 2015, 589(15): 1761-1765

A study of species formation of aqueous amines using NMR spectroscopy

Lijing Leng, Anli Xu , Jian Wang*, Hongkun Zhao

College of Chemistry & Chemical Engineering, YangZhou University, YangZhou, Jiangsu 225002, People's Republic of China
*E-mail: wjhg@yzu.edu.cn

In this study, the CO_2 absorption characteristics of two tertiary amines were studied using ^{1}H nuclear magnetic resonance (NMR) and quantitative ^{13}C NMR. The equilibrium experiments were conducted in the vapor-liquid equilibrium (VLE) apparatus, which was used to measure the CO_2 absorption capacities of aqueous solutions of N-methyldiethanolamine (MDEA), N,N-dimethylethanolamine (DMEA). The CO_2 loaded amines were used for NMR measurement to determine the distribution of species formed in the carbonated amine solutions. This process confirmed the reaction mechanisms of the individual tertiary amines in relation to CO_2 absorption capacities.

Keywords: Carbon dioxide; tertiary amine; Speciation

References:

[1] Wolfram, B.; Michael, M.; Hans, H. *Fluid. Phase. Equilib.* **2008**, **263**: 131.

N-Methylcarbamoyl Azide: Spectroscopy, X-ray Structure and Decomposition via Methylcarbamoyl Nitrene

Huabin Wan[1], Manabu Abe[2,*], Didier Bégué[3] and Xiaoqing Zeng[1,*]

[1] College of Chemistry, Chemical Engineering and Materials Science, Soochow University, 215123 Suzhou, P. R. China.

[2] Department of Chemistry, Graduate School of Science, Hiroshima University, 1-3-1 Kagamiyama, Higashi-Hiroshima Hiroshima 739-8526, Japan

[3] Institut des Sciences Analytiques et de Physico-Chimie pour l'Environnement et les Matériaux (IPREM), Université de Pau et des Pays de l'Adour, Pau, France.

[1]*Email: xqzeng@suda.edu.cn

[2]*Email: mabe@hiroshima-u.ac.jp

N-Methylcarbamoyl azide Me(H)NC(O)N_3 has been synthesized and structurally characterized. Both N_3 and CH_3 groups in the molecule adopt *syn* conformation with the C=O bond. Upon flash vacuum pyrolysis at 800 K, the azide mainly decomposes into Me(H)NNCO/N_2 and MeNCO/HN_3 through Curtius-rearrangement and retro-ene reaction, respectively. In contrast, 193 and 266 nm laser photolysis of Me(H)NC(O)N_3 in cryogenic matrices (Ar, Ne, and N_2) leads to stepwise Curtius-rearrangement via the intermediacy of carbamoylnitrene Me(H)NC(O)N, for which two conformers with the CH_3 group being in *syn* and *anti* conformations to the C=O bond have been unambiguously identified by matrix-isolation IR spectroscopy. Triplet multiplicity of Me(H)NC(O)N ($|D/hc|$ = 1.57 cm^{-1} and $|E/hc|$ = 0.012 cm^{-1}) and another two carbamoylnitrenes H_2NC(O)N ($|D/hc|$ = 1.59 cm^{-1} and $|E/hc|$ = 0.018 cm^{-1}) and Me_2NC(O)N ($|D/hc|$ = 1.55 cm^{-1} and $|E/hc|$ = 0.016 cm^{-1}) has been further established with matrix-isolation EPR spectroscopy. Subsequent visible light irradiation (420–460 nm) of Me(H)NC(O)N results in the exclusive formation of Me(H)NNCO. The molecular structures of Me(H)NC(O)N_3 and Me(H)NC(O)N, multiplicities of the nitrene, and the underlying mechanism for the decomposition of the azide are reasonably explained with quantum chemical calculations by utilizing the B3LYP, CBS-QB3, CCSD(T), and CASPT2 methods.

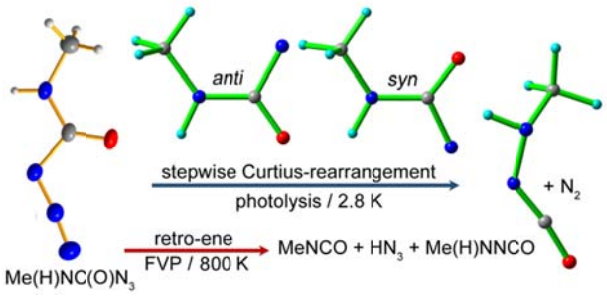

Keywords: azides • nitrenes • matrix-isolation • X-ray crystallography • photochemistry

References:

[1] Y. Park, Y. Kim, S. Chang, *Chem. Rev.* 2017, DOI: 10.1021/acs.chemrev.6b00644.

[2] X. Q. Zeng, E. Bernhardt, H. Beckers, K. Banert, M. Hagedorn, H. L. Liu, *Angew. Chem. Int. Ed.* 2013, *52*, 3503–3506.

XUV 泵浦-UV 探测方法研究 HD 的预解离动力学

汪杰[1]，韩媛媛[1]，莫宇翔[1,*]

[1]清华大学物理系，北京，100084

*Email: ymo@mail.tsinghua.edu.cn

氢分子的光解对于电子结构理论计算和光解动力学的研究具有重要意义。HD 分子在 14.72 eV[1]以上可以通过两个解离通道发生光解：HD+XUV→H(1*s*)+H(2*s*/2*p*)和 HD+XUV→D(1*s*)+D(2*s*/2*p*)。这两个通道的相互竞争为 HD 的光解带来了更加丰富的实验现象。就预解离而言，HD 涉及 $4p\pi D'^1\Pi_u$，$3p\pi D^1\Pi_u^{\pm}$ 和 $4p\sigma B''^1\Sigma_u^+$ 等多个能级，解离产物的角分布和分支比可以揭示这两个解离通道和三个电子态各自的特点。

利用 XUV 激光泵浦-UV 激光探测的方法，我们测量了 $4p\pi D'^1\Pi_u(\upsilon=1)$，$3p\pi D^1\Pi_u^{\pm}(\upsilon=4)$ 和 $4p\sigma B''^1\Sigma_u^+(\upsilon=2)$ 三个态解离产物 H 和 D 的产生效率谱，确认了 $3p\pi$ 和 $4p\sigma$ 态的 *P* 支和 *R* 支跃迁的 Fano 线型：$3p\pi$ 态的 *P* 支和 *R* 支 *q* 值符号相反，$4p\sigma$ 态的 *P* 支和 *R* 支 *q* 值符号相同。通过速度成像，可以看到 H 和 D 遵循同样的对称性，并且 $4p\pi D'^1\Pi_u$，$3p\pi D^1\Pi_u^+$ 和 $4p\sigma B''^1\Sigma_u^+$ 都主要通过 L-uncoupling 与 $3p\sigma B'^1\Sigma_u^+$ 发生相互作用。利用 2*s* 和 2*p* 的寿命差异，测量了各个跃迁产物的分支比 H(2*s*)/(H(2*s*)+H(2*p*))和 D(2*s*)/(D(2*s*)+D(2*p*))。分支比的测量结果表明，对于 $3p\pi D^1\Pi_u^+$ 和 $4p\sigma B''^1\Sigma_u^+$，D(2*s*)/(D(2*s*)+D(2*p*))略高于 H(2*s*)/(H(2*s*)+H(2*p*))；然而对于 $4p\pi D'^1\Pi_u$ 态，H(2*s*)/(H(2*s*)+H(2*p*))却远大于 D(2*s*)/(D(2*s*)+D(2*p*))，并且 $4p\pi D'^1\Pi_u$ 态的各个预解离跃迁都伴随着 HD 离子的产生，揭示了 $4p\pi D'^1\Pi_u$ 态解离的复杂性。

关键词：预解离；HD；Fano线型；角分布；分支比

参考文献

[1] Eyler E. E.; Melikechi N. *Phys. Rev. A*, **1993, 48(1)**: R18.

HD 直接解离产物的分支比震荡与量子干涉

汪杰[1]，莫宇翔[1,*]

[1]清华大学物理系，北京，100084

*Email: ymo@mail.tsinghua.edu.cn

氢分子的光解是电子结构理论计算和光解动力学理论的试金石。早在 1987 年，文献预测直接解离产物 H(2*s*)和 H(2*p*)的分支比在解离阈值附近随产物平动能的变化发生振荡[1]。对于 HD 分子， 由于有 H 和 D 两个解离产物，这两个产物的分支比及随平动能的变化关系，对于深入了解相关的动力学有更重要的意义，并对理论计算提供更多的检验标准。

实验采取了 XUV 激光泵浦-UV 激光探测的方法。XUV 光通过两束激光四波混频获得。用单光子电离方法探测解离产物 H(2*s*/2*p*)和 D(2*s*/2*p*)，并利用 2*s* 和 2*p* 寿命差异加以区分。我们测量了 HD 解离阈值以上 3300 cm^{-1} 内的解离产物分支比 H(2*s*)/(H(2*s*)+H(2*p*))和 D(2*s*)/(D(2*s*)+D(2*p*))，观察到了分支比的震荡现象。在靠近阈值的位置，H(2*s*)/(H(2*s*)+H(2*p*))和 D(2*s*)/(D(2*s*)+D(2*p*))呈现出不同的相位。实验结果可用散射模型解释。$2p\sigma B^1\Sigma_u^+$ 和 $3p\sigma B'^1\Sigma_u^+$ 两个势能面可简化成两个球形势阱，直接解离过程可以理解为波函数在这两个势阱上的散射，散射波函数的相互干涉造成了分支比的震荡。我们拟合了分支比震荡的实验曲线，获得了等效方势阱的宽度和深度参数，与从势能曲线转换而来的参数符合地很好。分支比的震荡直接呈现了解离通道的量子干涉效应，势阱散射模型则直观地展现了直接解离的物理过程，有助于加深人们对于光解过程的理解。

关键词：直接解离；HD；分支比；散射模型

参考文献

[1] Beswick J.A.; Glass-Maujean M. *Phys. Rev. A*. **1987, 35**: 3339.

宽带和频光谱技术对电子-声子相互作用的研究

王静静[1]，吴雪娇[2]，何玉韩[1]，郭伟[1]，张永燕[1]，刘晨西[1]，王朝晖[1,*]

[1] 固体表面物理化学国家重点实验室，谱学分析与仪器教育部重点实验室，厦门大学化学化工学院，福建厦门，361005

[2] 固体表面物理化学国家重点实验室，能源材料化学协同创新中心，厦门大学化学化工学院，福建厦门，361005

*Email: zhwang@xmu.edu.cn, zhwang2009@gmail.com

CdS是一种II-IV族半导体，室温下禁带宽度为2.42 eV，在光催化、印染、纺织、涂料、非线性光学等领域具有广泛应用。和频光谱技术是一种二阶非线性振动光谱技术，具有界面选择性[1]，已广泛用于材料、生物、电化学、催化等研究领域。本文使用宽带和频光谱技术（Broadband sum frequency generation, BB-SFG）[2]研究CdS气/固界面，测量了SFG谱峰强度随入射到样品表面的可见与红外脉冲相对延迟时间的变化，发现在负延时方向（可见脉冲先于红外脉冲到达样品表面）表现为双指数弛豫过程。当可见脉冲为Guass线型时，弛豫时间分别为0.29±0.11 ps和4.44±0.37 ps。长时间的弛豫时间对应于CdS样品的电子-声子散射时间。

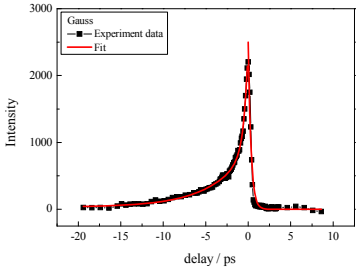

Fig. 1 Dephasing time

关键词： 宽带和频光谱；振动退相位；电子-声子散射

参考文献

[1] Zhu, X. D.; Suhr, H.; Shen, Y. R. Phys. Rev. B **1987, 35**, 3047.

[2] Wang, Z., Carter, J. A., Lagutchev, A., Koh, Y. K., Seong, N. H., Cahill, D. G., & Dlott, D. D. Science.**2007, 317(5839)**, 787-790.

The photoluminescence properties of 1,1,2,3,4,5-Hexaphenylsilole (HPS)

Lian Wang, Miaomiao Zhou, Song Zhang*, Bing Zhang*
Wuhan Institute of Physics and Mathematics Chinese Academy of Sciences, West No.30 Xiao Hong Shan,Wuhan, 430071

1,1,2,3,4,5-Hexaphenylsilole (HPS) is a typical molecular which exhibited aggregation-induced emission(AIE) behavior and used in sensors, cell imaging, highly efficient light emitters etc. The AIE property and decay dynamics of HPS in methanol, dimethyl sulfoxide and aniline are studied by time-resolved transient absorption spectrum and chemical calculations. Following the excitation at 400nm, the S_1 state is first populated in the Franck-Condon region. The rising trend of transient absorption spectra indicates that intramolecular torsional motions occurs on the S_1 potential energy surface with a time constant of tens of picoseconds. The kinetic traces of excited state absorption show that the S_1 state in the adiabatic region decays to the S_0 state through an internal conversion with a decay time of several picoseconds. It is found that the more viscous the solvent, the slower the intramolecular torsional motions. As a result, the relaxation of the excited states through the radiationless channel is effieciently blocked in aggragates, and the radiative depopulation becomes the dominant decay channel of the excited states. These results provided evidence that the AIE behavior is due to restricted intramolecular motion.

Experimental and Computational Assignment of FTIR Spectra of Dityrosine and Its Configuration

Wang Mohan[1], **Weng Yuxiang**[1,*]

Key Laboratory of Soft Matter Physics, Institute of Physics, Chinese Academy of Science, Beijing, 100190

Dityrosine bonds widely exist in natural tissues to maintain their properties such as elasticity, toughness, and energy storage capacity and so on. Therefore dityrosine cross-links are used to build biomaterials such as collagen, resilin, et al. [1]Fluorescence spectroscopy is commonly used as a nondestructive method to examine the existence of dityrosine, but quantitative analysis can not be easily achieved by fluorescence spectroscopy regarding to the overlapping of fluorescence of kynurenine. We achieved FTIR spectra of dityrosine in different pH condition and assigned its vibrational modes through DFT method. This facilitates both quantitative analysis of dityrosine and FTIR analysis of biomaterials contain dityrosine.

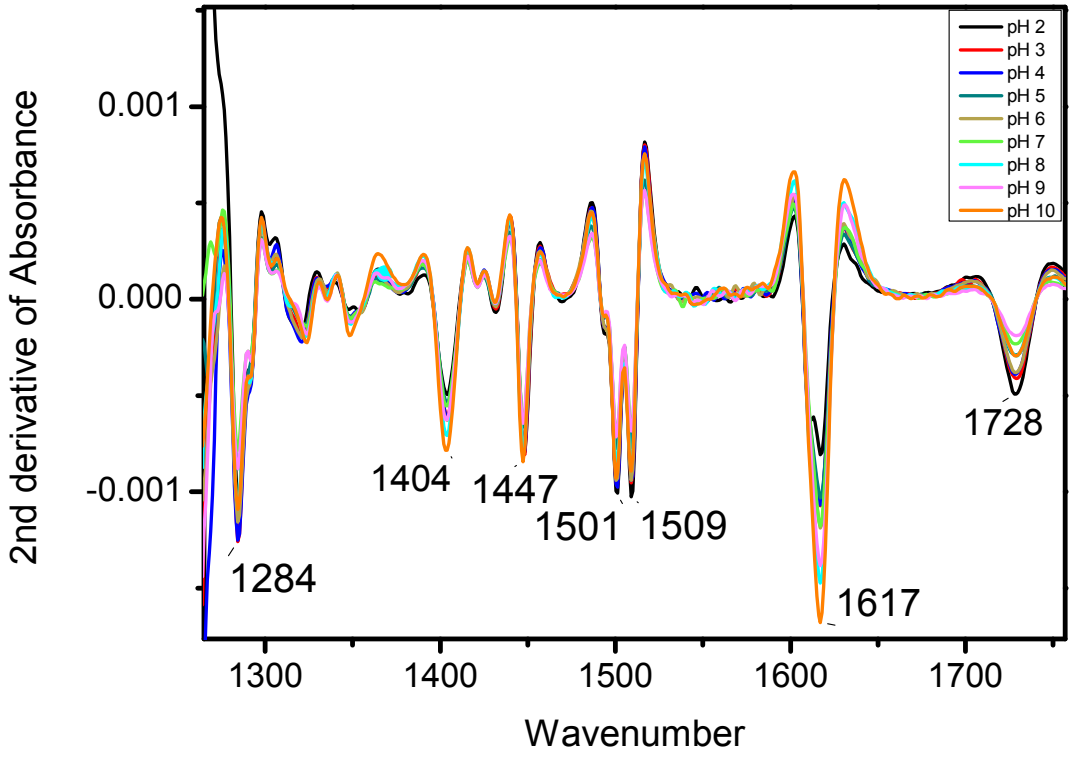

Fig. 1 FTIR Spectrum of Dityrosine in Different pH Conditions

Keywords: dityrosine; FTIR; DFT;cross-link

References:

[1] Benjamin P. Partlow; Matthew B. Applegate; Fiorenzo G. Omenetto; David L. Kaplan. *ACS Biomater. Sci. Eng.* **2016**, **2**: 2108.

非天然碱基对在 DNA 中光物理过程的理论研究

王倩，方维海,和崔刚龙*

北京师范大学化学学院，理论与计算光化学教育部重点实验室，北京市新街口外大街 19 号，100875

Email: qianwang@mail.bnu.edu.cn

非天然碱基是否像DNA和RNA中的碱基一样具有光稳定性是人们一直比较关心的科学问题。[1]最近，Marvin Pollum等人[2]从实验上对d5SICS和dNaM两个非天然碱基的光物理和光化学性质进行了系统的研究，发现两个分子在溶液和DNA中都具有非常高的三态量子产率，但是两者微观的激发态失活路径到目前仍然不清楚。[3]在本课题中，我们采用高精度的CASPT2//CASSCF结合量子力学/分子力学(QM/MM)的方法[4]系统地研究了d5SICS和dNaM在DNA环境中的光物理机理。通过计算，我们最终给出了几条可能的由激发单态到三态的无辐射弛豫通道，解释实验现象，给出了一些新的机理解释，为下阶段的实验研究提供了重要的理论参考。

关键词：碱基; d5SICS和dNaM ; 光物理反应机理;QM/MM

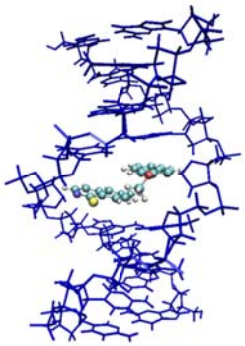

Fig.1 System are studied in this work.

参考文献

[1] J.J. Nogueira,;M. Oppel,;L. Gonzalez, ***Angew. Chem. Int. Ed.***, 2015,54,4375-4378.

[2] L. Li,; M. Degardin,; T. Lavergne, ;D.A. Malyshev, ;K. Dhami,; P. Ordoukhanian,; F.E. Romesberg, ***J. Am. Chem. Soc.***, 2014, 136, 826-829.

[3] X.P. Chang,; G. L. Cui,; W.-H. Fang,; W. Thiel, ***ChemPhysChem***, 2015, 16 ,933-937.

[4] X.P. Chang,; X.Y. Xie,; S.Y. Lin,; G. L. Cui, ***J. Phys. Chem. A***, 2016, 120,6129-6136.

作为电子给体材料的类寡聚噻吩小分子电荷分离效率的奇偶效应研究

王娴，郭前进，夏安东*

中国科学院化学研究所，北京市海淀区中关村北一街 2 号，100190

* Email: andong@iccas.ac.cn

太阳能电池器件的能量转换效率除了受到给受体材料的LUMO能级差的影响外，还与材料堆积尺寸和形貌相关。在自组装过程中，不同奇偶个数重复单元的分子的堆积形貌常见有物理化学性质的奇偶效应。本工作运用超快光谱和理论计算，详细探讨了噻吩链奇偶长度导致不同对称性的DRCN4T–DRCN8T系列小分子作为电子给体在有机太阳能电池中的光电转换过程。已报道DRCN5T与DRCN7T相较于同系列DRCN4T，DRCN6T和DRCN8T具备更高的能量转换效率（与$PC_{71}BM$共混，重量比1：0.8），且DFT量子计算得到基态奇数噻吩分子是轴对称结构，基态偶数噻吩分子是中心对称结构。将电子给体DRCN*n*T（*n*=4–8）和电子受体$PC_{71}BM$分子共混成膜，采用飞秒瞬态吸收光谱研究600 nm激发光照射下（选择激发电子给体分子）的激子（EX）弛豫动力学。研究发现激子在给体DRCN*n*T中瞬时激发产生，扩散至给受体的两相界面处，进一步在界面分离为空穴和电子，1ps内即产生电荷转移态（CT）和电荷分离态（CS）。通过全局拟合瞬态光谱得到电荷分离效率的奇偶更替特征。TDDFT进一步计算表明奇数分子的激发态与基态偶极矩差$\Delta\mu_{ge}$比偶数分子大。本工作实验和理论计算的结果证实了，分子基态和激发态偶极矩差别越大，则激子库伦束缚能越弱，将有利于激子分离和载流子的产生，同时激子分离产生的空穴和电子不容易复合，进而有利于得到高的能量转换效率。

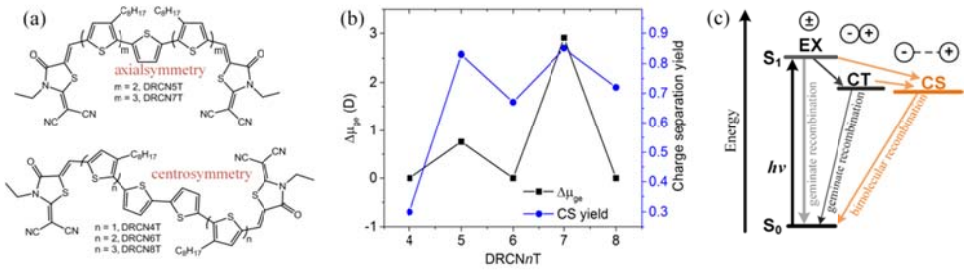

Fig. 1 (a) Molecular structures of DRCN*n*T (*n* = 4–8). (b) Odd–even trends of dipole moment change $\Delta\mu_{ge}$ and charge separation yield. (c) Proposed model of initially accessible electronic states in DRCN*n*T:$PC_{71}BM$ films.

关键词：类寡聚噻吩小分子；太阳能电池；奇偶效应；瞬态吸收光谱

参考文献

[1] Kan, B.; Li, M.; Zhang, Q.; Liu, F.; et al. *J. Am. Chem. Soc.* **2015**, **137**: 3886-3893.

[2] Zhang, Q.; Kan, B.; Liu, F.; Long, G.; et al. *Nature Photon.* **2014**, **9**: 35-41.

[3] Long, G.; Wu, B.; Solanki, A.; Yang, X.; et al. *Adv. Energy Mater.* **2016, 6**: 1600961.

[4] Wang, X.; He, G.; Li, Y.; Kuang, Z.; et al. *J. Phys. Chem. C*. 2017, 121: 7659-7666.

Photochromic Mechanism of a Bridged Diarylethene: Combined Electronic Structure Calculations and Nonadiabatic Dynamics Simulations

Ya-Ting Wang, Yuan-Jun Gao, Qian Wang, Ganglong Cui*

Key Laboratory of Theoretical and Computational Photochemistry, Ministry of Education, College of Chemistry, Beijing Normal University, Beijing 100875, China
Email: wangyating@mail.bnu.edu.cn

Intramolecularly bridged diarylethenes exhibit improved photocyclization quantum yields because the anti-syn isomerization that originally suppresses photocyclization in classical diarylethenes is blocked. Experimentally, three possible channels have been proposed to interpret experimental observation, but many details of photochromic mechanism remain ambiguous. In this work we have employed a series of electronic structure methods (OM2/MRCI, DFT, TDDFT, RI-CC2, DFT/MRCI, and CASPT2) to comprehensively study excited state properties, photocyclization, and photoreversion dynamics of 1,2-dicyano[2,2]metacyclophan-1-ene. On the basis of optimized stationary points and minimum-energy conical intersections, we have refined experimentally proposed photochromic mechanism. Only an S_1/S_0 minimum-energy conical intersection is located; thus, we can exclude the third channel experimentally proposed. In addition, we find that both photocyclization and photoreversion processes use the same S_1/S_0 conical intersection to decay the S_1 system to the S_0 state, so we can unify the remaining two channels into one. These new insights are verified by our OM2/MRCI nonadiabatic dynamics simulations. The S_1 excited-state lifetimes of photocyclization and photoreversion are estimated to be 349 and 453 fs, respectively, which are close to experimentally measured values: 240 ± 60 and 250 fs in acetonitrile solution. The present study not only interprets experimental observations and refines previously proposed mechanism but also provides new physical insights that are valuable for future experiments.

Keywords: photocyclization; photoreversion; isomerization; electronic structure methods; nonadiabatic dynamics simulations

References:

[1] Aloïse, S.; Sliwa, M.; Pawlowska, Z.; Réhault, J.; Dubois, J.; Poizat, O.; Buntinx, G.; Perrier, A.; Maurel, F.; Yamaguchi, S. *J. Am. Chem. Soc.* **2010**, **132**: 7379.
[2] Takeshita, M.; Jin-nouchi, H.; Ishikawa, J. *Chem. Lett.* **2009**, **38**: 982.
[3] Xia, S.-H.; Xie, B.-B.; Fang, Q.; Cui, G. L.; Thiel, W. *Phys. Chem. Chem. Phys.* **2015**, **17**: 9687.

光电子能谱研究镧系和锕系元素氟化物的电子结构

王永天[1]，李艳丽[1]，费泽杰[1]，刘洪涛[1,*]，唐紫超[2,*]

[1] 中国科学院上海应用物理研究所，熔盐化学与工程技术部，上海，201800

[2] 厦门大学化学化工学院，厦门，361005

[1]*Email: liuhongtao@sinap.ac.cn

[2]*Email: zctang@xmu.edu.cn

钍及熔盐堆（TMSR）是当前在发展的第四代核反应堆之一，核燃料均匀分散在液态熔盐中。其中氟化物熔盐由于其优良的热稳定性和中子特性，是熔盐反应堆的首选燃料载体和传热介质，但是反应堆运行中间涉及大量液态熔盐化学问题，其中直接影响熔盐堆安全运行的主要问题是堆内关键元素氧化还原形态变化导致的燃料沉积和熔盐对结构材料的腐蚀。其中关键元素包括核燃料钍、铀自身在熔盐中的化学价态和结构，贵金属裂变产物和腐蚀产物的存在形态，以及^{233}Pa 、^{239}Np和^{239}Pu等在堆内熔盐环境中的形态等。通常镧系和锕系元素在氟化熔盐中以配位和团簇负离子形态存在。由于氟盐的强腐蚀性，直接进行原位熔盐团簇配位结构研究难度大，本文将报道利用气相负离子光电子能谱研究镧系和锕系氟化物团簇结构和配位成键性质研究，气相模型体系的研究有助于对TMSR中熔盐蒸汽团簇形态和熔盐中氟化物成键特征深入理解。目前对于其研究多集中于镧系元素常见+3，+4价态氟化物。在前期的试验中我们利用激光溅射产生了不同配位数的La、Ho等的氧化物团簇,这说明激光溅射可产生La、Ho除常见+3价以外的其他价态，经飞行时间质谱选质进入光电子速度成像后得到了部分团簇的光电子能谱，后续通过密度泛函,从头算等方法可对其进行理论计算与验证。另外，我们即将搭建完成的高质量及能量分辨的双反射飞行时间质谱-光电子速度成像仪将帮助我们得到更精确的能谱数据，更准确的开展对镧系氟化物电子结构的研究。

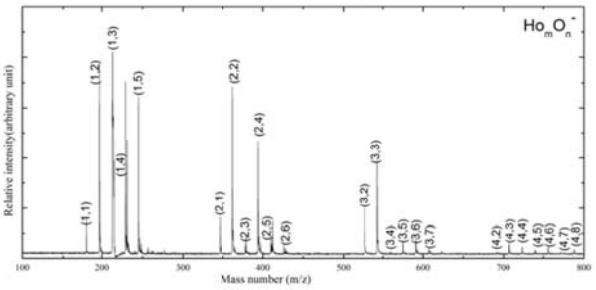

Fig. 1 Time-of-flight mass spectra for $Ho_mO_n^-$

关键词：镧系氟化物；光电子能谱；电子结构

参考文献

[1]. Li W-L, Liu H-T, Jian T, Lopez GV, Piazza ZA, Huang D-L, et al.Chem Sci. 2016,7(1):475-81.

[2] Li, Y. L., Zou, J. H., Xiong, X, G., Tang, Z. C., Liu, H. T. J. et al. Phys. Chem. A, 2017, 121 (10)

氮化碳中间体(Melem)及剥离产物的光物理性质研究

温静[1]，于安池[1]，吕荣[1,*]

[1]中国人民大学理学院化学系，100872

*Email: Lvrong@chem.ruc.edu.cn

氮化碳是一种新型非金属可见光响应催化剂,具有广阔的应用前景，但其光物理性质和光催化机理还存在一定的争议。本工作为了更清楚的了解氮化碳的结构及其形成过程，选取了双氰胺(Dicyandiamide，DCDA)和三聚氰胺(Sgm-Melamine)两种前驱体，运用时间相关单光子计数技术(TCSPC)结合紫外可见吸收光谱、荧光光谱及 X 射线粉末衍射等，从两种途径对氮化碳的性质进行研究。第一，从氮化碳的制备路径来研究，分别用 260 ℃煅烧 DCDA 和 400 ℃煅烧 Sgm-Melamine 来制备氮化碳中间体[1]；第二，用酸碱剥离氮化碳来研究[2]，用一定浓度的酸碱对这两种前驱体在不同温度下制备的氮化碳进行剥离。通过实验可得 DCDA 在 260 ℃煅烧下会形成三聚氰胺；Sgm-Melamine 在 400 ℃(M400)时会有蜜勒胺(Melem)形成，但需进一步纯化(M400-CH)。通过荧光光谱发现经酸碱回流剥离的氮化碳纳米片与两种前驱体制备的氮化碳中间体水溶液在 230-270 nm 激发时峰位置均在 370 nm 左右，并且经酸水热法剥离得到的氮化碳量子点和 Sgm-Melamine 水溶液的紫外可见吸收光谱、激发谱、荧光光谱相似度极高。由此可见剥离之后的产物与中间体的结构有一定的相似之处，但是它们之间具体的关联我们还需要进一步探究。

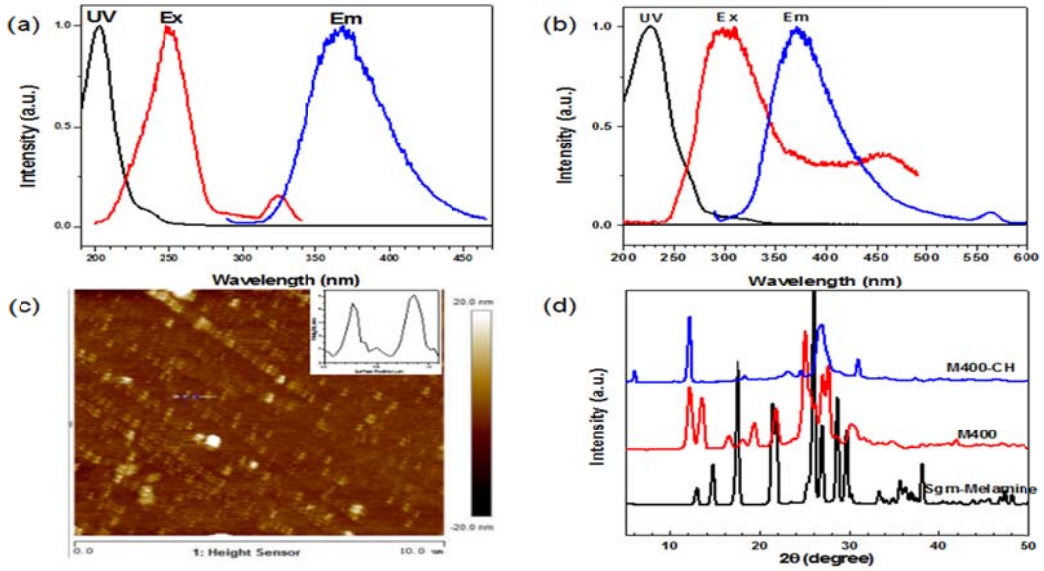

Fig. 1 UV-vis absorption (black), PL excitation (red) and PL emission (blue) of Sgm-Melamine (a). UV-vis absorption (black), PL excitation (red) and PL emission (blue) of C_3N_4 (550 ℃ Melamine)-H_2SO_4 nanosheet (b). AFM image of g-CN nanosheet. Inset : the corresponding height image of the nanosheet (c) . XRD of Sgm-Melamine, M400, M400-CH (d) .

关键词：氮化碳；中间体；飞秒瞬态吸收

参考文献

[1] Dirk Hollmann,*,†Michael Karnahl,†Stefanie Tschierlei,‡Kamalakannan Kailasam,§Matthias Schneider,†Jörg Radnik,†Kathleen Grabow,†Ursula Bentrup,†Henrik Junge,†Matthias Beller,†Stefan Lochbrunner,‡Arne Thomas,*,§and Angelika Brückner*,†*Chem. Mater.***2014, 26**, 1727−1733.

[2] Zhixin Zhou, Jianhai Wang, Jiachao Yu, Yanfei Shen, Ying Li, Anran Liu, Songqin Liu,and Yuanjian Zhang**J. Am. Chem. Soc.* **2015, 137**, 2179−2182.

Selective Dehydrogenation of Diaminobenzenes by Deep Ultraviolet Single Photons

Haiming Wu[1], Zhixun Luo[1,*]

[1]State Key Laboratory for Strucutral Chemistry of Unstable and Stable species, Institute of Chemistry, Chinese Academy of Sciences, Beijing, 100190
*Email: zxluo@iccas.ac.cn

Single-photon ionization mass spectrometry (SPI-MS) is known as an important technique available for chemical identification because organic molecules are readily fragmented under usual laser radiation.[1] The use of deep ultraviolet (DUV) radiation takes advantages for SPI-MS especially for the compounds with ionization potentials below the energy of a single DUV photon. The 177.3-nm all-solid-state DUV laser single-photon ionization based on our customed time-of-fight mass spectrometer (TOF-MS) system has a unique advantage in distinguishing diaminobenzenes isomers which possess ionization energies close to 7.0 eV.[2] The reasonable performance is attributed to the synergistic effect of short pulse duration, high single photon energy, and high photon flux of the all-solid-state DUV laser and distinguishing merits of TOF-MS. It is found that the dramatic selectivity of diaminobenzenes isomers pertains to varied photochemical processes initiated by the DUV laser radiation. A single-photon ionization process dominates for 1,4-diaminobenzene (PPD) resulting in a fragmentation-free mass spectrum; photo-induced dehydrogenation is observed for 1,2-diaminobenzene (OPD) and 1,3-diaminobenzene (MPD). The dramatic intensity ratio of the molecule parent ion relative to its dehydrogenation fragment reveals selective C-H activates under the DUV single photons.

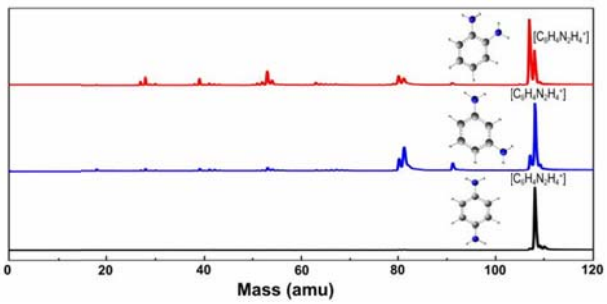

Fig. 1 Time-of-flight (TOF) mass spectra of collected diaminobenzenes under radiation of 177.3-nm laser source. Red, blue and black line presents 1,2-diaminobenzene (OPD), 1,3-diaminobenzene (MPD) and 1,4-diaminobenzene (PPD), respectively. The inserts are optimized neutral diaminobenzenes isomers. The molecular formulas of major molecular ion peaks are given aside the peaks.

Keywords: deep ultraviolet laser; time-of-fight mass spectrometer; diaminobenzenes isomers; single photon ionization

References:

[1] C. Yuan, X. Liu, C. Zeng, H. Zhang, M. Jia, Y. Wu, Z. Luo, H. Fu and J. Yao, *Rev Sci Instrum*, **2016**, **87**, 024102.

[2] J. Chen, Z. Luo, H. Fu and J. Yao, *J. Phys. Chem. A*, **2017**, DOI: 10.1021/acs.jpca.7b03635.

苯酞激发态非辐射动力学的拉曼强度分析和理论计算研究

吴刘霞，欧阳冰，郑旭明*

浙江理工大学，浙江省杭州市下沙 2 号大街 928 号，310018

*Email: zhengxuming126@126.com

锥形交叉点或者势能面交叉点是化学动力学中用于研究两个不同势能面之间的无辐射跃迁的有效途径，但从 F-C 区域到势能面交叉点的动力学过程仍然面临挑战。共振拉曼光谱技术结合 CASSCF 理论计算方法可以很清楚地得到物质在被激发后 50 飞秒之内的结构信息，在研究物质激发态结构动力学方面具有十分重要的作用[1]。我们利用含时波包理论分析进行共振拉曼强度分析，结合量子化学计算的结果，对苯酞在乙腈溶液中的激发态短时结构动力学进行了深入的研究。通过对 B-吸收带含时量子波包理论的绝对拉曼横截面积拟合得到简正模的位移量$|\Delta_i|$ $_6$（C_1=O_{10}）、 $_7$（C_7C_8+C_4C_5）、 $_8$（C_8C_9+C_5C_6）、 $_{15}$（ring breathing）最大值分别为 0.72、0.82、0.63、0.50，这与共振拉曼光谱得到的苯酞在 S3 态结构动力学基本沿着 C1=O10、C_7C_8、C_4C_5、C_8C_9、C_5C_6 的方向伸缩的结果一致。将在 F-C 区域中的 11 个简振模位移量转化成短时结构的内坐标形式，结合 CASSCF 计算得到交叉点结构信息 Figure3 揭示了苯酞在 F-C 区域的激发态的非辐射过程[2]，Figure4 的路径原理图所示。

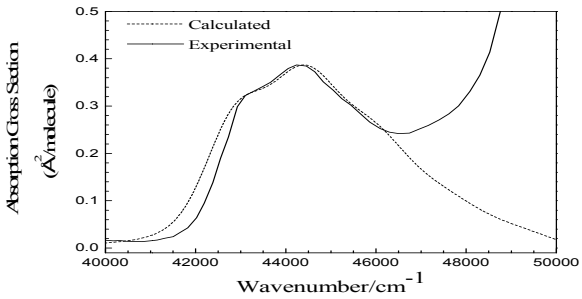

Figure 1.Comparison of the experimental and the calculated absorption spectra.

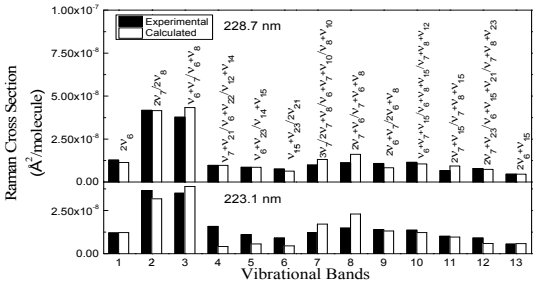

Figure 2.Comparison of the experimental and the calculated resonance Raman cross-sections of overtones and combination bands for the 223.1 and 228.7 nm resonance Raman spectra.

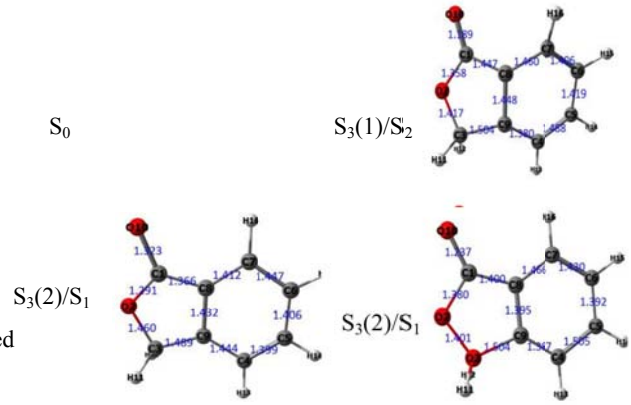

Figure 3. Geometric structures of the optimized singlet excited states and the curve-crossing points in singlet

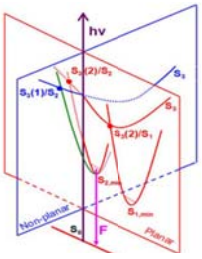

Figure 4. Schematic diagram of the decay dynamics of phthalide initiated from the $S_3(\pi\pi^*)$ state.

关键词：苯酞；CASSCF 计算；非辐射衰减动力学；共振拉曼光谱；拉曼强度分析；

参考文献

[1] Zhu,X ,M.; Zhang,S,Q.; Zhang, X.; *J. Chem. Phys.* **2005**,**109**, 3086 .

[2] Jiang, J.; Zhang,T. S.; Xue,J. D.; Zheng,X.; Cui,G.; Fang,W,H.; *J. Chem. Phys.* **2015**,**143**, 175103 .

碳酸二甲酯解离光电离研究

—阈值光电子-光离子符合技术的应用

吴向坤[1]，周晓国[1,*]，刘世林[1]，Patrick Hemberger[2]，Andras Bodi[2]

[1]微尺度物质科学国家实验室(筹)，中国科学技术大学化学物理系，安徽合肥，230026

[2]Laboratory for Femtochemistry and Synchrotron Radiation, Paul Scherrer Institute, 5232 Villigen, Switzerland

*Email: xzhou@ustc.edu.cn

应用阈值光电子-光离子符合（iPEPICO）技术[1]，我们研究了10.3-12.5 eV 光子能量范围内，能态选择的碳酸二甲酯（DMC）分子的电离-解离动力学。通过对DMC的阈值光电子谱（TPES）的振动结构进行Franck-Condon拟合，确认了电离过程中主要伴随O-C-O的弯曲振动与C=O的伸缩振动模式的激发，从而获得了DMC的电离能为10.47±0.01 eV。通过对电离-解离产物的相对丰度随着光能的变化得到了碳酸二甲酯的Breakdown曲线，结合统计解离模型拟合，我们得到了各主要解离产物的0 K出现势分别为：CH_2OH^+（m/z=31，AP_0 = 11.14 eV），$OHCH_2CH_2OH^+$ (m/z = 62，AP_0 = 11.16 eV)， CH_3CHOH^+ (m/z = 45，AP_0 =11.46 eV)，CH_3OCO^+ (m/z = 59，AP_0 = 11.47 eV)和$CH_3OH_2^+$ (m/z = 33，AP_0 = 11.54 eV)。进一步的反应路径计算也很好的解释了实验观察到的各解离过程。最终，我们通过热力学计算，获得了DMC的生成焓为Δ_fH_{0K}(DMC(g)) =−548.3 ± 1.5 kJ mol^{-1}，DMC$^+$的生成焓为Δ_fH_{0K}(DMC$^+$(g)) = 461.9 ± 1.8 kJ mol^{-1}。[2]

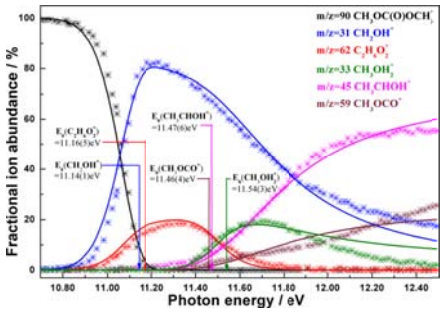

Fig. 1 Breakdown diagram of dimethyl carbonate between 10.70 and 12.50 eV. Crosses correspond to measured fractional abundances and continuous lines show the best fit model, based on which the appearance energies have been determined.

关键词：阈值光电子-光离子符合；光解离；生成焓

参考文献

[1] Bodi, A.; Johnson, M.; Gerber, T.; Gengeliczki, Z.; Sztaray, B.; Baer, T.; Rev. Sci. Instrum. 80, 034101, 2009

[2] Wu, XK.; Zhou, XG.; Hemberger, Patrick.; Bodi, Andras. *J. Phys. Chem.* **2017**, **121**: 2748.

A Cryogenic Ion Trap Mass Spectrometer for Infrared Photodissociation Spectroscopy of Mass-Selected Ions

Xiaonan Wu*, Zejian Huang, Guanjun Wang, Fanchen Kong, Xuan Wu, Di Zhang, Mingfei Zhou*

Department of Chemistry, Fudan University, 220 Handan Rd, Shanghai, 200433

*Email: wuxiaonan@fudan.edu.cn, mfzhou@fudan.edu.cn

Infrared photodissociation spectroscopy is emerging as an important tool in the structural characterization of organic or biological molecules. A new instrumental setup for measuring infrared photodissociation spectra of mass-selected ions is built in our lab, as shown in Fig 1. Ions are generated by electrospray ionization (ESI). After ions are selected by a quadrupole mass filter, they are sent into a low temperature 3D Paul trap (minimum temp. 10K). The ions are cooled and attached by messenger molecules (such as Ar gas) in the trap for a controlled time interval prior to being ejected. The ejected ions drift into a time of flight mass spectrometer (TOFMS). The ions of interest are mass selected, decelerated and dissociated by a tunable IR laser (Nd:YAG Pumped OPO/OPA). The fragment and parent ions are analyzed by a second collinear TOFMS. Infrared photodissociation spectrum is obtained by monitoring the yield of the fragment ions as a function of the dissociation IR laser wavelength and normalizing to parent ion signal.

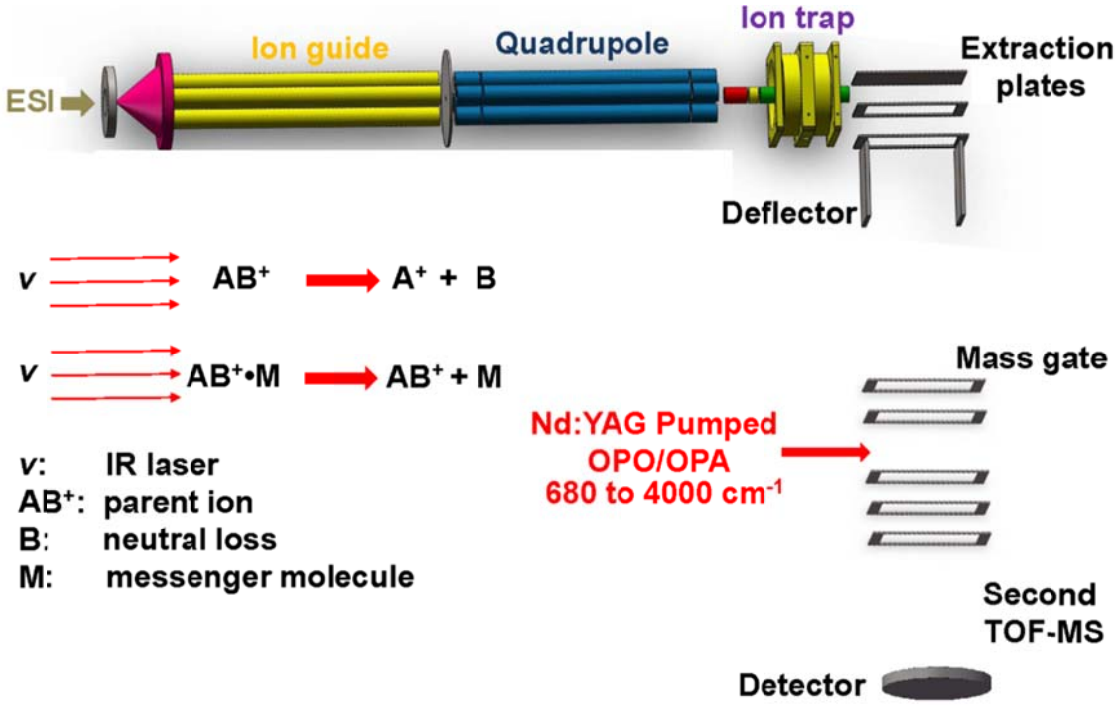

Fig. 1 Schematic diagram of the experimental setup.

References:

[1] C. T. Wolke, et al. *J. Phys. Chem. A* **2015**, *119*, 1859-1866.

[2] X.-B. Wang, et al. *Rev. Sci. Instrum.* **2008**, *79*, 073108.

Resonant Two-Photon Ionization and Mass-Analyzed Threshold Ionization Spectroscopy of 4-Chloro-2-fluoroanisole

Pei Ying Wu [1,2], **Wen Bih Tzeng** [1*]

[1]Institute of Atomic and Molecular Sciences, Academia Sinica, P.O. Box 23-166, 1 Section 4, Roosevelt Road, Taipei 10617, Taiwan

[2]Department of Chemistry, National Taiwan University, 1, Section 4, Roosevelt Road, Taipei 10617, Taiwan

*Email: wbt@sinica.edu.tw

We applied the resonant two-photon ionization and mass-analyzed threshold ionization spectroscopic techniques to record the vibronic and cation spectra of 4-chloro-2-fluoroanisole (4C2FAN). The cation spectra of 4C2FAN were obtained by ionizing via five levels of its electronically excited S_1 states. The band origin of the $S_1 \leftarrow S_0$ electronic transition of 4C2FAN appears 35227 ± 2 cm^{-1}; and the adiabatic ionization energy is determined to be 67218 ± 5 cm^{-1}.

The observed active vibrations of 4C2FAN in the S_1 and cationic ground D_0 states include methyl torsion, substituent-sensitive out-of-plane and in-plane ring bending and deformation vibrations. Comparison of the present data with those of multiply halogen substituted anisoles, phenols, and anilines reveals halogen substituent effect and additivity rule on electronic transition and ionization energies.

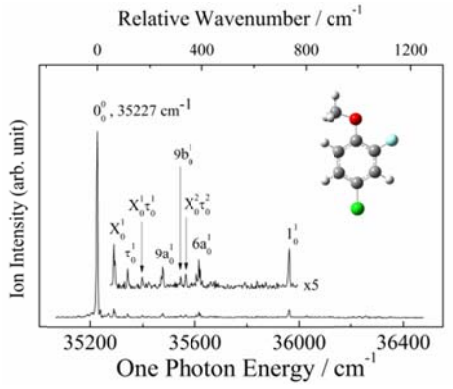

Fig. 1 Vibronic spectrum of 4-chloro-2-fluoroanisole. The 2C-R2PI experiment was performed by scanning the excitation laser while fixing the ionization laser at 624.40 nm (32031 cm^{-1}).

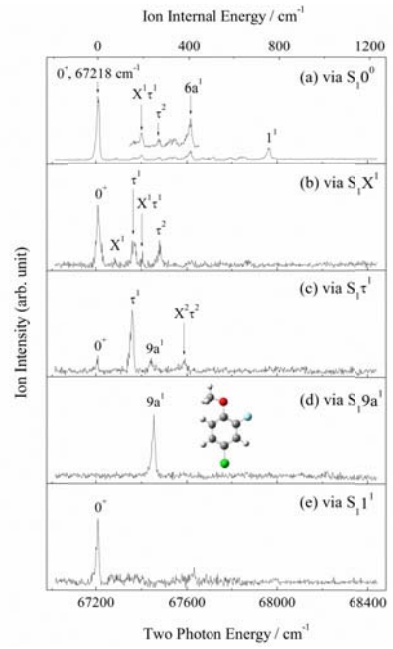

Fig. 2 MATI spectra of 4-chloro-2-fluoroanisole recorded by ionizing via the (a) 0^0, (b) X^1, (c) τCH_3, (d) $9a^1$, and (e) 1^1 levels in the S_1 state, respectively.

Keywords: resonant two-photon ionization, mass-analyzed threshold ionization, 4-chloro-2-fluoroanisole, vibronic spectrum, cation spectrum

INFRARED SPECTRA OF BARIUM CARBONYLS IN NEON MATRICES

Xuan WU, Mingfei Zhou
Department of Chemistry, Fudan University, Shanghai
200433, China

The reaction of Ba+CO has been studied for decades, however, only the product BaCO has been detected by broad banded chemiluminescence owing to its difficultyof charge transfer. Herein, we observed the infrared spectra of novel Barium Carbonyls in the solid Nematrices at 3.0 K. The products Ba(CO) n (n=1,2,3,4) and Ba 2 (CO) n (n=1,2) were identified by isotopic substitution (13 CO and C 16 O) and by correlation with B3LYP calculations. The complexes of barium dimer with CO are assigned within the spectrum of 1455 - 1370 cm -1 . It's worth noting that the intensities of features of Ba(CO) 2 diminished after 20-minute infrared (λ=1064 nm) irradiation, whereas those of Ba 2 (CO) 2 increased dramatically. Furthermore, energetic analysis for the possible reactions of barium atoms with CO molecules is also given.

Reference:

[1] Mingfei Zhou,Lester Andrews,Charles W. Bauschlicher, Jr.,Chem. Rev. 2001, 101, 1931−1961
[2] C. Gée, M. A. Gaveau, O. Sublemontier, J. M. Mestdagh,J.-P. Visticot,J. Chem. Phys., Vol. 107, No. 11, 15 September 1997
[3] John B. West, Helen M. Poland,J. Chern. Phys., Vol. 66, No.5, 1 March 1977

拉曼光谱法研究 γ-己内酯短程有序结构和ν(C=O)振动耦合相互作用力

许文文，王惠钢*，郑旭明

浙江理工大学“生态染整技术”教育部工程研究中心，浙江省“化学工程与技术”高校重中之重学科，浙江理工大学，中国，杭州，310018

Email: zdwhg@163.com

论文利用拉曼光谱法研究γ-丙内酯在二元混合溶液中的非一致效应(NCE)以及不同浓度时NCE大小($\Delta\nu_{NCE}$）的变化规律。采集了不同浓度γ-己内酯在CCl_4/DMSO中ν(C=O)的各项同性和各向异性拉曼光谱，发现随着浓度的降低C=O振动模的NCE渐渐消失，并且在CC_4溶液中随着γ-己内酯浓度的增加$\Delta\nu_{NCE}$呈现出一条向上凸的曲线，而在DMSO中则是一条向上的直线。这说明在CCl_4分子增强了γ-丙内酯分子二聚体的短程有序结构。采集了体积分数为0.5的γ-己内酯在不同极性溶剂中ν(C=O)的各项同性和各向异性拉曼光谱，发现随着极性的增强NCE效应不断变弱。因此，我们利用DFT/B3LYP-D3和PCM溶剂模型在6-311G(d,p)基组下计算了γ-己内酯单分子和二聚体的最优几何构型，并提出一种分子聚集态结构理论模型解释γ-己内酯分子中C=O振动模的NCE效应，浓度效应和溶剂效应，实验光谱现象与计算结果保持一致。

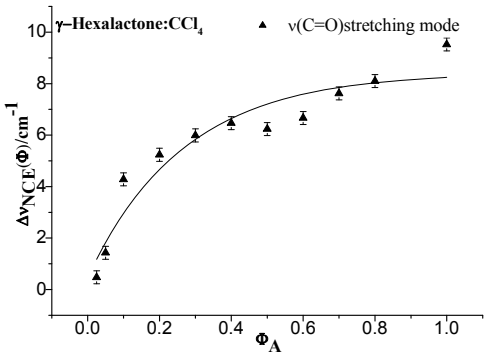

Fig. 1 Variation of NCE of C=O stretching mode of γ-Caprolactone as a function of solute volume fractions ($C_6H_{10}O_2$+CCl_4)

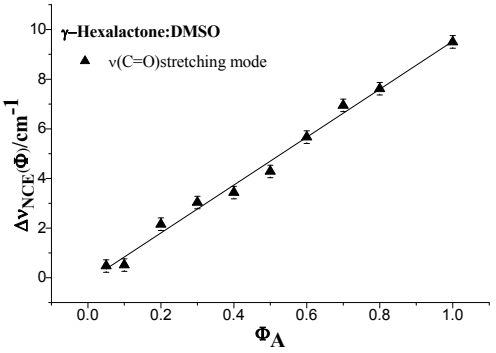

Fig. 2 Concentration dependence of the NCE of C=O stretching mode of γ-Caprolactone in the binary mixture (C6H10O2+ DMSO)

关键词：C=O伸缩振动；γ-己内酯；非一致效应；振动耦合；DFT计算

参考文献

[1] Wu, F., Wang, H., Zheng, X. *J. Raman Spectrosc* **2015**, ***46***: 591.

[2] Xu, W., Wu, F., Zhao, Y., Zhou, R., Wang, H., Zheng, X., Ni, B. *Scientific Reports* **2017**, ***7***: 43835.

[3] Zhou, R., Wu, F., Zhou, X., Wang, H., Zheng, X. *J. Mol. Struct.* **2017**, ***1129***: 205.

Quantum state tomography of high temporal resolution with THz streaking-assisted photoelectronic momentum distribution

Yizhu Zhang, Tian-Min Yan* and Y. H. Jiang

Shanghai Advanced Research Institute, Chinese Academy of Science, Shanghai, China
*Email: yantm@sari.ac.cn

An approach to retrieve the information of dynamics on a sub-femtosecond time scale from the photo-ionization is proposed by using the combination of the linearly polarized short XUV pulse with the THz streaking field. The method is theoretically verified under the strong field approximation. With the duration of the XUV pulse much shorter than a half cycle of the THz pulse, the photo-electron streaked by the THz field leads to the broadened momentum distribution and significantly enhanced coherence signal, ascribing the advantage of high time resolution to the method that allows using pulse of femtoseconds duration to resolve sub-femtosecond process. On the other hand, with the fixed center times of XUV and THz fields, scanning with the varying time delay allows for retrieving the elements of density matrix, implementing the so-called quantum process tomography, as shown in Fig. 1 for the two level model system. The longitudinal momentum distribution shows the evolution of both the population and coherence, providing important information such as the coherence frequencies and decaying rates of relevant states.

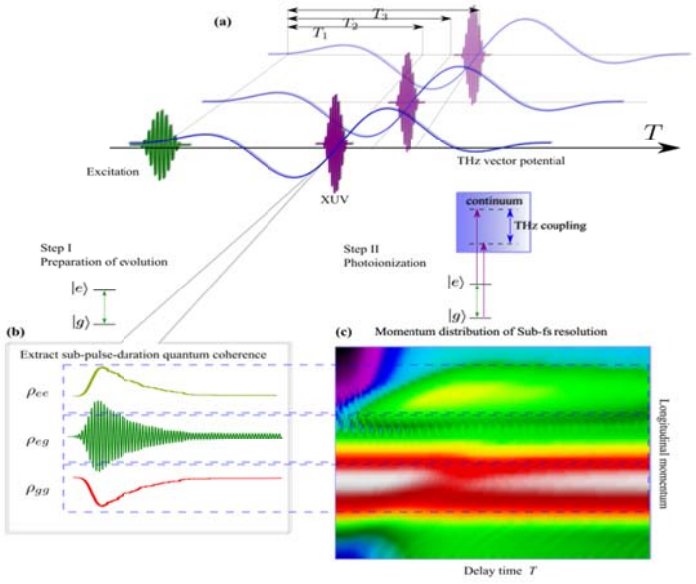

Fig. 1 Quantum process tomography of high temporal resolution retrieved from photoelectronic momentum distribution.

Keywords: free electron laser; terahertz; coherence; attosecond

A simulation study on exciton dissociation in organic photovoltaic cells

Yaming Yan, Linze Song, Qiang Shi

Beijing National Laboratory for Molecular Sciences, State Key Laboratory for Structural Chemistry of Unstable and Stable Species, Institute of Chemistry, Chinese Academy of Sciences, Zhongguancun, Beijing 100190, China

University of Chinese Academy of Sciences, Beijing 100049, China

Email:yanyaming@iccas.ac.cn;songlinze@icas.ac.cn;qshi@iccas.ac.cn

The quite high efficiency of exciton dissociation observed in organic photovoltaic solar cells is a confusing problem because of the high coulomb exciton binding energy in those materials [1-4]. By employing several lattice model systems, we investigate how several important factors affect the charge separation barrier in organic photovoltaic (OPV) cells. The combined effects of external electric field, dimensionality, and charge delocalization are found to reduce the free energy barrier for charge separation significantly. The dynamic disorder reduces charge carrier delocalization and results in increased charge separation barrier, while the effect of static disorder is more complex. It is found that, under a reasonable set of parameters, the charge separation barrier can be reduced to several k_BT. The current results also indicate that only a small energy offset between the band gap and the lowest energy charge transfer state is needed to achieve efficient free charge generation in OPV devices. Besides, we also performed quantum dynamic study, which reveal that hot vibronic exciton can fascinate the dissociation process.

Keywords: Organic photovoltaic, exciton dissociation, HEOM, IT-PIMC

References:

[1] T. M. Clarke and J. R. Durrant, *Chem. Rev.* **2010**,*110*, 6736.

[2] F. Gao and O. Inganäs, *Phys. Chem. Chem. Phys.* **2014***, 16*, 20291.

[3] C. Deibel, T. Strobel, and V. Dyakonov, *Adv. Mater.* **2010**, *22*, 4097.

[4] S. R. Cowan, N. Banerji, W. L. Leong, and A. J. Heeger, *Adv. Fun. Mater.* **2012**, *22*, 1116.

Time-resolved Photodissociation of Acetaldehyde Molecules by Ultraviolet Excitation

C.-H. Yang[1], S. Bhattacharyya[1], M. Roy[1], K. Liu[1,2*]

[1]Institute of Atomic and Molecular Sciences, Academia Sinica, Taipei, 10617, Taiwan
[2] Department of Physics, National Taiwan University, Taipei, 10617, Taiwan
*Email: kliu@po.iams.sinica.edu.tw

The broad near-UV absorption continuum of acetaldehyde (CH3CHO) spanning 240-330 nm has been studied extensively due to the significant roles of the resulting radical products in atmospheric chemistry. In this absorption range, the ground state of acetaldehyde is mainly excited to the first electronic excited singlet state (S_1) followed by fluorescence or radiationless processes such as internal conversion and intersystem crossing that then lead to different fragmentations[1-2]. Recently, a roaming pathway[1], which is anomalous compared with the conventional transition state mechanism, has been proven to play a significant role in the CO+CH_4 channel from photodissociation of acetaldehyde using static spectroscopy methods[1]. In order to take a different view of the roaming pathway in the time domain, the picosecond (ps) time-resolved time-of-flight (TOF) spectroscopy and velocity map ion imaging (VMI) are implemented to study time evolutions of fragments from the excitation of acetaldehyde to the S_1 state. A 10% gas mixture of acetaldehyde is expanded into the reaction chamber and subsequently pumped and probed by two time-delayed laser beams (pulse width ~1.7 ps). The probe wavelengths are chosen either at ~333 nm through 2+1 resonance enhanced multiphoton ionization (REMPI) of CH_3 or at ~230 nm through 2+1 REMPI of CO and 1+1 REMPI of HCO. In addition to resonance detection products, products from dissociative ionization are observed due to the relatively high peak intensities of ps pulses. From the TOF measurements, the CH_3^+ signals probed at the REMPI wavelength of ground state show an exponential growth with a rise time ~1.2 ns, ~800 ps, or ~500 ps at 286 nm, 276 nm, or 266 nm pump wavelength, respectively, which are presumably dominated by radiationless processes. From pump-probe vibrational state selected ion imaging data, the energy partitions of products are partially disentangled with picosecond time resolution.

Keywords: acetaldehyde; roaming; time-resolved; VMI; REMPI; radiationless

References:

[1] Lee, K. L. K.; Quinn, M. S.; Maccarone, A. T.; Nauta, K.; Houston, P. L.; Reid, S. A.; Jordan, M. J. T.; Kable, S. H. *Chem. Sci.* **2014, 5:** 4633.
[2] Toulson, B. W.; Kapnas, K. M.; Fishman, D. A.; Murray, C. *Phys Chem Chem Phys* **2017, 19:** 14276

Insights into Structural Properties and Vibrational Spectra of Ethylammonium Nitrate Ionic Liquid Confined in Single-Walled Carbon Nanotubes

Zheng Wan, Zhen Yang*

Institute of Advanced Materials (IAM), State-Province Joint Engineering Laboratory of Zeolite Membrane Materials, College of Chemistry and Chemical Engineering, Jiangxi Normal University, Nanchang 330022, People's Republic of China

*Email：yangzhen@jxnu.edu.cn

The structures and relevant vibrational spectra of an ethylammonium nitrate (EAN) ionic liquid (IL) confined in single-walled carbon nanotubes (SWCNTs) with various diameters have been investigated in detail by using classical molecular dynamics simulation. Our simulation results demonstrate that the EAN IL confined in larger SWCNTs can form well-defined multi-shell structures with an additional cation chain located at the center. However, a different single-shell hollow structure has been found for both the cations and the anions in the 1-nm SWCNT. For the cations confined in SWCNTs, the CH_3 groups stay closer to the nanotube walls because of their solvophobic nature while the NH_3^+ groups prefer to point toward the central axis. Accordingly, the NO_3^- anions tend to lean on the SWCNT surface with three O atoms facing to the central axis to form hydrogen bonds (HBs) with the NH_3^+ groups. In addition, in the 1-nm SWCNT, the CH_3 groups of cations exhibit an obvious blue shift of around 16 cm^{-1} for the C−H stretching mode with respect to the bulk value, and the N−H stretching mode of NH_3^+ groups is split into two characteristic peaks with one peak appearing at a higher frequency. Such blue shift is attributed to the existence of more free space for the C−H bonds of confined CH_3 groups. While the splitting phenomenon is due to the fact that more than 60% of the confined NH_3^+ groups have one dangling N−H bond. For the anions confined in the 1-nm SWCNT, the N−O stretching mode of NO_3^- has a maximum red shift of around 24 cm^{-1} with respect to the bulk value, which is attributed to enhanced HBs between anions and cations. Our simulation results reveal a molecular-level correlation between confined structural configurations and the corresponding vibrational spectra changes for the ILs confined in nanometer scale environments.

References:

[1] Zhou, G. B.; Li, Y. Z.; Yang, Z.; Fu, F. J.; Huang, Y. P.; Wan, Z.; Li L.; Chen, X. S.; Hu, N.; Huang L. L. *J. Phys. Chem. C* **2016**, 120, 5033−5041.

No-planar photodissociation path way of bromo-2,6-difluorobenzene

Rongrong Yin[1], BinJiang[1,*], Dongfeng Zhao[2,*]

[1]Department of Chemistry Physicis, University of Science and Technology of China, No. 96 Jinzhai Road, Hefei, Anhui, 230026, China

[2] Hefei National Laboratory for Physical Science at the Microscale, University of Science and Technology of China, No. 96 Jinzhai Road, Hefei, Anhui, 230026, China

*Email: bjiang@ustc.edu.cn; dzhao@ustc.edu.cn

The halobenzenes, C_6H_n-X_{6-n} (X = F, Cl, Br, I) have proven to be suitable model systems to study intramolecular light induced phenomena and have therefore received much experimental and theoretical attention. The previous one-dimensional potential energy curve indicates that the photodissociation of 1-Br-2,6-diFPh at 205 nm experiences a high barrier, which, however, disagree with the experimentally estimated fast timescale of the 1-Br-2,6-diFPh's photodissociation process, i.e. ~0.3 ps. In order to resolve this puzzle, we investigated the excited state potential energy surfaces of 1-Br-2, 6-diFPh at CASSCF/CASPT2 level, focusing on the nonplanar dissociation pathway. It is found that the geometrical changes of C-Br bond stretch and the bromine out-of-plane bending enable the mixing π^* and σ^* to lower the barrier. Our results suggest the photodissociation at 267 nm may occur fast via the nonplanar dissociation path and yield the perpendicular anisotropy parameters, as recently measured in the our collaborating experimental lab.[unpublished results]

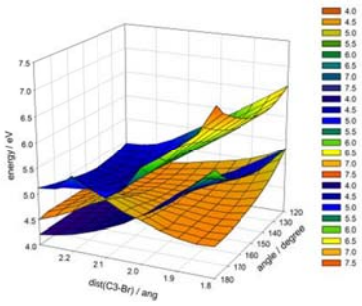

Fig. 1 The PESs of three excited states

Keywords: halobenzenes; photodissociation process; orbital mixing

References:

[1] O. A. Borg, Y. J. Liu, P. Persson, S. Lunell, D. Karlsson, M. Kadi, J. Davidsson, *J. Phys. Chem. A*. **2006**, **110**: 7045.

[2] O. Anders Borg, *Chemical Physics Letters*. **2007**, **436**: 57-62.

Isotopic Effects on the Photodissociation of CH_3I: a Nonadiabatic Dynamics Study

Angyang Yu*

School of Science, Liaoning University of Petroleum and Chemical Technology, Fushun, 113001
*Email: xintongyang2011@163.com

The nonadiabatic photodissociation dynamics of the triatomic (or pseudo-triatomic) system in multiple electronic states is a frontier topic in molecular reaction dynamics.[1,2] In the present work, the photodissociation dynamics of CH_3I and its isotopic species (CD_3I, CD_2HI and CDH_2I) in three electronic states of A band, namely, $^3Q_0$, $^1Q_1$ (A') and $^1Q_1$ (A''), have been investigated by employing a time-dependent quantum wave packet method, in which the time propagation of the wave packet is carried out using the split-operator scheme. The absorption spectra, product vibrational state distributions and product rotational state distributions of these species are calculated and compared. Additionally, the extent of nonadiabatic couplings has been analyzed.

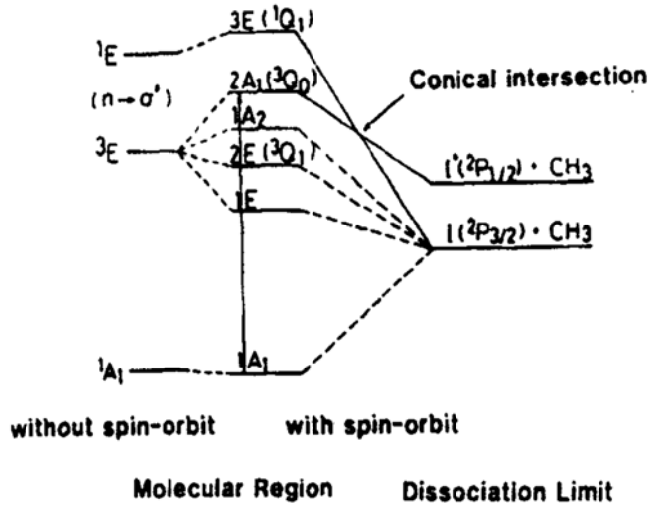

Fig. 1 Potential energy surface for CH_3I and its isotopic species

Keywords: Isotopic effects; Nonadiabatic photodissociation dynamics; Split-operator scheme

References:

[1] Alekseyev, A.B.; Liebermann, H.; Buenker, R.J. ***J. Chem. Phys.*** 2011**,** 134**: 044303.**

[2] Jiang, B.; Xie, D.Q. ***Prog. Chem.*** 2012**,** 24**: 1120.**

C-H…O interaction in methanol-water solution revealed from Raman spectroscopy and theoretical calculations

Yuanqin Yu[1], Wei Fan[2],Yuxi Wang[2], Xiaoguo Zhou[2], and Shilin Liu[2*]

1 Department of Physics, Anhui University, Hefei, Anhui 230039, China

2 Hefei National Laboratory for Physical Sciences at the Microscale, Department of Chemical Physics, University of Science and Technology of China, Hefei, Anhui 230026, China

*Email: yyq@ahu.edu.cn, slliu@ustc.edu.cn.

Hydrogen bond, as the most common weak interaction in molecules, plays an important role in physical, chemical, and biological processes. In addition to the conventional hydrogen bond, an unusual class of C-H…Y hydrogen bond termed with "improper blue-shifted hydrogen bond" has attracted much attention in recent years. In this paper, we investigated the origin of blue shift of CH_3 stretching vibration in methanol-water mixture by temperature-dependent Raman spectroscopy and quantum chemistry calculation. Based on the spectral response to temperature and the calculated structures for methanol-$(water)_n$ (n=1-4) clusters, we provide clear experimental evidence that the weak C-H…O interaction coexists with conventional O-H…O hydrogen bond in methanol-water solution and play a role in the determination of C-H blue shift. Moreover, the temperature-dependent measurements of methanol-water mixtures in both C-H and O-H stretching regions reveal that the C-H…O interaction behaves differently from the conventional O-H…O hydrogen bond upon the temperature increasing. The former is enhanced whereas the latter is weakened. These results will shed new light to the nature of C-H…O interaction and be helpful to understand hydrophilic and hydrophobic interactions of amphiphilic molecules in different environments.

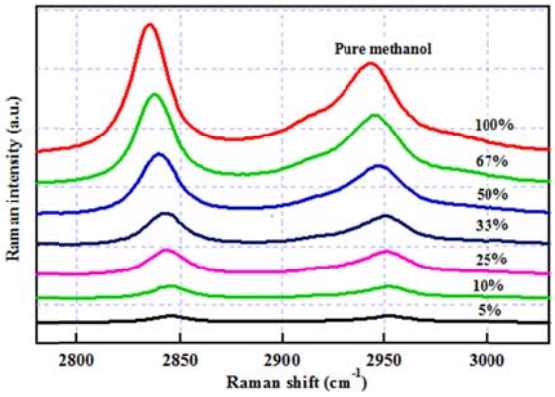

Fig. 1 Concentration-dependent Raman spectra of methanol-water mixtures in the C-H stretching region.

Keywords: C-H…O interaction; O-H…O hydrogen bond; methanol-water solution; temperature-dependent Raman spectroscopy.

References:

[1] Keefe, C. D.; Gillis, E. A. L.; MacDonald, L. *J. Phys. Chem. A*, 2009, *113*(11), 2544-2550.

[2] Shimoaka, T.; Katsumoto, Y. *J. Phys. Chem. A*, 2010, *114*(44), 11971-11976.

水在 C(010)态的光解动力学

常尧[1, 2]，苏抒[1]，王黑龙[1, 3]，陈志超[1]，王兴安[2]，袁开军[1*]，杨学明[1]

[1] 中国科学院大连化学物理研究所分子反应动力学国家重点实验室，大连市中山路 457 号，116023

2 中国科学技术大学化学物理系，合肥市金寨路 96 号，230026

3 大连海事大学物理系，大连市凌海路 1 号，116026

*Email: kjyuan@dicp.ac.cn

水分子的光解动力学研究过去三十年取得了极大的进展，尤其是在转动态分辨的水平上揭示了不同电子态上水分子的绝热和非绝热的解离动力学过程。水的C态是束缚态，寿命较长，是第一个可以观测到转动吸收谱的电子态，在其上的解离动力学显示出两个非绝热解离通道。转动量子数Ka（J_{KaKc}）控制着这两个非绝热解离通道的竞争。

最近我们实验室的超快光电子成像的工作显示H_2O的C（010）态具有非寻常的短寿命～300fs，而其同位素D_2O的C(010)态则依然具有长寿命～4ps。通过对比发现，除了以前发现的两个非绝热解离通道C→A和C→B之外，新的非绝热解离通道C(010)→D（000）→B在水的C(010)态解离过程占据主导作用，而在重水中该通道可以忽略不计。这个新的非绝热解离通道是由于能级共振造成的。我们通过可调谐的VUV光源对水和重水在120-122nm波段进行了光谱扫描，发现水的C(010)的吸收谱明显展宽，而重水的C(010)的吸收谱依然具有窄的转动吸收峰。通过高分辨的光解动力学研究，对比水和重水的动力学分析，揭示了振动激发在水的光解动力学的影响。另外我们利用极紫外自由电子激光光源也进行了水的光解动力学研究，光解波长117.5nm，水分子被激发到C(101)态，解离结果进一步说明了振动激发对解离动力学的影响。

关键词：非绝热解离；振动激发；极紫外自由电子激光

参考文献

[1] K. J. Yuan, R. N. Dixon, X. M. Yang*, Photochemistry of the Water Molecule: Adiabatic versus Nonadiabatic Dynamics. *Accounts Chem Res* 44, 369-378 (2011);

[2] K. J. Yuan, Y. Cheng, L. Cheng, Q. Guo, D. X. Dai, X. Y. Wang, X. M. Yang*, R. N. Dixon*, Nonadiabatic dissociation dynamics in H2O: Competition between rotationally and nonrotationally mediated pathways. *P NAS* 105, 19148-19153 (2008);

[3] S. Su, H. Z. Wang, Z. C. Chen, S. R. Yu, D. X. Dai, K. J. Yuan*, X. M. Yang*, Photodissociation dynamics of HOD via the (B)over-tilde ((1)A(1)) electronic state. *J Chem Phys* 143, (2015);.

Configuration Interconversion and Flipping of Hydrogen Bond in the Neutral Methylamine Dimer Revealed by Infrared Spectroscopy

Bingbing Zhang[#] ,Xiangtao Kong,[#] Shukang Jiang, Ling Jiang*
State Key Laboratory of Molecular Reaction Dynamics, Dalian Institute of Chemical Physics, Chinese Academy of Sciences, 457 Zhongshan Road, Dalian 116023, China
*Email: ljiang@dicp.ac.cn

Solvation clusters, produced and probed in the gas phase, are often taken as microscopic models for solutions. However, neutral solvation clusters are much more challenging to measure, due to difficulties in both size selection and signal detection [1-5]. Recently, infrared-vacuum ultraviolet (IR-VUV) spectroscopy of neutral clusters has aroused great interest [6-9].

Well-resolved IR spectrum of neutral methylamine dimer, $(CH_3NH_2)_2$, was measured in the C-H and N-H stretching region using the Dalian IR-VUV apparatus. Quantum chemical calculations and molecular dynamics simulations were performed to identify the structures and to assign the observed spectral features. Experimental and theoretical results reveal the dynamic nature of (CH3NH2)2 with the involvement of fast configuration interconversion and extensive flipping of hydrogen bond. The present work demonstrates a fundamental model to understand the microscopic details in the solvent-solvent interaction and the vibrational couplings among the biologically ubiquitous CH_3 and NH_2 groups [10].

Keywords: IR-VUV Spectroscopic; clusters; IRPD; Methylamine; Quantum chemical calculations

References:

[1] Esherick, P.; Owyoung. Chem. Phys. Lett. 1983, 103, 235-240.
[2] Page, R. H.; Shen, Y. R.; Lee, Y. T. J. Chem. Phys. 1988, 88, 4621-4636.
[3] Zwier, T. S. Annu. Rev. Phys. Chem. 1996, 47, 205-241.
[4] Ebata, T.; Fujii, A.; Mikami, N. Int. Rev. Phys. Chem. 1998, 17, 331-361.
[5] Buck, U.; Huisken, F. Chem. Rev. 2000, 100, 3863-3890.
[6] Matsuda, Y.; Mikami, N.; Fujii, Phys. Chem. Chem. Phys. 2009, 11, 1279-1290.
[7] Han, H. L.; Camacho, C.; Witek, H. A.; Lee, Y. P. J. Chem. Phys. 2011, 134, 144309.
[8] Hu, Y. J.; Guan, J. W.; Bernstein, E. R. Mass Spectrom. Rev. 2013, 32, 484-501.
[9] Hasegawa, H.; Mizuse, K.; Hachiya, M.; Matsuda, Y.; Mikami, N.; Fujii. Angew. Chem., Int. Ed. 2008, 47, 6008-6010.
[10] Zhang, B.; Kong, X.; Jiang, S.; Zhao, Z.; Yang, D.; Xie, H.; Hao, C.; Dai, D.; Yang, X.; Liu, Z.; Jiang, L. submitted.

High-resolution electronic spectra of yttrium oxide (YO)

I: identification of the $D^2\Sigma^+$ state

Deping Zhang, Q Zhang, B Zhu, J Gu, D Zhao,* and Y Chen *

Hefei National Laboratory for Physical Sciences at the Microscale,
Department of Chemical Physics, University of Science and Technology of China, Hefei, Anhui 230026, PR China
*Email: dzhao@ustc.edu.cn.

Yttrium oxide (YO) is an important constitute in atmospheres of cool stars, and has long been considered as a key indicator in defining the S-type stars. It is also one of the benchmark molecules used for laser cooling and molecular trapping in a magneto-optical trap (MOT). Here, we present the high resolution spectroscopic study on the $D^2\Sigma^+$–$X^2\Sigma^+$ electronic transition of YO in the 400–440 nm region using laser induced fluorescence. YO molecules are produced by corona discharge of oxygen between the tips of two yttrium needles in a supersonic jet expansion. An unambiguous spectroscopic identification of the $D^2\Sigma^+$–$X^2\Sigma^+$ transition becomes possible from a combined analysis of the moderate-resolution laser excitation spectrum and dispersed fluorescence spectrum. By using a home-made KTP crystal based single-longitude-mode optical parametric oscillator (OPO) as a narrowband light source, we have also recorded spectra of $D^2\Sigma^+$–$X^2\Sigma^+$ (0, 0) and (1, 0) bands with a spectral resolution of ~ 0.018 cm^{-1}, which allows to fully resolve the spin-rotational fine structure and partially resolve hyperfine nuclear spin splitting in the experimental spectra. Accurate spectroscopic constants for $D^2\Sigma^+$ v′ = 0 and 1 levels have been determined from a rotational analysis of the high resolution spectra. Severe perturbations are observed in the experimental spectra, and are considered to originate from interactions with at least one nearby $^{2/4}\Pi$ electronic state, e.g., the undetected $C^2\Pi$ state. We have also measured the radiative lifetimes of $B^2\Sigma^+$ v' = 0, and $D^2\Sigma^+$ v' = 0 and 1 states for the first time, based on which the $B^2\Sigma^+$–$X^2\Sigma^+$ (0, 0) and $D^2\Sigma^+$–$X^2\Sigma^+$ (0/1, 0) band oscillator strengths have been determined. The spectroscopic data presented here are of implications in astronomical observations of YO molecules in atmospheres of exoplanets and cool stars.

Keywords: YO; high-resolution spectra; laser excitation spectrum; dispersed fluorescence spectrum

References:

[1] Zhang, D. P.; Zhang, Q; Zhu, B. X.; Gu, J. W.; Suo, B. B.; Chen, Y; Zhao, D. F. *J. Chem. Phys.* **2017**, **146**:114303.
[2] Bernard, A.; Gravina, R.; *Astrophys. J. Suppl.* **1980**, **44**, 223.

Effect of Vibronically Induced Spin-Orbit Coupling on Nonradiative S-T Intersystem Crossing[#]

Song Zhang[1,2*], Lian Wang[1,2], Miaomiao Zhou[1,2], Bing Zhang[1,2]

[1] State Key Laboratory of Magnetic Resonance and Atomic and Molecular Physics, Wuhan Institute of Physics and Mathematics, Chinese Academy of Sciences, Wuhan, 430071

[2] University of Chinese Academy of Sciences, Beijing, 100049

*Email: zhangsong@wipm.ac.cn

Dibenzo compounds belongs to the group of heterocyclic fluorene analogs, which include heavy atoms on the symmetry axis.[1] Dibenzo compounds has attracted much attention since its polychlorinated derivatives as well as dibenzo-p-dioxin molecules are widely considered as harmful contaminants to people which are highly toxic environmental persistent chemicals.[2] Polychlorinated dibenzofurans present in by-products of combustion and other industrial processes, moreover they can persist a long time in environment and show great bioaccumulation and bioconcentration through food-chains.[3-5] In this work, we have investigated the ultrafast intramolecular rotation behavior of dibenzofuran in several different viscosity solutions using femtosecond time resolved spectroscopy. Ultrafast broadband absorption measurements were performed based on the Ti-sapphire femtosecond laser system. The second harmonic and the white light continuum pulses were used as the pump and probe lasers, respectively. The two laser beams were focused in the sample solution which flowed in a quartz cell with optical length of 1 mm. The angle between polarizations of both beams were set to a magic angle to avoid rotational diffusion effects. To describe properly the dynamics observed in the visible range, global fit analysis of all of the kinetics at different wavelength regions is performed with singular value decomposition. The heavy atom effect, which an increase in the probability of singlet-triplet intersystem crossing upon introduction of a many-electron atom in a hydrocarbon molecule, has been experimentally observed both in nonradiative $S_1 \rightarrow T_1$ intersystem crossing (ISC) and $T_1 \rightarrow S_0$ intersystem degradation transitions. In terms of the model of vibronically induced spin-orbit (VISO) interactions, which determine the $S_1(\pi\pi^*) \rightarrow T_n(\pi\pi^*)$ nonradiative transition, it is demonstrated that the intersystem crossing $S_1 \rightarrow T_1$ involves also the intermediate T_2 and T_3 triplet states and an effect of the heavy atom of dibenzo compounds on K_{ST} is established.

Keywords: dibenzo compounds; vibronically induced spin-orbit coupling; femtosecond time-resolved spectroscopy

References:

[1] E. A. Gastilovich, N. V. Korol'kova, V. G. Klimenko, and R. N. Nurmukhametov. *Opt. Spectrosc.*, **2009**, **106**: 311.

[2] Y. Q. Ye, C. Negishi, Y. Hongo, H. Koshino, J. Onose, N. Abe, and S. Takahashi. *Bioorg. Med. Chem.*, **2014**, **22**: 2442.

[3] 4L. L. Aylward, S. Hays, N. J. Karch, and D. J. Paustenbach. *Environ. Sci. Technol.*, **1996**, **30**: 3534.

[4] K. Y. Tsang, H. Diaz, N. Graciani, and J. W. Kelly. *J. Am. Chem. Soc.*, **1994**, **116**: 3988.

[5] L. J. Deng, J. Y. Li, G. X. Wang, and L. Z. Wu. *J. Mater. Chem. C*, **2013**, **1**: 8140.

High-resolution electronic spectra of yttrium oxide (YO)

II: spectroscopic study on the $[33.2]^2\Pi$ and $A'^2\Delta_{5/2}$ states

Qiang Zhang, D Zhang, B Zhu, J Gu, D Zhao*, and Y Chen*
Hefei National Laboratory for Physical Sciences at the Microscale,
Department of Chemical Physics, University of Science and Technology of China, Hefei, Anhui 230026, PR China
*Email: dzhao@ustc.edu.cn.

The $[33.2]^2\Pi_{1/2,\,3/2}$ and $A'^2\Delta_{5/2}$ electronic states of the astrophysically relevant yttrium oxide (YO) molecule have been experimentally studied at high resolution for the first time. The YO molecules are produced using the same method as in Part I of this work, i.e., by corona discharge of oxygen between the tips of two yttrium needles in a supersonic jet expansion. In this presentation, different spectroscopic detection schemes, including laser excitation spectroscopy, disperse fluorescence, optical-optical double resonance spectroscopy, and fluorescence depletion spectroscopy, are employed to identify the newly discovered $[33.2]^2\Pi$ state, and to precisely measure the ro-vibrational energies of the $A'^2\Delta_{5/2}$ state. The $A^2\Pi$ state is used as the intermediate resonance state in the optical-optical double resonance experiment to reveal the spin-orbital coupling nature of the $[33.2]^2\Pi$ state. To determine accurate spectroscopic constants of the 'optically dark' $A'^2\Delta_{5/2}$ state, a 'pump-probe' fluorescence depletion experiment is performed, where the newly discovered $[33.2]^2\Pi_{3/2}$ state is used in the pump scheme.

Keywords: YO; laser induced fluorescence; optical-optical double resonance

References:

[1] Field, R. W.; Revelli, M. A; *J Chem. Phys.* **1975, 63,** 3228.
[2] Bernard, A.; Gravina, R.; *Astrophys. J. Suppl.* **1983**, **52**, 443.

利用重氮基团红外探针研究局部水合环境的氢键动力学

张文凯 [1,*]

[1] 北京师范大学高等量子研究中心、物理学系，北京，100875

*Email:wkzhang@bnu.edu.cn

共价键结合的重氮基团广泛存在于生物体系中。重氮基团的C=N=N反对称伸缩振动具有很大的消光系数，并且出现在水的红外光谱窗口区。为了评估C=N=N反对称伸缩振动的溶剂化效应及其在生物体系研究中的应用，我们测量了一个模型重氮化合物2-重氮-3-氧代-丁酸乙酯在不同溶剂中的红外光谱。我们发现，C=N=N反对称伸缩振动的带宽和反映溶剂的极化率和氢键受体能力Kamlet-Taft溶剂参数存在线性依赖关系。因此，C=N=N反对称伸缩振动的带宽可以用来探测溶剂的这些性质。我们还发现C=N=N反对称伸缩振动的频率与溶剂中氢键供体基团的密度线性相关。我们还进一步利用超快红外光谱和二维红外光谱研究了天然氨基酸，6-重氮-5-氧代-L-正亮氨酸的C=N=N反对称伸缩振动的弛豫动力学和光谱扩散。C=N=N反对称伸缩振动的弛豫和光谱扩散时间常数与N=N=N反对称伸缩振动的弛豫和光谱扩散时间常数相似。我们得出结论，重氮基团的C=N=N反对称伸缩振动的频率和带宽可以分别用于探测氢键供体和溶剂的受体能力。这些研究结果表明，重氮基团可用作局部水合环境的特异性位点红外探针。

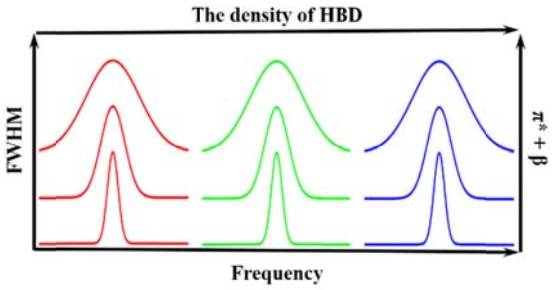

Fig. 1 重氮基团的带宽和频率可以探测溶剂的极化率和氢键给体基团的密度。

Precise phase determination in two-dimensional electronic spectroscopy

Yizhu Zhang*, T.-M. Yan, Y. H. Jiang

Shanghai Advanced Research Institute, Chinese Academy of Science, Shanghai, China
*Email: zhangyz@sari.ac.cn

In a typical two-dimensional electronic spectroscopy (2DES) experiment, the timing error of the coherence time and emission time when determining the absolute time zeros usually introduce extraneous spectral phase slopes and distort 2D spectrum. We develop new methods to calibrate the absolute phase at the exact interaction region at sub-wavelength accuracy. The new method is easily implemented without supplementary instrumental construction, only relying additional scanning and data post-processing algorithm. The new proposed methods are expected to improve the phasing procedure in 2DES in a more convenient way.

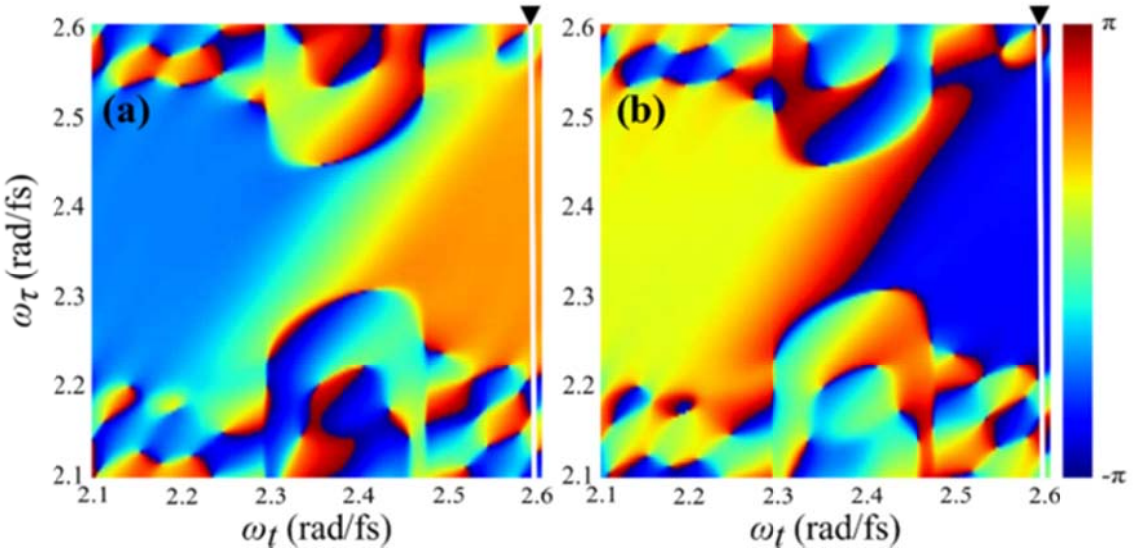

Fig. 1 The 2D profile of the phase components of the purely absorptive 2D spectra. (a) The phase component with the timing errors. (b) The phase with coherence time error $\Delta\tau$ = 1 fs.

Keywords: 2D spectroscopy; ultrafast spectroscopy

References:

[1] Q. Meng, Y. Zhang, T.-M. Yan, and Y. H. Jiang, "Post-processing phase-correction algorithm in two-dimensional electronic spectroscopy," Opt. Express, vol. 25, no. 6, pp. 6644–6652, 2017.
[2] Y. Zhang, T.-M. Yan, and Y. H. Jiang, "Precise phase determination with the built-in spectral interferometry in two-dimensional electronic spectroscopy," Opt. Lett., vol. 41, no. 17, p. 4134, 2016.

飞秒反向拉曼光谱色散线型的研究

张永燕，何玉韩，刘晨西，王静静，郭伟，王朝晖*

固体表面物理化学国家重点实验室，谱学分析与仪器教育部重点实验室，厦门大学化学化工学院，福建厦门，361005

*Email: zhwang@xmu.edu.cn

飞秒反向拉曼光谱(Femtosecond Inverse Raman pectroscopy，FIRS)是一种三阶非线型光谱，具有信号强，不易受荧光信号干扰(其信号位于拉曼泵浦光的短波一侧)等特点。然而研究发现当拉曼峰所在波长与电子跃迁发生共振时，FIRS 光谱的线型随泵浦波长而变化[1]，不同的研究都对此提出了不同的模型。β-胡萝卜素是类胡萝卜素的重要一员，在生物中具有捕光和光保护的作用。目前有多种超快光谱方法被用于 β-胡萝卜素激发态的研究[2]，因此本研究采用 β-胡萝卜素为模型体系对反向受激拉曼光谱的线型进行研究。β-胡萝卜素 $S_2 \leftarrow S_0$ 的最大吸收波长 λ_{Max} = 454 nm，0-0 跃迁的波长为 483 nm。Fig. 1 给出了不同泵浦波长下的 FIRS 光谱。由 Fig. 1 可知，共振拉曼峰的线型和强度随泵浦波长而变化。此外我们的研究还发现，不同振动模式的拉曼峰强在不同的泵浦波长下达到最大值。我们的研究结果表明 FIRS 的共振拉曼峰与激发态构型(Frank-Condon 因子和 Frank-Condon 位移)有关，因此可以借助电子激发态的理论和实验参数对 FIRS 机理进行进一步的研究。

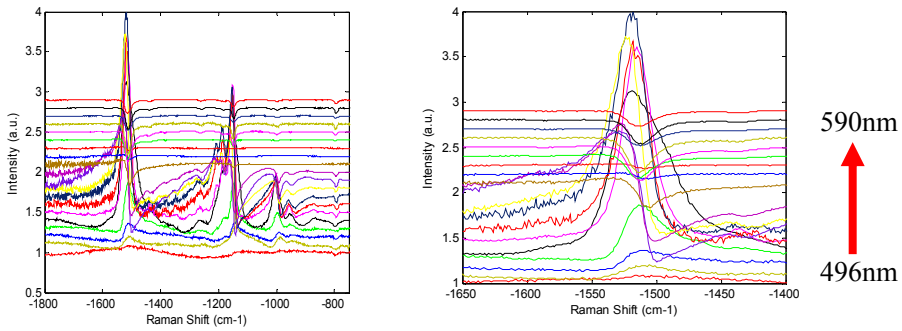

Fig. 1 不同泵浦波长下的FIRS光谱

关键词： 受激拉曼光谱；β-胡萝卜素；色散线型

参考文献

[1] Q. Cen, Y. He, M. Xu, J. Wang, Z. Wang, J. Chem. Phys. 2015, 142,114201

[2] S. Shim, R.A. Mathies, J. Phys. Chem. B 112 (2008) 4826

溶剂调控 2-环己烯酮双荧光现象的理论研究

张腾烁,郑旭明*

浙江理工大学化学系，浙江省杭州市下沙，310018

*Email: zxm@zstu.edu.cn

双荧光现象自发现以来就受到实验与理论化学家的广泛研究。N,N−二甲基氨基苯甲氰(DMABN)及其衍生物等一系列具有双荧光现象的物质均是通过 π 键连接的电子给受体。[1] 大量研究认为，两个发射带源于一个正常的局域态(LE)和一个分子内电荷迁移态(CT)。人们提出了很多理论模型来解释双荧光的现象，典型的有扭转的分子内电荷转移(TICT)、平面分子内电荷转移(PICT)模型。[2] 两类理论模型对大多数研究体系有成功的应用，但机理至今仍无明确定论。此类分子在光电开关、化学敏感器、荧光探针等分子器件开发方面的巨大潜力而持续受到关注。[3]

最近我们发现了 2-环己烯酮受溶剂调控的双荧光现象。其特殊之处在于，2-环己烯酮分子明显小于 DMABN 等具有较大共轭环的分子体系，且其电子给受体区分并不显著。对 2-环己烯酮双荧光现象的研究有助于进一步揭示双荧光发射的内在机质，并为设计具有非线性光学性质的分子提供有利参考。

我们通过量子化学计算方法，结合共振拉曼光谱技术对 2-环己烯酮在不同溶剂中的激发态驰豫路径进行了深入研究。如 **Fig. 1** 所示，溶剂极性对荧光发射光谱的跃迁能和强度都有极强的影响。高波数的荧光带几乎不随溶剂极性位移，强度随溶剂极性增强而显著下降；低波数的荧光带随溶剂极性的增强有较小的红移，强度增强。我们开展了 CASSCF 计算，选取两个 π 轨道、一个 n 轨道以及两个 π 反键轨道组成 6 电子 5 轨道的活化空间，获得了两个被认为具有荧光发射的 S_2-min 结构（如 **Fig. 2** 所示），以及多个系内转换及系间窜越交叉点。辐射跃迁与非辐射跃迁存在明显竞争。我们认为，溶剂极性对荧光量子产率的影响是由溶剂对激发态的稳定化作用的差异导致的，另外溶剂对基态（尤其是 S_2(P1)和 S_2(P2)结构下的 S0’和 S0”）势能面的移动，改变 S2-min 与 S0 的振动重叠积分，进而影响荧光的产率。

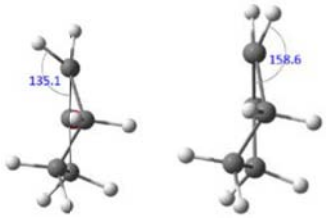

S_2(P1)-min　　S_2(P2)-min

Fig. 1 Absorption and emission spectrum of 2-cyclohexenone in different solvents

Fig. 2 S_2-min structures of 2-cyclohexenone

关键词：2-环己烯酮；双荧光；CASSCF；溶剂效应

参考文献：

[1] Rettig, W; Bliss, B; Dirnberger, K. *Chem. Phys. Letters*. **1999, 305(1)**: 8-14.

[2] Changenet, P; Plaza, P; Martin, M M; et al. *J. Phys. Chem. A*. **1997, 101(44)**: 8186-8194.

[3] Leresche, F; Von, Gunten, U; Canonica, S. *Environ Sci Technol*. **2016, 50(20)**: 10997-11007.

The Structure and Dynamics of Ions in Confined Water Environment Investigated by Infrared Spectroscopy

Dexia Zhou, Yuanchun Zhao, Hongtao Bian*

Key Laboratory of Applied Surface and Colloid Chemistry, Ministry of Education, School of chemistry and Chemical Engineering, Shaanxi Normal University, Xi'an, 710119
*Email: zdx161893@snnu.edu.cn

Water science has been the frontier of physics, chemistry, environmental science and biology studies. The hydrogen bond network of water molecule is crucial for its peculiar physical and chemical properties. However, in most of the biological related living systems, the hydrogen bond of water molecule is encountered by the biomolecules and separated in the confined environment. The water molecules confined in nanometer scale confinement showed distinct behavior compared with bulk water. The reverse micelles (RMs) provides a model systems for investigating the structure and dynamics of water molecule in confined environment. Here, we utilize the Infrared spectroscopy to study the structure and dynamics of azide (N3-) and thiocyanate (SCN-) anions in different reverse micelle systems where the anions were used as a vibrational probe to report the local structure of water molecules. At the same time, the diameter of the waterpool in different reverse micelles is measured by DLS.

The Infrared spectroscopy results demonstrated that RMs exhibit reduced polarity and a reduced and disrupted hydrogen bonding network compared to the bulk water. And Dynamic Light Scattering results showed that with the increase of ω0, the diameter of the waterpool in the reverse micelles increases. And after adding ions, the diameter of the pool in the reverse micelle has increased slightly compared to the reverse micelles without the addition of ions. The location and structure of the ions in the reverse micelle is the focus of our next study.

Keywords: confined water environment, reverse micelle system, IR(infra-red spectrum), SCN-and N3- ions, DLS

References:

[1] Zhang, S.; Li, S.; Zhou, W.; Zheng, L. *Chem. Phys.* **2011**, **135**: 14304.

[2] Das, A.; Parta, A.; Mitra, R. K. *Colloid and Polymer Science.* **2016, *294***: 715.

[3] Lepori, C. M.; Correa, N. M.; Silber, J. J.; Falcone, R. D. *Soft matter.* **2016**: ***12,*** 830.

[4] Das, A.; Patra, A.; Mitra, R. K. *The journal of physical chemistry. B.* **2013, *117***: 3593.

SC-KMC：一种兼顾精度和效率的表面催化动力学新方法

陈征[1]，王鹤[1]，徐昕[1,*]

[1] 复旦大学化学系，上海，200433

*Email：xxchem@fudan.edu.cn

动力学是连接微观基元反应和宏观催化性能的桥梁。工业条件下的表面催化，是个复杂的动态过程[1]，内禀地要求动力学方法能够精确地描述催化剂表面固有的结构和组成的不均匀性及由相互作用所引起的表面物种的空间相关性。当下，唯一在原理上能够满足该要求的是显格子动力学蒙特卡罗（on-lattice KMC）方法。然而，由于表面上存在各种过程(如迁移、快平衡、决速步等)，其时间尺度分离问题显著地制约了显格子动力学蒙特卡罗的实际可行性[2]。通过混合使用精确的显格子动力学蒙特卡罗和高效的隐格子动力学蒙特卡罗（off-lattice KMC），我们发展了一种自洽动力学蒙特卡罗(SC-KMC)方法，成功地克服了时间尺度分离的难题。SC-KMC 方法首先利用精确的显格子动力学蒙特卡罗模拟出给定覆盖度下的反应趋势，然后利用高效的隐格子动力学蒙特卡罗演化覆盖度和计算反应速率，最终互为函数的表面覆盖度及其相应的反应趋势实现自洽，体系到达稳态。基于“线性关系”[3]并考虑吸附物种间的相互作用，SC-KMC 被应用于描述过渡金属表面上的一类催化反应动力学。对一些简单体系，在给出和显格子动力学蒙特卡罗模拟一致结果的同时，SC-KMC 极大地提高了效率；然而 SC-KMC 可以处理显格子动力学蒙特卡罗无法模拟的复杂体系。模拟结果揭示了吸附物种间相互作用的重要性，表明相互作用不仅会显著地影响火山型曲线的形状，甚至会影响对催化剂理性设计最重要的山峰位置。该新方法为多相催化的理性设计提供了更精确、有效的手段。

关键词：多相催化；KMC；相互作用能；催化氨分解；火山型曲线

参考文献

[1] Li, H. P.; Fu, G.; Xu, X. *Phys. Chem. Chem. Phys.* **2012**, **14**: 16686.

[2] Stamatakis, M.; Vlachos, D. G. *ACS Catal.* **2012**, **2**: 2648.

[3] Wang, S.; *et.al. Phys. Chem. Chem. Phys.* **2011**, **13**: 20760.

Construction of potential energy surfaces for polyatomic molecules with Gaussian Process Regression: Active Data Selection

Yafu Guan[1], Shuo Yang[1], Dong H. Zhang[1,*]

[1]State Key Laboratory of Molecular Reaction Dynamics and Center for Theoretical Computational Chemistry, Dalian Institute of Chemical Physics, Chinese Academy of Sciences, Dalian 116023, People's Republic of China

*Email: zhangdh@dicp.ac.cn

Gaussian Process (GP) Regression is an efficient non-parametric method for constructing multi-dimensional potential energy surfaces (PESs) for polyatomic molecules. Since not only the posterior mean but also the posterior variance can be easily calculated, gaussian process regression provides a well-established model for active learning, through which PESs can be constructed more efficiently and accurately. We propose a strategy of active data selection for the construction of PESs with emphasis on low energy regions. Through a 1D example of potential curve for H_2, the validity of this strategy is verified. The PESs for two prototypically reactive systems, namely, the $H + H_2 \rightarrow H_2 + H$ and $H + H_2O \rightarrow H_2 + OH$ reactions are reconstructed. Only 103 and 920 points are assembled to reconstruct the two PESs respectively. The accuracy of the GP PESs is not only tested by fitting errors but also validated by quantum scattering calculations.

Keywords: Potential energy surface; Gaussian Process Regression; active learning

References:

[1] C. Jie and V. K. Roman, *Journal of Physics B: Atomic, Molecular and Optical Physics* 49, 224001 (2016).

[2] J. Chen, X. Xu, X. Xu, and D. H. Zhang, *The Journal of Chemical Physics* **138**, 154301 (2013).

[3] C. E. Rasmussen and C. K. I. Williams, *Gaussian processes for machine learning*, Adaptive computation and machine learning (MIT Press, Cambridge, Mass., 2006) pp. xviii, 248 p.

[4] B. Kolb, P. Marshall, B. Zhao, B. Jiang, and H. Guo, *The Journal of Physical Chemistry A* **121**, 2552 (2017).

[5] S. Sambu, M. Wallat, T. Graepel, and K. Obermayer, in *Proceedings of the IEEE-INNS-ENNS International Joint Conference on Neural Networks. IJCNN 2000. Neural Computing: New Challenges and Perspectives for the New Millennium*, Vol. 3, pp. 241-246 vol.3.

低能量离子–分子反应的离子速度成像装置

胡婕，吴春晓，王旭东，田善喜*

中国科学技术大学化学物理系，合肥微尺度物质科学国家实验室，安徽合肥，230026

*Email: sxtian@ustc.edu.cn

离子–分子反应是一类重要的化学过程，是星际空间和燃烧中的物质演化关键步骤之一。我们拟开展低能量离子与分子碰撞反应动力学实验研究，自主设计了离子速度成像装置，仪器包括离子束源、分子束源和产物离子成像三部分。此前，国际上的实验组采用电子–分子碰撞、激光溅射、等离子体放电等技术[1]产生正/负离子，但难以控制离子束的能量分散，导致产物离子速度切片成像模糊[2]。

为了获得离子–分子反应更多详细的立体动力学信息，我们设计并完成采用交叉束研究的低能量离子–分子反应速度成像装置的安装和部分调试工作。利用二次脉冲的能量补偿和一系列偏转、聚焦和限孔透镜获得能量、时间、空间分布均较窄的脉冲离子束后，与超声分子束进行单次碰撞，产物离子经设计的新型离子速度成像透镜系统得以获得更好的空间聚焦、动量和质量分辨。

关键词：离子–分子反应；离子束；离子速度成像

参考文献

[1] Z. Herman, *Int. J. Mass Spectrom.* **2001, 212**: 413

[2] Xie J.; Otto R.; Mikosch J.;Zhang J.; Wester R.; Hase W. L., *Acc. Chem. Res.* **2014, 47**: 2960

燃烧反应机理的多尺度粗粒化表达

吉琳*，宁安，张乃新

首都师范大学化学系，100048

*Email: jilin@mail.cnu.edu.cn

复杂燃烧反应微观机制的有效简化表达是连接燃烧化学机理研究和燃烧流体力学研究的关键桥梁。本项目基于燃烧的耗散结构本质，提出燃烧反应机理研究应以提炼宏观唯象机制上的反馈回路为目标，以“粗粒化”的思想研究燃烧反应动力学。拟发展包括反应“微态聚类”统计、介观多通路反应的“涨落化”的表示，以及宏观机制中反馈环路的提炼的三个层次的多尺度粗粒化具体方法。通过动力学蒙特卡洛（KMC）等方法实现具体反应过程的演化模拟，建立符合统计规律的燃烧反应机理多尺度粗粒化表达，实现机理模型的有效简化，从而达到将燃烧反应机理研究结果有效服务于燃烧流体力学研究的目的。

Stationary state distribution and efficiency analysis of Langevin dynamics in real dynamics and virtual dynamics regions

Dezhang Li[1], Xu Han[1], Yichen Chai[1], Cong Wang[2], Jian Liu[1, a)], Jiushu Shao[2, b)]

[1]Beijing National Laboratory for Molecular Sciences, Institute of Theoretical and Computational Chemistry, College of Chemistry and Molecular Engineering, Peking University, Beijing, 100871
[2]College of Chemistry and Center for Advanced Quantum Studies, Key Laboratory of Theoretical and Computational Photochemistry, Ministry of Education, Beijing Normal University, Beijing, 100875
a) Email: jinaliupku@pku.edu.cn
b) Email: jiushu@bnu.edu.cn

Langevin dynamics is a typical thermostat for canonical MD simulations. Various schemes may be proposed for numerical integration of the Langevin equation. Accuracy and efficiency of the simulation strongly replies on the numerical algorithm employed to solve the Langevin equation. In this article, we study twelve useful schemes for Langevin dynamics. For both the stationary state distribution and the characteristic correlation time of the one-dimensional harmonic system, we introduce two approaches to investigate the twelve schemes. They include a direct approach that is based on the trajectory of Langevin dynamics, and an indirect approach that employs the mean value and the phase space propagator. All the schemes are employed in the MD simulations of two model systems (harmonic potential and quartic potential).

Keywords: Langevin dynamics; numerical algorithms; stationary state distribution; characteristic correlation time

References:

[1] Leimkuhler, B.; Matthews, C. *J. Chem. Phys*. **2013**, **138**: 174102.
[2] Grønbech-Jensen, N.; Farago, O. *Mol. Phys*. **2013**, **111**: 983.
[3] Liu, J.; Li, D.; Liu, X. *J. Chem. Phys*. **2016**, **145**: 024103.

A novel time of flight spectrometer for crossed beam experiment of elementary chemical reactions

Lulu Li[1,2], Xing-an Wang[2], Chunlei Xiao[1,*], Xueming Yang[1,2,*]

[1]State Key Laboratory of Molecular Reaction Dynamics, Dalian Institute of Chemical Physics, Chinese Academy of Sciences, Zhongshan Road 457, Dalian, 116023

[2]Department of Chemical Physics, University of Science and Technology of China, Jinzhai Road 96, Hefei, 230026

*Email: chunleixiao@dicp.ac.cn, xmyang@dicp.ac.cn

We develop an apparatus in Dalian Coherent Light Source for investigating elementary chemical reaction using time of flight Rydberg tagging method. In this apparatus, the angle between the crossed beams can be minimized to 15 degree so we can study dynamics of chemical reaction at very low collision energy. For example, in the benchmark reaction $F+H_2 \rightarrow HF+H$, the collision energy can reach few cm^{-1}. Especially, we use a 15-channel detector covering 112 degree in laboratory frame which is a powerful tool for measuring differential cross section. Relying on the detector we can study some special reactions with low cross section and save valuable FEL machine time in DCLS.

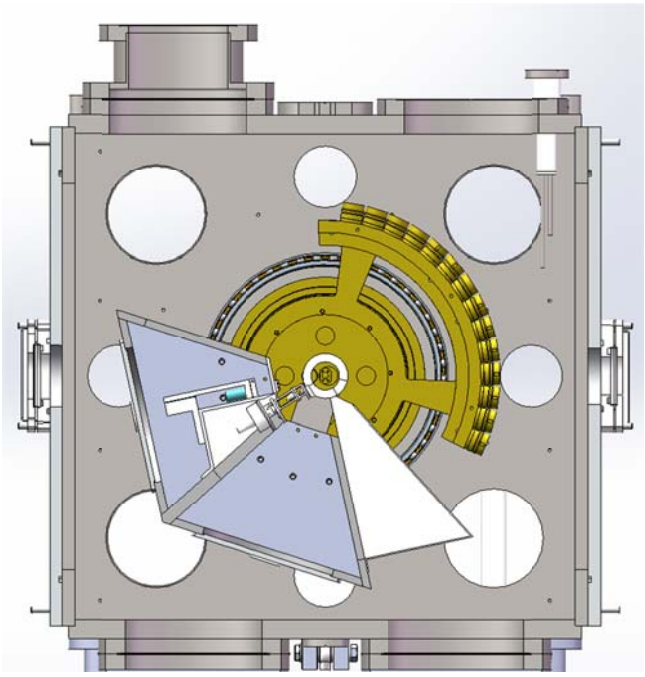

Fig. 1 Section view of the apparatus

Keywords: Crossed beam; Low collision energy; reaction dynamics; multichannel detectors;

References:

[1] Minghui Qiu; Li Che; Zefeng Ren; Dongxu Dai; Xiuyan Wang; Xueming Yang. Review of Science Instruments 76, 083107 (2005)

String Method Study on the Proton Transfer Process of a simplified model system from CcO D-channel

Runze Liu[1], Keli Han[1,*]

[1]Dalian Institute of Chemical Physics, 457 Zhongshan Road, Dalian, Post code 116023
*Email: klhan@dicp.ac.cn

The cytochrome c oxidase d-channel is responsible for the uploading of all pumping protons through the membrane. However, the water wire in the channel is often blocked by the two Asn residues near the entrance. The proton loading process could become complex because the rotation of Asn is coupled to the water wire reformation. We proposed a possible mechanism of loading a proton using Asn residue as an intermediate. Thus we build a simplified model system to investigate this process. Three residues Asp, Asn, and Asp are solvated in a water droplet and the proton transfer process goes upward through the rotation of Asn. The whole proton transfer process involves more than three collective variables to describe, so string method is the ideal approach for this study. Both SMCV[1] and FTSM[2] methods are carried out to calculate the minimum free energy path and the free energy profile with the contribution of entropy. The results are further validated by umbrella sampling results and higher DFT level method by FEP. Committor analysis shows that both O-H distances and rotation dihedrals are required to describe the process, and string method is capable of calculating such complex transfer process involves a "hard" degree of freedom (O-H-O bond distances) combined with a "soft" process (residue group rotation). Also our model reveals that the proton transfer through Asn is possible in biological systems and could be a potential competing mechanics of proton loading in d-channel of CcO. Further study is needed to perform in the real CcO d-channel.

Keywords: Proton transfer; SCC-DFTB; String method; SMCV; FTSM;

References:

[1] Maragliano, L.; Fischer, A.; Vanden-Eijnden, E.; Ciccotii, G.; *J. Chem. Phys.* 2006, 125:02406.
[2] Vanden-Eijnden, E.; Venturoli M.; *J. Chem. Phys.* 2006, 125:02406.

Ultrafast Liquid-jet Photoelectron Spectroscopy of Hydrated Electron: A New Method for Directly Tracking Electrons in Aqueous Solutions

Jinyou Long(龙金友)[1], Ziheng Qiu(邱梓恒) [1], Kai Liu(刘凯) [1],Bing Zhang(张冰)[1,*]

[1]State Key Laboratory of Magnetic Resonance and Atomic and Molecular Physics, Wuhan Institute of Physics and Mathematics, Chinese Academy of Sciences, Wuhan 430071, China
*Email: bzhang@wipm.ac.cn

Water is important for life, however, it is surprising that the seemingly simplest electronic structure quantity, that is, the binding energy (BE) of electrons in the highest occupied molecular orbital (HOMO), from given aqueous solutions is relatively unknown for a long time. This is because photoelectron spectroscopy (PES) of liquids is technically difficult due to the incompatibility of using volatile liquids with the high vacuum required for PES. Recently, ultrafast photoelectron spectroscopy from highly volatile liquids, especially from water and aqueous solutions, has become possible due to the development of the vacuum liquid microjet technique (shown in the inset of Fig.1)and has succeeded in the direct mearsurement of the BE of hydrated electron (e^{-1}(aq)), suggesting that it could be applied to study ultrafast dynamics of excited molecules in solutions [1].

Currently, we have also succeeded in building this kind of new experimental setup and extended our research field from the gas phase to the liquid phase. Herein, we describe a detailed spectrometer characterization based on the spectroscopy of nitric oxide in the gas phase, and then present the direct measurement of the vertical binding energy (VBE) of a hydrated electron in bulk water by using the time-resolved photoelectron spectroscopy (TRPES) of the charge-transfer-to-solvent (CTTS) reaction in aqueous NaI solution. More importantly, the observed time-dependent PKED also reveals a wealth of information on the ultrafast CTTS dynamics, i.e., the evolution of the solvated electrons (e^{-1}(aq)) (as shown in Fig.1).

Applications of liquid-jet PES go well beyond the example given here, including such as solvation of biological relevant molecules by water, aqueous electron attachment, charge-transfer and light-energy conversion processes. And thus we are looking forward to gaining new insights into the in situ photoreactions that are closely related to real life science within aqueous environment.

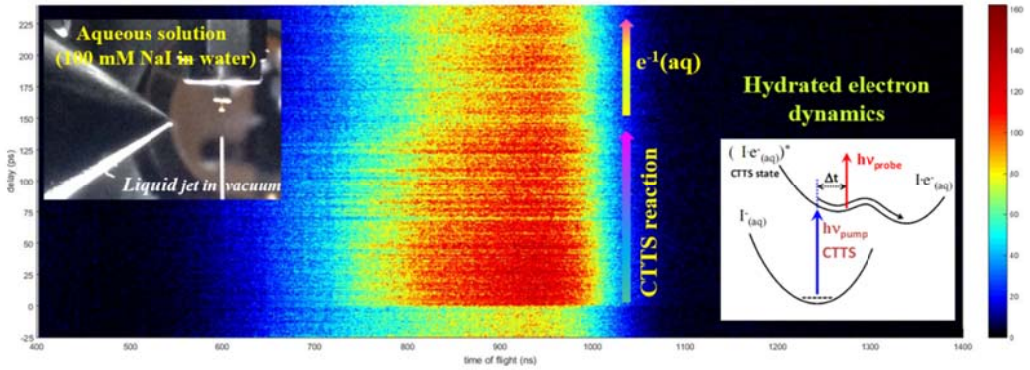

Fig. 1 Liquid-jet photoelectron spectroscopy of hydrated electron

Keywords: water; hydrated electron; aqueous solution; photoelectron spectroscopy

References:

[1] K. R. Siefermann et al., Nature Chem., 2, 274(2010).

微波化学反应动力学模型构建

马建毅

四川大学原子与分子物理研究所

Email: majianyi81@163.com

微波化学与传统加热化学相比有许多独特的优势。但由于微波的能量远低于任何化学反应所需要的能量，使得人们对微波作用何以显著的影响化学反应行为存有许多的疑问。虽然近 30 年来有许多机制被提出，但都不能圆满的解决微波化学的问题。我们用量子态识别的主方程方法构建了微波反应的动力学模型，包含的微波反应中可能存在的各种机制。结合 KMC 方法，我们对微波作用下的单分子解离过程进行了模拟。发现微波作用不仅可以激活体系中的快速反应量子态，还会使得反应物振转态分布严重地偏离平衡分布。这方面工作有望解决存在微波合成领域近 30 年的关于微波非热效应的争议。为了进一步研究微波作用的详细行为，我们以燃烧反应中最重要的反应 O+OH←→H+O_2 为例（图 1），用量子动力学的方法讨论了微波调控反应的可行性。

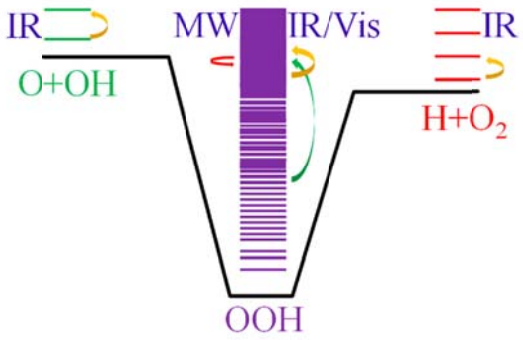

图 1 O+OH←→H+O_2 反应的微波调控

参考文献

[1]1Jianyi Ma, Master Equation Analysis of Thermal and Nonthermal Microwave Effects, *J. Phys. Chem. A* 2016, 120, 7989

Application of weak accelerating field to ion velocity map imaging

Wenke Qi [1,2], Pan Jiang [1,2], Dan Lin[1,2] , Min Cheng[1,*] , Yikui Du[1] , Qihe Zhu[1,*]

[1] Beijing National Laboratory of Molecular Sciences, State Key Laboratory of Molecular Reaction Dynamics, Institute of Chemistry, Chinese Academy of Sciences, Beijing 100190, China
[2] University of Chinese Academy of Sciences, Beijing 100049, China
*Email: chengmin@iccas.ac.cn#

A novel time-sliced ion velocity map imaging translational spectrometer using weak accelerating field has been designed to measure the speed and angular distributions of photodissociation products directly and simultaneously. The innovating of this approach is adopting a weak electric field (10~30 V/cm) rather than traditional strong electric field (100~300 V/cm) to accelerate ionic fragments before a period of field free expansion. The overall length of the flight path from the laser interaction region to the detector is merely 12 cm, therefore, it owns some unique advantages such as concise structure, easy to operate and maintain .Ions trajectories simulation and experimental study of multiphoton ionization and dissociation of O_2 at 224.999 nm was conducted as a standard system to calibrate ion images and examine the overall performance of the new approach. A weak accelerating field spreads the arrival time of O^+ over 0.36 μs, which provides sufficient time to conduct slicing. The resolution of velocity ($\Delta v/v$) in this experiment was calculated to be about 0.8%, which is superior to most previous reported results using strong accelerating field.

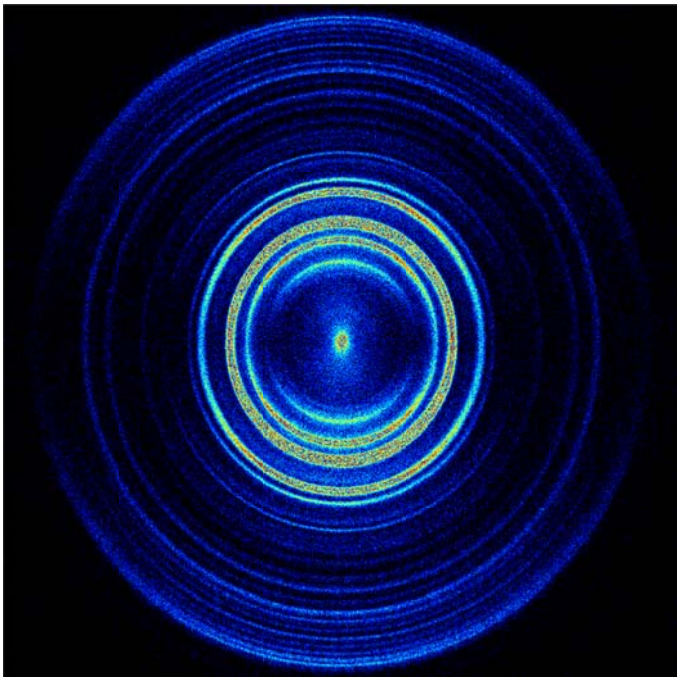

Fig. 1 Time-sliced image of O^+ from multiphoton ionization/dissociation of O_2 at 224.999 nm using photofragment translational spectrometer with weak accelerating field

Keywords: Velocity map imaging; Weak field accelerate; Photodissociation;

超快时间分辨紫外光电子能谱装置

商辰尧，王天骏，郝群庆，周传耀*，杨学明*

大连化学物理研究所分子反应动力学国家重点实验室，辽宁省大连市中山路，116023

[2]工作单位，地址，邮编

*Email: chuanyaozhou@dicp.ac.cn, xmyang@dicp.ac.cn

对超快电荷动力学和反应动力学最直接的探测方法是超快时间分辨的泵浦-探测技术。我们使用高次谐波产生技术，研制了一台超快时间分辨的极紫外光电子能谱装置，拟将其应用于与能源环境密切相关的表界面催化和光催化反应的超快动力学的研究中，如TiO_2表面的光催化等。

用UPS测量泵浦光诱导后表面吸附分子的分子轨道和催化剂本身的价带电子结构随泵浦光和UPS探测光之间延时的变化，探测表面过程的动力学，“实时”观测表界面催化和光催化过程，理解表界面催化和光催化的微观机制及影响因素，优化构效关系，为新型高效催化剂和光催化剂的合成提供理论基础。

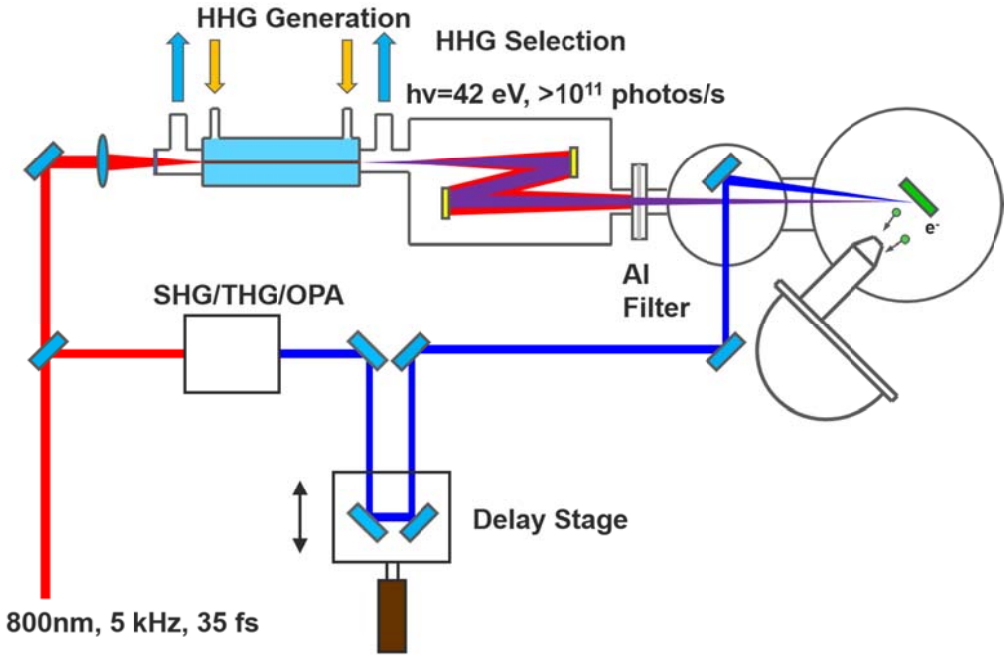

Fig. 1 Experimental setup

关键词：高次谐波；极紫外光电子能谱；光催化反应；二氧化钛

参考文献

[1] Mathias et al, Rev Sci Instrum, 78, 083105 (2007)

催化反应过程中反应中间体原位质谱探测系统的研制

施再发[1]，林水潮[1]，唐紫超*,[1]，郑兰荪[1]

[1] 固体表面物理化学国家重点实验室，厦门大学化学化工学院，厦门，361005

*Email: zctang@xmu.edu.cn

化学反应从反应物到最终生成物往往需要经过一系列的中间过程。对反应过程中自由基与反应中间体的认识是控制反应过程的关键。自由基和反应中间体不易分离和检测，目前一般都是通过量子化学计算等研究手段间接推测其存在。传统的核磁、高分辨质谱、高效气/液相色谱、红外光谱、激光荧光光谱等仪器只能用来进行终产物的分析与鉴别。目前还没有一个通用的、针对自由基和反应中间体的分析测试仪器。我们实验室搭建了一套原位中间体探测系统。该系统将常压反应器与飞行时间质谱联用，采用分子束取样技术可以对反应过程中的不稳定中间体、自由基进行原位取样，且分子间不发生碰撞，可以有效地冷却不稳定产物。电离池紧贴着采样锥，在分子束最强的位置采用真空紫外单光子进行电离，保证分子束的最大效率利用。该系统灵敏度高，分辨率优于 3000，可直接用于甲烷无氧转化、甲醇制烯烃过程中自由基和不稳定中间体的检测，为反应机理的推测提供可靠的实验依据[1]。

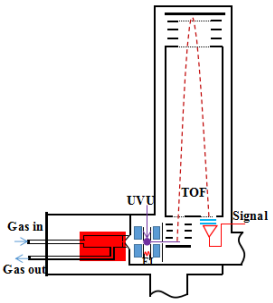

Fig. 1 Schematic diagra (TOF- time of flight mass spectrometry,UVU-Vacuum Vltraviolet)

关键词： 原位反应；分子束飞行时间质谱；自由基，中间体，反应机理

参考文献

[1] Guo X.; Fang G.; Li G.; Ma H.; Tang Z.; Bao X. et al. *Science.*2014, 344: 616

量子态分辨的分子束-表面解离动力学实验研究装置

吴家伟，申琦琦，汪涛*，杨学明*

中国科学院大连化学物理研究所分子反应动力学国家重点实验室 大连市中山路 457 号 116023

wtxlx04@dicp.ac.cn ; xmyang@dicp.ac.cn

分子在金属表面的解离吸附在多相催化、腐蚀等过程中占有非常重要的地位，通常是气体在金属表面各种反应的速控步骤。分子在金属表面的解离吸附，不仅取决于金属表面的性质，也取决于分子本身的平动能和所处的量子态。对于存在一定反应势垒的吸附过程，提高分子的平动能可以提高分子的吸附几率，而处于不同激发态的分子，也能提高反应活性，因而深入研究不同量子态分子在金属表面的反应动力学十分有助于加深对解离动力学的理解。

为了实现态分辨的分子束表面解离研究，我们设计了本装置。本装置共有四个真空腔室，第一级为束源室，用来产生超声分子束，第二级与第三级主要用来分子束质量提高，第四级为主腔室，用来进行反应与表征，表面的表征仪器有 LEED 与 AES 谱仪，信号的探测装置为四级杆质谱仪，窄线宽激光器来高效率制备不同量子态的分子束，从而实现量子态分辨的目的。由于氢分子比较简单，针对其的前期研究较多，在铜表面的解离吸附已经是检验动力学模型和电子结构计算精确性的一个基准体系，因此我们装置首先选择该反应进行研究，现在已经在信号测试中。

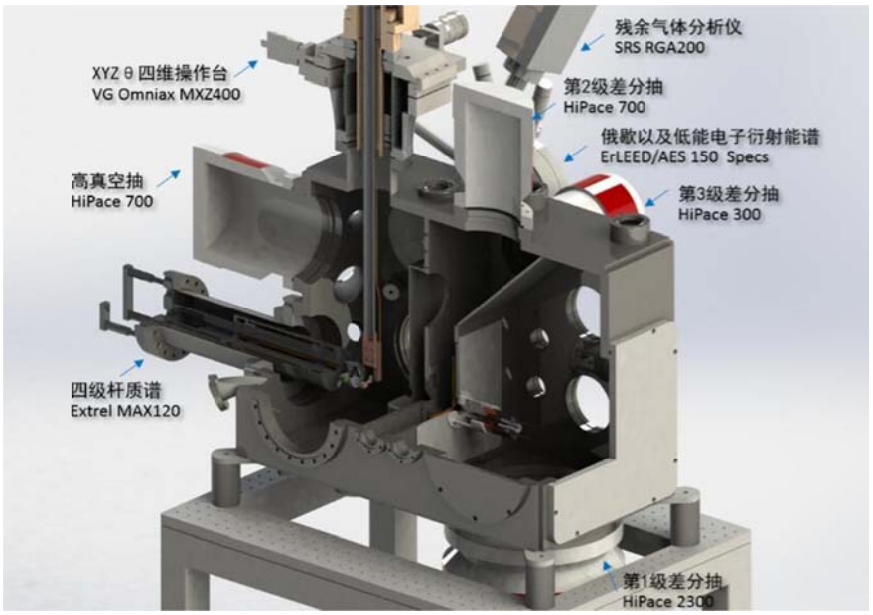

图 1. 实验装置图

参考文献

[1] Wang, T.; Yang, T.; Xiao, C.; Dai, D.; Yang, X. ***The Journal of Physical Chemistry Letters***, 2013, 368.

[2] Wang, T.; Chen, J.; Yang, T.; Xiao, C.; Sun, Z.; Huang, L.; Dai, D.; Yang, X.; Zhang, D. H. ***Science***, 2013, 342,1499.

兼顾精度和效率的催化剂理性设计新策略

——在理性设计双金属催化剂催化氨分解反应中的应用

王鹤[1]，陈征[1]，徐昕[1,*]

[1] 复旦大学化学系，上海，200433

*Email：xxchem@fudan.edu.cn

在理论上精确描述多相催化的基础上，寻找催化性质的描述子并研究这些描述子如何确定催化剂的活性和选择性，是基于计算的催化剂理性设计中最重要也最具挑战的难点。目前，应用最为广泛的策略[1]是，以某一个或两个表面吸附物种的吸附能作为描述子，基于拟合关系得出反应网络其他物种的能量，结合动力学方法描绘一维或二维的火山型曲线，以搜索最优催化剂。然而，已有文献报道[2]拟合关系的精度大大限制了该策略预测活性和选择性的能力。在大跨度的“催化地图”上确认最佳活性区域，应保证效率优先，基于拟合关系的策略可以满足要求。但在最佳活性区域中，通过穷举策略筛选催化剂依旧十分低效。因此，需要既能保证精度又能兼顾效率的新策略。我们通过引入能量跨度[3]的概念用以标准化反应网络中过程的概念并定量化过程，进而提出竞争过程能量跨度以及相应的决速态的概念，再以之为描述子实现催化剂的理性设计，同时利用自洽的动力学蒙特卡洛方法（SC-KMC）[4]快速预测新催化剂的活性。与此相比，单一的能量跨度[3]和决速态[5]并不能很好地指导催化剂设计，其原因是经典的 Sabatier 规律意味着最优催化剂通常是活化过程和脱附过程竞争的结果。我们通过过渡金属最密堆积面催化氨分解反应为例来阐明该策略，并从理论上预测了一些活性更好的催化剂。我们发现：新策略预测的活性和完整动力学得到的活性几乎一致；反应活性对决速态相关的相互作用能很敏感；考察基于拟合关系的策略，一些好的催化剂并不在其预测的峰值附近，原因是 N*的吸附能与竞争过程决速态 TS(NH_2-H)拟合关系不显著，导致 N*的吸附能并不是一个很好的描述子。

关键词：多相催化；描述子；竞争过程能量跨度；SC-KMC；氨分解

参考文献

[1] Medford, A. J.; Vojvodic, A.; Hummelshøj, J. S.; Voss, J.; Abild-Pedersen F.; Studt, F.; Bligaard, T.; Nilsson, A.; Nørskov, J. K. *J. Catal.* **2015**, **328**: 36.

[2] Sutton, J. E.; Vlachos, D. G. *J. Catal.* **2016**, **338**: 273.

[3] Amatore C., Jutand A. *J. Organomet. Chem.* **1999**, **576**: 254.

[4] Chen Z.; Wang H.; Su N. Q.; Xu X. in preparing.

[5] Kozuch, S.; Shaik, S. *Acc. Chem. Res.* **2011**, **44**: 101.

VUV 激光解吸/电离质谱成像（VUVDI-MSI）

王佳[1]，刘峰[1]，王朝英[2]，莫宇翔[1,*]

[1]清华大学物理系原子分子纳米科学教育部重点实验室，北京 100084

[2]清华大学化学系，北京 100084

*Email: ymo@mail.tsinghua.edu.cn

质谱成像广泛应用于材料，生物，药学等领域的研究。目前广泛使用的质谱成像方法为SIMS（二次离子质谱）和MALDI（基质辅助激光解吸电离飞行时间质谱）。SIMS的空间分辨率可达亚微米，但仅能获得小质量的样品碎片成像信息（m/z <500）；MALDI可以得到大质量（高达10^5 Da）母体离子，但由于基质效应，该方法的空间分辨率仅能达到微米级别，难于用于研究微小尺寸样品（如单细胞）。

为了获取高的空间分辨率以及较大质量的样品离子信号，我们实验室最近搭建了一台VUV激光解吸/电离质谱成像（VUVDI-MSI）装置。三束准直基频光通过恒温的四波混频汞蒸气池，产生波长为125.4 nm的高强度VUV激光（约为100微焦耳/脉冲）[1]。通过设计分光和聚焦光路，使得空间分辨率约为4微米，获得了大量样品分子的质谱以及指纹、果蝇大脑切片、小鼠食管组织切片、小鼠卵细胞、青蛙卵细胞，斑马鱼卵细胞等样品的VUV质谱成像。这些结果表明，VUV溅射光源具有波长可调，溅射深度较浅、不需要添加基质、且比SIMS灵敏度更高等优点。

关键词：VUV激光；四波混频； 质谱成像

参考文献

[1] D. R. Albert, D. L. Proctor and H. F. Davis, *Review of Scientific Instruments*, **2013**, **84**: 063104.

Revised M06-L Functional

Ying Wang[1], Xinsheng Jin[1], Haoyu S. Yu[2], Donald G. Truhlar[2] and Xiao He[1,3*]

[1]School of Chemistry and Molecular Engineering, State Key Laboratory of Precision Spectroscopy, East China Normal University, Shanghai, 200062, China

[2]Department of Chemistry, Chemical Theory Center, Nanoporous Materials Genome Center, and Minnesota Supercomputing Institute, University of Minnesota, Minneapolis, Minnesota, 55455-0431, USA

[3]NYU-ECNU Center for Computational Chemistry at NYU Shanghai, Shanghai, 200062, China

*Email: xiaohe@phy.ecnu.edu.cn

M06-L has proven to be one of the most accurate local functionals currently available, but it has room for improvement with regard to numerical stability and overall accuracy. Here we present a revised M06-L functional, named revM06-L, which gives both smoother potential energy curves and improved overall accuracy, especially for chemical reaction barrier heights, noncovalent interactions, and solid-state physics. We obtained the revM06-L functional by optimizing against a larger database than had been used for M06-L and by using smoothness restraints. The mean unsigned error (MUE) of revM06-L on 422 chemical energies is 3.07 kcal/mol, which is improved from 3.57 kcal/mol calculated by M06-L. The MUE of revM06-L for the chemical reaction barrier height database (BH76) is 1.98 kcal/mol, which is improved by more than a factor of 2 with respect to the M06-L functional. The revM06-L functional gives the best result among local functionals tested for the noncovalent interaction database (NC51), with an MUE of only 0.36 kcal/mol, and the MUE of revM06-L for the solid-state lattice constant database (LC17) is about half of that for M06-L. The revM06-L functional also predicts more accurate results than M06-L in 6 out of 7 diversified test sets not used for parameterization. We conclude that the revM06-L functional is well suited for a broad range of applications in chemistry and condensed matter physics.

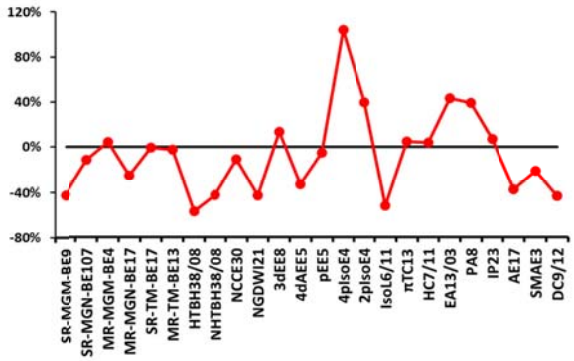

Fig. 1 The percentage change in MUEs of revM06-L relative to M06-L on atomic and molecular energetic databases

Keywords: DFT; local functional; M06-L; barrier height; noncovalent interactions; chemical energies

References:

[1] Zhao, Y.; Schultz, N. E.; Truhlar, D. G., J. *Chem. Theor. Comput*. **2006, 2:** 364-382.

[2] Yu, H. S.; He, X.; Truhlar, D. G., *J. Chem. Theor. Comput.* **2016, 12:** 1280-1293.

[3] Yu, H. S.; He, X.; Li, S. L.; Truhlar, D. G., *Chem. Sci.* **2016, 7:** 5032-5051.

[4] Zhao, Y.; Truhlar, D. G., *J. Chem. Phys.* **2006, 125:** 194101.

双原子-双原子非弹性散射中改良的 CS 近似

杨东铮[1]，张东辉[2]，谢代前[1,*]

[1] 南京大学化学化工学院, 理论与计算化学研究所, 介观化学教育部重点实验室, 南京, 江苏 210093, 中国
[2] 中国科学院大连化学物理研究所，分子反应动力学国家重点实验室理论与计算化学中心，大连，辽宁 116023，中国
*Email: dqxie@nju.edu.cn

由于大量的矩阵变换、操作，使用非含时全维量子力学方法求解四原子反应体系动力学方程十分困难。采用CS近似[1-2]方法使矩阵解耦分块，可以大大减少计算量。但在某些体系下，这样做会引入不可忽略的误差[3]。我们在CS近似的基础之上，提出了一种包含邻近K耦合的CS近似用于求解双原子-双原子体系非含时耦合方程组。在物体固定坐标系中，该方法沿用了原CS近似将矩阵按照量子数K来分块的思想实现矩阵解耦，所以其保持了原CS近似的占用内存小、传播速率快等优点。我们在BKMP势能面[4]上做了*para-ortho* H_2+H_2和*para*-H_2+HD的数值测试。结果表明，包含邻近K耦合的CS近似与严格解的差异程度远远小于原CS近似与严格解的差异，尤其是在两个双原子分子初始转动量子数之和j_1+j_2较大时。我们期望这种把科里奥利耦合加入CS近似当中的方法也可以在其他体系应用。

关键词：非含时方法；耦合方程组；CS近似；科里奥利耦合

参考文献

[1] R. T. Pack, *The Journal of Chemical Physics* 60 (2), 633-639 **(1974)**.
[2] P. McGuire and D. J. Kouri, *The Journal of Chemical Physics* 60 (6), 2488-2499 **(1974)**.
[3] G. Hahne, *Journal of mathematical physics* 25 (8), 2567-2575 **(1984)**.
[4] A. Boothroyd, P. Martin, W. Keogh and M. Peterson, *The Journal of chemical physics* 116 (2), 666-689 **(2002)**.

原子、分子以及自由基的高效电离探测——大连相干光源光束线

杨家岳[1]，李钦明[1]，俞盛锐[3]，史磊[1]，魏珅[2]，杜学维[2]，贺博[2]，李朝阳[2]，汪啸[2]，刘群[2]，刘良宝[2]，余永[1]，丁洪利[1]，王光磊[1]，陶凯[1]，王秋平[2]，戴东旭[1]，张未卿[1,*]，杨学明[1,*]

[1]中国科学院大连化学物理研究所，大连市中山路457号，116023
[2]中国科学技术大学国家同步辐射实验室，合肥市合作化南路42号，230029
[3]浙江师范大学，杭州市萧山区宁围镇萧山高教园耕文路1108路，311231
*Email: weiqingzhang@dicp.ac.cn; xmyang@dicp.ac.cn

绝大多数原子、分子以及自由基的电离能集中在10ev附近，对应的光波波长在极紫外波段。因此获得高品质的极紫外激光可以实现它们的高效探测。最近，已经建成并成功出光的大连相干光源是目前世界上首套HGHG模式的极紫外波段自由电子激光用户装置，可以为用户提供高品质的极紫外激光。该激光波长范围为50-150nm，单脉冲能量大于100μJ，脉宽1ps，脉冲重复频率1-50Hz。为了把光源产生的高品质激光传输到实验站，达到用户科学研究的需求，我们设计建造了一套高效的激光传输系统，该套光束线系统是国内首条自由电子激光光束线（Fig.1）。该光束线系统可以对光源产生的极紫外激光能量进行实时测量，可连续调节末端实验站的激光脉冲能量，并且实现光源超高真空系统与末端实验站用户装置不同真空度之间的对接。另一方面，通过精心设计的光谱仪，我们可以实现光谱的实时在线诊断（光谱分辨率大于10000）。目前，大连相干光源光束线一共有4条分支，极紫外自由电子激光已经成功传输到实验站末端，并满足用户需求。

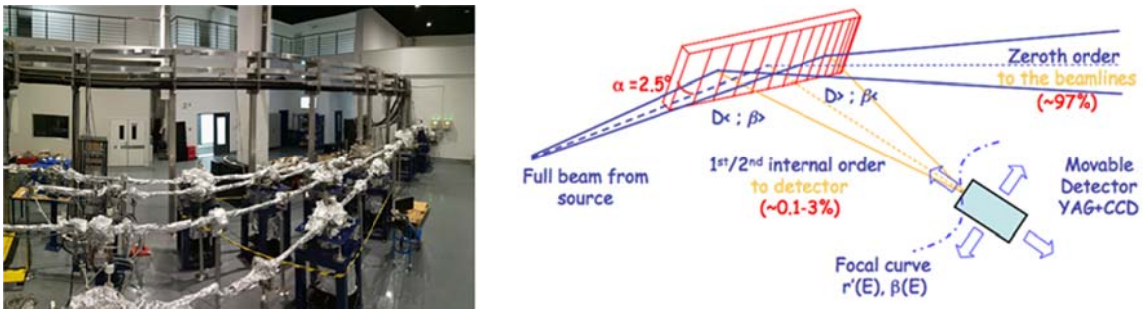

Fig. 1 Photo of beamlines and schematic diagram of spectrometer

关键词：大连相干光源；自由电子激光；极紫外；光电离

Double-Hybrid Density Functionals for Noncovalent Interactions

Feng Yu*

School of Science, Xi'an Technological University, No. 4 Jinhua North Road, Xi'an, 710032
*Email: fengyu@xatu.edu.cn

Noncovalent interactions play important roles in the physical and life sciences, and therefore, developing and assessing advanced density functionals for noncovalent interactions are very important for theoretical and computational chemistry.[1,2] In this abstract, we briefly summarize some representative double-hybrid density functionals (DHDFs) fitted by us for noncovalent interactions. Moreover, the recommended basis sets and corresponding counterpoise (CP) corrections[3] for these DHDFs are also presented as follows.

- B2NC-PLYP: 6-311+G(2df,2p) (non-CP), aug-cc-pVTZ (non-CP).[4]
- 1DH/LS1DH-PWB95-NC: def2-QZVP (non-CP), def2-TZVPP (half-CP).[5]
- DSD/DOD-PBEP86-NL: def2-QZVP (non-CP), cc-pVXZ (X=5, 6) (non-CP), cc-pVXZ (X=T, Q) (half-CP), aug-cc-pVXZ (X=T, Q) (half-CP), def2-TZVPP (half-CP), def2-TZVPPD (half-CP).[6,7]

Keywords: Noncovalent Interactions; Double-Hybrid Density Functionals (DHDFs)

References:

[1] Su, N. Q.; Xu, X. *Annu. Rev. Phys. Chem.* **2017**, **68**: 155.
[2] Goerigk, L.; Grimme, S. *WIREs Comput. Mol. Sci.* **2014**, **4**: 576.
[3] Boys, S. F.; Bernardi, F. *Mol. Phys.* **1970**, **19**: 553.
[4] Yu, F. *J. Phys. Chem. A* **2014**, **118**: 3175.
[5] Yu, F.; Fu, L.-X. *Int. J. Quantum Chem.* **2016**, **116**: 1166.
[6] Yu, F. *J. Chem. Theory Comput.* **2014**, **10**: 4400.
[7] Yu, F.; Fu, L.-X.; Yang, Y. *Int. J. Quantum Chem.* **2017**, e25417. https://doi.org/10.1002/qua.25417.

双光子激发时间分辨成像技术原位监测纳米载体的活体输运过程

张超杰[1]，王川西[2]，高智悦[2]，付利民[1]，张建平[1,*]，王远[2,*]

[1]中国人民大学，北京市海淀区中关村大街 59 号，100872

[2]北京大学，北京市海淀区颐和园路 5 号，100871

[1]*Email: jpzhang@chem.ruc.edu.cn

[2]*Email: wangy@pku.edu.cn

纳米载药体由于其优异的药物载运效率与肿瘤靶向性，以及药物释放的可控性和低毒性，在肿瘤诊断和治疗领域备受瞩目。纳米载药体在活体内富集代谢过程、与肿瘤组织靶向结合及其代谢规律是该领域的重要科学问题[1]。然而，由于原位、无损的活体成像技术的制约，对相关科学问题的认识尚不充分。最近，我们基于双光子敏化稀土纳米发光探针$Eu(tta)_3bpt$@SMA[2]，以及时间分辨光谱技术，研制出无损伤、深穿透、大视场的活体成像系统。

我们利用稀土配合物发光的长寿命和不受环境影响的特点，以800 nm飞秒激光对活体小动物实行快速线聚焦扫描，借助增强式电子耦合器件的高速时间门控技术[3]消除了自发荧光和本体散射光的干扰，研制了双光子激发时间分辨活体荧光成像系统（Two Photon Excited Time-Resolved in vivo Fluorescence Imaging System, TPE-TR）。我们监测到了纳米荧光探针在小鼠不同部位的输运过程，研究了纳米发光探针在小鼠体内的富集位点和代谢规律，所得信息有助于促进纳米药物研发和纳米载药体使用。预期该技术在医学诊断、药物研发、生物学、化学等科学研究领域有广阔的应用空间。

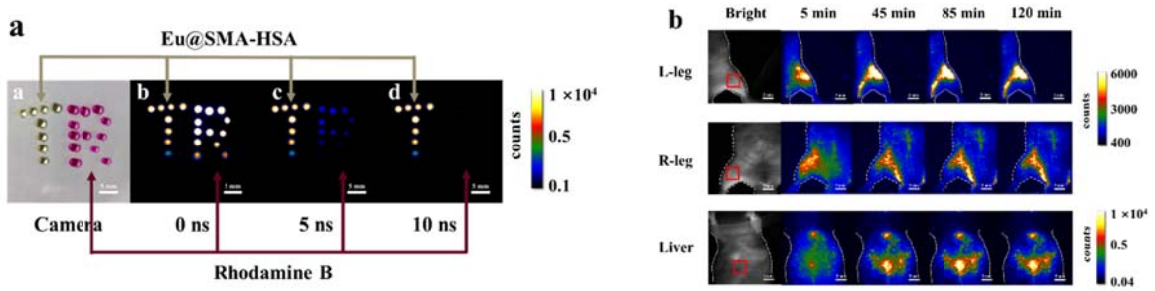

Fig. 1 (a) Camera image and TPE-TR images of a spot pattern printed with Eu@SMA-HSA nanoparticle carrier (T) and with Rhodamine (R). (b) TPE-TR images of Eu@SMA-BSA carrier in a living mouse at the left leg, right leg and liver sites. Scale bars: 5 mm. Region of interests (ROI) are indicated with red frames.

关键词： 双光子激发；活体成像；发光纳米探针；输运过程；代谢过程

参考文献

[1] Wang, R.; Zhou, L.; Wang, W.; Li, X.; Zhang, F. *Nat commun* **2017**, **8:** 14702.

[2] Yang, W.; Fu, L. M.; Wen, X.; Liu, Y.; Tian, Y.; Liu, Y. C.; Han, R. C.; Gao, Z. Y.; Wang, T. E.; Sha, Y. L.; Jiang, Y. Q.; Wang, Y.; Zhang, J. P. *Biomaterials* **2016**, **100**: 152-61.

[3] Sayyadi, N.; Care, A.; Connally, R. E.; Try, A. C.; Bergquist, P. L.; Sunna, A. *Sci Rep* **2016**, **6**: 27564.

A single-longitudinal-mode optical parametric oscillator for high resolution spectroscopy of free radicals

Qiang Zhang, D. Zhang, B. Zhu, J. Gu, D. Zhao*, and Y. Chen*

Hefei National Laboratory for Physical Sciences at the Microscale,
Department of Chemical Physics, University of Science and Technology of China, Hefei, Anhui 230026, PR China
*Email: dzhao@ustc.edu.cn.

We present the development of a tunable, narrow-bandwidth optical parametric oscillator (OPO) system and its applications in high resolution spectroscopy of free radicals. The OPO system employs a bulk KTP crystal as the nonlinear optical material and a compact grazing-incidence-grating cavity as the oscillator. The second harmonic output of an injection-seeded nanosecond Nd:YAG laser with a spatially optimized beam profile is used to pump the OPO system. The OPO cavity length is precisely controlled by monitoring both the beam position and the mode structure of the signal output, ensuring a stable single-longitudinal-mode operation of the system with a broad tuning range. The output of the OPO covers a tunable wavelength of 660 to 2700 nm, with a typical pulse duration of ~5 ns, a FT-limited bandwidth ~150 MHz, and a total pulsed energy of ~ 2.5 mJ at a pump energy of 40 mJ. The newly developed OPO system has been applied to the laser induced fluorescence study on high resolution electronic spectra of CuSH and YO in a supersonic jet expansion. By frequency doubling of the signal output, fully resolved spectra of the CuSH $B^1A' - X^1A'$ and the YO $D^2\Sigma^+ - X^2\Sigma^+$ electronic transition bands has been recorded for the first time.

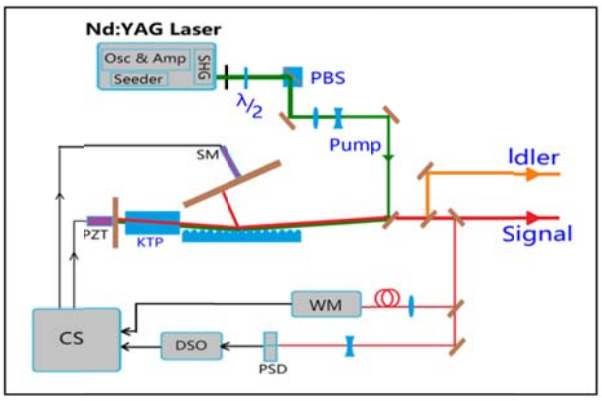

Fig. 1 A schematic view of the geometry of the home-made OPO system

Keywords: OPO; narrow-bandwidth; high resolution spectroscopy

References:

[1] Bosenberg W. R.; Guyer D. R., *Appl. Phys. Lett.* **1992**, **61**: 387.

[2] Zhang, D. P.; Zhang, Q; Zhu, B. X.; Gu, J. W.; Suo, B. B.; Chen, Yang; Zhao, D. F. *J. Chem. Phys.* **2017**, **146**:114303.

多氯代多环芳烃的电加热合成方法

张小闽[1]，李淑娟[2]，陈应[3]，林水潮，唐紫超[1,*]，郑兰荪

厦门大学化学化工学院化学系，固体表面物理化学重点实验室
福建省厦门市思明区思明南路 422 号，361005
*Email: zctang@xmu.edu.cn

自从 1985 年，美国的 Smally、Curl 和英国的 Kroto 等在激光脉冲蒸发石墨[1]的实验过程中发现了富勒烯 C_{60} 以来，富勒烯边引起了科学界的广泛关注和极大的兴趣。目前已经有的方法有石墨激光汽化法、石墨电弧放电法、太阳能法、火焰燃烧法、多环芳烃热裂解法、液相电弧法、辉光放电法和微波等离子体法等等。研究表明多氯代碳簇和富勒烯在同一个反应条件下由氯仿生成，应有着同样的生长机理，且是富勒烯形成过程中的反应中间体。因此对多氯代多环芳烃的合成和研究对探究富勒烯的形成机理具有重大的意义。本文提出一种能条件可控的、操作简单的和生成产物温度的合成富勒烯中间体多氯代多环芳烃的合成方法，得到了 $C_{10}Cl_8$,$C_{12}Cl_8$，$C_{16}Cl_{10}$,$C_{20}Cl_{10}$,$C_{24}Cl_{l2}$ 等一系列的多氯代多环芳烃。

关键词：多氯代多环芳烃；富勒烯；电加热合成方法

参考文献

[1] H. W. Kroto, J. R. Health, S. C. O'Brien, R. F. Curl, R. E. Smalley, *Nature* 1985, 318,162-163.

A Hybrid Learning Algorithm for Atomistic Neural Networks to Fit Potential Energy Surface

Yaolong Zhang[1], Xueyao Zhou[1], Bin Jiang[1,*]

1. Department of Chemical Physics, University of Science and Technology of China, Hefei, Anhui 230026, China

*Email: bjiangch@ustc.edu.cn

Atomistic dimensional neural networks (ANNs) have been widely used to fit the potential energy surface. ANNs can be used for fitting a very large system including thousands of atoms by designing a different neural networks for different atom with distinct element. Levenberg-Maquardt (LM) algorithm is a powerful neural network training algorithm. However, its efficient is still insufficient for a very large system. Extreme Learning Machine is a recently proposed algorithm which resolves the weights in one shot by a linear equation and is thus extremely fast. However its accuracy remains a bottleneck because of its random nature. This work attempts to take advantages of both algorithms and constructs the ANNs with a modified version of Behler and Parrinello symmetry functions[1]. This so-called LM-ELM algorithm performs one ELM halfway forward and one LM halfway backward iteratively, thus reduces the time-consuming LM steps.[2] The LM-ELM algorithm has been tested using the PES of $H+H_2$ and H_2CC systems, which performs better in the convergence speed and generalization ability comparing to the sole LM algorithm.[3]

Keywords: Potential Energy Surface; Levenberg-Marquardt algorithm; Extreme Learning Machine algorithm; Atomistic DimensionalNeural Network

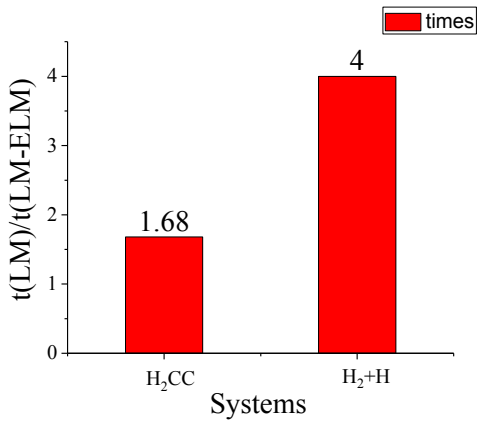

Fig.1 The trend of the ratio of assumed time of L-M algorithm to ELM_L-M algorithm with the fitting system

References:

[1] Smith, J.S., O. Isayev, and A.E. Roitberg, ANI-1: an extensible neural network potential with DFT accuracy at force field computational cost. Chemical Science, 2017. **8**(4): p. 3192-3203.

[2] Huawei ChenFan Jin in Springer, Vol.3971, Eds.: J. Wang et al. Overflag Berlin Heidelberg, **2006**, pp. 509-514.

[3] Yaolong Zhang, Xueyao Zhou, Bin Jiang, (in prepration)

Thermochromatium tepidum 光合膜人工模拟体系的构造及其激发态能量传递动力学

戴玲[1]，谭黎明[1]，石莹[1]，王鹏[1*]，张建平[1]，王征宇[2]

[1]中国人民大学化学系，北京市中关村大街 59 号，100872；
[2]茨城大学理学部，日本水户市文京 2-1-1，310-8512

紫色光合细菌光合膜chromatophore是由外周捕光天线蛋白LH2，核心复合物LH1-RC以一定比例形成的高度有序、二维平面阵列结构，承担着光吸收、激发态能量传递及电荷分离等功能。用细胞膜模拟体系——脂质体将不同的光合膜蛋白以不同比例重新组装成人工膜体系，再与天然chromatophore对比研究，可以进一步阐明光合膜超分子组装的构-效关系。本研究将中等嗜热紫色光合细菌Thermochromatium （Tch.） tepidum 的LH2及LH1-RC以不同比例组装进由大豆卵磷脂构成的脂质体中（样品S1、S2），采用一系列稳态和瞬态光谱手段将它们与Tch. tepidum的chromatophore（样品S3）对比研究，结果表明：人工膜S1和S2样品的LH1-RC/LH2比例分别高于和低于天然膜chromatophore（样品S3）；飞秒时间分辨吸收动力学结果表明，选择性激LH2的B800，人工脂质体的LH2内B800→B850、LH2→LH1（B850→B915）激发态能量传递速率都比chromatophore中相应的过程快，而三种样品中LH1→RC（B915→RC）激发态能量传递速率则非常接近；B800、B850、B915间的激发态能量传递效率对比研究表明，两种人工膜体系的LH2内B800→B850激发态能量传递效率均比天然膜chromatophore中高，而LH2→LH1、LH1→RC的激发态能量传递效率则都比chromatophore中低，其中样品S1更为接近chromatophore；人工膜体系中LH2的取向不像天然膜体系中保持完全一致，以及光合膜蛋白的不同混合比例（S1和S2）导致人工膜上蛋白宏观二维阵列的疏密程度不同，是造成三种样品在激发态动力学上产生不同规律的根本原因。

葡萄球菌肠毒素 B 与亲和体的分子识别动力学模拟研究

丁俊杰[1*]，高川，丁晓琴，童朝阳，李大禹，潘里，董华

[1]北京药物化学研究所，国民核生化灾害防护国家重点实验室，北京昌平，102205

*Email: djj224@163.com

亲和体是一种新型的由58个氨基酸残基组成的蛋白质配体。具有3个α螺旋结构，其中第一及第二螺旋中的13个特定位点，可被随机突变形成理论上可与任何靶分子结合的亲和体。亲和体可作为抗体的替代品，用于蛋白质识别、实验诊断、分子显像及靶向治疗等。本文采用分子模拟方法，对我们应用噬菌体展示方法获得的9个葡萄球菌肠毒素B（SEB）亲和体进行三维结构搭建和优化，采用蛋白-蛋白对接的DS Protein Docking方法和分子动力学模拟，研究亲和体与SEB的相互作用模型及分子识别机制。SEB三维结构来自PDB结构数据库（PDB ID：3W2D），亲和体三维结构的搭建，以PDB结构数据库中的亲和体晶体结构（PDB ID:2B88）为模板，进行定点突变，然后进行分子力学和分子动力学（MD）优化获得。分子对接计算结果表明，两组数据实验值Log（A450）和分子对接结合自由能E-Rdock的协方差为-0.556，相关系数为-0.510，说明两者具有一定的相关性。对亲和能力最强的亲和体affi-SEB17与SEB复合物进行50ns的分子动力学模拟，探讨新型亲和体与SEB的分子识别机制。图1示出亲和体affi-SEB17与SEB分子对接及动力学优化后的分子识别模式图。亲和体的13个特定位点均处于三维结构的外侧面，这样更利于与目标蛋白结合。亲和体affi-SEB17的13个特定位点所在的第一和第二个α螺旋与SEB的第二结构域相互作用。计算结果表明，affi-SEB17与SEB共产生18个不同类型的非键相互作用，包括氢键作用、静电作用和疏水作用，在18个非键相互作用中，13个特定位点有11个，占据了整个相互作用的61%。affi-SEB17与SEB相互作用中共有6个位点（9、13、17、24、28、35）属于13个特定位点，见图1（B）。研究结果为进一步设计亲和体虚拟库和筛选高亲和力的亲和体提供模板和理论指导。

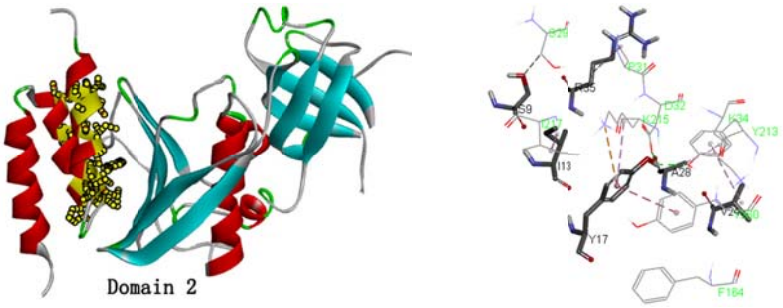

（A） （B）

Fig. 1 Docking and MD results of most potent affibody affi-SEB17 with SEB model

关键词：亲和体；葡萄球菌肠毒素B（SEB）；分子识别；分子动力学模拟（MD）

参考文献

[1] Lofblom J; Feldwisch J; Tolmachev V; et al. Affibody molecules:Engineered proteins for therapeutic, diagnostic and biotechnological applications. *FEBS Lett,* **2010, 584(12):** 2670.

[2]李爽; 郝志明. 新型蛋白质配体-亲和体研究进展. 生物化学与生物物理进展, **2012, 39(2)**: 137.

New energy transfer channel from carotenoids to chlorophylls in purple bacteria

Jin Feng, Yuchen Ma *

School of Chemistry and Chemical Engineering, Shandong University, Jinan 250100
*E-mail: myc@sdu.edu.cn

It has long been controversial whether there is an intermediate dark state between the S2 and S1 states of carotenoids.1 Recent two-dimensional electronic spectroscopy (2DES) measurements further substantiate its existence and its involvement in the energy transfer (ET) from carotenoids to chlorophylls.2 However, there is still considerable debate on the origin of this dark state and how it regulates the ET process. On the basis of ab initio calculations on excited-state dynamics using many-body Green's function theory3,4 and simulated 2D electronic spectrum of carotenoids, we identify that the dark state could be assigned to a completely new Ag+ state.5 ET capability of this state is clarified through Förster-Dexter theory, which may help to solve the long-standing argument on the contribution of each pathway to the total carotenoid-to-chlorophyll ET efficiency in purple bacteria. Moreover, groups on the conjugation backbone of carotenoids are found to affect significantly the excited-state levels and the ET process.

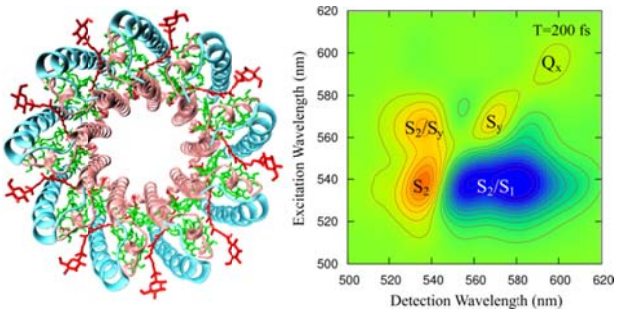

Fig.1 Structure of LH2 complexes (left) and simulated 2D electronic spectrum (right) of *Rhodopseudomonas acidophila*

Keywords: carotenoids, chlorophylls, energy transfer, many-body Green's function theory, 2DES

References:

[1] Cerullo, G. *et al*. *Science* **2002**, *298*, 2395.
[2] Ostroumov, E.E. *et al*. *Science* **2013,** *340*, 51
[3] Leng, X.; Jin,F.; Wei, M. and Ma, Y.C.; *WIREs Comput. Mol. Sci,* **2016**, *6*, 532
[4] Ma, Y. C.; Liu, C. B.; *Prog. Chem.*, **2012**, *24*, 981
[5] Feng, J.; Ma, Y. C.; *et al.*; *Nat. Commun.*, DOI:10.1038/s41467-017-00120-7

蓖麻毒素与单链抗体的相互作用分子动力学模拟研究

高川[1]，丁俊杰，童朝阳，丁晓琴，穆睎惠，刘志伟，刘冰，汪将

[1]北京药物化学研究所，国民核生化灾害防护国家重点实验室，北京昌平，102205

*Email: g.ch.chuan@263.net

单链抗体(Scfv)作为一种小分子基因工程抗体，其分子量小，穿透力强，特异性好，成为抗体工程中最流行的技术之一，单链抗体为特异性识别与检测毒素提供了便捷的技术平台。我们应用噬菌体展示方法获得蓖麻毒素单链抗体。包被蓖麻毒素，用ELISA检测随机挑选出来20个克隆，挑选亲和力最高的克隆扩增提取质粒后进行DNA测序，获得完整单链抗体Scfv16的基因序列，具有735个碱基，编码245个氨基酸残基。而后应用分子模拟方法，研究新型单链抗体Scfv16与蓖麻毒素的相互作用机制。对蓖麻毒素单链抗体Scfv16，进行重链、轻链、CDR区的识别研究，同时对蓖麻毒素A链进行构象表位预测和结构功能分析。采用同源模建及分子动力学方法，构建并优化单链抗体Scfv16三维结构，结合Profile-3D和拉氏图方法，评价单链抗体三维结构与其一维序列的兼容性和模型的合理性。利用蛋白-蛋白分子对接方法和50ns的分子动力性模拟方法，研究单链抗体Scfv16与毒素的识别及相互作用模型。结果表明，蓖麻毒素A链具有13个可能的构象表位，毒素结合到单链抗体的重链上，毒素与单链抗体Scfv16分子识别，主要是蓖麻毒素A链的第7、8表位的残基，与单链抗体重链的CDR2区的残基，形成氢键、π-π相互作用和疏水作用。本研究为蓖麻毒素抗体的结构设计提供了重要的线索和理论依据，对毒素类新型抗体的研究和开发具有理论指导价值。

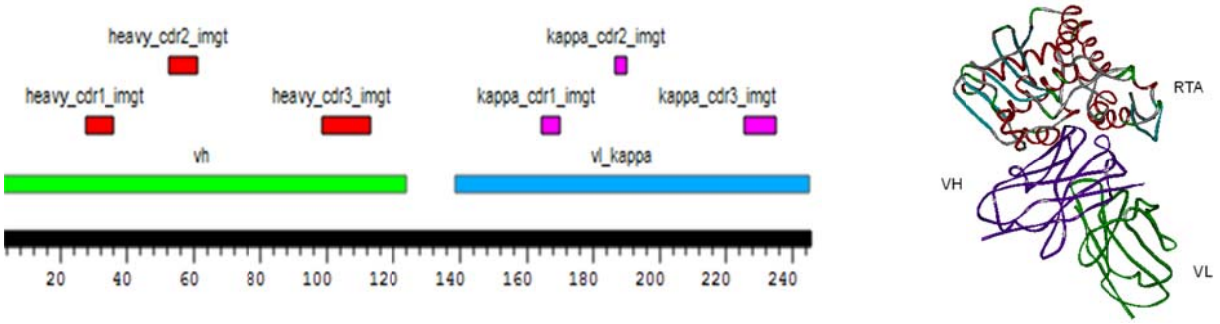

(A) (B)

Fig. 1 Predicting of single-chain antibody Scfv16 CDR domain (A) and Ricin-Scfv16 recognition model (B)

关键词： 蓖麻毒素；单链抗体；分子动力学模拟（MD）；分子对接

参考文献

[1] Rudolph, M J.;Vance, D. J.;Cheung J.,et al. *J Mol Biol.* **2014, 426**: 3057.

[2] Hu W.G.; Yin. J.; Chau D.; Negrych LM，et al. *PLoS One* **20l2, 7**：e45595.

激光解吸/后电离质谱在生物医学中的应用

陆桥，胡勇军*

华南师范大学生物光子学研究院激光生命科学教育部重点实验室，广州，510631

*Email: yjhu@scnu.edu.cn

对生物组织中的药物分析的传统方法，都需要对样品进行复杂的前处理，包括萃取、离心、浓缩等。这些过程不仅浪费时间，而且难以实现原位检测。本文中所介绍的激光解析-真空紫外单光子电离质谱(LDPI-MS)为这一难题的解决展示了很好的应用前景[1]。在激光解吸/后电离质谱技术中, 解析和电离过程在空间和时间上是相互独立的, 这样可以方便的对每一过程进行单独优化。本课题组自主搭建的质谱仪配备一个三维进样平台，可对生物组织进行质谱成像。在实验中，样品杆在电机的带动下缓缓的在质谱仪中的电离区进行移动。三维平台可以实现XYZ三维方向上随意速度步长的精密移动。如图1所示，成像时，三维平台采取往返扫描模式，直到整个样品表面被扫描完。在这个过程中，三维平台的移动速度以及步长由样品大小决定。每个点的扫描时间为1.6 s，包括采集，传输，处理以及样品重置。对于在本论文中的成像实验，样品大小为 6×6 mm^2，因此三维平台在Y轴方向上的移动速度为25 μm/s，在X轴上的步长为 300 μm。成像数据经过Matalab软件处理获得质谱成像图。

众所周知，上皮癌细胞由于快速分裂增殖，需要大量的叶酸来用于DNA合成，会比正常细胞成倍分泌叶酸受体。叶酸受体与叶酸具有高度亲和性，因此，对已接种乳腺癌的小鼠注射20 mg/kg的叶酸溶液时，叶酸受体高表达区域即肿瘤组织会吸收大量的叶酸，而正常组织的叶酸含量较低[2]。由于基质的干扰限制了MALDI-MS对叶酸等小分子化合物的检测，而LDPI-MS可以实现对这类化合物的直接检测。通过激光解吸/后电离质谱成像(LDPI-MSI)与H&E染色实验对比（如图2所示），我们清楚地发现肿瘤组织中的叶酸质谱信号强于邻近的正常组织。这种分子成像方法对肿瘤的临床医学诊断和外科手术治疗具有潜在的应用价值。

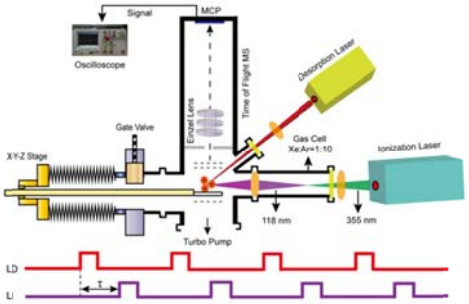

Fig. 1 Schematic drawing of the LDPI-MSI. Schematic diagram of the laser desorption postionization mass spectrometer imaging apparatus and the sample hold with an X-Y-Z stage. The lower panel illustrates the laser trigger sequence.

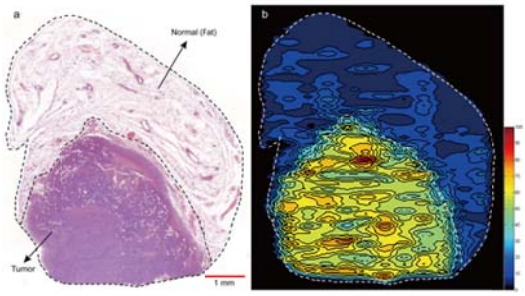

Fig. 2 LDPI-MS images of the tissue sections. The image (a) shows the H&E staining of the The image (a) shows the H&E staining of the tissue section and (**b**) depicts spatial distribution of FA dominate ion at *m/z* 265.

关键词：激光解吸/后电离；质谱；成像；叶酸；叶酸受体；肿瘤诊断

参考文献

[1] G. L. Gasper, L. K. Takahashi, J. Zhou, M. Ahmed, J. F. Moore, L. Hanley. *Anal. Chem*. **2010, 82**: 7472.

[2] Chen, C.; Ke, J.; Zhou, X. E.; Yi, W.; Brunzelle, J. S.; Li, J.; Yong, E. L.; Xu, H. E.; Melcher, K. *Nature* **2013, 500**：486-489.

气液界面鞘磷脂与胆固醇相互作用的高分辨宽带和频振动光谱研究

李亦易[1,2]，刘鸣华[3]，郭源[1,2,*]，张贞[1,*]

[1] 中国科学院化学研究所北京分子科学国家实验室，北京市海淀区中关村北一街 2 号，100190

[2] 中国科学院大学，北京市石景山区玉泉路 19 号（甲），100049

[3] 中国科学院化学研究所胶体、界面与化学热力学院重点实验室，北京市海淀区中关村北一街 2 号，100190

[*]Email: guoyuan@iccas.ac.cn; zhangz@iccas.ac.cn

鞘磷脂分子是细胞质膜的重要组成部分。鞘磷脂分子在生物膜界面上的结构变化及其与胆固醇之间的相互作用直接影响生命过程中细胞膜的生物学功能。我们在以往的研究中发现钙离子与极性头基PO_2^-的结合影响气/液界面鞘磷脂单分子膜的结构和取向[1]，但气液界面的鞘磷脂与胆固醇之间相互作用的研究尚不多见。利用本组自行研制的高分辨和频振动光谱(HR-BB-SFG-VS)研究了气液界面胆固醇对鞘磷脂（egg sphingomyelin, ESM）分子的构象和取向的影响，从分子水平理解鞘磷脂单分子膜与胆固醇相互作用的分子机理。胆固醇使ESM两条烃链中的鞘氨醇骨架变得有序，而对另一条N-linked的饱和脂肪酸烃链几乎没有影响。胆固醇的插入破坏了鞘氨醇骨架上羟基与头基上PO_2^-基团之间形成的分子内氢键，使鞘氨醇骨架末端甲基的取向更加直立；同时胆固醇末端亲水的羟基与鞘磷脂头基上的PO_2^-基团形成了分子间氢键，使得ESM极性头基上的PO_2^-基团的取向更平行于界面。为了进一步验证这一分子机理，我们通过改变鞘磷脂单分子膜亚相的pH，破坏鞘氨醇骨架上羟基与头基上PO_2^-基团之间的分子内氢键后研究界面上ESM的取向，发现ESM鞘氨醇骨架的取向变得更加直立， N-linked的饱和脂肪酸烃链几乎没有影响，头基的PO_2^-基团取向变得更加直立，支持了胆固醇与ESM单分子膜之间相互作用的分子机理。本研究首次从分子水平上阐明了气液界面鞘磷脂与胆固醇相互作用的机理，加深了胆固醇对细胞膜结构和功能影响机制的认识。

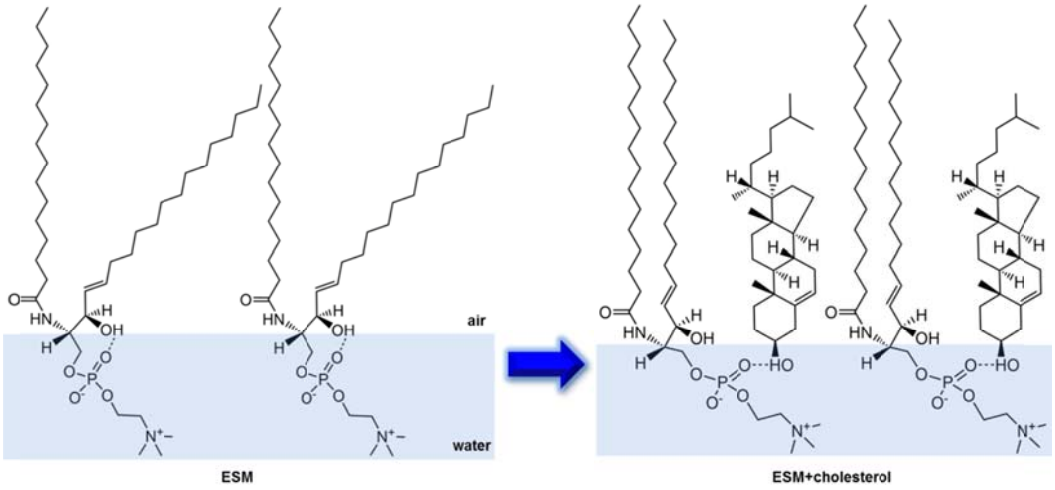

Fig. 1 Molecular mechanism of cholesterol interacting with the headgroup and hydrocarbon chains of ESM.

关键词：鞘磷脂；胆固醇；相互作用；高分辨和频振动光谱

参考文献

[1]R. J. Feng, L. Lin, Y. Y. Li, M. H. Liu, Y. Guo, Z. Zhang, *Biophysical Journal* **2017**, *112*, 2173-2183.

激光烧蚀分子束质谱法对生物药物分子及其团簇的探测研究

李裕健，宋文韬，胡勇军*

华南师范大学生物光子学研究院，激光生命科学教育部重点实验室 中国 广州

*Email: yjhu@scnu.edu.cn

采用超声分子束质谱方法在气相中研究生物或药物分子及其分子间相互作用，有助于我们在分子水平理解生物分子识别过程的物理化学本质。由于生物或药物分子大多为热不稳定的固体物质，需要寻找一种快速气化生物分子的方法。基于激光解析/烧蚀的气化方法，在采用分子束质谱技术开展对生物分子及其团簇的探测研究过程中得到广泛应用。本课题组在原有超声分子束电离质谱实验装置的基础上，自主设计并组装一种新的激光烧蚀气化装置，并应用分子束质谱法对一些生物或药物分子及其团簇进行了初步探测。该实验过程中，检测过程可以分为两步，首先利用532或1064 nm的激光去照射生物或药物分子使之气化，在载气的载带下经过漏勺形成超声分子束。经过一定时间的延迟后，再采用118 nm真空紫外光对分子束中的生物或药物分子及其团簇进行“软”电离。通过飞行时间质谱仪以及信号采集装置来优化和采集单分子及其团簇离子信号。目前本课题组对一些碱基，如胞嘧啶，腺嘌呤和一些药物分子如9-苯基吖啶，1-5二氨基蒽醌等进行了初步的探测研究，并探测获得相应分子及其团簇的飞行时间质谱图。

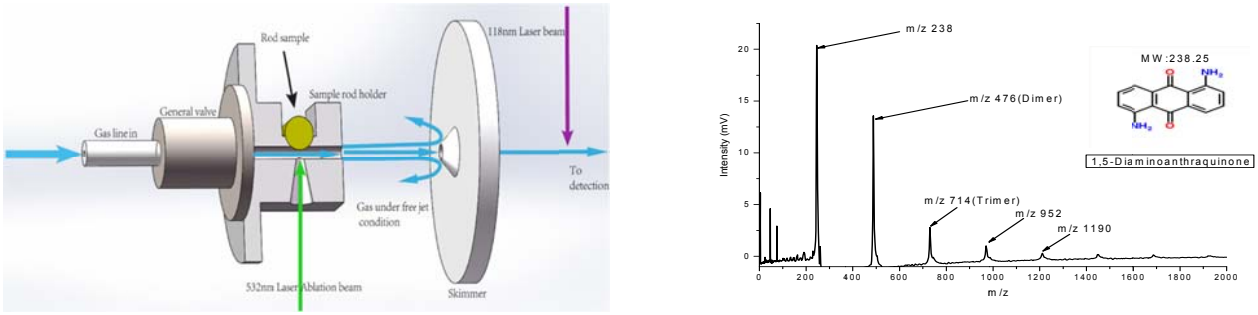

Fig.1 A. Scheme of the laser vaporization-molecular beam source. B. Time-of-flight mass spectrum of 1,5-Diaminoanthra- quinone and it’s cluster.

关键词：激光烧蚀；超声分子束；团簇；药物分子

参考文献

[1] Tomonari Wakabayashi, Takamasa Momose, and Tadamasa Shida. *J. Chem. Phys.* 1999, **111**: 14.

[2] Michael A. Duncan. *Rev. Sci. Instrum.* 2012, **83**: 041101.

[3] Mukarakate e t al . *Rev. Sci. Instrum*. 2011, **82:** 033104.

6-硫代鸟嘌呤脱氨反应机理的理论研究

吴丽丹*，陈来林，吴伟虹，沈鑫海

上饶师范学院化学与环境科学学院，江西上饶，334001

*Email: wulidan1987@iccas.ac.cn

本文利用量子化学从头算的方法计算了6-硫代鸟嘌呤和水、OH^-、OH^-/H_2O及质子化的6-硫代鸟嘌呤和水的脱氨反应机理。计算得到六条反应路径，各路径所涉及的反应物、中间体、过渡态及产物利用HF/6-31+G(d)、 M062X/6-31+G(d)、B3LYP/6-31+G(d) 和 B3LYP/6-311++G(d, p)方法进行了优化，并利用以上方法对每一条反应路径的活化能、焓及活化Gibbs自由能进行了计算。与6-硫代鸟嘌呤和水及质子化的6-硫代鸟嘌呤和水发生脱氨反应相比，6-硫代鸟嘌呤和OH^-发生脱氨反应的能垒更低，说明6-硫代鸟嘌呤最容易发生脱氨反应的形式是去质子化的6-硫代鸟嘌呤。在额外一个水分子的帮助下，6-硫代鸟嘌呤和OH^-/H_2O发生脱氨反应的能垒进一步降低，即具有最低的反应能垒，被视为6-硫代鸟嘌呤脱氨的最优反应路径。

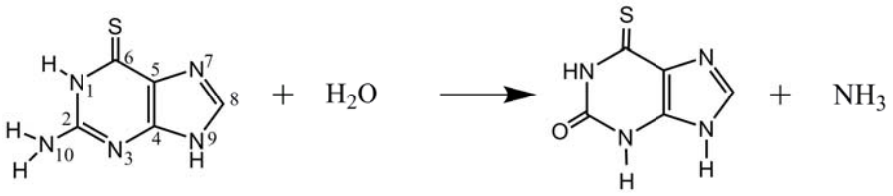

Fig. 1 Deamination Reaction of 6-thioguanine

关键词：6-硫代鸟嘌呤；脱氨反应；量子化学；反应机理

参考文献

[1] Zou, X.; Zhao, H.; Yu, Y.; Su, H. *J. Am. Chem. Soc.* **2013**, **135**: 4509.

[2] Ren, X.; Li, F.; Jeffs, G.; Zhang, X.; Xu, Y.; Karran, P. *Nucleic Acids Res.* **2010**, **38**: 1832.

[3] Yu, Y.; Liu, K.; Zhao, H.; Song D. *J. Phys. Chem. A* **2013**, **117**: 5715.

蛋白质超粗粒化模型的发展

夏飞[*,†,§]，曹泽星[‡]，张增辉[†]

[†]化学与分子工程学院，华东师范大学，邮编 200062

[‡]厦门大学化学化工学院，厦门大学，邮编 361005

[§]上海纽约大学-华师大联合计算中心，上海纽约大学，邮编 200062

*Email: fxia@chem.ecnu.edu.cn

粗粒化模型被广泛地应用于蛋白质结构与功能的研究，发展蛋白质的粗粒化模型为生物大体系的多尺度模拟提供了重要的理论工具。近期，我们尝试了发展了蛋白质超粗粒化模型，超粗粒化模型跟目前国际上的粗粒化模型相比具有更低的分辨率。我们已经发展了针对蛋白质体系超粗粒化的快速优化方法(FM-CG)与算法(SLIO)，利用这些方法可以优化得到蛋白质体系的超粗粒化表达。我们进一步利用经验的势能函数对超粗粒化粒子进行了参数化，并构建了蛋白质有效的超粗粒化模型。我们将运用发展的超粗粒化模型来模拟研究蛋白质复合物的动力学性质与功能。

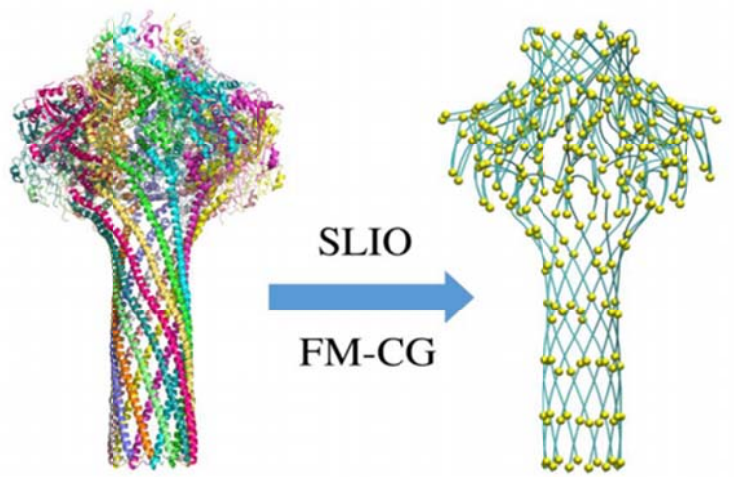

Fig 1. 超大蛋白质复合物的快速粗粒化

关键词：超粗粒化模型；蛋白质功能；多尺度模拟

参考文献

[1] Zhang, Y. W.; Cao, Z. X.; Xia, F.* Chem. Phys. Lett. 2017, 681, 1.

[2] Zhang, Y. W.; Cao, Z. X.; Zhang, J. Z. H.; Xia, F.* J. Chem. Inf. Model. 2017, 57, 214.

[3] Li, M.; Zhang, J. Z. H.; Xia, F.* J. Chem. Theory Comput. 2016, 12, 2091.

[4] Li, M.; Zhang, J. Z. H.; Xia, F.* J. Comput. Chem. 2016, 37, 795.

拉曼光谱研究溶菌酶纤维化结构与进程

邢蕾[1]，范伟[2]，周晓国[1,2*]，刘世林[1,2*]

[1]合肥微尺度物质科学国家实验室

[2]化学物理系，中国科学技术大学，安徽合肥，230026

*Email: xzhou@ustc.edu.cn

蛋白质依赖于其稳定的球状结构发挥正常的生物功能。然而在某些条件下，其结构会发生展开并错误折叠[1,2]，其中最被广泛研究的即为蛋白质纤维化。它由大量分子间β-sheet 沿着纤维轴生长而构成。这一结构被 ThT 荧光光谱以及 CD 光谱所证实，其细长纤维样的形貌也被 AFM 技术所证实。这一刚性有序的结构被认为与神经退行性疾病有着密切的联系，如阿尔兹海默病，帕金森症等[3,4]。尽管这一结构变化过程被普遍接受，但是关于其微观层次的分子结构变化以及其特征时间一直以来都没有明确结论。本文以溶菌酶蛋白为模型[5]，利用拉曼光谱同时对其纤维化过程中三级结构以及二级结构的变化进行了观测。我们采用 1340-1360cm^{-1} 范围 Trp 侧链残基的吲哚环伸缩振动表征蛋白质三级结构的变化，927cm^{-1} 范围 N-C_α-C 基团以及 1650cm^{-1} 范围 Amide I 基团的拉曼光谱指针表征蛋白质二级结构的变化。结合 ThT 荧光光谱以及 AFM 图谱，我们定量分析了微观结构以及宏观结构的变化，从而得到溶菌酶蛋白纤维化过程的反应历程及主要中间状态的特征时间：溶菌酶纤维化过程中，其三级结构首先变化，形成部分展开态，随后二级结构中α-helix 在 10h 左右开始减少，而β-sheet 则在 40h 左右开始大量增多，最终在 160h 左右纤维样达到饱和，这说明α-helix 结构可能并不是直接转化为β-sheet 结构，而是优先转化为 random coil 结构。

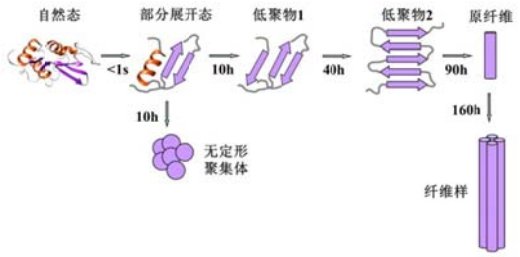

Fig. 1 Mechanism of amyloid fibrillation of lysozyme

关键词：蛋白质纤维化；溶菌酶；拉曼光谱

参考文献

[1] Dobson, C. M. *Nature* **2003**, **426**: 884.

[2] Chiti, F.; Dobson, C. M. *Annu. Rev. Biochem.* **2006**, **75**: 333.

[3] Dobson, C. M. *Trends in biochemical sciences* **1999**, **24**: 329.

[4] Soto, C. *Nature Reviews Neuroscience* **2003**, **4**: 49.

[5] Swaminathan, R.; Ravi, V. K.; Kumar, S.; Kumar, M. V. S.; Chandra, N. *Adv Protein Chem Struct Biol* **2011**, **84**: 63.

小分子多元醇对嗜热紫色光合细菌 *Tch. tepidum*-LH2 激发态动力学的影响

于洁[1]，昌玉强[1]，于龙江[2]，周璇[1]，王鹏[1]，张建平[1,*]，王征宇[2,*]

[1] 中国人民大学，北京市海淀区中关村大街 59 号，100872

[2] 日本茨城大学，日本茨城，310-85112

*Email: jpzhang@chem.ruc.edu.cn; wang@ml.ibaraki.ac.jp

*Tch. tepidum*是发现于美国黄石国家公园的紫色光合细菌，生理温度约为50°C[1]，其外周捕光天线LH2具有非均一的脱辅基蛋白和类胡萝卜素[2]，,LH2中每个结构单元里有三个细菌叶绿素，吸收分别在800 nm以及850 nm处，分别称为B800及B850，目前该细菌的LH2晶体结构未知。通常对LH2的研究是将LH2从膜蛋白中提取出后，置于含有一定比例表面活性剂的缓冲溶剂中，但是对于在缓冲溶液中的LH2，上下两端的N-端及C-端会暴露于缓冲溶液中，与水分子直接接触。.甘油是一种高效的生物防腐剂和防冻剂，可以使蛋白保持结构完整和生物活性，但同时也影响了蛋白的三级、四级结构。为了更好的研究LH2中的能量传递，研究者通常选择在低温下进行试验，经常在缓冲溶液中加入一部分的甘油，保证冷冻样品的光学质量。但是人们经常忽略一个事实，甘油可以改变缓冲溶液中的氢键网络和水的活度，通过与蛋白表面残基和氢键的作用，影响蛋白的水合层，从而影响蛋白的状态。本文研究了*Tch. tepidum* LH2在加入不同比例的甘油以及山梨醇的缓冲溶液中的激发态动力学行为，随着甘油比例的增加，B800向B850传能速度变快，且基态漂白回复逐渐变快，但对于加入山梨醇的样品，传能速度与漂白回复速度都有一些变快但并不明显，只是在加入80%比例的山梨醇时有一个突变行为。小分子多元醇会对蛋白水合状态以及聚集程度有影响，不同的小分子多元醇对样品有不同的影响，本工作有助于进一步了解光合细菌的环境适应性。

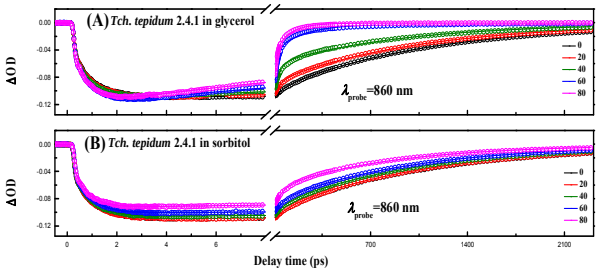

Fig. 1 Kinetics traces at BLC of B850 for the LH2 complexes with different percent low-molecular complexes weight polyols.

关键词： 小分子多元醇；激发态动力学；紫色嗜热细菌；能量传递

参考文献

[1] Madigan, M.T. *Science*. 1984,225(4659),313-315

[2] Zeng, X., Choudhary,M., Kaplan, S. *J. Bacteriol*. 2003,185(20),6171-6184

[3]Hussels, M., Brecht, M. *Biochemistry*. 2011, 50(18),3628-3637

Dynamic Protein Conformations Preferentially Drive Energy Transfer along Active Chain of the Photosystem-II Reaction Center

Lu Zhang[1,2], Daniel-Adriano Silva[2], Houdao Zhang[3], Alexander Yue[2], YiJing Yan[3*] and Xuhui Huang[2*]

[1]State Key Laboratory of Structural Chemistry, Fujian Institute of Research on the Structure of Matter, Chinese Academy of Sciences, Fuzhou, Fujian, China

[2]Department of Chemistry, Hong Kong University of Science and Technology, Kowloon, Hong Kong
[3]Hefei National Laboratory for Physical Sciences at the Microscale, University of Science and Technology of China, Hefei, China

One longstanding puzzle concerning photosystem II, a core component of photosynthesis, is that only one of the two symmetric branches in its reaction centre is active in electron transfer. To investigate the effect of the photosystem II environment on the preferential selection of the energy transfer pathway (a prerequisite for electron transfer), we have constructed an exciton model via extensive molecular dynamics simulations and quantum mechanics/molecular mechanics calculations based on a recent X-ray structure. Our results suggest that it is essential to take into account an ensemble of protein conformations to accurately compute the site energies. We identify the cofactor CLA606 of active chain as the most probable site for the energy excitation. We further pinpoint a number of charged protein residues that collectively lower the CLA606 site energy. Our work provides insights into the understanding of molecular mechanisms of the core machinery of the green-plant photosynthesis.

Reference:

[1]Zhang, L. et al. Dynamic protein conformations preferentially drive energy transfer along active chain of the photosystem II reaction centre. Nat. Commun. 5:4170 doi: 10.1038/ncomms5170 (2014).

胆酸钠对 *Rhodobacter* (*Rba.*) *sphaeroides* 2.4.1 的 chromatophore 膜的通透性的影响

周璇，王鹏，付立民，张建平*

中国人民大学，北京市海淀区中关村大街 59 号，100872

*Email: jpzhang@chem.ruc.edu.cn

作为一种表面活性剂，胆酸钠(Sodium Cholate)与脂膜的相互作用受到研究者的广泛关注。研究表明，胆酸钠可以有效地改变脂质体膜的通透性。在我们的实验中中发现胆酸钠也可以改变 *Rba. sphaeroides* 2.4.1 的 chromatophore 膜的通透性。我们的实验探究了 chromatophore 样品 carotenoid band-shift 信号(生物活性的标志)对胆酸钠(Sodium Cholate)的响应情况，利用此响应情况表征胆酸钠对 chromatophore 膜通透性的影响程度。并且利用动态光散射技术(DLS)探究了不同浓度的胆酸钠对 chromatophore 粒径大小的影响，结果表明，加入的胆酸钠浓度在一定范围时，chromatophore 粒径大小保持稳定，结构未被破坏，且 carotenoid band-shift 信号受到显著影响。

关键词：胆酸钠；*Rba.sphaeroides*；chromatophore；通透性